National Library of Canada
Bibliothèque nationale du Canada

Canadian Theses Service
Service des thèses canadiennes

Ottawa, Canada
K1A 0N4

NOTICE

The quality of this microform is heavily dependent upon the quality of the original thesis submitted for microfilming. Every effort has been made to ensure the highest quality of reproduction possible.

If pages are missing, contact the university which granted the degree.

Some pages may have indistinct print especially if the original pages were typed with a poor typewriter ribbon or if the university sent us an inferior photocopy.

Reproduction in full or in part of this microform is governed by the Canadian Copyright Act, R.S.C. 1970, c. C-30, and subsequent amendments.

AVIS

La qualité de cette microforme dépend grandement de la qualité de la thèse soumise au microfilmage. Nous avons tout fait pour assurer une qualité supérieure de reproduction.

S'il manque des pages, veuillez communiquer avec l'université qui a conféré le grade.

La qualité d'impression de certaines pages peut laisser à désirer, surtout si les pages originales ont été dactylographiées à l'aide d'un ruban usé ou si l'université nous a fait parvenir une photocopie de qualité inférieure.

La reproduction, même partielle, de cette microforme est soumise à la Loi canadienne sur le droit d'auteur, SRC 1970, c. C-30, et ses amendements subséquents.

NL-339 (r. 88/04) c

Canada

UNIVERSITY OF ALBERTA

BEHAVIOUR OF SALINE FROZEN SOILS

BY

© ELISABETH G. HIVON

A THESIS
SUBMITTED TO THE FACULTY OF GRADUATE STUDIES AND RESEARCH
IN PARTIAL FULFILLMENT OF THE REQUIREMENTS FOR THE DEGREE
OF DOCTOR OF PHILOSOPHY

DEPARTMENT OF CIVIL ENGINEERING

EDMONTON, ALBERTA
SPRING 1991

National Library of Canada
Bibliothèque nationale du Canada

Canadian Theses Service
Service des thèses canadiennes

Ottawa, Canada
K1A 0N4

The author has granted an irrevocable non-exclusive licence allowing the National Library of Canada to reproduce, loan, distribute or sell copies of his/her thesis by any means and in any form or format, making this thesis available to interested persons.

The author retains ownership of the copyright in his/her thesis. Neither the thesis nor substantial extracts from it may be printed or otherwise reproduced without his/her permission.

L'auteur a accordé une licence irrévocable et non exclusive permettant à la Bibliothèque nationale du Canada de reproduire, prêter, distribuer ou vendre des copies de sa thèse de quelque manière et sous quelque forme que ce soit pour mettre des exemplaires de cette thèse à la disposition des personnes intéressées.

L'auteur conserve la propriété du droit d'auteur qui protège sa thèse. Ni la thèse ni des extraits substantiels de celle-ci ne doivent être imprimés ou autrement reproduits sans son autorisation.

ISBN 0-315-66771-0

Canada

UNIVERSITY OF ALBERTA

RELEASE FORM

NAME OF AUTHOR: Elisabeth G. Hivon

TITLE OF THESIS: BEHAVIOUR OF SALINE FROZEN SOILS

DEGREE : Doctor of Philosophy

YEAR THIS DEGREE GRANTED: Spring 1991

PERMISSION IS HEREBY GRANTED TO THE UNIVERSITY OF ALBERTA LIBRARY TO REPRODUCE SINGLE COPIES OF THIS THESIS AND TO LEND OR SELL SUCH COPIES FOR PRIVATE, SCHOLARLY OR SCIENTIFIC RESEARCH PURPOSES ONLY.

THE AUTHOR RESERVES OTHER PUBLICATION RIGHTS, AND NEITHER THE THESIS NOR EXTENSIVE EXTRACTS FROM IT MAY BE PRINTED OR OTHERWISE REPRODUCED WITHOUT THE AUTHOR'S WRITTEN PERMISSION.

Elisabeth Hivon

Permanent address:

1460 Boul. de l'Entente #808
Québec, Québec
Canada
G1S 4V2

Date: March 27, 1991

UNIVERSITY OF ALBERTA

FACULTY OF GRADUATE STUDIES AND RESEARCH

THE UNDERSIGNED CERTIFY THAT THEY HAVE READ, AND RECOMMEND TO THE FACULTY OF GRADUATE STUDIES AND RESEARCH FOR ACCEPTANCE, A THESIS ENTITLED *BEHAVIOUR OF SALINE FROZEN SOILS* SUBMITTED BY *ELISABETH G. HIVON* IN PARTIAL FULFILLMENT OF THE REQUIREMENTS FOR THE DEGREE OF DOCTOR OF PHILOSOPHY.

DC Sego.

Dr. D.C. Sego (supervisor)

Dr. N.R. Morgenstern (co-supervisor)

Dr. D. Chanasyk

Dr. G. Lock

Ted S Vinson

Dr. T. Vinson

Date: March 22, 1991

A mes parents,

avec amour et reconnaissance.

ABSTRACT

This thesis presents the results of an investigation of the distribution and mechanical behaviour of saline frozen soils. A better understanding of these soils will help the geotechnical engineer working in northern areas.

The first part of the thesis presents a database of the salinity measurements from the Northwest Territories. Correlations between salinity and physical properties show that salinity decreases with an increase in moisture content, and that high salinities are found in marine or glacial sediments associated with a period of marine transgression. The occurrence of saline permafrost was shown to be associated with the Quaternary geology .

Two aspects of the mechanical behaviour were investigated in detail; the deformation response under constant strain rate compression and the time dependent deformation response under constant stress compression. Three soils were studied at four different salinities: a fine uniform sand, a silty sand and a very fine silty sand at salinities of 0, 5, 10, 30 ppt.

For the constant strain rate tests, test temperatures were -12°C, -10°C, -7°C and -5°C. An important difference between the behaviour of the sand and the silty sands was observed: the sand behaved in a brittle manner while the silty sands displayed a strain-strengthening behaviour up to strain levels of 15%, with an initial yield point at about 1% strain which corresponds to the onset of ice failure. This difference in behaviour is related to the location of the unfrozen water within the frozen soil.

The strength of all soils was shown to decrease with an increase in salinity and temperature, or with an increase in unfrozen water content which was measured using time-domain reflectometry. Relationships between strength and temperature or unfrozen water content are presented.

Time dependent (creep) behaviour was studied at -7°C. The soils studied followed the minimum strain rate creep theory. An increase in minimum strain rate, or a decrease in

time to failure, were observed with an increase in salinity and stress. Three models from the literature were investigated to predict the strain-time relationship. Sayles' (1968) and Gardener et al.'s (1984) models gave fairly good predictions up to failure. Vyalov et al.'s (1988) model can not predict strain-time relationship for the silty sands and gave a poor prediction for the sand. All creep parameters were related to salinity or unfrozen water content. The use of a stress exponent n=3 in an equation similar to the flow law of ice was shown to be invalid for the soils studied.

ACKNOWLEDGEMENTS

The author would like to thank sincerely Dr. Dave Sego for his help, patience and most valuable support during the course of this thesis. His technical knowledge and his great disponibility made him the ideal supervisor. Dr. Morgenstern also deserves many thanks for his interest and support of the subject. The whole academic staff of the geotechnical section were very helpful during the last five years.

The author would like to thank the technical staff, and especially Mr. Gerry Cyre and Mrs. Christine Hereygers. Without their input and help, the laboratory portion of this thesis would have never been completed and the author still would be locked up in a freezer. The support staff of the department of civil engineering were of great assistance during the course of this research.

To all my friends and collegues, who went through the difficult and happy moments of this adventure, thank you! Very special thanks must go to Kevin Biggar and Jean Hutchinson who had to share a cold room with me, and much more. Their friendship will stay with me for the rest of my life. To my friend and former office mate, Tai Wong, I want to offer my sincere thanks for his enormous help and patience regarding computer matters. To Chris B., Angie and Chris G. thank you for your friendship, love and support.

The Natural Science and Engineering Research Council, the Alberta Research Council, the Department of Energy, Mines and Resources and the Alberta Heritage Fund, all made this research possible through their financial assistance to the author.

Finalement, les derniers remerciements, mais les plus importants, doivent aller à mes proches du Québec et à ma famille. Catherine, Véro, Caroline et Renée merci de tout mon coeur de votre support et amitié. A Michel, qui a du endurer les derniers mois, merci. Ton amour et patience m'ont permis de passer au travers des derniers moments. A mes parents, à qui je dois cette thèse, les mots ne suffisent pas pour décrire ma gratitude. Votre amour et support m'ont permis de survivre ces cinq longues années.

TABLE OF CONTENTS

Chapter Page

1. INTRODUCTION 1
   1.1. Background 1
   1.2. Scope of Study 2

2. DISTRIBUTION OF SALINE PERMAFROST 5
   2.1. Introduction 5
   2.2. Database 6
      2.2.1. Data Collection 6
      2.2.2. Database Entries 7
   2.3. Results 13
      2.3.1. Introduction 13
      2.3.2. Summary of Data 14
      2.3.3. Salinity versus Moisture Content 14
      2.3.4. Salinity versus Depth 15
   2.4. Interpretation 17
      2.4.1. Introduction 17
      2.4.2. Quaternary Geology of Baffin Island 17
      2.4.3. Quaternary Geology of Northwestern Canadian Shield 19
      2.4.4. Quaternary Geology of the Canadian Interior Plains 20
      2.4.5. Explanation of the Salinity Distribution 23

3. LITERATURE REVIEW 39
   3.1. Physical behaviour of frozen soils 39
      3.1.1. Unfrozen water in non-saline frozen soils 39
      3.1.2. Influence of salinity on pore fluid of frozen soils 41
      3.1.3. Direct measurement of unfrozen water content 45
      3.1.4. Electrical properties of saline frozen soils 51
   3.2. Mechanical properties of ice 52
      3.2.1. Compressive strength of polycrystalline ice 53
      3.2.2. Compressive strength of sea ice 55
      3.2.3. Creep behaviour of polycrystalline ice 60
      3.2.4. Creep behaviour of saline and sea ice 65
   3.3. Mechanical properties of non-saline frozen soils 66
      3.3.1. Compressive strength of non-saline frozen soils 66
      3.3.2. Creep of non-saline frozen soils 71
   3.4. Mechanical properties of saline frozen soils 82
      3.4.1. Compressive strength of saline frozen soils 82
      3.4.2. Creep behaviour of saline frozen soils 85

4. LABORATORY PROCEDURE 95
   4.1. Scope of testing program 95
   4.2. Sample preparation 95
   4.3. Determination of physical properties 97
      4.3.1. Moisture Content and Density 97
      4.3.2. Salinity Determination 97
      4.3.3. Unfrozen Water Content Determination- TDR testing 98
      4.3.4. Electrical conductivity 99
   4.4. Unconfined constant strain rate compression tests 100
      4.4.1. Description of equipment 100
      4.4.2. Test procedure 102

4.5. Constant stress compression tests 103
  4.5.1. Description of equipment 103
  4.5.2. Test procedure 103

5. EXPERIMENTAL RESULTS 112
5.1. Introduction 112
5.2. Moisture content, density and salinity 112
5.3. Unfrozen water content 116
5.4. Unconfined constant strain rate compression test results 117
5.5. Constant stress compression test results 121

6. ANALYSIS AND INTERPRETATION OF TEST RESULTS 159
6.1. Unfrozen water content 159
6.2. Behaviour of frozen saline soils under uniaxial constant strain rate compression 161
  6.2.1. Stress-strain behaviour of frozen saline soils 161
  6.2.2. Influence of density on the compressive strength and secant modulus 163
  6.2.3. Influence of temperature on compressive strength and secant modulus 164
  6.2.4. Influence of the unfrozen water content on compressive strength and secant modulus 170
6.3. Time dependent deformation of frozen saline soils under uniaxial compression 174
  6.3.1. Time dependent deformation of frozen saline soils 174
  6.3.2. Analysis of strain-time relationships 176
  6.3.3. Variation of the creep parameters with salinity or unfrozen water content 180
6.4. Comparison between constant stress test (creep) and constant strain rate test 189
6.5. Ultimate strength of frozen soils 191

7. CONCLUSION AND RECOMMENDATIONS 263
7.1. Conclusion 263
7.2. Practical implications of the results 267
7.3. Recommendations for future work 268

8. BIBLIOGRAPHY 270

APPENDIX A
Database of salinity measurements from the Northwest Territories 286

APPENDIX B
Results of the unconfined constant strain rate compression tests 303

APPENDIX C
Results of the constant stress (creep) compression tests 330

APPENDIX D
Constant stress test analysis 373

APPENDIX E
Strain vs Time predictions 419

LIST OF TABLES

Table Page

2.1 Geological sub-units for Baffin Island 26

2.2 Geological sub-units for the Northwestern Canadian Shield 27

2.3 Geological sub-units for the Canadian Interior Plains 28

2.4 Summary of salinity data 29

5.1 Physical properties of strength samples 123

5.2 Physical properties of creep samples 126

5.3 Physical properties of 1988 TDR samples 127

5.4-a Physical properties of 1990 TDR moisture content samples 128

5.4-b Physical properties of 1990 TDR salinity samples 128

5.5 Physical properties of additional tests 129

5.6 Unfrozen water content results from the 1988 and 1990 TDR testing programs 130

5.7 Constant strain rate compression test results 132

5.8 Constant strain rate compression test results of additional tests 135

5.9 Constant stress compression test results 136

6.1 Physical properties for soil B-5 at different densities 192

6.2 Compression strength for various sands 193

6.3 Strength vs Temperature regression coefficients 194

6.4 A vs Salinity regression coefficients 194

6.5 Ratio of normalized strength 195

6.6 Modulus vs Temperature regression coefficients 196

6.7 C vs Salinity regression coefficients 196

6.8 Creep strain to failure 197

6.9 Creep parameters 198

6.10 B and n values for $\dot{\varepsilon}_m = B\sigma^n$ 199

6.11 Sayles' creep parameter M 199

6.12 Regression coefficients for the $\dot{\varepsilon}_1$ vs σ relationships 200

6.13 Regression coefficients for the ε_1 vs σ relationships 200

6.14 Average c values for Gardener's strain predictions 201

6.15 B and n values from Gardener and from Flow law 201

6.16 Comparison CSR tests and creep tests results 202

6.17 Ultimate strength results 202

LIST OF FIGURES

Figure Page

2.1 Map of salinity measurement sites in the Northwest Territories 30
2.2 Salinity vs Moisture content 31
2.3 Salinity vs Moisture content according to soil type 32
2.4 Salinity vs Depth 33
2.5 Salinity vs Depth according to soil type 34
2.6 Salinity vs Depth for Region I 35
2.7 Salinity vs Depth for Region II 36
2.8 Salinity vs Depth for Region III excluding Holman and Richards Island 37
2.9 Salinity vs Depth for Richards Island 38
3.1 Distribution of unfrozen water in frozen soils 89
3.2 Idealized TDR trace 90
3.3 Typical ductile stress-strain curve for polycrystalline ice under constant strain rate 91
3.4 Influence of strain rate on the strength of ice at -7°C 92
3.5 Schematic of Assur sea ice model 93
3.6 a) Steady-state creep curve b) Non steady-state creep curve 94
4.1 Grain size distribution of soils tested 105
4.2 Split freezing mold used to consolidate and freeze sample 106
4.3 Schematic of sample consolidation and freezing apparatus 107
4.4 a) Schematic of TDR equipment b) Details of connection head 108
4.5 Modified triaxial cell 109
4.6 Schematic of unconfined compression test set-up 110
4.7 Schematic of constant stress compression test set-up 111
5.1 1988 TDR unfrozen water contents 137
5.2 1990 TDR unfrozen water contents 138
5.3 TDR results comparison 1990-1988 for Soil A 139
5.4 TDR results comparison 1990-1988 for Soil B 140
5.5 Average TDR unfrozen water contents 141
5.6 TDR unfrozen water contents according to soil type 142
5.7 Stress vs Strain 143
5.8 Unconfined compression strength vs Temperature 144
5.9 Unconfined compression yield strength vs Temperature 145
5.10 Unconfined compression strength vs Salinity 146
5.11 Unconfined compression yield strength vs Salinity 147

5.12 Secant modulus vs Temperature 148
5.13 Secant modulus vs Salinity 149
5.14 Volume change vs Strain 150
5.15 Compression test results for tests A and F 151
5.16 Compression test results for tests B and C 152
5.17 Compression test results for tests C, D, E, G and H 153
5.18 a) 10% Strength vs Density for Soil B 5 ppt at -7°C 154
b) Secant modulus vs Density for Soil B 5 ppt at -7°C 154
5.19 a) Yield strength vs Density for Soil B 5 ppt at -7°C 155
b) Yield strength vs Moisture content for Soil B 5 ppt at -7°C 155
5.20 Strain vs Time curves 156
5.21 log strain rate vs log time curves 157
5.22 a) Original Strain vs Time curve for test CR-76 158
b) Corrected Strain vs Time curve for test CR-76 158
6.1 Sodium chloride (NaCl) - Water (H_2O) binary phase diagram 203
6.2 Comparison between TDR results for Soil A and phase diagram prediction for unfrozen water content 204
6.3 Comparison between unfrozen water content measured by TDR and predicted by Banin and Anderson's (1974) equation for Soil B 205
6.4 Comparison between unfrozen water content measured by TDR and predicted by Banin and Anderson's (1974) equation for Soil C 206
6.5 Comparison between unfrozen water content measured by TDR and predicted using phase diagram and unfrozen water content at a salinity of 0 ppt for Soil B 207
6.6 Comparison between unfrozen water content measured by TDR and predicted using phase diagram and unfrozen water content at a salinity of 0 ppt for Soil C 208
6.7 Comparison of strength vs temperature for different sands at a salinity of 0 ppt 209
6.8 Comparison of strength vs temperature for different sands at salinities other than 0 ppt 210
6.9 Strength vs Temperature ratio for Soil A 211
6.10 10% Strength vs Temperature ratio for Soil B 212
6.11 Yield strength vs Temperature ratio for Soil B 213
6.12 10% Strength vs Temperature ratio for Soil C 214
6.13 Yield strength vs Temperature ratio for Soil C 215
6.14 Parameter B_s vs Salinity 216
6.15 Parameter A vs Salinity 217
6.16 Parameter A vs Salinity regressions 218
6.17 Normalized strength vs Temperature 219

6.18 Normalized yield strength vs Temperature 220

6.19 Strength ratio R vs Salinity 221

6.20 Comparison between strength predicted using ice area ratio and measured strength 222

6.21 Secant modulus vs Temperature for Soil A 223

6.22 Secant modulus vs Temperature for Soil B 224

6.23 Secant modulus vs Temperature for Soil C 225

6.24 Parameter D vs Salinity 226

6.25 Parameter C_M vs Salinity 227

6.26 Parameter C_M vs Salinity regressions 228

6.27 Comparison of strength vs unfrozen water content for different sands 229

6.28 Strength vs Unfrozen water content 230

6.29 a) Strength vs Unfrozen water content for Soil A 231
b) Normalized strength vs Unfrozen water content for Soil A 231

6.30 10% Strength or Yield strength vs Unfrozen water content 232

6.31 Strength vs corrected Unfrozen water content for Soils B and C 233

6.32 a) Normalized 10% strength vs Unfrozen water content for Soil B 234
b) Normalized Yield strength vs Unfrozen water content for Soil B 234

6.33 a) Normalized 10% strength vs Unfrozen water content for Soil C 235
b) Normalized Yield strength vs Unfrozen water content for Soil C 235

6.34 Secant modulus vs Unfrozen water content 236

6.35 Secant modulus vs Unfrozen water content regressions 237

6.36 Creep strain to failure vs Stress 238

6.37 Comparison between measured strain and predicted strain using Vyalov bilinear or linear approach 239

6.38 Comparison between measured strain and predicted strain for Soils A, B and C at 5 ppt 240

6.39 Strain rate at failure vs Stress ratio 241

6.40 Sayles' M creep parameter for Soil A 242

6.41 Sayles' M creep parameter for Soils B and C 243

6.42 Strain rate 1 hour predicted by Sayles' equation vs Stress ratio 244

6.43 Strain rate 10 minute predicted by Sayles' equation vs Stress ratio 245

6.44 E vs Salinity regressions 246

6.45 E vs Unfrozen water content regressions 247

6.46 Strain 1 hour (measured strain) vs Stress ratio 248

6.47 Strain 10 minute (measured strain) vs Stress ratio 249

6.48 a) G vs Salinity for Soil A 5, 10 ppt, Soil B, Soil C 0, 5, 10 ppt 250
b) G vs Unfrozen water content for Soil A 5, 10 ppt, Soil B, Soil C 0, 5, 10 ppt 250

6.49 a) Flow law parameter B vs Salinity 251
b) Flow law parameter B vs Unfrozen water content 251

6.50 a) Flow law parameter n vs Salinity 252
b) Flow law parameter n vs Unfrozen water content 252

6.51 a) Flow law parameter B vs Salinity regressions 253
b) Flow law parameter B vs Unfrozen water content regressions 253

6.52 a) Flow law parameter n vs Salinity regressions for Soils B and C 254
b) Flow law parameter n vs Unfrozen water content regressions for Soils B and C 254

6.53 Gardener's creep parameter c vs Stress 255

6.54 Comparison between measured strain and predicted strain using Gardener's approach with the specific c value or the average c value 256

6.55 Time to failure vs Stress ratio 257

6.56 a) K vs Salinity for Soils A, B, C 251
b) K vs Unfrozen water content regressions for Soils A, B, C 251

6.57 a) Parameter n from Gardener vs Salinity for Soils B and C 259
b) Parameter n from Gardener vs Unfrozen water content regressions for Soils B and C 259

6.58 Creep results comparison between Soil A 30 ppt and Pharr and Godavarti (1987) results 260

6.59 Comparison between strain rate vs strain curves from Pharr and Godavarti (1987) and the prediction using the results from this study 261

6.60 1/Ultimate strength vs Time 262

B.1 Compression results Soil A 0 ppt T = -12°C and -10°C 304

B.2 Compression results Soil A 0 ppt T = -7°C and -5°C 305

B.3 Compression results Soil A 5 ppt T = -12°C and -10°C 306

B.4 Compression results Soil A 5 ppt T = -7°C and -5°C 307

B.5 Compression results Soil A 10 ppt T = -12°C and -10°C 308

B.6 Compression results Soil A 10 ppt T = -7°C and -5°C 309

B.7 Compression results Soil A 30 ppt T = -12°C and -10°C 310

B.8 Compression results Soil A 30 ppt T = -7°C and -5°C 311

B.9 Compression results Soil B 0 ppt T = -12°C and -10°C 312

B.10 Compression results Soil B 0 ppt T = -7°C and -5°C 313

B.11 Compression results Soil B 5 ppt T = -12°C and -10°C 314

B.12 Compression results Soil B 5 ppt T = -7°C and -5°C 315

B.13 Compression results Soil B 10 ppt T = -12°C and -10°C 316

B.14 Compression results Soil B 10 ppt T = -7°C and -5°C 317

B.15 Compression results Soil B 30 ppt T = -12°C 318
B.16 Compression results Soil B 30 ppt T = -10°C 319
B.17 Compression results Soil B 30 ppt T = -7°C 320
B.18 Compression results Soil B 30 ppt T = -5°C 321
B.19 Compression results Soil C 0 ppt T = -12°C and -10°C 322
B.20 Compression results Soil C 0 ppt T = -7°C and -5°C 323
B.21 Compression results Soil C 5 ppt T = -12°C and -10°C 324
B.22 Compression results Soil C 5 ppt T = -7°C and -5°C 325
B.23 Compression results Soil C 10 ppt T = -12°C and -10°C 326
B.24 Compression results Soil C 10 ppt T = -7°C and -5°C 327
B.25 Compression results Soil C 30 ppt T = -12°C and -10°C 328
B.26 Compression results Soil C 30 ppt T = -7°C and -5°C 329
C.1 Creep results test CR-45 Soil A 0 ppt at σ = 4581 kPa 331
C.2 Creep results test CR-92 Soil A 0 ppt at σ = 3927 kPa 332
C.3 Creep results test CR-95 Soil A 0 ppt at σ = 2836 kPa 333
C.4 Creep results test CR-59 Soil A 5 ppt at σ = 1026 kPa 334
C.5 Creep results test CR-51 Soil A 5 ppt at σ = 1026 kPa 335
C.6 Creep results test CR-60 Soil A 5 ppt at σ = 855 kPa 336
C.7 Creep results test CR-67 Soil A 5 ppt at σ = 570 kPa 337
C.8 Creep results test CR-86 Soil A 10 ppt at σ = 887 kPa 338
C.9 Creep results test CR-47 Soil A 10 ppt at σ = 761 kPa 339
C.10 Creep results test CR-87 Soil A 10 ppt at σ = 634 kPa 340
C.11 Creep results test CR-64 Soil A 30 ppt at σ = 888 kPa 341
C.12 Creep results test CR-70 Soil A 30 ppt at σ = 666 kPa 342
C.13 Creep results test CR-72 Soil A 30 ppt at σ = 555 kPa 343
C.14 Creep results test CR-83 Soil B 0 ppt at σ = 2825 kPa 344
C.15 Creep results test CR-71 Soil B 0 ppt at σ = 2354 kPa 345
C.16 Creep results test CR-81 Soil B 0 ppt at σ = 2119 kPa 346
C.17 Creep results test CR-84 Soil B 5 ppt at σ = 1890 kPa 347
C.18 Creep results test CR-49 Soil B 5 ppt at σ = 1718 kPa 348
C.19 Creep results test CR-9 Soil B 5 ppt at σ = 1546 kPa 349
C.20 Creep results test CR-17 Soil B 5 ppt at σ = 1546 kPa 350
C.21 Creep results test CR-32 Soil B 5 ppt at σ = 1546 kPa 351
C.22 Creep results test CR-82 Soil B 10 ppt at σ = 1359 kPa 352
C.23 Creep results test CR-50 Soil B 10 ppt at σ = 1235 kPa 353
C.24 Creep results test CR-33 Soil B 10 ppt at σ = 1112 kPa 354

C.25 Creep results test CR-38 Soil B 10 ppt at σ = 1112 kPa 355
C.26 Creep results test CR-75 Soil B 30 ppt at σ = 678 kPa 356
C.27 Creep results test CR-77 Soil B 30 ppt at σ = 559 kPa 357
C.28 Creep results test CR-88 Soil B 30 ppt at σ = 442 kPa 358
C.29 Creep results test CR-79 Soil C 0 ppt at σ = 2240 kPa 359
C.30 Creep results test CR-65 Soil C 0 ppt at σ = 2036 kPa 360
C.31 Creep results test CR-36 Soil C 0 ppt at σ = 1832 kPa 361
C.32 Creep results test CR-96 Soil C 5 ppt at σ = 2006 kPa 362
C.33 Creep results test CR-66 Soil C 5 ppt at σ = 1839 kPa 363
C.34 Creep results test CR-62 Soil C 5 ppt at σ = 1672 kPa 364
C.35 Creep results test CR-89 Soil C 5 ppt at σ = 1672 kPa 365
C.36 Creep results test CR-94 Soil C 5 ppt at σ = 1504 kPa 366
C.37 Creep results test CR-55 Soil C 10 ppt at σ = 1372 kPa 367
C.38 Creep results test CR-52 Soil C 10 ppt at σ = 1235 kPa 368
C.39 Creep results test CR-68 Soil C 10 ppt at σ = 1098 kPa 369
C.40 Creep results test CR-76 Soil C 30 ppt at σ = 1222 kPa 370
C.41 Creep results test CR-78 Soil C 30 ppt at σ = 1008 kPa 371
C.42 Creep results test CR-91 Soil C 30 ppt at σ = 794 kPa 372
D.1 Creep test CR-45 Soil A 0 ppt at σ = 4581 kPa 377
D.2 Creep test CR-92 Soil A 0 ppt at σ = 3927 kPa 378
D.3 Creep test CR-95 Soil A 0 ppt at σ = 2826 kPa 379
D.4 Creep test CR-59 Soil A 5 ppt at σ = 1026 kPa 380
D.5 Creep test CR-51 Soil A 5 ppt at σ = 1026 kPa 381
D.6 Creep test CR-60 Soil A 5 ppt at σ = 855 kPa 382
D.7 Creep test CR-67 Soil A 5 ppt at σ = 570 kPa 383
D.8 Creep test CR-86 Soil A 10 ppt at σ = 887 kPa 384
D.9 Creep test CR-47 Soil A 10 ppt at σ = 761 kPa 385
D.10 Creep test CR-87 Soil A 10 ppt at σ = 634 kPa 386
D.11 Creep test CR-64 Soil A 30 ppt at σ = 888 kPa 387
D.12 Creep test CR-70 Soil A 30 ppt at σ = 666 kPa 388
D.13 Creep test CR-72 Soil A 30 ppt at σ = 555 kPa 389
D.14 Creep test CR-83 Soil B 0 ppt at σ = 2825 kPa 390
D.15 Creep test CR-71 Soil B 0 ppt at σ = 2354 kPa 391
D.16 Creep test CR-81 Soil B 0 ppt at σ = 2119 kPa 392
D.17 Creep test CR-84 Soil B 5 ppt at σ = 1890 kPa 393
D.18 Creep test CR-49 Soil B 5 ppt at σ = 1718 kPa 394

D.19 Creep test CR-9 Soil B 5 ppt at σ = 1546 kPa 395
D.20 Creep test CR-17 Soil B 5 ppt at σ = 1546 kPa 396
D.21 Creep test CR-32 Soil B 5 ppt at σ = 1546 kPa 397
D.22 Creep test CR-82 Soil B 10 ppt at σ = 1359 kPa 398
D.23 Creep test CR-50 Soil B 10 ppt at σ = 1235 kPa 399
D.24 Creep test CR-33 Soil B 10 ppt at σ = 1112 kPa 400
D.25 Creep test CR-38 Soil B 10 ppt at σ = 1112 kPa 401
D.26 Creep test CR-75 Soil B 30 ppt at σ = 678 kPa 402
D.27 Creep test CR-77 Soil B 30 ppt at σ = 559 kPa 403
D.28 Creep test CR-88Soil B 30 ppt at σ = 442 kPa 404
D.29 Creep test CR-79 Soil C 0 ppt at σ = 2240 kPa 405
D.30 Creep test CR-65 Soil C 0 ppt at σ = 2036 kPa 406
D.31 Creep test CR-36 Soil C 0 ppt at σ = 1832 kPa 407
D.32 Creep test CR-96 Soil C 5 ppt at σ = 2006 kPa 408
D.33 Creep test CR-66 Soil C 5 ppt at σ = 1839 kPa 409
D.34 Creep test CR-62 Soil C 5 ppt at σ = 1672 kPa 410
D.35 Creep test CR-89 Soil C 5 ppt at σ = 1672 kPa 411
D.36 Creep test CR-94 Soil C 5 ppt at σ = 1504 kPa 412
D.37 Creep test CR-55 Soil C 10 ppt at σ = 1372 kPa 413
D.38 Creep test CR-52 Soil C 10 ppt at σ = 1235 kPa 414
D.39 Creep test CR-68 Soil C 10 ppt at σ = 1098 kPa 415
D.40 Creep test CR-76 Soil C 30 ppt at σ = 1222 kPa 416
D.41 Creep test CR-78 Soil C 30 ppt at σ = 1008 kPa 417
D.42 Creep test CR-91 Soil C 30 ppt at σ = 794 kPa 417
E.1 Comparison between measured and predicted strain for Soil A 0 ppt 420
E.2 Comparison between measured and predicted strain for Soil A 5 ppt 421
E.3 Comparison between measured and predicted strain for Soil A 10 ppt 423
E.4 Comparison between measured and predicted strain for Soil A 30 ppt 424
E.5 Comparison between measured and predicted strain for Soil B 0 ppt 425
E.6 Comparison between measured and predicted strain for Soil B 5 ppt 426
E.7 Comparison between measured and predicted strain for Soil B 10 ppt 428
E.8 Comparison between measured and predicted strain for Soil B 30 ppt 430
E.9 Comparison between measured and predicted strain for Soil C 0 ppt 431
E.10 Comparison between measured and predicted strain for Soil C 5 ppt 432
E.11 Comparison between measured and predicted strain for Soil C 10 ppt 434
E.12 Comparison between measured and predicted strain for Soil C 30 ppt 435

LIST OF SYMBOLS AND ABBREVIATIONS

TDR:	Time-domain reflectometry
NMR:	Nuclear magnetic resonnance
CSR:	constant strain rate
$NaCl$, $CaCl_2$:	Sodium, calcium chloride
ppt:	parts per thousand
ka:	1 000 years
a.s.l.:	above sea level
m, m^3:	meters, cubic meters
g, kg, Mg:	gram, kilogram, megagram
ml, l:	milliliter, liter
kJ/kg:	kilo Joule/ kilogram
s or sec:	seconds
kPa, kN:	kiloPascal, kiloNewton
lb:	pounds
K:	thermal conductivity
m.c.or w.c.:	moisture content
W_u or $w.c._u$:	gravimetric unfrozen water content
θ_u:	volumetric unfrozen water content
γ_{total}:	total (bulk) density
ρ_d or γ_d :	dry density
ρ_w:	water density
e, S_r:	void ratio, degree of saturation
A_{ice}:	ice area ratio
v_b:	volumetric brine content
S:	salinity
T or θ:	temperature
σ:	stress
σ_3:	confining pressure
σ_o, σ_{max} :	instantaneous, maximum strength
σ_f:	failure stress
E:	Young's modulus
$\dot{\varepsilon}$, $\dot{\varepsilon}_m$:	strain rate, minimum strain rate
ε, ε_o, ε_f, ε_m, ε_c:	strain, instantaneous strain, failure strain strain at minimum strain rate, creep strain

t, t_f, t_m:	time, time to failure, time to minimum strain rate
$\dot{\varepsilon}_c$, σ_c, E_c:	proof strain rate, proof stress, proof modulus (from Ladanyi,1972)
n, x:	strain rate stress exponent, modulus stress exponent
B:	flow law parameter
Q:	activation energy
$\sigma_{10\%}$, σ_y, σ_∞ :	resitance at 10% strain, yield, residual strength
σ_{ult} (or σ_{lt}):	ultimate or long-term strength
E_s, $E_{s\ 50\%}$:	secant modulus, secant modulus at 50% of failure strain
$t_{10\%}$, $\dot{\varepsilon}_{10\%}$:	time to 10% strain, strain rate at 10% strain
R:	ratio of strength of a soil to the strength at 0 ppt salinity for a given temperature
R_{max}, $R_{10\%}$, R_y:	strength ratio for maximum strength, 10% strength, yield strength
T_1, σ_1:	reference temperature (-10°C), reference stress (1 000 kPa)
A, B_s:	Strength-Temperature correlation coefficients
A_2, B_2:	Parameter A-Salinity correlation coefficients
C_M, D:	Modulus-Temperature correlation coefficients
C_2, D_2:	Parameter C_M-Salinity correlation coefficients
$\sigma_{max\ o}$, $\sigma_{10\%\ o}$, $\sigma_{y\ o}$:	maximum, 10% or yield strength for 0 ppt salinity at a given temperature
c, k:	Pharr and Merwin's (1987) strength parameters
M:	Sayles' creep time exponent
$\dot{\varepsilon}_1$, ε_1 :	strain rate, strain 1 hour
$\dot{\varepsilon}_{10\ min}$, $\varepsilon_{10\ min}$:	strain rate, strain 10 minutes
c, K:	Gardener et al.'s (1984) creep parameters
α, a:	Vyalov et al's (1988) creep parameters
E, F:	$\dot{\varepsilon}_1$ vs Stress ratio correlation coefficients
G, H:	ε_1 vs Stress ratio correlation coefficients

1. INTRODUCTION

1.1. BACKGROUND

The increased interest in the exploration of hydrocarbon reserves in the Beaufort Sea in the late '70s left the geotechnical community with some interesting problems related to the design of offshore structures. The construction of artificial islands requires the hydraulic placement of large amounts of sand fill. In order to reduce the amount of sand needed, consideration was given to artificial freezing of the submerged sand. The behaviour of these artificially frozen islands was not well understood then, because of the presence of saline pore fluid. Investigations started on the influence of salinity on the compressive behaviour of saline frozen sands. Moreover, since these structures have to sustain important ice loads for long periods of time, the time dependent behaviour of frozen saline soils (creep) was also of great interest.

Different investigators such as Sego et al.(1982), Sego and Cherenko (1984), Pharr and Godavarti (1985) and Pharr and Merwin (1985) investigated the behaviour of saline coarse-grained frozen soils in the early '80s.

The concern with saline frozen ground is not limited to the design of artificial islands. The presence of saline pore fluid in the continous permafrost underlying many coastal communities also causes great concern to the geotechnical engineer involved in northern work. Foundation design for facilities servicing these northern communities or supporting the oil field industry in these regions require a better understanding of the behaviour of saline permafrost. Nixon (1988) reported on the problems related to a pile foundation at Clyde River , NWT, because of the presence of saline permafrost. Nixon and Lem (1984) observed that creep rates can be accelerated by factors of 10 to 100 as salinity increases from 0 ppt to 30 ppt.

Another important aspect of understanding the behaviour of frozen saline soils is the effect of artificial ground freezing on soils containing saline pore fluid. The development of inground storage facilities for liquified natural gases (LNG) in Japan caused some concern, since most of these storage areas are located in coastal environment, where the soils have saline pore fluid. As the concrete containers used to store the LNG are filled, the ground surrounding the tank freezes. Since the pore fluid in the soils is saline, a better understanding of the behaviour of saline frozen ground is necessary to determine properly the pressures on the tanks and the heave of the ground surface. Ogata et al. (1983) studied the effect of salinity on artificially frozen soils and attempted to correlate the influence of salinity to the concept of unfrozen water content. Since artificial freezing is becoming a more popular means of ground improvement, a better understanding of the effect of saline pore fluid on the behaviour of these artificially frozen soils would be important in regions where the soils are of marine origin, since the ground water contains salts in such environment. A case study of ground freezing for a tunneling project in marine clays in Norway was presented by Aas (1980).

1.2. SCOPE OF STUDY

Realising the paucity of the available data on the behaviour of frozen saline soils, a comprehensive testing program was planned in an attempt to provide a more global explanation of the effects of salinity and temperature on the behaviour of frozen saline soils. The scope of the thesis is two-fold. In the first part, the thesis will provide a better understanding of the variation of pore fluid salinity in nature, and will explain the interrelation between the presence and distribution of these salinities and the geology of the region where they are found. Secondly, the thesis will present an improved explanation of the combined effects of salinity and temperature on the strength and deformation of saline soils. As a result of this improved understanding of the mechanical behaviour of frozen saline soils, the estimation of the parameters required in analytical or numerical studies for stress and deformation predictions in saline frozen soils will be made easier in the future.

The author believes that the distribution of saline permafrost can be explained by the Quaternary geology of the regions where saline permafrost is found. The author's initial assumption, with respect to the mechanical behaviour, is that the unfrozen water content can provide a means of explaining the influence of salinity and temperature on the response to loading of saline frozen soils.

The thesis first introduces a study of the available information on the distribution of permafrost in northern Canada in Chapter 2. This study has resulted in the establishment of a data base of the measurements of in-situ salinity in the Northwest Territories. A brief explanation of the database will be presented and some correlations between physical properties and salinity are introduced. A tentative explanation of the distribution of saline permafrost based on Quaternary geology is also given, since the main cause of salinity in soils is marine submergence.

Chapter 3 presents a complete review of the literature available pertaining to the saline permafrost. The effect of unfrozen water on the physical behaviour of frozen soils is discussed and the influence of salinity on the unfrozen water is introduced. A review of available measuring methods of unfrozen water content is presented with special emphasis on the time-domain reflectometry (TDR) method. A review of the mechanical properties of ice (polycrystalline and sea ice) is presented as it relates to the mechanical behaviour of frozen soils which is then discussed. Both the compressive strength and the time dependent deformation behaviour are included. Finally, the relevant research work which has been carried out to date on the behaviour of saline frozen soils is reviewed.

Chapter 4 presents the laboratory testing program. The method of sample preparation and freezing is discussed. Three soils were studied at four different salinities; a fine sand, a silty sand and a very fine silty sand or sandy silt at nominal salinities of 0, 5, 10 and 30 ppt are described. A description of the time-domain reflectometry equipment is included, along with a description of the equipment used for the constant strain rate (CSR) unconfined compression tests and the time dependent constant stress (creep) tests .

The experimental results are presented in Chapter 5. The physical properties are first introduced followed by the results of the unfrozen water content determination. The unconfined compression constant strain rate test results include peak strength, yield strength, strength at 10% strain, strain to failure, yield strain and the secant modulus. A brief section on the influence of density on the strength is included. For the constant stress creep tests, the strain rate at failure, time to failure and strain to failure are summarized.

Chapter 6 presents the interpretation and discussion of the experimental results. The first section is concerned with the unfrozen water content. A method to predict unfrozen water content using the phase diagram of sodium chloride is introduced. The second portion of this chapter discusses the unconfined compression strength of the three soils studied. Available methods from the literature are used and modified to correlate strength, temperature and salinity. The variation of strength with unfrozen water content is discussed. The constant stress test results are then discussed using three theories previously outlined in the literature. These are modified to include the influence of unfrozen water content in the determination of the creep parameters.

The findings of the thesis are summarized in the conclusion and a list of recommendations for future work is presented.

2. DISTRIBUTION OF SALINE PERMAFROST

2.1. INTRODUCTION

This Chapter describes a database of the distribution of saline permafrost in Arctic Canada. The database contains information related only to the Northwest Territories since the Yukon and northern Quebec governments have no salinity measurements available which could be included.

The presence of saline permafrost has caused concerned to the geotechnical engineering community for the past few years since salt in the pore water affects the behaviour of frozen soils. The database is intended to provide a comprehensive source of information on the distribution of saline permafrost for interested parties who have to deal with construction and development in Northern communities. A constant updating of the database should be carried out as additonal information becomes available, since new information will assist in our understanding of the distribution as well as the impact of saline permafrost on engineered works.

This Chapter presents the methodology followed for gathering the information and an explanation of the contents of the database. Thereafter, a few correlations between the salinity and some physical properties of the permafrost are presented, and this is followed by a preliminary geological explanation for the occurrence of saline permafrost in the different northern regions.

It is important to mention that the information presented here was obtained for onshore communities. Data also exists for offshore locations (especially in the Beaufort Sea) but this study concentrates on measurements obtained from subsurface investigation on land.

2.2. DATABASE

2.2.1. Data Collection

The scope of the project was to gather the available measurements of salinity and initiate a database of this information for the entire Canadian Arctic. However as previously mentioned, no data are presently available for the Yukon nor for northern Quebec. Therefore, the data collected and contained in the database is for communities in the Northwest Territories.

The first step in gathering the information for the database was to visit the offices of the Architecture Division of the Department of Public Works of the Northwest Territories, in Yellowknife. There a complete review of all site investigation and engineering reports commissioned by the Territorial government was undertaken. None of the engineering reports, except for a few water well drilling test, contained any reliable information about saline permafrost. The same is true for most site investigation reports prepared prior to 1983. However, recently most geotechnical consultants who work in the north have become more aware of the importance of saline permafrost , and usually perform salinity measurements on selected samples (the techniques of salinity determination will be discussed in the following section). Therefore, a large number of entries for the database were compiled during the visit .

Subsequently, visits to consultants offices (especially Thurber Consultants Ltd., Calgary) proved beneficial since a great deal of information was made available which was not contained in the reports reviewed in Yellowknife. Finally additional information was gathered while in Ottawa, at the Geological Survey of Canada from Dr. S. R. Dallimore for sites on northern Richards Island, and at the Geophysics Division of the Department of Energy, Mines and Resources from M. Burgess for sites along the Norman Wells - Zama Lake pipeline. Salinity measurement carried out by K. Biggar at the University of Alberta on samples from the pile load testing conducted in Iqaluit in 1988, are also included.

2.2.2. Database Entries

A hard copy of the database is presented in Appendix A. The database was established using Microsoft Excel Version 2.2., © Microsoft Corporation. In the next few pages, each one of the entries (fields) used in the database will be briefly explained.

2.2.2.1. Community, Project and Location

These three fields are used to identify where the boreholes were drilled, for what project the drilling and sampling were completed and the location of the community by latitude and longitude. This information will assist others in using the database for their project or research.

2.2.2.2. Geological Setting Units

The entries under geological setting describe the general geology of the studied sites. As seen on the map of the location of measurement sites, Figure 2.1, three major zones comprise all locations:

1- Baffin Island
2- Northwestern Canadian Shield (West Hudson Bay and East Arctic Coast)
3- Canadian Interior Plains (Mackenzie Valley and Delta, Victoria Island)

The Quaternary geology of these regions will be explained in Section 2.4, where it is used to assist in providing a preliminary interpretation of the occurence and distribution of salinity. Only a brief description of the stratigraphy will be given here, for more details refer to Fulton (1989).

I- Baffin Island

According to Andrews (1989), most of Baffin Island is underlain by the Precambrian Shield. On northern Baffin Island, the Proterozoic rocks are covered by Paleozoic to Cretaceous sedimentary rocks. Central Baffin Island is formed almost completely of Archean granite-gneiss. Locally around Foxe Basin, some Paleozoic limestone can outcrop. Southern Baffin Island consists mostly of the Precambrian Shield.

There is a cover of Paleozoic limestone which extends from Foxe Basin eastward to Iqaluit (Frobisher Bay).

In general, the surficial deposit cover is thin over most of Baffin Island except along the outer coast in the region of the fiords. The outer east coast is formed of deltaic and outwash materials (sand, gravel, mud) associated with some glacial (till, moraine) and glacio-marine (interglacial periods) sediments (e.g. raised beaches) which were deposited by marine transgression and regression during interstadial periods. The glacial tills can be differentiated into two distinct lithologies; a sandy gravelly till derived from Precambrian bedrock; and a silt and clay rich till derived from the Paleozoic limestone. Some eolian deposits can be found on southern Baffin Island.

Taking this general description into consideration, Baffin Island was divided into two geological sub-units; one for the northern part and one for the southern part, as shown in Table 2.1

For more details on the surficial geology of Baffin Island , papers by Dyke et al. (1982) and Hodgson and Haselton (1974) should be reviewed.

II- Northwestern Canadian Shield

The northwestern Canadian Shield covers the area of the craton which lies west of Hudson Bay and the Gulf of Boothia (Southampton Island is included in this region). The most western community of interest for this study is Gjoa Haven. According to Dyke and Dredge (1989), the bedrock consists of a variety of Precambrian rocks locally covered by Paleozoic sedimentary rocks (usually carbonates).

In the northern part of the region (Somerset Island), an extensive cover of residuum and colluvium mantles the bedrock. The glacial materials consists of till, glacial lacustrine and glacial marine sediments.

The till is variable in composition and thickness. It is thickest where it overlies Paleozoic or Proterozoic sedimentary rocks. Glacio-fluvial materials are widespread throughout the area but their distribution is not uniform. Numerous eskers are present over most of Keewatin and eastern Mackenzie districts, indicating the ice flow direction. Some small glacial lakes developed as the Keewatin Ice sector retreated, but no significant amount of lacustrine sediments were deposited. Since most of Hudson Bay, Committee Bay, Pelly Bay and Chantrey Inlet were submerged by sea after the Late Wisconsin glaciation, glacial marine deposits can be found over most of the area. However, the marine cover around Hudson Bay is generally thin (a few meters) compared to the very thick extensive glacial marine deposition (up to 100 m) from Committee Bay to Chantrey Inlet. Coarser ice contact glacio-marine sediments also exist in the form of deltas in the region of the marine limit in northern Keewatin. Beside glacial marine sediments (raised gravel and sand beaches) some other post-glacial sediments are found over the area. These are terraced and active alluvium and delta sediments as well as some eolian sands.

For this region, three geological sub-units have been established for the sites with saline pore fluid measurements and are presented in Table 2.2: one for Hudson Bay communities, one for the eastern Arctic Coast, and one for Southampton Island.

For more detailed information on the surficial geology of the northwestern Shield, Geological Survey of Canada maps 8-1980 (Eskimo Point) and 3-1985 (Baker Lake) should be examined.

III. Canadian Interior Plains

This area is found between the Canadian Shield and the Cordillera. Vincent (1989) gives a detailed description of the geology. The bedrock varies spatially over the region; the platform areas are based on Paleozoic to Mesozoic sedimentary rocks (carbonates, shales and sandstones); the bedrock on Victoria Island is Proterozoic carbonates, shales sandstones and diabase. In the Mackenzie Delta, Cenozoic unconsolidated to poorly consolidated materials (terrestrial and marine silts, sands and gravels) are found throughout the region. The alluvial sands and gravels of the Beaufort Formation are Miocene in age.

The Quaternary deposits over the region vary according to topographic position. In low areas along the Mackenzie and Liard River valleys, flood plain, terrace and delta (including the Mackenzie Delta) sediments are extensive and large areas of glacio-lacustrine silts and sands are also found close to Great Slave and Great Bear Lakes. At slightly higher elevations, some till plains (fluted and drumlinized moraines) form the surficial deposits. On higher land, ground hummocky moraine with localized glacio-fluvial deposits covers most of the plateaus and hills.Four geological sub-units presented in Table 2.3 describes these sites.

For a more comprehensive understanding of the surficial geology of this area, some reports and maps should be looked up (Rampton and Bouchard, 1975), Rampton, 1988, Geological Survey of Canada maps 3-1978 and 32-1979.).

2.2.2.3. Terrain Type

From the available information, a terrain type accordingly to the Canadian Landform Classification System (Cruden and Thomson, 1987) has been assigned for most entries. In many cases, the interpretation was difficult and questionable, so a question mark is placed beside the terrain type symbol, if doubt existed as to its interpretation. Moreover, the qualifying descriptor which should be placed as a superscript is put in brackets in the database because the program does not allow superscript.(e.g. F "G" means fluvio-glacial). The qualifying descriptor m beside bedrock (R) means that the rock is metamorphic.

These are the genetic materials most often used in the database:
R: bedrock
M: moraine (usually till)
F: fluvial
W: marine
C: colluvium
L: lacustrine

2.2.2.4. Borehole number, Depth and Date

These three entries are used to identify and locate the salinity measurements: the borehole number from where the salinity sample was taken , the date it was drilled and the sample depth. The depth is given using the soil surface as reference and is not a geodetic elevation since the control information was not available in the data sources. For some locations, the borehole entry is a pit number since only an open pit was dug.

2.2.2.5. Soil Classification

The soil classification system used is the Modified Unified Soil Classification System (USCS).

2.2.2.6. Temperature, Density, Moisture Content and Salinity

The ground temperature information available and presented in the database is limited to the information presented in the engineering reports reviewed and does not include all of the thermal information available throughout the Northwest Territories. Only temperature information from locations where salinity measurements were carried out has been included. This temperature information was included to indicate the ground temperature distribution and its variation with location and time. For a limited number of sites, temperature data for different dates are included to show how the permafrost temperature varies throughout the year.

Limited density data are included for samples on which bulk or dry densities were determined. The different densities are identified. The moisture contents are almost always included as it has an influence on the in-situ salinity. The moisture content is given in percent by dry weight of soil solids. Finally, the salinity of the tested samples is given in parts per thousand (ppt). In most cases, the salinity was obtained by a conductivity measurement (see Section 2.2.2.8. for details) and consequently the nature of the dissolved salts is unknown. In general the calibration for the conductivity measurement is carried out using NaCl (sodium chloride) as the reference, so the salinity is more or less an equivalent NaCl concentration.

2.2.2.7. Consultant

Under this heading, the name of the consulting firm responsible for the site investigation and report is included. In some cases, where the data is not from a consultant report, the source of information is given.

2.2.2.8. Comments

This column includes pertinent information not contained in the other fields. The consultant file number was given when available. Also for some sites, the method of drilling is indicated. The most important entry in this field is the method of salinity determination. Four methods used by the various agencies that provided information are briefly described here;

Method 1: ASTM D4542-85	Standard Test Method for : Pore Water Extraction and Determination of Soluble Salt Content of Soils by Refractometer.

The procedure for this method is presented below in a simplified form:

1- Take about 50 g of moist soil and place into soil press.
2- Slowly apply pressure to press and collect extracted pore water using a clean syringe.
3- Filter the extracted pore water and place a few drops of clean water on the platform of the refractometer.
4- Measure salinity using refractometer.

This method is very convenient since it is fast and simple. However, it has some limitations. The moisture content of the soil should be greater than 14% to have sufficient pore water available. To avoid this problem it is possible to add some distilled water to the soil and proceed. The moisture content of both the normal sample and the "humidified" sample should be determined. Knowing the salinity of the humid sample, the salinity of the original sample can be back calculated. The original salinity is equal to the "humidified" salinity multiplied by the ratio of the "humidified" moisture content by the original moisture content. Another problem with this procedure is that it is not applicable to coarse-grained materials, since they contain such small volumes of pore water. Finally, a reliable reading of the refractometer is difficult and can cause some slight variation of the reported salinity from user to user. Nevertheless, this method is recommended for its simplicity by the author.

Method 2: Method presented by Rhoades (1982) and used for analysis of NRC samples from the Norman Wells-Zama Lake Pipeline.

1- Determine moisture content of the sample (ASTM D2216).
2- Take a 100 g of dry soil.
3- Mix with 100 ml of distilled water.
4- Let stand for 24 hours.
5- Extract the pore water using pressurized nitrogen.
6- Determine the electrical conductivity using KCl as the standard.

Method 3: Method used by most consultants (in particular Thurber Cons. Ltd.)

This method is very similar to method 2.

1- Determine moisture content of the sample (ASTM D2216)
2- Measure conductivity of distilled water for calibration.
3- Take ± 100 g of dried and ground soil.
4- Add and mix 100 ml of distilled water
5- Let stand until the soil settles down.
6- Determine the electrical conductivity using NaCl as the standard.

Method 4: Method used by the Geological Survey of Canada.

1- Extract pore water from the sample using either a soil press (see method 1) or a centrifuge.
2- Measure directly the conductivity of the pore water using NaCl as the standard.

2.3. RESULTS

2.3.1. Introduction

Various comparisons can be made from the data; a limited number of these comparisons are presented, since they illustrate a number of important results. Firstly, a summary of the salinity values for each community will be given, and the relationship between community location and salt concentration will be discussed. The variation of the measured salinity with moisture content and depth are reviewed, as well as, the influence of soil type and terrain type on the measured salinity.

2.3.2. Summary of Data

Table 2.4 summarizes the range of salinity encountered at each community. High salinities are observed in all communities located on Baffin Island (units I-a, I-b) and in the northwestern Canadian Shield (units II-a, II-b, II-c) except at Coral Harbour, Gjoa Haven, Spence Bay and Whale Cove. The salinity values for the sites in the Mackenzie Delta are generally lower than the salinity of sea water. Along the Mackenzie valley, the salinity values are relatively low. The explanation for these variations of the salinity will be discussed in Section 2.4.

2.3.3. Salinity versus Moisture Content

The salinity depends on the moisture content of the soil, since the salinity is defined as the mass of salt divided by the mass of one litre of water. For a relatively dry unsaturated soil, high salinity would be expected since the mass of water is low. The opposite should be true for high moisture content soils. Thus the salinity of an ice rich soil would be expected to be low. This trend of decreasing salinity with increasing moisture content is shown in Figures 2.2. The first graph (Figure 2.2 a) contains all the data for moisture content less than 300%. To facilitate the data analysis, all data with moisture content higher than 300% was eliminated because the salinity of theses samples is always extremely low. The other two graphs, Figures 2.2 b) and 2.2 c), have cut off moisture content values of 100% and 50% respectively, to display the relationship in more details.

The relationship between salinity and moisture content for different soil textures as defined using the classification system is given in Figure 2.3. The highest salinities can be observed in low moisture content sands. The variation in the measured salinities with moisture content is similar for all three soil types.

2.3.4. Salinity versus Depth

Figure 2.4 presents a plot of all the salinity data versus the depth of the sample. As can be seen on Figure 2.4 a), the bulk of the data is located in the upper 20 to 30 m. This reflects the fact that most site investigations for engineering purposes are concerned with the top 10 m of soil since few foundations are placed below this depth. In Figure 2.4 b), the data from the three different geological regions show that higher salinities in the upper 10 m are found in Regions I and II. Region III contains some high salinities below 10 m. An important point is that the salinity is low in the top 2 m, i.e. salinities are less than 5 ppt. This is usually the extent of the active layer (layer which thaws during the warm season), suggesting that salt leaching takes place in that zone. Thus sampling for salinity determination should be performed at depths greater than the limit of the active layer to ensure representative measurements of the salinity of the permafrost at depth. Figure 2.5 shows the distribution of salinity vs depth accordingly to soil types. The salinity distribution is very similar for all three soil types. The only differences are that more sand samples have very high salinities (>30 ppt), and more clay samples have high salinities at depth greater than 10 m as compared to silt samples.

It is also of interest to look at the salinity distribution as a function of terrain type since it is an indication of the depositional environment of the soil. High salinities would be expected for marine soils, for glacial soils (till, fluvial and lacustrine deposits) which were deposited just prior to a period of marine transgression and for carbonate bedrock. Since the behaviour of hard rock is not of our concern, only unconsolidated materials will be considered.

For Regions I and II, the soil salinities found in marine sediments were compared to salinities found in glacial sediments. Figure 2.6 shows that for both types of sediments in Region I, relatively high salinities were observed. As it will be discussed later, most coastal regions of Baffin Island have been submerged by the sea during the last glaciation explaining the high salinities in the glacial sediments. As shown by Figure 2.7, only a few salinity measurements were available for marine sediments in Region II. For the glacial sediments, more than half had salinities in excess of 10 ppt. This suggests that the sediments were associated with a marine environment at some time during their history.

For Region III, some difficulties were encountered, when sites close to the Mackenzie Delta were investigated especially Richards Island. This is the reason why Richards Island will be discussed separately. For Region III (except Richards Island), the data reveals that, except for Holman Island, no marine sediments were present. The salinities at Holman vary between 3 and 5.7 ppt which are relatively low values for marine sediments. Figure 2.8 presents the distribution of salinity vs depth for sites along the Mackenzie River. The majority (≈90%) of the salinity measurements have low values. The higher salinities (>10 ppt) are all associated with low moisture content soils or with sites close to the delta: Arctic Red River, Fort McPherson and Inuvik. As shown in Figure 2.9, most salinity measurements from Richards Island are low (<5 ppt). Some high values are found in both terrain types (glacial and marine). To understand these occurences better, a brief review of the stratigraphy of this site would be beneficial. The stratigraphy is believed to consist of recent alluvial and/or marine deposits, underlain by a sequence of fine sediments (probably till/diamicton) of glacio-marine origin, overlying a thick sequence of Pleistocene sands. These sands are one of the source of confusion since there is no agreement in the literature as to their origin, i.e. glacio-fluvial or marine. These sands are probably glacio-fluvial sediments because high salinities are observed only occaisonally. The second problem in attempting to correlate salinity and terrain type is the presence of a till/diamicton unit. In the literature, this unit is described to be of glacio-marine origin. It is therefore impossible to separate if these sediments belong to a glacial or marine environment. In Figure 2.9, these values are included in both graphs. Finally, it should be kept in mind that all the boreholes on Richards Island were drilled along the coast, which is influenced by sea water.

2.4. INTERPRETATION

2.4.1. Introduction

To understand the salinity distribution within the Northwest Territories one must understand the relationship between a particular location and its Quaternary geological history. As for the description of the geological setting units (Section 2.2), three major regions in the Northwest Territories will be discussed;

1 - Baffin Island

2 - Northwest Canadian Shield

3 - Canadian Interior Plains

A significant part of the information presented hereafter is from Dyke and Prest (1987) and from their accompanying maps 1702A and 1703A available from the Geological Survey of Canada.

2.4.2. Quaternary Geology of Baffin Island

As previously stated, Baffin Island is part of the northeastern Canadian Shield, which implies that its bedrock is mostly Precambrian metamorphic rocks. Locally a cover of Paleozoic and Tertiary sediments are found. The nature of the bedrock influences the composition of the surficial glacial deposits (Andrews, 1989).

This region was not completely covered by the Late Wisconsin (last) glaciation and consequently a number of older (Early Wisconsin and older) deposits are found within the area. Extensive evidence suggests that Baffin Island was covered by several glaciations prior to the Foxe Glaciation (Wisconsin age). Cross-sections along the east coast expose sequences of relatively complete Quaternary deposits composed of alternating glacial and marine (transgressive and regressive) deposits. The Clyde Foreland Formation is a good example of such a sequence.

The lobe of the Laurentide Ice Sheet that covered Baffin Island is called the Foxe Glacier Complex. The Foxe Glaciation which was centred over Foxe Basin is divided into three periods; early, middle and late. The early Foxe Glaciation dates from prior to 54ka, and some authors suggest that a stade or stades of this glaciation could be Pre - Wisconsin. The sediments of this period are fossiliferous marine deposits associated with glacial materials (lateral moraines and ice proximal deposits).

Little information is available on the middle Foxe glaciation. However, some middle Foxe marine glacial sediments are assumed to be present on the west coast of the Island.

The most relevant period of the Foxe Glaciation is the late Foxe glacial events (which corresponds to late Wisconsin). More information is available to explain this period even if the cause of its onset is unknown. It is believed that the eastern margin of the Foxe ice was relatively stable between 18ka and 8ka (when deglaciation started). Maps 1703A and 1702A show an interesting evolution of the ice movement during the late Wisconsin. It is important to observe that the east coast and Cumberland Peninsula where ice free prior to 18ka. The sea level during the Late Wisconsin and Holocene period seems to have been close to present sea level. This means that the surficial deposits are older than late Foxe age. However, ice covered the rest of the Island and some part of the south eastern Continental Shelf for a long period during Late Wisconsin (until 8ka).

Around 11ka, the sea level was above the present shoreline on southeastern Baffin Island (for example, the sea was at +79m a.s.l. at the outer part of Iqaluit). Around 9000 years ago, some regions of the east coast (mostly Cumberland Peninsula) might also have been below sea level. Around 8400 years ago, the Laurentide Ice Sheet started to break up due to sea advance in the Hudson Strait. Consequently, during the period between 8400 and 5000 years ago, the ice cover over Baffin Island retreated to more or less its present location. The Barnes and Penny Ice Caps are the remnants of this Laurentide Ice Sheet. Several glacial lakes developed on Baffin Island during deglaciation.

The sea level variation is quite complex in southern Baffin Island. Most of the area is undergoing isostatic rebound. However, it is believed that present day submergence is taking place at the outer tip of Cumberland Peninsula. A transition zone (i.e. initial emergence and subsequent submergence) is proposed for northern and southern Cumberland Peninsula and outer Frobisher Bay (Iqaluit).

The sites from this region with available salinity measurements are: Arctic Bay, Broughton Island, Cape Dorset, Clyde River, Iqaluit, Pangnirtung and Pond Inlet.

2.4.3. Quaternary Geology of Northwestern Canadian Shield

The region described by the name Northwestern Canadian Shield extends west of the Hudson Bay and Gulf of Boothia. The bedrock, as for the eastern Shield, is Precambrian rocks covered locally by Paleozoic to Cretaceous sedimentary rocks (mostly carbonates) (Dyke and Dredge, 1989). This part of the Shield was completely covered during the Late Wisconsin glaciation by the Keewatin Sector of the Laurentide Ice Sheet. At its maximum extent, the Keewatin Sector was in contact with the Cordilleran Ice on the west and with the Baffin and Labrador Ice to the north and east.

Several pre-Late Wisconsin events can be recognized throughout the region. On the Boothia Peninsula (Spence Bay), a sequence of marine deltaic and glacial sediments pre-date Wisconsin glaciation (probably Sangamon Interstade for the marine sediments). Over the Keewatin District, numerous till Sections older than Late Wisconsin (>27ka) can be found underlying the surface material.

The late Wisconsin Keewatin Ice is assumed to have extended from Eastern Banks Island to Foxe Basin in the east and to Manitoba and Ontario in the south. The Keewatin Sector remained stable to its maximum extent until around 11ka. By that time, deglaciation had started on Victoria Island, and the sea was entering northwest of Prince of Wales Island. The southern limit of the Keewatin Ice Sheet was retreating quite rapidly in contact with glacial Lake Agassiz. During the period 10ka to 8400 years ago, the Keewatin Ice retreated rapidly as the sea entered Hudson Strait and as Lake Agassiz expanded. The northern part of the Ice Sheet retreated most significantly as it was flooded by a postglacial sea. By 8400 years ago, the major Keewatin Ice Dome had moved to Hudson Bay. During the 8400 to 8000 year interval, Lake Agassiz joined with the sea arm in Hudson Strait to form the Tyrell Sea. Around 8000 years ago, the major remnant of Keewatin Ice was located near Baker Lake along the Hudson Bay shore. By 5000 years ago, the entire region was ice-free and marine submergence was extensive.

The maximum sea level evolved during a long period throughout the region ; from 12.6 ka in the northwest (Victoria Island) to about 8000 year for the Tyrell Sea. The southwest and west part of Victoria Island was submerged for a period from 12ka to approximately 10ka . The 11ka shoreline on southwest Victoria Island can be found at an elevation of about 115m. Around 7000 to 8000 years ago, the marine submergence was quite extensive and covered western Hudson Bay and the Arctic Coast from Coronation Gulf to the Gulf of Boothia. The maximum extent of the Tyrell Sea took place around 5000 to 6000 years ago. For example, the shoreline was at +160m a.s.l. 8000 years ago around Bathurst Inlet and the highest shorelines west of Hudson Bay vary between 120 to 180m a.s.l. (Lee, 1962). Marine submergence decreased slowly in this region as the ice completely retreated (5000 years ago). Land emergence continues to take place at present.

The following sites with salinity measurements are part of this region; Baker Lake, Coral Harbour, Eskimo Point, Gjoa Haven, Pelly Bay, Rankine Inlet, Repulse Bay, Spence Bay and Whale Cove.

2.4.4. Quaternary Geology of the Canadian Interior Plains

The Canadian Interior Plains which are bounded by the Canadian Shield on the east and the Cordillera on the west cover the Mackenzie Valley and Delta as well as Banks and Victoria Islands (Vincent, 1989). Stratigraphic evidence suggests that this region might have undergone three full glaciations since the beginning of the Quaternary age. Non-glacial deposits underlie the oldest till. The bedrock consists of sedimentary rocks (mostly carbonates, shales and sandstones) of Paleozoic to Mesozoic age. Some unconsolidated Cenozoic deposits are present in the Mackenzie Delta and on central and western Banks Island. Locally the bedrock is formed of Proterozoic sedimentary or volcanic rocks not covered by Phanerozoic material.

Evidence of two full pre-Wisconsin glaciations and interglaciations are present on Banks and Victoria Islands. The oldest galciation, Banks Glaciation, (older than 730 ka, early Pleistocene) was extensive, completely covering Banks Island except for the northwest part. This glaciation left a till unit which is overlain by marine and glacio-marine sediments of the interglaciation period. The second pre-Wisconsin glaciation (Thomsen Glaciation, probably middle Pleistocene) covered the southern and eastern parts of Banks Island. Unglaciated areas may have been submerged during this period. On the mainland, limited evidence of pre-Wisconsin glaciation are also present in the District of Mackenzie and Yukon. Glacio-marine and glacio-fluvial sediments of limited extent can also be found along the coastal zones of the Mackenzie District.

The chronology of Wisconsin glaciation over the Interior Plains is a source of wide controversy in the literature. Some authors suggest that the early Wisconsion glaciation was the most extensive advance, while others state that the extent of the late Wisconsin advance was more important. During early Wisconsin, parts of the Tuktoyaktuk Peninsula, of Banks Island and Melville Island were not glaciated since the glacial till found on Banks Island is believed to be of early Wisconsin age. Victoria Island was (except for central Prince Albert Peninsula and parts of the Shaler Mountains) covered by ice during the late Wisconsin. The region north of Great Bear Lake and northward to the Mackenzie Delta and the southern Tuktoyaktuk Peninsula was covered by early Wisconsin Ice. During deglaciation, some marine sediments were deposited on top of the ice depressed shelf. Some sediments overlying early Wisconsin material are thought to be interstadial deposits (middle Wisconsin).

The limit of the late Wisconsin advance indicates that most of Banks Island, northwestern Victoria Island (this is debatable), important areas of the Yukon, and large extent of land directly south of the Beaufort Sea and the Amundsen Gulf escaped glaciation during that period. The rest of the region was covered by the western margin of the Keewatin Sector of the Laurentide Ice Sheet which coalesced with the Cordilleran Ice Sheet until about 13ka. Around 12ka, most of the north part of the Mackenzie valley and a large portion of northwest Victoria Islands were deglaciated. Then by 10ka, the entire Mackenzie valley was ice free and glacial Lake MacConnell was at its maximum extent.

An important aspect of the late Wisconsin glaciation is the variation of the sea level within the Mackenzie Delta. Two major attempts to explain the evolution of the sea level are presented by Forbes (1980) and Hill et al (1985). Hill et al (1985) suggests that the sea level rose some 140m in the last 27 000 years (the sea level was at - 40m at 14ka). A short sea level regression between 13ka and 12ka took place and brought the sea level back down to -70 m. Then at 11ka, the submergence started again to bring the level to - 50m at 9ka. Hill et al (1985) has estimated that the total average subsidence (due to basin subsidence, subsidence along shallow growth faults, sediment loading and consolidation subsidence) was approximately 35m, and that consequently the glacio-eustatic effect accounted for 105m of the rise of the relative sea level during the last 27 000 years. He also states that a late Wisconsin re-advance of the Ice Sheet is necessary to explain the evolution of the sea level subscribing to the idea that Late Wisconsin glaciation was very extensive.

Parts of southwest and west Victoria Island were under marine submergence during the 12ka to 10ka period. Later (after 9 000 years), as the ice retreated eastward, the east and south part of the Island became submerged. There is some controversy about whether Holman Island was ever submerged.

The salinity sites that are located in the Interior Plains are: Arctic Red River, Fort Good Hope, Fort McPherson, Fort Norman, Fort Simpson, Holman Island, Inuvik, Jean Marie Creek, Manner Creek, Richards Island, Table Mountain, Tuktoyaktuk, and Wrigley.

2.4.5. Explanation of the Salinity Distribution

It is believed that the Quaternary geology of the Northwest Territories controls the understanding of the salinity distribution.

All the communities on Baffin Island have relatively high salinities,i.e. salinity greater than 5 ppt. As explained in Section 2.4.2., some parts of Baffin Island were not glaciated during the late Wisconsin but the entire Island was covered by ice at some point in the late Quaternary history. There is some controversy about the marine submergence of Baffin Island. It is believed that Arctic Bay, and Pond Inlet were possibly submerged and that Iqaluit, Pangnirtung and Cape Dorset were probably submerged during the late Wisconsin, which explains the high present day salinities. The marine submergence history for Clyde River and Broughton Island is more obscure, but it is believed by the author that a period of marine submergence that pre-dated the late Wisconsin must have occurred since high salinities are also found at these two sites. Moreover, the terrain type at these two locations is believed to be glacio-marine which would support the idea of submergence.

The entire coastal region of the northwestern Canadian Shield was under marine submergence after the late Wisconsin glaciation. So the high salinities present at these sites (except for Coral Harbour, Gjoa Haven, Spence Bay and Whale Cove), are easily explained by the presence of some diluted sea water in the pore fluid in the surficial materials. Most of the low salinities measured at Gjoa Haven, Spence Bay and Whale Cove (0.02 to 1.1 ppt) originated from shallow samples located within the active layer where low salinities are expected and are not representative of the material at depth. The remaining low salinities could be caused by leaching of the salts from the surficial deposits which consist of thick beach sands of high permeability.

Sites in the Interior Plains regions should be discussed in groups. As stated in Section 2.4.4., it is not known if Holman Island was submerged or not. The visual description of the sample used for the salinity measurement suggest that the sediments are of marine origin. According to Section 2.3.4., the salinities at this site are relatively low for marine sediments suggesting that salt leaching could have taken place through the coarse beach deposits which cover the area.

The Mackenzie Delta is an estuarine environment suggesting that the sea water salinity would be lower than normal sea water salinity of 35 ppt. Therefore, sites in the Mackenzie Delta should have salinities lower than sea water. This is the case for Tuktoyaktuk. However, as revealed in Section 2.3.4., Richards Island presents occasional high salinities (>10 ppt) . These higher values are usually associated with samples from greater depth. A possible explanation for these occurrences is that some diffusion from sea water of higher salinity at depth (below the zone of influence of the fresh water) has taken place into the frozen material located along the coast. However, as mentioned in Section 2.3.4., no agreement exists in the literature on the stratigraphy and glacial history of Richards Island, and consequently a rational explanation for these high salinities is difficult with the information available for this study. Another important point to mention is that the delta region was never submerged, i.e. the delta is in a phase of marine transgression.

Along the Mackenzie River, low salinities are expected since the area is above sea level and was never submerged. This is what has been observed at all sites except for Arctic Red River, Fort McPherson and Inuvik where salinity in excess of 10 ppt are frequently observed. These sites are located closer to the Mackenzie Delta than other sites along the Mackenzie Valley. The salinity measurements listed in the database were from fine-grained materials (mostly clays) at temperatures warmer than -4.5°C. This suggest that unfrozen water exists in the permafrost causing a significant increase in the diffusion coefficient of sea water salts. It is believed (Murrmann, 1973) that ions can diffuse in frozen ground through a continous unfrozen water film, especially in fine-graines soils. Since the three sites of interest, Arctic Red River, Fort McPHerson and Inuvik are relatively close to the delta, it is possible that the observed high salinitiesare a consequence of sea salt diffusion through the permafrost at depth. This long-term diffusion should be investigated more since it could be related to the diffusion of contaminated pore fluid through cryogenic barriers.

TABLE 2.1
GEOLOGICAL SUB-UNITS for BAFFIN ISLAND

UNIT	COMMUNITY	GEOLOGICAL UNITY
I-a	Arctic Bay Pond Inlet	The bedrock consists of Paleozoic to Cretaceous sedimentary rocks (limestone, dolomite, sandstone) over Precambrian gneiss and granite of the Shield. The bedrock is usually covered by a thin layer of glacial deposits in the form of ground or end moraines. The till is usually overlain by scree (drift from bedrock), marine deposits such as beach and terrace sediments and/or by glacio-fluvial or recent alluvial sediments deposited in old glacier outwash channels. Very little glacio-lacustrine deposits are present.
I-b	Broughton Island Cape Dorset Clyde River Iqaluit Pangnirtung	The bedrock is the Precambrian Shield formed of metamorphic granite and gneiss. The surficial cover is a glacial sandy to gravelly till of varying thickness. Locally, some pre-Late Wisconsin till can be observed. Raised marine beaches can be found at some sites. In Pangnirtung area, thick glacio-marine sediments occur. A wide variety of active and inactive alluvial and fluvio-glacial sediments are distributed over the area. Some recent marine mud sedimentation takes place in the fiords.

TABLE 2.2
GEOLOGICAL SUB-UNITS for the NORTHWESTERN CANADIAN SHIELD

UNIT	COMMUNITY	GEOLOGICAL UNIT
II-a	Baker Lake Eskimo Point Rankine Inlet Repulse Bay Whale Cove	The bedrock is either metamorphic gneiss and granite of the Shield or a complex of volcanic and sedimentary rocks of Proterozoic age. A relatively thin cover of glacial deposits (usually a ground moraine) overlie the bedrock . Some glacial marine and raised beach sands mantles the till.
II-b	Gjoa Haven Pelly Bay Spence Bay	The bedrock is formed of a thin cover of Paleozoic (Ordovician to Silurian) carbonate limestones and/or dolomites over the Precambrian metamorphic gneiss and granite. The bedrock is overlain locally by thin glacial till and glaciolacustrine deposits. The surface deposits are glacial marine and sand beach deposits of varying thickness.
II-c	Coral Harbour	Two major physiographic units form this region: 1- The Precambrian Uplands composed of granite and gneiss covered by glacial till; 2- Paleozoic limestone covered by post-glacial beaches and raised glacial outwash deposits.

TABLE 2.3
GEOLOGICAL SUB-UNITS for the CANADIAN INTERIOR PLAINS

UNIT	COMMUNITY	GEOLOGICAL UNIT
III-a	Arctic Red River Fort McPherson Fort Norman Fort Good Hope Fort Simpson Inuvik Jean Marie Creek Manner Creek Paulatuk Table Mountain Wrigley	The bedrock is formed of Paleozoic (Devonian to Cretaceous) sedimentary rocks (dolomite, limestone, shale). It is covered by some glacial deposits which are locally overlain by glacio-fluvial deposits. Post-glacial fluvial , lacustrine and marine materials blanket the sediments at some sites. In communities located along the Mackenzie River, some recent fluvial and or deltaic deposits (flood plains, low terraces) complete the stratigraphy. At Fort Good Hope, Fort Norman and Fort Simpson, a cover of eolian deposits (dunes and sand ridges) overlay the older sediments.
III-b	Tuktoyaktuk	The bedrock is a Cretaceous Sedimentary Basin. A thick unit of pre-glacial Pleistocene marine and fluvial (deltaic) sediments is capped by a glacial till and fluvio-glacial deposits. Glacio-lacustrine deposits locally covers the area. Some very limited recent marine sediments can be found. (It should be kept in mind that the eastern third of the Tuktoyaktuk Peninsula was not glaciated during Late Wisconsin.)
III-c	Richards Island	The bedrock is the same as for unit III-a. Two physiographic units are found in this area: 1- The modern delta which is a thick sequence of alluvial silts and fine sands locally interbedded with organics or recent marine sediments; 2- The Pleistocene Coastlands (similar to Tuktoyaktuk Peninsula) which consists of fine to medium sand of marine deltaic origin. In the Uplands and along ridges, these deposits are overlain by till and/or mudflow debris. In low topographic areas, the marine sand is covered by organics and recent lacustrine sediments.
III-d	Holman Island	The bedrock is formed of a gabbro intrusion which cuts through the Proterozoic sedimentary sequence. Low lying areas are covered by smooth and hummocky till plains with well developed ice contact landforms. Some glacio-marine sediments can be observed.

TABLE 2.4
SUMMARY of SALINITY DATA

COMMUNITY	UNIT	SALINITY RANGE (ppt)
Arctic Bay	I-a	1.0 - 32.0
Arctic Red River	III-a	1.2 - 70.4
Baker Lake	II-a	4.1 - 30.0
Broughton Island	I-b	0.6 - 22.0
Cape Dorset	I-b	0.4 - 25.2
Clyde River	I-b	0.6 - 44.5
Coral Harbour	II-c	1.3 - 7.5
Eskimo Point	II-a	0.8 - 38.3
Fort Good Hope	III-a	0.7 - 2.6
Fort McPherson	III-a	0.4 - 22.7
Fort Norman	III-a	0.4 - 0.8
Fort Simpson	III-a	0.5 - 0.9
Gjoa Haven	II-b	0.2
Holman Island	III-d	3.0 - 5.7
Inuvik	III-a	1.2 - 41.0
Iqaluit	I-b	0.1 - 24
Jean Marie Creek	III-a	0.18
Manner Creek	III-a	0.02 - 0.23
Pangnirtung	I-b	0.1 - 31.3 (up to 208ppt at very low m.c.)
Pelly Bay	II-b	12.0 - 33.7
Pond Inlet	I-a	0.2 - 23.4
Rankine Inlet	II-a	2.6 - 30.6
Repulse Bay	II-a	0.5 - 10.4
Richards Island	III-c	0.03 - 30.2
Spence Bay	II-b	0.02
Table Mountain	III-a	0.24 - 1.28
Tuktoyaktuk	III-b	0 - 9.1
Whale Cove	II-a	0.1 - 1.1
Wrigley	III-a	0.6

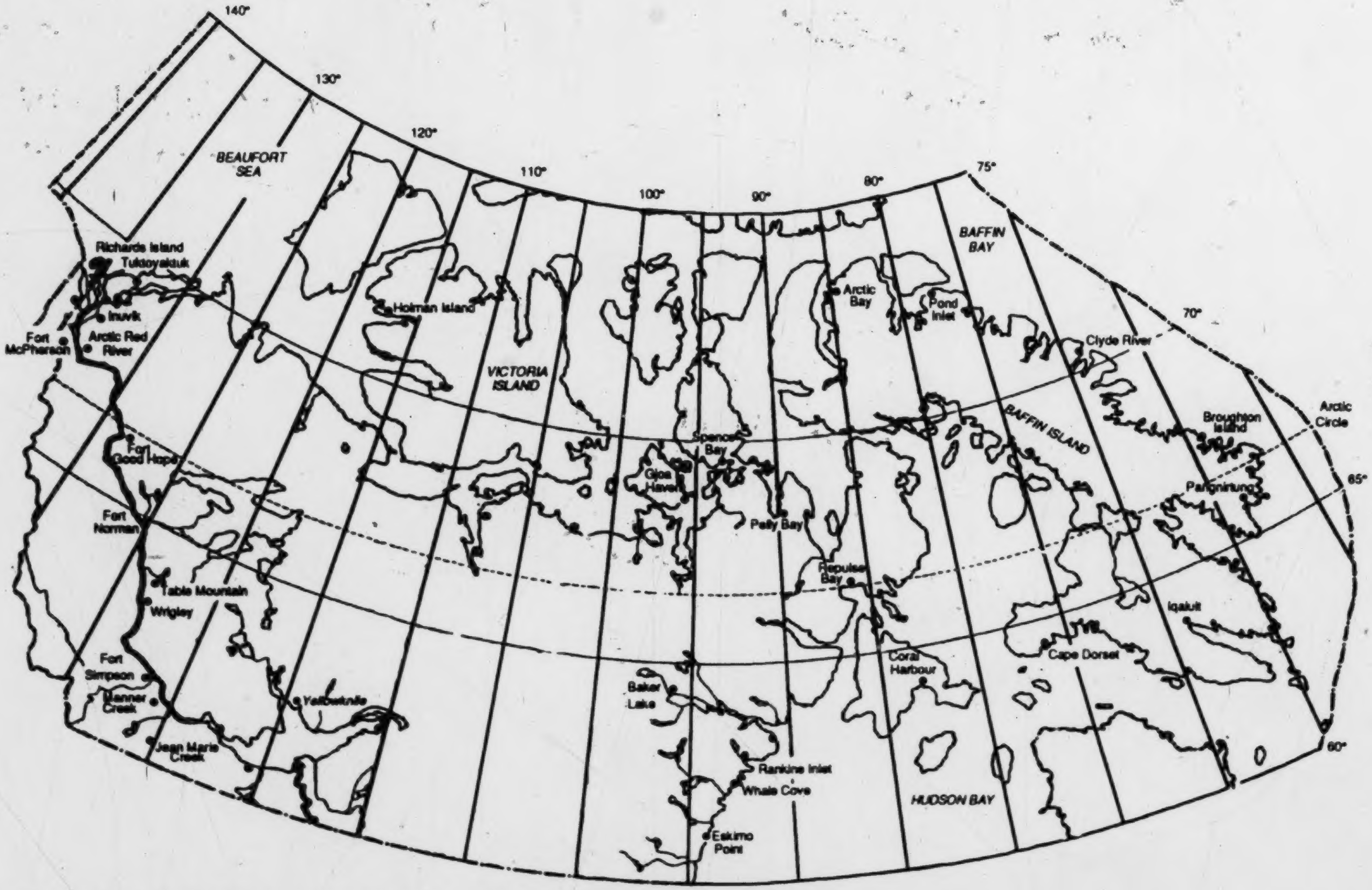
140°
130°
120°
110°
100°
90°
80°
75°
70°
65°
60°
Arctic Circle
BEAUFORT SEA
BAFFIN BAY
BAFFIN ISLAND
VICTORIA ISLAND
HUDSON BAY
Richards Island
Tuktoyaktuk
Inuvik
Fort McPherson
Arctic Red River
Fort Good Hope
Fort Norman
Table Mountain
Wrigley
Fort Simpson
Manner Creek
Jean Marie Creek
Yellowknife
Holman Island
Arctic Bay
Pond Inlet
Clyde River
Broughton Island
Pangnirtung
Iqaluit
Cape Dorset
Coral Harbour
Repulse Bay
Pelly Bay
Spence Bay
Gjoa Haven
Baker Lake
Rankine Inlet
Whale Cove
Eskimo Point

Figure 2.1: Map of salinity measurement sites in the Northwest Territories adapted from Map 38 in Atlas of the Northwest Territories, Canada, 1966.

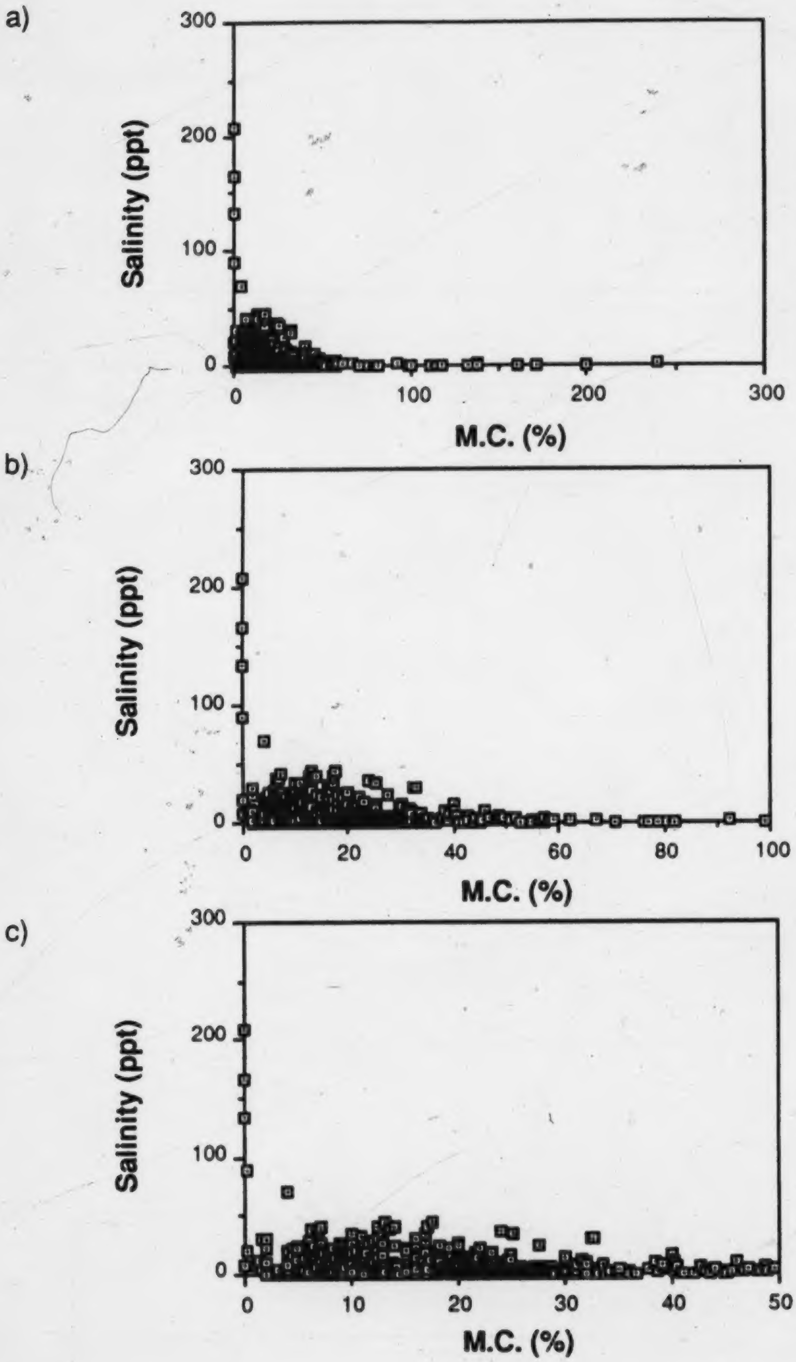

Figure 2.2: Salinity vs Moisture Content
a) m.c. < 300% b) m.c. < 100% c) m.c. < 50%

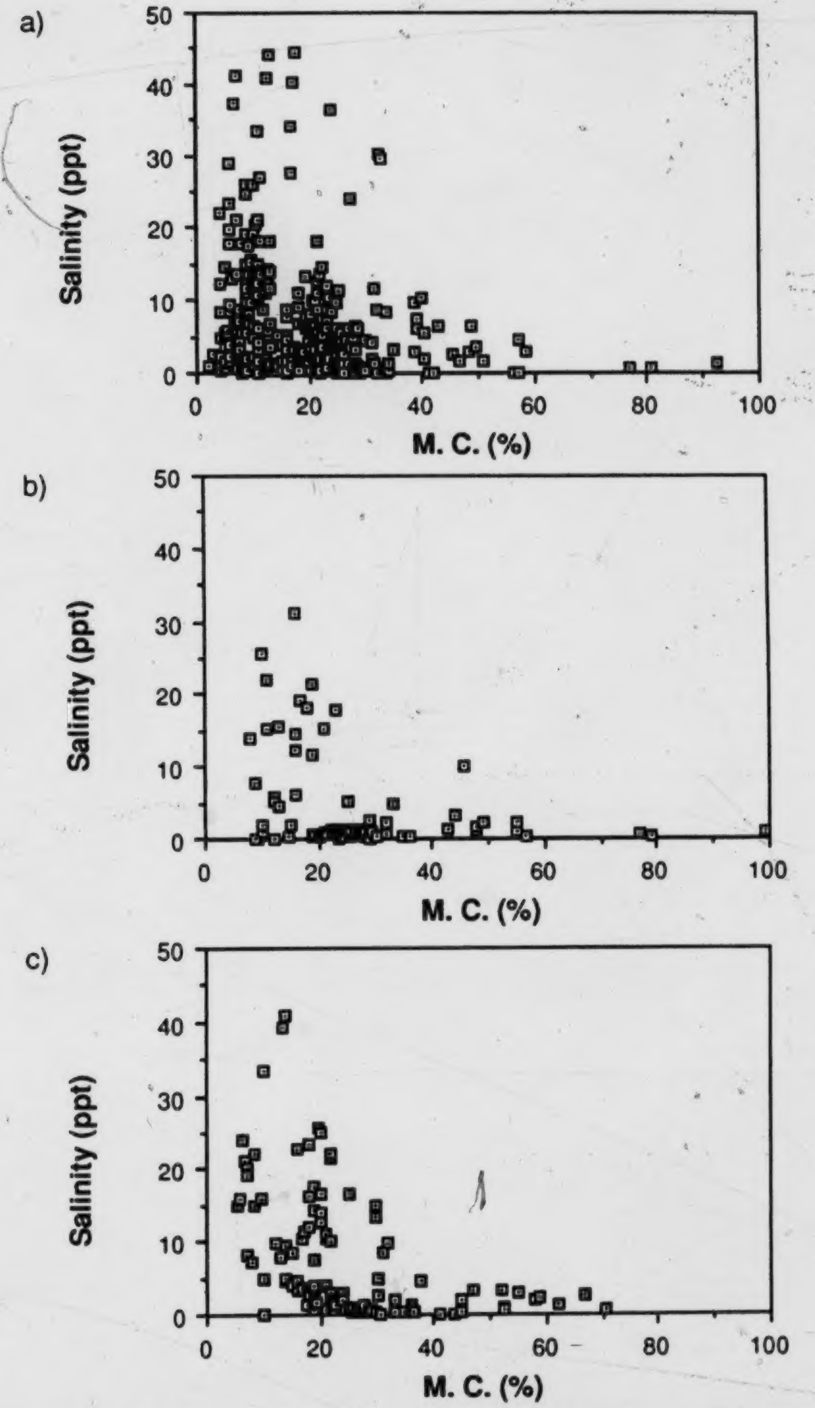

Figure 2.3: Salinity vs Moisture Content according to soil type
a) sand b) silt c) clay

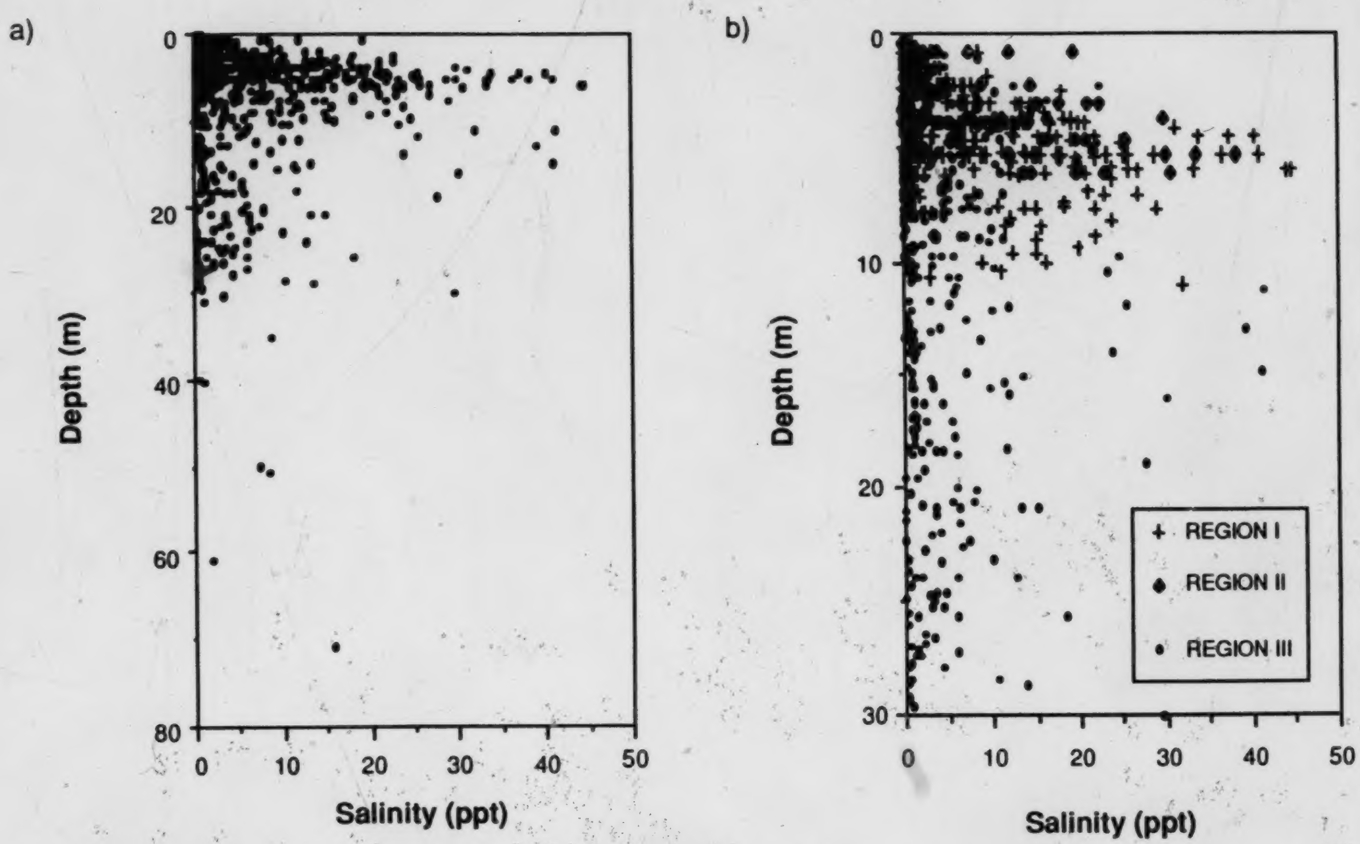

Figure 2.4: Salinity vs Depth a) all entries b) according to regions

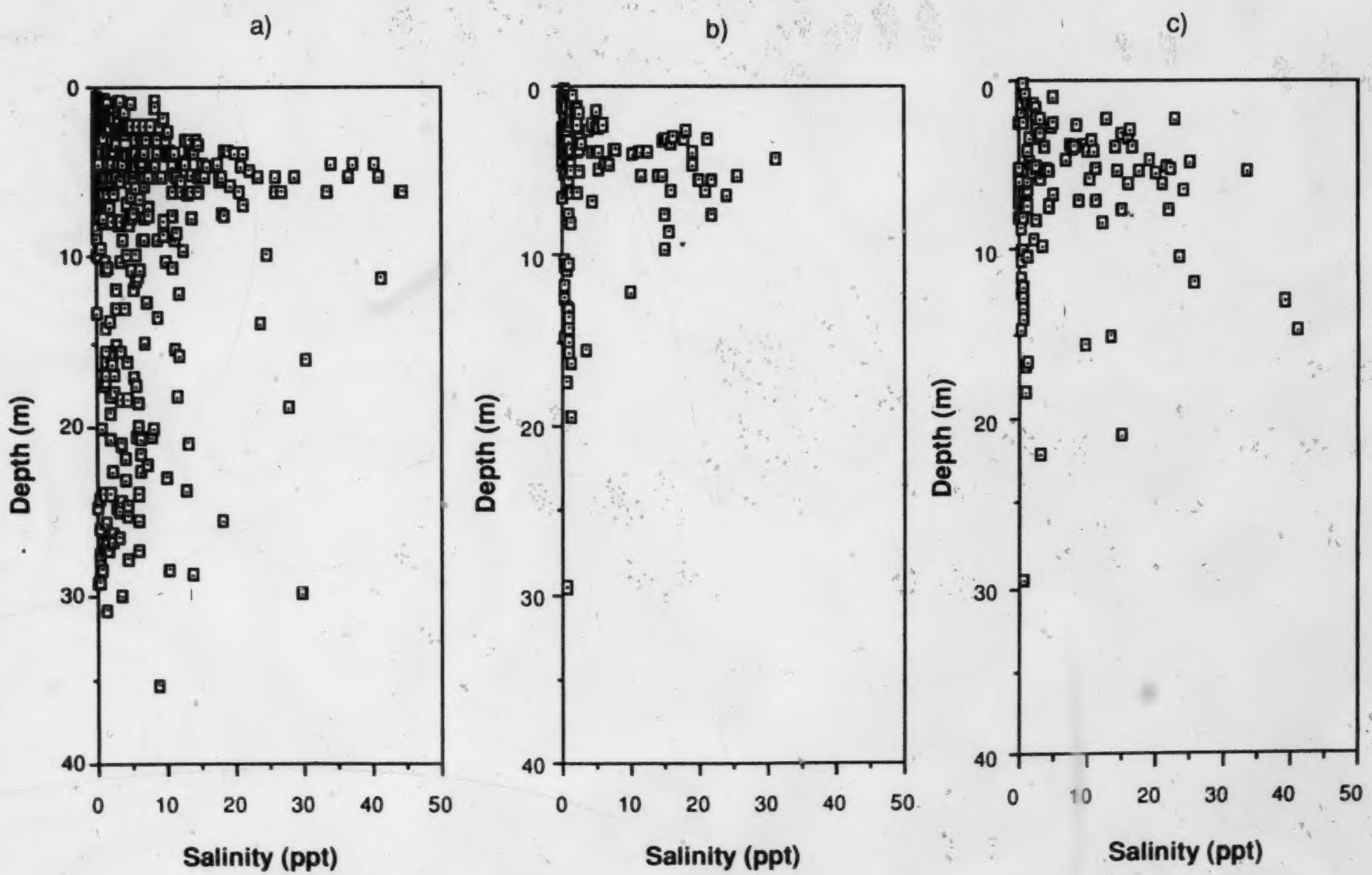

Figure 2.5: Salinity vs Depth according to soil type a) sand b) silt c) clay

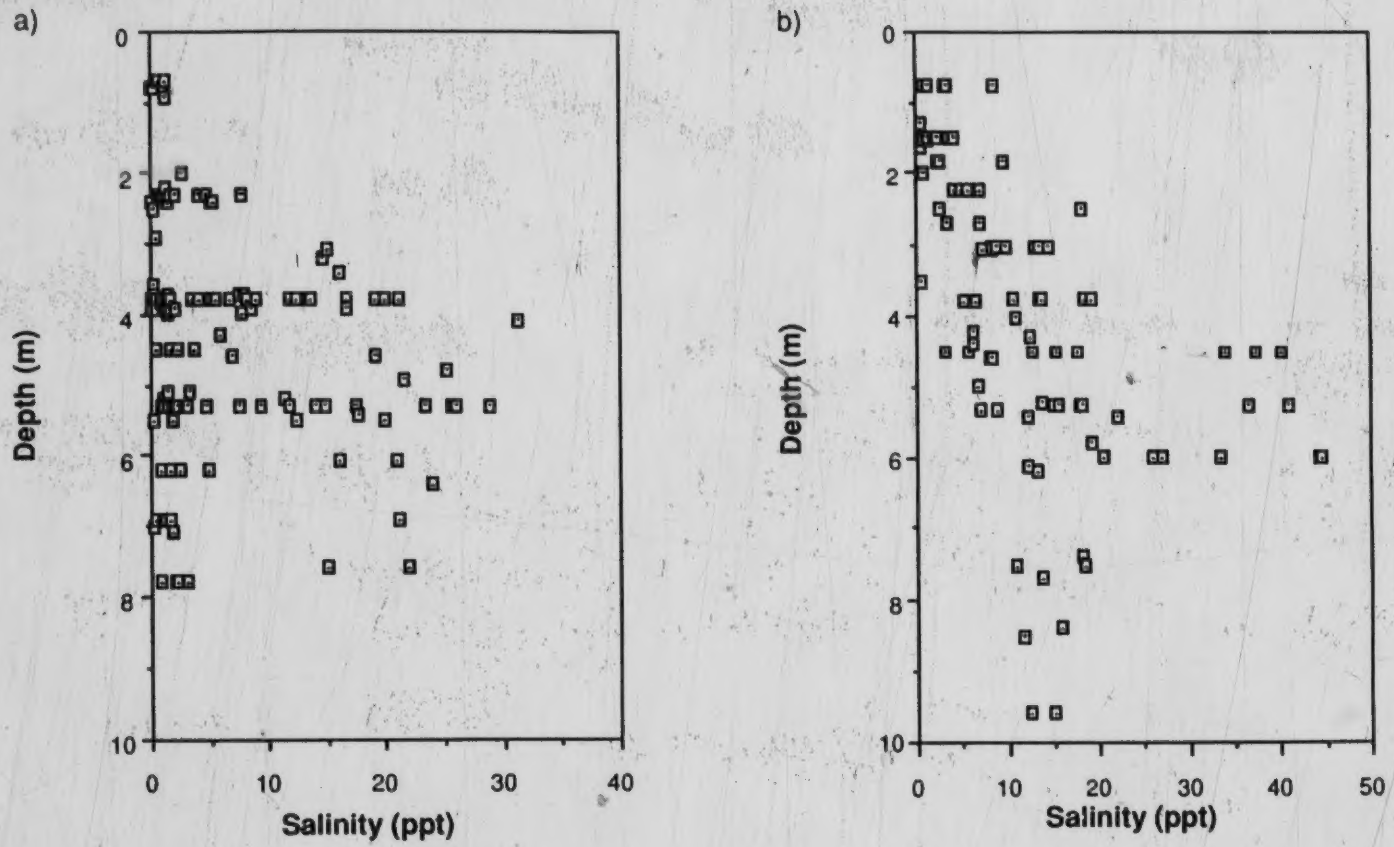

Figure 2.6: Salinity vs Depth for Region I a) glacial deposits b) marine deposits

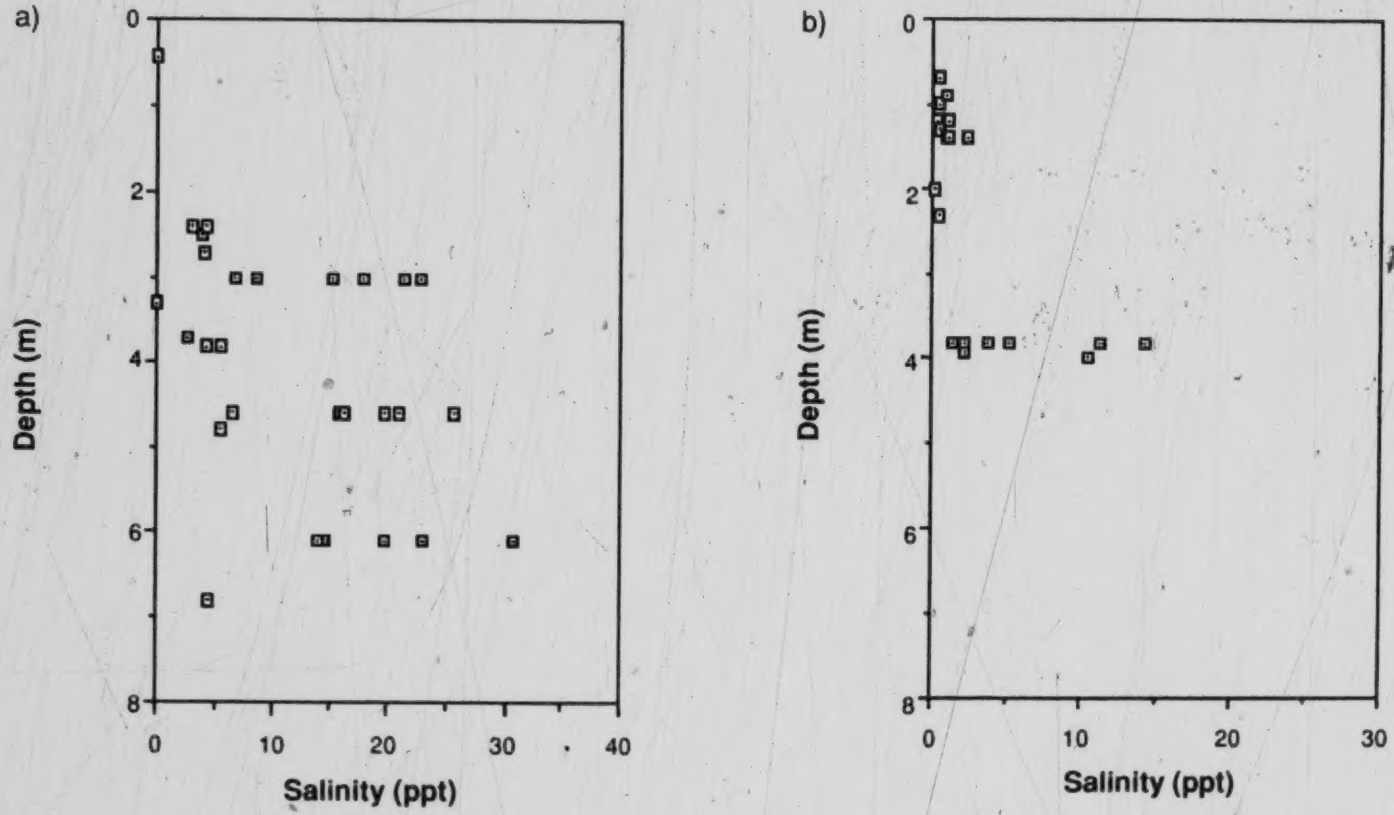

Figure 2.7: Salinity vs Depth for Region II a) glacial deposits b) marine deposits

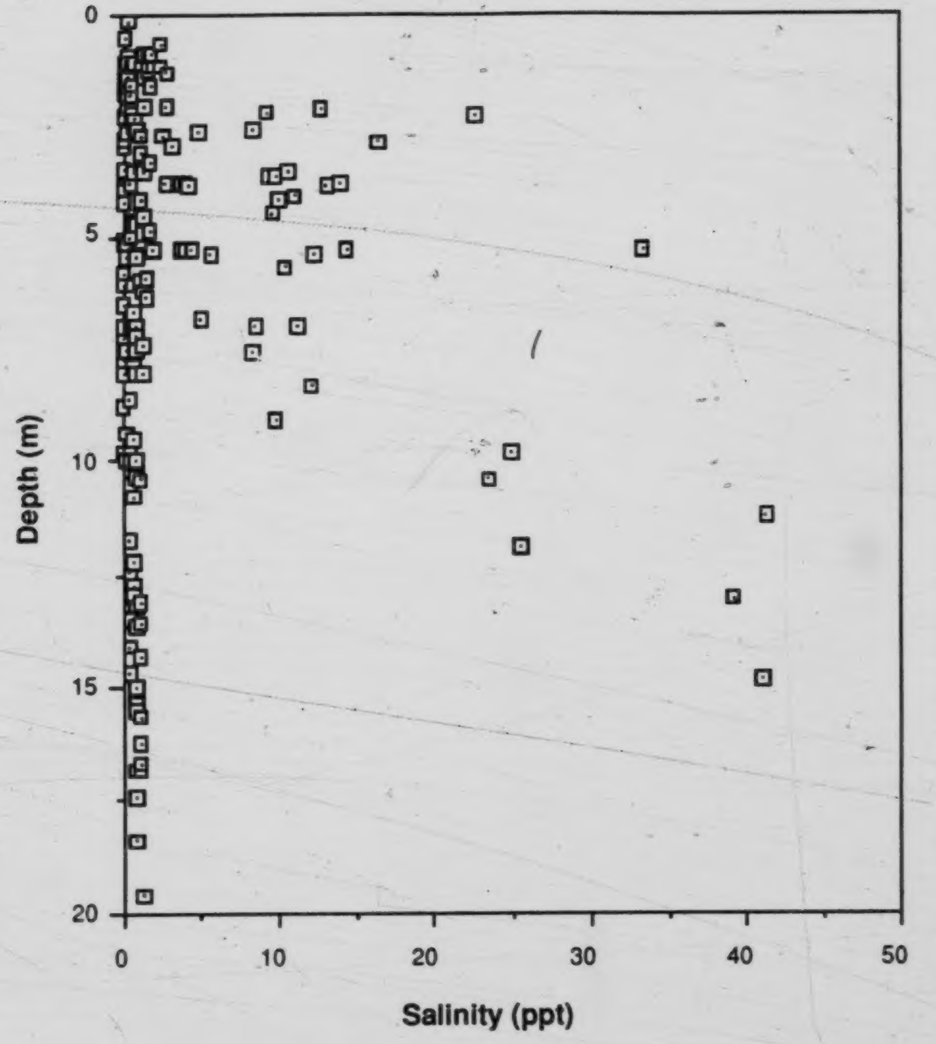

Figure 2.8: Salinity vs Depth for Region III excluding Holman and Richards Islands

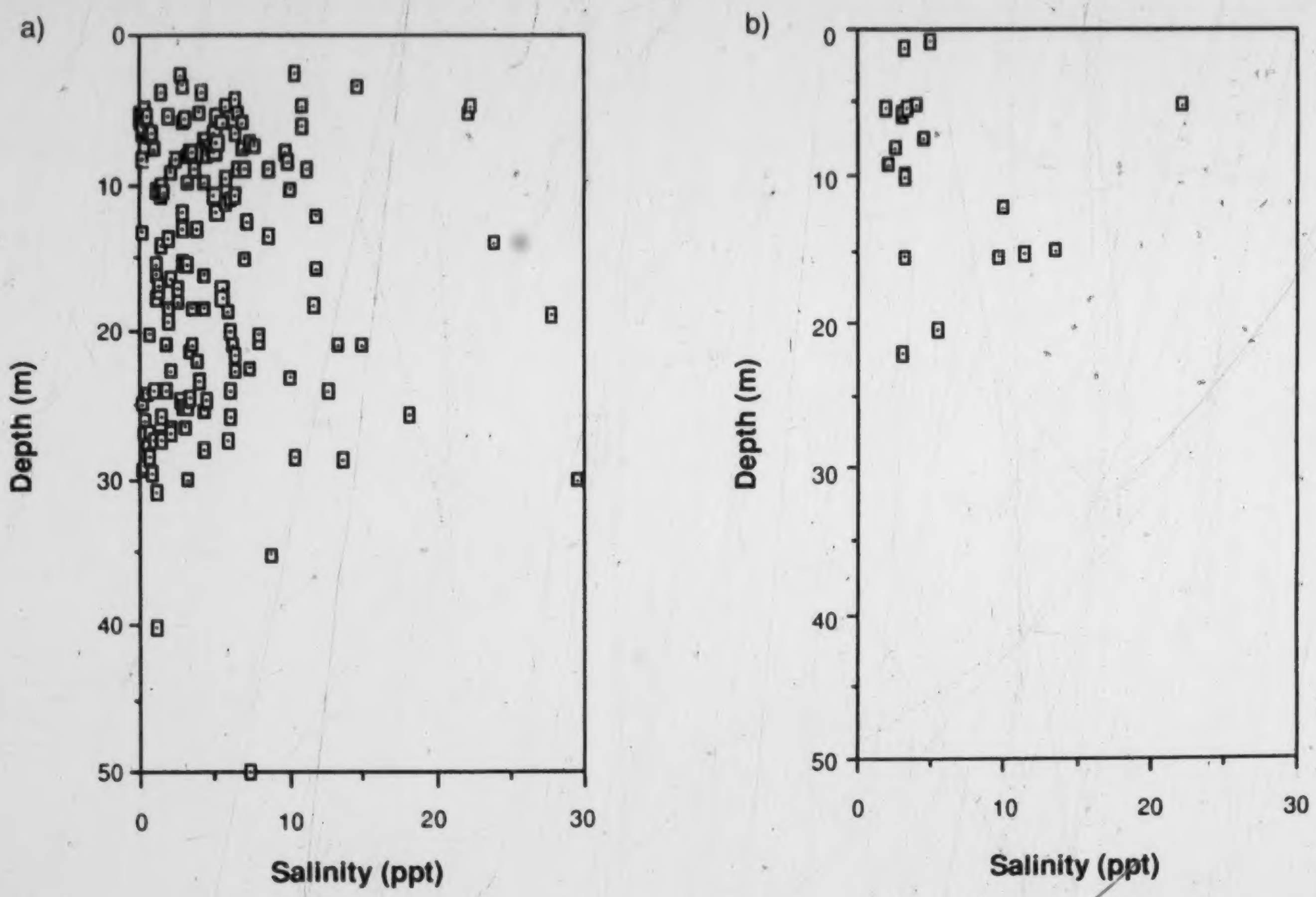

Figure 2.9: Salinity vs Depth for Richards Island a) glacial deposits b) marine deposits

3. LITERATURE REVIEW

3.1. PHYSICAL BEHAVIOUR OF FROZEN SOILS

3.1.1. Unfrozen water in non-saline frozen soils

It is commonly accepted that frozen soils are formed of soil grains, ice, unfrozen water and air (for unsaturated soils). As stated by many authors (Anderson and Tice (1972), Nerseova and Tsytovich (1963), Vershinin et al. (1960), Hoekstra (1969)) the amount of unfrozen water will be governed by the temperature of the soil, the pressure, the specific surface area of the soil grains, the mineralogical and chemical composition of the soil, the arrangement of the soil particles, the density, the solute concentration and composition of the pore fluid. In non-saline soils, the amount of unfrozen water is mainly governed by the specific surface area and grain arrangement which control the development of capillary and adsorption forces. Consequently, the amount of unfrozen water found in non-saline coarse soils is usually negligible because of the large voids and small adsorption forces. Nerseova and Tsytovich (1963) distinguished between three states of soil water: the gaseous state, the bounded state (weakly or strongly bounded) and the free state. They defined the weakly bounded water as the adsorbed water which goes through a phase change when subjected to sub-zero temperature and the strongly bounded water as the water which stays in the liquid phase even at sub-zero temperatures. The free water freezes at 0°C at one atmosphere.

Anderson and Tice (1972) and Dillon and Andersland (1966) suggested two methods to predict the unfrozen water content based on specific surface area and temperature. Dillon and Andersland also included the activity of the soil, a coefficient to consider the type of clay mineral present, and the freezing point depression of the pore water. Tice et al. (1976) proposed a method for predicting phase composition curves based on liquid limit measurements. They stated that the relationship is valid for soils with a liquid limit less than 100 or with no excessive soluble salts. Some problems could occur when the prediction is applied to smectite type clays.

Numerous authors have used thermodynamic principles (surface tension, free energy, etc.) to evaluate the phase composition of frozen soils. Each author uses a different version of the Gibbs equation, the Kelvin equation or the Clausius-Clayperon equation to model gas-water-ice systems. Colbeck (1981) gave an extensive explanation of the cold capillary systems based on the Laplace's equation of surface forces using different equilibrium assumptions. For a liquid-solid flat interface at equilibrium (saturated soil), he gives the following form of the Clausius-Clayperon equation;

$$T_m = \frac{T_o}{L}\left(\frac{1}{\rho_l} - \frac{1}{\rho_s}\right)P \qquad (3.1)$$

where: T_m: freezing temperature (K)
T_o: freezing temperature of pure water (K)
ρ_l, ρ_s: liquid (water), solid (ice) densities
P: vapor pressure
L: latent heat of fusion

Keune and Hoekstra (1967) and Hoekstra (1969) used partial molar free energy of ice and liquid water in conjunction with the moisture characteristic curve of liquid water (relation between moisture content and soil water tension) and osmotic pressure to establish a method to evaluate unfrozen water content. Freezing point depression can be predicted using free energy and activity of components (Low et al. (1968)), pressure differences between water phases in the system (Kinosita and Ishizaki (1980), Miller (1980)), or suction (Williams (1963)). Miller gave the following for the freezing temperature equation.

$$\left(\frac{L}{273}\right)T = \frac{(P_{H_2O})}{\rho_w} - \frac{(P_i)}{\rho_i} \qquad (3.2)$$

where: L: latent heat of fusion (kJ/kg)
T: freezing temperature
P_{H2O}: vapor pressure in free water
P_i: vapor pressure in ice
ρ_w, ρ_i: water, ice densities

3.1.2. Influence of salinity on pore fluid of frozen soils

Wilson and Vinson (1983) gave a very good explanation of the effect of the presence of salt on the formation of ice. They explained how solutes can fit into the Ice Ih lattice only in two ways, depending on the solute size, shape, charge and valence. If the solute can not fit in the lattice (as it is the case for NaCl), it is rejected into the liquid phase. The degree of concentration of the solution will depend on the rate of solute rejection (which is controlled by the rate of advance of the interface into the solution and the proportion of salts incorporated in the ice) and the rate of solute diffusion. This solute exclusion causes an increase in salinity of the liquid phase according to the salt binary phase diagram. The freezing of a saline solution is consequently a progressive process where the amount of liquid decreases as the concentration of the solution increases causing a continous decrease in freezing point. The initial freezing takes place at the freezing point of the original solution; freezing continues until the eutectic point of the given solution is attained. Many authors (Baker and Osterkamp (1988), Kay and Perfect (1988), Kay and Groenevelt (1983)) gave explanations of the effect of solute rejection on the advance of freezing front. A combination of diffusion, dispersion and convection govern the transport of the solute in the liquid phase. This migration of solute causes a gradient of freezing point leading to the formation of alternating brine layers and ice lenses under given conditions. It should be kept in mind, that since the presence of solute increases the unfrozen water content, the hydraulic conductivity of a saline frozen soil is higher than for a non-saline frozen soil. Sheeran and Yong (1975) gave a good explanation of the salt exclusion process in a single pore: the ice forms in the centre of the pore moving towards the adsorbed water layer. They explained that for pore fluid with high solute concentration, the development of brine islands within the ice is possible. Colbeck (1985) observed the development of ice-water interfaces in freezing glass beads. He suggested that since the ice does not seem to be strongly bonded to the beads, a thin liquid film could exist around the bead. Wilson and Vinson (1983) following an approach by Anderson (1967) stated that ice nucleation occurs at some distance from the soil particle, where water is only slightly affected by the diffuse double layer. The ice crystal then grows away from the soil surface into the pore space, rejecting solutes which concentrate at the ice-soil interface. However, other authors (Gilpin (1980), Hoekstra (1969)) including the present author, do not agree with the presence of such a liquid film around the soil grain in granular coarse materials since the thermal conductivity of quartz is larger than that of ice: K_{quartz}=8.4 W/mK, K_{ice}=2.2 W/mK and for a wide range of soil mineral K_s=2.9 W/mK (according to Farouki (1981)). The author believes that the ice would form directly in contact with the soil grain since it cools down faster than the pore fluid. In fine-grained soils, the presence of the adsorbed water film is almost universally accepted. Some authors (Farouki (1981)) even suggested that the adsorbed water could have a thermal conductivity higher than that of ice. Figure 3.1 shows an illustration of Sheeran and Yong's (1975) approach and the modification suggested by this author for coarse-grained soils.

The initial freezing temperature of a saline fluid was given by Cheung (1979):

$$\Delta T = \frac{R\,T_0^2}{L_f} X_2 \quad \text{where } X_2 = \frac{W_2/M_2}{W_1/M_1 + W_2/M_2} \tag{3.3}$$

where: ΔT: freezing point depression (K)
T_0: freezing temperature of pure water (K)
L_f: latent heat of fusion
R: gas constant
W_1, W_2: weights of solvent and solute
M_1, M_2: molecular weights of solvent and solute

Other similar equations for the freezing point depression of a saline solution are also given by Chen and Nagy (1987) and Banin and Anderson (1974) . Cheung also gave an expression for the shift in freezing point depression due to salt exclusion during freezing. Moreover, he gives an equation to predict the freezing point depression in clays due to osmotic pressure using the double-layer theory. However this is beyond the scope of the present work. Velli and Grishin (1982) presented a much simpler way to predict freezing point depression for three types of salts (sea salt, NaCl and $CaCl_2$).

$$T_{f.p.} = a\,K_{is} \tag{3.4}$$

where: a = 57 for sea salt
= 62 for NaCl
= 32.5 for $CaCl_2$
K_{is}: concentration of interstial solution
= Z / W+Z
Z: soil salinity % by dry weight
W: total water content (%)

This relationship is believed to be valid for clays with a moisture content greater than the liquid limit or for sands with a moisture content larger than the saturated moisture content. Loch (1979) presented an excellent thermodynamic explanation of the equilibrium of ice and water in porous media (non-saline and saline). He presented a modification of the classical Clausius-Clapeyron equation which allows for a pressure difference between the two phases of water (solid and liquid). For a binary system of salt and water, he uses the chemical potentials of the two components to express the Gibbs free energy. The variation of chemical potential of the water is given by:

$$d\,\mu_w = -\overline{S}\,d\,T + \overline{V}\,d\,P - R\,T\,d\left(\frac{n_s}{M_s\,n_w}\right) \tag{3.5}$$

where: μ_w : chemical potential of water
$\overline{S}$: entropy for 1 g of water
T : temperature
$\overline{V}$: volume for 1 g of water
P : hydrostatic pressure
R : gas constant
n_s, n_w : mass of salt and water
M_s : molecular weight of salt

Loch then introduced his definition of osmotic pressure, π:

$$\pi = R\,T\left(\frac{n_s}{M_s\,n_w\,\overline{V}}\right) \tag{3.6}$$

Equation 3.5 then becomes:

$$d\,\mu_w = -\overline{S}\,dT + \overline{V}\,dP - \overline{V}\,d\pi_v = -\overline{S}\,dT + \overline{V}\,dP_w \tag{3.7}$$

where: $P_w = P - \pi$: total potential

The integration for small change in temperature gives,

$$\mu_w = -\overline{H}\,\frac{\Delta T}{T_o} + \overline{V}\;P_w \tag{3.8}$$

where: $\overline{S} = \frac{\overline{H}}{T}$ and $\overline{H}$: enthalpy/ unit mass
T_o:freezing temperature of pure water

The chemical potential of the ice is given by,

$$\mu_i = -\overline{H_i}\,\frac{\Delta T}{T_o} + \overline{V_i}\;P + \overline{V_i}\,\sigma_{iw}\frac{\partial A}{\partial V} \tag{3.9}$$

where: σ_{iw}: interfacial energy for ice-water
A: surface area

For two phases in equilibrium, the chemical potentials are equal; $\mu_w = \mu_i$

$$\overline{V_i}\left(P + \sigma_{iw}\frac{\partial A}{\partial V}\right) - \overline{V}\,P_w = -\left(\overline{H} - \overline{H_i}\right)\frac{\Delta T}{T_o} \tag{3.10}$$

Since,

$$\overline{H} - \overline{H_i} = L_f \qquad \text{where: } L_f\text{: latent heat of fusion} \tag{3.11}$$

and by definition,

$$P_i = P + \sigma_{iw}\frac{\partial A}{\partial V} \tag{3.12}$$

Loch got the following form for the modified Clausius-Clapeyron equation,

$$\overline{V_i}\,P_i - \overline{V}P_w = -\frac{L_f}{T_o}\,\Delta T \tag{3.13}$$

Finally, Patterson and Smith (1983) used a simplified version of the method originally proposed by Banin and Anderson (1974) for the special case of sodium chloride. The method predicts the freezing point (T_n) of a saline soil when the unfrozen water content (θ_i) of the soil at its natural salinity is known. In other words, the method predicts the temperature at which a given unfrozen water content will occur for different salinities. The temperature T_n is given by;

$$T_n = T_i + \frac{S_o \Delta}{\theta_i / \theta_o} \tag{3.14}$$

where: T_n: new freezing temperature at which θ_i will occur
T_i: freezing temperature of the soil at its natural salinity
θ_i: volumetric unfrozen water content for the soil at its natural salinity
θ_o: volumetric water content for the thawed soil
S_o: salinity (g/l)
Δ: -5.867×10^{-2} °C/ g NaCl/l

It this author opinion, the best thermodynamic approach to use is Loch's (1979) method, since it is complete and considers the influence of salt within the pore fluid simply by using the concept of chemical potentials. Velli and Grishin, as well as Banin and Anderson equations are empirical in nature but easier to use in practice.

3.1.3. Direct measurement of unfrozen water content

The theoretical methods of unfrozen water content prediction presented in the previous section require extensive physical chemistry calculations which are beyond the scope of this study. This is why a direct method of measurement of the unfrozen water content was used.

3.1.3.1. Direct methods

Anderson and Morgenstern (1973) gave a good overview of the methods developed to measure unfrozen water content. They mentioned dilatometry (Bouyoucos, 1916, Koopmans and Miller, 1966), adiabatic calorimetry (Williams, 1964), X-ray diffraction (Anderson and Hoekstra, 1965), heat capacity (Nersesova and Tsytovich, 1963), nuclear magnetic resonance (Wu, 1964), differential thermal analysis (Anderson and Tice, 1971), and isothermal calorimetry (Anderson and Tice, 1973).

Each method has a set of assumptions and limitations. The dilatometry method, which relates the volume expansion of a sample to the amount of unfrozen water, assumes that the water remains inert during freezing, that the sample is fully saturated and that soil water expands to the same extent as pure water. Since adsorbed water has a density less than that of pure water, the dilatometry method can lead to an overestimation of the unfrozen water content. The adiabatic calorimetry method, which measures the heat exchange between a frozen sample and a liquid at a known temperature, relies on three major assumptions: 1) the heat capacities and temperature coefficients of all components are known, 2) during thawing, the absorption of latent heat is the only transfer process, and 3) the latent heat of melting ice is constant and equals 333.7 kJ/kg. Each of these assumptions suggests that the theoretical thermodynamic basis of that method is not fully understood. Similar to the dilatometry method, the adiabatic calorimetry sometimes leads to an overestimation of the unfrozen water content. However, it is still the most widely used method. The third method reviewed was the X-ray diffraction method. This technique does not have a wide applicability since it can be effective only on expanding lattice clays, and it usually slightly underestimates the unfrozen water content. Anderson (1966) developed a method based on the measurement of the heat capacity of the frozen soil, which seems to be less dependent on unverifiable assumptions as compared to the previous methods discussed. The method, which was used only once, assumes that over a certain range of temperatures, the unfrozen water content is independent of the total water content. The nuclear magnetic resonance (NMR) method takes advantage of the fact that water has a very narrow spectral line compared to that of ice. The main assumption is again that the amount of unfrozen water is independent of the total water content. Since 1973, many authors (Oliphant and Tice, 1982), Tice et al., 1980, Tice et al., 1978 a,b, Tice et al., 1988 and Mel'nichenko et al., 1981) have improved the method using both steady and pulsed NMR to determine unfrozen water content. Two similar methods are the differential thermal analysis (DTA) (Anderson and Tice, 1971) and the differential scanning calorimetry (DSC) (Horigychi, 1985) which use a comparison between the temperature response of a frozen sample and an inert reference temperature sample when both systems are exposed to a uniformly changing temperature. The exotherm corresponding to the amount of latent heat yielded is proportional to the amount of ice formed. This method has two important limitations; first only one point on the moisture characteristic curve can be obtained, and secondly a true thermodynamic equilibrium is never established. The isothermal calorimetry method was developed to circumvent these problems. The method, which is limited to temperature above -10°C, tries to achieve equilibrium by maintaining a constant temperature and to control nucleation in order to get more than one point on the phase composition curve.

All the above methods require extensive equipment and complex analysis. Moreover, most of these studies have been carried out on clay soils which limits their applicability. Moreover, except for NMR, all methods are limited to laboratory measurements of unfrozen water content. Finally, very little consideration has been given to the influence of dissolved salts in the pore fluid on the measured unfrozen water content. These limitations are the reason why a more recent method which correlates the dielectric properties of a soil to its water content, the time-domain reflectometry method (TDR), was used.

3.1.3.2. Time-domain reflectometry

The time-domain reflectometry is a wide-frequency bandwidth technique used to evaluate the dielectric constant of a material. TDR was originally used as a tool to detect faults along electrical transmission lines. According to Davis and Annan (1977), the complex dielectric constant, K*, is expressed as;

$$K^{*} = K' + j\left(K'' + \frac{\sigma_{dc}}{\omega\,\varepsilon_o}\right) \tag{3.15}$$

where: K^*: complex dielectric constant
K': real part of dielectric constant
K'': dielectric losses
σ_{dc}: d.c. electrical conductivity
ω: angular frequency
ε_o: free-space permittivity

The second or imaginary term of the equation represents the dielectric and conductive losses in the measuring system. Over the frequency range used in TDR (10^6 to

10^9 Hz), the real part of the dielectric constant, K', is almost independent of frequency, and the dielectric losses are one to two orders of magnitude lower than K'. The technique measures what is called the "apparent" dielectric constant K_a, which is a combination of the real and imaginary parts.

Electromagnetic theory shows that in a non-magnetic low loss material, the propagation velocity is given by;

$$V = \frac{C}{(K_a)^{0.5}} \tag{3.16}$$

where: V: propagation velocity (m/sec)
C: free-space electromagnetic wave velocity = 3×10^8 m/sec

As stated by Patterson and Smith (1981), the TDR measures the propagation velocity and the reflection voltage of the transverse electromagnetic wave. The TDR unit provides a small pulse (step voltage) which travels unchanged along the transmission line until it comes in contact with a dielectric discontinuity (impedance mismatch) which causes a partial reflection and a partial transmission of the signal. The vertical axis in Figure 3.2 represent the reflection ratio which is defined as the ratio of the reflected voltage to the incident voltage. The travel time (tt) of the reflected wave along the transmission line can be evaluated from the signal trace, distance AB in Figure 3.2, and consequently the propagation velocity can be calculated knowing the length of the transmission lines (L) using;

$$V = \frac{L}{(tt)} \tag{3.17}$$

Combining equations 3.16 and 3.17, the apparent dielectric constant can be expressed as;

$$K_a = \left(\frac{C\,(tt)^2}{L}\right) \tag{3.18}$$

The concept of using the dielectric constant to evaluate the moisture content of soils arose from the fact that the dielectric constant of soil grains (K'_{soil} = 2 to 4) is much lower than the dielectric constant of free water ((K'_{water} = 80 at 20 °C). Moreover, it has been established (Davis and Annan, 1977), Hoekstra and Delaney, 1974) that the dielectric constant is weakly dependent on soil type, density, temperature or pore water salinity, but is strongly dependent on the liquid water content.

Topp et al. (1980) established a relationship between the apparent dielectric constant (K_a) and the volumetric water content (θ_v) of soils, which is defined as the ratio of the volume of water to the total volume of soil . They proved that except for very fine-grained or organic soils, this relationship holds over a wide range of soil types and textures and is independent of temperature and salinity. Smith and Tice (1988) explained that for high specific surface area materials (very fine-grained soils), the value of the apparent dielectric constant decreases because of the large amount of adsorbed water which has a dielectric constant lower than 80. The authors also observed that saline pore fluids increased signal attenuation since saline pore fluid has a higher electrical conductivity than a non-saline pore fluid.

Since ice and soil grains have similar dielectric constants (K_{ice} = 3.2 and K'_{soil} = 2 to 4), Patterson and Smith (1981) extended the use of TDR to the evaluation of the volumetric unfrozen water in frozen soils. These authors used a combined TDR-dilatometry method on ice-water mixtures and frozen soils to verify the validity of the equation proposed by Topp et al. (1980). Fairly good agreement was observed between the two techniques. The authors also showed good correlation between the TDR results and previously published unfrozen water content data using other measuring techniques. Smith and Tice (1988) observed that Patterson and Smith (1981) carried out their experimentation at temperature above -4°C. It was recognized by Patterson and Smith (1981) that the relationship proposed by Topp et al. (1980) could not predict unfrozen water content temperatures lower than -4°C because of the very low unfrozen water contents. In low moisture frozen soils, ice which has a dielectric constant of 3.2 is substituted for air which has a dielectric constant of 1. Moreover, a value of 80 for the dielectric constant of bulk water was used by Topp et al. (1980) which was shown to be wrong by Smith and Tice (1988) who measured a value of approximately 72. Smith and Tice (1988) recognized the need for a different calibration for frozen soils, and used a comparison between NMR and TDR to establish the following equation.

$$\theta_u = -1.458\mathrm{x}10^{-1} + 3.868\mathrm{x}10^{-2}K_a - 8.502\mathrm{x}10^{-4}K_a^2 + 9.92\mathrm{x}10^{-6}K_a^3 \qquad (3.19)$$

These authors established that the error using equation 3.19 is ± 0.03 cm^3cm^{-3}. They also showed that the equation could be used for a wide variety of soils. Van Loon et al. (1990 b) used the dispersion theory applied to parallel planes to validate theoretically the use of the dielectric constant or TDR to measure unfrozen water content. Their first attempt using a value for the dielectric constant of water of 88 was not in agreement with the prediction by Smith and Tice (1988). However by modifying the value of K_w to 65, they obtained a good agreement (r^2=0.984) with the Smith and Tice's prediction.

Patterson and Smith (1983 and 1985) extended the application of the TDR technique for unfrozen water content determination to saline frozen soils. They observed that the main difficulty with the method was an increase in signal losses for highly saline soils (salinity > 5 ppt) caused by the increase in pore water electrical conductivity. The high signal attenuation makes it difficult to determine the open circuit response from the TDR trace, and consequently the evaluation of the travel time becomes less accurate. A compromise between long transmission lines which increase the precision of the travel time and short transmission lines which improve the definition of the open circuit response had to be made to solve this problem. When using line length of 50 to 150 mm, Patterson and Smith (1983, 1985) obtained good agreement between the volumetric unfrozen water content measured using TDR and that measured using dilatometry.

Two transmission line configurations can be used: an unbalanced coaxial line or a balanced parallel transmission line. The coaxial configuration constrains the magnetic field to within the sample. However, this configuration is only applicable for laboratory testing. The parallel configuration is more versatile (laboratory and field) even if the extent of the magnetic field is unknown. The parallel configuration requires the use of a transformer called a "balun" to establish the connection between the coaxial line hooked to the TDR unit and the parallel lines within the sample. The choice of the "balun" should be made carefully in order to match as closely as possible the impedance of the coaxial line to that of the parallel line to avoid additional signal attenuation. Smith and Patterson (1979) give the following equation (from Chipman (1968)) to calculate the impedance, Z_o, of parallel transmission line:

$$Z_o = \frac{276}{K'} \log_{10}\left(\frac{S}{2a} + \sqrt{\left(\frac{S}{2a}\right)^2 - 1}\right) \qquad (3.20)$$

where: S: spacing between conductors
a: radius of the conductors

3.1.4. Electrical properties of saline frozen soils

Few papers have been published on the electrical conductivity of frozen saline soils. Some authors (Hayhoe and Balchin (1986)) have used electrical resistance measurement of freezing soils to monitor the advance of the freezing front. To understand the effect of the different soil constituents on the electrical conductivity of frozen soil, a brief review of the unfrozen saline soil electrical properties may be useful. The electrical conductivity of a saline unfrozen soil is the result of the combined effects of the electrical conductivity of the soil grains which depends on the surface chemistry of the particles, the electrical conductivity of the pore fluid which is a function of its salinity and the amount of air present for an unsaturated soil. Bottraud and Rhoades (1985) gave an equation for the electrical conductivity (σ_a) of the soil mass as a function of volumetric water content (θ) for a saturated soil;

$$\sigma_a = \sigma_s + T\,(\sigma_w\,\theta) \qquad (3.21)$$

where: σ_a, σ_s, σ_w: electrical conductivities of soil mass, mineral grains, water
θ : volumetric total water content
T : transmission coefficient (pore geometry factor)
$T = a\,\theta + b$ (a,b : fitting parameters)

This author believes that, following the same reasoning, Equation 3.21 could be modified to model the electrical conductivity of frozen soils, by using the total and unfrozen water contents. Equation 3.21 would then take the form:

$$\sigma_a = \sigma_s + T\left[\, \sigma_w\, \theta_u + \sigma_i\left(\theta - \theta_u\right)\right] \tag{3.22}$$

where σ_i : electrical conductivity of ice
θ_u: unfrozen water content

As stated before, the mineral phase electrical conductivity is primarily a function of the surface conductance and exchangeable cations with the mineral. The water conductivity is a direct measurement of the pore fluid salinity. Therefore an increase in salinity of the pore water, increases the conductivity of the fluid and consequently the electrical conductivity of the bulk soil. Equation 3.22 has never been verified experimentally, and is simply a suggested possible extension of Equation 3.21.

Van Loon et al. (1990 a) suggested a new method of measuring frozen soil electrical conductivity using TDR results which corrects for all impedance mismatches. The electrical conductivity is function of the ratio between the reflection ratio of the signal in air to the reflection ratio in the soil, and the dielectric constant of the soil. This method shows great promise for the determination of electrical conductivity in frozen soils, but is only in the first stages of development and verification.

3.2. MECHANICAL PROPERTIES OF ICE

To understand better the mechanical behaviour of ice a brief review of the crystal structure of ice is necessary. The following is from Weeks and Ackley (1982). In the ice structure, each oxygen atom is located at the centre of a tetrahedron with four other oxygen atoms located at each of the apices. This tetrahedral coordination of the oxygen atoms leads to a crystal structure having hexagonal symmetry. The oxygen atoms are concentrated in parallel planes referred to as basal planes. The direction perpendicular to these planes is called the c-axis. Rupture between two parallel planes requires that only two oxygen bonds be broken, as opposed to four bonds in any perpendicular directions to the basal plane, causing a much lower shear resistance in the direction parallel to the basal planes. Two hydrogen atoms are believed to be shared by four oxygen atoms. This distribution of the hydrogen atoms respects the Bernal-Fowler rules: 1) two hydrogen atoms are near each oxygen atom; and 2) only one hydrogen atom can be on the line connecting two oxygen atoms. Any breach of these rules will result in defects in the crystal structure. Hydrogen bonding between water molecules is the cause of the very open ice structure (lower density than liquid water).

3.2.1. Compressive strength of polycrystalline ice

Most of the evaluation of ice strength has been carried out using uniaxial compression tests since ice is considered to be a frictionless material (at low $\dot{\varepsilon}$) (Sego and Morgenstern, 1985), and consequently is not influenced by confining pressure, σ_3. However, as stated by Goughnour and Andersland (1968) an increase in σ_3 will cause an increase in the strength of ice at high strain rates, $\dot{\varepsilon}$, because the confinement will restrict the propagation of cracks. The stress-strain curve of polycrystalline ice displays two yield points when the strain rate is low (less than 10^{-4} s^{-1}) (Mellor and Cole, 1982, Mellor and Cole, 1983, and Mellor, 1979). Figure 3.3 shows a typical stress-strain curve for ice under ductile yielding. The first yield point at a strain, $\varepsilon = 0.3$ to 0.4 %, is associated with the onset of internal cracking, which allows the release of elastic strain energy from within the sample. In compression, the cracks usually form in the direction parallel to the major principal stress axis. Three types of failure, which depend on the test strain rate can develop in ice. At high strain rates, the failure is usually brittle and the accumulated strain before failure is mostly elastic; usually only the first yield point develops for strain rate larger than 10^{-4} s^{-1} (Mellor and Cole (1982)). The second type of failure is a combination of the brittle and ductile deformations, which take place for strain rates in the transition zone between brittle and ductile behaviours (approximately between 10^{-4} to 5.5×10^{-5} s^{-1}). For medium to low strain rate, the deformation is usually ductile, and the accumulated strain is mostly irrecoverable and the strain energy is dissipated within the sample. For ductile yielding in compression, it is widely accepted that the strain to failure, ε_f , is 1% independently of strain rate. This allows the time to failure to be evaluated as the ratio of strain at failure to strain rate. However as mentioned by Mellor and Cole (1983), ε_f is not completely invariant with respect to $\dot{\varepsilon}$, and the time to failure then depends on the ice strength, σ_{max}, which is a function of strain rate. The ratio $(\sigma / \dot{\varepsilon})_{max}$ should be used to characterize the peak of the stress-strain curve. The strength increases with an increase in strain rate in the ductile range up to the ductile-brittle transition after which the strength is more or less constant within this region (Mellor, 1979). Figure 3.4 illustrates this phenomenon. The ductile-brittle transition is a function of the stress level, strain rate and accumulated strain. A decrease in strength with an increase in strain rate beyond the brittle-ductile transition can be observed and is due to imperfections caused by the sample preparation or compliant loading system which are used. The ratio of the strength at the first yield point, σ_{1y} to the maximum (peak) strength, σ_{max} is also function of strain rate. Mellor and Cole (1983) state that for $\dot{\varepsilon}$ larger than 10^{-4} s^{-1}, $\sigma_{1y} / \sigma_{max} \approx 1$; for $\dot{\varepsilon}$ between 10^{-4} s^{-1} and 10^{-6} s^{-1}, $\sigma_{1y} / \sigma_{max} \approx 0.7$; for $\dot{\varepsilon} < 10^{-6}$ s^{-1}, $\sigma_{1y} / \sigma_{max} \geq 1$.

The residual strength of ice is also influenced by the failure mode. For ductile deformation where failure occurs by flow and internal cracking, the residual strength, σ_∞ , is less than the peak strength at which internal cracking propagation is initiated. For very low strain rate, where yielding is purely flow, $\sigma_\infty \approx \sigma_{max}$. Flow is defined according to Orth (1988) as the diffusive flux of matter through and around the surface of crystal grains.

At large strain rate , the strength of ice tends to be independent of temperature. However, in the ductile range, the strength of ice is a function of temperature, i.e. as temperature decreases the strength increases, following Mellor (1979) equation:

$$\sigma = \left[\frac{\dot{\varepsilon}}{A\ f(\theta)}\right]^{\frac{1}{n}} \tag{3.23}$$

Due to the ice crystal structure which was briefly explained in the introduction to this section, ice strength is anisotropic. Ice sheared in a direction parallel to the basal plane will glide and cleave more easily than ice sheared in the c-axis (perpendicular to basal plane) direction. Fabric anisotropy can also develop during straining as recrystallization of the ice crystal can occur after undergoing large strains. This softening effect reduces the load carrying capacity of the ice. Sego and Morgenstrern (1983) believed that there are no structural changes in the ice at strains less than about 1%.

Another important strength characteristic of the ice is its deformation modulus. At low temperature or high strain rate, the secant modulus is almost a constant giving a good approximation of the true Young's modulus, E. However, at warm temperature or low strain rate (ductile behaviour), the stress-strain curve is not linear, and the secant modulus underestimated the true Youngs's modulus. Mellor and Cole (1983) believed that the initial tangent modulus is almost equal to E, if the deformations are measured directly on the sample and the testing apparatus give good precision and resolution. Moreover, they believed that the real Young's modulus, E, is independent of temperature or strain rate.

Many authors have attempted to correlate uniaxial constant strain rate compression test results to creep tests results. These comparison will be discussed in the section on the time dependent (creep) behaviour.

3.2.2. Compressive strength of sea ice

Sea ice differs from pure polycrystalline ice due to the presence of salt ions in the water from which the ice forms. This leads to the development of brine pockets. The sea ice cover is formed by dendritic ice crystals joining together. The ice cover then thickens developing three zones (Weeks and Assur, 1967 and Schwarz and Weeks, 1977); 1) surface zone where the c-axes are vertical or randomly oriented, 2) the transition zone and 3) the columnar zone where the crystals c-axes are mostly horizontal and the ice mass is formed by the joining of ice platelets. The last zone is the most important, since horizontal c-axis crystals grow faster due to a higher thermal conductivity in the direction perpendicular to the c-axis (parallel to the basal plane). As sea ice forms, solutes are rejected and formed zones of high concentration brine, which may become entrapped within the growing ice. As stated by Schwarz and Weeks (1977), these brine channels, layers or pockets decrease the cross-sectional area of ice to ice bonding thus creating planes of weakness. Weeks and Ackley give a detailed explanation of the evolution of the salinity profile within the ice sheet as it matures. Different factors control the removal of salt from the ice with time; 1) initial amount of entrapped salt in the ice, 2) migration of liquid inclusions through the ice crystals, 3) brine expulsion (or squeezing) due to differential volume changes in the different phases making up the ice, 4) brine drainage which is the dominant mechanism, 5) flushing due to pressure head provided by surface meltwater.

Mellor (1983) explained that the mechanical behaviour of sea ice is governed by the same variables as for non-saline ice (i.e. temperature, strain rate, grain size and structure) with the addition of the influence of salinity, the geometry of pore structures and the variation of brine volume with temperature which all affect porosity. In saline ice, the influence of temperature is more important than in pure ice, since temperature controls the brine volume as well as the strength of pure ice. Nawar et al. (1983), Cox et al. (1985) noted that sample orientation also influence the strength of sea ice. They observe that the compressive strength of samples loaded in the direction of elongation (i.e. parallel to brine channels) is much higher than for samples loaded perpendicular to elongation axis (i.e. parallel to c-axis). These authors also mentioned that sea ice strength usually decreases as salinity increases, since an increase in salinity results directly in an increase in porosity which controls sea ice strength. However for sea ice of very low salinity, an increase of strength with an increase in salinity may be observed since the sample fails in a brittle manner.

Assur (1958) proposed a model explaining the strength of sea ice as a function of plane porosity which is controlled by brine and air porosity. His model was later improved and modified (Weeks and Assur, 1967, Assur and Weeks, 1964, Schwarz and Weeks, 1977, Weeks and Ackley, 1982). A brief description of the model with various improvements is presented. The strength of the sea ice is given by:

$$\frac{\sigma_f}{\sigma_o} = 1 - \psi \tag{3.24}$$

where: σ_f : failure strength for sea ice
σ_o : strength of imaginary material which fails like sea ice but contains no brine
ψ : plane porosity
$= \text{fct}\,(\upsilon_b + \upsilon_a)$
υ_b, υ_a : brine and air porosity

Assuming that $\upsilon_b >> \upsilon_a$, Equation 3.24 becomes

$$\frac{\sigma_f}{\sigma_o} = 1 - c\,\upsilon_b^{\,k} \tag{3.25}$$

The plane porosity has to be expressed as a function of brine porosity using a simplified model of the brine inclusion geometry. Such a model was given by Assur (1958) and is illustrated in Figure 3.5. Defining F_g as the average area of brine inclusion in the BG plane, Assur gives:

$$\upsilon_b = \frac{F_g}{a_o\, b_o\, g_o} \tag{3.26}$$

Defining,

$$\beta_o = \frac{a_o}{b_o} \quad \text{and} \quad \gamma = \frac{g}{g_o}$$

the reduction in cross-sectional area is given by;

$$\psi = \frac{2\, r_b\, g}{b_o\, g_o} = \frac{2\, r_b\, \gamma}{\beta_o\, a_o} \tag{3.27}$$

The variation of r_b and γ with υ_b can be described accordingly to three classes of assumptions:

1) -Geometric similarity is maintained along the B-axis
-r_g and γ remain constant
Then,

$$r_b \;\alpha\; \upsilon_b \text{ and consequently } \frac{\sigma_f}{\sigma_o} = 1 - c\,\upsilon_b \tag{3.28}$$

2) -Average length and spacing of brine pockets remain constant
-The change in υ_b is reflected in BC cross-section
Then,

$$\frac{\sigma_f}{\sigma_o} = 1 - c\,\upsilon_b^{0.5} \tag{3.29}$$

3) -Brine pockets remain of similar shape
Then,

$$\frac{\sigma_f}{\sigma_o} = 1 - c\,\upsilon_b^{2/3} \tag{3.30}$$

For all classes of assumption,

$$c = \upsilon_o^{-k} \qquad \text{where: } k = 1,\ 1/2,\ 2/3 \tag{3.31}$$

which gives with $\rho = 2\,r_b / F^{0.5}$ and $\alpha_o = a_o / F^{0.5}$,

$$\upsilon_o = 1 / \rho\, a_o \qquad \text{for } k=1 \tag{3.32a}$$

$$\upsilon_o = \beta_o / (\rho^2 \gamma) \qquad \text{for } k=1/2 \tag{3.32b}$$

$$\upsilon_o = (\beta_o / \rho^3 \gamma\, a_o)^{1/2} \qquad \text{for } k=2/3 \tag{3.32c}$$

Two major models have been used to date to analyze strength results; the constant width model and the elliptical cylinders model.

For the constant width model,

$$F = 4\, r_a r_b \quad \text{and} \quad \upsilon_o = 2\, r_a / a_o = d_o / a_o \tag{3.33}$$

where: d_o: minimum width of parallel brine layer before it splits to form individual brine pockets
≈ cst ≈ 7 x 10^{-3} cm

$$\sigma_f = \sigma_o \left(1 - \frac{\upsilon}{\upsilon_o}\right) \tag{3.34}$$

For the elliptical cylinders model,

$$\varepsilon = r_b / r_a \quad \text{and} \quad F = \pi\, r_b\, r_a = \pi\, r_b^2 / \varepsilon \tag{3.35}$$

$$\sigma_f = \sigma_o \left(1 - 2\sqrt{\frac{\varepsilon\gamma}{\pi\beta_o}}\,\sqrt{\upsilon_b}\right) \tag{3.36a}$$

For a cylinder with no interruption of the brine pocket, $\varepsilon = 1$ and $\gamma = 1$ then,

$$\sigma_f = \sigma_o \left(1 - \frac{2}{\sqrt{\pi}\,\beta_o} \sqrt{\upsilon_b} \right) \tag{3.36b}$$

Assur and Weeks (1964) gave equations predicting the plate width a_o, as a function of growth velocity, depth in ice sheet and temperature gradient. Cox and Weeks (1982) provided equations to predict the gas and brine volumes in sea ice based on mass, density, volume and salinity of each of the components (air, brine, ice, salt, solid salts). The value of σ_o can be determined by the value of fresh ice strength divided by a stress concentration factor due to brine pockets. At very cold temperatures, precipitation of solid salts can develop causing an increase in strength by salt bridging across brine pockets.

The deformation modulus of sea ice is also affected by the presence of brine pockets. As for pure ice, the stress-strain curve does not give an accurate evaluation of the true Young's modulus. The best estimation of the Young's modulus is by using the initial tangent modulus. As stated before, the true Young's modulus is not strongly affected by temperature but is very much a function of porosity in sea ice. In the case of sea ice, the porosity which depends on air content (not a function of temperature) and brine content (function of temperature) is controlled by temperature (Mellor (1983)). Therefore, the true Young's modulus, **E**, decreases as the porosity increases or the temperature increases. Schwarz and Weeks (1977) recommended the use of dynamic methods to measure the elastic modulus in order to get more consistent results than are achieved by using static measurements. Schwarz and Weeks (1977) established, from static measurements, that **E** is inversely proportional to υ_b. Weeks and Acley (1982) assumed that air porosity is negligible, that brine cylinders are continous and that the brine porosity is equal to relative cross-sectional area of brine, to find a relation between E, the elastic modulus and υ_b;

$$\mathbf{E} = \mathbf{E_1} + (1 / K - \mathbf{E_1})\, \upsilon_b \tag{3.37}$$

where: $\mathbf{E_1}$: bulk modulus of pure ice
$K = \varepsilon / p$
ε : strain, p: pressure in brine pockets

Ice behaviour is an important component in the understanding of frozen soil behaviour since ice is the major component of the pore fluid in the soil. Moreover, the influence of salt on the development of brine channels in sea ice is similar to the influence of salt in the pore fluid of saline frozen soils. The reduction of strength as a function of brine volume is a most important concept in the understanding of the strength of frozen saline soils.

3.2.3. Creep behaviour of polycrystalline ice

Creep deformations are defined as the deformation response with time of a material under constant stress, without any volume change. The evolution of strain and strain rate with time provide an understanding of the material response to the applied stress. The process of creep in ice is believed to be a combination of grain-boundary migration (sliding), crack formation, dislocation glide and recrystallisation. It is generally accepted that the response of ice to constant stress follows four stages:

1) Instantaneous elastic strain, usually called ε_0
2) Primary creep stage with a deceleratng strain rate
3) Secondary creep stage
4) Tertiary creep stage whit accelerating strain rate up to failure

Some authors (Glen, 1955, Ladanyi, 1972) believed that the strain rate during secondary creep is constant. However, more recently, most authors, as stated in the review by Mellor (1979), believe that the secondary creep stage is only an inflection point where the transition between decelerating and accelerating strain rate takes place, i.e. a point where the strain rate is minimum. Figure 3.6 shows the two approaches. The primary creep stage is believed to be a period where the strain hardening effect dominates (Mellor and Cole, 1982, Goughnour and Andersland, 1968). It is believed that the deceleration is an effect of delayed elasticity with a recoverable component of time dependent elastic strain. During primary creep, there is a point where deceleration is maximum, i.e. $\ddot{\varepsilon}$ is minimum. At this point the strain softening of the ice starts to prevail leading eventually to failure. As for uniaxial strength, it is generally accepted that creep failure in ice takes place at a strain of approximately 1%, for ice loaded in the ductile strain rate region.

A large number of models have been developed to predict the creep behaviour of ice, some based on primary creep, others based on secondary creep, others trying to combine both stages.

Azizi (1989) used the creep law proposed by Hult (1966) for metals to predict the primary creep of polycrystalline ice in unconfined uniaxial compression. He states that the secondary creep is reduced to an inflection point. The creep strain is predicted by;

$$\varepsilon_c = K\,\sigma^a\,t^b \tag{3.38}$$

By differentiating Equation 3.38, the strain rate can be obtained;

$$\frac{d\,\varepsilon_c}{d\,t} = \dot{\varepsilon}_c = b\,K\,\sigma^a\,t^{b-1} \tag{3.39}$$

The Andrade equation (1910) has been widely used to predict primary and secondary strain in ice.

$$\varepsilon = \varepsilon_0 - \beta\,t^{1/3} - \kappa\,t \qquad \text{for } \left|\beta t^{1/3}\right| << 1 \tag{3.40}$$

Ting and Martin (1979), as well as Sego and Morgenstern (1983), studied the applicability of the Andrade equation to predict secondary strain rate from short term tests. By differentiating Equation 3.40, the strain rate is given by;

$$\dot{\varepsilon} = \frac{d\,\varepsilon}{d\,t} = -\kappa - \frac{1}{3}\,\beta\,t^{-2/3} \tag{3.41}$$

These authors observed that for short term tests, the Andrade equation could not predict the correct value of κ and that in general the calculated κ values were less than the measured secondary strain rate and κ was usually not a constant. They concluded that the Andrade equation could be used to predict transient (primary) creep only.

Gardener et al. (1984) proposed an onset of tertiary creep model similar to the ones proposed by Fish (1982), Assur (1980), Ting (1983). The creep rate is a function of time, and the creep strain predicted gives an excellent fit to experimental data up to the inflection point. The creep strain at a given time is predicted by;

$$\frac{\varepsilon_c}{\varepsilon_m - \varepsilon_o} = \left(\frac{t}{t_m}\right)^c \exp\left[\left(c^{1/2} - c\right)\left(\frac{t}{t_m} - 1\right)\right] \tag{3.42}$$

where: $\varepsilon_c, \varepsilon_m, \varepsilon_o$: creep,minimum,initial strain
t, t_m: time,time to minimum strain rate
c: dimensionless parameter describing shape of the curve

By differentiating Equation 3.42, an expression for c can be derived as a function of the minimum strain rate, $\dot{\varepsilon}_m$;

$$c = \left(\frac{\dot{\varepsilon}_m t_m}{\varepsilon_m - \varepsilon_o}\right)^2 \tag{3.43}$$

This equation respects that the strain second derivative with respect to time equals zero at t_m; the slope of the strain rate vs time curve is zero at the inflection point

The most well known flow law to predict constant secondary strain rate is Glen's (1955) flow law which was used by many authors (Sego and Morgenstern (1983), Morgenstern et al.(1980)) to predict secondary creep rate

$$\dot{\varepsilon} = B\,\sigma^n \tag{3.44}$$

Glen stated that B was a function of temperature and ice type and that n could be function of stress level, but that a value of n=3 could be used for stresses in the range 60 to 1500 kPa. Sego (1980) proved that this assumption was valid for ice at temperature higher than -1°C. Mellor (1979) used Equation 3.44 to predict minimum strain rate using different values of n for different stress levels.

Nixon and McRoberts (1976) used a bilinear flow law to show the dependence of n to stress level;

$$\dot{\varepsilon}_e = B_1\,\sigma_e^{n_1} + B_2\,\sigma_e^{n_2} \tag{3.45}$$

where: $\dot{\varepsilon}_e, \sigma_e$: effective shear strain rate, shear stress

McRoberts (1978, 1988) proposed to use a different flow law developed by Glen (1975) to model the dependency of secondary strain rate to temperature. He stated that using n=3 was valid for ice at low stresses but that a value of n=6 should be used at high stresses (>400 kPa) in conjunction with the bilinear flow law.

$$\dot{\varepsilon} = \frac{A\,\sigma_d{}^n}{(1 - T)^m} \tag{3.46}$$

where: σ_d : deviatoric stress
T : temperature (°C)
A, n, m: constants

Creep is largely affected by temperature, since it is considered to be a thermally activated process (Mellor, 1979). Following this idea, Fish (1983) developed a thermodynamic creep model. He defined creep strain rate as a function of temperature, activation energy and change in entropy, and assumed that the creep process is isothermal and that volumetric and instantaneous strains are small. His equation is an expansion of the basic Arrhenius equation which describes thermally activated processes;

$$\dot{\varepsilon} = A \exp\left(\frac{-Q}{RT}\right) \tag{3.47a}$$

where: A: constant
Q: activation energy
R: gas constant
T: temperature

Mellor (1979) showed that at temperature warmer than -10°C the relationship between ln $\dot{\varepsilon}$ and 1/T is not linear proving that Q is not a constant as assumed in the Arrhenius' equation. The Arrhenius equation is based on properties which appear at temperature much larger than 273K where ice does not exist. However, Barnes et al. (1971) showed that the Arrhenius equation proposed by Glen (1955) was not valid for temperature warmer than -2.8°C, but that it could be used to model the influence of temperature on the flow law if the value of the activation energy, Q, is changed for certain temperature ranges.

$$\dot{\varepsilon} = A\sigma^n \exp\left(\frac{-Q}{RT}\right) \tag{3.47b}$$

They recommended to use Q=120 kJ/mol for temperature between -2.8°C and -8°C, and a value of Q = 78 kJ/mol for temperatures colder than -8°C. For temperatures close to

0°C, they suggested to use a relationship of the form proposed by Voytkovskiy, i.e. $\dot{\varepsilon} \alpha$ 1/ 1+T.

Sego and Morgenstern (1983) introduced the concept of grain size ratio, GSR = D_d / D_s (D_d:average crystal size, D_s: average sample size), which accounts for variations in the size of sample to the ice being tested.

As mentioned in Section 3.2.1., many authors have tried to correlate results from constant strain rate tests with results from creep tests (constant stress). The strain to failure is believed to be the same for both type of tests under ductile yielding, i.e. ε_f = 1 %. Failure in CSR tests is defined as the peak stress value, and in creep test as the point of minimum strain rate. In both cases, failure should be characterized by a maximum value of the ($\sigma / \dot{\varepsilon}$) ratio (Mellor, 1979). Mellor and Cole (1982) established that for different stress levels, the slope of the $\log\dot{\varepsilon}_m$ vs $\log t_m$ is -1. Assuming that the deceleration in primary creep is due to delayed elasticity, these authors state that the irrecoverable creep strain can be considered constant and is equal to $\dot{\varepsilon}_m t_m$. It is believed (Mellor and Cole, 1982, 1983) that from creep curves a stress-strain curve could be built or vice versa, as long as the different stress paths do not affect the structure and texture of the ice. To study this effect of stress path, Cole (1983) used a comparison between normal creep tests and two-mode creep tests: up to failure, i.e. maximum stress, a constant deformation rate test was applied to the sample, and after failure a constant load test was performed. He observed that both types of tests gave good agreement for the behaviour in the tertiary stage indicating that material behaviour is practically independent of the stress path used during this study. This conclusion was quite surprising to the author, since in a normal creep test prior to the inflection point, the sample experiences a strain rate higher than the minimum strain rate. This should cause more structural damage to the sample as compared to a sample under two-mode testing. However, in this study, the stress and strain rate range used produce mostly ductile yielding even though some brittle internal cracking took place, which did not significantly affect the sample behaviour. The author believed that the major deformation mechanism for ductile yielding is dislocation glide with some cracking.

Mellor and Cole (1983) compared times to failure from both type of tests. They found a reasonable agreement between the two sets of results. They also proved by plotting $\log\dot{\varepsilon}$ vs $\log\sigma$ for a constant time, that using a simple linear power law (Newtonian viscosity) to correlate strain rate and stress was unrealistic. Cole (1983) studied the effect of stress application rate on creep behaviour of ice. He observed that the primary creep strain rate was most affected by an increase in the loading rate, because of the increased micro-fracturing activity due to high loading rate.

3.2.4. Creep behaviour of saline and sea ice

Few studies of the creep behaviour of sea ice are available in the literature. It is even more difficult to find information about to behaviour of non-marine saline ice. Mellor (1983) established that at low stresses (< 1 Mpa) the creep deformation of sea ice is ductile with no micro-cracking. For the high stress range, the deformation is also ductile but some micro-cracks form. He observed, that similar to polycrystalline ice, the yield point is almost always at $\varepsilon = 1\%$, and that the minimum strain rate should correspond to the peak strength in a CSR tests. Cox et al. (1985) extended Mellor's (1983) work to multi-year sea ice; he observed that the minimum strain rate increases with an increase in stress level, and an increase in temperature. However $\dot{\varepsilon}_m$ decreases with and increase in strain to failure and time to failure.

The only reference on non-marine saline ice that the author could find was a study by Pharr and Godavarti (1987) who compared laboratory prepared saline ice to frozen saline sand. The authors insisted on the fact that the structure of laboratory saline ice is very different from sea ice which is columnar ice with vertical brine channels. They observed that ice creeps plastically up to a strain of 25% without reaching failure. The saline ice deformed uniformly with very little barreling and no signs of cracking. Significant brine drainage took place causing a decrease in overall salinity. The laboratory saline ice was weaker than natural sea ice because sea ice has a much lower salinity and a different structure. The presence of brine significantly increases the creep rate.

3.3. MECHANICAL PROPERTIES OF NON-SALINE FROZEN SOILS

3.3.1. Compressive strength of non-saline frozen soils

The strength of frozen soils is a combination of ice strength in the pores and soil matrix strength depending on the concentration of soil in the ice. Goughnour et al. (1968) stated that at low sand concentration the frozen soil behaviour is very similar to that of polycrystalline ice and as the sand concentration increases friction, dilatancy and sand-ice cohesion start to control the frozen soil behaviour. The strength of frozen soils is governed by the soil type, grain size distribution, density, moisture content, temperature, confining pressure, strain rate, and unfrozen water content which is a combination of some of these parameters. As for unfrozen soils, the soil type and grain size distribution are important with respect to the nature of the strength (cohesive or frictional strength) and the amount of unfrozen water (fine-grained soils having much higher unfrozen water content than coarse-grained soils). The effect of moisture content on strength has been studied by Shusherina et al. (1969). For silts and sands, they found that an increase in moisture content caused an increase in strength up to complete saturation after which the strength started decreasing with a further increase in moisture content. This can be explained by the fact that as moisture content increases past saturation, the strengthening effect of the soil skeleton on ice decreases because of the decrease in density and the increase in unfrozen water. For clays, the same increase was observed but after full saturation, the strength remained constant. The effect of moisture content on strength is influenced by temperature, composition and level of saturation. For fully saturated samples, a further increase in water content lead to a behaviour similar to ice. When the strength of the soil is lower than the strength of ice under identical conditions, it suggests that the strengthening effect of the soil skeleton is overturned by the weakening effect of unfrozen water.

As stated earlier, the strength of frozen soil is a result of ice strength (cohesion), friction and cohesion of the soil particles as well as soil-ice bonding. It is generally accepted (Andersland and AlNouri, 1970) that the cohesion is time, stain rate and temperature dependent as opposed to friction which is usually constant. Roggensack and Morgenstren (1978) established that for ice-poor materials the friction angle in the thawed state, ϕ_{thawed}, is practically equal to the friction angle in the frozen state, ϕ_{frozen}. In ice-rich soils, ϕ_{thawed} is usually larger than ϕ_{frozen} since the ice hinders the full mobilization of the friction in the soil. Goughnour and Andersland (1968) suggested an explanation for the effect of increasing sand content on the mobilization of strength. They observed a drastic change in behaviour as the sand volume content surpassed 42%. For concentration lower than 42%, the frozen soil strength can be predicted by the ice strength multiplied by a constant stress factor which is function of the sand volume for a given temperature and strain rate. For sand concentration higher than 42%, the stress concentration factor is also a function of strain. They introduced three mechanisms of strengthening of sand-ice samples versus pure ice; 1) since the sand particles are almost undeformable under the considered stresses, a larger deformation rate is imposed on the ice matrix, causing an increase in ice strength; 2) friction of the sand particles at their contact points provides some additional resistance which is function of the degree of dispersion and the normal stress; 3) dilatancy is impeded during deformation by the ice matrix causing an effect similar to an increase in effective normal stress.

Ladanyi and Morel (1988) described an effect similar to this which they called internal confinement. They observed that the strength of a frozen sand could not be predicted by adding the strength of the ice and the strength of the same sand in the unfrozen state. They concluded that the tensile strength of ice causes a dilatancy hardening, which makes a frozen sand under unconfined compression behave like it is under confinement. This strengthening effect continues as long as the volume increases or the limiting cohesion of the ice (tensile strength) is exceeded. Ting et al. (1983) presented another study of the mechanisms of strength in frozen sands. He believed that strength has three components; firstly the ice strength, secondly the soil strength and thirdly the interaction of the ice and soil. As discussed in Section 3.2.1. , the ice strength is a function of temperature, strain rate and grain size. The soil provides the frictional and cohesive component of the resistance. The ice-soil interaction causes three strengthening effects; the ice strengthened by the presence of the soil particles, the soil is strengthened by the presence of the ice and the tension in the unfrozen water film increases the effective normal stress. As for the previous two authors, Ting et al. (1983) explained the interaction between ice and soil the hindrance of dilatancy. An increase in density results in an increase in the strength because of a larger number of grain contacts and enhanced dilatancy during shear. It should be kept in mind, that dilatancy effects are not present during the deformation of fine-grained soils.

The unconfined compressive strength is a function of strain rate and temperature. Other parameters such as density, degree of saturation also affect the strength. Many authors have investigated the effects of strain rate and temperature on frozen soil strength. Ersoy and Torgrol (1978) noted that the effect of strain rate is less significant than the effect of temperature on the measured strength. As the strain rate increases and the temperature decreases, the deformation behaviour of the frozen soil goes from ductile to brittle. The strain rate at which this transition takes place is a function of the soil type. Shibata et al. (1985) suggested that the increase in strength due to a decrease in temperature is due to an increase in ice strength since the slope of soil strength versus temperature and ice strength versus temperature are practically equal. The stress-strain curve of a frozen soil is characterized by an initial yield point which represents the initial fracturing of the pore ice at a strain of approximately 1% (Zhu and Carbee, 1987, Sayles, 1973) followed by a second peak at failure. In the case of sands, Sayles noted that the second peak represents the maximum development of friction between sand particles and/or between sand and ice. Parameswaran (1980) stated that at high strain rate and low temperature there is a small drop in stress after the initial yield because a lower stress in needed to maintain a nominal strain rate. For low strain rates, the development of the frictional component is progressive and there is no drop in stress after the initial yield. Roggensack and Morgenstern (1978) observed that in direct shear the frictional component of the strength decreases with an increase in shear rate, since for high deformation rate most of the strength is provided by ice cohesion. Baker (1979) suggested that in the range of strain rate between 10^{-7} $\sec^{-1}$ and 10^{-2} $\sec^{-1}$, a linear relationship exits between log of strength and log of strain rate of the form;

$$\sigma_{max} = A\,\dot{\varepsilon}^{b} \tag{3.48}$$

Parameswaran (1980) presented a relationship similar to Equation 3.48. Baker (1979) also observed that the strain to failure is a function of the time to failure or strain rate.

$$\varepsilon_f = C\,t_f^{d} \tag{3.49}$$

where: C, d: constants

Zhu and Carbee (1987) also mentioned that the strain to failure is relatively insensitive to temperature changes.

Fish (1984, 1985) presented an equation to predict the maximum strength as a function of strain rate and temperature. The temperature dependency is analyzed using the activation energy concept, i.e. rate process theory. The strength, σ_{max}, is given by:

$$\sigma_{max} = \sigma_o \left(\frac{\dot{\varepsilon}\,t_o}{\varepsilon_m}\right)^{1/m} \quad \text{and} \quad t_o = \frac{h}{\kappa T} \exp\left(\frac{E}{RT}\right) \tag{3.50 a,b}$$

where: σ_o: instantaneous strength ($\dot{\varepsilon}_o = 6\text{x}10^{-2}\text{s}^{-1}$)
ε_m: strain to failure
$\dot{\varepsilon}$: strain rate in s^{-1}
m: strain hardening parameter
h, κ: Planck, Boltzmann constants
T: temperature (K)
E: activation energy in kcal/mol
R: gas constant

The strain hardening parameter, m, reflects the number of micro defects that can be accumulated in a unit volume of material before failure develops. Fish expressed the variation of activation energy as a function of the variation of the unfrozen water content. Parameswaran (1980) stated that the temperature dependency of strength can not be explained by a thermally activated theory of deformation because of the variation of the activation energy with temperature and deformation mechanisms but that a simple power law as proposed by Tsytovich (1975) is acceptable. This idea is supported by Zhu and Carbee (1987) who used Sayles (1974) equation for compressive strength;

$$\sigma_m = A\left(\frac{\theta}{\theta_o}\right)^m \quad \text{and} \quad A = \frac{\alpha A_o}{\alpha + A_o\left(\ln \dot{\varepsilon}_o/\dot{\varepsilon}\right)} \tag{3.51 a,b}$$

where: A: parameter with units of stress
A_o: A at $\dot{\varepsilon}_o = 1.1\times10^{-3}\ s^{-1}$
θ: temperature in °C
θ_o: reference temperature = -1°C
m: temperature dependence exponent
$1/\alpha$: slope of $\ln \dot{\varepsilon}$ vs $1/A$

The influence of the confining pressure on the compressive strength of frozen soils is studied by triaxial testing. Baker et al. (1981) observed that, for frozen sands, in the low range ($\sigma_3 < 0.35$ MPa), the confinement has little effect on the peak strength. For σ_3 between 0.35 and 40 MPa, the peak strength and the yield strength increases as the confining pressure increases, due to closure of microcracks and voids, and a larger resistance to dilatancy (increase of friction with confinement). However, a further increase of σ_3, decreases the strength due to pressure melting causing an increase in unfrozen water content. However, confining pressures larger than 40 MPa are unrealistically high for geotechnical purposes. Goughnour and Andersland (1968) studied the behaviour of sand-ice systems and concluded that at high strain rate, an increase of σ_3 causes an increase in strength, but that at low strain rate, the opposite effect takes place. In the case of purely cohesive materials, the confinement has no influence on the development of strength because of the absence of dilatancy (Gregersen et al., 1983).

Lade et al. (1980) examined the effect of σ_3 on the failure criterion for frozen soils, on the strain to failure and the volumetric change. At low to medium confining stresses, the failure envelope is convex as opposed to concave at high σ_3. In the convex region, an increase of strain rate will cause an increase in strength. In general, the strain to failure will increase as the confining stress increases. The volume of the sample will decrease more significantly during deformation as the confining pressure increases.

The deformation moduli are also influenced by the same parameters, i.e. strain rate, temperature and σ_3. There is some confusion in the literature on the effect of decreasing temperature on the moduli. Goughnour and Andersland (1968) observed a decrease in the elastic Young's modulus measured from the elastic recoverable strain as the temperature decreases. However Parameswaran (1980), Shibata (1985) and Zhu and Carbee (1987) obtained the opposite result. The initial tangent modulus, E_i, measured by Parameswaran in sand increased with a decrease in temperature and an increase in strain rate. The same relationship between E_i and temperature was uncovered by Zhu and Carbee for silts. However, these authors state that the increase in E_i with an increase in strain rate is so small, that it can be considered insignificant, as was also mentionned by Lade et al. (1980). Shibata (1985) measured three different moduli, the Young's modulus, E, the shear modulus, G, and the bulk modulus, K, and observed that they all increase with a drop in temperature. Moreover, these three moduli are all linear functions of the maximum strength. The Poisson's ratio increases with an increase in temperature, which is similar to ice . Finally, Lade et al. (1980) pointed out that the secant modulus increases with an increase in confining pressure, σ_3.

3.3.2. Creep of non-saline frozen soils

As defined for ice, creep is the deformation response without volume change of a material to constant stress with time. It is believed that in frozen soils, the creep phenomenon is related to the presence of pore ice. Weaver and Morgenstern (1981) pointed out that in general the creep deformation of frozen soil is less than for ice but that in the case of very low solid content, the creep of ice could be less than the creep of the ice with soil, because the size of the ice crystals is reduced in the soil-ice mixture causing a decrease in ice strength which can not be compensated by the soil strength. Ting et al. (1983), Sayles (1988) mentioned that the long-term creep strength is provided by the friction and cohesion of the soil which are invariant with time, and that the ice matrix provides short-term resistance to rapidly applied loads. This ice cohesion is the contribution of strength which decreases with time.

Vyalov and Tsytovich (1955) explained that creep deformations in frozen soils are caused by pressure melting of the ice at point of stress concentration, i.e. grain contacts, followed by migration of the resulting melt water to a point of lower stress where the water refreezes. This has two effects on the structural arrangement of the frozen soil; a strengthening effect and a weakening effect. The strengthening effect is the result of a denser particle packing and the weakening effect is caused by a decrease in structural cohesion of the ice and possibly an increase in unfrozen water which surrounds the soil particles. As defined by Vyalov (1963), if the strengthening effect exceeds the weakening effect, then the creep behaviour is "damped" or attenuating, i.e. the strain rate decelerates continuously and rupture is never reached. This situation occurs when the stress level is lower than the long-term strength of the frozen soil. If the applied stress surpasses that critical stress, then accelerating creep develops and the sample eventually fails. Shields et al. (1985) observed that the volumetric strain is an indication of the type of creep. For attenuating creep, the volume of the sample decreases as opposed to an increase in volume for non-attenuating creep. Dilatancy can consequently be used as an indication of the start of failure. It is generally accepted that, except for ice-rich soils, the secondary creep stage is limited to a point of minimum strain rate. However, as mentioned for the creep of ice, some authors still use the steady state secondary creep approach because of its simplicity (Ladanyi, 1972). Orth (1988, 1985) stated that there are two mechanisms which explain the deformation of ice; the dislocation glide limited to discrete obstacles which is a thermally activated process and diffusional flow which is only a valid explanation at very low stresses. This is the reason why a number of authors have expressed the temperature dependence of creep mathematically using the rate process theory (thermal activation).

The creep behaviour of frozen soil is influenced by a number of the same parameters as its strength, i.e. temperature, confining stress, density and also by the applied stress level. The minimum strain rate or secondary strain rate (in the case of steady-state secondary creep) increases with an increase in stress level or temperature and a decrease in confining pressure. However, if σ_3 exceeds a certain critical level where pressure melting starts, then the strain rate increases with an increase in σ_3. At high axial stress level, the strain rate is considered independent of density but at low to medium stresses the strain rate decreases as the density increases.

The time to failure, t_m, (or the time to secondary creep) will increase with a decrease in applied stress or in temperature. The time to failure will also increase with an increase in density, especially in the low to medium stress range. It is generally accepted that the strain to failure for a given soil is more or less independent of the minimum strain rate or temperature. However, contrary to many authors, Rein and Hathi (1978) showed that the strain to failure decreases with an increase in applied stress. These authors insist on the fact that this variation should be included in all time dependent deformation models.

A wide number of creep models have been developed during the last thirty years; some are based on primary creep, some on steady-state secondary creep and others on tertiary creep.

One of the most famous creep theories is the primary creep theory proposed by Vyalov (1963) based on the hereditary creep theory. He established a rheological model to define the total creep strain given by:

$$\varepsilon = \varepsilon_o + \varepsilon_1(t) + \varepsilon_2(t) + \varepsilon_3(t) \qquad (3.52)$$

where: ε_o: instantaneous elastic strain represented by a spring
ε_1: visco-elastic strain represented by a spring in parallel with a dashpot
ε_2: visco-plastic strain represented by

a braking element in series with
a dashpot
ε_3: failure strain

Vyalov (1963) gave the following equation for creep strain, assuming a small initial elastic strain;

$$\varepsilon_c = \left[\frac{\sigma t^{\lambda}}{\omega\left(\frac{\theta}{\theta_o} + 1\right)^{k}} \right]^{1/m} \qquad (3.53)$$

This equation express the stress and temperature dependency of the creep strain. Vyalov also extended his equation to complex stress states. Sayles (1988) stated that this equation slightly underpredicts the measured strains, but that it gives the best available prediction for primary creep strain. Vyalov (1988, a) developed an other approach to strain prediction using the hardening theory (accumulated strain) which he believes is the most effective in predicting stress-strain behaviour of frozen soils. The strain rate is given by:

$$\dot{\varepsilon} = \frac{\alpha\, a^{1/\alpha}}{\varepsilon^{1/\alpha - 1}} \left[1 + \left(\frac{\varepsilon}{a}\right)^{1/\alpha} \frac{1}{t_f} \right]^2 \qquad (3.54)$$

where: α, a: deformation parameters
t_f : strengthening parameter, time to failure

For a constant stress, α, a and t_f are constant, and the strain and strain rate are given by;

$$\frac{\varepsilon}{a} = \left(\frac{t}{1 - t/t_f}\right)^{\alpha} \quad \text{and} \quad \dot{\varepsilon} t^2 = \frac{\alpha}{a^{1/\alpha}} \varepsilon^{1 + 1/\alpha} \qquad (3.55\text{ a, b})$$

Sayles (1968, 1973, 1974) also developed a strain equation based on primary creep strain;

$$\dot{\varepsilon} = \dot{\varepsilon}_R \left(\frac{t_R}{t}\right)^{1/M} \qquad (3.56\text{ a})$$

and by integrating for M≠1,

$$\varepsilon - \varepsilon_R = \dot{\varepsilon}_R t_R{}^{1/M} \left(\frac{M}{M-1}\right) \left(t^{(M-1)/M} - t_R^{(M-1)/M}\right) \qquad (3.56\text{ b})$$

where: ε_R, $\dot{\varepsilon}_R$: reference strain, strain rate
t_R: reference time

$$M = \text{fct}\,(\theta, \sigma) = c\,\sigma^{1/w}$$

If t_R is taken as 1 hour and ε_R, $\dot{\varepsilon}_R$ are taken as the strain and strain rate after 1 hour, Equation 3.56 becomes;

$$\dot{\varepsilon} = \dot{\varepsilon}_1\, t^{-1/M} \quad \text{and} \quad \varepsilon = \varepsilon_1 + \dot{\varepsilon}_1\left(\frac{M}{M-1}\right) t^{(M-1)/M} \tag{3.57 a, b}$$

$\dot{\varepsilon}_1$ can be determined graphically or be using the following equation;

$$\dot{\varepsilon}_1 = \left(\frac{\sigma}{\sigma_1}\right)^{1/k} \quad \text{and} \quad \sigma_1 = \sigma_{01}\left(\theta + 1\right)^{\alpha} \tag{3.58 a,b}$$

where: σ_1: stress at $\dot{\varepsilon}_1 = 1$
σ_{01}: σ_1 at $\theta = 0°C$

Defining $\psi = M\text{-}1/\,M$, the strain equation is given by;

$$\varepsilon = \dot{\varepsilon}_1 \frac{t^{\psi}}{\psi} + \varepsilon_o = \left(\frac{\sigma}{\sigma_{o1}\left(\theta + 1\right)^{\alpha}}\right)^{1/k} \frac{t^{\psi}}{\psi} + \varepsilon_o \tag{3.59}$$

Since M is taken as a function of stress, Sayles' equation is similar to Azizi (1989) equation (Equation 3.38) where creep strain is a power function of stress and time.

As presented in Section 3.2.3, Gardener et al. (1984) proposed a new creep equation for tertiary creep strains which is an improvement on Fish (1982) equation (see Equations 3.74 and 3.75). According to Sayles (1988), this new equation by Gardener gives a good prediction for time greater than 70% of the time to failure. The creep strain is given by Equation 3.42 which is repeated here;

$$\frac{\varepsilon_c}{\varepsilon_m - \varepsilon_o} = \left(\frac{t}{t_m}\right)^{c} \exp\left[\left(c^{1/2} - c\right)\left(\frac{t}{t_m} - 1\right)\right] \tag{3.42}$$

where: ε_m, t_m: strain, time to inflection point
c: parameter describing shape of curve

$$c = \left(\frac{\dot{\varepsilon}_m\, t_m}{\varepsilon_m - \varepsilon_o}\right)^{2} \tag{3.43}$$

Gardener et al. (1984) suggested that for a given soil over a limited stress range c could be taken as a constant. Therefore, the time to failure can be expressed as;

$$t_m \;\alpha\; \frac{\varepsilon_m - \varepsilon_o}{\varepsilon_m} \tag{3.60}$$

If the value of creep strain to failure, $\varepsilon_m - \varepsilon_o$, is assumed to be constant, and a power law is used to relate the minimum strain rate and the stress ($\dot{\varepsilon}_m = B\,\sigma^n$), then the time to failure is given by the following equation according to Gardener et al.;

$$t_m = K / \sigma^n \qquad \text{and} \qquad K = (\varepsilon_m - \varepsilon_o) / B \qquad (3.61\ \text{a,b})$$

where: K: constant

Fish (1983, 1985) developed a creep equation to predict the strain rate in the primary creep stage using on rate process theory. This equation is simply the same equation as Equation 3.50 written to express strain rate as a function of stress activation energy and change in entropy. Sayles (1988) observed that this approach is valid for stress level much larger than the ultimate long-term strength of the soil, and that at $\sigma \approx \sigma_{ult}$, the prediction by Fish is very poor.

The conclusion reached by Ting and Martin (1979) that the Andrade equation is valid only to predict primary creep in ice is also valid for frozen soil. Consequently, Equation 3.40 could be used to predict primary creep if the last term is neglected.

Orth (1988, 1985) studied the micromechanical processes occurring in crystalline bodies under stress to establish an equation for the minimum strain rate as a function of stress and temperature;

$$\dot{\varepsilon}_m(\sigma, T) = \dot{\varepsilon}_\alpha \exp\left[\left(\frac{k_1}{T} + \ln \dot{\varepsilon}_\alpha\right)\left(\frac{\sigma}{\sigma_\alpha(T)} - 1\right)\right] \qquad (3.62)$$

where: T: temperature in K
$\dot{\varepsilon}_\alpha$: reference $\dot{\varepsilon}$ $\dot{\varepsilon}_\alpha = 1\%\ \text{min}^{-1}$
$\sigma_\alpha(T)$: stress under which $\dot{\varepsilon}_m = \dot{\varepsilon}_\alpha$ at T
K_1: characteristic temperature
K_1 = constant for T<268.4 K

Orth also found that the time to failure could easily be calculated using;

$$\dot{\varepsilon}_m t_m = c \quad \text{or} \quad t_m = c / \dot{\varepsilon}_m \qquad (3.63)$$

where: c: constant

Finally, this author mentioned that triaxial stresses can be ignored for practical purposes, since grain friction develops only at large strains ($\varepsilon > 10\%$) which is a unacceptable level of deformation in practice.

As stated before, some creep theories based on secondary creep are still present in the literature and could be applied to ice-rich frozen soils. Andersland and AlNouri (1970) developed an equation for steady-state creep rate as a function of temperature, deviatoric stress and mean normal stress. This relation is very similar to a rate process theory formulation.

$$\dot{\varepsilon} = A \exp\left(-\frac{L}{T}\right) \exp(\,(N\,D)) \exp(-m\,\sigma_m\,) \tag{3.64}$$

where: T: absolute temperature (K)
A, L, N, m; parameters
L=U/R
U: activation energy
R: gas constant
$D = (\sigma_1 - \sigma_3)\,\sigma_m$
$\sigma_m = 1/3\,(\sigma_1 + \sigma_2 + \sigma_3)$

Ladanyi's (1972) presented a modification a the flow law for ice to predict the creep strain of frozen soils. He introduced a proof strain rate, $\dot{\varepsilon}_c = 10^{-5}\ \mathrm{min}^{-1}$,and a proof stress, σ_c, to express to steady-state secondary strain rate;

$$\frac{\dot{\varepsilon}}{\dot{\varepsilon}_c} = \left(\frac{\sigma}{\sigma_c}\right)^n \tag{3.65}$$

Using this relation, the total creep strain can be obtained by;

$$\varepsilon = \frac{\sigma}{E} + \varepsilon_k\left(\frac{\sigma}{\sigma_k}\right)^n + \dot{\varepsilon}_c\left(\frac{\sigma}{\sigma_c}\right)^n t \tag{3.66}$$

The first term of the equation represents the elastic instantaneous strain, the second term the plastic instantaneous strain and the last term the secondary creep deformation. Sayles (1988) considered this equation to be valid for the evaluation of secondary creep deformation for some ice-rich materials. To take the influence of temperature into consideration, Ladanyi used Andersland and AlNouri's (1970) equation to correct σ_c for different temperatures. The secondary strain rate is then;

$$\dot{\varepsilon} = \dot{\varepsilon}_c\left(\frac{\sigma}{\sigma_{co}}\right)^n \exp\left[\frac{L\,(273-T)}{273\,T}\right] \tag{3.67}$$

Ladanyi also extended his theory to take into account multi-axial state of stress.

McRoberts (1978, 1988) used a bilinear form of Equation 3.46 to predict the secondary creep rate for ice-rich silt and show the dependence of n to stress level;

$$\dot{\varepsilon} = \frac{A_1 \sigma_d^{n_1}}{((1 - T)^{1.8}} + \frac{A_2 \sigma_d^{n_2}}{((1 - T)^{1.8}} \tag{3.68}$$

Berggren and Furuberg (1985) presented a new approach for predicting creep strains using the concept of degree of mobilization which is the ratio of applied stress to a reference stress, $f = \sigma / \sigma_\theta$, and time resistance which is defined as $R = dt / d\varepsilon$. These authors believed that a primary and secondary steady-state period would develop. The primary creep strain is given by;

$$\varepsilon = \varepsilon_o + \frac{1}{r} \ln t \qquad \text{for } t < t_p \tag{3.69}$$

where: r: slope of R vs t in the primary stage
t_p: time of primary creep

Both parameters, r and t_p are stress dependent and their dependencies are given by;

$$r = r_f (f)^{-i} \quad \text{and} \quad t_p = t_{pf} (f)^{-j} \tag{3.70}$$

where: r_f and t_{pf}: r and t_p for f=1

The reference stress can either be measured from a constant strain rate test or it can be evaluated using;

$$\sigma_\theta = \sigma_u \left(\frac{w_s}{w_u}\right)^u \tag{3.71}$$

where: σ_o: reference stress
σ_u: strength for unfrozen soil
w_s: water content at full saturation
w_u: unfrozen water content
u: exponent

The secondary creep rate is a constant, and the secondary creep strain is given by;

$$\varepsilon_s = \frac{1}{r\, t_p} (t - t_p) \tag{3.72}$$

The tertiary creep is not modelled in this theory because it represents the start of instability. The temperature dependence is expressed through the value of σ_θ.

Recently, some authors have attempted to model the entire creep curve by developing tertiary creep models. Assur (1980) proposed the following equation for strain rate as a function of time;

$$\dot{\varepsilon}(t) = \left(\frac{\dot{\varepsilon}_m}{\varepsilon^{\beta}}\right)\left(\frac{t_m}{t}\right)^{\beta} \exp\left(\frac{\beta t}{t_m}\right) \qquad (3.73)$$

where: β: constant

Zhu and Carbee (1987) observed that this equation is valid for ice-rich soils or for short-term tests in ice-poor materials. However, the relation underpredicts primary and tertiary creep strain for ice-poor material in long-term testing.

Fish (1982) presented a very similar tertiary creep model. The normalized form of his equation is;

$$\frac{\dot{\varepsilon}}{\dot{\varepsilon}_m} = \left(\frac{t}{t_m}\right)^{-\delta} \exp\left[\delta\left(\frac{t}{t_m} - 1\right)\right] \qquad (3.74)$$

where: δ: constant

This equation requires that the integration be done by series expansion in order to get an exact form for the creep strain. However, a simplified form can be obtained;

$$\varepsilon_c \approx \frac{\dot{\varepsilon}_o}{1 - \delta} t^{1-\delta} \exp\left(\frac{t\,\delta}{t_m}\right) \qquad (3.75)$$

where: $\dot{\varepsilon}_o$: initial strain rate

This relationship is only valid at short times, i.e. $t / t_m << 1$, and it does not respect the fact $\dot{\varepsilon}_m$ is a minimum at t_m.

Ting (1983, a) developed another similar tertiary creep model, which uses the minimum strain rate and the time to minimum strain rate. The strain rate as a function of time is given by;

$$\dot{\varepsilon} = A\, t^{-m} \exp\left(\beta\, t\right) \tag{3.76}$$

where: A, m and β: constants

The integration to obtain strain also requires a series expansion. The parameters m and β are given by the following;

$$m = \beta\, t_m \quad \text{and} \quad \beta = \frac{\ln\left(\frac{\dot{\varepsilon}_o}{\dot{\varepsilon}_m}\right)}{t_m \ln\left(\frac{t_m}{t_o}\right) + (t_o - t_m)} \tag{3.77 a, b}$$

where: t_o: initial non-zero reference time
$\dot{\varepsilon}_o$: strain rate at t_o

The parameter A is a function of temperature and saturation which can be determined by experiments. This model is of interest because it considers saturation. Even though this model can predict $\dot{\varepsilon}_m$ and t_m, Sayles (1988) indicated that it gives a good prediction only at the start of the test but that it generally underpredicts the remainder of the creep curve. Moreover, this model is not applicable at low stresses, since the creep behaviour is damped.

As mentioned earlier, frozen soils differ from ice by the fact that they have some long-term strength provided by their frictional resistance. A few authors have tried to predict that long-term strength. The first equation, and probably the one still most in use, is the one proposed by Vyalov (1963);

$$\sigma(t) = \frac{\beta}{\ln \frac{t + t^*}{B}} \approx \frac{\beta}{\ln \frac{t}{B}} \tag{3.78}$$

Sayles (1988) stated that this equation gives a reasonable prediction when the parameters B and β are determined experimentally on the specific sample. However, it should be kept in mind, that this equation is not consistent with a long-term strength of frozen soils since σ(t) → 0 as t → ∞. Ladanyi (1972) predicts a failure strength, σ_f, for ice-rich soils where secondary creep strain dominates and which respect $\dot{\varepsilon}_f = \varepsilon_f\, t_f$.

$$\sigma_f \equiv \sigma_c \left(\frac{\dot{\varepsilon}_f}{\dot{\varepsilon}_c}\right)^{1/n} \tag{3.79}$$

Sayles (1988) suggested that for models which define failure at the inflection point on the creep curve, t_m is the time to failure and the strength could be defined as;

$$t_m = A\,\sigma^n \tag{3.80}$$

where A, n: temperature dependent parameters

The effect of temperature, θ, on the ultimate long-term strength, σ_{lt}, has been studied by Vyalov (1959). The relationship has the following simple form;

$$\sigma_{lt} = C\,\theta^n \tag{3.81}$$

where: C, n: constants

More investigation has to be carried out to determine the long-term strength of frozen soils.

The correspondence between creep tests and constant strain rate tests was mentioned in Section 3.2.3. In ice, the peak strength to strain rate ratio from CSR tests corresponds to the stress to minimum strain rate ratio in creep tests, because it has been established by Cole (1983) that deformation of ice at low strain levels was practically independent of stress path. Few authors have established this same relationship for frozen soils. Sayles (1988) mentioned studies by Perkins and Ruedrich (1974) and Ladanyi (1981) who suggest that peak strength from a CSR test corresponds to the point of inflection in a creep test. He also pointed out that Fish (1983) and Rein (1985) suggested that both types of curves are completely equivalent. Rein (1985) proved that the constant strain rate curve can be predicted using a maximum stress function and a shape function. He established that correspondence between CSR results and creep results exist only at high stresses and strain rates. He suggested that at low stresses and strain rates, the discrepancies between the two types of tests are due to one of the following reasons: the material behaviour depends on loading history, the material behaviour changes drastically at low stresses and strain rates or the differences in testing procedure affect significantly the material behaviour at low stresses and strain rates. It should be kept in mind that Fish considered the frozen soil as a viscous material, i.e. no frictional resistance. Zhu and Carbee (1987) also mentioned the correspondence between the two following ratios; (σ_{peak} / $\dot{\varepsilon}$) from CSR test and (σ / $\dot{\varepsilon}_{min}$) from creep test. These ratios are both maximum at the point of failure. It is important to note that these observations were made on non-frictional materials.

3.4. MECHANICAL PROPERTIES OF SALINE FROZEN SOILS

3.4.1. Compressive strength of saline frozen soils

The behaviour of saline frozen soils is also governed by the presence of ice and solid grains. However, there is an additional component which influences the behaviour of saline frozen soils, the presence of a relatively important quantity of brine or unfrozen water within the soil matrix. This unfrozen water is caused by the influence of freezing point depression and salt exclusion within the saline pore fluid. The amount of unfrozen water is controlled by a combination of the initial pore fluid salinity and soil temperature. As the initial salinity and temperature increase, the amount of unfrozen water increases. This increase in unfrozen water is generally believed to cause a decrease in compressive strength (Ogata et al., 1983, Pharr and Merwin, 1985, Stuckert and Mahar, 1984). Ogata et al. (1983) suggested that for granular soils, the concept of unfrozen water provides a unifying concept for the prediction of compressive strength at temperature higher than the eutectic point (-21.3°C for NaCl) . At temperature lower than the eutectic point, the precipitation of salts reverses the behaviour, and causes an increase in salinity to increase the strength, since salts crystals increases the cohesion between soil grains. For cohesive soils, he notices that using the unfrozen water content does not provide a unique relationship for different soil types, and that using the thickness of the unfrozen water film could be used to explain the decrease in strength with an increase in unfrozen water content. He defines the unfrozen water film thickness, δ, as:

$$\delta = W_u / S_s \rho_w \qquad (3.82)$$

where: W_u: unfrozen water content (% wt.)
S_s: specific surface area
ρ_w: density of water

Pharr and Merwin (1985) used the idea of volumetric brine content, ν_b, which was developed for sea ice to predict the strength of saline frozen Ottawa sand. Their reasoning is that since brine can not support load, the plane porosity is a good indicator of strength reduction. They suggested the use Equation 3.25 without pre-determining the value of the exponent k, since the shape of the brine inclusions is unknown. They proposed a plot of log $(1-\sigma_f/\sigma_o)$ vs log ν_b to determine the values of k and c. σ_o is a temperature dependent function which represent the strength of a brine free sand having the same structure as a saline sand. They used the following correlation between σ_o and temperature, T;

$$\sigma_o = A + B \log_{10}(-T) \tag{3.83}$$

Their final relationship is given by;

$$\sigma_f = \{3.76 + 7.53 \log_{10}(-T)\}\{1 - 1.02\, \nu_b^{0.109}\} \tag{3.84}$$

with: σ_f in MPa
T in °C

and,

$$\nu_b = \frac{S/\rho_b S_b}{S/\rho_b S_b + (1 - S/S_b)/\rho_i} \tag{3.85}$$

where: S: salinity of solution before freezing
ρ_i: density of ice at given temperature
S_b, ρ_b: salinity and density of brine in equilibrium with ice at given temperature (from phase diagram)

Stuckert and Mahar (1984) used the concept of volumetric ice content to model the influence of temperature and salinity on the compressive strength of saline granular soils. They believed that the presence of brine reduces the volume of ice available to provide particle bonding. They used a loosely packed particle arrangement in order to avoid any particle interaction which could provide some strength. They defined the volumetric ice content and the ice area ratio (A_{ice}) as follows;

$$\frac{V_{ice}}{V_{void}} = 1 - \frac{S_o}{S_T} \quad \text{and} \quad A_{ice} = \frac{\text{area of contact ice}}{\text{total cross-section area}} \qquad (3.86\text{ a,b})$$

where: S_o: initial salinity
S_T: equilibrium salinity at a given temperature

They established a relationship between volumetric ice content and ice area ratio based on spherical particles and an ideal cubical particle arrangement. For such an ideal material, the compressive strength is given by;

$$\sigma_{max} = A_{ice} \times S_{ice} \qquad (3.87\text{ a})$$

where: S_{ice}: strength of ice
$= 300 - 30\ T(°C)$ in psi (3.87 b)

For a non-ideal soil, the void ratio is different than for the cubical arrangement, and consequently a void ratio correction should be applied to the strength equation;

$$\sigma_{max} = A_{ice} \times e_{soil} / e_{sphere} \times S_{ice} \qquad (3.88)$$

Sego and Chernenko (1984) presented a study of the influence of salinity and confining pressure on the cohesion and friction angle of frozen saline sands. They observed that cohesion is linearly dependent with salinities between 0.2% and 0.8% and then increases drastically at salinity close to 0. The angle of friction proved to be almost independent for salinities larger than 0.2%. As for unfrozen sands, an increase in confining pressure increases the strength of frozen sands due to the enhanced friction. These authors also used the soil strength minus the frictional component of strength which they defined as q_o, to study the behaviour of the material at no confinement, in order to compare their results with other results from the literature;

$$q_o = q - (p - p_o) \tan \alpha \qquad (3.89)$$

where: $q = (\sigma_1 - \sigma_3)_f / 2$
$p = (\sigma_1 + \sigma_3)_f / 2$
$\tan \alpha = q / p$
$p_o = x / (1 - \tan \alpha)$
x : intercept at p=0

They observed that q_o also decreases dramatically with an increase in salinity. The effect of confining pressure was also investigated by Furuberg and Berggren. Since these authors studied clays, they observed that the confining pressure had no influence on the strength of frozen clays.

Sego et al. (1982) studied the effect of strain rate on the peak strength and deformation modulus of frozen saline sands. They used the equation proposed by Ladanyi (1972) to evaluate the variation of the proof stress, σ_c, and the stress exponent, n, with salinity. They noticed a decrease in n values as the salinity increases and a drastic decrease in proof stress with an increase in salinity. The secant Young's modulus follows a similar power law.

$$\frac{\dot{\varepsilon}}{\dot{\varepsilon}_c} = \left(\frac{E}{E_c}\right)^x \qquad (3.90)$$

where: $\dot{\varepsilon}$, $\dot{\varepsilon}_c$: strain rate, proof strain rate
E, E_c: Youn'g secant modulus, proof modulus
x: modulus exponent

The modulus increases with an increase in strain rate and decreases with an increase in salinity. The proof modulus (value of E for $\dot{\varepsilon}$ = 0.001%/hour) decreases significantly with an increase in salinity and the exponent x decreases slightly with an increase in salinity. The exponent x does not vary as much as the stress exponent for the same increase in salinity suggesting that the modulus is not as affected by salinity changes as the strength. These authors also observed that the strain to failure was independent of salinity.

Tsytovich and Samuel'son (1973) made an interesting observation on the influence of soils type on the behaviour of frozen saline soils. They noticed that for sands the decrease in strength with an increase in salinity is very sharp, as opposed to a more gradual decrease in strength for silty or clayey soils.

3.4.2. Creep behaviour of saline frozen soils

As for non-saline frozen soils, saline soils creep under constant stress due to the presence of ice in the pores of the soil matrix. Aas (1980) used a concept similar to Vyalov's attenuating creep, when he introduced the critical shear stress which is the transition between small creep deformation at a constant creep rate and large uncontrolled deformation in a frozen saline clay. As stated by Pharr and Godavarti (1987), the creep deformation of saline frozen materials is controlled by the plasticity of the ice-brine mixture. The presence of the brine increases the creep rate of the pore ice, leading to an increased creep rate for any saline frozen soil as compared to a similar non-saline soil. These same authors compared the behaviour of laboratory saline ice to saline frozen sands, and noticed that the addition of sand to laboratory ice does not improve the creep behaviour and only promotes the development of tertiary creep. The behaviour of both types of material seem very similar at small strains (<2%). They believed that the sand only acts as a stress concentrator generating tensile stresses leading to internal cavitation, when the sample is under no confinement.

Nixon and Lem (1984) were among the first authors to investigate the creep behaviour of fine-grained saline frozen soils. They used the concept of secondary steady-state creep rate to study the influence of salinity on creep. They applied Equation 3.44 ($\dot{\varepsilon} = B\,\sigma^n$) to their results to study the variation of B and n with salinity. They established that the stress exponent n is a function of stress range and soil type and appears to be independent of salinity. They decided to fix n = 3 and then investigate the variation of B, the creep coefficient, with salinity. B, which is an indication of the creep velocity, increases with an increase in salinity and temperature. They finally mentioned that at temperature close to the freezing point depression where the unfrozen water content is high, it would be important to differentiate between consolidation and creep effects.

Nixon and Pharr (1984) examined the creep behaviour of saturated saline frozen gravel. They observed that neither a secondary creep stage nor a minimum strain rate developed during testing. Consequently, they selected two arbitrary creep parameters, i.e. the strain rate at 10% strain, $\dot{\varepsilon}_{10\%}$, and the time to 10% strain, t_m, to investigate the effects of temperature, stress and salinity on the creep behaviour. They observed that the temperature influence is more pronounced at high temperatures. For an increase in temperature from -8°C to -4°C, they noticed a decrease in $t_{10\%}$ and an increase of $\dot{\varepsilon}_{10\%}$ by two orders of magnitude. They modelled the stress dependency by using the following equations;

$$\dot{\varepsilon}_{10\%} = A \exp(\alpha\sigma) \quad \text{and} \quad t_{10\%} = B \exp(-\beta\sigma) \tag{3.91 a,b}$$

where: A, α, B, β: constants

The creep resistance decreases (represented by an increased $\dot{\varepsilon}_{10\%}$ and a decreased $t_{10\%}$) with an increase in salinity due to a larger equilibrium brine fraction associated with higher salinities. Nixon and Pharr (1984) used a concept similar to Stuckert and Mahar's (1984) ice content concept to unify their creep results. They used the ice fraction by weight which is a combination of the temperature (in °C) and salinity (in ppt) effects, to characterize $t_{10\%}$ and $\dot{\varepsilon}_{10\%}$. The ice fraction is defined as;

$$f_{ice} = \frac{W_{ice}}{W_{total\ water}} = 1 - 0.001\ S\left[1 - \frac{54.11}{T}\right] \tag{3.92}$$

Furuberg and Berggren (1988) used Equations 3.69 to 3.72 to study the creep behaviour of frozen saline clays. These equations are readily applicable to saline frozen soils since they include the influence of unfrozen water on the reference strength. As the salinity increases, the unfrozen water content increases and consequently the reference strength σ_θ decreases and there is an increase in primary creep deformation as these authors observed. Since, these authors believed that if secondary creep develops, failure will eventually take place, they define the creep long-term strength, σ_L, as the upper stress limit of primary creep.

$$\sigma_L = \sigma_\theta \left(\frac{t_{pf}}{t_p}\right)^{1/j} \tag{3.93}$$

Furuberg and Berggren stated that the long-term strength is governed by the presence of unfrozen water.

The strength and time dependent behaviour of frozen saline soils have been modelled using different approaches all based on the concept of a reduction of ice content due to the presence of unfrozen water content. An increase in salinity or unfrozen water content reduces the strength of the frozen saline soil. The time dependent deformation behaviour is also worsened by an increase in salinity. The resistance to constant stress decrease with an increase in salinity as indicated by an increase in strain rate at failure and a reduction of time to failure.

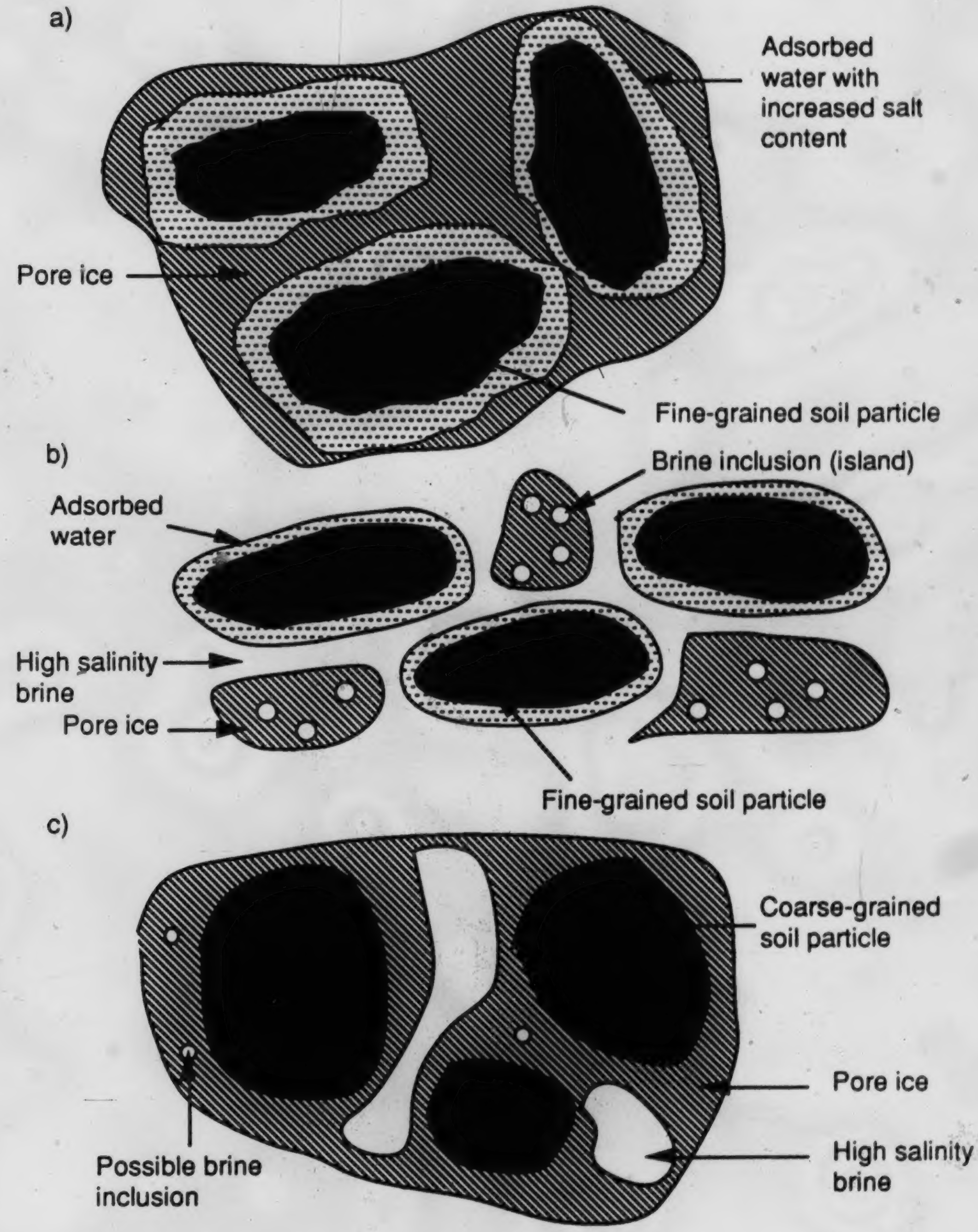
a)
Adsorbed water with increased salt content
Pore ice
Fine-grained soil particle
b)
Brine inclusion (island)
Adsorbed water
High salinity brine
Pore ice
Fine-grained soil particle
c)
Coarse-grained soil particle
Pore ice
High salinity brine
Possible brine inclusion

Figure 3.1: Distribution of unfrozen water in frozen soils
a) Low salt concentration pore fluid in fine-grained soil
b) High salt concentration pore fluid in fine-grained soil
a) and b) after Sheeran and Yong (1975)
c) High salt concentration pore fluid in coarse-grained soil

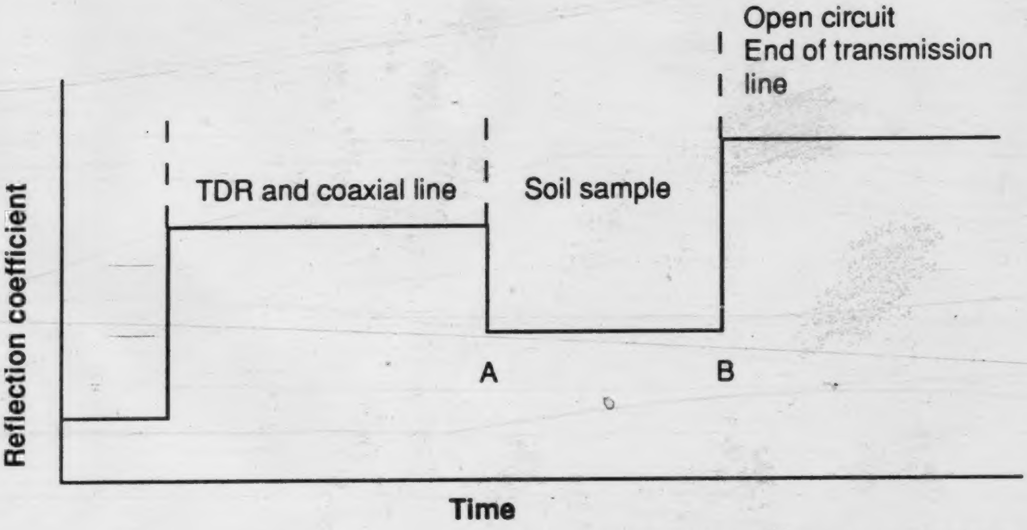
Open circuit
End of transmission line
TDR and coaxial line
Soil sample
Reflection coefficient
A
B
Time

(modified from Topp et al. (1980))

Figure 3.2: Idealized TDR trace

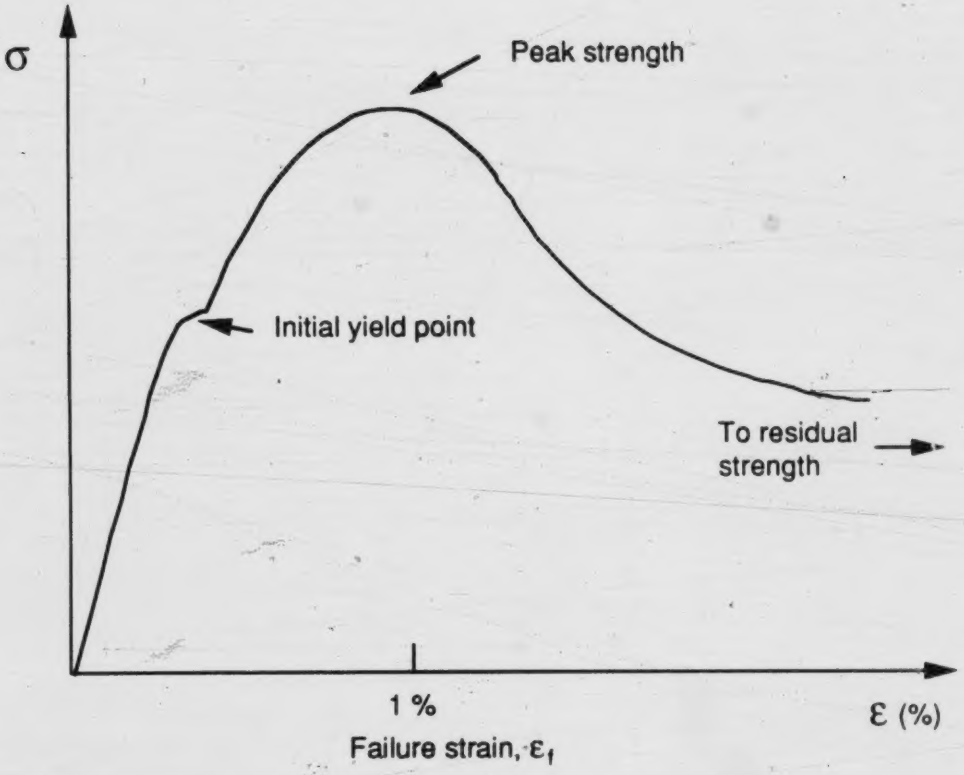

Figure 3.3: Typical ductile stress-strain curve for polycrystalline ice under constant strain rate (modified from Mellor and Cole (1982))

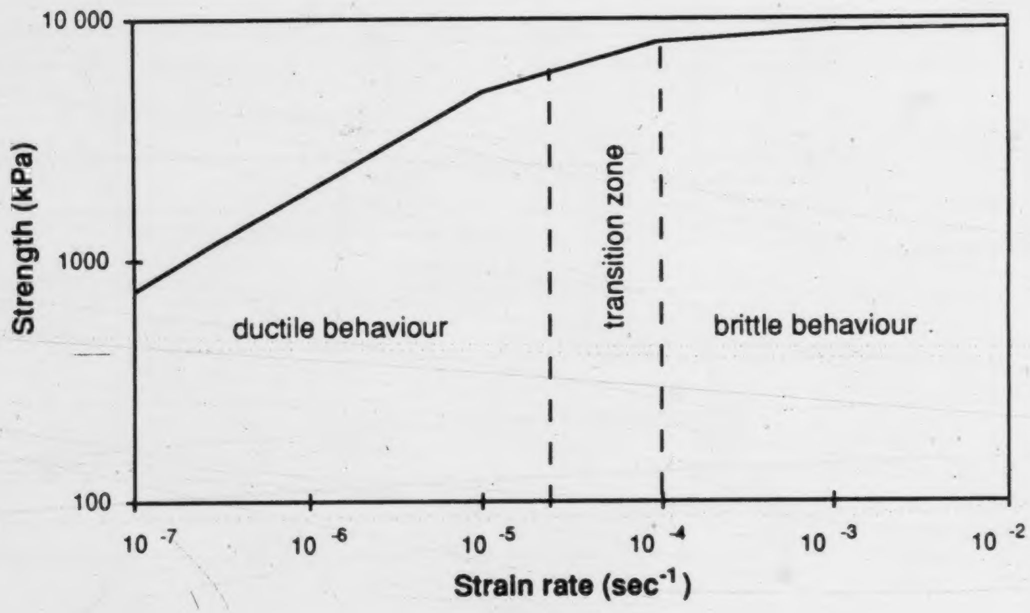

Figure 3.4: Influence of strain rate on the strength of ice at -7°C (modified from Mellor, 1979)

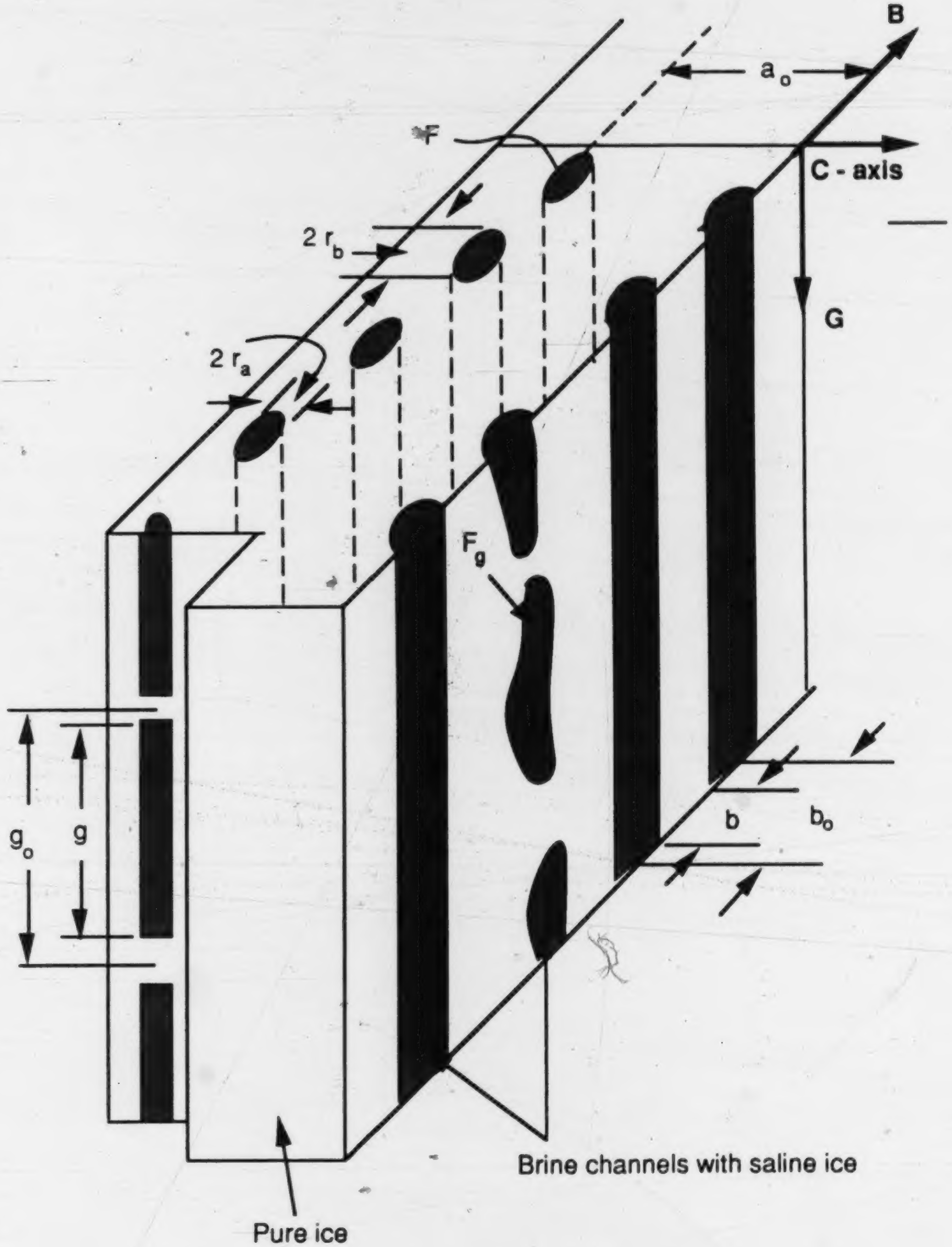
B
a_o
F
C - axis
$2r_b$
G
$2r_a$
F_g
g_o
g
b
b_o
Brine channels with saline ice
Pure ice

Figure 3.5: Schematic of Assur sea ice model (modified from Assur (1958))

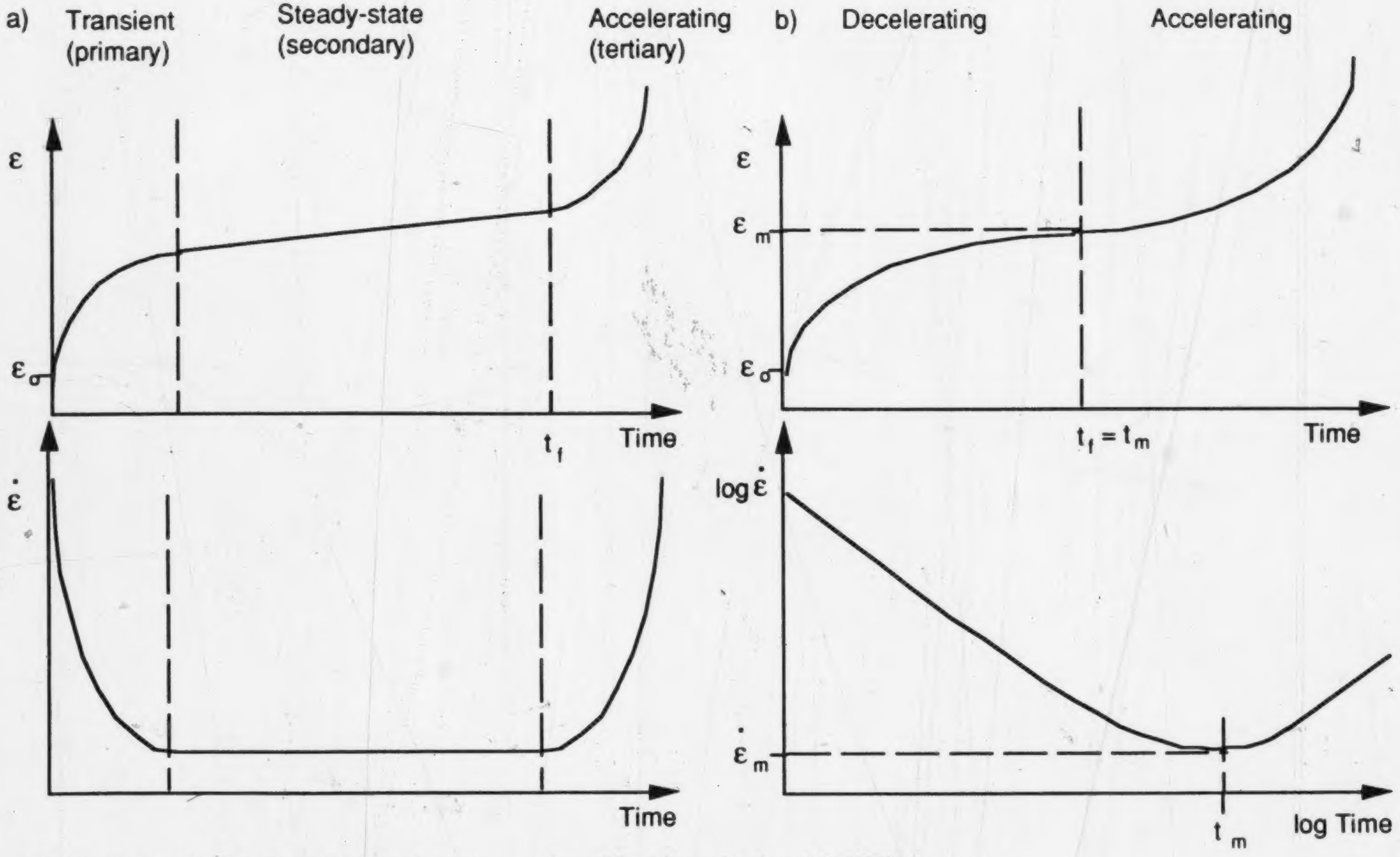

Figure 3.6 : a) Steady-state creep curve (modified from Ladanyi (1972))
b) Non-steady state creep curve (from Ting (1983))

4. LABORATORY PROCEDURE

4.1. SCOPE OF TESTING PROGRAM

The objective of the laboratory program was to investigate the influence of soil grain size, salinity and temperature on the mechanical behaviour of frozen soils. Moreover, a study of the unfrozen water content of each soil was undertaken to understand its influence on the mechanical behaviour and its relationship to soil type, salinity and temperature. The range of values for each parameter was selected to be as representative as possible of field conditions present in permafrost environments. The mechanical behaviour of interest to this study were the stress-strain response under unconfined compression at constant strain rate (CSR), and the time dependent deformation under constant stress (creep behaviour).

4.2. SAMPLE PREPARATION

Three soils were selected to be as representative as possible of soils found in Arctic communities. However, no fine-grained soils (clay) were studied since the presence of clay minerals complicates the interpretation of the mechanical behaviour and was beyond the objective of this study. The grain size curves of each soil are presented in Figure 4.1. Soil A is a uniform sand with a coefficient of uniformity of 2.2. The sand is a locally available mortar sand which has a grain size distribution comparable to the range of grain size of marine sands found in the Beaufort Sea, and was similar to the sand tested and reported by Sego et al. (1982) and Sego and Cherenko (1984). Soil C is a very fine silty sand or sandy silt, called the Devon Silt, and is available in the Edmonton region. Soil B is a half and half mixture of soils A and C, creating a silty sand.

The soils were air dried for at least a week prior to being mixed for sample preparation. The sand was vibrated over a #10 sieve to remove all lumps, and the fine silty sand (Soil C) was soaked in the appropriate saline solution for 24 hours before being mixed. The soils were then mixed with the pore fluid which was a solution of 0, 5, 10 or 30 ppt of pure sodium chloride (NaCl) dissolved in distilled water. Soil A was submerged in the solution, and a vibratory table was used for ten minutes to remove air from the mixture. Soils B and C were mixed in a industrial mixer with the solution until a fluid paste was obtained. Both methods were used to achieve a high degree of saturation.

The prepared slurry was then poured into a split PVC mold (see Figure 4.2) which allowed either top or top and bottom drainage. For Soil A, only top drainage was used because of the high permeabiltity of the material. For Soils B and C, filter paper strips were placed on the walls of the mold to allow for radial, as well as top and bottom drainage. A load plate was placed at the top of the sample, and a consolidation pressure of approximately 80 kPa was applied to the sample. The consolidation process was continued until at least 90% primary consolidation was achieved. The samples were then frozen uni-directionnally by circulating liquid nitrogen through a freezing plate placed beneath the base plate of the cell (Figure 4.3). The samples were frozen after 4 to 5 hours. After freezing of the sample was completed, the split mold was opened, the sample extracted, then sprayed with distilled water which immediately froze (to reduce moisture loss during storage) and wrapped in two layers of plastic film. The samples were stored in a freezer maintained at a temperature of -15°C until required for testing. Before testing (except for TDR), the sample was taken to a cold room at a temperature of -25°C, where a diamond blade saw and carbon-bit milling machine were located. Thin slabs of approximately 15 mm from the ends of the sample were sawed off. The samples were then trimmed using a milling machine to achieve square ends and a height-diameter ratio of 2 (i.e. a height of approximately 200 mm, with a diameter of 100 mm). A height-diameter ratio of 2 was selected to ensure a uniform stress distribution in the center of the sample, and to avoid as much as possible end effects.

Throughout this study, samples will be referred by their soil type, i.e. Soil A, B or C and by their nominal salinity 0, 5 10 or 30 ppt. For example, a sample referred to as B-5 is a sample of Soil B (silty sand) with an initial salinity of 5 ppt.

4.3. DETERMINATION OF PHYSICAL PROPERTIES

4.3.1. Moisture Content and Density

For each sample tested (TDR, unconfined and creep compression), the moisture content and the total and dry densities were determined. After testing, the still frozen sample was cut into five slabs: three were used to determine the moisture content distribution throughout the sample (i.e. top, middle and bottom), and the remaining two slabs were kept for possible future testing. The moisture content was determined following the ASTM D2216. Since the shape of the sample was cylindrical, the total density was determined by weighing and measuring the volume of the sample before testing. The dry density was simply calculated from the total density and average moisture content. An attempt to determine liquid limits on Soil C was carried out, but because of the low plasticity silt used, no reliable results were obtained. Therefore soils B and C were low plasticity soils.

4.3.2. Salinity Determination

On the TDR samples, the post-testing total salinity of thawed samples was determined to verify if the freezing method yielded a uniform salinity distribution. For the samples tested in 1988, three salinities measurements (top, middle, bottom) were performed for each sample. The moisture contents of the salinity samples were not determined, and consequently the moisture content correction given by Equation5.1 could not be applied to these samples. For the 1990 samples, only two salinity samples (top and bottom) were used but the moisture contents of each one was also measured.

The procedure used to determine salinity is the method describe in Section 2.2.2.8, method 1: ASTM Standard D4542-85 (pore fluid extraction and salinity measurement using refractometer). The filter papers used during extraction were very fine cellulosic membrane filters, and two types of refractometers were used: Endeco Refractometer (type 102) with a precision of ±0.1 ppt (for 1988 testing) and a AO Scientific Instrument Hand Refractometer (model 10419) with a precision of ±1 ppt (for 1990 testing).

4.3.3. Unfrozen Water Content Determination- TDR testing

As discussed in Chapter 3, numerous methods are available to determine unfrozen water content. Time-domain reflectometry (TDR) was chosen for its simplicity and availability of equipment. Two groups of tests were performed: one at the laboratories of the Geotechnical Division of the National Research Council in Ottawa during April 1988, and the second at the University of Alberta in March 1990. The second set of testing was necessary because Soil C was not tested in 1988.

The samples were prepared according to Section 4.3.2. except that parallel transmission lines were inserted in the samples just before consolidation. These lines were stainless steel rods of 2 mm in diameter and were spaced 20 mm apart in the sample. The length of the lines was 80 mm for the samples tested in 1988 and 100 mm for the ones tested in 1990. To monitor soil temperature, thermocouples (1988) or RTD's (resistance-temperature devive) (1990), were used.

The equipment used in both cases was a Tektronix 1502 TDR unit connected to a Hewlett-Packard XY plotter. The horizontal axis of the TDR trace represents travel time and was calibrated using either an air line (1988) or a polypropylene line (1990) of known lengths. The connection between the parallel balanced transmission lines in the samples and the coaxial line connected to the TDR unit was made through a *balun*. In 1988, an Anzac TP-101 *balun* was used (primary impedance 50 ohms and secondary impedance 50 ohms), and in 1990 two types of *baluns* were used: an Anzac TP-101 and an Anzac TP-103 (primary impedance 50 ohms and secondary impedance 200 ohms), to see which allowed a better impedance match between the coaxial line and the frozen sample.. The entry point of the signal in the sample (point A) was establised by shorting the parallel transmission lines at the top of the sample. Figure 4.4 presents a schematic of the equipment used during a test and Figure 3.2 already presented an idealized TDR trace.

Samples of the three soil types (A, B, C) at four salinities (0, 5, 10, 30 ppt) were tested through the temperature range of -12°C to -1°C by warming up using one degree steps. At each temperature, two sets of readings were taken at six hour time intervals. Over the temperature range of -7°C to -1°C, one set of readings was taken after the sample was inverted end for end for six hours to avoid gravity migration of the unfrozen water and to maintain a uniform soil moisture distribution.

The TDR method yields a volumetric unfrozen water content. To convert volumetric unfrozen water to gravimetric unfrozen water, the following relationship should be applied;

$$\theta_u = \frac{\rho_d}{\rho_w} \text{w.c.}_u \tag{4.1}$$

where: θ_u : volumetric unfrozen water content

ρ_d: dry density of the soil

ρ_w: density of water

w.c._u: gravimetric unfrozen water content

4.3.4. Electrical conductivity

Originally, the electrical conductivity of the frozen samples was going to be measured by a Wheaton half-brige configuration, using a strain indicator to maintain zero voltage and a resistor box to balance the sample resistivity. These measurements would allow an attempt at determining the real salinity of the unfrozen pore fluid in the frozen soil. However, the calibration of the saline solutions (from 30 to 200 ppt) at sub-zero temperatures gave a very wide scatter in resistivity values which made the measurements inapplicable to an equation of the form of Equation 3.22. Moreover, the electrical conductivity of the pore ice could not have been evaluated properly since it was impossible to determine if brine inclusions existed. Finally, at cold temperature, a large relative error on the amount of unfrozen water exists since the values of θ_u are so small. Consequently, the idea of measuring the electrical conductivity of the samples was abandoned.

4.4. UNCONFINED CONSTANT STRAIN RATE COMPRESSION TESTS

4.4.1. Description of equipment

The unconfined compression tests were performed using standard triaxial cells for 100 mm samples, modified to accomodate a temperature-control system. All the testing was carried out in a cold room which allowed temperatures in the range of -1°C to -20°C. The samples were loaded by a constant displacement rate loading frame (Figure 4.6). The displacement, load, temperature,and volume change were all monitored using a Helios data acquisition system.

Figure 4.5 shows the modified triaxial cell used. The cooling coil was connected to a constant temperature bath which consisted a refrigeration/heating unit, antifreeze (glycol) reservoir, a pump and a control panel allowing temperature adjustments. Antifreeze was pumped by the bath and then circulated through the cooper coil placed inside the triaxial cell. Using this set up the temperature of the cell fluid (light mineral oil), which was monitored by a RTD, could be controlled to within ±0.3°C of the desired nominal temperature, avoiding fluctuations caused by temperature variations in the cold room.

Two constant displacement loading frames were used: a Wykeham Farrance Ltd. 5 000 kg (50 kN) stepless compression test machine and a Wykeham Farrance Ltd. 10 000 kg (100 kN) stepless compression test machine. The higher capacity frame was needed for the non-saline samples. The displacement of the sample was measured using a 24 volt LVDT (linear voltage displacement transducer). The LVDT had to be initially positioned so that the output was in the linear range of the LVDT. The load, which was applied through a steel ram in contact with the sample, was measured using a load cell of appropriate capacity (1 000 lb (4.5 kN), 2 000 lb (9.0 kN), 5 000 lb (22.5 kN), 20 000 lb

(90 kN)). Steel ball bearings were used at each end of the rams to ensure vertical load application to the sample.

The volume change of the samples was measured indirectly from the displaced cell fluid to evaluate volume change. The cell was connected by a valve to a plastic tube which reached a small oil-water reservoir outside the cold room, in which an oil-water interface formed. The reservoir was linked to the volume change device (also located outside the cold room) which was filled with water and measured volume change via a LVDT displacement. The use of oil as a cell fluid was necessary to avoid freezing within the cell and ensure that a sufficient thermal mass surrounded the sample.

All LVDT's, load cells and RTD's were calibrated in the cold room under conditions similar to those used during testing. The volume change devices were calibrated at room temperature since they were filled with water.

Neoprene membranes were used for all tests since latex membranes are weakened by oil. The stiffness of the membrane was measured using the method proposed by Bishop and Henkel (1962) and all strengths were corrected for the membrane stiffness. The neoprene membranes were held in contact with the bottom and top load plates by 100 mm diameter O-rings tighten with hose-clamps.

As stated previously, a data acquisition system, consisting a Helios Fluke box (which transforms the analog signal to a digital signal) and an Operand AT computer, was used to record all electronic signals. The program Labtech Notebook, © Laboratory Technologies Corporation, was used to log the digital output of each channel and allowed the user to choose sampling interval, display of the readings and organization of the data files. These data files were directly compatible with Lotus 123 format, © Lotus Development Corporation, permitting easy data reduction and manipulation.

4.4.2. Test procedure

The test sample was taken out of the cold room where it had been machined and placed on the base plate of the triaxial cell. A neoprene membrane was slipped over the sample, and the top load plate was placed at the top of the sample. O-rings were placed around the upper part of the bottom and top platens to provide good contact between the membrane and the sample. Then hose-clamps were tighten around the O-rings to avoid any movement of the O-rings during testing. The sample fixed to the base of the triaxial cell (Figure 4.5 b) was brought into the cold room where the top portion of the triaxial cell was placed over the sample. The cell was closed using the long cell screws, and then filled with light mineral oil through the shaft opening. Once the cell was filled, the ram was pushed in until contact was established with the ball bearing placed on the load platen. The volume change line was hooked up, and a small pressure was applied to the oil-water reservoir in order to push out any air remaining in the cell through the air vent. Once oil was coming out of the vent, the valve was closed and the pressure released. The valve was then reopened.

The cell was placed on the moving ram of the compression test machine. A ball bearing was placed at the end of the ram and the moving ram of the loading frame was moved up until the ball bearing was almost in contact with the load cell, (Figure 4.6). The LVDT was then adjusted to give an output in its linear range. The displacement rate was adjusted so a strain rate of 0.8 %/hour could be acheived. The temperature bath was then set at the test temperature (-5°C, -7°C, -10°C or -12°C), and the sample was left under these conditions for at least 12 hours to achieve temperature equilibrium. The test was then started. After approximately 20 hours, which was equivalent to about 16% strain, the test was stopped, and the moving ram lowered so that the cell could be taken out. The cell fluid was drained by applying a small air pressure through the air vent. The top of the cell was unscrewed and removed. The sample was taken out of the cold room, where the hose-clamps and O-rings where removed prior to cutting the membrane. The sample was then drawed, measured and photographed. It was then placed in another cold room where it was cut using a diamond saw into cubes of approximately 300mm x 300mm x 100mm which were used as moisture content samples.

4.5. CONSTANT STRESS COMPRESSION TESTS

4.5.1. Description of equipment

Equipment similar to that used during the unconfined CSR compression tests was used for the creep tests. Consequently only the differences in the test equipment will be described here. The same modified triaxial cells were used except that the copper cooling coil were removed to avoid the samples contacting the coils at large axial strains during the tests. The room temperature was maintained at -7°C, for all tests. Since the constant temperature bath was not used the cell fluid temperature (which was monitored with an RTD) could only be maintained within ± 0.4 °C of the nominal temperature.

As shown in Figure 4.7, a static load frame was used and the load was applied through a bellofram which was filled with oil. The load was applied to the bellofram using air pressure which was controlled through two air pressure regulators placed outside the cold room.

The deformation of the sample was measured using a 7 volt LVDT which was fixed to loading ram. The load was monitored using a load cell (2 000 lb (9.0 kN), 5 000 lb (22.5 kN), 20 000 lb (90 kN). The same data acquisition system was used for these tests.

4.5.2. Test procedure

The samples were set up in the same manner as in the CSR compression tests. The volume change was measured only during a limited number of tests. For the tests where it was not measured, the cell was not completely filled with oil (a gap of approximately 20 mm was left at the top of the cell to allow for sample expansion). For the tests where volume change was measured, the same procedure as previously described was followed. The height of the static frame was adjusted using the threaded rods so that the cell and the load cell could both fit. The cell was placed on the bottom plate of the static frame. A very small pressure was applied to the bellofram to bring the bellofram ram close to the ball bearing at the end of the ram in contact with the sample. Once this was completed, the bellofram valve was closed and the cell was centered with respect to the load cell. The LVDT was fixed to the loading shaft and adjusted to give an output in its linear range. The sample was left overnight to reach temperature equilibrium. A small load was applied to the bellofram to bring the ram in contact with the ball bearing. The load was then increased to achieve the desired axial stress level. Throughout the whole test the load had to be adjusted as the sample underwent strain in order to maintain a constant applied stress and not a constant load. The test was continued until the sample reached the tertiary creep deformation stage, and then stopped. The sample was disassembled following the same procedure as for the compression tests.

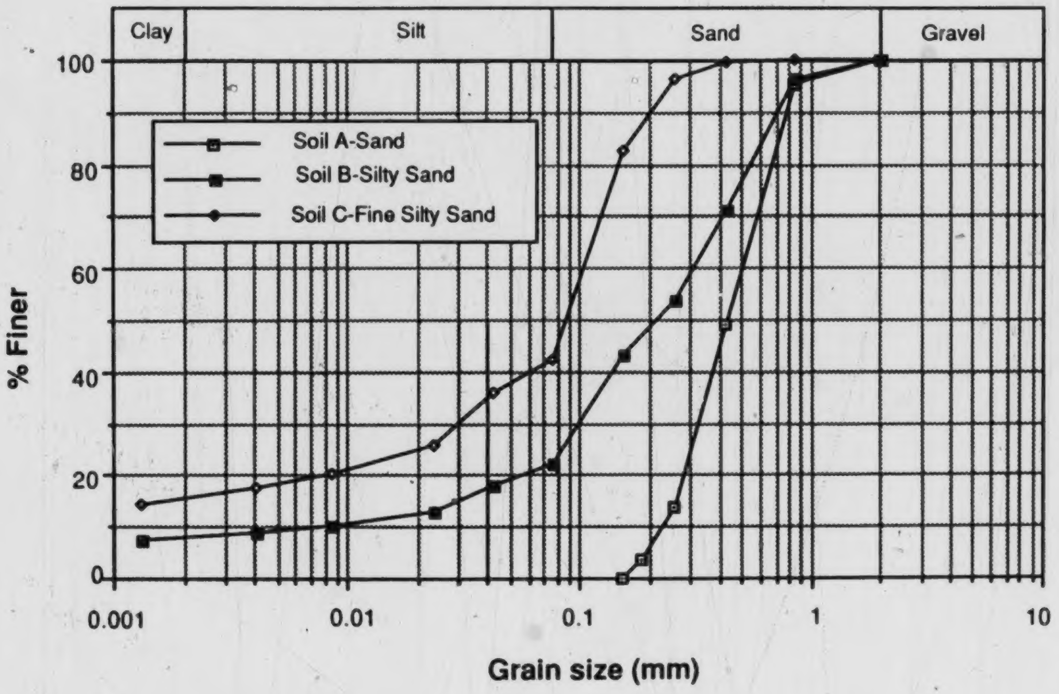

Figure 4.1: Grain size distriubtion of soils tested

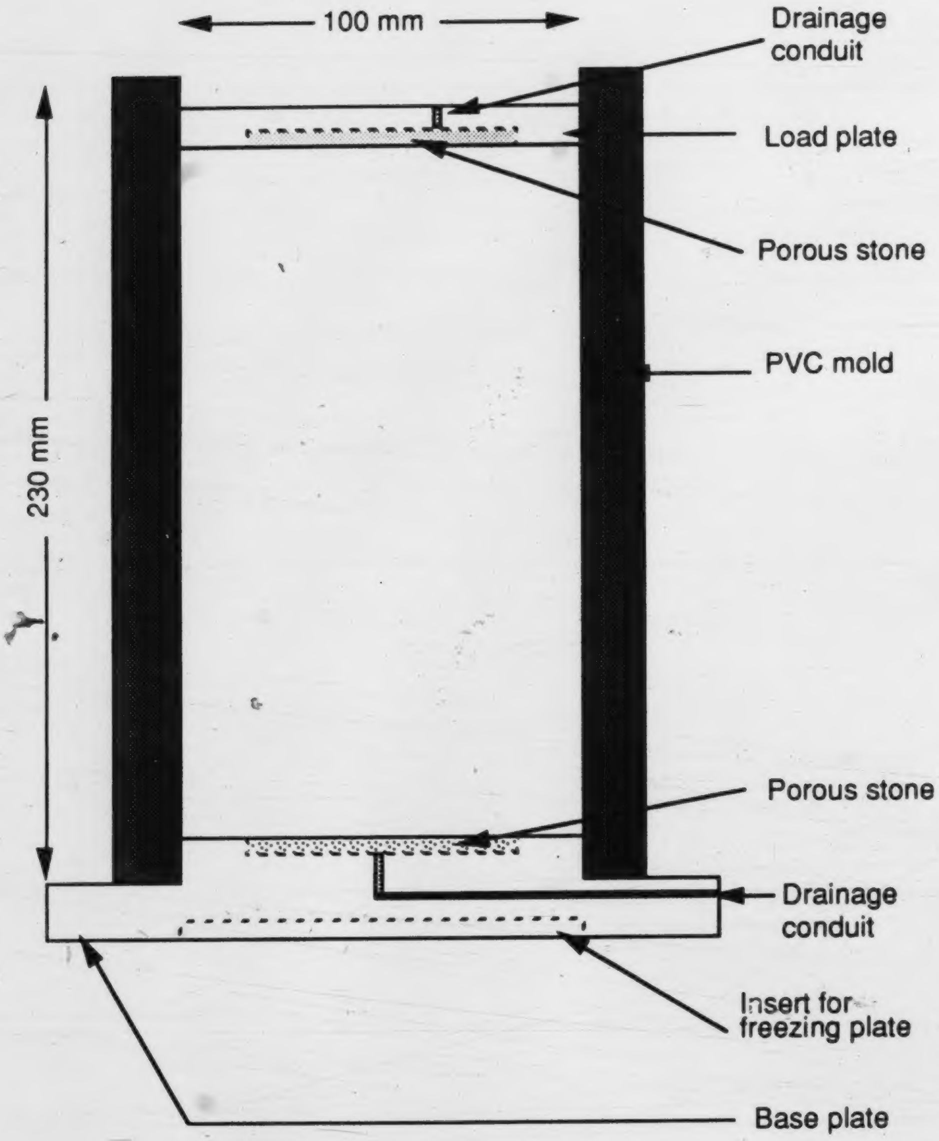
100 mm
Drainage conduit
Load plate
Porous stone
PVC mold
230 mm
Porous stone
Drainage conduit
Insert for freezing plate
Base plate

Figure 4.2: Split freezing mold used to consolidate and freeze sample

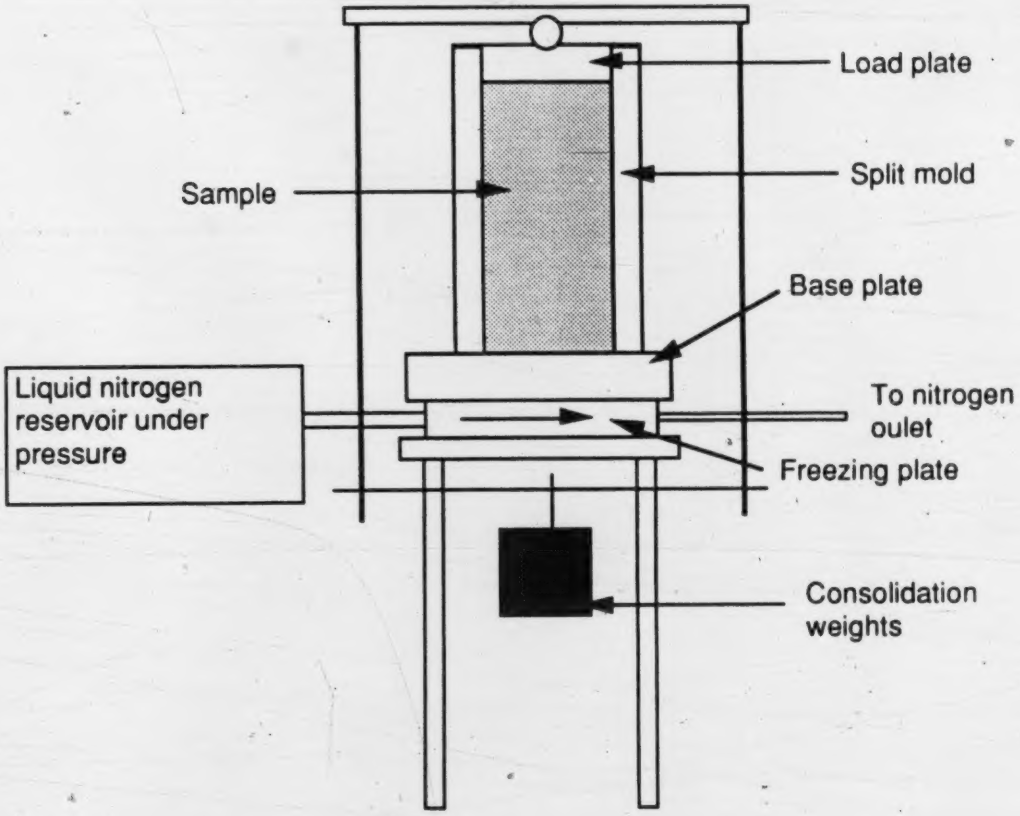
Load plate
Split mold
Sample
Base plate
Liquid nitrogen reservoir under pressure
To nitrogen oulet
Freezing plate
Consolidation weights

Figure 4.3: Schematic of sample consolidation and freezing apparatus

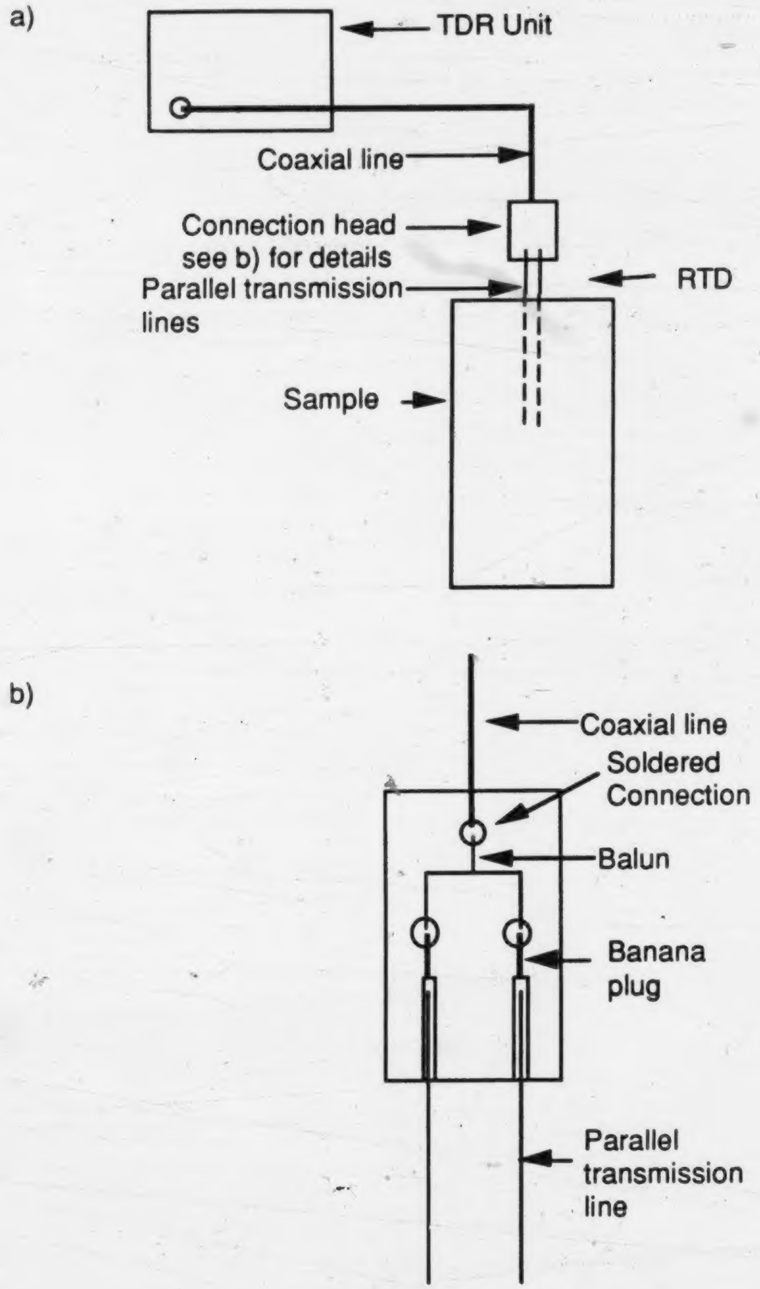
a)
TDR Unit
Coaxial line
Connection head
see b) for details
Parallel transmission
lines
RTD
Sample
b)
Coaxial line
Soldered
Connection
Balun
Banana
plug
Parallel
transmission
line

Figure 4.4: a) Schematic of TDR equipment b) Details of connection head

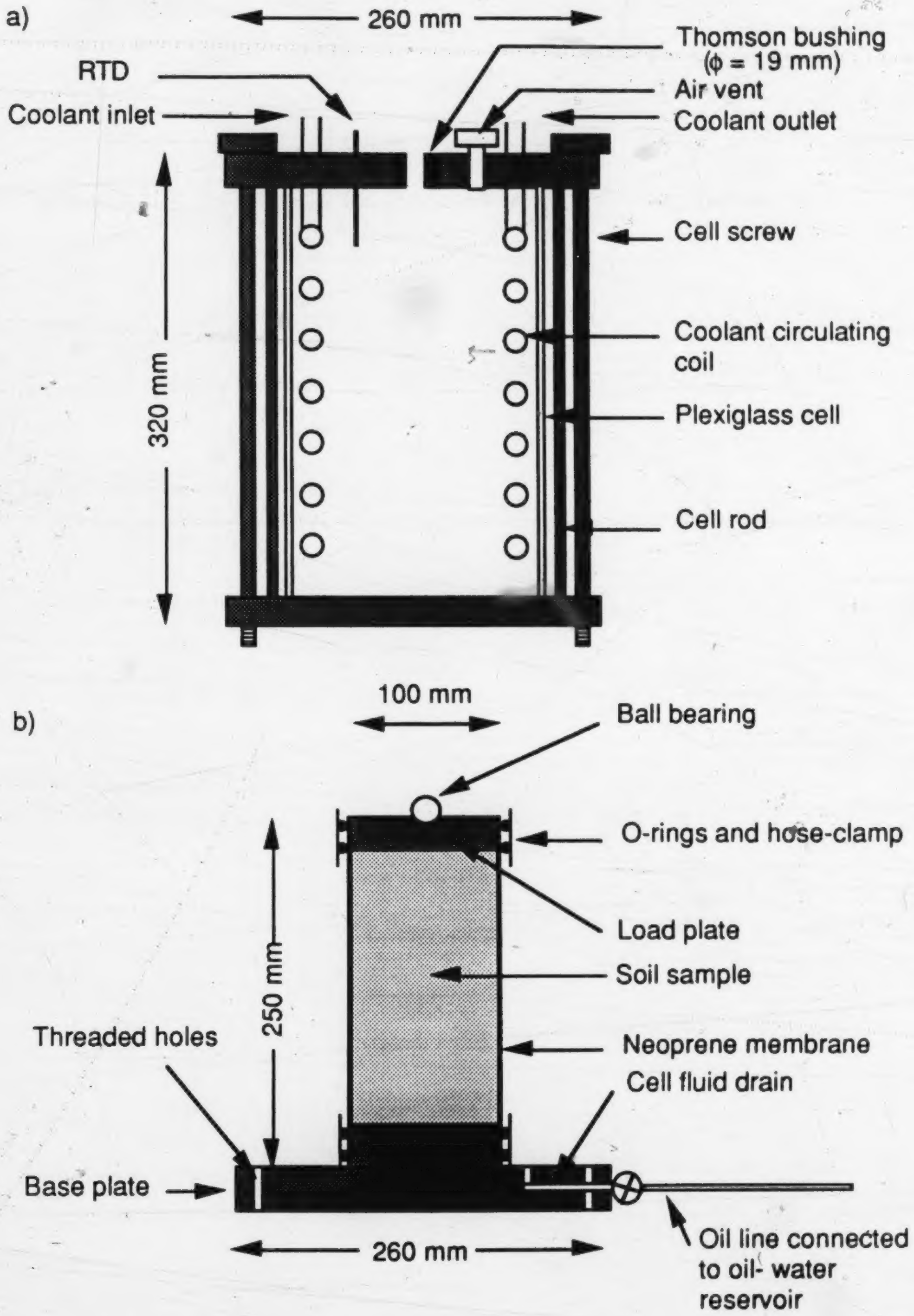
a)
260 mm
Thomson bushing
(ϕ = 19 mm)
RTD
Air vent
Coolant inlet
Coolant outlet
Cell screw
Coolant circulating coil
320 mm
Plexiglass cell
Cell rod
b)
100 mm
Ball bearing
O-rings and hose-clamp
Load plate
Soil sample
250 mm
Threaded holes
Neoprene membrane
Cell fluid drain
Base plate
260 mm
Oil line connected to oil- water reservoir

Figure 4.5: Modified triaxial cell: a) exterior cell layout b) sample setup

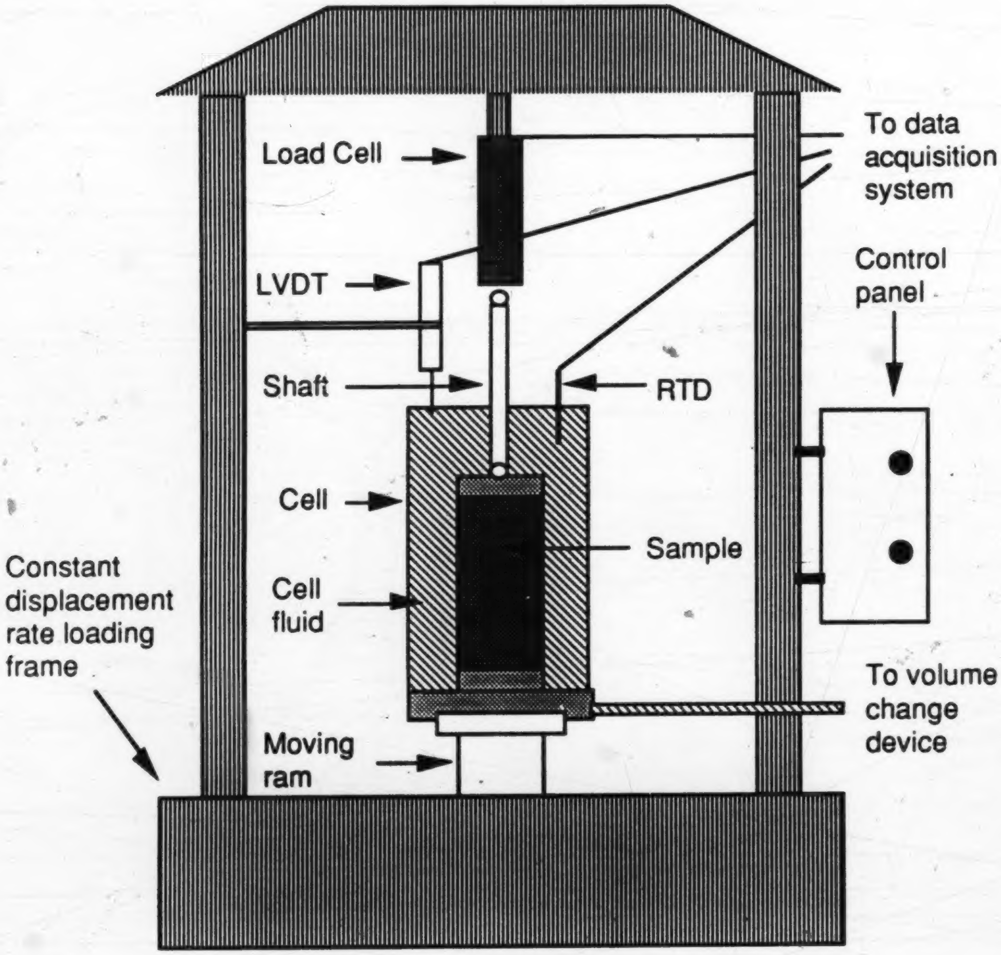
To data acquisition system
Load Cell
LVDT
Control panel
Shaft
RTD
Cell
Sample
Constant displacement rate loading frame
Cell fluid
To volume change device
Moving ram

Figure 4.6: Schematic of unconfined compression test set-up

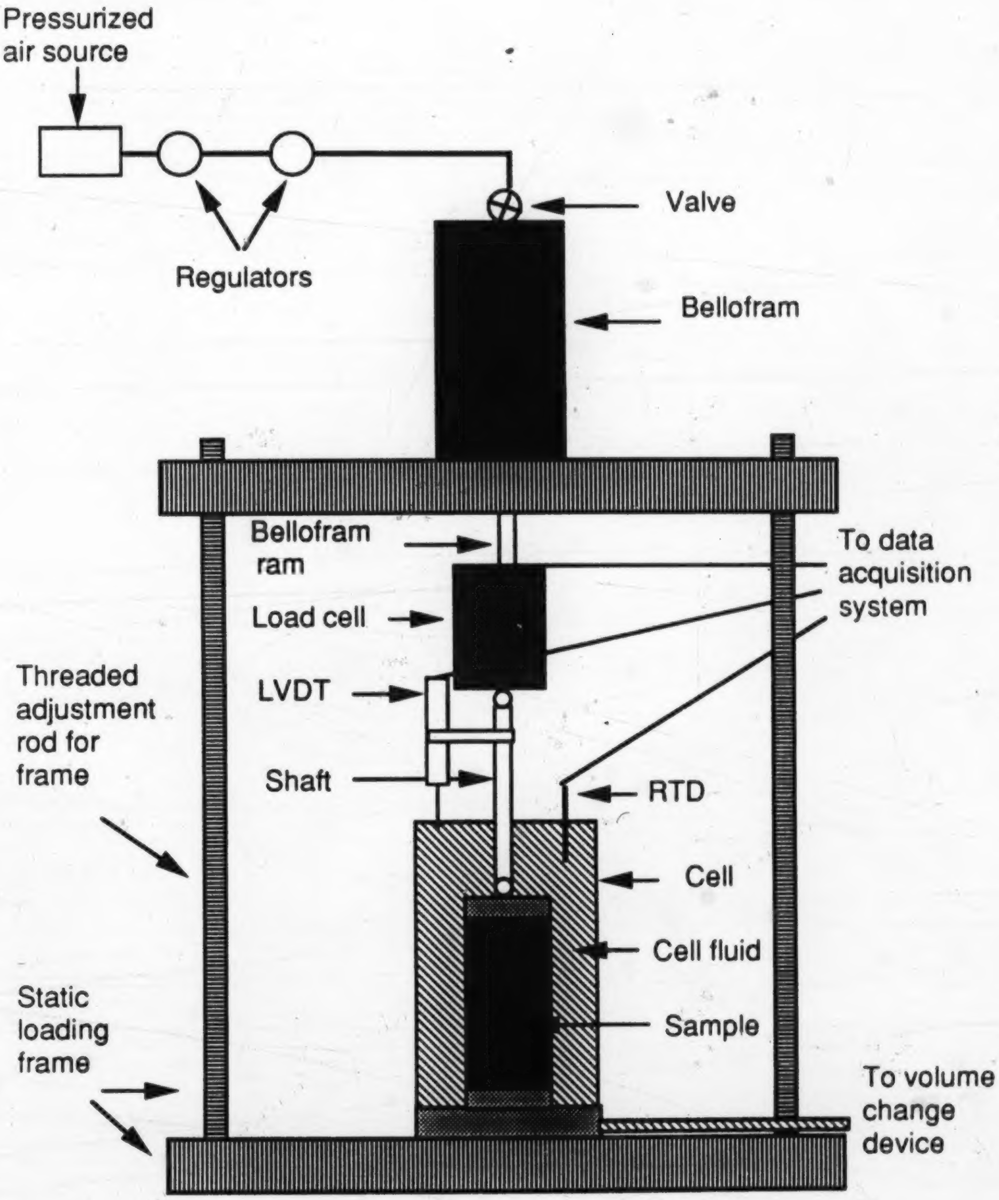
Pressurized air source
Valve
Regulators
Bellofram
Bellofram ram
To data acquisition system
Load cell
Threaded adjustment rod for frame
LVDT
Shaft
RTD
Cell
Cell fluid
Static loading frame
Sample
To volume change device

Figure 4.7: Schematic of constant stress compression test set-up

5. EXPERIMENTAL RESULTS

5.1. INTRODUCTION

In this chapter, the raw experimental results are presented. Analysis of the test results is presented in Chapter 6.

5.2. MOISTURE CONTENT, DENSITY AND SALINITY

For each sample tested in unconfined compression (constant strain rate or creep), the total density was evaluated prior to the start of the test and the gravimetric total moisture content was evaluated after the test at three locations in the sample (top, middle and bottom of sample). The total density was evaluated by measuring and weighing the sample. Moreover, the degree of saturation of each sample was evaluated assuming a value of G_s of 2.67. It should be kept in mind that the degree of saturation was calculated using values of the volume of water and not the volume of ice. Consequently, the 9% volume expansion of the water when it becomes solid is not considered. This explains the lower than 100% saturation values obtained. To convert water degree of saturation to ice degree of saturation, the value should simply be multiplied by 1.09. For the TDR samples, in addition to determine density, moisture content and saturation, the thawed salinity was also measured as described in Chapter 4.

Tables 5.1 and 5.2 present the total density, moisture content and degree of saturation values for the constant strain rate (CSR) and creep tests respectively. The results will be discussed for each soil type.

For Soil A, in the CST tests, the average density was 2.05 Mg/m^3, with a maximum value of 2.09 Mg/m^3 and a minimum value of 2.03 Mg/m^3. The mean degree of saturation was 88.2% (or 96.1% ice saturation). The average moisture content was 17.4% with an average variation of 0.8% within a given sample, i.e. between top, middle and bottom measurements. The maximum variation within a sample was 2.2%. For the creep tests, very similar values were obtained. The mean density was 2.06 Mg/m^3, with maximum and minimum values of 2.08 Mg/m^3 and 2.03 Mg/m^3 respectively. The average degree of saturation was 87.6% (or 95.5% ice saturation). The average moisture content value was 17.1% with an average and maximum variations of 0.7% and 3.5% respectively within the sample.

Soil B displayed similar values to those for Soil A. For the CSR tests, the average total density was 2.08 Mg/m^3 with maximum and minimum of 2.14 Mg/m^{3}and 1.99 Mg/m^3. The saturation was 89.0% (or 97.0% ice saturation) on average. Moisture content varied between 13.9% and 21.1% with an average of 16.6%. The variation within the sample was 1.7% on average with a maximum observed variation of 4%. For the creep samples, the mean density was 2.06 Mg/m^3 and varied between 2.09 Mg/m^3 and 2.04 Mg/m3. The mean saturation was 87.6% (95.5% ice saturation). The range of moisture content was from 14.5% to 20.6% with an average value of 16.8% and a mean and maximum variations of 1.4% and 4.2% respectively within the sample.

Soil C had a lower total density ranging between 1.94 Mg/m^3 and 2.01 Mg/m^3 with an average value of 1.98 Mg/m^3 for the CSR samples. The average saturation was 91.8% which is full ice saturation. The moisture contents were higher than for the other soils, varying from 19.2% to 27.5% with an average of 22.2%. In general the variations of the moisture content within the samples were more important with a mean value of 2.3% and a maximum value of 7.2%. The creep samples showed the same trends with an average moisture content of 1.96 Mg/m^3 , and maximum and minimum values of 1.98 Mg/m^3 and 1.93 Mg/m^3. The degree of saturation was 88.8% corresponding to ice saturation of 97.3%. The moisture content ranged between 19.0% and 25.5% averaging 22.1%. The variations within the samples were not as large as in the CSR samples with a mean variation of 2.0% and a maximum deviation of 5.2%.

Tables 5.3 and 5.4 present the moisture content, density, saturation and salinity of the TDR samples for 1988 and 1990 respectively. It should be kept in mind, as mentionned in Chapter 4, that no moisutre content correction was applied on the salinity measurements for the 1988 samples.

For 1988 TDR samples of Soil A, the moisture contents varied between 17% and 18.7% with small variations within the samples, and the total densities were equal to 2.05 Mg/m^3. The average degree of saturation was 86.2% (ice saturation 93.9%). The measured salinities were close to the nominal salinities. For the 1988 Soil B samples, the mean total density and moisture content were 2.06 Mg/m^3 and 16.5% respectively. No important variations of moisture content within the samples were observed. Sample B-5 had a relatively low degree of saturation 81.1% as compared to 87.3% and 91.9% for samples B-10 and B-30. Except for sample B-5, the measured salinities were within 20% of the nominal mixing salinity. For sample B-5, the measured salinity gave an average value of 8.6 ppt, which can be explained by the sample loosing moisture during storage. No moisture content measurement was carried out on the salinity sample which makes it impossible to verify if the lost of moisture was the real cause of salinity increase.

The 1990 TDR A samples had average total density and moisture content of 2.07 Mg/m^3 and 16.4% respectively. Except for sample A-30 which underwent severe fluid migration at warm temperatures during testing, the moisture content did not vary significantly throughout the samples. Samples A-0, A-5, A-10 had a degree of saturation of 88.0%. Sample A-30 had a lower saturation of 85.4%. However, as previously stated since the sample was completely thawed at the end of the TDR testing much moisture was lost and the measured values are undoubtedly too low. The moisture content of each salinity sample was measured allowing the corrected salinity values to be measured. These corrected values gave salinities close to the mixing salinities within the precision of the refractometer (± 1 ppt). To evaluate the corrected salinity for the moisture content of the salinity sample, the following equation should be applied;

$$\text{Corrected salinity} = \frac{\text{m.c.}_{\text{salinity sample}}}{\text{average m.c.}_{\text{m.c. sample}}} \times \text{measured salinity} \tag{5.1}$$

The 1990 TDR B samples densities ranged from 2.07 Mg/m^3 to 2.12 Mg/m^3 with an average of 2.09 Mg/m^3. The average moisture content and degree of saturation were 16.0% and 88.3% respectively. As for Sample A-30, Sample B-30 underwent severe downward migration of the unfrozen water at warm temperatures causing an important lost of moisture at the top of the sample explaining the low moisture content at this location. This value was excluded from the averaging and saturation calculations. For Samples B-5 and B-30, the corrected salinities are within 1 ppt (precision of the refractometer) of the nominal values. Sample B-10 had corrected measured salinities approximately 20% to 30% higher than the mixing salinities.

The 1990 TDR C samples had relatively low densities averaging 1.92 Mg/m^3 and relatively high moisture content with a mean of 23.9%. The degree of saturation is usually high (average 89.3%) except for sample C-5 which had a degree of saturation of 82.7%. Sample C-30 did not display the same low moisture content at the top of the sample because the permeability of Soil C was lower than for Soils A and B limiting the downward movement of water at warm temperatures. The corrected salinities were within 1 ppt of the nominal salinities except for the bottom samples of C-10 and C-30 which displayed salinities 20% to 30 % higher than the mixing values.

In general the measured salinities even after a correction for moisture content were slightly higher than the mixing salinities. This situation can be explained by ice sublimation. Even if the samples were wrapped in plastic bags, air could get in contact with the samples surfaces causing ice sublimation during the 3 weeks of TDR testing. This decrease in moisture caused a relative increase in salt content resulting in an increased salinity.

Despite the small variations within samples, the distribution of salinity was fairly uniform and the measured salinity was close to the mixing nominal salinity. This shows that the freezing method using liquid nitrogen to achieve very fast rates of freezing was succesful in avoiding salt rejection and an uneven salinity distribution.

As it will be explained in Section 5.4, some additional tests were run to study the behaviour at large strains and the effect of density on the strength. The physical properties of these samples are presented in Table 5.5. Samples for tests A, B and F were used to determine the stress-strain behaviour at large strains. The physical properties of these samples were consistent with the physical properties of the same soils from the main testing program. Samples from tests C, D, E, G and H which were used to study the influence of density on strength, had densities varying between 1.93 Mg/m^3 and 2.08 Mg/m^3, with degree of saturation between 80.8% to 89.4%.

5.3. UNFROZEN WATER CONTENT

The unfrozen water content was determined using time-domain-reflectometry as explained in Chapter 4. Two series of test were carried out, the first one in 1988, the second in 1990. In 1988, only Soils A and B were tested. Table 5.6 presents the results from both series of tests and Figures 5.1 and 5.2 illustrate the variation of unfrozen water content with temperature for each soil type for 1988 and 1990 respectively. In order, to examine the consistency of the results, a comparison of the two sets of data are presented in Figures 5.3 and 5.4 for Soils A and B.

The unfrozen water content increases with an increase in salinity and temperature for all soils. For temperature lower than -7°C, the variation of the unfrozen water content with temperature is small. The comparison between the 1988 and 1990 results shows good consistency. For Soil A, Figure 5.3 shows that for salinities of 5 ppt and 10 ppt, the differences between the two sets of readings are less than 1.5%, except at a temperature of -1°C where the differences are 3% for a salinity of 5 ppt and 3.8% for a salinity of 10 ppt. For a salinity of 30 ppt, the difference increase from about 1% at -12°C to 3% at -2°C. Figure 5.4 displays the good agreement between 1988 and 1990 results for Soil B with salinities of 5 and 10 ppt. The maximum difference is about 2%. For both series of test, a reading at -1°C was not possible for sample A-10. For a salinity of 30 ppt, the difference are quite significant. For the range of temperature of -6°C to -12°C, the 1990 unfrozen water content are approximately 5% larger than the 1988 values. For temperature between -4°C and -1°C, the opposite situation occurs, and the 1988 values are larger than the 1990 ones by up to 10% at -2°C. It is believed that the 1988 values at warm temperatures, when the sample is practically thawed, are excessively high since the total volumetric water content for Soil B-30 is 31.3%. Figure 5.5 present the average unfrozen water content using results from both series of tests for Soils A and B. The 1988 values for B-30 at -2°C and -1°C were rejected. This averaging process is possible since for each soil the difference in total moisture content is never greater than 1.5%.

Figure 5.6 presents the influence of soil type or grain size on the unfrozen water content for each studied salinity. For Soils A and B, the average values from 1988 and 1990 were used. A decrease in grain size causes a small increase in unfrozen water content. It should be kept in mind that the variation in soil type is not very large since only sands or sandy silts were studied. In general, a consistent increase of unfrozen water can be observed from Soil A to Soil B to Soil C. The only exception is for Soils A and B at a salinity of 10 ppt. In this case, the unfrozen water content for the two soils are practically equal at temperatures warmer than -7°C.

5.4. UNCONFINED CONSTANT STRAIN RATE COMPRESSION TEST RESULTS

Over a hundred unconfined compression strength tests were performed, in order to determine the influence of salinity and temperature on the strength of the three selected soils. All tests were conducted at a strain rate of 0.8 %/hour.

Results of all the tests are given in Table 5.7. Where data was not available the value is omitted and when the results are uncertain a question mark is inserted beside the value. Figure 5.7 shows a typical stress-strain curve for each soil at a temperature of -10°C. The stress-strain, temperature vs strain and volume change vs strain curves from all the tests are presented in Appendix B. The difference in the stress-strain behaviour between Soil A and Soils B and C is important to identify. Soil A behaves in a brittle manner with strain-weakening after the peak resistance is attained. As for Soils B and C, they display a strain-strengthening behaviour after an initial yield point at a strain of approximately 1%. This initial yield is believed to represent the onset of failure of the ice matrix. Since Soils B and C do not reach a maximum resistance, an arbitrary resistance had to be selected to represent the soil strength. The resistance at 10% strain was chosen and will be referred to as the 10% strength.

Figure 5.8 illustrates the variation of strength (peak for Soil A and 10% for Soils B and C) as a function of temperature. Figure 5.9 gives the same variation for the yield strength for Soils B and C. The results are also presented as a function of salinity in Figures 5.10 and 5.11. For a given salinity, the strength decreases with an increase in temperature. This effect is not very pronounced for a salinity of 30 ppt. For Soil A, the largest portion of the strength loss with an increase in salinity occurs between 0 and 5 ppt. Approximately 65% of the strength is lost with this increase of salinity. For Soils B and C, the loss of strength is more gradual as the salinity increases.

Since the material is not linear elastic (i.e. recoverable deformations), it is difficult to define a modulus of deformation. It was decided that a secant modulus would be used to compare the Soils. For Soil A, the secant modulus was defined as the slope of the line joining the initial point on the stress-strain curve to the point at 50% of the strain to failure, which gave a line almost tangent to the initial part of the stress-strain curve. This modulus will be referred to as the secant modulus at 50% strain to failure, $E_{s50\%}$. For Soils B and C, the secant modulus was taken as the slope of the line joining the initial point of the stress-strain curve to the initial yield point. Since a wide scatter exist in the modulus values, it was decided to use average values in all the plots. Moreover, the questionable values were rejected from the averaging process. Figure 5.12 and 5.13 present the variation of the modulus with temperature and salinity respectively.

For Soil A, there is a decrease in modulus with an increase in temperature (Figure 5.12). The major loss in modulus takes place between temperatures of -10°C and -7°C. The value of the modulus for Soil A-5 at -12°C is considered to be questionable. For Soil A-30, the modulus does not vary significantly with a change in temperature as compared to the other salinities. Soil B displays the same general trend, except for Soils B-5 and B-10 which have modulus values almost equal at -7°C and -5°C. Soil C also undergoes a decrease in modulus with an increase in temperature.

For Soil A at all temperatures, a major decrease in modulus with an increase in salinity is observed between salinities of 0 to 5 ppt (Figure 5.13). The values of the moduli at -12°C and -10°C, as well as at -7°C and -5°C are almost equal. For Soil B, there is also a general trend that shows that the modulus decreases with an increase in salinity. The moduli values for temperatures of -7°C and -5°C are practically equal except for Soil B-0 at -5°C which shows a low value. For Soil C, a decrease in modulus with an increase in salinity is also observed.

The volumetric change of the sample, measured by cell fluid displacement, was monitored in most tests. It should be kept in mind that this measuring method does not measure the actual volume change but simply the amount of fluid displaced during sample deformation. Figure 5.14 shows the volume change versus strain for the same three tests as presented in Figure 5.7. These are typical of volumetric deformations for most tests. Soil A displays a dilatant behaviour starting at a strain level between 1% and 2%. The total volume change varied between 150 to 200 ml for a total strain between 14% to 16%. The volumetric deformations do not vary significantly with either temperature or with salinity. Soil B present a very similar volumetric change behaviour. However, Soil B does not dilate as much as Soil A. In general the total volume increase varies between 20 ml to 50 ml at a strain level of 15%. The onset of the dilatancy occurs at strains slightly larger, i.e. between strains of 1 to 4%. For Soil C, the total dilatancy varies between 10 ml to 25 ml at a strain of 15%. Dilatancy usually starts at a strain of 2 to 3%, for this soil. As for Soil A, Soils B and C the volumetric deformations do not seem to be affected by a variation of temperature or salinity. As can be seen from the test results, Soil B and C sometimes display a very small decrease in volume at the very start of the test (1 ml to 3 ml). The author believes that these small decreases in volume are caused by some adjustment in the measuring system at the beginning of the test.

After completion of the initially planned testing, some additional tests were run to investigate two aspects of the behaviour of the frozen soils under constant strain rate compression; first, the strain level at which Soils B and C would experience a drop in strength, i.e. these tests were continued to a strain level of up to 25%; and secondly, the influence of density on the yield and 10% strength. Table 5.8 presents the results of these tests. Figure 5.15 shows the results of the large strain tests on Soils B-30 and C-30. It is interesting to note that no loss of strength was observed even at strain levels greater than 20%. Figure 5.16 demonstrates that for Soils B-5 and C-5 there is some strain-weakening at a strain level of approximately 16%. For these two sets of tests, the volume changes were not measured. Figure 5.17 shows the results of the five tests run on Soil B-5 at different densities, at a temperature of -7°C. Figure 5.18 a) is a plot of the 10% strength as a function of the total density and Figure 5.18 b) present the variation of the secant modulus with density. In these figures, results from tests 65, 71 and 75 were also included since they were tests of the same material at the same temperature. A general decrease in 10% strength is observed with a decrease in density. The secant modulus is shown to be independent of density. As for the yield strength, Figure 5.19a) shows its variation with respect to total density, and Figure 5.19b) presents yield strength versus moisture content. No significant variation of yield strength is observed except at very low density or high moisture content.

5.5. CONSTANT STRESS COMPRESSION TEST RESULTS

A total of 43 creep tests were run at a temperature of -7°C. The stress level was chosen as a percentage of the peak strength or the 10% strength. Except for soils of salinities of 30 ppt, the percentage of strength varied between 50% to 120%. For soils at a salinity of 30 ppt, higher percentage of the strength had to be used. Table 5.9 presents the results of all creep tests. The strain vs time, strain rate vs time and temperature and volume change (when measured) vs time plots from all tests are shown Appendix C. Figure 5.20 shows an example of the strain versus time for each type of soil and Figure 5.21 presents the log strain rate versus log time for the same tests. Time to failure, strain to failure or strain rate to failure are defined as the point where acceleration in the strain rate is observed, i.e. the point of minimum strain rate.

The temperature control for these tests was slightly more difficult, since the copper cooling coil had to be removed from the cells, to allow more room for sample deformation. However, for the valid tests, a temperature variation of less than ±0.3°C could be achieved, in most cases. As explained in Chapter 3, a lot of controversy exists in the literature between the concepts of secondary creep (steady-state creep) or minimum strain rate. In general, the author believes that a real constant strain rate does not develop as can be seen in Appendix C. However, some tests displays a very small variation of the strain rate with time and consequently a pseudo secondary strain rate could be estimated. In Table 5.9, the author uses the term minimum strain rate to indicate the strain rate developped just before failure or acceleration of the strain rate. The strain rate was calculated using a five point linear regression.

It should be noted that Soils B and C at a salinity of 30 ppt did not reach failure, and that a continously decreasing strain rate was observed up to a strain of at least 20%. Consequently, an arbitrary strain level had to be chosen; a strain level of 12% was selected to compare strain rates. From Table 5.9, a few observation can be made. Firstly, in general the strain to failure seems relatively independent of stress level. For all soils, a decrease in stress causes a decrease in the minimum strain rate and an increase in time to failure.

It should be mentioned that the creep results from test CR-76 had to be corrected since the LVDT ran out of travel at a strain of approximately 13%, preventing the sample from further straining. The original and corrected strain vs time curves for test CR-76 are shown in Figure 5.22.

The volume change during testing was not measured for each test. In cases where it was measured the following observations were made; Soil A displayed a dilatant behaviour practically from the start of the test; for Soils B and C, the paucity of the results makes establishing a trend very difficult; however, the author believes that for some tests it could be suggested that contractant behaviour takes place up to failure where dilatancy starts. However, the observations are not conclusive since the amount of observations is insufficient.

TABLE 5.1
PHYSICAL PROPERTIES OF STRENGTH SAMPLES

Test	Soil	γ_{total} (Mg/m^3)	S_r (%)	e	Top M.C. * (%)	Middle M.C. (%)	Bottom M.C. (%)
27	A-0	2.03	87.0	0.56	17.3	17.5	19.5
28	A-0	2.05	88.3	0.53	16.9	17.2	19.0
36	A-0	2.06	89.4	0.52	16.9	16.7	18.7
49	A-0	2.06	89.4	0.52	16.5	17.7	18.1
62	A-0	2.06	---	---	---	---	---
76	A-0	2.04	89.9	0.55	17.4	19.0	19.2
82	A-0	2.06	90.3	0.53	17.0	18.3	18.7
87	A-0	2.04	90.6	0.55	19.2	19.3	17.9
93	A-0	2.04	89.7	0.55	18.0	18.3	19.2
140	A-0	2.02	85.3	0.55	18.1	17.6	17.1
23	A-5	2.06	87.0	0.52	16.9	16.2	17.4
43	A-5	2.07	87.9	0.51	16.4	16.9	16.8
53	A-5	2.05	87.3	0.52	17.1	16.6	17.5
60	A-5	2.04	87.2	0.54	16.7	18.1	18.4
66	A-5	2.04	87.7	0.53	17.5	17.8	17.4
90	A-5	2.09	88.6	0.48	15.5	16.2	16.0
95	A-5	2.04	87.1	0.53	17.1	17.1	17.9
19	A-10	2.06	88.4	0.53	16.9	17.6	17.7
37	A-10	2.07	87.7	0.51	16.4	16.7	16.8
42	A-10	2.06	87.0	0.51	16.1	16.8	17.2
52	A-10	2.05	87.1	0.53	17.1	17.5	17.2
74	A-10	2.06	88.7	0.52	17.0	16.8	17.6
80	A-10	2.05	89.2	0.54	17.9	18.0	18.0
86	A-10	2.06	87.5	0.52	16.7	17.1	17.4
137	A-10	2.04	88.3	0.54	17.4	17.2	19.0
26	A-30	2.05	---	---	---	---	---
45	A-30	2.05	87.4	0.53	16.4	17.3	18.6
56	A-30	2.05	87.9	0.53	17.5	17.1	17.9
70	A-30	2.05	89.6	0.54	17.9	18.5	18.1
83	A-30	2.07	88.1	0.50	17.3	14.6	17.7
91	A-30	2.08	88.6	0.49	16.7	15.5	16.7
21	B-0	2.12	88.3	0.45	14.3	14.5	15.8
25	B-0	2.09	86.7	0.48	15.1	14.8	16.8
35	B-0	2.06	87.5	0.52	15.8	16.5	18.4
41	B-0	2.06	87.3	0.51	15.9	16.1	18.3
51	B-0	2.12	90.0	0.45	14.1	14.8	16.2
55	B-0	2.11	88.4	0.45	13.8	15.2	16.0
63	B-0	2.09	89.0	0.48	15.2	16.4	16.7
64	B-0	2.06	86.7	0.51	16.1	17.5	16.2
78	B-0	2.08	90.5	0.50	15.8	16.6	18.4
88	B-0	2.07	91.0	0.52	15.9	17.0	19.9
97	B-0	2.09	92.5	0.50	16.1	16.6	19.4

Table 5.1 (con't)

Test	Soil	γ_{total} (Mg/m^3)	S_r (%)	e	Top M.C. (%)	Middle M.C. (%)	Bottom M.C. (%)
16	B-5	2.03	85.3	0.55	16.2	17.9	18.3
30	B-5	2.05	86.0	0.53	15.4	17.7	17.7
47	B-5	2.10	91.1	0.48	15.9	16.4	17.0
57	B-5	2.09	89.5	0.49	15.6	16.5	17.2
65	B-5	2.03	87.6	0.55	17.3	18.5	18.7
71	B-5	2.10	88.8	0.48	14.9	15.3	17.3
75	B-5	2.09	88.5	0.48	14.8	16.1	17.1
89	B-5	2.09	88.0	0.48	15.1	15.8	17.0
94	B-5	2.09	90.4	0.49	15.6	16.2	17.7
111	B-5	2.11	91.0	0.47	15.2	15.7	16.9
128	B-5	2.12	88.9	0.45	14.3	15.0	15.8
15	B-10	2.00	83.9	0.57	16.9	18.6	18.5
34	B-10	2.07	88.0	0.50	16.0	16.6	16.8
50	B-10	2.05	86.8	0.53	15.9	17.1	18.3
67	B-10	2.01	87.5	0.58	18.4	19.4	19.6
77	B-10	2.03	92.7	0.58	19.7	20.0	20.3
105	B-10	2.14	93.1	0.44	15.0	15.5	15.5
129	B-10	2.11	90.4	0.46	14.8	15.6	16.3
134	B-10	2.11	95.5	0.49	15.2	20.5	16.5
13	B-30	2.06	88.4	0.51	16.0	17.0	17.9
14	B-30	2.05	85.7	0.52	15.0	17.4	17.5
54	B-30	2.06	84.0	0.50	14.6	15.4	17.1
59	B-30	2.07	91.4	0.52	16.5	17.6	18.9
69	B-30	2.06	85.7	0.51	15.3	16.1	17.3
73	B-30	2.07	87.0	0.50	15.1	15.9	17.6
79	B-30	2.06	89.6	0.53	16.4	17.6	19.2
81	B-30	2.07	90.3	0.52	16.7	17.4	18.3
84	B-30	1.99	89.8	0.62	21.1	21.2	20.7
85	B-30	2.12	90.1	0.46	14.3	15.9	16.0
96	B-30	2.12	89.1	0.44	13.8	14.9	15.6
104	B-30	2.10	89.6	0.48	16.9	15.9	15.5
112	B-30	2.12	90.4	0.45	14.7	15.3	15.3
113	B-30	2.10	87.9	0.47	14.2	15.5	16.8
114	B-30	2.10	91.0	0.48	16.6	16.5	16.6
115	B-30	2.13	91.9	0.45	14.8	15.5	16.2
117	B-30	2.11	90.1	0.47	14.4	15.7	17.0
141	B-30	2.09	88.1	0.48	15.2	16.1	16.6
98	C-0	1.95	89.3	0.68	20.8	21.8	25.4
102	C-0	1.96	90.0	0.67	20.6	23.2	24.4
106	C-0	1.97	91.6	0.66	20.7	23.6	23.4
109	C-0	1.95	92.4	0.70	21.4	23.9	27.2
122	C-0	1.94	92.1	0.71	20.3	25.6	27.5
124	C-0	1.98	92.7	0.65	20.3	22.4	24.7
126	C-0	1.98	90.7	0.64	19.8	21.8	23.3

Table 5.1 (con't)

Test	Soil	γ_{total} (Mg/m^3)	S_r (%)	e	Top M.C. (%)	Middle M.C. (%)	Bottom M.C. (%)
133	C-0	2.00	90.2	0.61	22.2	20.4	19.7
135	C-0	1.99	87.6	0.60	23.8	16.5	19.2
100	C-5	1.97	92.5	0.66	20.4	22.9	25.7
107	C-5	1.96	92.5	0.69	21.9	24.0	26.1
121	C-5	1.97	89.0	0.65	21.1	23.7	20.3
123	C-5	1.99	93.1	0.64	20.4	22.3	24.3
130	C-5	1.99	91.1	0.63	23.3	21.1	19.6
99	C-10	1.99	94.0	0.65	24.5	23.1	21.1
101	C-10	1.99	92.2	0.64	23.3	21.2	21.6
110	C-10	2.00	94.3	0.64	21.6	21.9	24.0
116	C-10	2.00	92.3	0.62	20.0	21.4	23.1
120	C-10	1.99	92.5	0.64	20.6	21.7	24.1
125	C-10	2.01	92.2	0.60	19.3	20.0	23.3
127	C-10	2.01	92.8	0.60	19.8	20.4	22.8
132	C-10	2.01	93.1	0.62	19.9	20.8	23.9
139	C-10	1.97	91.5	0.66	21.5	22.4	24.3
103	C-30	1.99	93.8	0.65	21.4	22.2	25.0
108	C-30	1.99	92.9	0.65	20.5	22.5	24.5
118	C-30	1.97	93.3	0.68	21.9	23.7	25.5
119	C-30	2.00	92.0	0.63	23.0	21.4	20.4
138	C-30	2.00	91.3	0.61	19.7	20.3	22.9

*: moisture content

TABLE 5.2
PHYSICAL PROPERTIES OF CREEP SAMPLES

Test	Soil	γ_{total} (Mg/m^3)	S_r (%)	e	Top M.C. (%)	Middle M.C. (%)	Bottom M.C. (%)
CR-45	A-0	2.051	87.9	0.53	16.6	18.1	17.5
CR-92	A-0	2.066	88.2	0.51	16.9	17.1	16.6
CR-95	A-0	2.075	87.7	0.50	16.9	16.5	15.9
CR-59	A-5	2.069	87.7	0.50	16.2	16.8	16.7
CR-51	A-5	2.072	93.6	0.53	16.8	20.3	18.3
CR-60	A-5	2.058	86.4	0.51	16.7	16.6	16.5
CR-67	A-5	2.047	87.7	0.53	17.3	17.8	17.4
CR-86	A-10	2.074	89.2	0.50	16.5	16.6	17.4
CR-47	A-10	2.070	89.6	0.51	17.5	17.3	16.7
CR-87	A-10	2.049	88.6	0.53	17.1	17.7	18.4
CR-64	A-30	2.049	---	0.56	---	---	---
CR-70	A-30	2.063	87.7	0.51	17.1	16.4	16.9
CR-72	A-30	2.03	84.2	0.54	16.3	18.0	16.7
CR-83	B-0	2.055	86.6	0.52	15.6	16.8	17.9
CR-71	B-0	2.062	89.3	0.52	16.2	16.7	19.3
CR-81	B-0	2.071	87.0	0.50	15.9	16.6	16.3
CR-84	B-5	2.062	85.4	0.50	15.1	16.1	17.1
CR-49	B-5	2.064	89.4	0.52	16.4	17.0	18.6
CR-9	B-5	2.053	84.4	0.51	14.5	16.3	17.6
CR-17	B-5	2.056	83.5	0.50	14.8	15.5	16.9
CR-32	B-5	2.060	86.0	0.51	14.9	16.5	17.7
CR-82	B-10	2.092	88.9	0.48	15.7	16.3	16.0
CR-50	B-10	2.056	92.1	0.54	16.4	19.0	20.6
CR-33	B-10	2.069	---	0.55	---	---	---
CR-38	B-10	2.083	89.6	0.49	16.0	16.2	17.6
CR-75	B-30	2.062	90.3	0.52	16.8	18.1	18.3
CR-77	B-30	2.068	89.0	0.51	16.5	17.2	17.4
CR-88	B-30	2.038	85.1	0.53	15.7	17.2	18.0
CR-79	C-0	1.953	88.1	0.67	19.6	21.8	24.8
CR-65	C-0	1.961	88.4	0.66	22.8	21.8	20.8
CR-36	C-0	1.958	---	---	---	---	---
CR-96	C-5	1.974	89.0	0.64	20.8	21.3	22.1
CR-66	C-5	1.961	88.7	0.66	19.8	22.4	23.6
CR-62	C-5	1.957	88.5	0.66	21.0	21.5	23.6
CR-89	C-5	1.965	88.2	0.65	20.1	21.0	23.4
CR-94	C-5	1.967	87.0	0.64	19.0	21.1	22.6
CR-55	C-10	1.952	88.2	0.67	20.3	22.1	24.1
CR-52	C-10	1.966	91.5	0.67	24.4	22.8	21.6
CR-68	C-10	1.962	88.4	0.66	19.9	22.2	23.2
CR-76	C-30	1.965	90.4	0.66	22.0	22.5	23.0
CR-78	C-30	1.951	89.0	0.68	21.6	22.5	23.7
CR-91	C-30	1.934	88.8	0.70	21.3	23.4	25.5

TABLE 5.3
PHYSICAL PROPERTIES of 1988 TDR SAMPLES

Soil	γ_{total} (Mg/m^3)	S_r (%)	e	Sample Location	M.C. (%)	Measured Salinity (ppt)
A-5	---	---	---	Top	17.8	5.2
				Middle	18.5	---
				Bottom	19.7	4.6
A-10	2.05	87.4	0.53	Top	16.5	9.8
				Middle	17.9	---
				Bottom	17.2	12.0
A-30	2.04	85.5	0.53	Top	17.2	28.1
				Middle	17.4	---
				Bottom	16.4	27.7
B-5	2.04	81.1	0.52	Top	15.6	9.9
				Middle	15.7	6.6
				Bottom	16.3	8.7
B-10	2.08	87.3	0.49	Top	15.4	12.8
				Middle	15.8	12.3
				Bottom	16.2	12.5
B-30	2.07	91.9	0.52	Top	17.0	32.7
				Middle	18.3	29.3
				Bottom	18.1	31.0

TABLE 5.4-a
PHYSICAL PROPERTIES of 1990 TDR MOISTURE CONTENT SAMPLES

Soil	γ_{total} (Mg/m^3)	S_r (%)	e	Top M.C. (%)	Middle M.C. (%)	Bottom M.C. (%)
A-0	2.067	88.0	0.51	17.7	16.1	16.5
A-5	2.061	88.1	0.52	16.8	17.3	17.1
A-10	2.095	88.0	0.47	15.0	16.0	16.0
A-30	2.072	85.4	0.49	10.7	16.1	21.2
B-0	2.072	86.5	0.50	14.7	16.4	17.5
B-5	2.078	85.3	0.48	14.6	15.5	16.2
B-10	2.119	89.4	0.45	15.1	14.8	15.4
B-30	2.081	91.8	0.50	---	16.7	17.6
C-0	1.952	87.7	0.66	19.7	21.3	23.9
C-5	1.902	82.7	0.71	20.1	22.0	24.0
C-10	1.887	90.1	0.79	24.9	28.4	26.9
C-30	1.918	90.1	0.74	22.1	26.1	27.2

TABLE 5.4-b
PHYSICAL PROPERTIES of 1990 TDR SALINITY SAMPLES

Soil	Top M.C. (%)	Bottom M.C. (%)	Measured Salinity Top (ppt)	Measured Salinity Bottom (ppt)
A-5	17.6	17.4	5.7	6.1
A-10	15.6	16.5	10	10.3
A-30	12.5	20.3	29.9	31.6
B-5	15.5	15.7	6.2	5.9
B-10	14.6	15.0	13.1	11.8
B-30	11.5	16.5	30.7	30.9
C-5	21.0	21.7	6	6.1
C-10	25.1	27.5	10.8	11.9
C-30	23.3	25.6	30.9	31.7

TABLE 5.5
PHYSICAL PROPERTIES of ADDITIONAL TESTS

Test	Soil	γ_{total} (Mg/m^3)	e	S_r (%)	Top M.C. (%)	Middle M.C. (%)	Bottom M.C. (%)
A	B-30	2.056	0.51	86.3	15.7	16.6	17.5
B	C-5	1.960	0.65	86.9	19.4	20.7	23.6
C	B-5	2.033	0.54	84.9	16.1	16.9	18.4
D	B-5	2.045	0.52	85.0	15.4	16.8	17.7
E	B-5	2.003	0.57	83.7	16.6	18.5	18.7
F	C-30	1.940	0.68	86.4	20.0	22.1	23.8
G	B-5	1.932	0.71	89.4	24.4	23.9	23.2
H	B-5	2.080	0.46	80.8	13.1	14.2	14.8

TABLE 5.6
UNFROZEN WATER CONTENT RESULTS from the 1988 and 1990 TDR TESTING PROGRAMS

Year	Soil	Temperature (°C)	θ_u (% vol.) for 0 ppt	θ_u (% vol.) for 5 ppt	θ_u (% vol.) for 10 ppt	θ_u (% vol.) for 30 ppt
1990	A	-12	0	0.51	1.40	7.50
	A	-11	0	0.48	1.51	7.93
	A	-10	0	0.41	1.72	8.49
	A	-9	0	1.01	2.41	8.89
	A	-8	0	1.30	2.82	9.40
	A	-7	0	1.07	3.06	10.3
	A	-6	0	1.01	3.31	11.2
	A	-5	0	1.22	4.42	12.2
	A	-4	0	2.00	5.48	14.1
	A	-3	0	3.27	6.70	16.7
	A	-2	0	3.98	9.42	23.0
	A	-1	0	8.55	---	32.8
	B	-12	2.20	2.21	2.40	11.0
	B	-11	2.25	2.28	2.77	12.0
	B	-10	2.08	2.41	2.67	13.0
	B	-9	2.23	2.72	3.21	13.8
	B	-8	2.35	3.00	3.42	14.2
	B	-7	2.43	3.20	3.37	14.5
	B	-6	2.63	3.32	4.07	15.3
	B	-5	2.87	3.42	5.36	17.6
	B	-4	2.97	3.85	5.99	21.3
	B	-3	3.07	4.40	7.08	20.8
	B	-2	3.81	5.23	10.1	21.0
	B	-1	4.89	9.16	19.1	---
	C	-12	3.00	3.50	3.80	12.7
	C	-11	3.12	3.48	3.93	13.0
	C	-10	3.30	3.59	4.10	14.8
	C	-9	4.26	4.46	5.32	16.3
	C	-8	4.77	5.29	6.15	17.8
	C	-7	5.00	6.08	6.71	19.6
	C	-6	5.14	6.50	7.59	23.2
	C	-5	5.40	6.80	8.23	27.1
	C	-4	6.00	7.42	9.35	30.3
	C	-3	5.86	8.11	10.2	35.6
	C	-2	6.30	8.81	15.2	---
	C	-1	7.81	12.6	21.6	---

Table 5.6 (con't)

Year	Soil	Temperature (°C)	θ_u (% vol.) for 0 ppt	θ_u (% vol.) for 5 ppt	θ_u (% vol.) for 10 ppt	θ_u (% vol.) for 30 ppt
1988	A	-12		1.23	3.04	6.60
	A	-11		1.50	2.79	6.37
	A	-10		1.65	2.96	7.27
	A	-9		1.85	2.85	7.93
	A	-8		1.46	3.78	8.30
	A	-7		1.65	4.16	8.40
	A	-6		1.67	4.61	8.54
	A	-5		2.34	5.88	8.96
	A	-4		3.20	7.12	10.5
	A	-3		3.95	9.10	13.1
	A	-2		4.54	14.5	20.0
	A	-1		5.77	---	35.2
	B	-12		1.51	4.38	6.81
	B	-11		2.48	4.17	7.04
	B	-10		2.97	4.43	7.50
	B	-9		3.40	5.01	7.79
	B	-8		3.88	5.66	8.62
	B	-7		4.02	5.37	9.32
	B	-6		3.80	5.61	10.7
	B	-5		4.56	6.14	16.3
	B	-4		4.77	6.81	23.4
	B	-3		5.66	7.82	32.6
	B	-2		6.01	9.70	41.3
	B	-1		9.18	20.5	45.8

TABLE 5.7
CONSTANT STRAIN RATE COMPRESSION TEST RESULTS

Test	Soil	T (°C)	σ_{max} (kPa)	ε_{max} (%)	$E_{s\,50\%}$ (MPa)
49	A-0	-12	6156	4.2	221
93	A-0	-12	6034	4.1	245
53	A-5	-12	2429	3.1	112
60	A-5	-12	2184	3.1	101
95	A-5	-12	2200	3.7	89.1
52	A-10	-12	1307	2.4	82.9
56	A-30	-12	860	5.2	28.0
28	A-0	-10	5789	3.4	281
36	A-0	-10	5684	4.9	149
87	A-0	-10	5957	4.0	244
43	A-5	-10	1981	2.9	80.7
90	A-5	-10	2148	3.3	130
37	A-10	-10	1124	2.7	55.6
42	A-10	-10	1204	2.0	84.0
45	A-30	-10	676	6.4	17.9
91	A-30	-10	646	4.4	21.9
62	A-0	-7	4280	---	---
76	A-0	-7	4384	4.0	181
82	A-0	-7	4426	3.6	186
66	A-5	-7	1140	3.6	58.4
86	A-10	-7	738	5.9	22.4
74	A-10	-7	882	6.0	26.6
80	A-10	-7	830	4.6	32.0
137	A-10	-7	932	4.5	36.1
70	A-30	-7	444	4.6	13.0
27	A-0	-5	3340	2.9	188
140	A-0	-5	3163	3.0	172
23	A-5	-5	1004	3.3	51.2
19	A-10	-5	667	5.3	21.3
26	A-30	-5	376	6.4	8.06
83	A-30	-5	369	5.5	10.3

Table 5.7 (con't)

Test	Soil	T (°C)	σ_y (kPa)	ε_y (%)	$\sigma_{10\%}$ (kPa)	E_s (MPa)
51	B-0	-12	2245	---	4744	---
55	B-0	-12	2278	1.2	4616	196
97	B-0	-12	2275	1.5	3751	149
57	B-5	-12	1702	1.1	3536	155
94	B-5	-12	1732	1.1	3671	156
111	B-5	-12	1586	0.9	3421	187
50	B-10	-12	1073	1.0	2406	107
105	B-10	-12	1101	0.6	2769	186
54	B-30	-12	306	0.5	1076	58.8
59	B-30	-12	320	0.5	985	61.5
96	B-30	-12	320	0.5	1180	59.3
104	B-30	-12	316	0.7	1071	43.9
35	B-0	-10	1904	1.0	3480	190
41	B-0	-10	1855	1.2	3190	155
88	B-0	-10	2029	1.3	3350	150
30	B-5	-10	1260	1.1	2590	114
47	B-5	-10	1135	0.9	2632	126
89	B-5	-10	1420	1.0	3170	150
34	B-10	-10	880	1.1	2126	80.0
113	B-30	-10	160	0.4	597	38.1
115	B-30	-10	200	0.4	876	47.6
117	B-30	-10	202	0.8	914	24.9
63	B-0	-7	1247	1.5	2249	83.7
64	B-0	-7	1212	1.4	2447	86.6
78	B-0	-7	1201	1.3	2620	95.3
65	B-5	-7	809	---	1415	---
71	B-5	-7	765	1.2	1831	63.7
75	B-5	-7	821	1.1	1900	75.3
67	B-10	-7	369	0.9	857	41.5
77	B-10	-7	513	1.4	892	37.7
134	B-10	-7	550	1.2	1578	47.8
69	B-30	-7	92	---	352	---
73	B-30	-7	94	0.5	383	18.4
79	B-30	-7	95	0.9	339	11.2
81	B-30	-7	88	0.5	406	16.3
114	B-30	-7	108	0.7	532	15.2
21	B-0	-5	689	1.0	2115	68.9
25	B-0	-5	644	1.0	1877	61.9
16	B-5	-5	401	0.6	1158	66.8
128	B-5	-5	472	0.6	1453	74.9
15	B-10	-5	304	0.7	581	42.2
129	B-10	-5	303	0.5	1134	58.3
13	B-30	-5	32	0.4	191	9.1
14	B-30	-5	42	0.6	176	6.70
84	B-30	-5	54	0.7	114	8.29
85	B-30	-5	52	0.4	330	12.7
112	B-30	-5	39	0.5	406	7.19
141	B-30	-5	48	0.6	260	7.88

Table 5.7 (con't)

Test	Soil	T (°C)	σ_y (kPa)	ε_y (%)	$\sigma_{10\%}$ (kPa)	E_s (MPa)
98	C-0	-12	2109	1.2	3045	176
102	C-0	-12	2006	1.3	2850	152
100	C-5	-12	1798	1.1	2970	159
99	C-10	-12	1212	1.0	2462	119
101	C-10	-12	1342	1.0	2543	137
103	C-30	-12	364	0.7	950	51.3
106	C-0	-10	1664	1.3	2368	127
109	C-0	-10	1638	1.4	2491	116
107	C-5	-10	1438	1.3	2333	110
121	C-5	-10	1403	1.6	2270	88.2
110	C-10	-10	1051	2.1	2048	50.0
116	C-10	-10	1075	1.6	2095	66.4
120	C-10	-10	921	1.3	1847	69.8
108	C-30	-10	253	1.7	575	14.6
118	C-30	-10	335	1.3	766	26.4
133	C-0	-7	1167	1.3	2059	92.6
135	C-0	-7	1126	1.0	2013	112
130	C-5	-7	910	1.1	1749	79.8
127	C-10	-7	629	1.3	1379	48.4
139	C-10	-7	665	0.7	1365	102 ??
138	C-30	-7	156	0.7	611	21.4
122	C-0	-5	870	1.5	1270	59.6
124	C-0	-5	---	---	1523	---
126	C-0	-5	781	1.2	1524	66.2
123	C-5	-5	636	1.5	1326	41.8
125	C-10	-5	---	---	1093	---
132	C-10	-5	357	1.0	1087	35.7
119	C-30	-5	96	0.5	349	18.5

TABLE 5.8
CONSTANT STRAIN RATE COMPRESSION TEST RESULTS
of
ADDITIONNAL TESTS

Test	Soil	Temperature (°C)	σ_y (kPa)	ε_y (%)	σ_{max} (kPa)	E_s (MPa)
A	B-30	-6.0	53	0.2	381	26.5
B	C-5	-6.6	860	1.2	1694	71.7
C	B-5	-6.6	770	1.0	1785	77.0
D	B-5	-6.6	792	1.0	1706	79.2
E	B-5	-6.6	790	1.2	1418	65.8
F	C-30	-6.9	177	1.1	467	16.1
G	B-5	-6.8	948	1.3	1179	72.9
H	B-5	-6.9	811	1.1	2314	73.7

TABLE 5.9
CONSTANT STRESS COMPRESSION TEST RESULTS

Test	Soil	Average Temperature (°C)	Stress Level (% of strength)	σ (kPa)	t_f (hr)	ε_f (%)	$\dot{\varepsilon}_{min}$ (%/hour)
CR-45	A-0	-6.87	105%	4581	1.7	3.9	1.175
CR-92	A-0	-7.10	90%	3927	12	4.0	0.12
CR-95	A-0	-6.94	65%	2836	514	3.4	0.0031
CR-59	A-5	-7.09	90%	1026	14	4.7	0.189
CR-51	A-5	-6.96	90%	1026	12	4.1	0.166
CR-60	A-5	-7.02	75%	855	34	5.4	0.0859
CR-67	A-5	-7.10	50%	570	414	9.1	0.0121
CR-86	A-10	-6.82	105%	887	12	6.0	0.324
CR-47	A-10	-7.07	90%	761	17	4.6	0.145
CR-87	A-10	-7.04	75%	634	62	8.0	0.0774
CR-64	A-30	-6.93	200%	888	0.20	5.3	16.1
CR-70	A-30	-6.91	150%	666	1.5	6.7	2.48
CR-72	A-30	-6.92	125%	555	3.9	5.9	0.671
CR-83	B-0	-6.97	120%	2825	2.8	12.7	0.843
CR-71	B-0	-6.95	100%	2354	20	10.9	0.104
CR-81	B-0	-6.92	90%	2119	110	10.9	0.0171
CR-84	B-5	-6.80	110%	1890	5.8	9.4	0.331
CR-49	B-5	-7.18	100%	1718	17	8.5	0.0623
CR-9	B-5	-6.88	90%	1546	47	8.1	0.0345
CR-17	B-5	-7.07	90%	1546	91	9.5	0.0157
CR-32	B-5	-6.94	90%	1546	108	10.0	0.021
CR-82	B-10	-6.86	110%	1359	6.1	9.2	0.332
CR-50	B-10	-6.95	100%	1235	16	8.4	0.0808
CR-33	B-10	-7.06	90%	1112	24	7.3	0.0528
CR-38	B-10	-7.13	90%	1112	44	6.6	0.0222
CR-75	B-30	-6.87	200%	678	0.76	12	6.73
CR-77	B-30	-6.88	165%	559	1.3	12	3.33
CR-88	B-30	-6.92	130%	442	4.9	12	0.83
CR-79	C-0	-6.96	110%	2240	23	18.5	0.181
CR-65	C-0	-6.85	100%	2036	70	15.3	0.0266
CR-36	C-0	-7.12	90%	1832	375	11.6	0.0011
CR-96	C-5	-6.85	120%	2006	3.5	12.8	0.757
CR-66	C-5	-6.78	110%	1839	3.7	11.7	0.9
CR-62	C-5	-7.13	100%	1672	4117	12.6	0.132
CR-89	C-5	-6.88	100%	1672	4237	13.7	0.070
CR-94	C-5	-7.10	90%	1504	645	11.4	0.0045
CR-55	C-10	-6.96	100%	1372	4.7	10.7	0.448
CR-52	C-10	-6.92	90%	1235	17	10.7	0.103
CR-68	C-10	-6.94	80%	1098	48	9.1	0.0203
CR-76	C-30	-6.91	200%	1222	0.06	12	110
CR-78	C-30	-6.98	165%	1008	0.12	12	60.4
CR-91	C-30	-6.97	130%	794	0.23	12	27.2

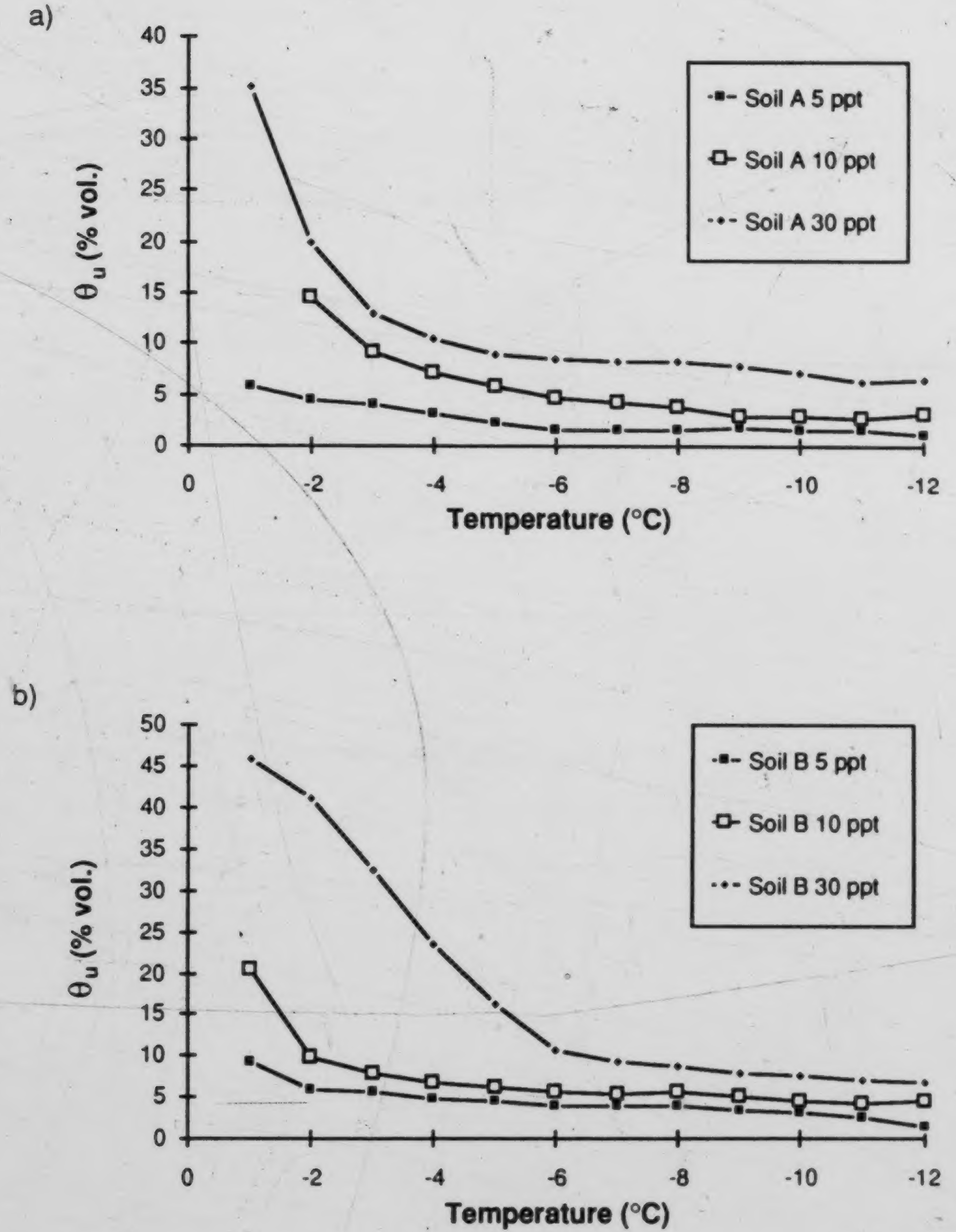

Figure 5.1: 1988 TDR unfrozen water contents a) Soil A b) Soil B

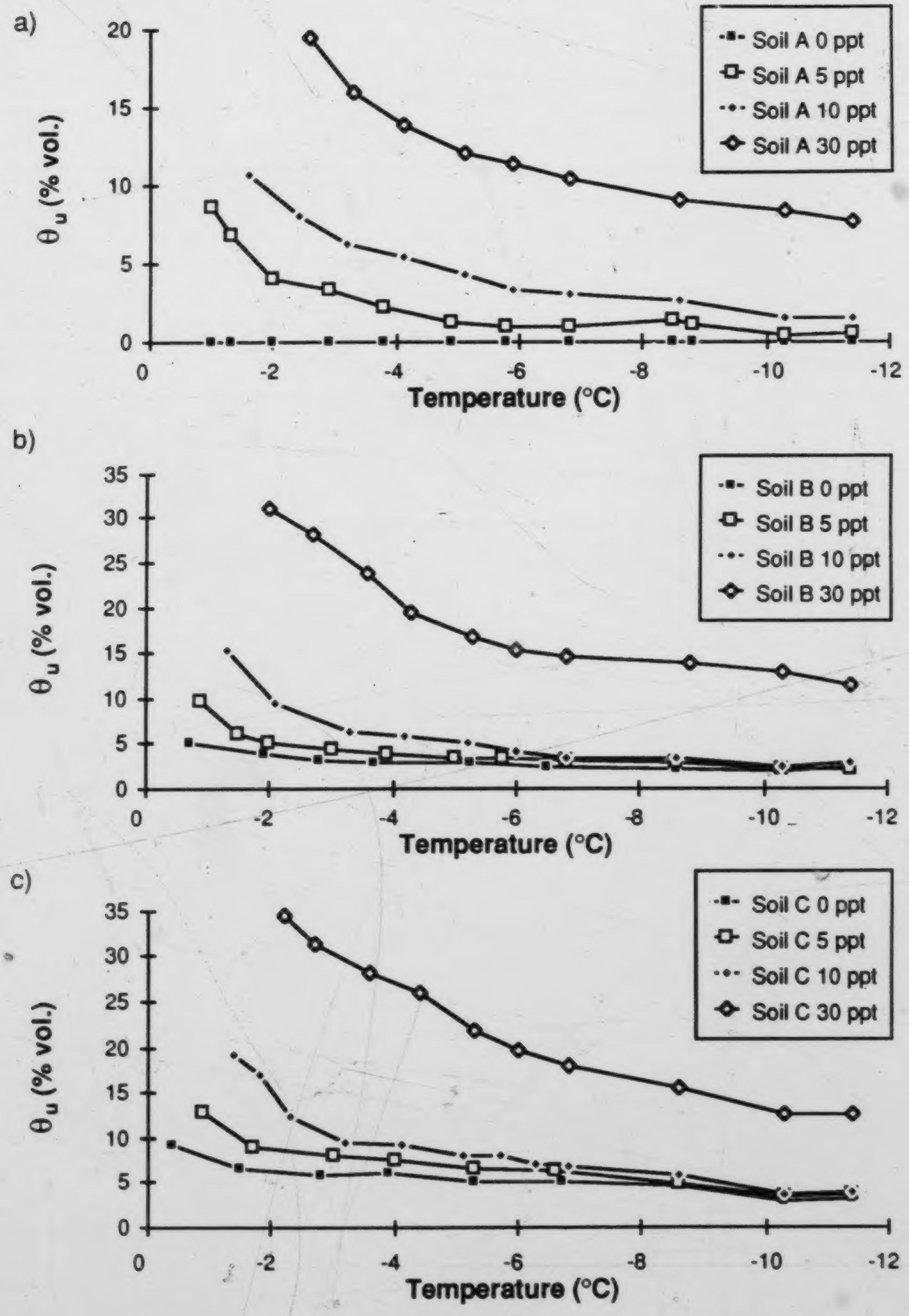

Figure 5.2: 1990 TDR unfrozen water contents a) Soil A b) Soil B c) Soil C

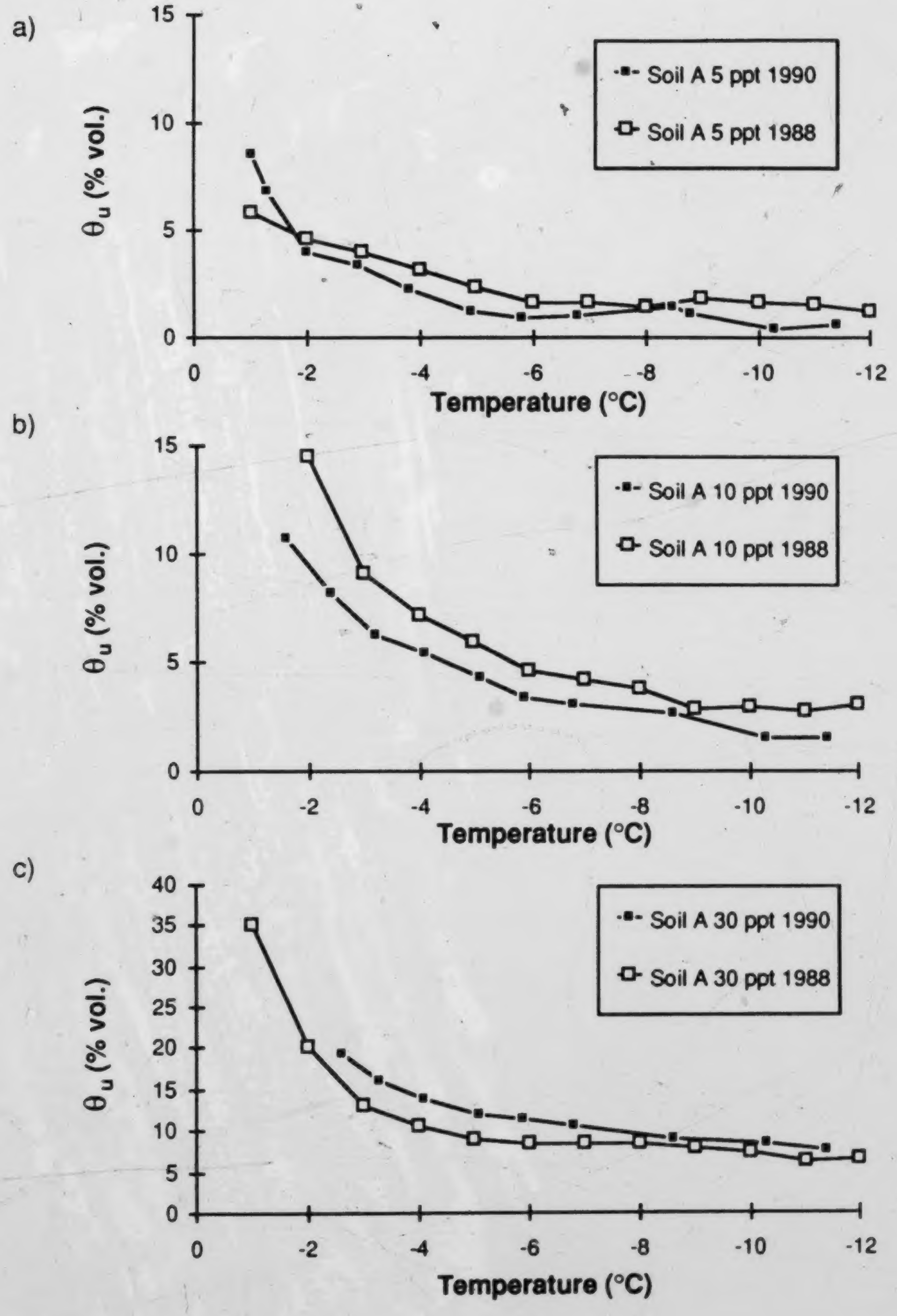

Figure 5.3: TDR results comparison 1990-1988 for Soil A
a) 5 ppt b) 10 ppt c) 30 ppt

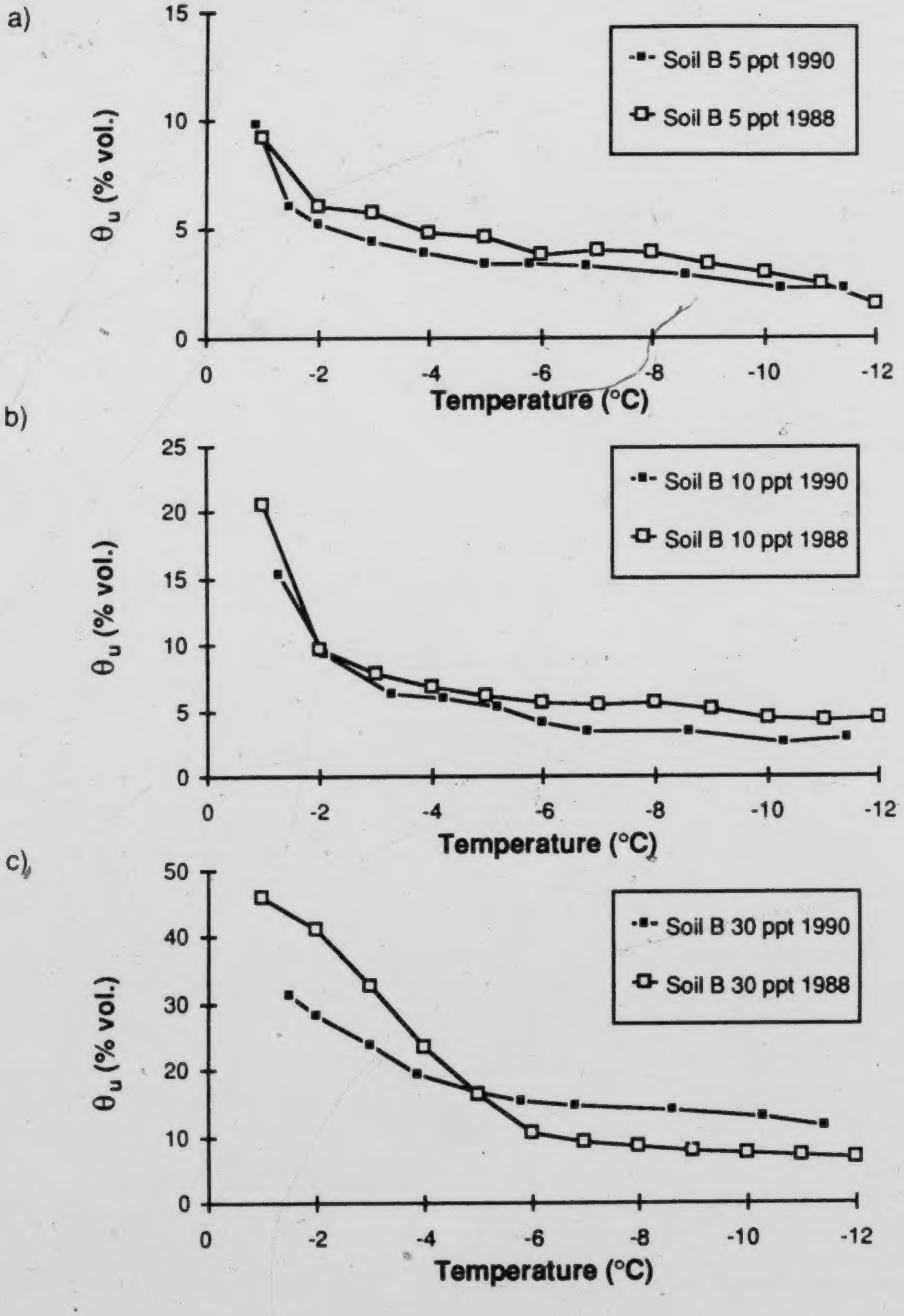

Figure 5.4: TDR results comparison 1990-1988 for Soil B
a) 5 ppt b) 10 ppt c) 30 ppt

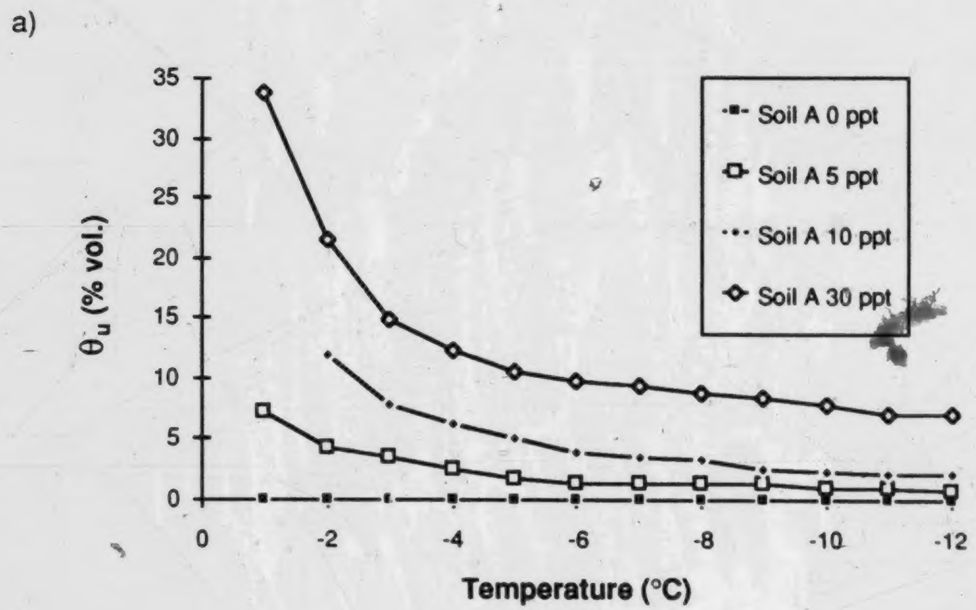
a)
35
30
25
20
15
10
5
0
θu (% vol.)
0
-2
-4
-6
-8
-10
-12
Temperature (°C)
Soil A 0 ppt
Soil A 5 ppt
Soil A 10 ppt
Soil A 30 ppt
b)
35
30
25
20
15
10
5
0
θu (% vol.)
0
-2
-4
-6
-8
-10
-12
Temperature (°C)
Soil B 0 ppt
Soil B 5 ppt
Soil B 10 ppt
Soil B 30 ppt

Figure 5.5: Average TDR unfrozen water contents a) Soil A b) Soil B

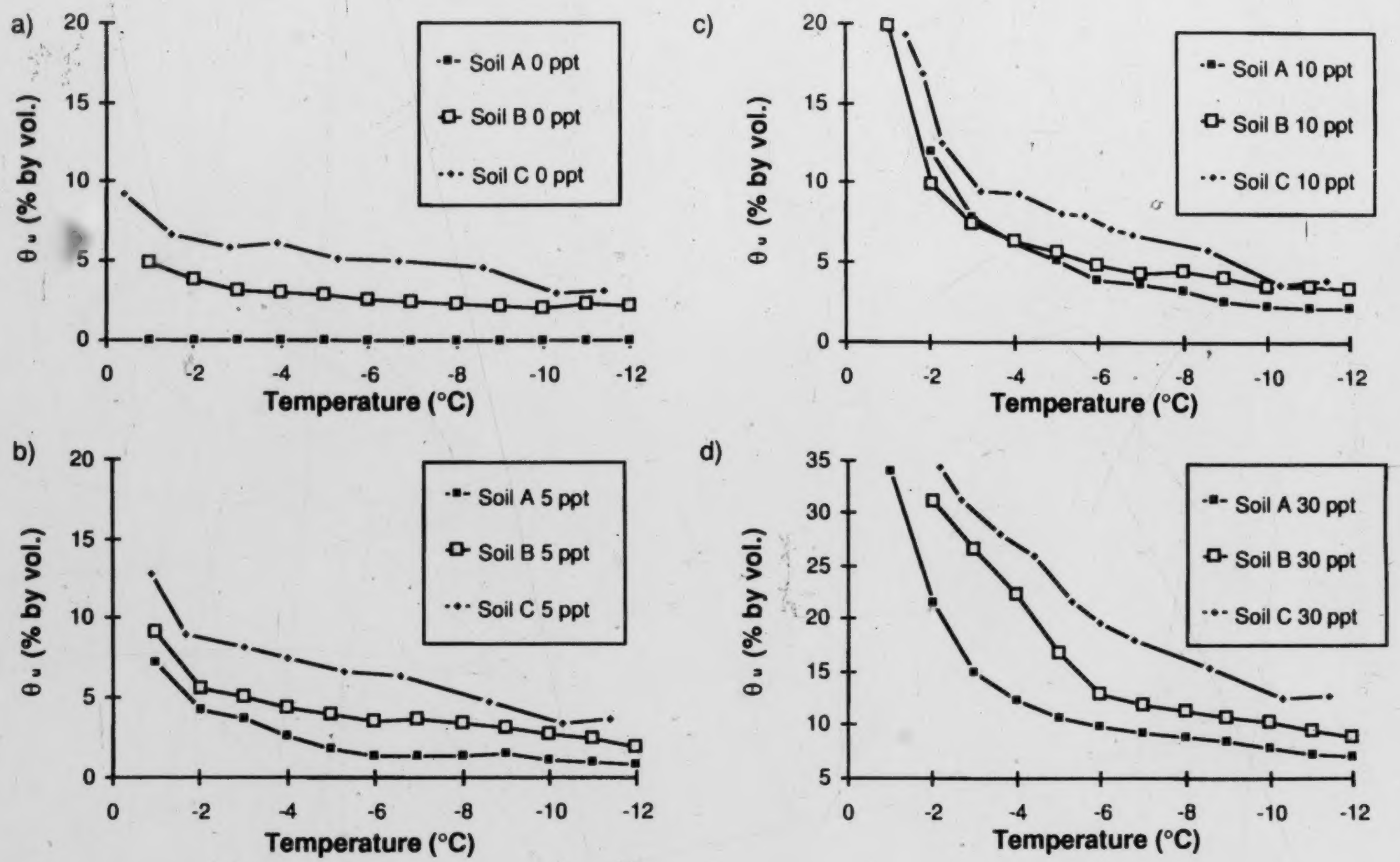

Figure 5.6: TDR unfrozen water contents according to soil type a) 0 ppt b) 5 ppt c) 10 ppt d) 30 ppt

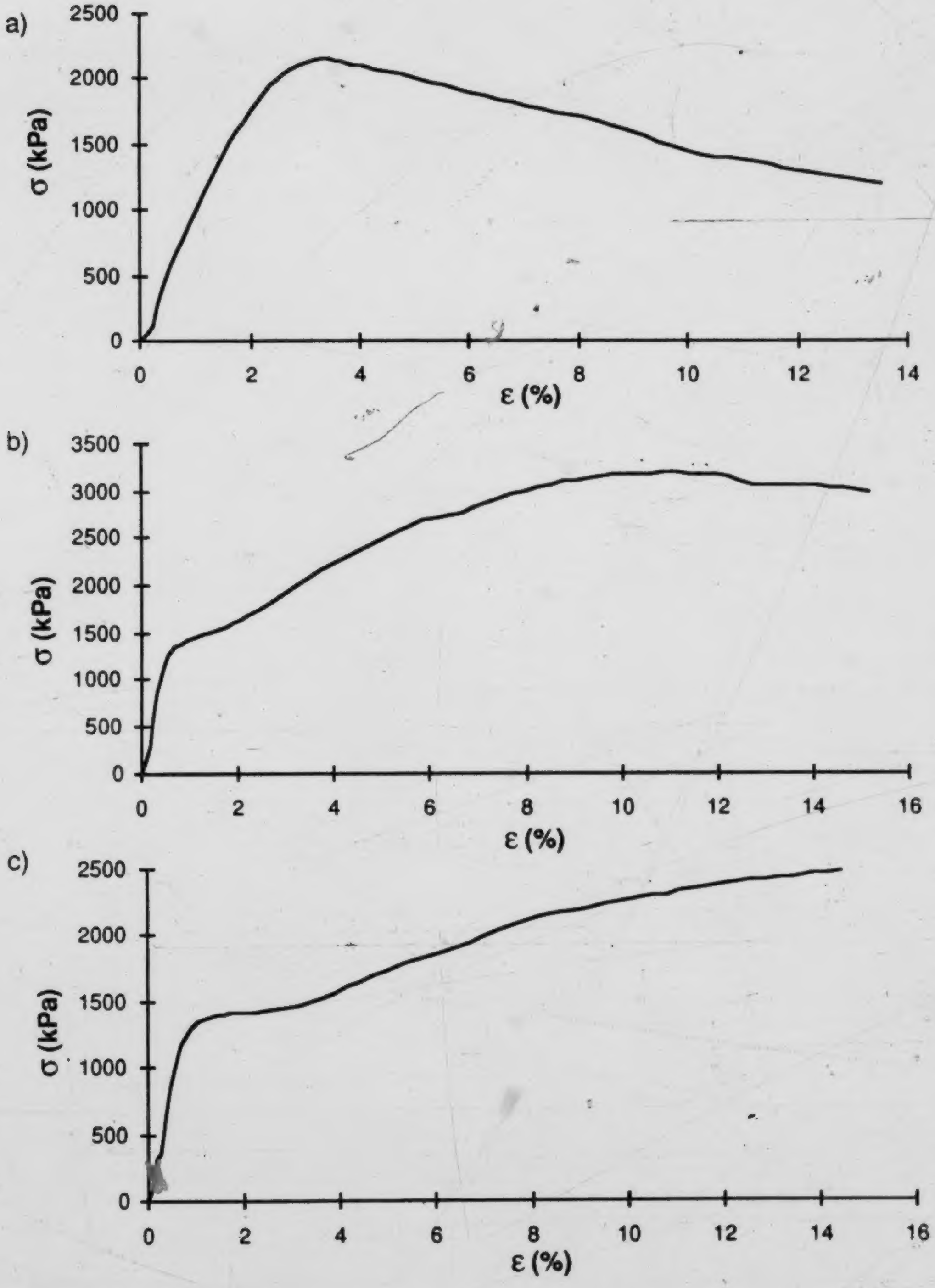

Figure 5.7: Stress vs Strain
a) Test 90, soil A 5 ppt at -10°C b) Test 89, soil B 5 ppt at -10°C
c) Test 121, soil C 5 ppt at -10°C

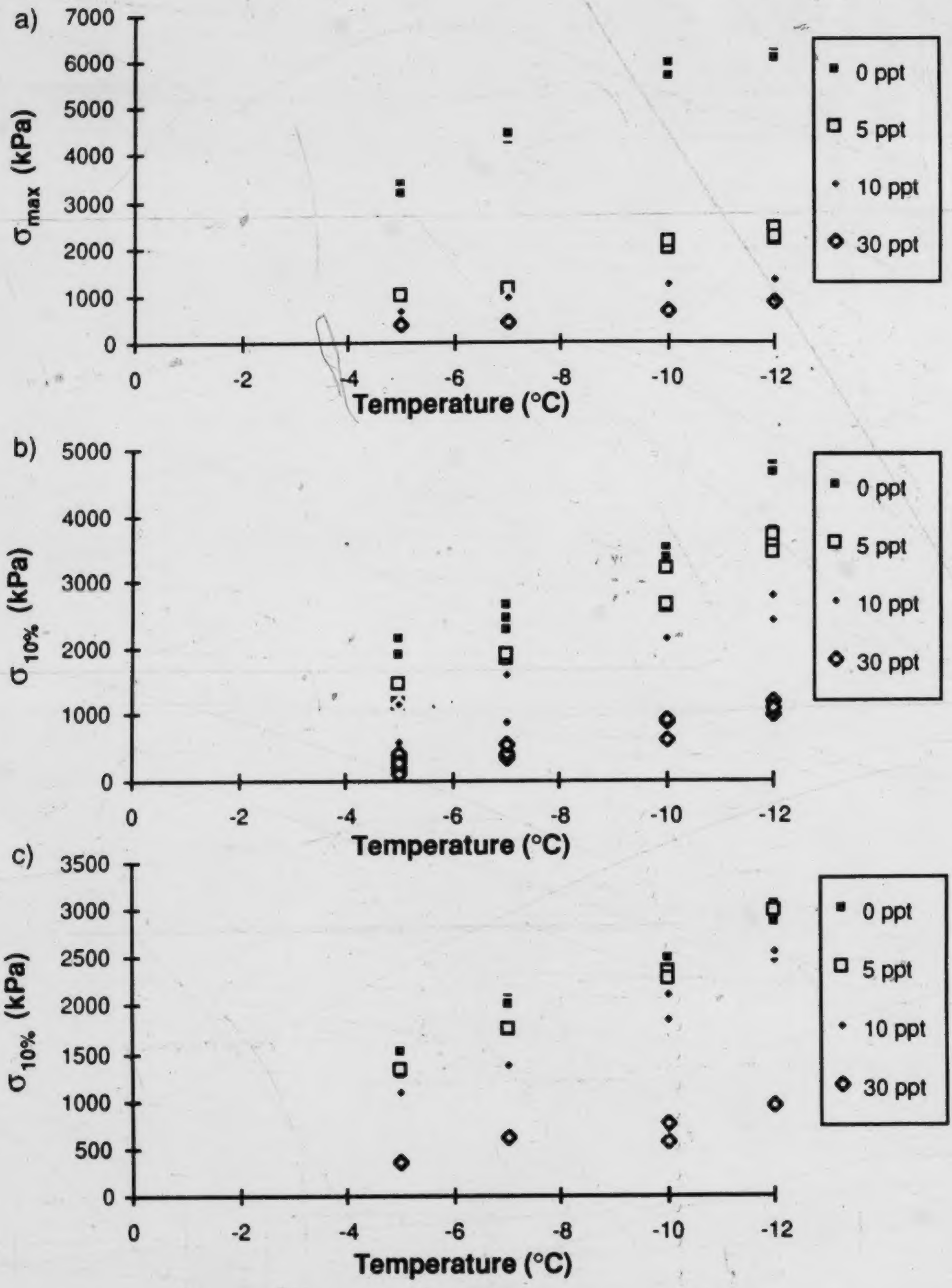

Figure 5.8: Unconfined compression strength vs Temperature
a) Soil A peak strength vs temperature
b) Soil B 10% strength vs temperature
c) Soil C 10% strength vs temperature

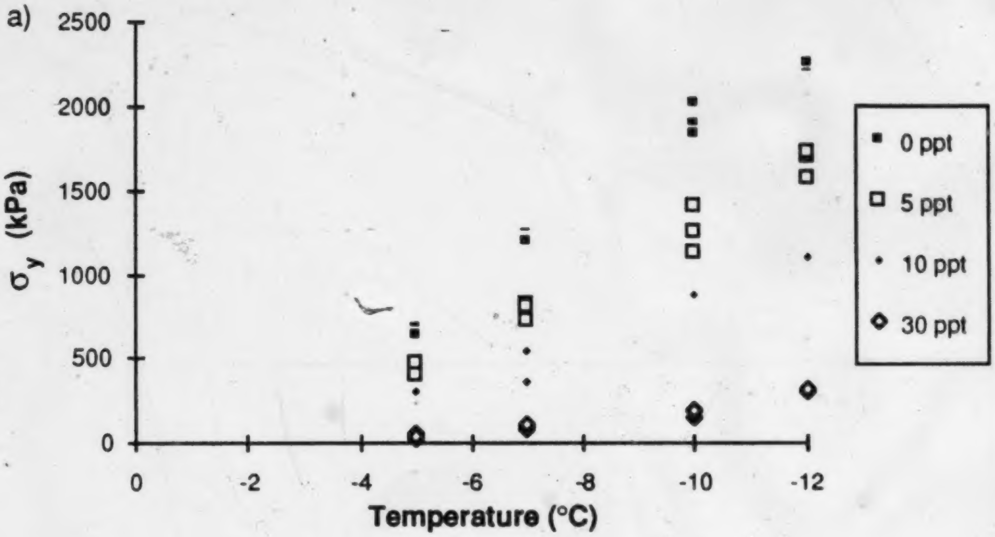

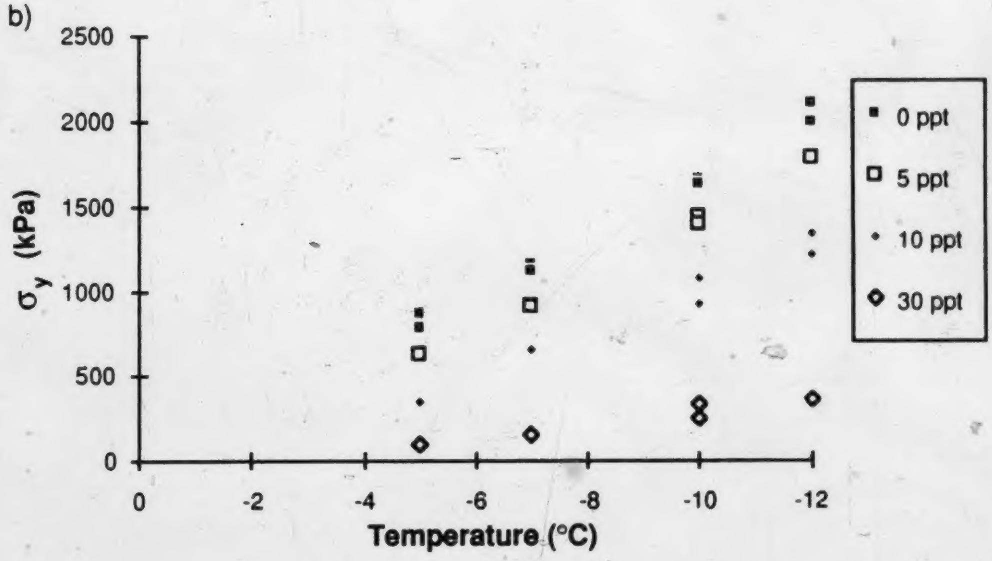

Figure 5.9: Unconfined compression yield strength vs Temperature
a) Soil B b) Soil C

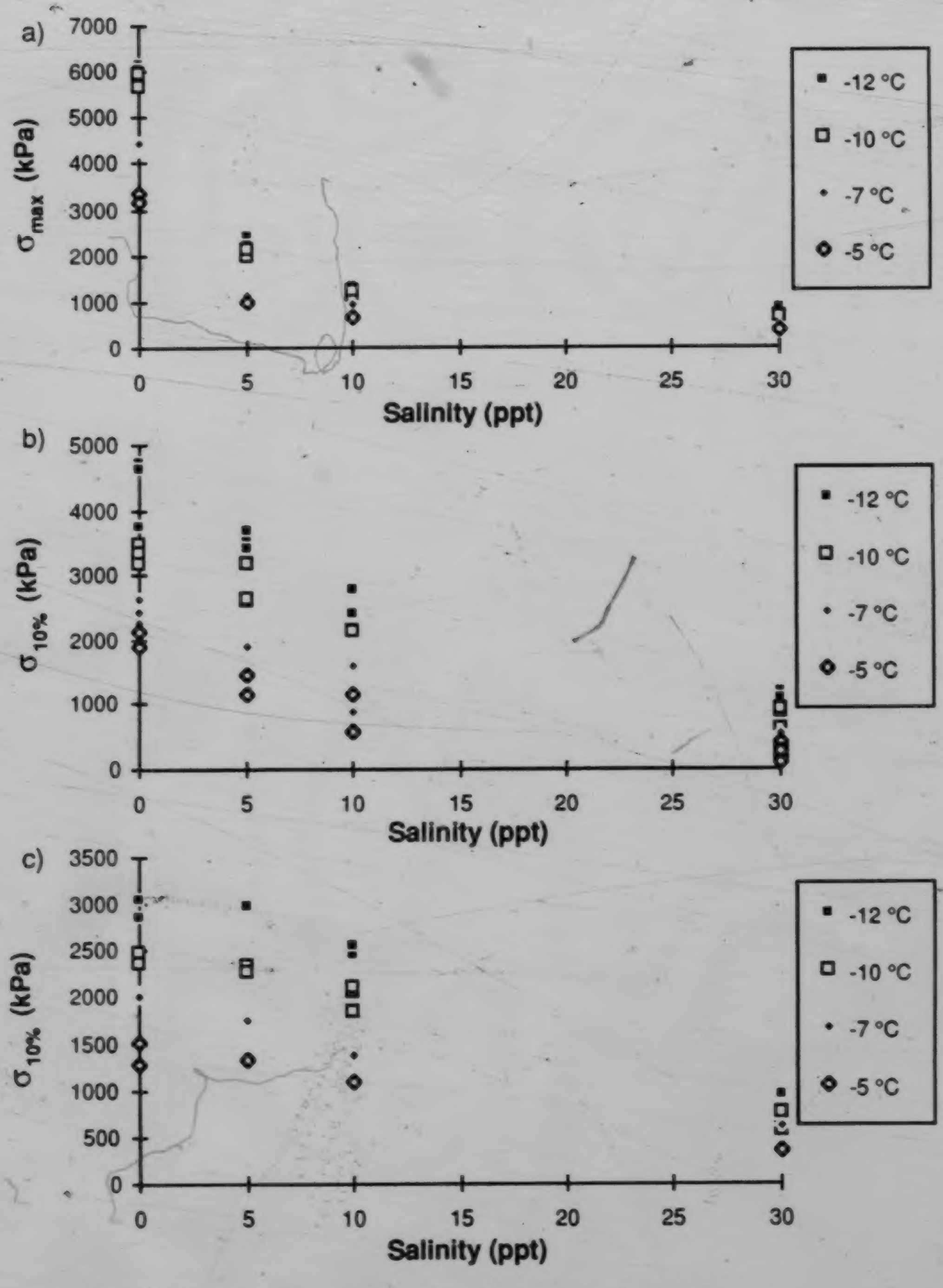

Figure 5.10: Unconfined compression strength vs Salinity
a) Soil A peak strength vs salinity
b) Soil B 10% strength vs salinity
c) Soil C 10% strength vs salinity

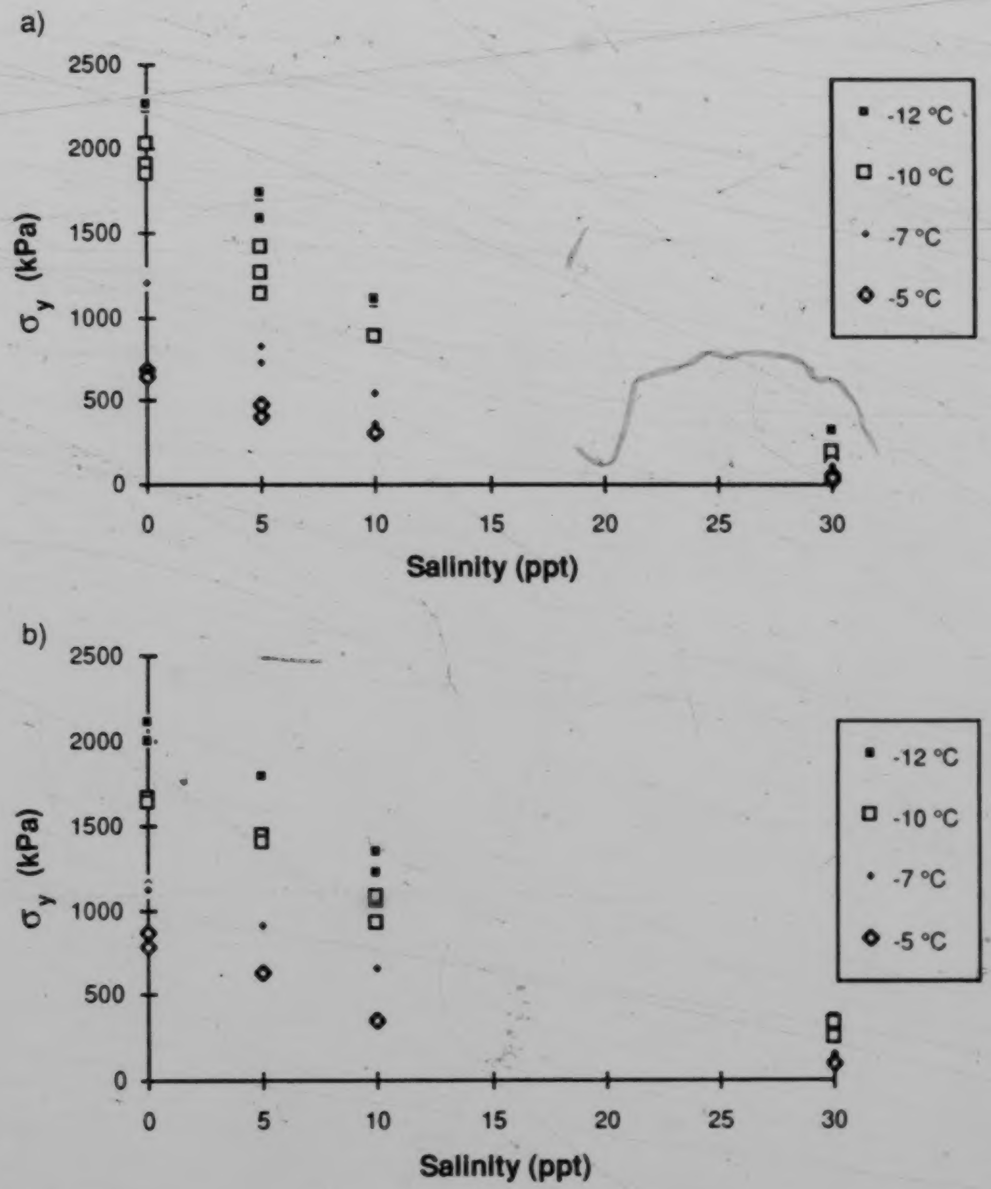

Figure 5.11: Unconfined compression yield strength vs Salinity
a) Soil B b) Soil C

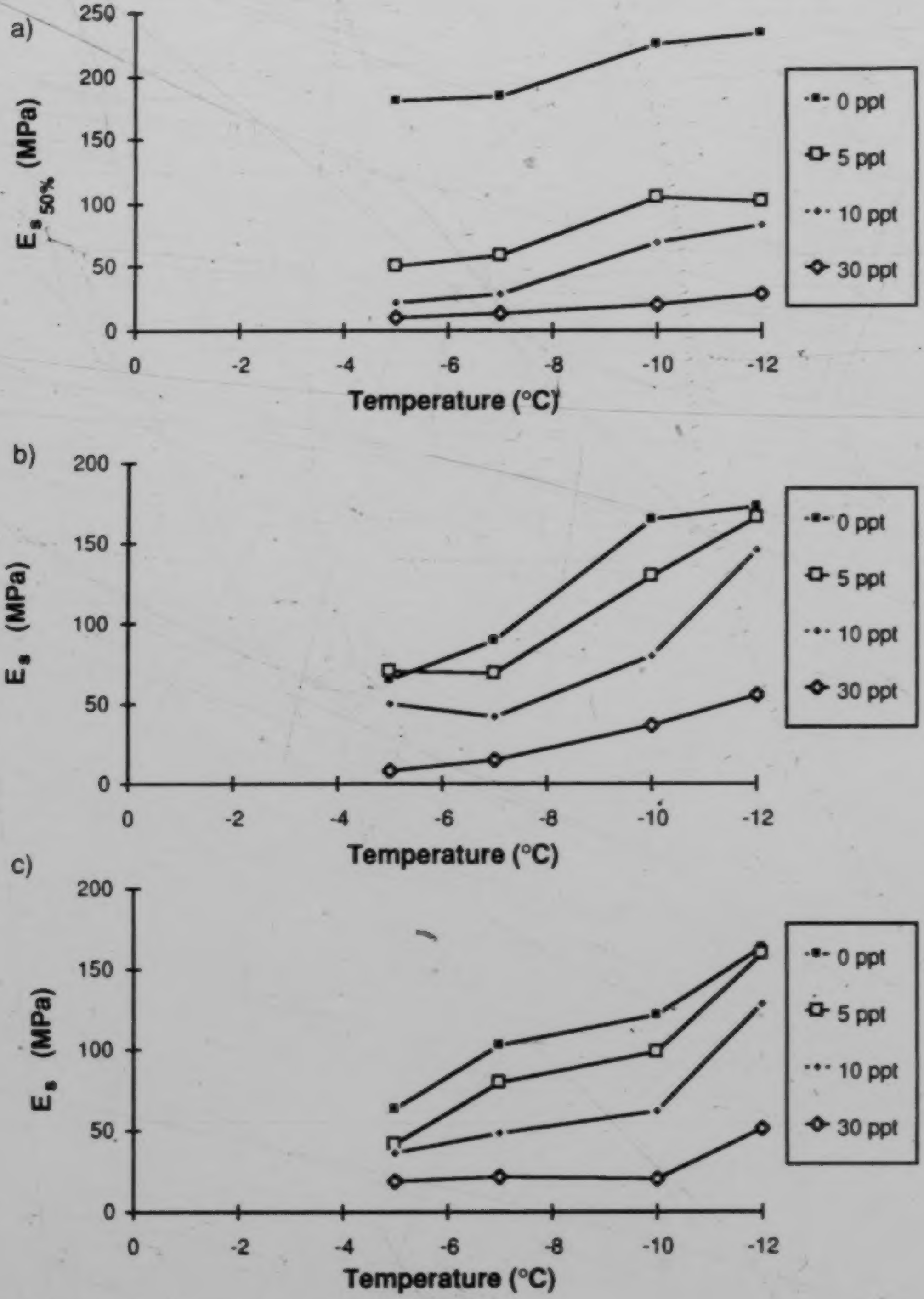

Figure 5.12: Secant modulus vs Temperature
a) Soil A b) Soil B c) Soil C

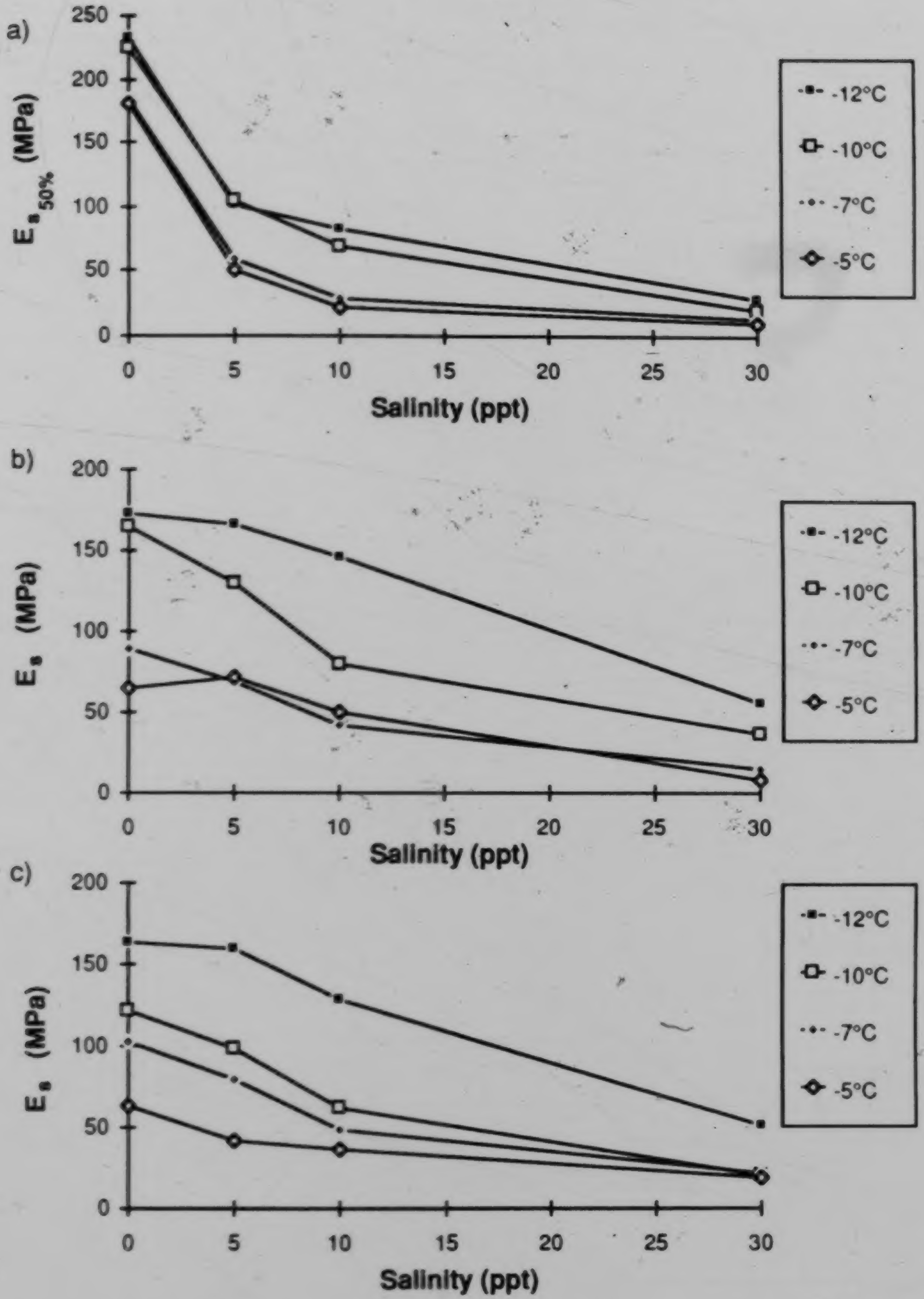

Figure 5.13: Secant modulus vs Salinity
a) Soil A b) Soil B c) Soil C

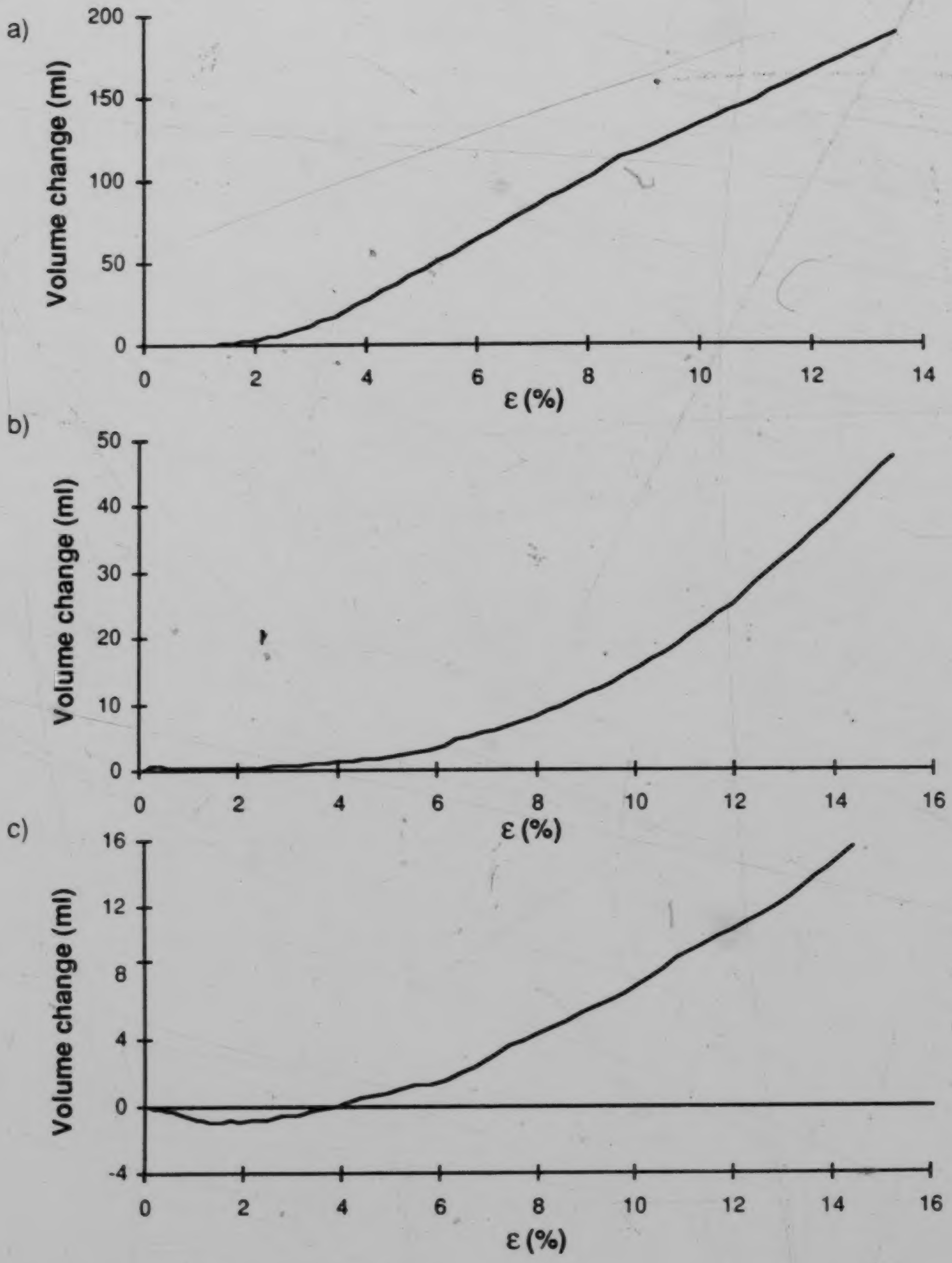

Figure 5.14: Volume change vs Strain
a) Test 90, soil A 5 ppt at -10°C b) Test 89, soil B 5 ppt at -10°C
c) Test 121, soil C 5 ppt at -10°C

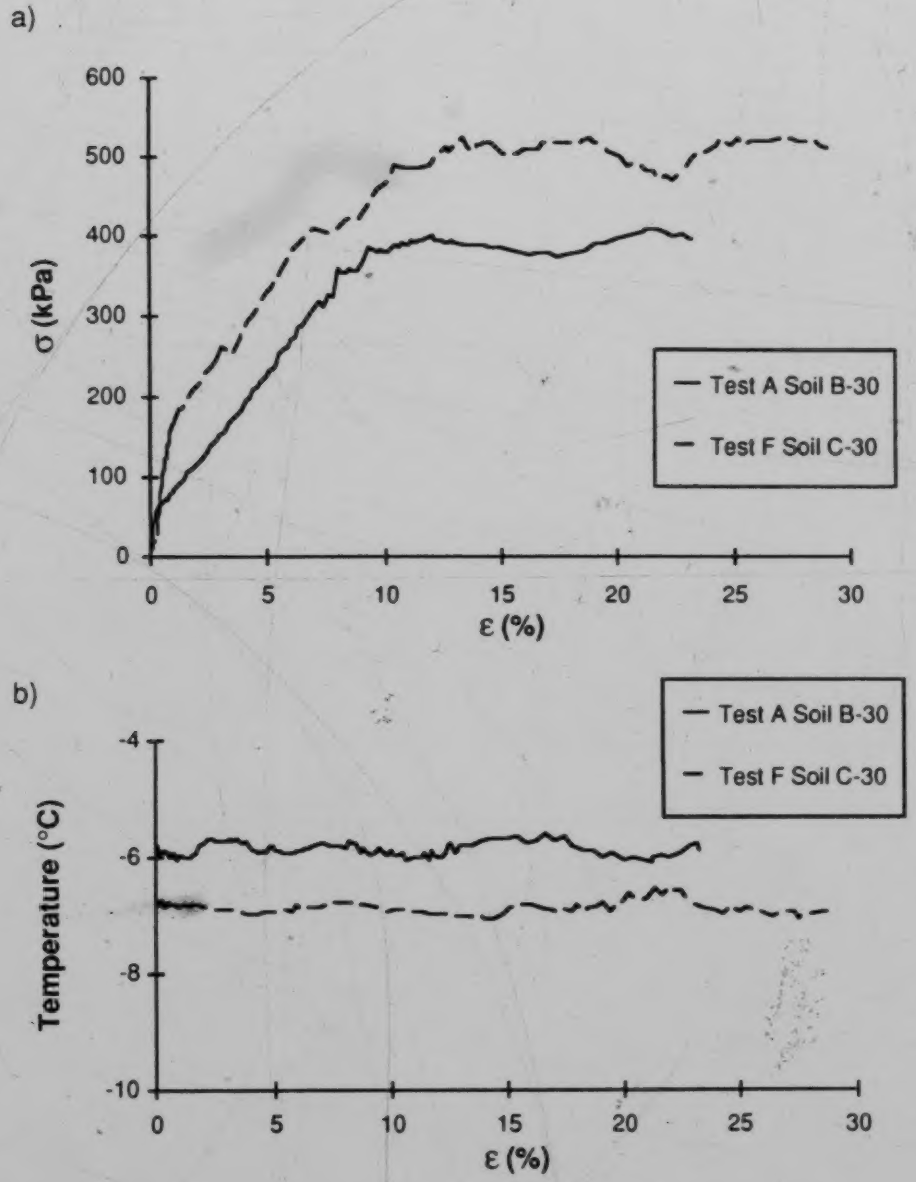

Figure 5.15: Compression test results for tests A and F
a) Stress vs Strain b) Temperature vs Strain

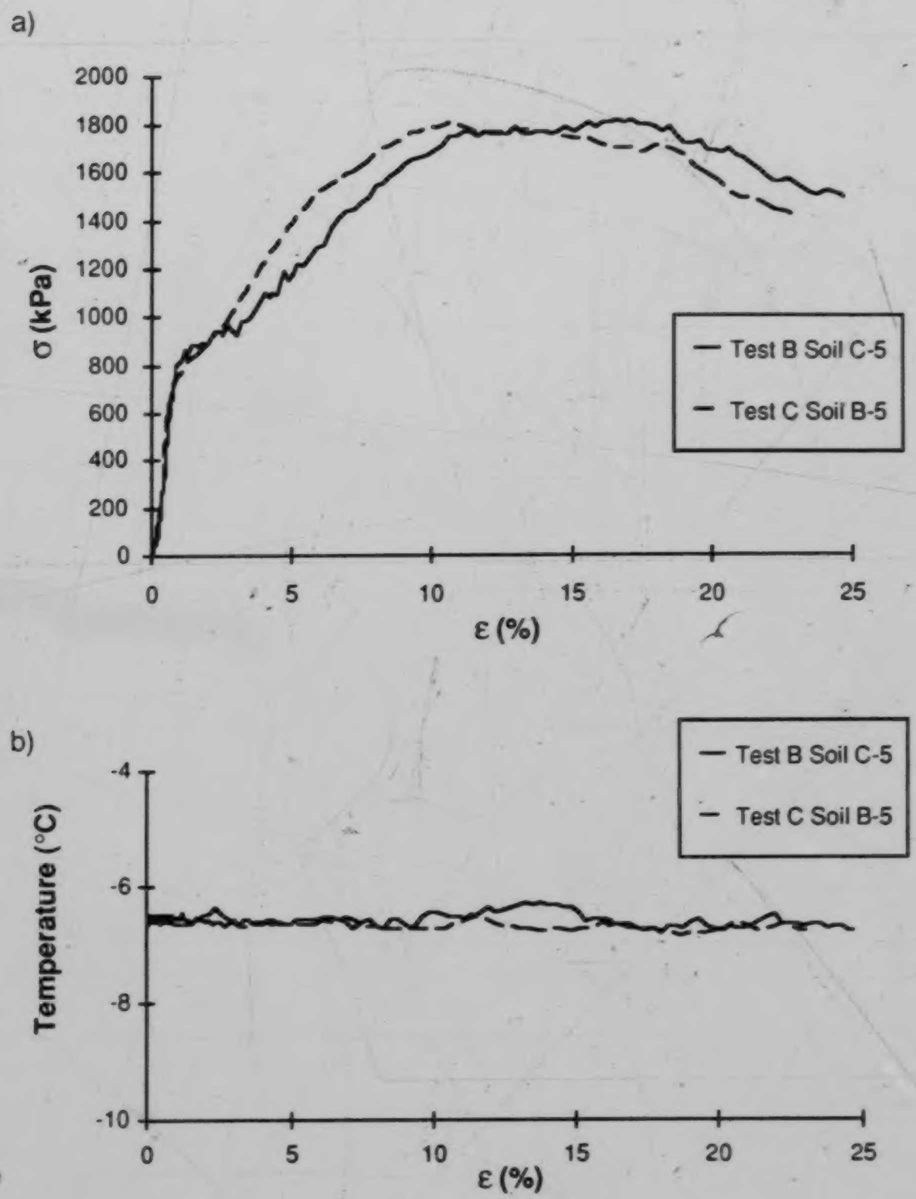

Figure 5.16: Compression test results for tests B and C
a) Stress vs Strain b) Temperature vs Strain

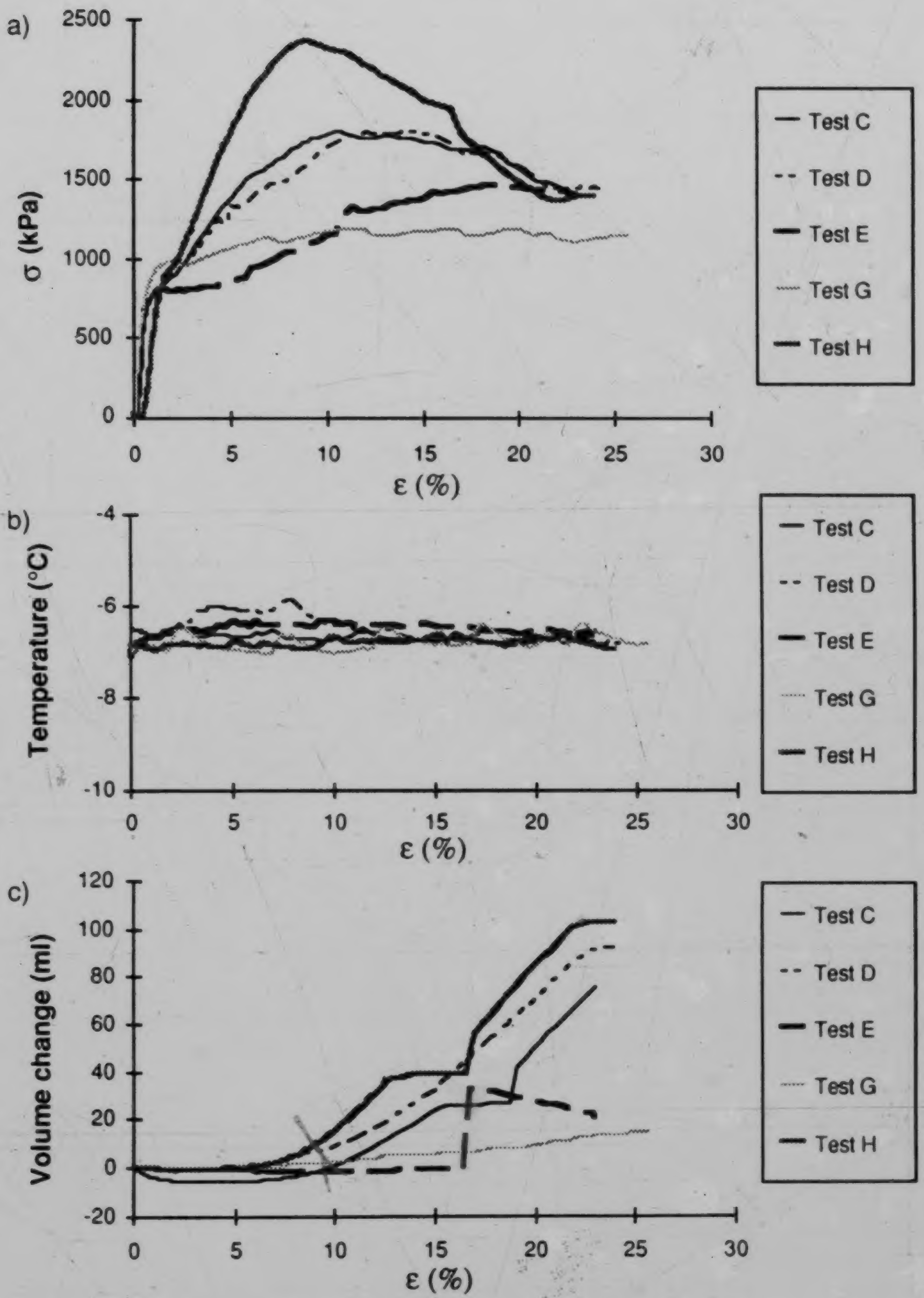

Figure 5.17: Compression test results for tests C, D, E, G and H
a) stress-strain curve b) temperature vs strain
c) volume change vs strain

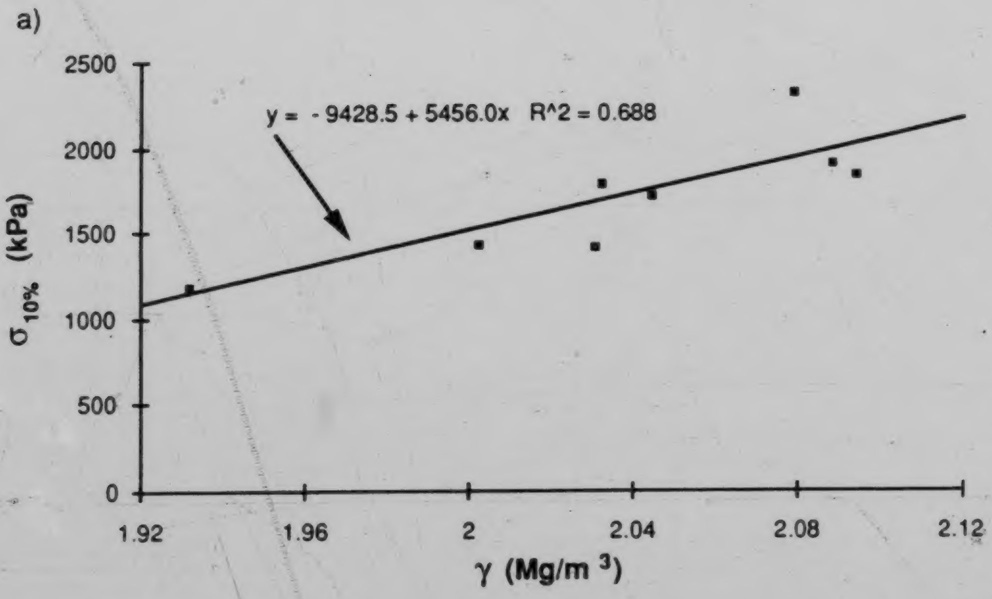

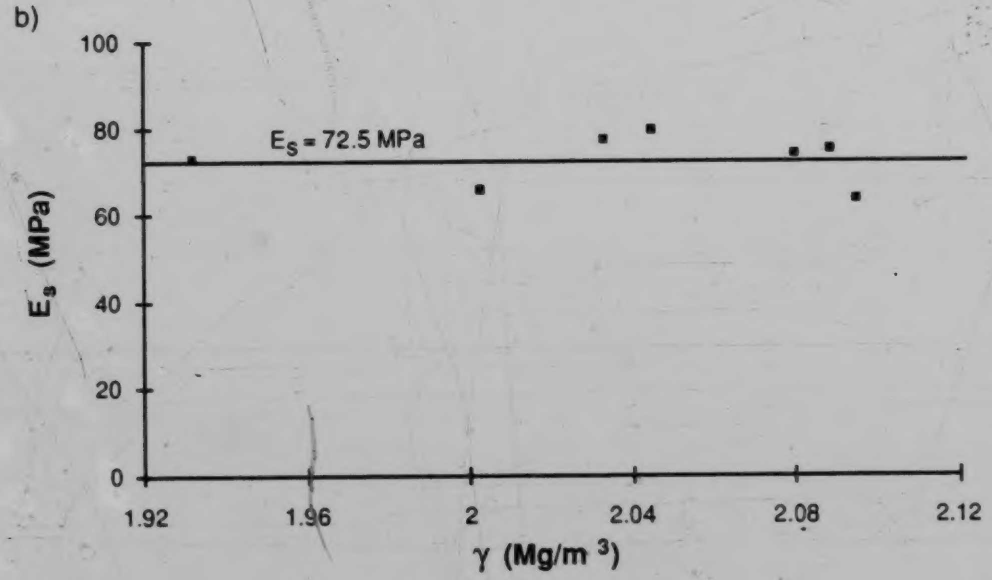

Figure 5.18: a) 10% Strength vs Density for soil B 5 ppt at -7°C
b) Secant modulus vs Density for soil B 5 ppt at -7°C

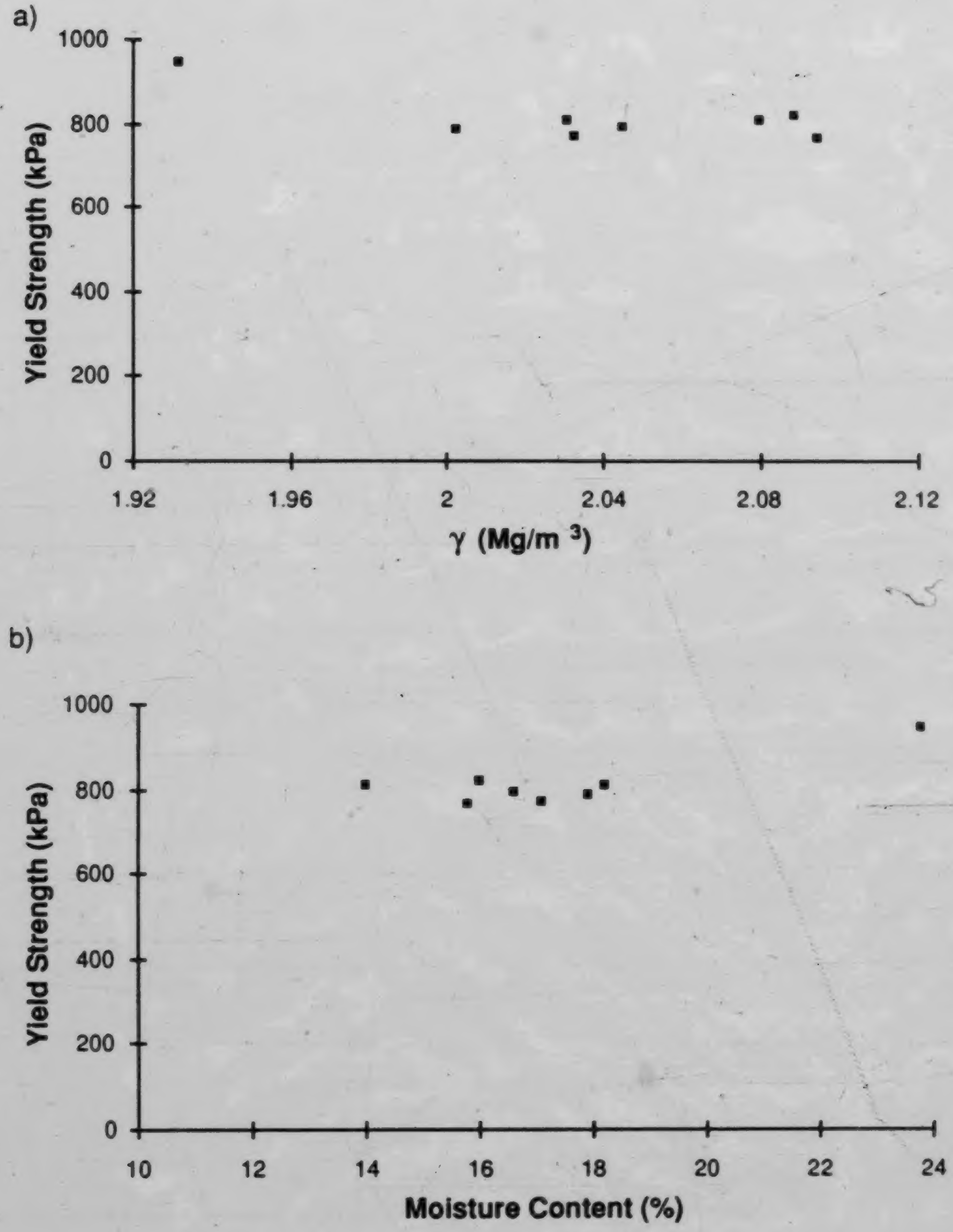

Figure 5.19: a) Yield strength vs Density for soil B 5 ppt at -7°C
b) Yield strength vs Moisture content for soil B 5 ppt at -7°C

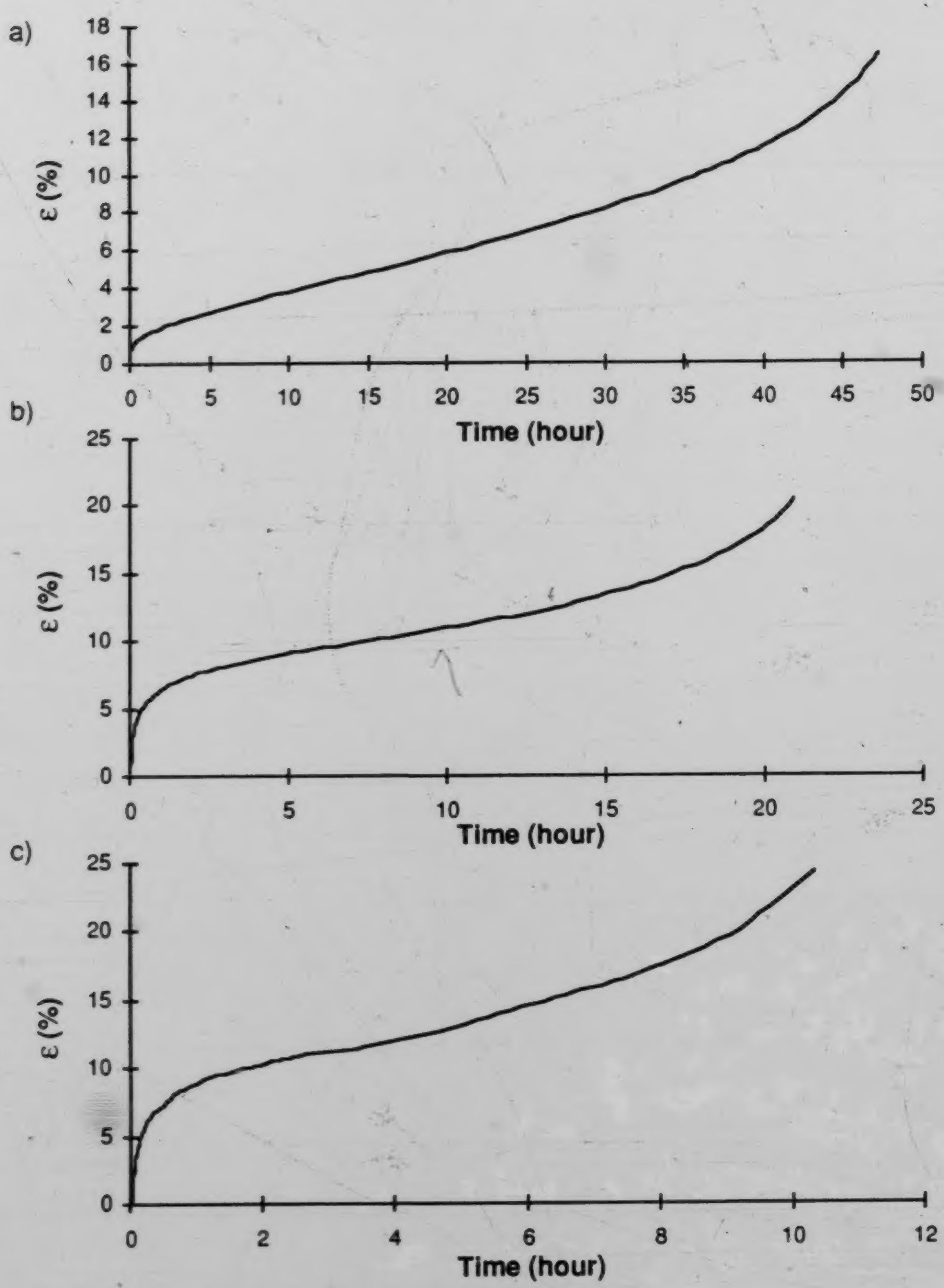

Figure 5.20: Strain vs Time curves
a) Creep test CR-59, soil A 5 ppt b) Creep test CR-84, soil B 5 ppt
c) Creep test CR-66, soil C 5 ppt

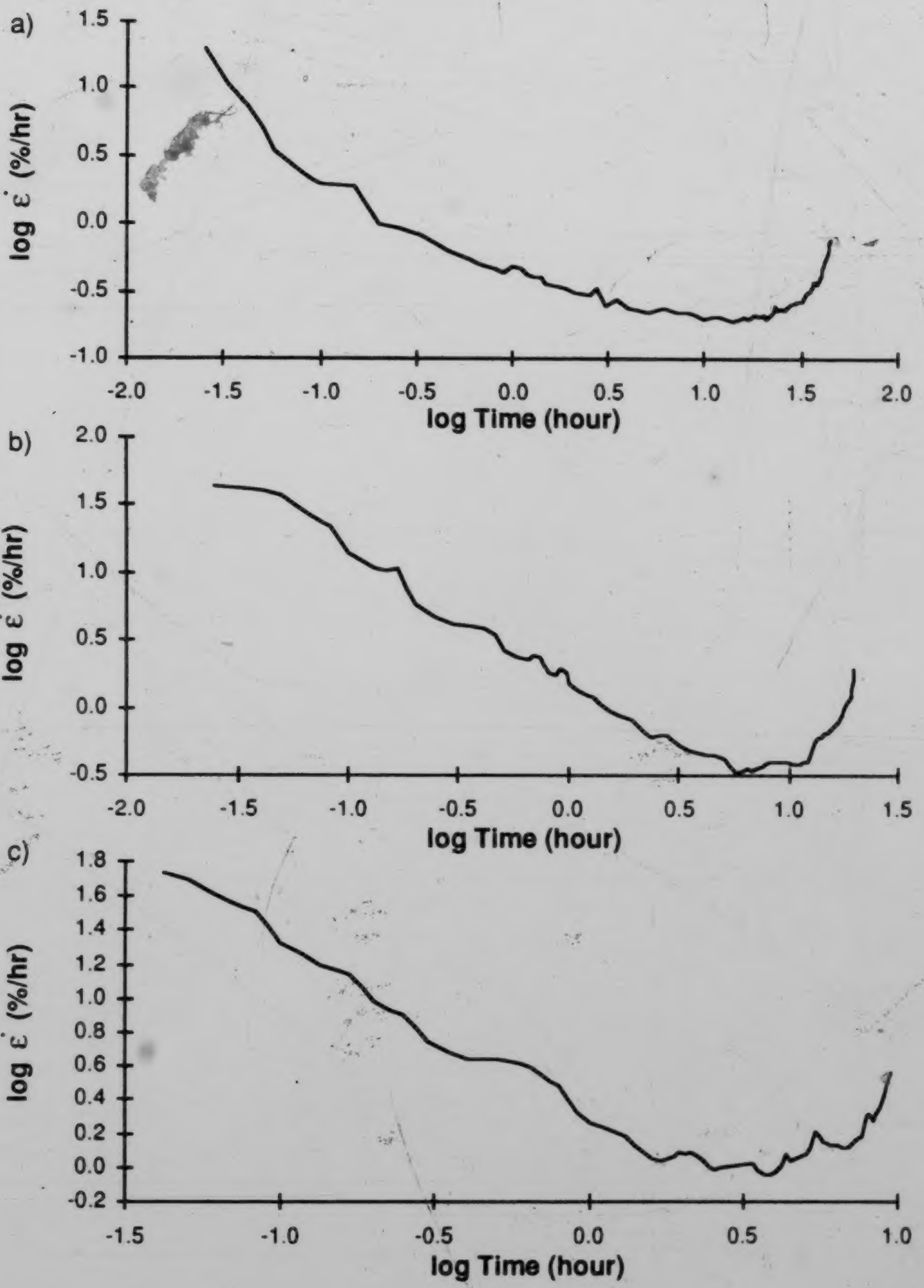

Figure 5.21: Log strain rate vs log time curves
a) Creep test CR-59, soil A 5 ppt b) Creep test CR-84, soil B 5 ppt
c) Creep test CR-66, soil C 5 ppt

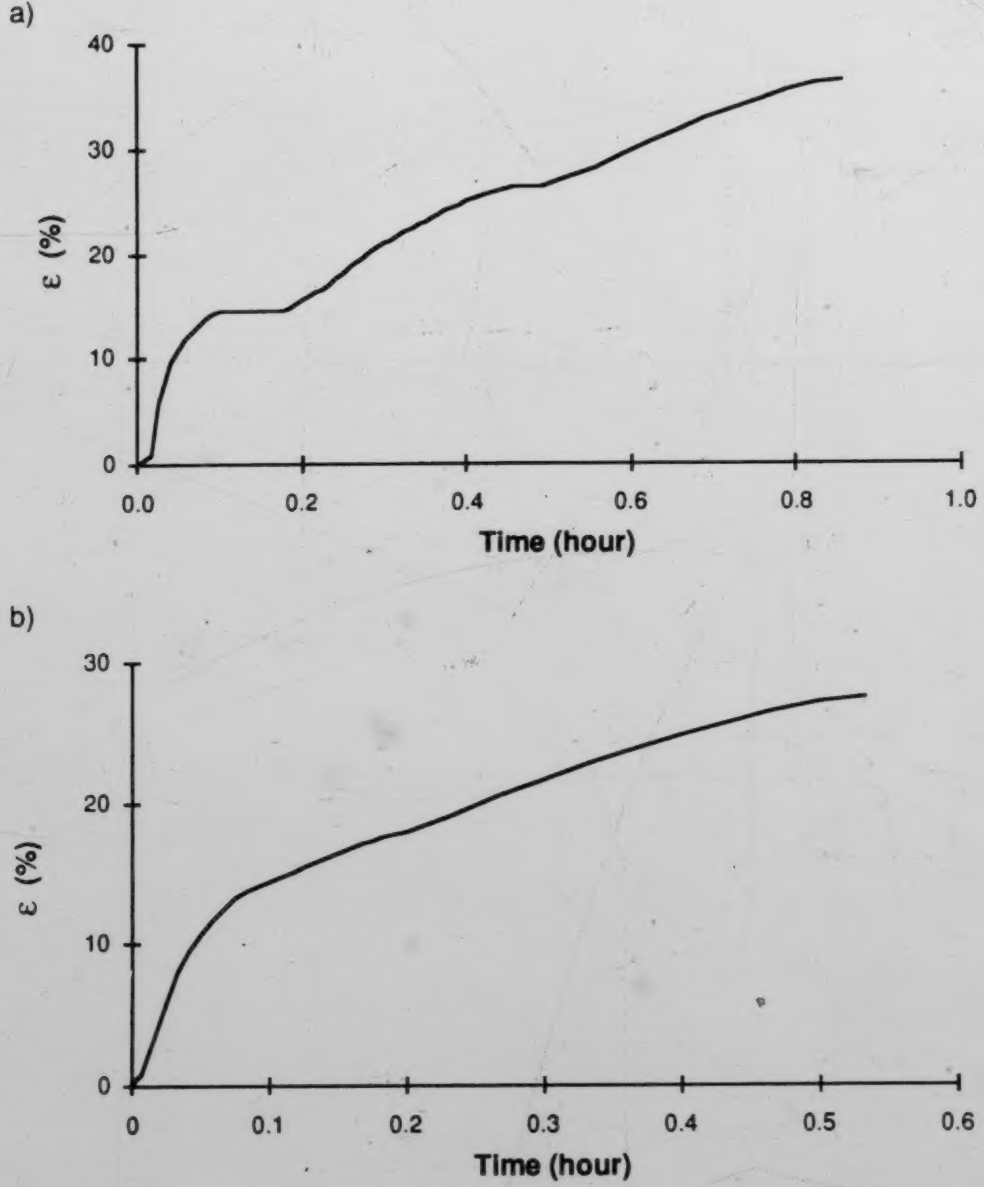

Figure 5.22: a) Original Strain vs Time curve for test CR-76
b) Corrected Strain vs Time curve for test CR-76

6. ANALYSIS AND INTERPRETATION OF TEST RESULTS

6.1. UNFROZEN WATER CONTENT

The results of the determination of the unfrozen water content by time-domain reflectometry were presented in Chapter 5. As stated, an increase in temperature and a decrease in grain size causes an increase in unfrozen water content. In this section, a method to predict the unfrozen water content of saline soils using data obtained experimentally will be presented.

Many authors have used the phase diagram of sodium chloride (Figure 6.1) to predict the unfrozen water content in saline frozen soils. This method is only valid for coarse grained soils which do not contain fines, since fine-grained particles affect the equilibrium state of the saline solution because of surface tension effects in the bound water around the particles and capillary effects within the free water.

Equation 3.85 was used to predict the volumetric brine content, v_b , at temperatures between -1°C and -12 °C for samples with initial salinities of 5, 10 and 30 ppt. The density of the ice was assumed constant at a value of 0.917 Mg/m^3. To modify the volumetric brine content to the unfrozen water content in a soil, the v_b value has to be multiplied by the soil porosity times the degree of ice saturation. This prediction was compared to the measured unfrozen water content of Soil A which is a fine sand with no fine-grained particles. Figure 6.2 shows the good agreement between the prediction and the experimental data. At 10 ppt salinity, the prediction slightly underpredicted the measured value. These comparisons shows that for coarse-grained materials the phase diagram can be used to give a good estimations of the unfrozen water content. Instead of using Equation 3.85, which requires the values of densities of the brine at each temperature, the following equation can be used to give a first approximation:

$$\theta_u\ (\%\ \text{vol.}) = \frac{S_o}{S_{eq}}\ (\text{m.c.})\ (\gamma_d) \tag{6.1}$$

where: S_o, S_{eq} : initial salinity, equilibrium brine salinity
m.c.: thawed soil moisture content
γ_d: dry density

This direct approach should not be used to predict the unfrozen water content for soils with fine-grained particles. The soils tested in the present study were non-plastic, therefore it was not possible to use Anderson and Tice's (1972) prediction for unfrozen water content of non-saline soils based on specific surface area or Tice et al.'s (1976) method based on liquid limit measurements. An attempt to carry out liquid limits measurement proved impossible due to the non-plastic nature of the test Soils B and C. Therefore the unfrozen water content for Soils B and C at 0 salinity had to be measured in the laboratory. Once these values were known, two methods were used to predict the phase composition curves at salinities of 5, 10 and 30 ppt.

The first method was proposed by Patterson and Smith (1983) based on a study by Banin and Anderson (1974) (Equation 3.14). This method takes the phase composition curve at a given natural salinity and uses it to predict the unfrozen water content for other salinities. In this case, the natural salinity was assumed to be 0, and the phase composition curves for salinities of 5, 10 and 30 ppt were calculated. The equation takes a given unfrozen water content and predicts its freezing temperature for different salinities. The predicted curves are compared to the measured unfrozen water content in Figures 6.3 and 6.4, for Soils B and C respectively. Figures 6.3 and 6.4 show that for salinities of 5 and 10 ppt, the prediction using Equation 3.3 is good for both types of soils. One problem, with this method is that as salinity increases, the values of unfrozen water content at warm temperatures can not be evaluated. This is shown to occur for a salinity of 30 ppt (Figures 6.3 and 6.4). Values of unfrozen water content at temperatures warmer than -10°C could not be evaluated, and consequently a comparison over the complete temperature range of the tests was not possible. The predicted values for a salinity of 30 ppt underestimate the measured unfrozen water content. Therefore, this method should only be used for soils salinity less than 10 ppt.

The second method investigated is simply to add the unfrozen water content measured for the non-saline soil to the unfrozen water content predicted by the phase diagram for a given soil salinity and temperature. The unfrozen water content at 0 ppt is due to the unfrozen water bonded to the fine-grained particles at any temperature. Figures 6.5 and 6.6 show the comparison between the measured unfrozen water contents and the predicted values, for Soils B and C respectively. The prediction gives reliable estimation of the unfrozen water content with differences between predicted and measured values less than 20%. In the case of Soil C 10 ppt, the prediction tends to overestimate the value of unfrozen water. The difference between predicted and measured values for Soils B 30 ppt in the temperature range of -3°C to -5°C was the largest difference observed. This procedure offers a reliable method for predicting the unfrozen water content of a soil without extensive measurement or thermodynamic calculations.

6.2. BEHAVIOUR OF FROZEN SALINE SOILS UNDER UNIAXIAL CONSTANT STRAIN RATE COMPRESSION

6.2.1. Stress-strain behaviour of frozen saline soils

The results of the uniaxial tests performed on the frozen soils were presented in Chapter 5. As stated, Soil A deformed as a brittle material in contrast to Soils B and C which displayed a strain-strengthening behaviour with an initial yield point at a strain of 1%. The difference in behaviour is believed to be related to the presence of fine-grained particles in Soils B and C. Soil A is a frictional material in the unfrozen state, and its strength in the frozen state is provided by a combination of cohesion caused by the ice and particle friction. For Soils B and C, the presence of a small amount of fines provides some particles cohesion in addition to particle friction and ice cohesion.

The main difference in the deformation behaviour is due to the location of the unfrozen water relative to the particles. As shown in Figure 3.1, coarse-grained materials have ice directly in contact with the soil grains and brine islands within the ice due to brine exclusion from the saline pore fluid. Non-saline fine-grained soils have unfrozen water bonded to the surface of the soil grain. If a fine-grained soil has low salinity, the ice forms a continous "cement" around the soil particles with its bonded water and causes an increase in salinity of the adsorbed water. At high salinity , the adsorbed water still exists, but the ice matrix becomes discontinous "floating" in a high salinity brine. For Soil A, the ice distribution is presumed to be as shown in Figure 3.1 c). In the case of Soils B and C, it is believed that a combination of these two models developed. Consequently, the presence of fine particles in Soils B and C allows for a more ductile mechanical behaviour since the unfrozen water act as a lubricant between the soil grains, as the sample deforms.

In Soil A, the ice matrix cohesion and grain to grain friction contributions to the resistance are believed to act simultaneously. Once the peak resistance is reached, the ice matrix cohesion and the grain friction decrease. In Soil A, no initial yield point is observed at a strain of 1%. Since the soil particles provide some resistance even at very small strains in the case of a frictional material, no loss of resistance is observed as the ice starts to fail. For Soils B and C, at very low strains (less than 1%), most of the resistance is provided by the ice cohesion which starts to fail at a strain of 1%, where the particle friction and cohesion start to provide some resistance. The resistance for Soils B and C reaches a maximum at a strain of approximately 10% to 12%. As shown in Figure 5.15 and 5.16, the resistance at large strains depends on the salinity. At high salinity, i.e. 30 ppt, the soil does not show a decrease in resistance even at strains larger than 20%. This could be explained by the very low ice content, and the fact that most of the resistance is provided by grain friction rather than ice cohesion. However, at a 5 ppt salinity, some loss of resistance can be observed at strains between 15% and 17%. This is explained by the higher ice content at this salinity which provides some resistance due to ice cohesion which does not fail completely until the high strain levels are reached.

The volume change behaviour of the soils during shearing supports the above discussion about the contribution of the cohesion of ice and the grain to grain friction to the resistance. The volume change was obtained by recording cell fluid displaced during the test. Since direct measurements of the volume change of the sample were not made, only qualitative conclusion about the contribution of the volume change to the measured resistance can be made. The volume change indicates that dilation occurs as the soil deforms. As mentioned in Chapter 5, the volume change of Soil A was larger than the volume change of Soil B which was larger than the volume change of Soil C. This observation is consistent with the observation that Soil A behaves as a frictional material which dilates as it deforms. The presence of fines reduces the diltancy of Soils B and C, since these soils are more cohesive in nature.

As explained in Chapter 3, the ice matrix provides some internal confinement as the soil dilates. This internal confinement develops more in Soil A due to its more dilatant behaviour, leading to a higher peak resistance as the maximum confinement develops. When the ice reaches its maximum tensile strength, confinement can no longer be maintained, and the soil fails in a brittle manner. In Soils B and C, since the soil does not dilate to the same extent full mobilization of the internal confinement develops more gradually leading to the strain-strengthening effect observed in the unconfined compression tests.

As mentioned in Chapter 5, neither the test salinity nor temperature affected the volume change behaviour. This is understandable since the dilatancy is caused by grain to grain friction which is not a function of temperature nor salinity.

6.2.2. Influence of density on the compressive strength and secant modulus

As mentioned in Chapter 5, a few tests were run to investigate the influence of density on the compressive behaviour of the soils. Soil B at a salinity of 5 ppt was chosen to study this dependency. Table 6.1 summarizes the physical properties of the samples tested. Tests 65, 71 and 75 were also included since they were tests of the Soil B 5 ppt at -7°C. The equivalent ice porosity is defined as the ratio of the volume of soil grains and air to the total volume. Figure 5.18 a) shows a general increase in the 10% strength with an increase in sample density. The phenomenon is easily understood, since a higher density results in more grain to grain contacts which cause an increase in the inter particle friction and the measured resistance. Test H (density of 2.08 Mg/m^3) gave a slightly higher 10% strength then would be expected. This can be explained by its lower degree of saturation (Table 6.1). Since less ice was present in the pore space, more interparticle friction developed leading to a higher resistance.

Figure 5.19 shows that for densities greater than 2.0 Mg/m^3 or moisture content lower than 19%, the yield strength remains constant with an average of 794 kPa. The strength at yield is provided by the ice resistance. For all these tests, a fairly constant volumetric ice content of 31.7% was measured in the soils. Test G was run at a density of 1.93 Mg/m^3 (average moisture content of 23.8%) and gave a yield strength of 948 kPa. This soil had the same degree of saturation as the other tests but had a void ratio of 0.71 as compared to an average void ratio of 0.51 for the other tests, leading to a higher ice content by volume of 40.5%. This higher ice content provided more ice bonding leading to a higher yield strength. Another way to understand the contribution of the ice to the yield strength is to consider the equivalent ice porosity of the samples. Test G had an equivalent ice porosity of 59.5% as compared to an average ice porosity of 68.3% for the other samples. This difference could also explain the higher yield strength observed in test G. Finally, as shown by Figure 5.18 b), the secant moduli obtained from these tests appear to be independent of density for Soil B.

6.2.3. Influence of temperature on compressive strength and secant modulus

The variations of strength and yield strength with temperature were presented in Chapter 5. In this section, a method to predict the variation of strength with temperature will be presented. As stated in the previous section, density influences the 10% strength for Soils B and C and the yield strength when the moisture content is larger than 19%. This finding suggests that the results of tests #65, #16, #67, #77 and #15 be excluded because of density influences.

To assist in understanding the influence of temperature on the measured strength, the results obtained in this study for the pure sand (Soil A) are compared with data available in the literature for similar sands. Table 6.2 present the results from these tests and Figures 6.7 and 6.8 compare the strength vs test temperature for non-saline and saline frozen sands, respectively. The scatter in results is important because of the large variation in strain rate used during the different studies. For example, all tests by Stuckert and Mahar (1984) were run at a strain rate almost forty times the strain rate used during this study. As stated in Chapter 3, the strength of frozen soils is dependent on strain rate since the ice matrix strength is highly strain rate dependent. However, for strain rates of the same order of magnitude, the results of the present study are in good agreement with previously published data.

To establish a correlation between strength and temperature, different strength-temperature relationshships were investigated. The best correlation was obtained by a relationship of the form proposed by Sayles (1974) and presented in Equation 3.51 a). However, instead of using $T_1 = -1°C$ as proposed by Sayles, $T_1 = -10°C$ was used since it is more representative of the temperature range under study. The relationship has the form;

$$\sigma = A\,(T/T_1)^{B_S} \quad \text{or} \quad \log\sigma = \log A + B_S \log(T/T_1) \qquad (6.2)$$

where: A, B_S: soil parameters
T/T_1: temperature ratio
T_1: -10°C

Figures 6.9 to 6.13 present the result of the regressions between log strength and log temperature ratio for Soils A, B and C respectively, also including the regression for yield strength vs temperature. The regressions were polynomial regressions of degree 1 calculated by the computer program Cricket Graph, © Cricket Software Inc. Figure 6.14 shows that the slopes of the regression lines, parameter B_S, are almost independent of salinity except for a salinity of 30 ppt for Soils B and C. Figure 6.15 presents the variation of the A parameter with salinity. The A parameter is the strength at a temperature of -10°C and is expected to decrease with an increase in salinity as observed. Figure 6.16 present a linear regression between the A parameter and salinity. For Soil A, which represents the coarse-grained frictional material, the best fit is given by a power law of the form:

$$A = A_2 (1+S)^{B_2} \tag{6.3a}$$

where: A_2, B_2: regression coefficient
S: salinity in ppt

For Soils B and C, a simple linear polynomial is appropriate.

$$A = A_2 + B_2 S \tag{6.3b}$$

Table 6.3 summarizes the strength vs temperature regression results, and Table 6.4 presents the parameter A vs salinity regression coefficients. By combining these results, the following equations can be used to predict the variation of strength with temperature for the soils studied . The strengths (σ) are in kPa, the salinity, S, is in ppt and the temperature is in °C. These equations are valid for a strain rate of 0.8%/hour.

For Soil A $\quad \sigma_{max} = 5\,595\,(1+S)^{-0.602}\,(T/T_1)^{0.89}$ (6.4a)

For Soil B at 0, 5, 10 ppt $\quad \sigma_{10\%} = (3\,305 - 87.5\,S)\,(T/T_1)^{0.96}$ (6.4b)

$\sigma_y = (1\,621 - 50.6\,S)\,(T/T_1)^{1.44}$ (6.4c)

For Soil B at 30 ppt $\quad \sigma_{10\%} = (3\,305 - 87.5\,S)\,(T/T_1)^{1.79}$ (6.4d)

$\sigma_y = (1\,621 - 50.6\,S)\,(T/T_1)^{2.21}$ (6.4e)

For Soil C at 0, 5, 10 ppt $\quad \sigma_{10\%} = (2\,616 - 62.1\,S)\,(T/T_1)^{0.87}$ (6.4f)

$\sigma_y = (1\,613 - 45.7\,S)\,(T/T_1)^{1.21}$ (6.4g)

For Soil C at 30 ppt $\quad \sigma_{10\%} = (2\,616 - 62.1\,S)\,(T/T_1)^{0.97}$ (6.4h)

$\sigma_y = (1\,613 - 45.7\,S)\,(T/T_1)^{1.57}$ (6.4i)

The difference in B_S between salinities of 0, 5, 10 ppt and a salinity of 30 ppt is believed to be caused by a change in behaviour of the soil as the unfrozen water content increases over a critical value. This critical unfrozen water content could not be determined since a large gap in salinities existed between values of 10 and 30 ppt. The soil unfrozen water content at a salinity of 30 ppt was more dependent on the variation in temperature, which caused a larger value of B_S which is the slope of the relationship between strength and temperature. The variations in strength for 30ppt is more important because the change in unfrozen water content with a change in temperature was more important at 30 ppt than at other salinities.

Table 6.2 includes the predicted strength using Equation 6.4 a) for the strengths of the sands from other studies at similar strain rates. The predicted strengths give an acceptable prediction of the strength for Sego et al.'s (1982) results except at a salinity of 10 ppt (for one sample tested at a strain rate 5 times slower than the strain rate used in this study) and 35 ppt where the predicted values overestimate the measured strengths by more than 100%. Comparing the results to Sego and Cherenko (1984) strengths good agreement is observed between predicted and measured values. The predicted strengths for the conditions tested by Goughnour and Andersland (1968) give good agreement for a temperature of -12°C but underpredicts the strength by 100% at a temperature of -4°C. However, the test at -4°C was run at a strain rate twice as fast as the strain rate valid for Equation 6.4 a).

Another approach to relate the strength and temperature was to used the normalized strength, or strength ratio, R, which is defined as the ratio of the strength of the soil at a given temperature to the strength of the same soil at a salinity of 0 ppt at the same temperature. Figure 6.17 presents the normalized peak strength for Soil A, and the normalized 10% strength for Soils B and C as a function of temperature. Figure 6.18 shows the normalized yield strength as a function of temperature for Soils B and C. The normalized strength for a given salinity can be considered independent of temperature for each soil. Two points do not follow the trend; Soil B 5 ppt for yield strength at a temperature of -12°C and Soil C 10 ppt for yield strength at a temperature of -5°C. Table 6.5 gives the value of the strength ratio, R, for each soil at each temperature and the average ratio. R decreases with an increase in salinity according to a power law for Soil A and is linearly related to salinity for Soils B and C. Figure 6.19 gives the R vs salinity relationships for each soil. R can be predicted using the following regressions;

For Soil A $R_{max} = 0.987\ (1 + S)^{-0.628}$ (6.5a)

For Soil B $R_{10\%} = 0.936 - 0.0254\ S$ (6.5b)

$R_y = 0.868 - 0.0274\ S$ (6.5c)

For Soil C $R_{10\%} = 1.027 - 0.0244\ S$ (6.5d)

$R_y = 0.940 - 0.0271\ S$ (6.5e)

The salinities (S) are in ppt and the equations are valid for a strain rate of 0.8%/hour.

Using these values of R and the value of the strength for a non saline soil at given temperature, it is possible to calculate the strength of the same soil at other salinities and the same temperature.

Stuckert and Mahar (1984) developed a relationship between the strength of sands and the ice area ratio which depends on the volumetric ice content. Using their equations given in Equations 3.86 to 3.88, the strength for Soil A was estimated. The method requires an estimate of the ice strength which Stuckert and Mahar predict using Equation 3.87 b). Figure 6.20 compared the result of the prediction to the laboratory measured strengths of Soil A. A prediction using ice strength values from the literature (Goughnour and Andersland ,1968 , Mellor , 1979, Cole , 1983 and Mellor and Cole, 1982) was also included. At a salinity of 0 ppt, both predictions seriously underpredict the strength. The same phenomenon was observed by Stuckert and Mahar. For a salinity of 0 ppt, this method predicts a resistance equal to the ice strength and does not consider any particle interaction. Moreover, this method was developed for loosely packed soils where grain to grain contacts were minimum. In the soil tested in the present study, the packing was relatively dense causing grain to grain contacts leading to the development of friction and internal confinement. For salinities of 10 and 30 ppt, the prediction using calculated ice strength overpredicted the frozen soil strength. However, when the ice strength from the literature were used, good agreement was obtained between measured and predicted soil strengths. For a salinity of 5 ppt, the predicted values using the calculated ice strength agreed with the measured values for temperature of -12°C and -10°C. For temperature of -7°C and -5°C, the measured strengths were well predicted when ice strength from the literature were used. This discrepancy in the prediction can not be explained.

As shown in Figure 5.12, the secant modulus also varies with temperature. A reasonably good fit was obtained when a linear polynomial was used for the regression between the secant modulus and the temperature.

$$E_S = C_M + D\,(T + 10°C) \qquad (6.6)$$

where: E_S: secant modulus in MPa
C_M, D: regression coefficients
T: temperature in °C

The reason to use T+10°C, instead of T, is the same as using T_1 = -10°C for the strength vs temperature regression, i.e. the intercept will give a value in the range of test temperatures. The intercept of the regression, parameter C_M, will be the secant modulus at a temperature of -10°C. Figure 6.21 to 6.23 show the regression for the secant modulus vs T+10°C for Soils A, B and C respectively. As shown by Figure 6.24, the value of D can be considered constant for each soil at salinities of 0, 5 and 10 ppt. Figure 6.25 indicates that the value of the coefficient C_M varies with salinity and the best regressions for each soil are presented in Figure 6.26. For Soil A, the best fit is given by a power law of the form:

$$C_M = C_2\,(1 + S)^{D_2} \qquad (6.7a)$$

where: C_M: in MPa
C_2, D_2: regression coefficient
S: salinity in ppt

For Soils B and C, a simple linear polynomial is appropriate.

$$C_M = C_2 + D_2 S \qquad (6.7b)$$

A summary of the modulus vs temperature regression results is presented in Table 6.6, and the parameter C_M vs salinity regression coefficients are given in Table 6.7. By substituting the results of Equation 6.7 into Equation 6.6, the following predictions are obtained for the variation of modulus with temperature for the soils tested. These relationships are valid for strain rates equal to 0.8%/hour. The secant modulus, E_s, is in MPa, the salinity, S, in ppt and the temperature, T, in °C.

For Soil A at 0, 5, 10 ppt $E_{s\,50\%} = 251\ (1+S)^{-0.65} - 8.83\ (T+10)$ (6.8a)

For Soil A at 30 ppt $E_{s\,50\%} = 251\ (1+S)^{-0.65} - 2.58\ (T+10)$ (6.8b)

For Soil B at 0, 5, 10 ppt $E_s = (145 - 3.62\ S) - 15.0\ (T+10)$ (6.8c)

For Soil B at 30 ppt $E_s = (145 - 3.62\ S) - 6.89\ (T+10)$ (6.8d)

For Soil C at 0, 5, 10 ppt $E_s = (129 - 3.27\ S) - 13.4\ (T+10)$ (6.8e)

For Soil C at 30 ppt $E_s = (129 - 3.27\ S) - 3.91\ (T+10)$ (6.8f)

Such relationships could be used in foundation design or settlement calculations where a deformation modulus is required. Moreover, these could be input into numerical analysis used to predict the deformation response under load of a saline frozen soil.

6.2.4. Influence of the unfrozen water content on compressive strength and secant modulus

In the previous section, the influence of temperature and salinity on the strength of frozen saline soils were considered as two different physical parameters. It is possible to combine the effect of salinity and temperature by investigating the variation of the strength of the soil with the unfrozen water content present in the soil. Only a few authors have investigated the correlation between unfrozen water content and strength in sands. The results of their investigations are compared to the results from this study in Figure 6.27. The same trend of a decrease in strength with an increase in unfrozen water content is observed. However, the strengths quoted by Ogata et al. (1983) and Pharr and Merwin (1985) were significantly higher since the strain rates used in their studies were at least 50 times higher than the strain rate used in this study. The data from the two studies found in the literature are comparable to each other.

Two approaches will be used to discuss to establish the interrelationship between the strength and the unfrozen water content. First, the best fit between unfrozen water content and strength will be established using linear polynomial regressions. Second, the approach proposed by Pharr and Merwin based on the brine porosity in sea ice mechanics will be discussed.

Figure 6.28 shows the variation of strength vs unfrozen water content for each soil. The decrease in resistance with an increase in unfrozen water content appears to follow an exponential law.

Figures 6.29 a) and 6.30 present the regression of the log strength vs log unfrozen water content. For Soil A, the points for 0 salinity were rejected since they artificially shifted the regression line upwards, when the log $(1+\theta_u)$ function was used. A good fit is observed between the regression line and the measured values for Soils B and C for both the 10% strength and the yield strength. For Soil A, more scatter is observed around the regression line. However, the concept of using unfrozen water content to relate the influence of both temperature and salinity on the strength of a given soil shows promise. The following equations can be used to predict the strength of the different soils. The strengths are in kPa, and the unfrozen water contents are given in % by volume. The relationships are valid for a strain rate of 0.8%/hour.

For Soil A $\quad \sigma_{max} = 1\,819\,(\theta_u)^{-0.574}$ (6.9a)

For Soil B $\quad \sigma_{10\%} = 7\,761\,(\theta_u)^{-1.084}$ (6.9b)

$\sigma_y = 5\,607\,(\theta_u)^{-1.580}$ (6.9c)

For Soil C $\quad \sigma_{10\%} = 8\,468\,(\theta_u)^{-0.954}$ (6.9d)

$\sigma_y = 9\,016\,(\theta_u)^{-1.389}$ (6.9e)

The concept of corrected unfrozen water content should be introduced at this point. The corrected unfrozen water content is defined as the unfrozen water content at a given temperature minus the unfrozen water content of the same soil at a salinity of 0 ppt at the same temperature. This concept was developed to investigate if the variation of strength vs unfrozen water content for Soils B and C would be the same when the unfrozen water generated by the presence of fines is subtracted from the total unfrozen water content. In other words, this will determine if the soil type has an influence on the strength-unfrozen water content relationship.

Figure 6.31 presents a comparison of the log strength vs log corrected unfrozen water content regression between Soils B and C. As for Soil A, the values of 0 unfrozen water content were rejected. Despite the fact that the points seem to establish one trend, the regressions indicate a fairly important difference between the regressions for each soil. This supports Ogata et al. (1983) observation that for fine-grained soils the unfrozen water concept is not a unifying concept between different soil types. This conclusion can be explained by the particle interactions which are not solely control by the unfrozen water content. An increased amount of fines would cause an increase in soil cohesion resulting in a higher resistance as compared to a soil with a lesser amount of fines.

The approach developed by Pharr and Merwin (1985) useson Equation 3.25.

$$\frac{\sigma_f}{\sigma_o} = 1 - c\, v_b^{k} \qquad (3.25)$$

They predicted the 0 ppt strength, σ_o, using a relationship between the strength and the log of temperature of the form given in Equation 3.83. They used Equation 3.85 to calculate the brine content over a range of salinities of 0 to 48 ppt and temperatures of -2.5°C to -15°C, and established the c and k coefficients. For frozen Ottawa sand, they obtained, the following regression:

$$\frac{\sigma_f}{\sigma_o} = 1 - 1.02\, v_b^{0.109} \qquad (6.10)$$

In the present study, the 0 ppt strength was not calculated but actually measured. Consequently, the σ_f / σ_o ratio is the same as the normalized strength or strength ratio, R, introduced in Section 6.2.3. Moreover, the measured values of unfrozen water content were used as brine content. Figures 6.29 b), 6.32 and 6.33 give the correlation between log(1-R) and log unfrozen water content. The strength ratio can be predicted using the unfrozen water content (% by volume) for a strain rate of 0.8%/hour using the following equations;

For soil A
$$\frac{\sigma_{max}}{\sigma_{max_o}} = 1 - 0.670\, \theta_u^{0.130} \tag{6.11a}$$

For soil B
$$\frac{\sigma_{10\%}}{\sigma_{10\%_o}} = 1 - 0.105\, \theta_u^{0.815} \tag{6.11b}$$

$$\frac{\sigma_y}{\sigma_{y_o}} = 1 - 0.194\, \theta_u^{0.619} \tag{6.11c}$$

For soil C
$$\frac{\sigma_{10\%}}{\sigma_{10\%_o}} = 1 - 0.0174\, \theta_u^{1.294} \tag{6.11d}$$

$$\frac{\sigma_y}{\sigma_{y_o}} = 1 - 0.0633\, \theta_u^{0.916} \tag{6.11e}$$

The result from Equation 6.11a) can be compared to Equation 6.10 which was obtained for frozen Ottawa sand. The dependency of the strength to the unfrozen water content is indicated by the slope of the line (k value). The two sands have similar values of k (0.13 vs 0.109). The c parameter in Equation 3.25 which represents the (1-R) value for θ_u =1. The c values for the sand from this study and the Ottawa sand tested by Pharr and Merwin are of the same order of magnitude (0.67 vs 1.02).

The results of the regression of the Pharr and Merwin's approach give, in general, coefficients of correlation between strength and unfrozen water content which are lower than the coefficients of correlation for the regressions between log strength and log θ_u. Therefore, since good correlation between strength and unfrozen water content was established using Equation 6.9, using unfrozen water content to predict the strength of a given soil appears to give a reliable method when based on limited experimental work.

The modulus of deformation should also depend on the unfrozen water content and the relationship between the secant modulus and the unfrozen water content would be useful. Figure 6.34 shows the variation of the secant modulus with unfrozen water content. As with the variation of strength, the secant modulus decreases with an increase in unfrozen water content and it appears to follow a power law. Figure 6.35 presents the linear polynomial regressions for the log secant modulus versus the log unfrozen water content for each soil. As was the case for the secant modulus vs temperature regressions the scatter is quite important. However, the regressions indicate a definite trend in the decrease of the secant modulus with an increase in unfrozen water content. Figure 6.35 gives the following relationships between the secant modulus, in MPa, and the unfrozen water content (% by volume). It should be kept in mind that these were established for a strain rate of 0.8%/hour.

For Soil A $E_{s\,50\%} = 102.5\,(\theta_u)^{-0.863}$ (6.12a)

For Soil B $E_s = 353.4\,(\theta_u)^{-1.161}$ (6.12b)

For Soil C $E_s = 426.4\,(\theta_u)^{-1.045}$ (6.12c)

Because of the important scatter in these regressions, more work should be carried out to establish the validity of Equations 6.12. More care should be given to the determination of the deformation moduli in future studies.

6.3. TIME DEPENDENT DEFORMATION OF FROZEN SALINE SOILS UNDER UNIAXIAL COMPRESSION

6.3.1. Time dependent deformation of frozen saline soils

Chapter 5 presented the results of the constant stress tests. As mentioned, the concept of secondary (steady-state) creep is not appropriate to study the time dependent behaviour of ice-poor soils. Consequently, the analysis will be based on either a primary or a tertiary creep model.

Before going any further, the author would like to clarify some confusion which is present in the literature concerning "creep" of frozen soils. Creep in the strict sense of the word is the time dependent deformation of a material without any volume change. Consequently, in a frozen soil, only the ice matrix undergoes creep. Other time dependent deformations take place such as rearrangement of the soil particles leading to a change in void ratio. Moreover, in highly saline soils, some consolidation may take place which increases the time dependent deformations. The volume change observed in the constant stress test are not related to the creep phenomenon itself but to rearrangement within the soil matrix. These distinctions are theoretically important, but from a phenomelogical stand-point it is impossible to distinguish between the different time dependent deformations. Therefore when the word creep deformation is used, it encompasses all time dependent deformations. The creep models used for frozen soils attempt to predict all time dependent deformations without distinguishing between the source of the time dependent deformation.

The results presented in Chapter 5 indicate that an increase in stress and an increase in salinity cause a decrease in the time to failure and an increase in the strain rate at failure. As mentioned in Chapter 5, Soils B and C at a salinity of 30 ppt did not reach failure but displayed attenuating creep to accumulated strains in excess of 20%. The author believes that, due to the high unfrozen water content present Soils B and C at salinities of 30 ppt, their behaviour was very plastic causing large time dependent deformations under constant stress. Since the amount of ice was less than in the other soils, the strengthening effect due to particle rearrangement as they underwent deformation dominated over the weakening effect caused by a loss of ice resistance. Shields et al. (1985) suggest that the onset of dilatancy could be an indication of the start of tertiary creep. In the case of Soil A, the dilatant behaviour started at the beginning of the test. Therefore, dilatancy could not be an indication of the start of tertiary creep, but dilatancy could indicate that the soil will eventually undergo tertiary creep. For Soils B and C, the paucity of the volume change results does not allow any conclusive observations. However, in creep test CR-65, the dilatant behaviour started at the onset of tertiary creep.

Contrary to the observations from Rein and Hathi (1978), the strain to failure does not indicate any consistent trend with respect to applied stress, except for Soil C 0 ppt which shows an increase in strain to failure with an increase in stress. Figure 6.36 shows the variation of accumulated creep strain at failure as defined by Gardener et al. (1984) (total strain to failure - instantaneous strain) with applied stress. The strain to failure for Soils B and C at a salinity of 30 ppt were not included since these soils did not reach tertiary creep. Table 6.8 present the creep strain to failure for each soil at each salinity. Except for Soil A, the strain to failure decreases with an increase in salinity. For Soil A at a salinity of 0 ppt, the average creep strain to failure was 2.7% indicating a very brittle behaviour due to the complete absence of unfrozen water in this soil at the test temperature of -7°C. Soil A at salinities of 5 and 10 ppt had almost the same average strain to failure, 5.5% compared to 5.9%. Soil A 30 ppt had a slightly lower strain to failure, i.e. 4.8%.

6.3.2. Analysis of strain-time relationships

Four models from the literature were considered to study the measured time dependent deformation data. First, Sayles' (1968) primary creep strain model was selected since it present a form similar to other authors (for example Azizi, 1989). Second, Vyalov (1988) primary creep strain model based on hardening theory was also used. The third model investigated was Gardener et al.'s (1984) tertiary creep model. Brief consideration was also given to Berggren and Furuberg (1985) secondary creep model.

Detailed examples of the calculation required by Sayles, Vyalov, and Gardener models are presented in Appendix D. The caculated strain vs time curves are compared to the measured curves in Appendix E.

Berggren and Fururberg (1985) method is based on the evaluation of the resistance, which is defined as the derivative of time with respect to strain, i.e. **R** = dt / dε. By considering the **R** vs time graphs from Appendix D, it is obvious that Berggren and Furuberg's model could not reliably predict creep strain for the studied soils, because of the irregularity in the curve. Moreover, no steady-state secondary stage where **R** is constant developed in the constant stress tests. Consequently no further consideration will be given to this model.

For Soil A, Vyalov's $\log (\dot{\varepsilon}\, t^2)$ vs $\log \varepsilon$ plots gave a straight line as predicted by the model. However, for Soils B and C, a bilinear line was obtained. An attempt will be made to predict creep strain using constants (α and **a**) for each part of the bilinear curve. The result will be discussed later.

Gardener's model require the evaluation of the **c** parameter as defined by Equation 3.43. The initial instantaneous strain is require to calculate **c**. Since the mode of loading in the constant stress tests was different from the mode of loading in the constant strain rate tests, the secant modulus from the CSR tests could not be used to predict an initial instantaneous strain. Therefore, an equivalent instantaneous strain was defined as the strain after 120 seconds into the creep test minus the strain after 30 seconds. For Soil A 0 ppt, the instantaneous strain was taken as the strain after 600 seconds minus the strain at 30 seconds, since the load application was very progressive. For Soil C 30 ppt, because of the high stresses used and the low resistance the strain after 90 seconds minus the strain after 30 seconds was used as the initial strain. Equation 3.42 gives the creep strain as a function of time according to Gardener et al. (1984) method. In order to compare the predicted strains to the measured strains the initial strain has to be added to the creep strain.

Table 6.9 presents all the creep parameters necessary to predict the strain vs time for Sayles (1968), Vyalov et al. (1988) and Gardener et al.(1984) models. The strain rate after 1 hour, $\dot{\varepsilon}_1$, calculated by Sayles' method and the strain rate after 1 hour measured are also included. The measured strain after 1 hour, ε_1, which is required in Sayles' computation is also listed. For tests CR-64, CR-76 and CR-78, the measured strain rates after 1 hour were not available since the tests were stopped before a period of one hour had elapsed. For these tests and the other tests on the same type of soil, i.e. Soil A 30 ppt and Soil C 30 ppt, the strain rates after 10 minutes, $\dot{\varepsilon}_{10\,min}$, predicted by Sayles and measured as well as the strain after 10 minutes are included, and indicated by an asterix. Values of α and **a** are not included for Soils B and C, since it will be shown that Vyalov's method is not applicable for these soils. Figure 6.37 shows Vyalov's prediction for creep tests CR-

71 (Soil B 0 ppt) and test CR-36 (Soil C 0 ppt). Two approaches were used; first, values of α and $\mathbf{a}$ were estimated for both parts of the bilinear line in the $\log \dot{\varepsilon}\, t^2$ vs $\log \varepsilon$ graphs (α_1, α_2, $\mathbf{a}_1$, $\mathbf{a}_2$) ; secondly, single values for α and $\mathbf{a}$ (α_{avg}, $\mathbf{a}_{avg}$) were obtained by fitting a line through all the points. Detailed calculations for test CR-71 are included in Appendix D. The values obtained for each test were:

Test 71 $\alpha_1 = 0.967$ $\mathbf{a}_1 = 24.3$
$\alpha_2 = 0.16$ $\mathbf{a}_2 = 6.36$
$\alpha_{avg} = 0.33$ $\mathbf{a}_{avg} = 5.75$

Test 36 $\alpha_1 = 0.781$ $\mathbf{a}_1 = 13.6$
$\alpha_2 = 0.068$ $\mathbf{a}_2 = 7.73$
$\alpha_{avg} = 0.34$ $\mathbf{a}_{avg} = 5.38$

Figure 6.37 shows that both approaches give very poor prediction of the measured strain vs time curve. This is the reason why α and $\mathbf{a}$ values for Soils B and C are not given and Vyalov's method is not used to predict the strain vs time curves for Soils B and C.

Appendix E presents the predicted strain vs time curves compared to the measured strain-time relationships. For Soil A, three predictions are included; Sayles', Vyalov's and Gardener's. For Soils B and C, only prediction by Sayles and Gardener are presented, as explained previously. Vyalov's method can only predict the beginning of the strain-time curve. In most cases, Vyalov's prediction departs from the measured curve much before the time to failure. In a few rare cases (CR-92, CR-95), Vyalov's equation seems to model adequately the observed strains up to failure, for Soil A. One of the drawbacks of Vyalov's equation is the impossibility of predicting strains for times greater than the time to failure. Equation 3.55 a) shows that for times close to time to failure, t_f, the denominator of the right side of the equation becomes very small or equals zero for $t=t_f$. Therefore, the predicted strains become excessively large at $t \approx t_f$ which is not coherent with the observed behaviour of the samples. Because of the very poor performance of this method, no further discussion pertaining to it will be included.

As shown in Appendix E, the strain predicted by Sayles' method and Gardener's method, both provide a very good fit to the measured strains, up to the initiation of failure. An example for each soil type is given in Figure 6.38 Sayles' method usually give a very good fit at the beginning of the test and up to the time to failure after which it starts to underpredict the measured strains. Some problems were observed for the following tests; in test CR-17 the predicted strains are at least 3% to high up to the time to failure; in test CR-32, CR-89 and CR-94, the predicted strains give a good fit at the start of the test, but underpredict the measured strains after strains of 7% to 9% were reached. Gardener's method does not predict the beginning of the measured strain curves as well as Sayles' method does. In general, it overpredicts the strain up to a time of 40% to 70% of the time to failure. However, Gardener's method usually predicts more accurately the strains after the time to failure has been reached. This observation is in agreement with the statement made by Sayles (1988) which said that Gardener's method provides a good prediction for times greater than 70% of the time to failure. Finally, for Soils B and C at a salinity of 30 ppt, Gardener's method gave a poorer prediction of the measured strains than Sayles' method, especially for test CR-76. Since both methods predict with accuracy different parts of the strain curve, they will both be considered further in Section 6.3.3.

Before closing this section, brief consideration will be given to the flow law of ice, Equation 3.44, as a tool to predict minimum strain rate. A value of n=3 (stress exponent) was shown to be acceptable for ice or ice-rich soils. However, the following discussion will show that the extension of n=3 for saline ice-poor frozen soils, such as used by Nixon and Lem (1984), is not valid. Figure 6.39 present the relationship between minimum strain rate and stress divided by 1 000 kPa on a log-log plot representing the equation;

$$\dot{\varepsilon}_{min} = B\left(\sigma / \sigma_1\right)^n \qquad (3.44b)$$

where: σ_1 = 1000 kPa
n: stress exponent
B: minimum strain rate at σ=1 000 kPa

The reason to divide the applied stress, σ, by 1 000 kPa is to get an intercept which is in the region of stresses used in the tests. Consequently, the B values represent the minimum strain rate for a stress of 1 000 kPa. Table 6.10 give the B and n values obtained for each soil at the different salinities. The n value is shown not to be equal to 3. In general, an increase in B values and a decrease in n values are observed with an increase in salinity. This dependency will be discussed in the following section.

6.3.3. Variation of the creep parameters with salinity or unfrozen water content

Before starting this discussion, it is important to note that all the following results are valid for a test temperature of -7°C. Sayles' creep parameters will be discussed first. Referring to Table 6.9, the strain rates after 1 hour predicted by Sayles' equation are in general in very good agreement with the measured strain rates after 1 hour. Figures 6.40 and 6.41 present the variation of the parameter **M** as a function of stress. Sayles predicted that **M** increases with an increase in stress for non-saline sands but that **M** is practically independent of stress for silts and clays. This is exactly what is observed here. For Soil A 0 ppt, **M** increases with stress, but **M** is practically a constant for Soil A 5, 10 30 ppt and Soils B and C. However for Soils B and C at a salinity of 30 ppt, the constant **M** value is slightly higher than for the other salinities. This author believes that as soon as some unfrozen water exists in the soil, the dependency of **M** on stress disappears. The dependency of **M** on stress for non-saline Soil A is given by;

$$M = 7.59 \times 10^{-8} \sigma^{2.076} \quad \text{with } \sigma \text{ in kPa} \qquad (6.13)$$

Table 6.11 gives the values for **M** for each soil at each salinity and an average **M** value for each soil which are; for Soil A 5, 10, 30 ppt, M_{avg} = 2.34; for Soil B 0, 5,10 ppt, $M_{avg} = 1.00$; for Soil B 30 ppt, $M_{avg} = 1.45$; for Soil C 0, 5, 10 ppt, $M_{avg} = 0.94$; and for Soil C 30 ppt, $M_{avg} = 1.19$.

Following Sayles' approach, the predicted strain rate after 1 hour is plotted as a function of stress ratio in Figure 6.42. For Soils A 30 ppt and C 30 ppt, measured values of strain rate after 1 hour were not always available since some of these tests were stopped before 1 hour had elapsed. For these two soils, the relationship between strain rate after 10 minutes and the stress is also shown in Figure 6.43. The value of strain rate predicted by Sayles for test CR-76 was rejected from the regressions, since the curve had to be completely corrected as discussed in Chapter 5. The regression between strain rate at 1 hour and stress has the following form;

$$\dot{\varepsilon}_1 = E\,(\sigma / \sigma_1)^F \qquad (6.14)$$

Again the stress is divided by $\sigma_1 = 1\,000$ kPa, in order to have E as the strain rate after 1 hour for a stress of 1 000 kPa. Table 6.12 presents the E and F values for each soil. For Soil A 5 and 10 ppt, and for Soils B and C the values of F can be considered constants with; F = 1.67 for Soil A 5 and 10 ppt, F = 2.22 for Soil B and F = 2.61 for Soil C. The value of E, the strain rate after 1 hour for an applied stress of 1 000 kPa, increases with an increase in salinity. Figures 6.44 and 6.45 present the relationship between E and salinity or unfrozen water content, respectively. The E value for Soil A 0 ppt was rejected from the regression for Soil A because of the different mode of deformation observed for this soil. It is interesting to note that the relationship between E and salinity is practically constant for the three soils. For a temperature of -7°C, the strain rate at 1 hour can be given by the following equations which relate the strain rate at 1 hour to salinity and stress ratio or unfrozen water content and stress ratio;

For Soil A 0 ppt $\quad \dot{\varepsilon}_1 = 7.2 \times 10^{-4}\,(\sigma / \sigma_1)^{4.87}$ (6.15a)

For Soil A 5, 10 ppt $\quad \dot{\varepsilon}_1 = 10^{(-0.64 + 0.056\,S)}\,(\sigma / \sigma_1)^{1.67}$ (6.15b)

or

For Soil A 5, 10 ppt $\quad \dot{\varepsilon}_1 = 10^{(-0.65 + 0.18\,\theta_u)}\,(\sigma / \sigma_1)^{1.67}$ (6.15c)

For Soil A 30 ppt $\dot{\varepsilon}_1 = 10^{(-0.64 + 0.056\,S)} (\sigma / \sigma_1)^{3.69}$ (6.15d)

or

For Soil A 30 ppt $\dot{\varepsilon}_1 = 10^{(-0.65 + 0.18\,\theta_u)} (\sigma / \sigma_1)^{3.69}$ (6.15e)

For Soil B $\dot{\varepsilon}_1 = 10^{(-0.64 + 0.056\,S)} (\sigma / \sigma_1)^{2.22}$ (6.15f)

or

For Soil B $\dot{\varepsilon}_1 = 10^{(-1.00 + 0.17\,\theta_u)} (\sigma / \sigma_1)^{2.22}$ (6.15g)

For Soil C $\dot{\varepsilon}_1 = 10^{(-0.64 + 0.056\,S)} (\sigma / \sigma_1)^{2.61}$ (6.15h)

or

For Soil C $\dot{\varepsilon}_1 = 10^{(-1.10 + 0.13\,\theta_u)} (\sigma / \sigma_1)^{2.61}$ (6.15i)

where: $\dot{\varepsilon}_1$: in %/hour
σ and σ_1 : in kPa
S: salinity in ppt
θ_u: unfrozen water content in % by volume

For Soils A 30 ppt and C 30 ppt, the strain rate after 10 minutes can also be used. It is given by;

For Soil A 30 ppt $\dot{\varepsilon}_{10\,\mathrm{min}} = 30.9\ (\sigma / \sigma_1)^{4.70}$ (6.16a)

For Soil C 30 ppt $\dot{\varepsilon}_{10\,\mathrm{min}} = 38.9\ (\sigma / \sigma_1)^{1.50}$ (6.16b)

Sayles' method can be used to predict the strain rate after 1 hour which is needed in the computation of the strain-time relationship but it can not predict the strain after 1 hour which is also required. Therefore, the measured strain after 1 hour has to be used. For Soils A 30 ppt and C 30 ppt, the values of strain after 1 hour were not always available as mentioned before. The values of strain after 10 minutes of testing will be used for Soils A 30 ppt and C 30 ppt. Figure 6.46 present the variation of strain 1 hour with stress ratio (stress/ 1 000kPa) and Figure 6.47 presents the strain after 10 minutes as a function of stress for Soils A and C 30 ppt. A regression of the following form has been established for all soils;

$$\varepsilon_1 = G\ (\sigma / \sigma_1)^{H} \qquad (6.17)$$

Table 6.13 lists the G and H regression coefficients. For Soils A 5, 10 ppt, B and C 0, 5, 10 ppt, the slope of the regression H can be considered independent of stress with

H = 1.64 for Soil A 5, 10 ppt, H = 1.84 for Soil B and H= 1.99 for Soil C 0, 5, 10 ppt. The parameter G, which is the strain after 1 hour for an applied stress of 1 000 kPa, increases with an increase in salinity or unfrozen water content. Figure 6.48 present the relationship between log G and salinity or unfrozen water content. The values for Soil A 0 ppt were rejected, and the values for Soils A and C at 30 ppt were not included since values of strain 1 hour were not available for these two soils. The following equations give the strain after 1 hour or strain after 10 minutes as a function of salinity and stress ratio, or unfrozen water content and stress ratio, for a temperature of -7°C;

For Soil A 0 ppt $\varepsilon_1 = 0.083\ (\sigma / \sigma_1)^{2.35}$ (6.18a)

For Soil A 5, 10 ppt $\varepsilon_1 = 10^{(0.087 + 0.021S)}\ (\sigma / \sigma_1)^{1.64}$ (6.18b)

or

For Soil A 5, 10 ppt $\varepsilon_1 = 10^{(0.13 + 0.047\,\theta_u)}\ (\sigma / \sigma_1)^{1.64}$ (6.18c)

For Soil A 30 ppt $\varepsilon_{10\ min} = 6.22\ (\sigma / \sigma_1)^{2.18}$ (6.18d)

For Soil B $\varepsilon_1 = 10^{(0.097 + 0.044\,S)}\ (\sigma / \sigma_1)^{1.84}$ (6.18e)

or

For Soil B $\varepsilon_1 = 10^{(-0.15 + 0.13\,\theta_u)}\ (\sigma / \sigma_1)^{1.84}$ (6.18f)

For Soil C 0, 5, 10 ppt $\varepsilon_1 = 10^{(0.17 + 0.053\,S)}\ (\sigma / \sigma_1)^{1.99}$ (6.18g)

or

For Soil C 0, 5, 10 ppt $\varepsilon_1 = 10^{(-1.39 + 0.31\,\theta_u)}\ (\sigma / \sigma_1)^{1.99}$ (6.18h)

For Soil C 30 ppt $\varepsilon_{10\ min} = 13.8\ (\sigma / \sigma_1)^{1.21}$ (6.18i)

where: ε_1 : in %
σ and σ_1 : in kPa
S: salinity in ppt
θ_u: unfrozen water content in % by volume

By using Equation 3.57 (or Equation 3.56 if t_R is taken as 10 minutes), the strain vs time curve can be predicted when the stress and salinity (or unfrozen water content) are known simply by substituting the results of Equations 6.15 and 6.18 into Equation 3.57 or the results of 6.16 and 6.18 into Equation 3.56.

The results from the correlation between minimum strain rate and stress will be discussed here, since they will be used in the discussion of Gardener's method which follows. Figures 6.49 and 6.50 present the variation of the B and n values (listed in Table 6.10) with salinity or unfrozen water content, respectively. For Soil A, except at a salinity of 0 ppt, the n value can be considered constant with values of 5.2. For Soil A at 0 ppt, which represent the case of a non-saline frictional material, the logB value is -8.1 and n equals 12.2. The non-saline Soil A will be rejected from all regressions since its behaviour was different from all the other soils because of the absence of unfrozen water within the sample. Establishing trends for B as functions of salinity or unfrozen water content did not result in highly reliable fits to the data. Figure 6.51 present two correlations; one between B and the salinity (rejecting 0 ppt salinity); the second one between B and the unfrozen water content. The regressions between B and salinity gave good correlations, but the regressions between B and unfrozen water content gave fairly poor correlations.

For Soil A 5, 10, 30 ppt $\log B = -3.13 + 3.11 \log S$ (6.19a)
For Soil B 5, 10, 30 ppt $\log B = -9.39 + 7.48 \log S$ (6.19b)
For Soil C 5, 10, 30 ppt $\log B = -11.4 + 8.98 \log S$ (6.19c)
For Soil A 5, 10 ,30 ppt $\log B = -1.40 + 2.81 \log \theta_u$ (6.19d)
For Soil B $\log B = -9.90 + 11.1 \log \theta_u$ (6.19e)
For Soil C $\log B = -19.5 + 17.5 \log \theta_u$ (6.19f)

where $B = \dot{\varepsilon}_{min}$ for $\sigma = 1\,000$ kPa in %/hour
S: salinity in ppt
θ_u: unfrozen water content in % by volume
T: test temperature = -7°C

As stated before n is considered a constant for Soil A 5, 10 and 30 ppt. For Soils B and C, the variation of n with salinity or unfrozen water content are presented in Figure 6.52. First a linear relationship between n and salinity is presented which gives fairly good coefficient of correlations. The second regression between log n and log unfrozen water content also gave good correlations. The relationships are given by the following equations, for a temperature of -7°C;

For Soil B $n = 13.8 - 0.29\ S$ (6.20a)

For Soil C $n = 23.1 - 0.69\ S$ (6.20b)

For Soil B $\log n = 1.45 - 0.68 \log \theta_u$ (6.20c)

For Soil C $\log n = 2.51 - 1.60 \log \theta_u$ (6.20d)

where S: salinity in ppt

θ_u: unfrozen water content in % by volume

Correlations using unfrozen water content have been presented to allow for future work at other temperatures. The unfrozen water content approach combines the effects of salinity and temperature as discussed in Section 6.2.4. However, the correlations between B or n and unfrozen water content did not give as good correlation as the relationships between B or n and salinity. The above observations suggest that using a value of n = 3 is definitely not valid for the saline frozen soils studied.

Finally, the parameters from Gardener's strain prediction equation will be discussed. Gardener et al. (1984) assumed that the parameter **c** was a constant for a given soil over a fairly wide range of stresses. Figure 6.53 shows that this assumption can be considered valid for the three soils studied except at salinities of 30 ppt. Creep test CR-36, for Soil C 0 ppt does not follow this trend, and its **c** value is an order of magnitude too low. This value will not be included for the averaging process. Table 6.14 gives the average value of **c** for each soil. The **c** value can practically be considered constant for a given soil type with; **c** = 0.37 for Soil A, **c** = 0.040 for Soil B and **c** = 0.046 for Soil C. Figure 6.54 shows two examples of strain curves where the prediction of strain was done using the specific **c** value for that soil or the average **c** value for that soil type. For test CR-36, the agreement is poor, but the strains up to failure are predicted within 1% of the measured strains. This is an extreme case, since the average **c** value for Soil C 0 ppt is an order of magnitude different from the specific **c** value for test CR-36. For test CR-82, the prediction using the average **c** value is very acceptable. The following linear relationships exist between c and applied stress for Soils A, B and C at salinities of 30 ppt at temperature of -7°C.

For Soil A 30 ppt $c = -0.50 + 0.0014\,\sigma$ (6.21a)

For Soil B 30 ppt $c = -0.248 + 0.00085\,\sigma$ (6.21b)

For Soil C 30 ppt $c = -0.85 + 0.0014\,\sigma$ (6.21c)

As explained in Chapter 3, since the creep strain to failure, $\varepsilon_m - \varepsilon_o$, is assumed constant, the time to failure is proportional to the inverse of the strain rate at failure (Equation 3.60).

$$t_m \; \alpha \; \frac{\varepsilon_m - \varepsilon_o}{\dot{\varepsilon}_m} \tag{3.60}$$

Gardener et al. (1984) used the flow law of ice to correlate the minimum strain rate to stress, and obtain Equation 3.61 a) for the time to failure as a function of stress;

$$t_m = K / \sigma^n \tag{3.61a}$$

Gardener established that K should be given by;

$$K = (\varepsilon_m - \varepsilon_o) / B \tag{3.61b}$$

The parameters B and n are the same as discussed previously. The present author does not agree with Equation 3.61b). Since Equation 3.60 could be expressed as follows;

$$t_m = \phi \frac{\varepsilon_m - \varepsilon_o}{\dot{\varepsilon}_m} \tag{3.60}$$

and the minimum strain rate is given by;

$$\dot{\varepsilon}_m = B\,\sigma^n \tag{3.44}$$

Therefore,

$$K = \phi \frac{\varepsilon_m - \varepsilon_o}{B} \tag{6.22}$$

Gardener et al. (1984) neglected to include the constant, ϕ, in Equation 3.61 b).

The creep strain at failure was shown to be practically a constant for a given soil (see Figure 6.36). Figure 6.55 present the variation of the time to failure with the stress ratio (stress divided by 1 000 kPa). Table 6.15 gives the values for K and n, and compares the B and n values given by Gardener and by the flow law. The n values determined by the two approaches are fairly close, except for Soil C 0 ppt. The B values as expected do not correspond for the reason explained above. Therefore, an attempt to correlate K to the B parameter from the flow law is not valid. A decrease in K is observed with an increase in salinity. Figure 6.56 presents the regression between K and salinity or unfrozen water content. The values for Soil A 0 ppt were not included, and the values for salinities of 0 ppt were not included in the K vs salinity relationship. The K value can be predicted using the following equations at a temperature of -7°C;

For Soil A 5, 10, 30 ppt $\log K = 3.34 - 2.87 \log S$ (6.23a)

For Soil B 5, 10, 30 ppt $\log K = 8.87 - 6.69 \log S$ (6.23b)

For Soil C 5, 10, 30 ppt $\log K = 11.1 - 8.29 \log S$ (6.23c)

For Soil A 5, 10 ,30 ppt $\log K = 1.73 - 2.59 \log \theta_u$ (6.23d)

For Soil B $\log K = 9.48 - 9.97 \log \theta_u$ (6.23e)

For Soil C $\log K = 14.45 - 12.5 \log \theta_u$ (6.23f)

where K = time to failure for $\sigma = 1\,000$ kPa in hours
S: salinity in ppt
θ_u: unfrozen water content in % by volume

As noticed for the n value from the flow law, the n value for Soil A 5, 10, 30 ppt can be considered as constant equal to 5.8, as opposed to 5.2 for the flow law n value. The n value for Soils B and C was shown to decrease with an increase in salinity or unfrozen water content. Figure 6.57 shows the same trends, but the regression are much poorer since more scatter exists in the n values from Gardener's equation compared to the n values from Equation 3.44. This author recommends using the flow law (Equation 3.44) to obtain the n values.

The only results in the literature that could be compared to the results presented herein are from Pharr and Godavarti (1987), who tested saline Ottawa sand at a salinity of 32 ppt and a temperature of -8°C. All other creep tests on saline materials were run under conditions much different from the present conditions to allow comparison. Figure 6.58 presents the variations of time to failure, strain rate at a strain of 2% and time to strain of 2% with stress for Soil A 30 ppt and the results from Pharr and Godavarti. Very good agreement is observed between the two sets of data points. The strain rate vs strain curves predicted using the results from the previous section for Sayles' and Gardener's methods are compared to the measured strain rate vs strain curves from Pharr and Godavarti (1987) tests in Figure 6.59. The following values for the creep parameters were obtained using Equations 6.16, 6.18, 6.21, 3.60 and 6.23 and a salinity of 32 ppt (test salinity used by Pharr and Godavarti);

for Sayle's method:

$M = 2.34$
$\dot{\varepsilon}_{10\,min} = 30.9\ (\sigma / \sigma_1)^{4.70}$ for σ = 1 034 kPa, 931 kPa, 828 kPa 586 kPa, 469 kPa, 345 kPa (stress studied by Pharr and Godavarti (1987))
$\varepsilon_{10\,min} = 6.22\ (\sigma / \sigma_1)^{2.18}$ for the same stresses

for Gardener's method:

$c = -0.50 + 0.0014\ \sigma$ for the same stresses
$t_m = K / (\sigma / \sigma_1)^n$ for the same stresses
$n = 13.8 - 0.29\ S = 4.52$ for S = 32 ppt
$\log K = 3.34 - 2.87 \log S = 0.105$ for S = 32 ppt

The strain to failure which was used in Gardener's method was 4.8% and the instanteneous strain was taken as 1%. Figure 6.59 shows that for the high stresses, i.e. 1 034, 931 and 828 kPa, the prediction by Sayles and Gardener methods gave strain rate vs strain relationship similar to the measured ones. However, neither method could predicted definitely the time to failure, nor showed an definite acceleration of the strain rate. This is to be expected since in the strain time predictions, the tertiary creep was never well modelled. For the low stress, 586, 469 and 345 kPa, both methods underpredicted the strain rates by at least one order of magnitude. For a stress of 345 kPa, Gardener's method could not be used since the predicted value of c using Equation 6. 21 was negative. The reason for this severe underprediction is that the stresses are lower than the range of stresses studied, and stress probably affects the values of M and c at lower stresses. The method developed would give a better correlation for the strain vs time curves. However, these curves were not presented in the paper by Pharr and Godavarti (1987) and consequently could not be compared to the strain-time prediction.

This section shows how Sayles' (1968) and Gardener et al.'s (1984) models could be used to predict the strain-time relationship for saline frozen soils with a minimum of experimantal data. Since Sayles' equation has been shown to predict well small time dependent deformations, this method should be used in conjunction with equations of the form of Equations 6.13, 6.15, 6.16 and 6.18 to predict strains when relatively small strains are expected, or when the strains have to be limited to a given level as it is the case in foundation design. If time to failure or strain to failure are of interest in a design project, Gardener's method would provide a better tool. Using Equtions 3.42 or 3.61 a) in conjunction with equations of the form of Equations 6.20 and 6.23 could give a good evaluation of the strain or time to failure.

6.4. COMPARISON BETWEEN CONSTANT STRESS TEST (CREEP) AND CONSTANT STRAIN RATE TEST

In Chapter 3, it was mentioned that some authors have tried to establish correspondence between constant stress tests and CST tests. The point of minimum strain rate and the point of maximum resistance both give a maximum value for the stress to strain rate ratio in the CSR tests or constant stress tests. The total strains and time to failure have been compared to see if they agree between the two tests. For CSR tests conducted at different strain rates, it is possible to compare the stress-strain rate relationship obtained from each test.

In the present case, since only one strain rate was investigated in the series of CSR tests, it is impossible to establish a stress strain rate relationship for the constant strain rate tests. Therefore the only comparison possible, is to investigate if, when a stress level comparable to the peak strength is applied in a creep test, the minimum strain rate is comparable to the applied strain rate in CSR tests, which was 0.8%/hour. To do so, the relationship established between minimum strain rate and stress in Section 6.2.2 will be used to predict the strain rate at a stress level equal to the peak strength or 10% strength. To predict the time to minimum strain rate, t_m, the relation established in Section 6.2.3 from Gardener will be used. For Soils B and C, a major difference exists between the two types of tests; in the CSR tests, the sample did not reach failure at strains as high as 15%; in the creep tests, failure was reached at strains between 8% and 15%. This difference alone suggests that correspondence between the two tests can not be established for these soils.

Table 6.16 presents a summary of all comparable results between the CSR tests and the creep tests. The values in parentheses in the table refer to actual measured values when the applied stress was equal to the maximum strength or 10% strength. The predicted minimum strain rates are consistently lower than the applied strain rate in the CSR tests except for Soil C 30 ppt. The strains at minimum strain rate for the creep tests are in general slightly larger than the strain to failure in the CSR tests, for Soil A. It should be kept in mind that for Soils B and C at a salinity of 30 ppt, failure never took place in the creep tests, and that a strain of 12% was arbitrarily selected.

This author believes that because of the discrepancies in modes of deformation and in strain rates at peak or minimum, correspondence between constant strain rate tests and constant stress tests can not be established. As mentioned in Chapter 3, the authors who to date have established correspondence have done so on non-frictional materials (ice or fine-grained soils). In this author's opinion, for frictional materials, correspondence between the two types of tests is not valid and the stress path and accumulated strains have a definite influence on the development of failure.

6.5. ULTIMATE STRENGTH OF FROZEN SOILS

As opposed to ice, frozen soils have some long-term strength. Vyalov (1963) proposed Equation 3.78 to predict the ultimate strength given a time to failure. Using his approach, the variation of the inverse of stress as a function of time to failure is plotted in Figure 6.60 for the three tested soils. The slope of the lines give the inverse of β and the intercept is equal to $-1/\beta(\log B)$. The values of β and B were calculated and are listed in Table 6.17. For Soil A 5, 10 and 30 ppt, the value of β is almost a constant. For Soils B and C, β decreases with an increase in salinity. However, the variation of β and B with salinity is not the point of interest here. The minimum long-term strength of the material should be equal to the strength of the unfrozen soil. Therefore, the minimum long-term strength should not be affected by the salinity, since the unfrozen strength is practically independent of salinity. For Soil A, the 100 or 1 000 year strength is practically the same for salinities of 5, 10 and 30 ppt, but differs greatly from the 100 or 1 000 year strength of Soil A 0 ppt. For Soils B and C, the 1 000 year strength decreases with an increase in salinity. Therefore, the calculated long-term strength seems to be a function of salinity for time period of up to 1 000 years. In practical applications where the design life is usualy set to 30 years, the use of long-term strength is acceptable as an upper bound on the strength for the stability criteria.

TABLE 6.1
PHYSICAL PROPERTIES for SOIL B-5 at DIFFERENT DENSITIES

Test	Soil	Total Density (Mg/m^3)	S_r (%)	Avg M.C. (%)	e	Ice content (% vol.)	Ice porosity (% vol.)
C	B-5	2.03	84.9	17.1	0.54	32.4	67.6
D	B-5	2.04	85.0	16.6	0.52	31.7	68.3
E	B-5	2.00	83.7	17.9	0.57	33.1	66.9
G	B-5	1.93	89.4	23.8	0.71	40.5	59.5
H	B-5	2.08	80.8	14.0	0.46	27.9	72.1
65	B-5	2.03	87.6	18.2	0.55	34.1	65.9
71	B-5	2.10	88.8	15.8	0.48	31.2	68.8
75	B-5	2.09	88.5	16.0	0.48	31.4	68.6

TABLE 6.2
COMPRESSION STRENGTH for VARIOUS SANDS

Author	Salinity (ppt)	Temperature (°C)	Strain rate (sec^{-1})	Strength (kPa)	Strength predicted by equation 6.4a) (kPa)
present study	0	-12	$2.2x10^{-6}$	6095	
	0	-10	$2.2x10^{-6}$	5810	
	0	-7	$2.2x10^{-6}$	4363	
	0	-5	$2.2x10^{-6}$	3252	
	5	-12	$2.2x10^{-6}$	2271	
	5	-10	$2.2x10^{-6}$	2065	
	5	-7	$2.2x10^{-6}$	1140	
	5	-5	$2.2x10^{-6}$	1004	
	10	-12	$2.2x10^{-6}$	1307	
	10	-10	$2.2x10^{-6}$	1164	
	10	-7	$2.2x10^{-6}$	845	
	10	-5	$2.2x10^{-6}$	667	
	30	-12	$2.2x10^{-6}$	860	
	30	-10	$2.2x10^{-6}$	661	
	30	-7	$2.2x10^{-6}$	444	
	30	-5	$2.2x10^{-6}$	373	
Stuckert and Mahar (1984)	0	-2.3	$8.5x10^{-5}$	2379	
	0	-5	$8.5x10^{-5}$	4206	
	6	-3	$8.5x10^{-5}$	1586	
	6	-6	$8.5x10^{-5}$	2413	
	10	-3	$8.5x10^{-5}$	1276	
	10	-6	$8.5x10^{-5}$	2100	
	30	-3	$8.5x10^{-5}$	620	
	30	-12	$8.5x10^{-5}$	2210	
Sego et al. (1982)	0	-7	$1.9x10^{-6}$	5335	4073
	0	-7	$3.5x10^{-7}$	4379	4073
	10	-7	$8.8x10^{-6}$	1080	962
	10	-7	$4.2x10^{-7}$	510	962
	35	-7	$2.2x10^{-6}$	166	471
	35	-7	$2.3x10^{-6}$	214	471
	35	-5	$2.3x10^{-6}$	236	349
	35	-5	$2.1x10^{-6}$	191	349
Sego and Cherenko (1984)	0	-7	$2.2x10^{-6}$	6184	4073
	10	-7	$2.2x10^{-6}$	1011	962
	35	-7	$2.2x10^{-6}$	474	471
Goughnour and Andersland (1968)	0	-12	$2.2x10^{-6}$	7584	6581
	0	-4	$4.4x10^{-6}$	5000	2475

TABLE 6.3
STRENGTH vs TEMPERATURE REGRESSION COEFFICIENTS

Soil	Salinity (ppt)	Strength	A (kPa)	B_S
A	0	σ_{max}	5611	0.75
A	5	σ_{max}	1919	1.03
A	10	σ_{max}	1140	0.81
A	30	σ_{max}	676	0.91
B	0	$\sigma_{10\%}$	3499	0.89
B	5	$\sigma_{10\%}$	2845	1.06
B	10	$\sigma_{10\%}$	2168	0.93
B	30	$\sigma_{10\%}$	773	1.79
B	0	σ_y	1862	1.38
B	5	σ_y	1285	1.50
B	10	σ_y	857	1.46
B	30	σ_y	203	2.21
C	0	$\sigma_{10\%}$	2529	0.79
C	5	$\sigma_{10\%}$	2388	0.87
C	10	$\sigma_{10\%}$	2023	0.95
C	30	$\sigma_{10\%}$	731	0.97
C	0	σ_y	1675	1.04
C	5	σ_y	1426	1.19
C	10	σ_y	1012	1.40
C	30	σ_y	283	1.57

TABLE 6.4
A vs SALINITY REGRESSION COEFFICIENTS

Soil	Strength	A_2 (kPa)	B_2
A	σ_{max}	5 595	-0.63
B	$\sigma_{10\%}$	3 305	-87.5
B	σ_y	1 621	-50.6
C	$\sigma_{10\%}$	2 616	-62.1
C	σ_y	1 613	-45.7

TABLE 6.5
RATIO of NORMALIZED STRENGTH

Soil	Salinity (ppt)	T (°C)	R σ_{max} or $\sigma_{10\%}$	R_{avg} σ_{max} or $\sigma_{10\%}$	R σ_y	R_{avg} σ_y
A	0	-12	1.00	1.00		
A	0	-10	1.00			
A	0	-7	1.00			
A	0	-5	1.00			
A	5	-12	0.37	0.33		
A	5	-10	0.36			
A	5	-7	0.26			
A	5	-5	0.31			
A	10	-12	0.21	0.20		
A	10	-10	0.20			
A	10	-7	0.19			
A	10	-5	0.21			
A	30	-12	0.14	0.12		
A	30	-10	0.11			
A	30	-7	0.10			
A	30	-5	0.11			
B	0	-12	1.00	1.00	1.00	1.00
B	0	-10	1.00		1.00	
B	0	-7	1.00		1.00	
B	0	-5	1.00		1.00	
B	5	-12	0.81	0.79	0.74	0.68
B	5	-10	0.84		0.66	
B	5	-7	0.76		0.65	
B	5	-5	0.73		0.66	
B	10	-12	0.59	0.61	0.48	0.46
B	10	-10	0.64		0.46	
B	10	-7	0.65		0.44	
B	10	-5	0.57		0.46	
B	30	-12	0.25	0.20	0.14	0.10
B	30	-10	0.24		0.10	
B	30	-7	0.17		0.08	
B	30	-5	0.15		0.07	
C	0	-12	1.00	1.00	1.00	1.00
C	0	-10	1.00		1.00	
C	0	-7	1.00		1.00	
C	0	-5	1.00		1.00	
C	5	-12	1.01	0.94	0.87	0.82
C	5	-10	0.95		0.86	
C	5	-7	0.86		0.79	
C	5	-5	0.92		0.77	
C	10	-12	0.85	0.78	0.62	0.56
C	10	-10	0.82		0.62	
C	10	-7	0.67		0.56	
C	10	-5	0.76		0.43	
C	30	-12	0.32	0.29	0.18	0.16
C	30	-10	0.28		0.18	
C	30	-7	0.30		0.14	
C	30	-5	0.24		0.12	

TABLE 6.6
MODULUS vs TEMPERATURE REGRESSION COEFFICIENTS

Soil	Salinity (ppt)	C_M (MPa)	D
A	0	218.2	-8.54
A	5	91.5	-8.41
A	10	65.1	-9.53
A	30	21.5	-2.58
B	0	148.2	-16.9
B	5	130.9	-14.6
B	10	100.1	-13.6
B	30	39.3	-6.89
C	0	132.4	-13.2
C	5	117.6	-15.2
C	10	86.2	-11.8
C	30	33.8	-3.91

TABLE 6.7
C vs SALINITY REGRESSION COEFFICIENTS

Soil	C_2 (MPa)	D_2
A	251	-0.65
B	145.3	-3.62
C	129.3	-3.27

TABLE 6.8
CREEP STRAIN TO FAILURE

Soil	Salinity (ppt)	Average failure creep strain (%)
A	0	2.7
A	5	5.5
A	10	5.9
A	30	4.8
B	0	10.9
B	5	8.1
B	10	7.0
B	30	n/a
C	0	13.9
C	5	11.1
C	10	8.8
C	30	n/a

n/a: not applicable

TABLE 6.9
CREEP PARAMETERS

Test	Soil	M	$\dot{\varepsilon}_1$ (%/hr) predicted	$\dot{\varepsilon}_1$ (%/hr) measured	ε_1 (%) meas.	α	a	c	ε_0 (%) $\varepsilon_{120s}-\varepsilon_{30s}$
CR-45	A-0	3.66	1.36	1.36	2.96	0.38	2.69	0.57	1.25
CR-92	A-0	1.67	0.47	0.46	2.04	0.22	2.02	0.27	1.33
CR-95	A-0	1.22	0.12	0.21	0.96	0.14	1.02	0.33	0.62
CR-59	A-5	2.60	0.46	0.49	1.54	0.28	1.46	0.39	0.43
CR51	A-5	2.29	0.46	0.46	1.65	0.32	1.62	0.28	0.38
CR-60	A-5	2.29	0.36	0.40	1.28	0.32	1.27	0.33	0.30
CR-67	A-5	2.04	0.21	0.39	0.61	0.43	0.58	0.31	0.04
CR-86	A-10	2.57	0.74	0.70	1.82	0.39	1.84	0.47	0.55
CR-47	A-10	2.50	0.48	0.43	1.04	0.52	0.96	0.30	0.13
CR-87	A-10	2.41	0.38	0.40	1.03	0.50	1.00	0.37	0.14
CR-64	A-30	2.38	16.2*	16.4*	4.75*	0.49	10.6	0.73	1.53
CR-70	A-30	2.31	2.63	2.66	5.44	0.6	4.90	0.42	0.98
			5.7*	6.01*	2.62*				
CR-72	A-30	2.02	1.35	1.27	3.30	0.35	3.22	0.27	0.86
			3.30*	3.04*	1.70*				
CR-83	B-0	0.796	2.54	2.76	10.4			0.037	0.40
CR-71	B-0	1.02	1.63	1.69	5.96			0.042	0.73
CR-81	B-0	0.932	1.29	1.17	5.96			0.034	0.74
CR-84	B-5	1.06	1.58	1.48	6.44			0.068	2.03
CR-49	B-5	0.927	1.21	1.28	5.48			0.018	0.79
CR-9	B-5	1.16	0.96	0.70	4.96			0.048	0.69
CR-17	B-5	0.996	1.24	n/a	5.12+			0.026	0.72
CR-32	B-5	1.03	0.97	1.23	4.16			0.060	0.76
CR-82	B-10	1.12	1.49	1.56	6.16			0.063	1.11
CR-50	B-10	0.967	1.27	1.28	5.00			0.029	0.80
CR-33	B-10	1.06	0.92	0.95	4.10			0.037	0.68
CR-38	B-10	0.977	0.80	0.82	3.78			0.028	0.78
CR-75	B-30	1.46	5.06	5.42	13.8			0.34	3.24
CR-77	B-30	1.44	3.94	3.95	10.9			0.20	2.00
CR-88	B-30	1.44	2.43	2.39	7.20			0.14	1.09
CR-79	C-0	1.02	2.40	2.10	10.9			0.062	1.72
CR-65	C-0	0.925	1.77	1.02	9.31			0.018	1.35
CR-36	C-0	0.832	1.47	1.66	6.56			0.0014	0.55
CR-96	C-5	0.955	2.11	1.67	9.90			0.060	2.02
CR-66	C-5	1.01	2.25	1.84	8.92			0.104	1.38
CR-62	C-5	1.01	1.44	1.32	8.46			0.037	0.91
CR-89	C-5	0.944	1.31	1.21	7.24			0.047	1.69
CR-94	C-5	0.785	1.01	1.0+	5.70			0.075	0.77
CR-55	C-10	1.01	1.79	1.70	8.00			0.056	1.8
CR-52	C-10	0.968	1.33	1.24	7.23			0.033	1.27
CR-68	C-10	0.913	1.08	1.08	5.62			0.014	0.90
CR-76	C-30	1.10	26.1*	17.1*	17.7*			0.86	5.2
CR-78	C-30	1.19	39.4*	39.1*	13.9*			0.56	3.52
CR-91	C-30	1.28	6.77	9.43	21.8			0.26	3.44
			27.5*	26.5*	10.5*				

+: estimated value *: value of strain or strain rate after 10 minutes

TABLE 6.10
B and n VALUES for $\dot{\varepsilon}_m = B\,\sigma^{n}$

Soil	Salinity (ppt)	B (%/hour)	n
A	0	8.3×10^{-9}	12.2
A	5	0.162	4.6
A	10	0.511	4.2
A	30	36.8	6.7
B	0	9.0×10^{-7}	13.3
B	5	7.9×10^{-5}	12.9
B	10	0.010	11.0
B	30	49.9	4.9
C	0	2.4×10^{-10}	25.6
C	5	5.4×10^{-6}	18.3
C	10	0.0054	14.0
C	30	57.9	3.25

TABLE 6.11
SAYLES' CREEP PARAMETER M

Soil	Salinity (ppt)	M	M_{avg}
A	0	$=7.59 \times 10^{-8}\,\sigma^{2.076}$	
A	5	2.30	2.34
A	10	2.50	2.34
A	30	2.24	2.34
B	0	0.92	1.00
B	5	1.04	1.00
B	10	1.03	1.00
B	30	1.45	1.45
C	0	0.93	0.94
C	5	0.94	0.94
C	10	0.96	0.94
C	30	1.19	1.19

TABLE 6.12
REGRESSION COEFFICIENTS for the $\dot{\varepsilon}_1$ vs σ RELATIONSHIPS

Soil	Salinity (ppt)	E (%/hour)	F	E for $\dot{\varepsilon}_{10\ min}$ (%/hour)	F for $\dot{\varepsilon}_{10\ min}$
A	0	7.2×10^{-4}	4.87		
A	5	0.443	1.36		
A	10	0.902	1.98		
A	30	11.9	3.69	30.9	4.70
B	0	0.218	2.36		
B	5	0.447	1.92		
B	10	0.641	2.88		
B	30	10.2	1.72		
C	0	0.326	2.45		
C	5	0.322	2.87		
C	10	0.857	2.26		
C	30	13.2	2.85	38.9	1.50

TABLE 6.13
REGRESSION COEFFICIENTS for the ε_1 vs σ RELATIONSHIPS

Soil	Salinity (ppt)	G (%)	H	G for $\varepsilon_{10\ min}$ (%)	H for $\varepsilon_{10\ min}$
A	0	0.083	2.35		
A	5	1.56	1.64		
A	10	1.99	1.64		
A	30			6.22	2.18
B	0	1.17	2.06		
B	5	2.43	1.53		
B	10	3.10	2.24		
B	30	25.7	1.53		
C	0	1.44	2.54		
C	5	2.90	1.83		
C	10	4.93	1.61		
C	30			13.8	1.21

TABLE 6.14
AVERAGE c VALUES for GARDENER'S STRAIN PREDICTIONS

Soil	Salinity	c_{avg}
A	0	0.39
A	5	0.33
A	10	0.38
A	30	$= -0.50 + 0.0014\ \sigma$
B	0	0.038
B	5	0.044
B	10	0.039
B	30	$= -0.248 + 0.00085\ \sigma$
C	0	0.040
C	5	0.065
C	10	0.034
C	30	$= -0.85 + 0.0014\ \sigma$

TABLE 6.15
B and n VALUES from GARDENER and from FLOW LAW

Soil	Salinity	Gardener			Flow Law	
	(ppt)	n	K (hour)	B	n	B (%/hour)
A	0	11.9	1.25×10^8	1.2×10^{-7}	12.2	8.3×10^{-9}
A	5	5.9	14.6	0.38	4.6	0.162
A	10	5.0	5.50	1.07	4.2	0.511
A	30	6.4	0.098	49.0	6.7	36.8
B	0	12.5	1.17×10^6	9.3×10^{-6}	13.3	9.0×10^{-7}
B	5	13.1	2.29×10^4	3.5×10^{-4}	12.9	7.9×10^{-5}
B	10	8.2	79.4	0.088	11.0	0.010
B	30	4.4	0.124	80.6	4.9	49.9
C	0	14.0	1.62×10^6	8.6×10^{-6}	25.6	2.4×10^{-10}
C	5	18.1	4.57×10^5	2.4×10^{-5}	18.3	5.4×10^{-6}
C	10	10.5	134.9	0.065	14.0	0.0054
C	30	3.1	0.116	69.0	3.2	57.9

TABLE 6.16
COMPARISON CSR TESTS and CREEP TESTS RESULTS

Soil		CSR			CREEP	
	$\sigma_{\text{max or 10\%}}$ (kPa)	t_{failure} (hour)	$\varepsilon_{\text{failure}}$ (%)	$\dot{\varepsilon}_{\text{min}}$ at $\sigma_{\text{max or 10\%}}$ (%/hour)	t_m (hour)	ε_m (%)
A-0	4363	5.2	3.8	0.552	3.1	3.8
A-5	1140	5.1	3.6	0.295	6.5	5.8
A-10	845	6.8	5.2	0.251	13.1	6.2
A-30	444	6.0	4.6	0.156	17.8	6.0
B-0	2354	12.6	10	0.084 (0.104)	26.2 (20.0)	11.5
B-5	1718	12.6	10	0.081	19.0	9.1
B-10	1235	12.9	10	0.096 (0.081)	14.9 (16.1)	7.9
B-30	402	12.6	10	0.561	0.22	12
C-0	2036	12.8	10	0.018 (0.027)	83.4 (70.0)	15.1
C-5	1749	12.7	10	0.149	1.3	12.4
C-10	1372	13.1	10	0.444 (0.448)	5.0 (4.7)	10.2
C-30	611	12.9	10	8.97	0.54	12

( ): actual measured value

TABLE 6.17
ULTIMATE STRENGTH RESULTS

Soil	Salinity (ppt)	β	B	σ_{ult} 10 years (kPa)	σ_{ult} 100 years (kPa)	σ_{ult} 1000 years (kPa)
A	0	18139	0.00022	2109	1889	1711
A	5	1934	0.172	339	288	251
A	10	1724	0.113	293	250	219
A	30	1965	0.0013	251	223	200
B	0	13459	0.000045	1449	1308	1192
B	5	10309	0.000017	1061	962	880
B	10	4831	0.0016	624	553	496
B	30	1054	0.01961	158	138	122
C	0	12180	0.000081	1348	1214	1104
C	5	15748	1.6E-08	1236	1146	1069
C	10	5587	0.00043	672	600	542
C	30	1328	0.0052	184	161	144

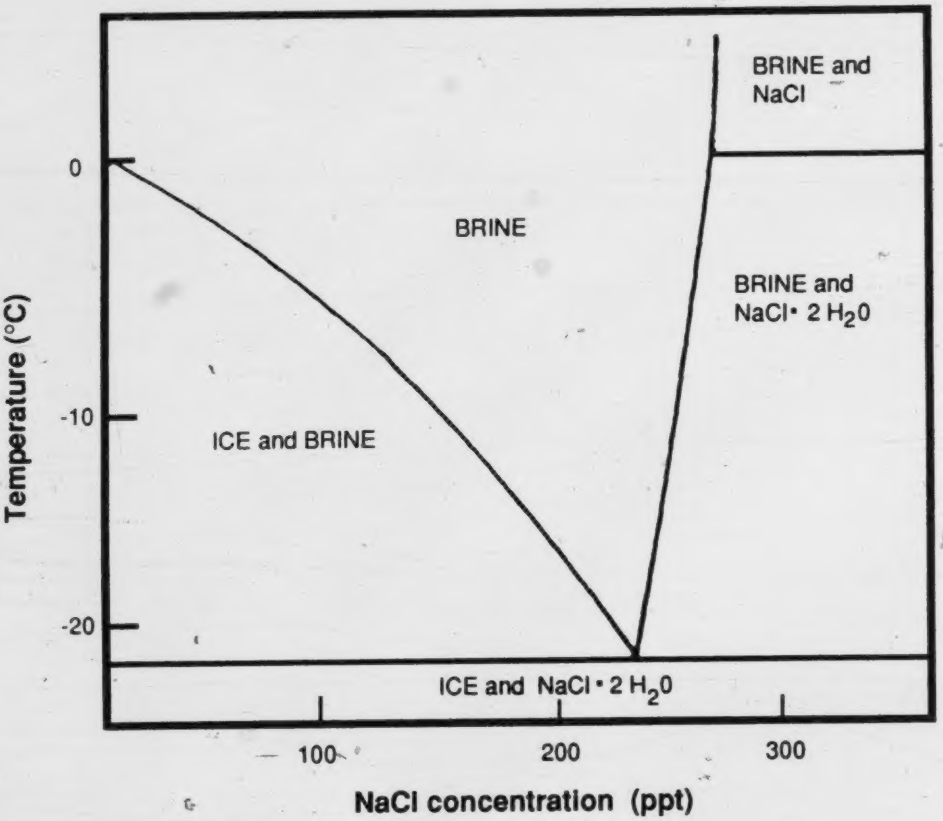

Figure 6.1: Sodium Chloride (NaCl)-Water (H_2O) binary phase diagram

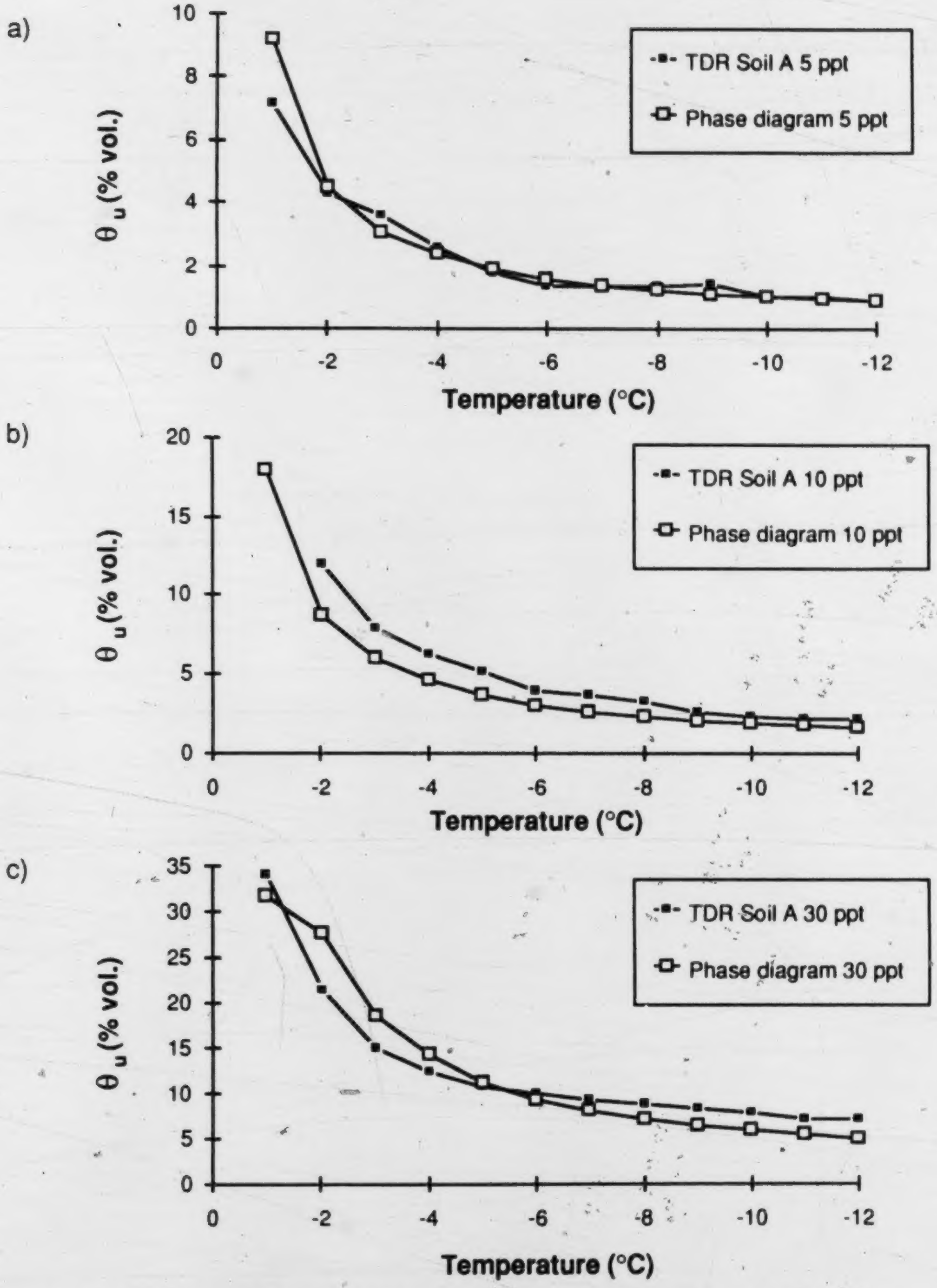

Figure 6.2: Comparison between TDR results for soil A and phase diagram prediction for unfrozen water content a) 5 ppt b) 10 ppt c) 30 ppt

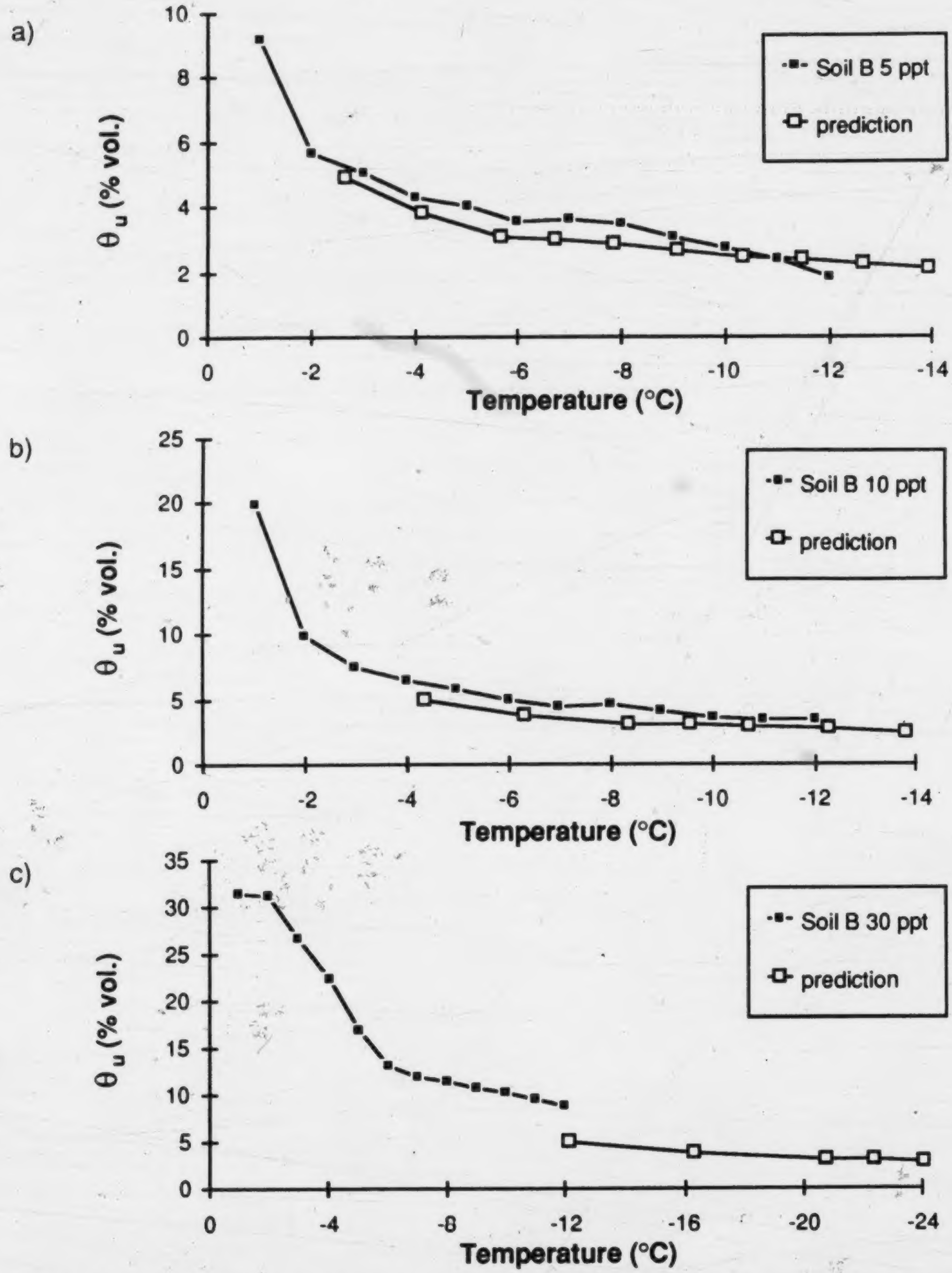

Figure 6.3: Comparison between unfrozen water content measured by TDR and predicited by Banin and Anderson's (1974) equation based on unfrozen water content at a salinity of 0 ppt for soil B
a) 5 ppt b) 10 ppt c) 30 ppt

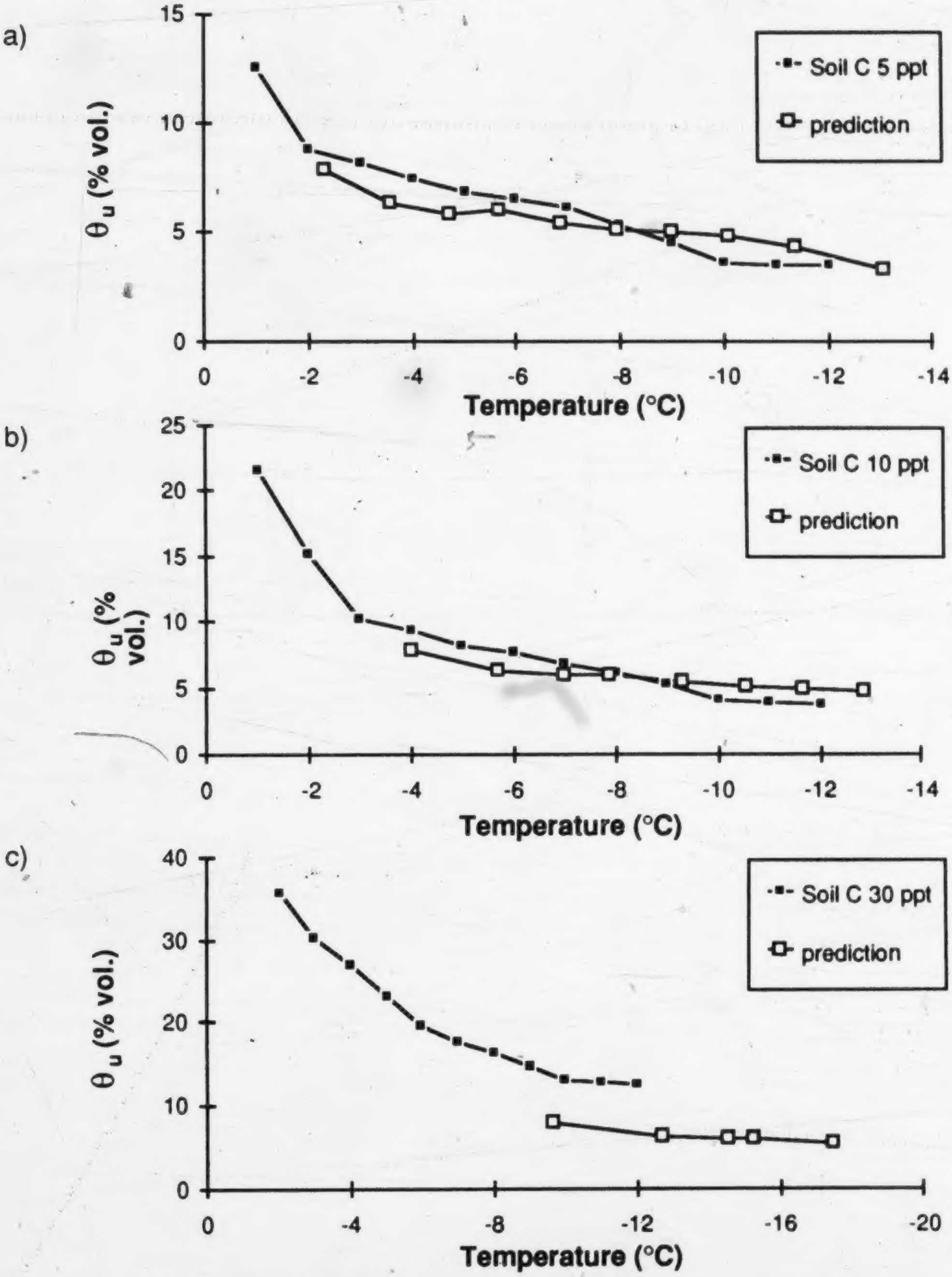

Figure 6.4: Comparison between unfrozen water content measured by TDR and predicited by Banin and Anderson's (1974) equation based on unfrozen water content at a salinity of 0 ppt for soil C
a) 5 ppt b) 10 ppt c) 30 ppt

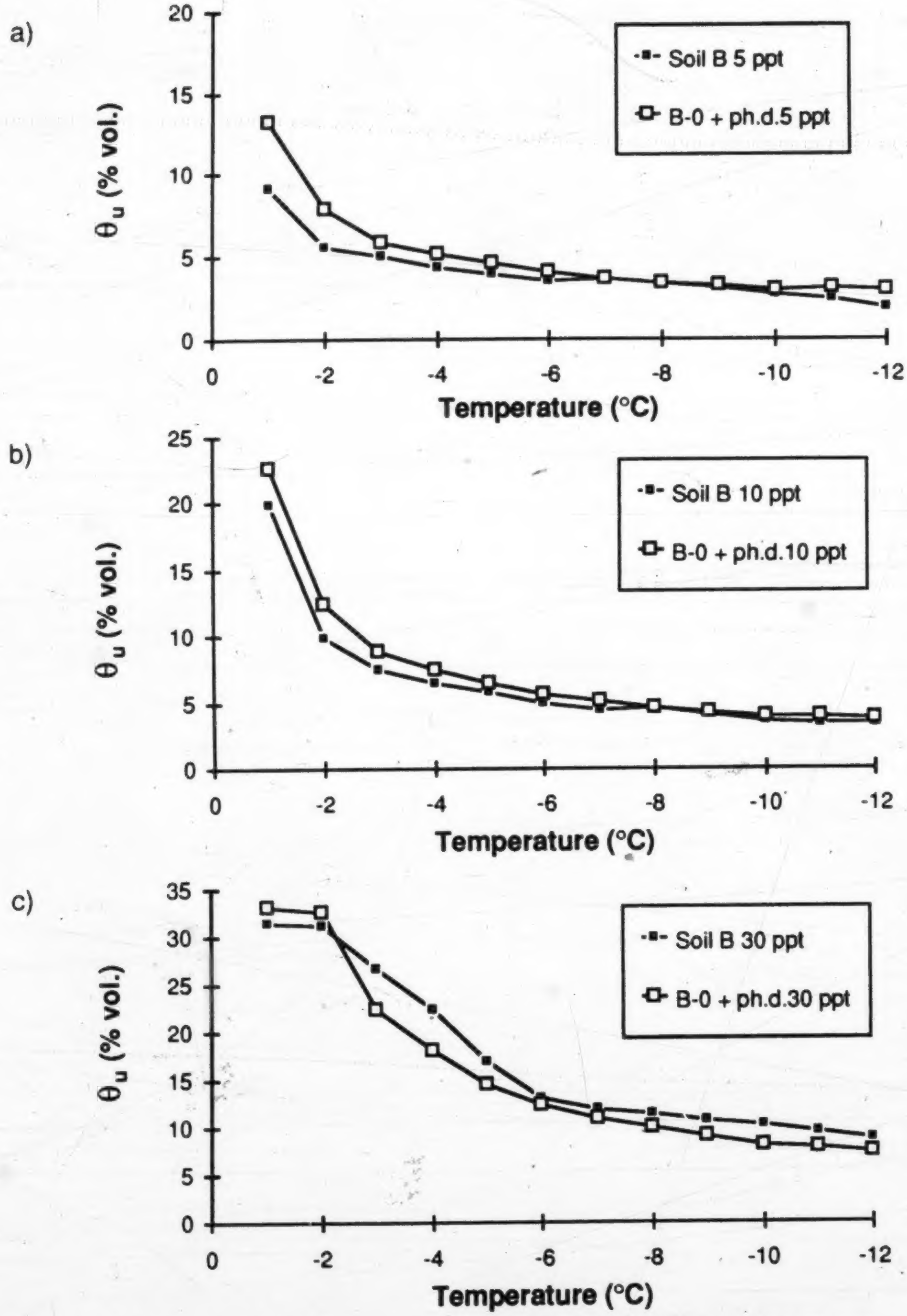

Figure 6.5: Comparison between water content measured by TDR and predicited using phase diagram and unfrozen water content at a salinity of 0 ppt for soil B a) 5 ppt b) 10 ppt c) 30 ppt

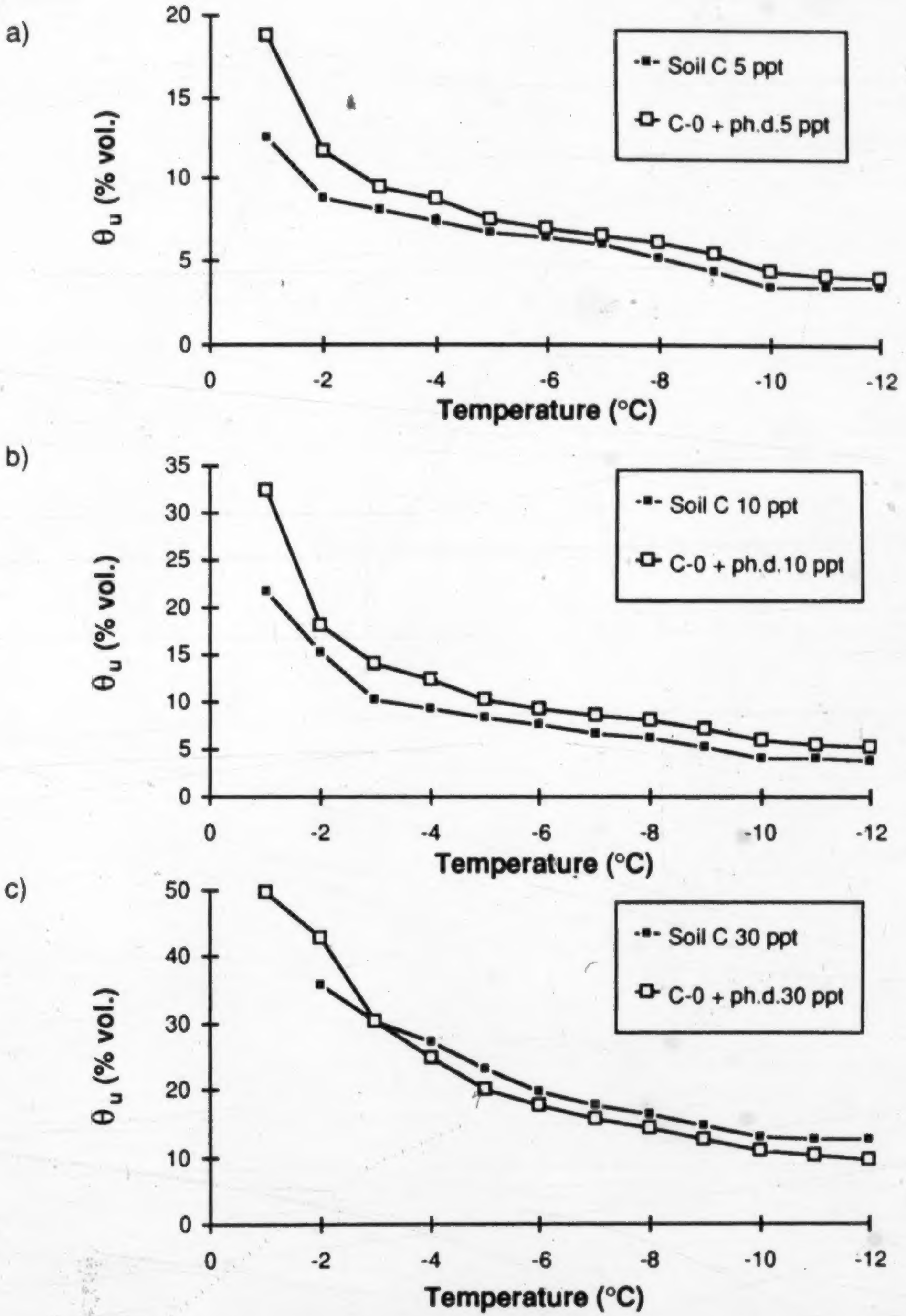

Figure 6.6: Comparison between unfrozen water content measured by TDR and predicited using phase diagram and unfrozen water content at a salinity of 0 ppt for soil C a) 5 ppt b) 10 ppt c) 30 ppt

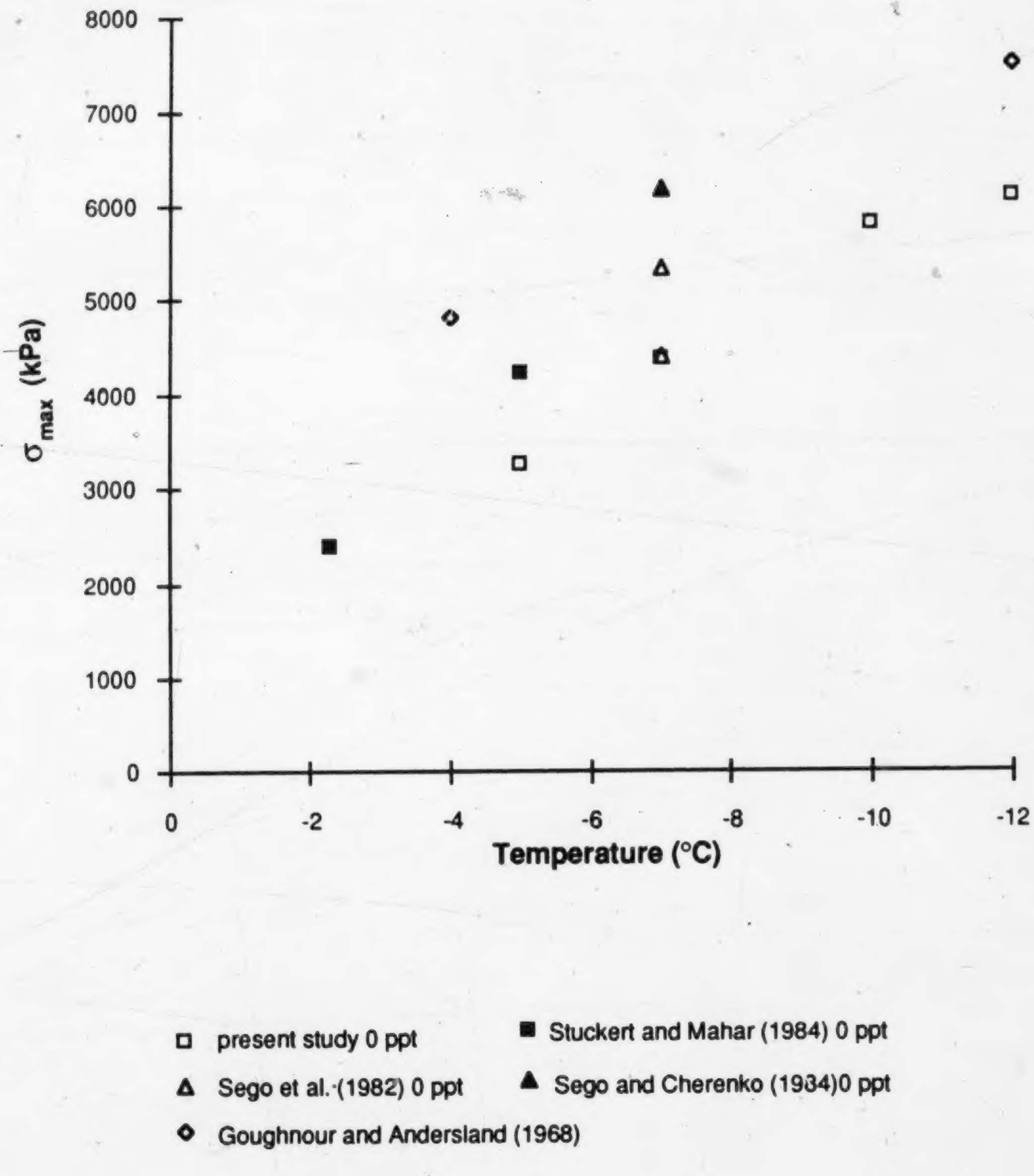

Figure 6.7: Comparison of strength vs temperature for different sands at a salinity of 0 ppt

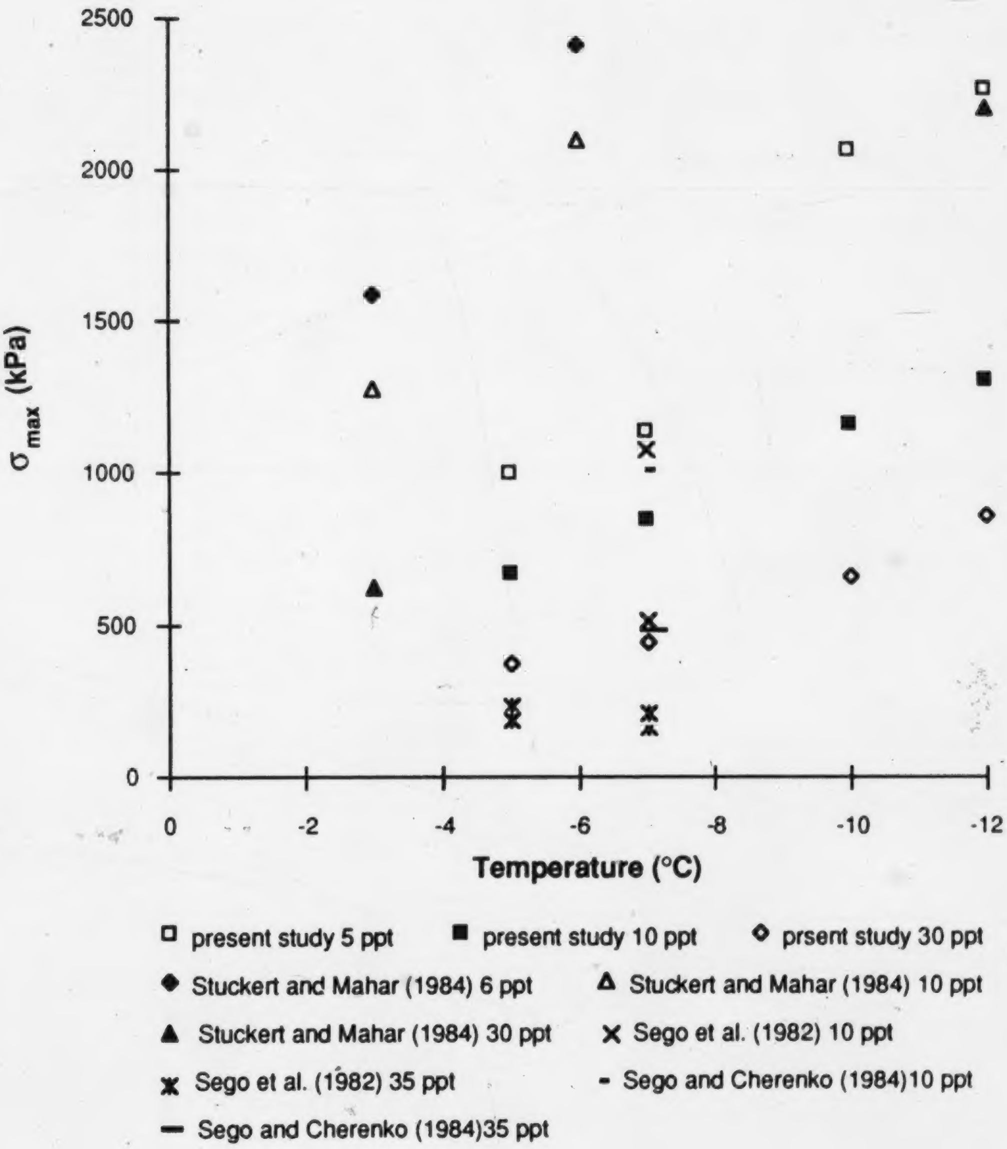

Figure 6.8: Comparison of strength vs temperature for different sands at salinities other than 0 ppt

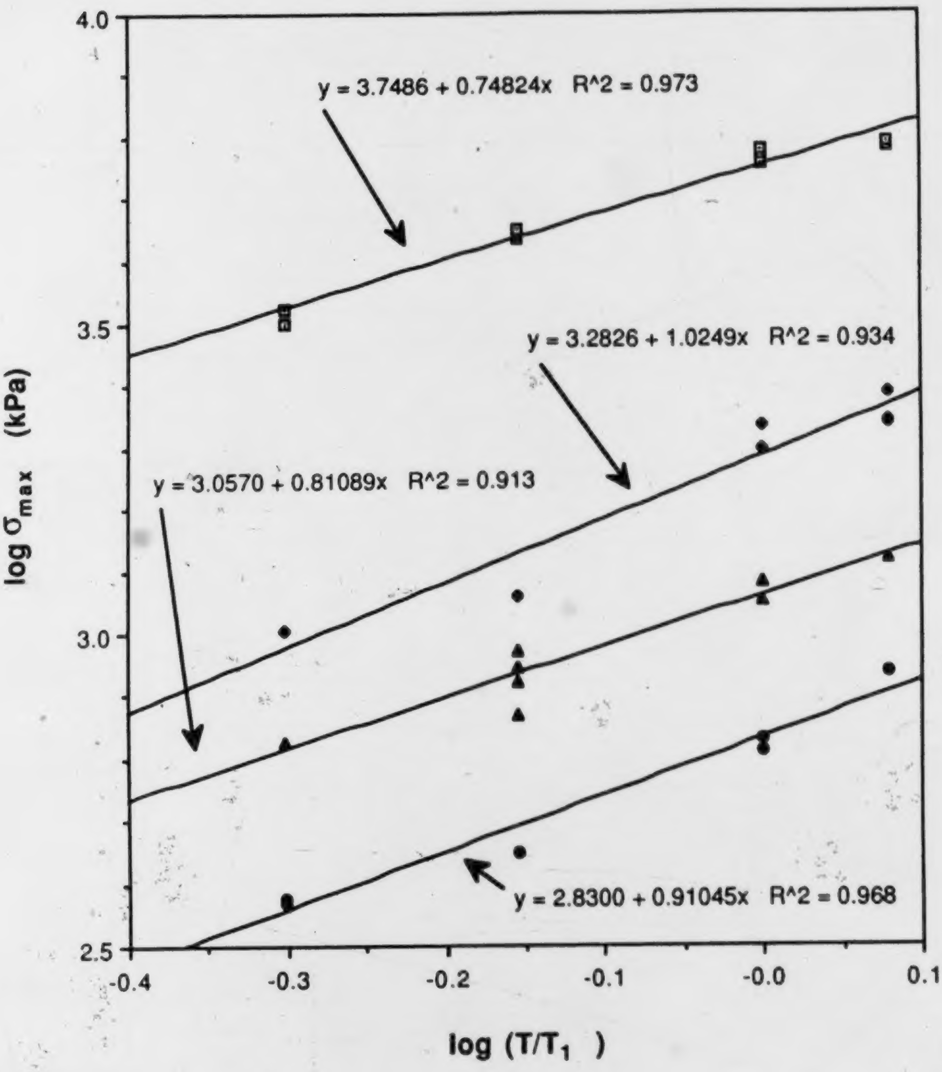

Figure 6.9: Strength vs Tempereterature ratio for soil A

▣ 0 ppt ● 5 ppt ▲ 10 ppt ● 30 ppt

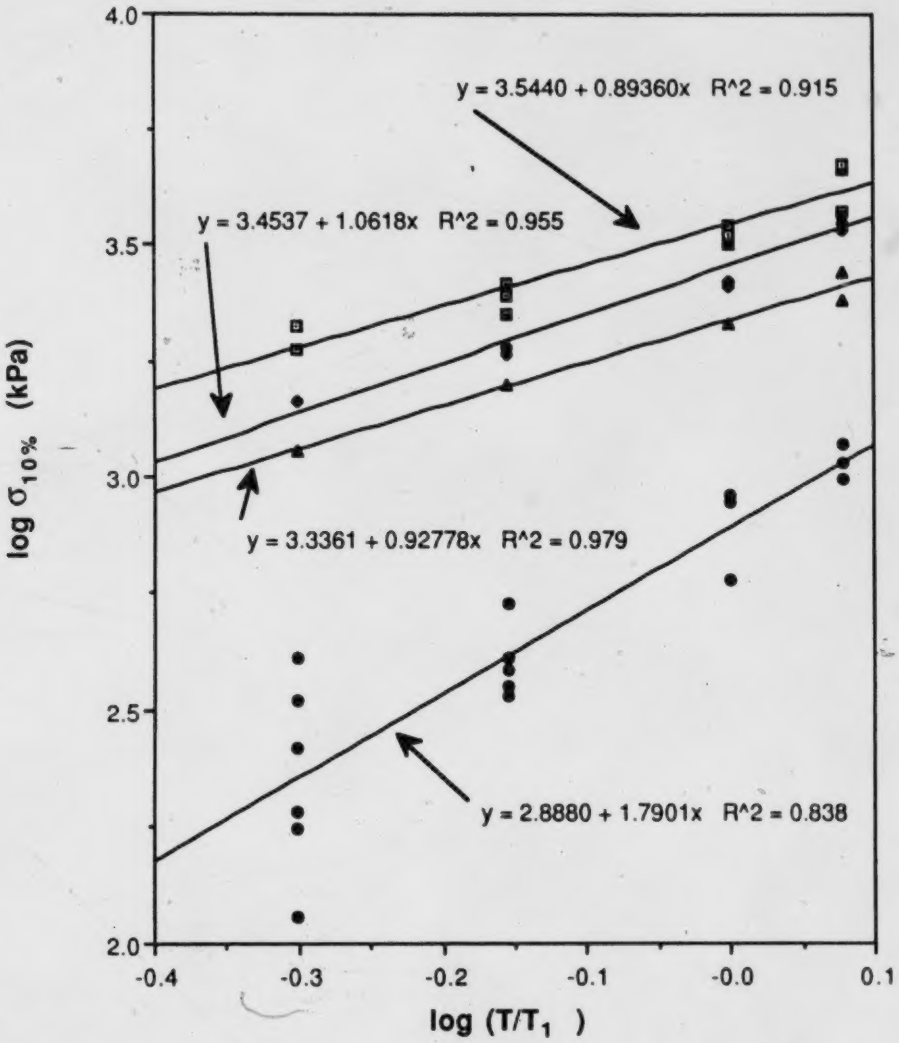

Figure 6.10: 10% Strength vs Tempereratature ratio for soil B
▣ 0 ppt ● 5 ppt ▲ 10 ppt ● 30 ppt

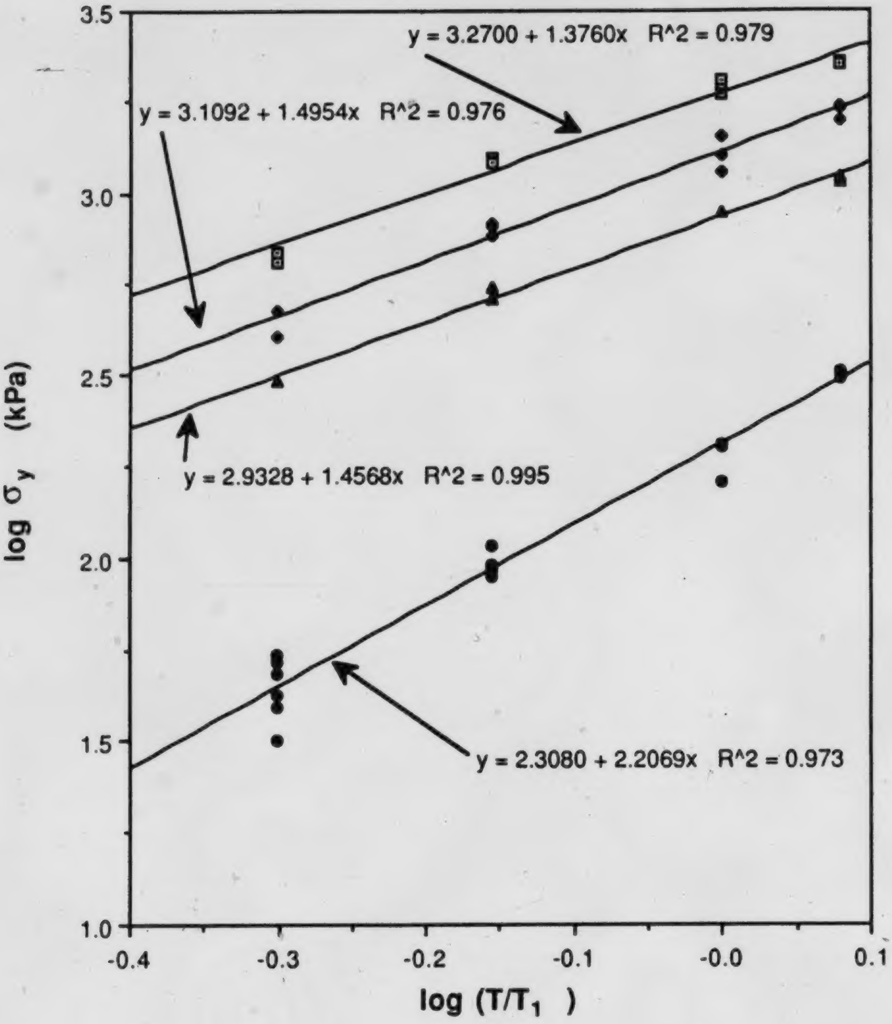

Figure 6.11: Yield strength vs Tempererature ratio for soil B

▫ 0 ppt ◆ 5 ppt ▲ 10 ppt ● 30 ppt

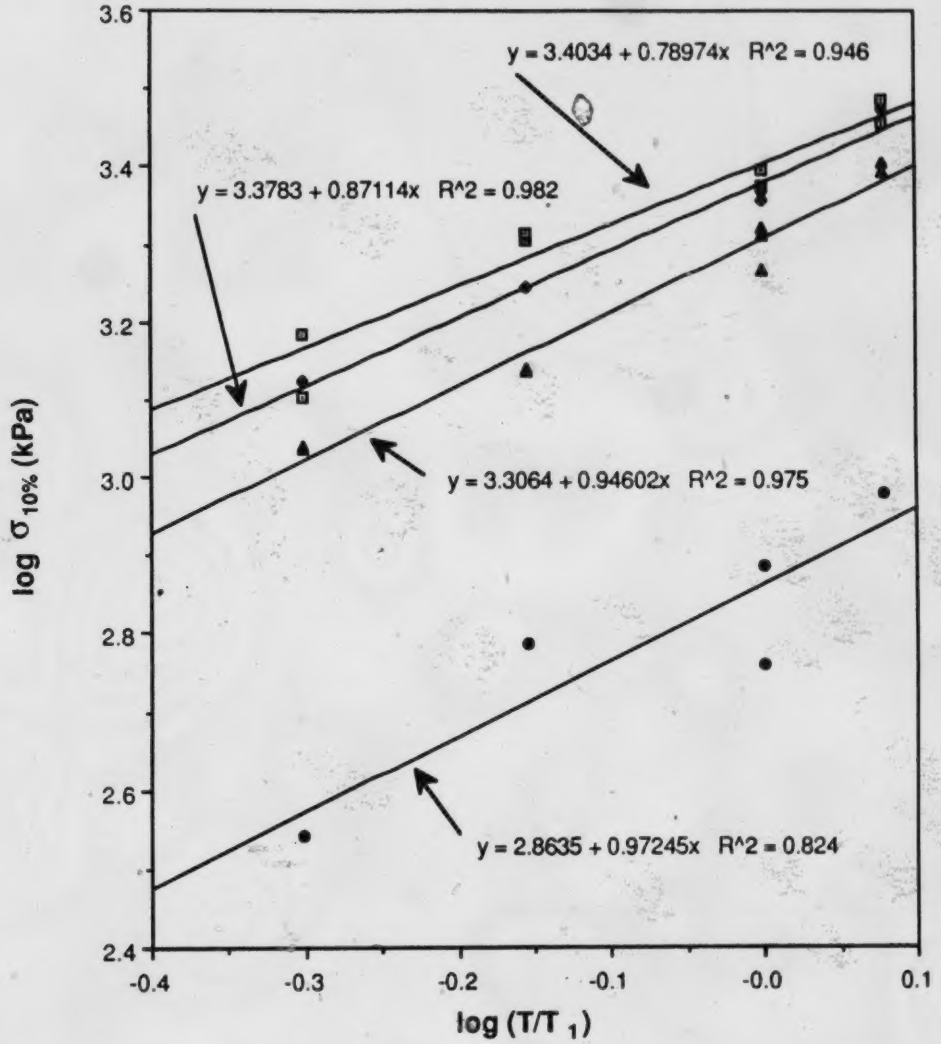

Figure 6.12: 10% Strength vs Tempererature ratio for soil C

▣ 0 ppt ◆ 5 ppt ▲ 10 ppt ● 30 ppt

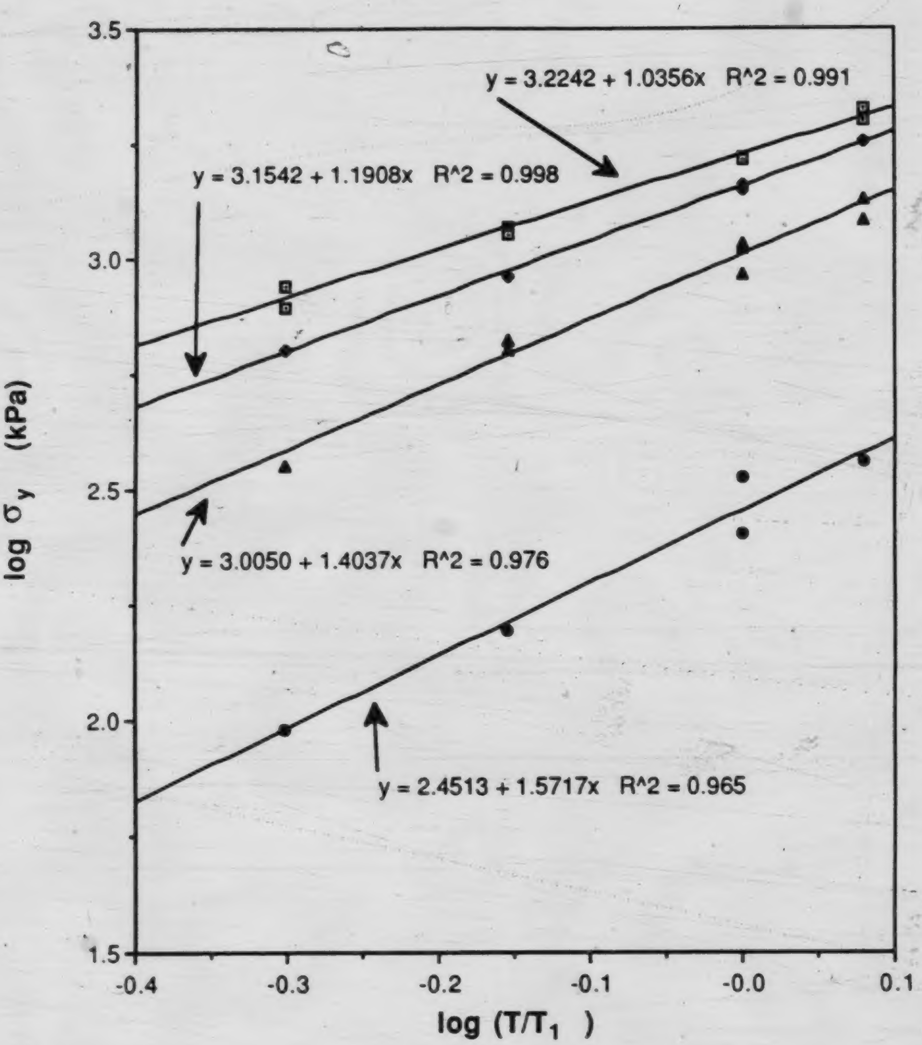

Figure 6.13: Yield strength vs Tempererature ratio for soil C

▣ 0 ppt • 5 ppt ▲ 10 ppt ● 30 ppt

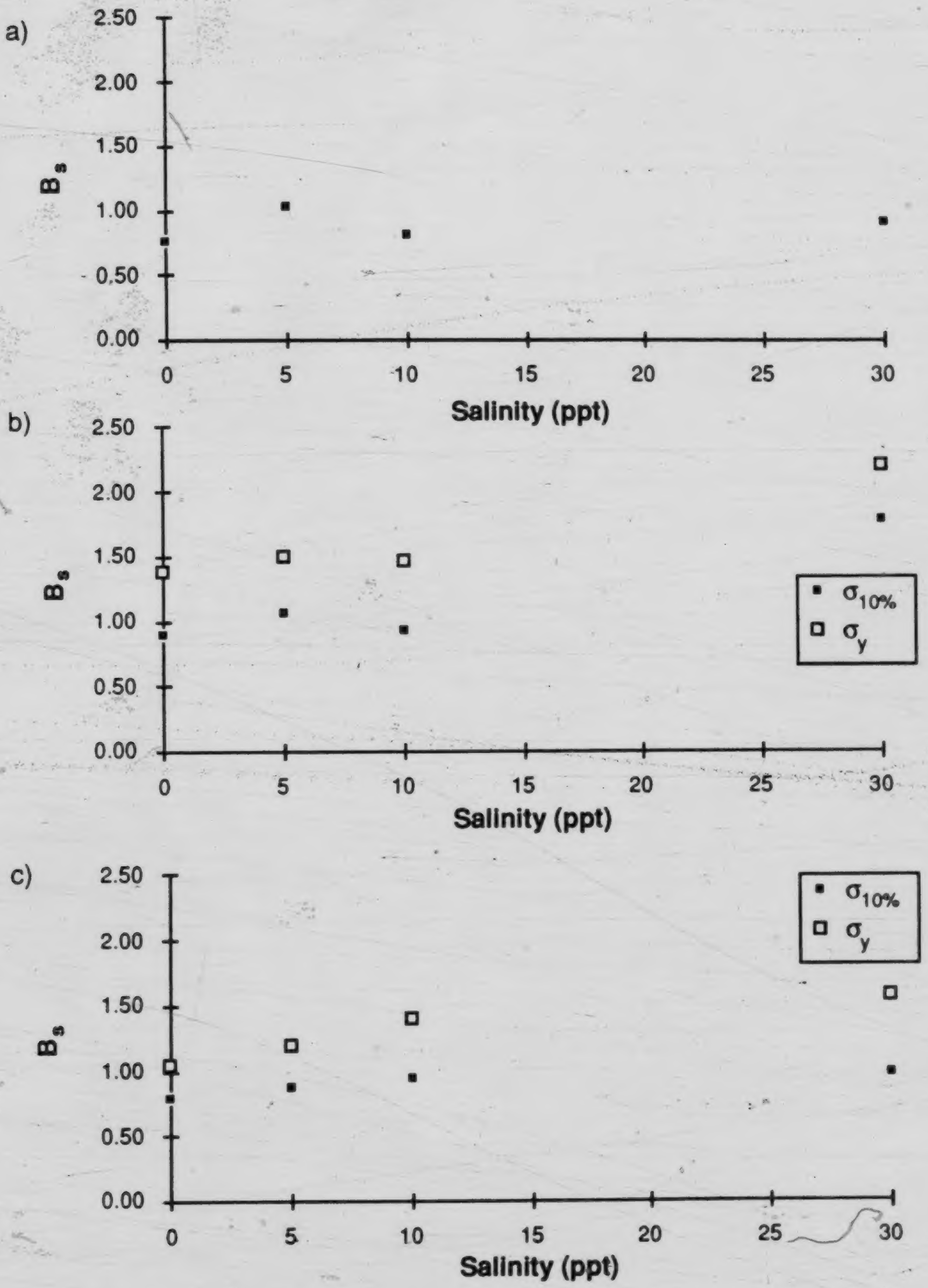

Figure 6.14: Parameter B_s vs Salinity a) Soil A b) Soil B c) Soil C

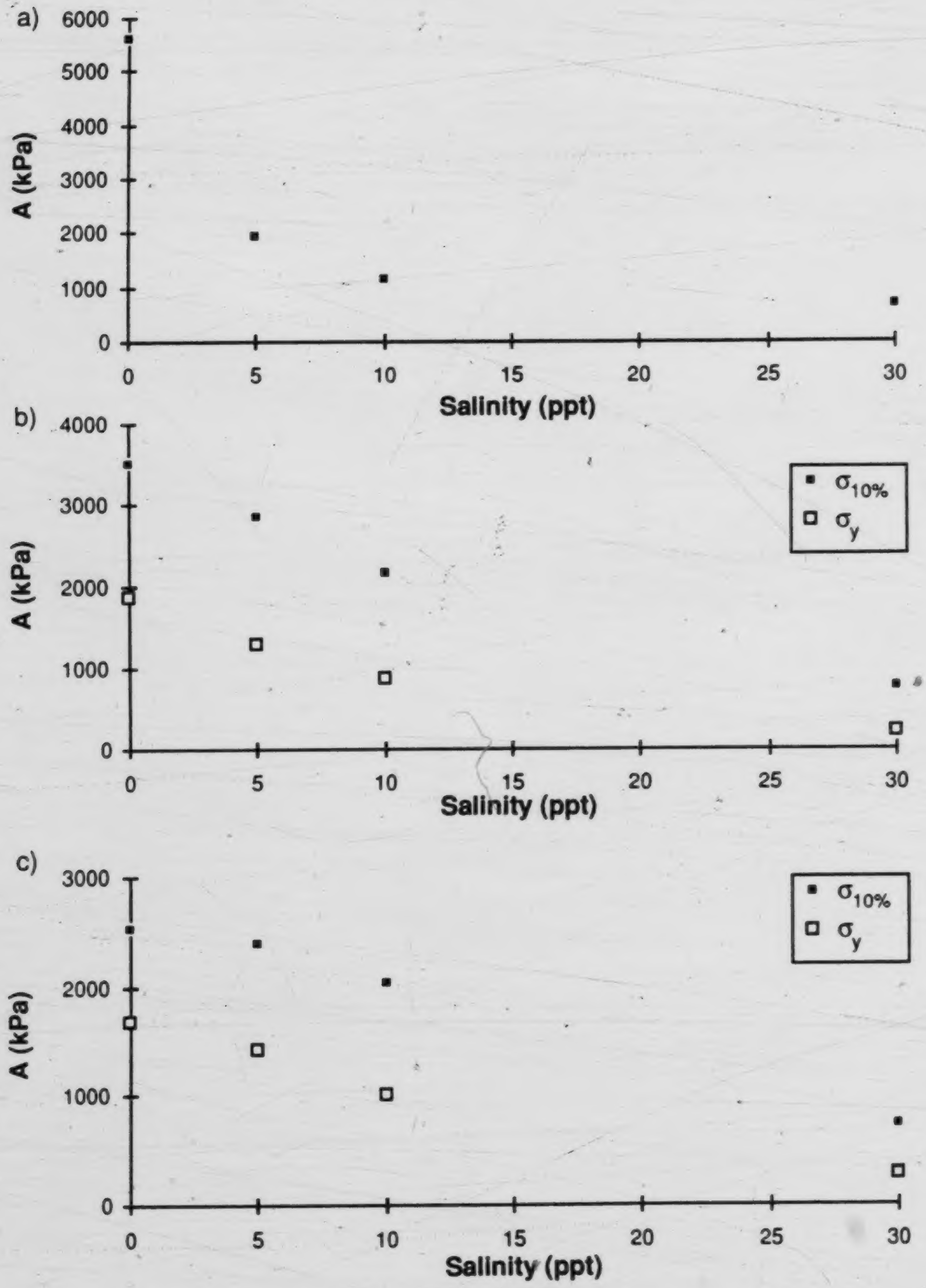

Figure 6.15: Parameter A vs Salinity a) Soil A b) Soil B c) Soil C

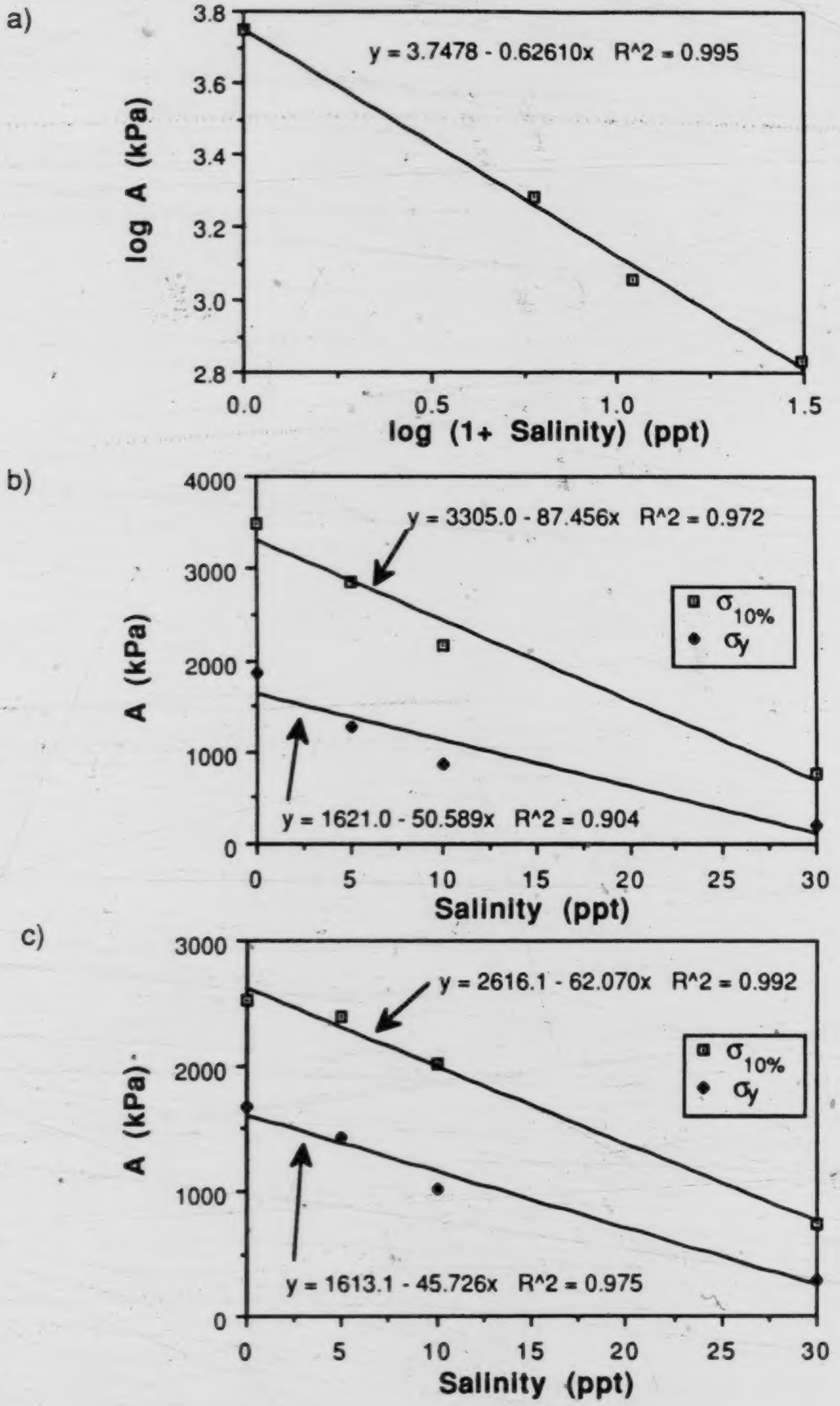

Figure 6.16: Parameter A vs Salinity regressions a) Soil A b) Soil B c) Soil C

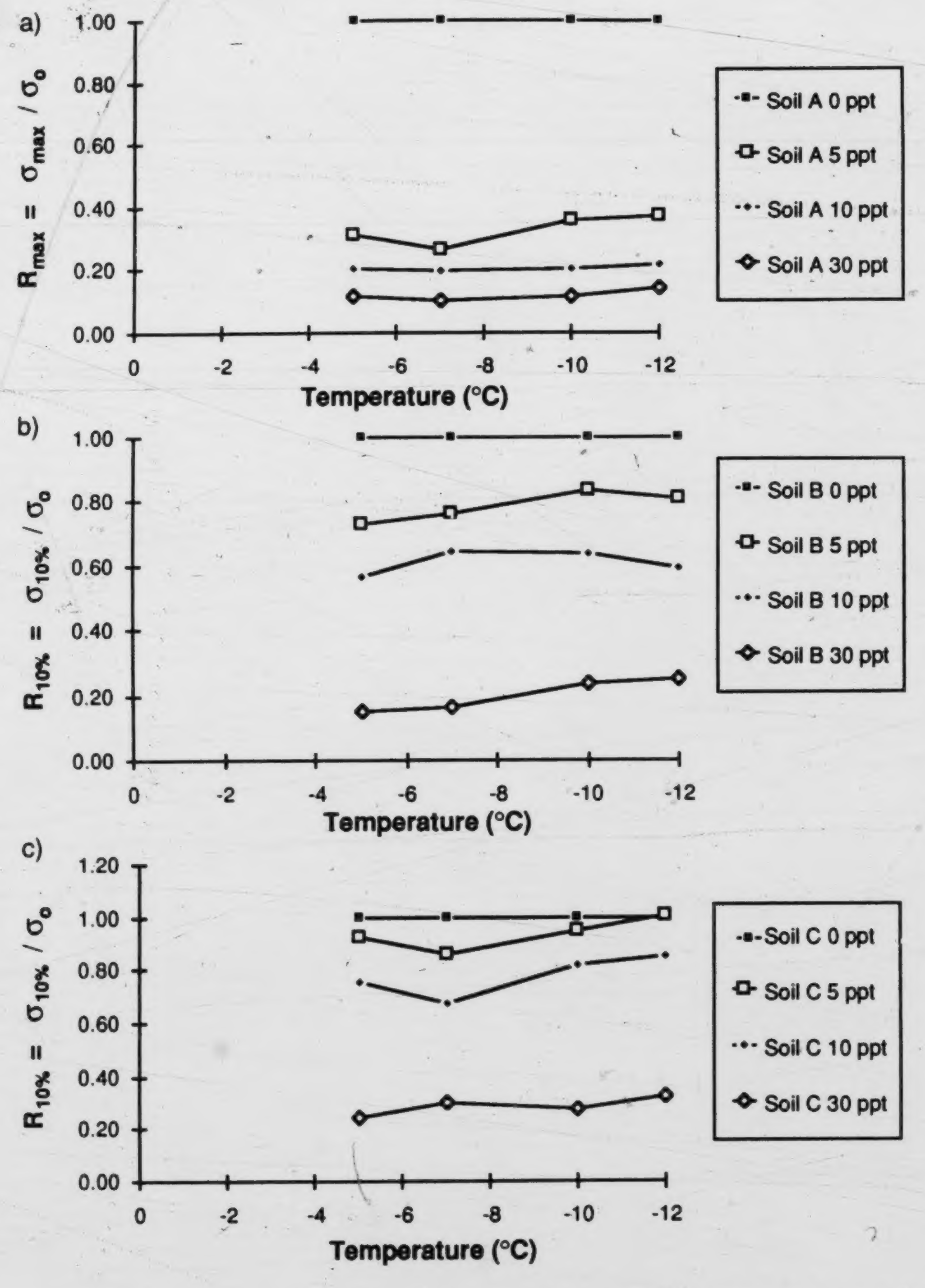

Figure 6.17: Normalized strength vs Temperature a) Soil A b) Soil B c) Soil C

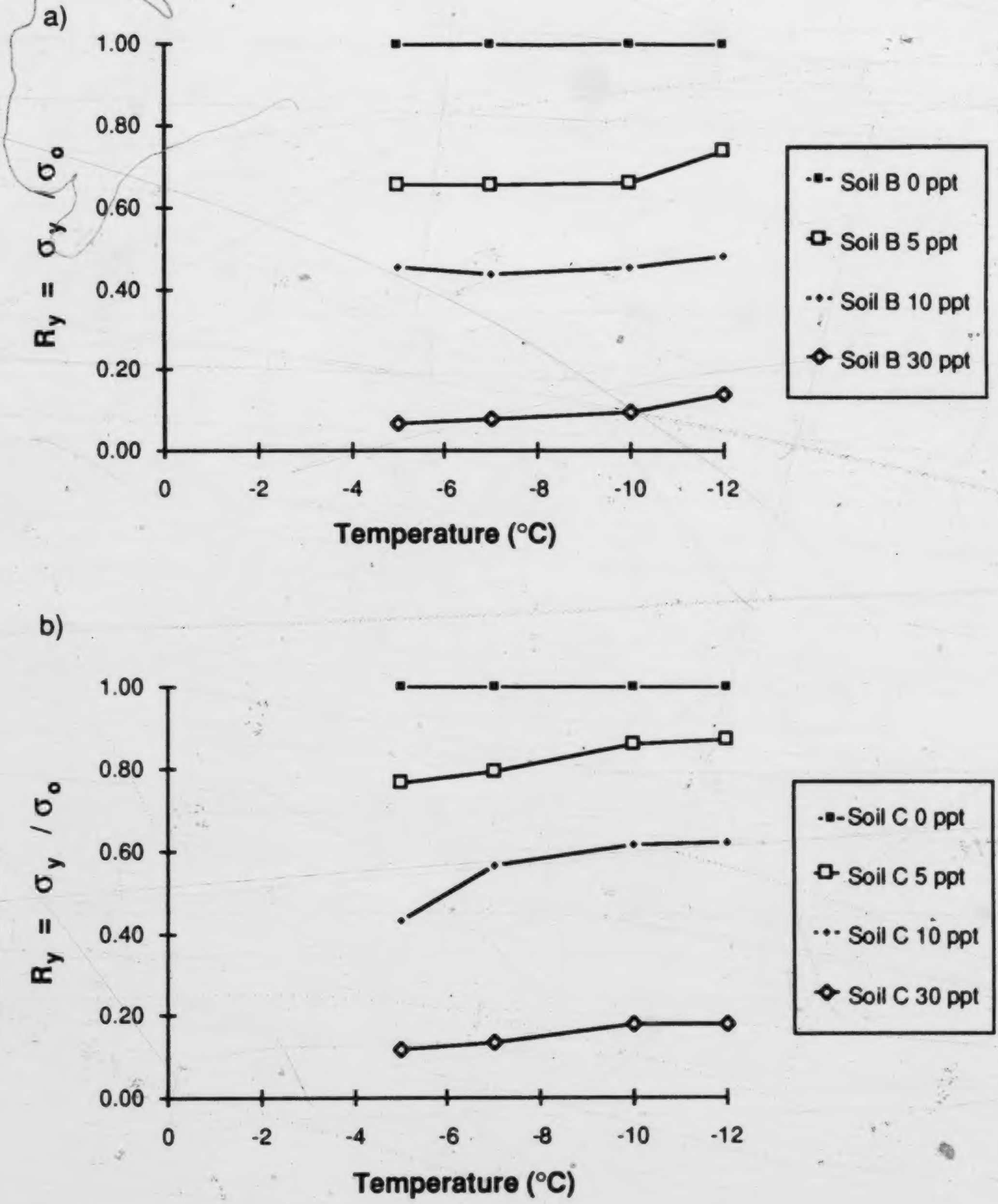

Figure 6.18: Normalized yield strength vs Temperature a) Soil B b) Soil C

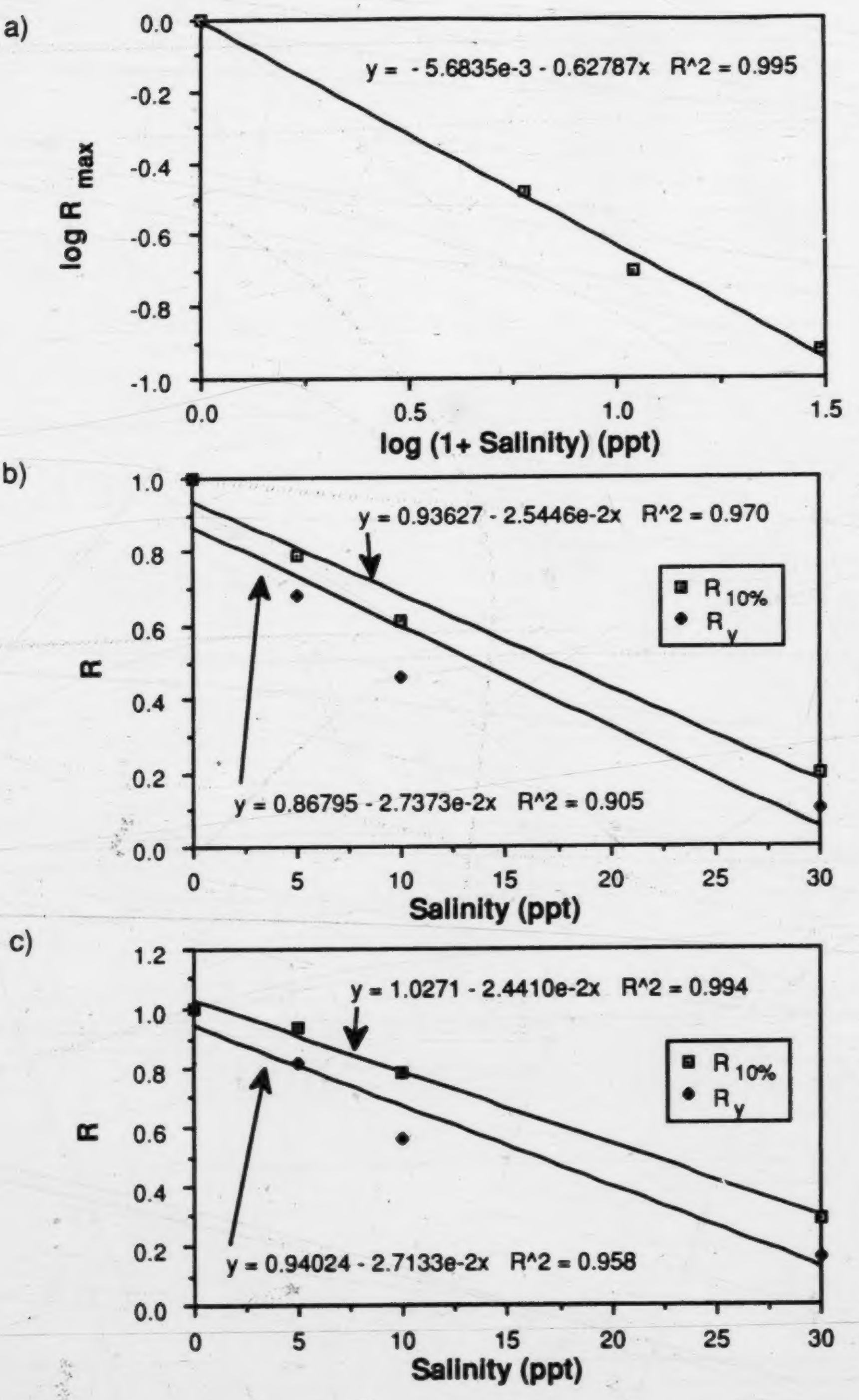

Figure 6.19: Strength ratio R vs Salinity a) Soil A b) Soil B c) Soil C

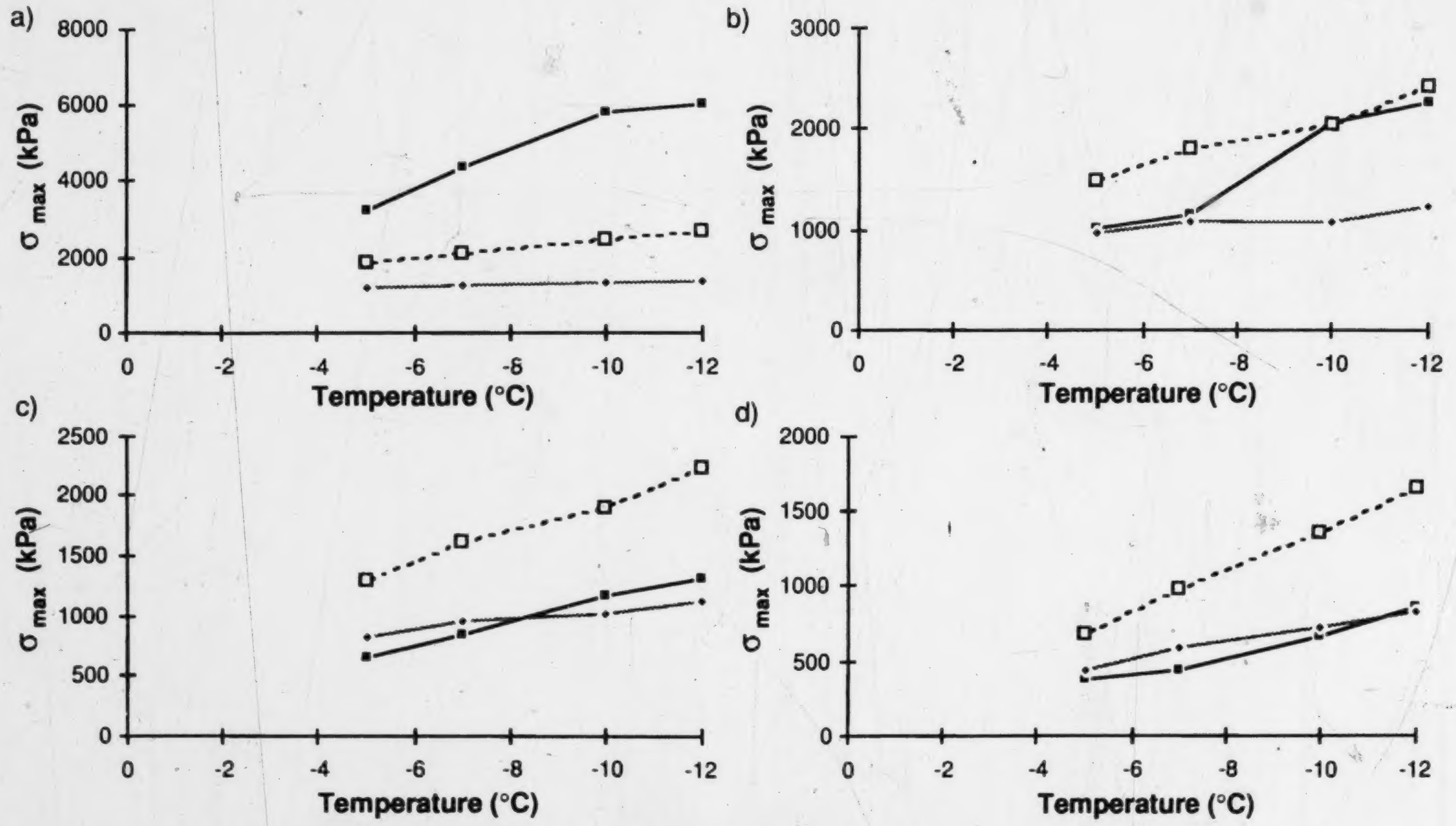

Figure 6.20: Comparison between strength predicted using ice area ratio and measured strength
a) soil A 0 ppt b) soil A 5 ppt c) soil A 10 ppt d) soil A 30 ppt
— measured strength --- predicted strength using calculated ice strength
— predicted strength using measured ice strength

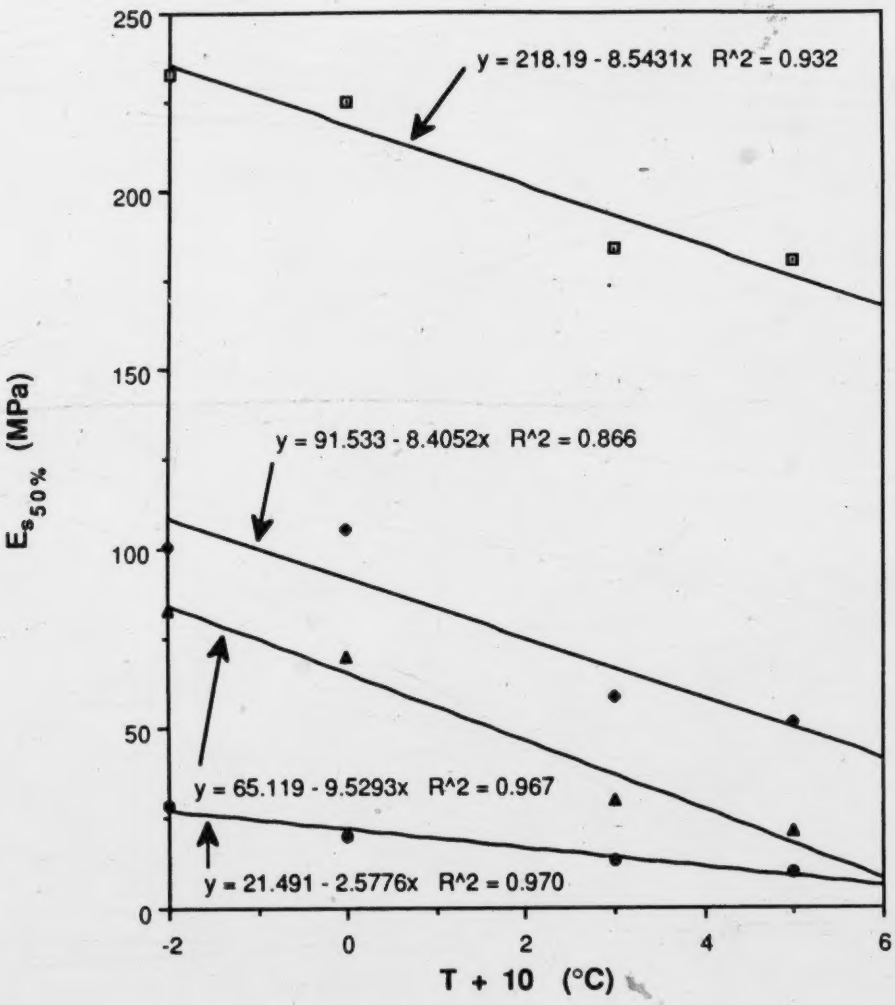

Figure 6.21: Secant modulus vs Temperature for soil A
▫ 0 ppt ◆ 5 ppt ▲ 10 ppt ● 30 ppt

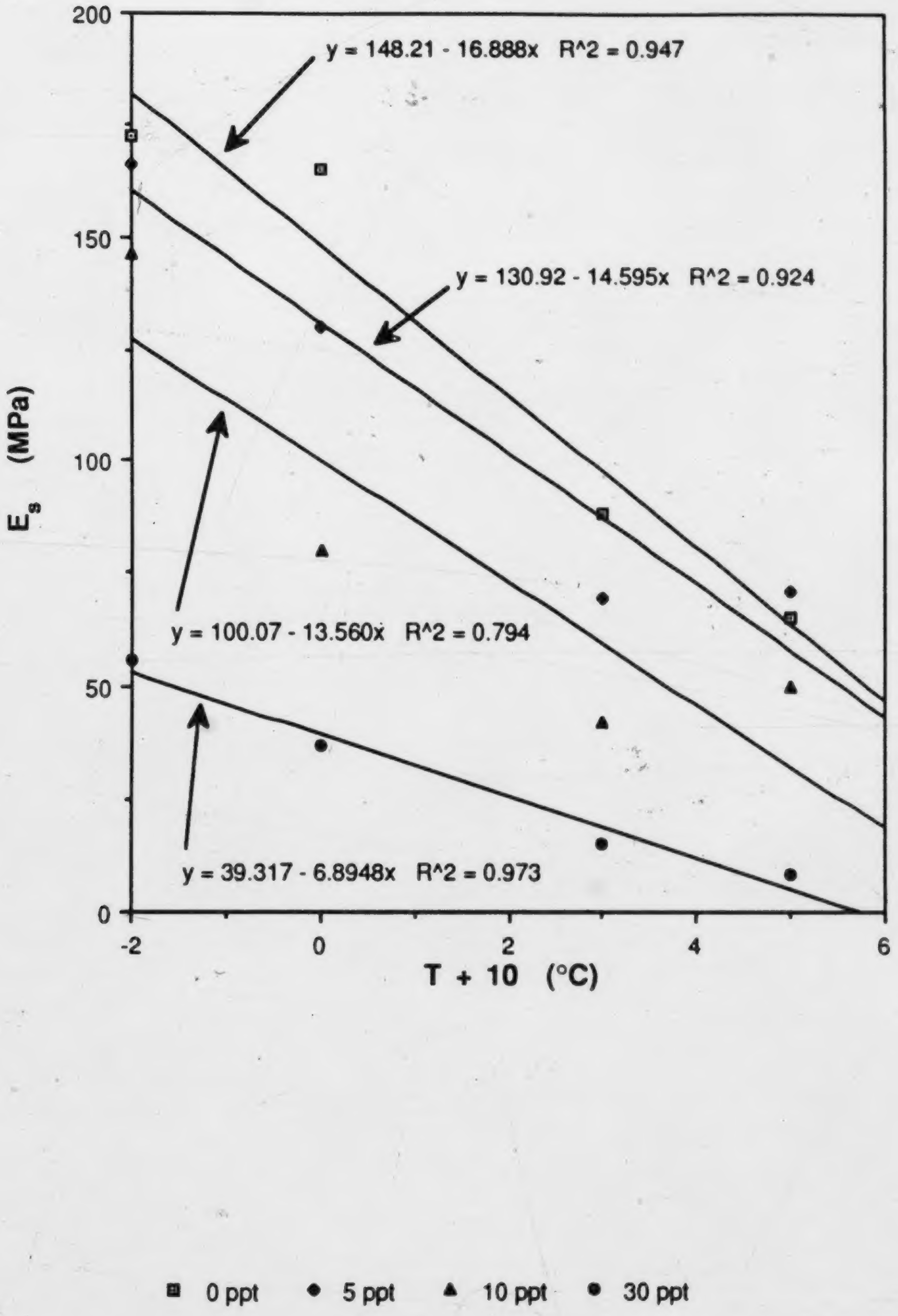

Figure 6.22: Secant modulus vs Temperature for soil B

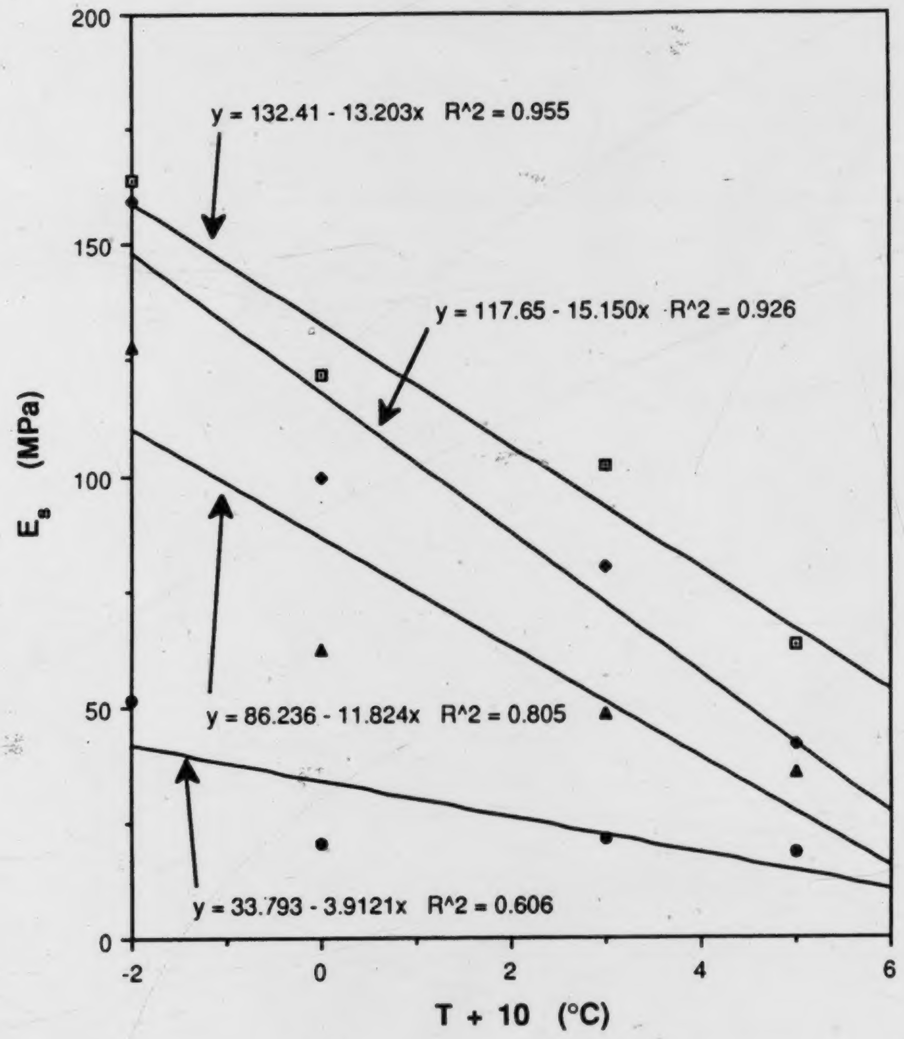

Figure 6.23: Secant modulus vs Temperature for soil C

▣ 0 ppt ◆ 5 ppt ▲ 10 ppt ● 30 ppt

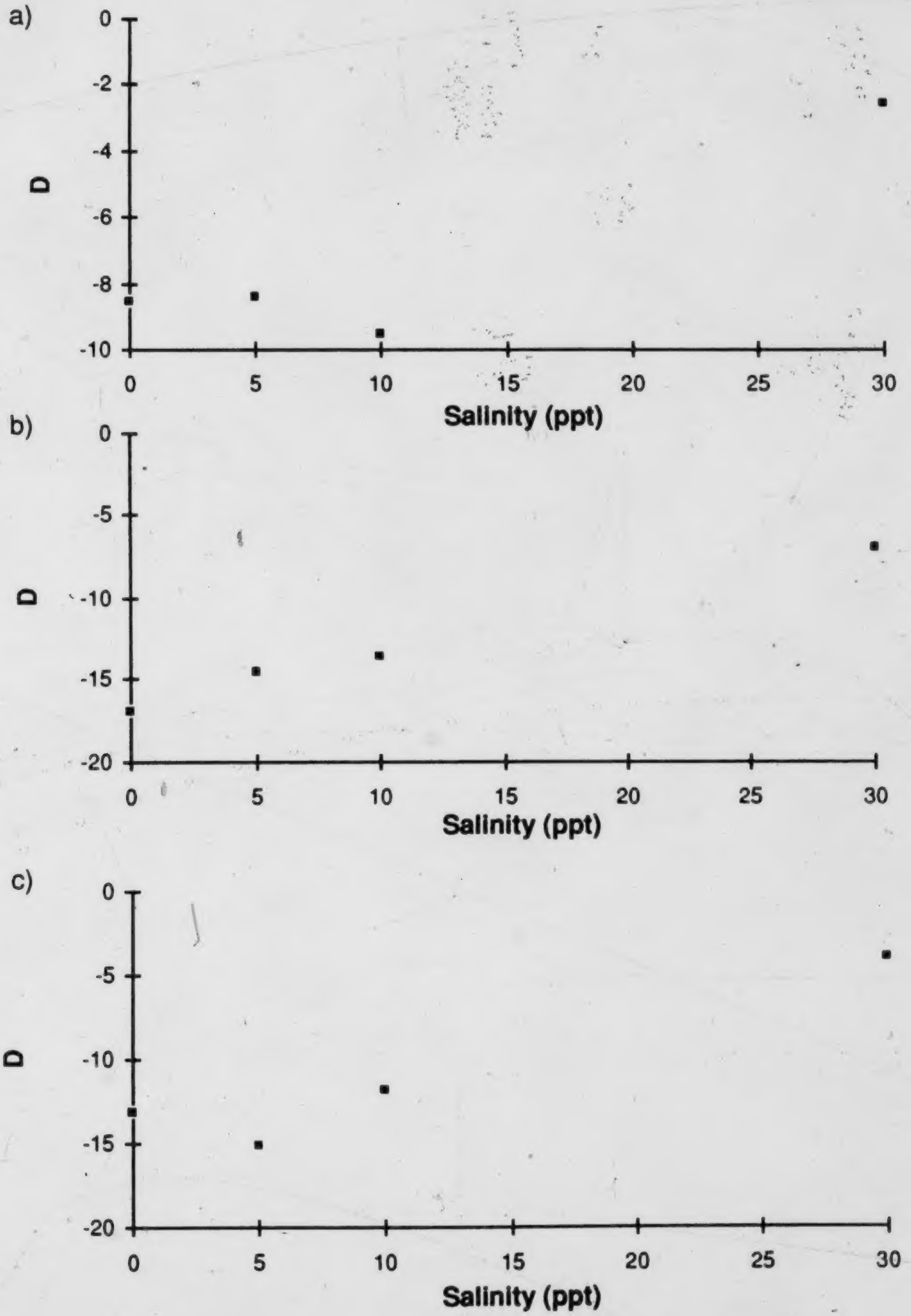

Figure 6.24: Parameter D vs Salinity a) Soil A b) Soil B c) Soil C

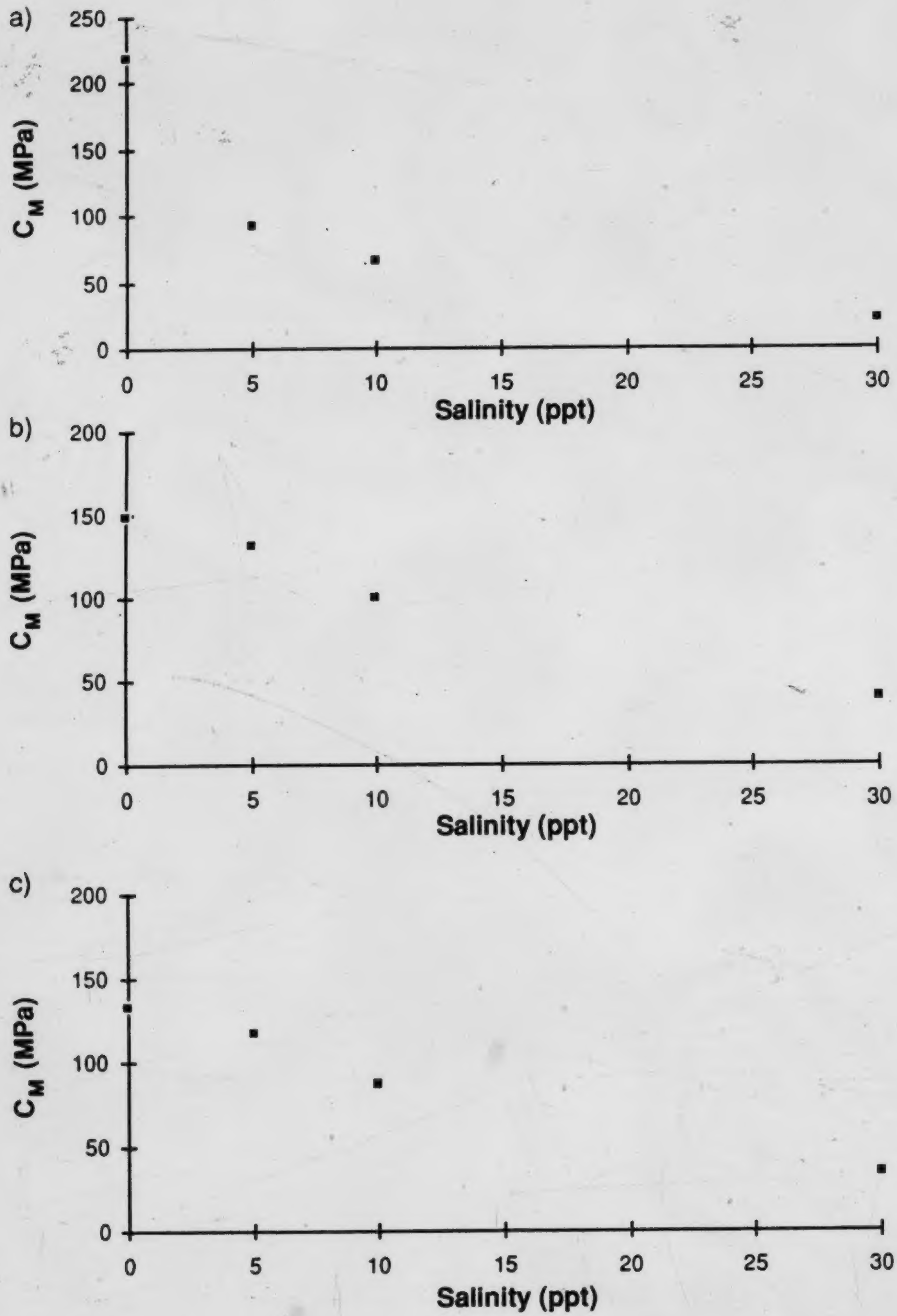

Figure 6.25: Parameter C_M vs Salinity a) Soil A b) Soil B c) Soil C

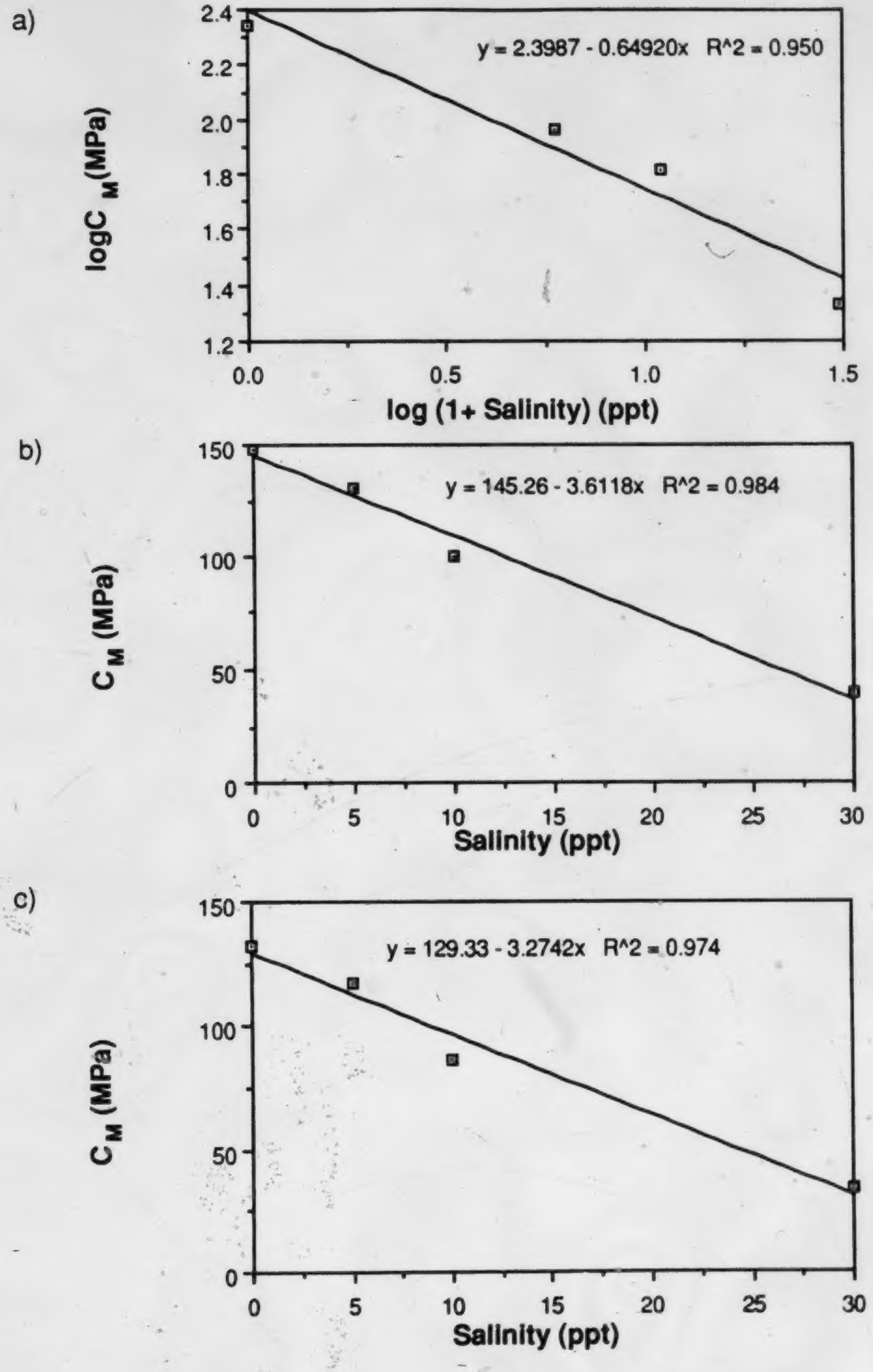

Figure 6.26: Parameter C_M vs Salinity regressions a) Soil A b) Soil B c) Soil C

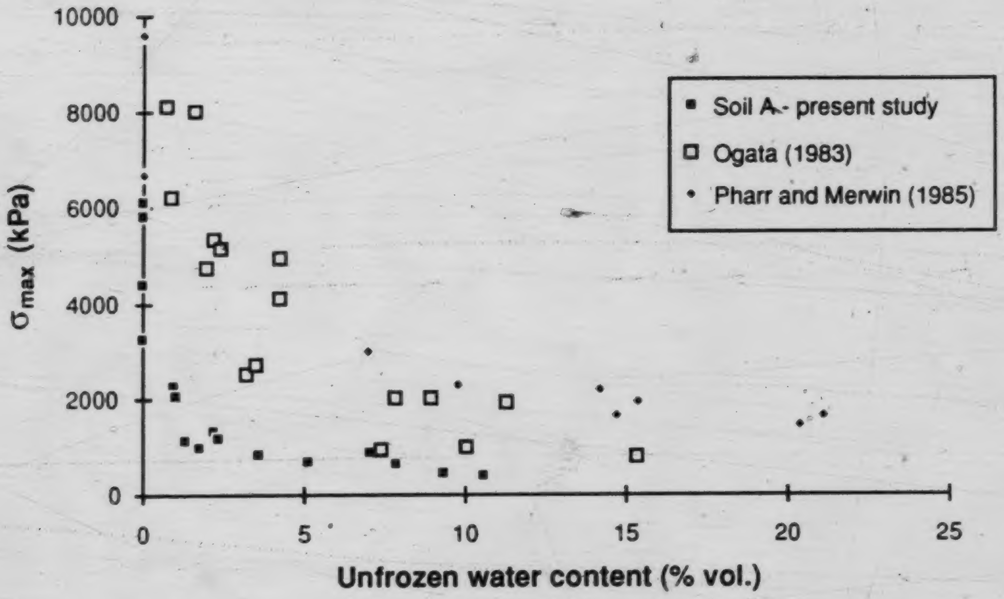

Figure 6.27: Comparison of strength vs unfrozen water content for different sands

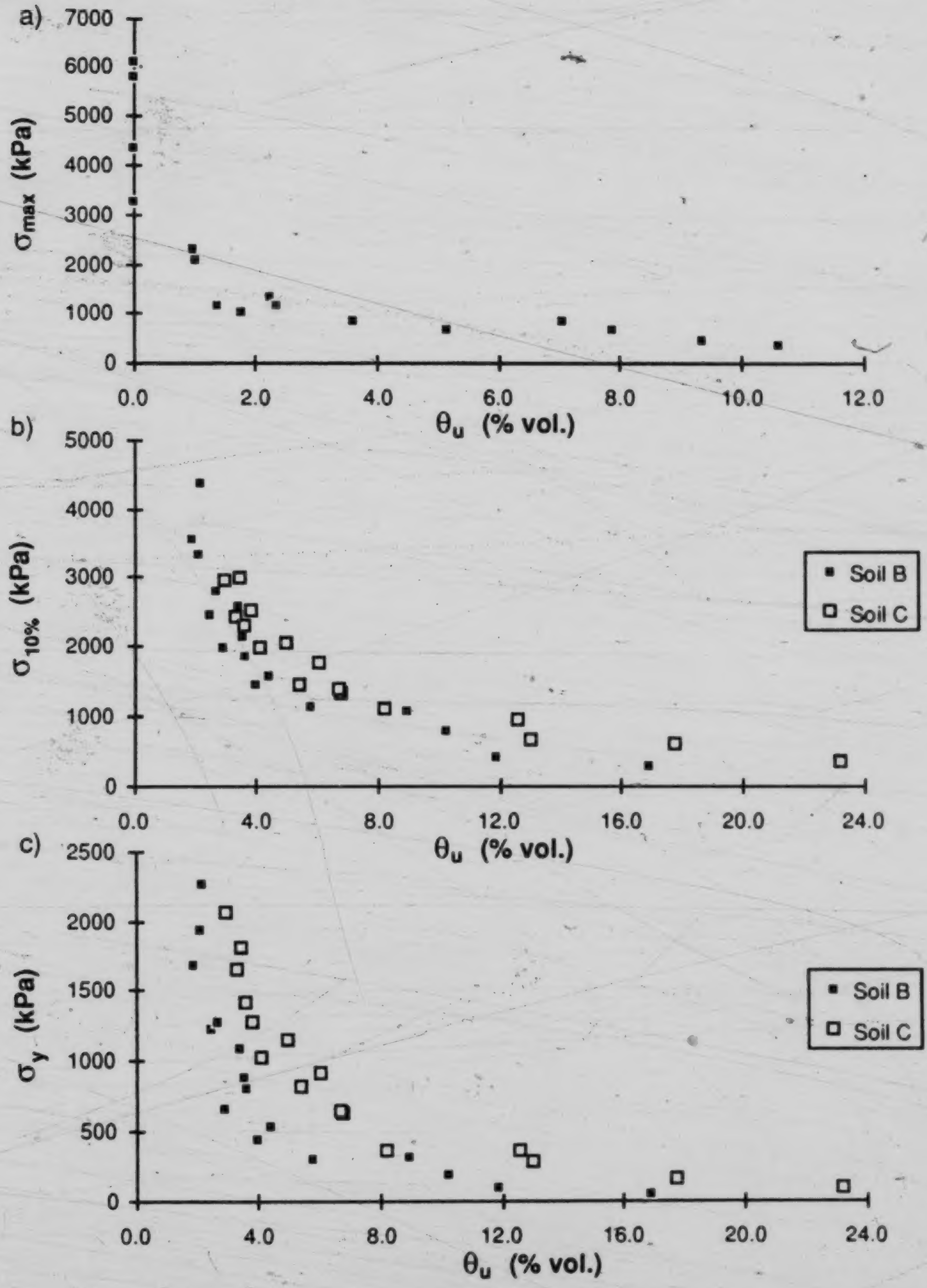

Figure 6.28: Strength vs Unfrozen water content
a) Soil A peak strength
b) Soils B and C 10 % strength c) Soils B and C yield strength

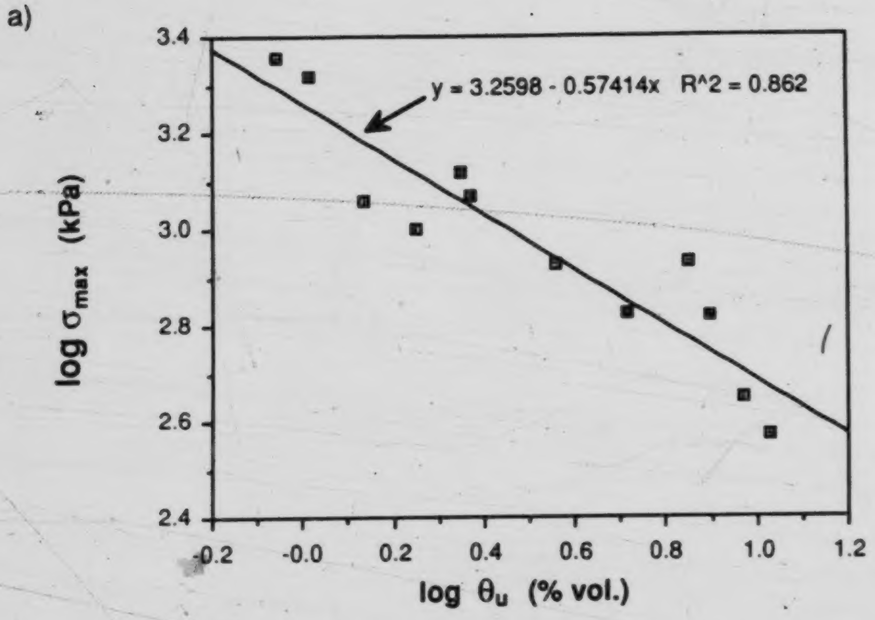

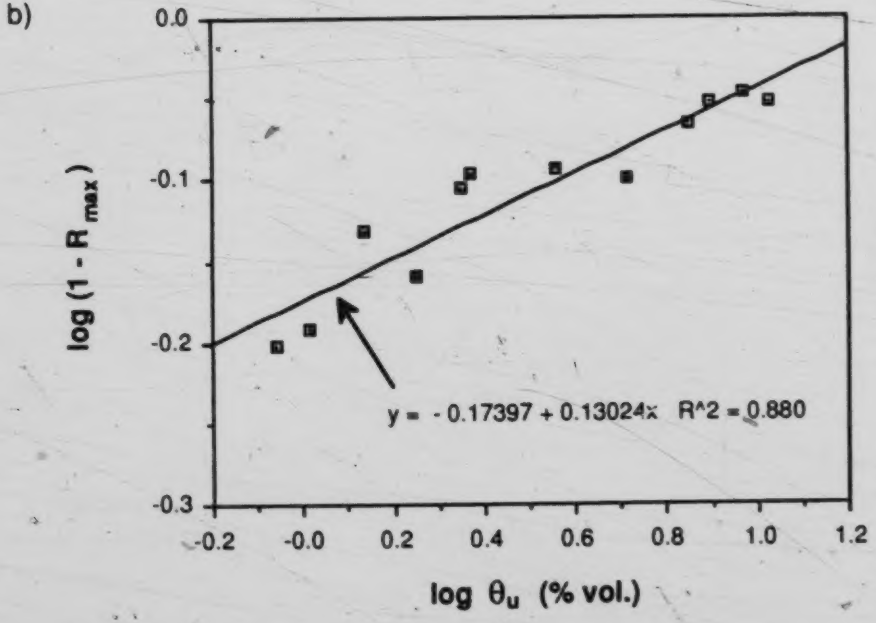

Figure 6.29: a) Strength vs Unfrozen water content for soil A
b) Normalized strength vs Unfrozen water content for soil A

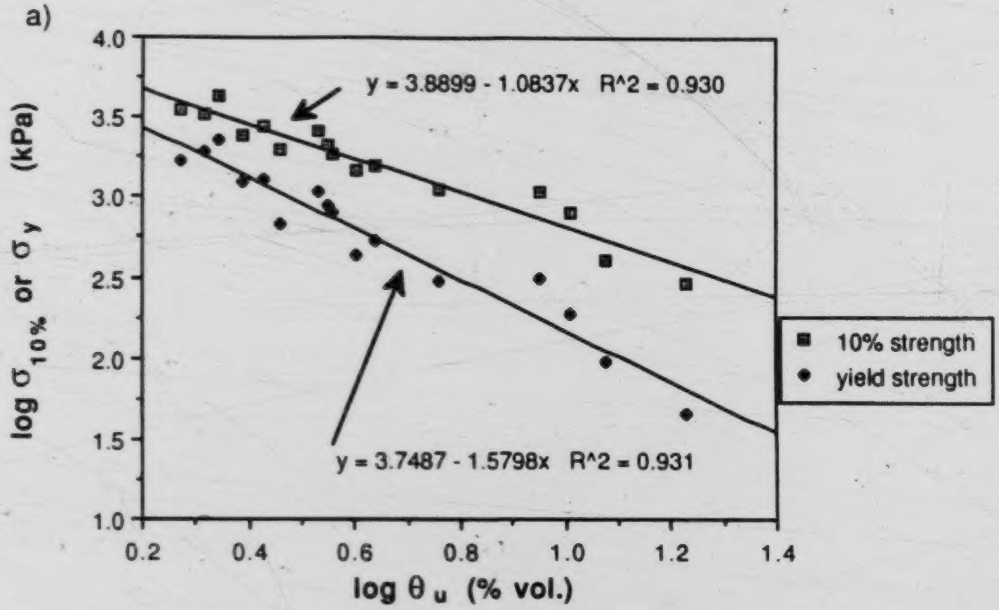

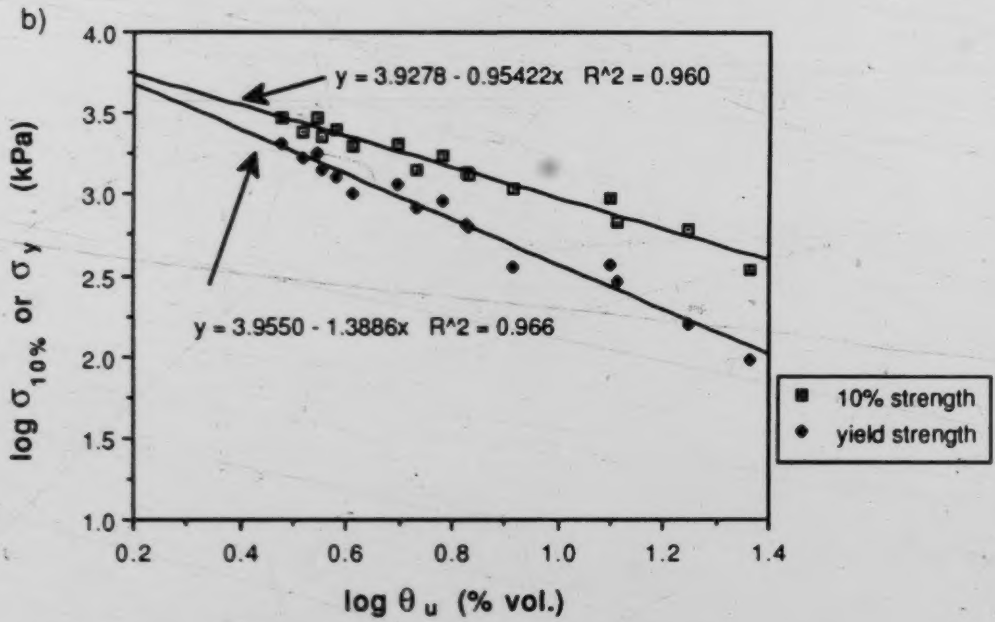

Figure 6.30: 10% Strength or Yield Strength vs Unfrozen water content
a) Soil B b) Soil C

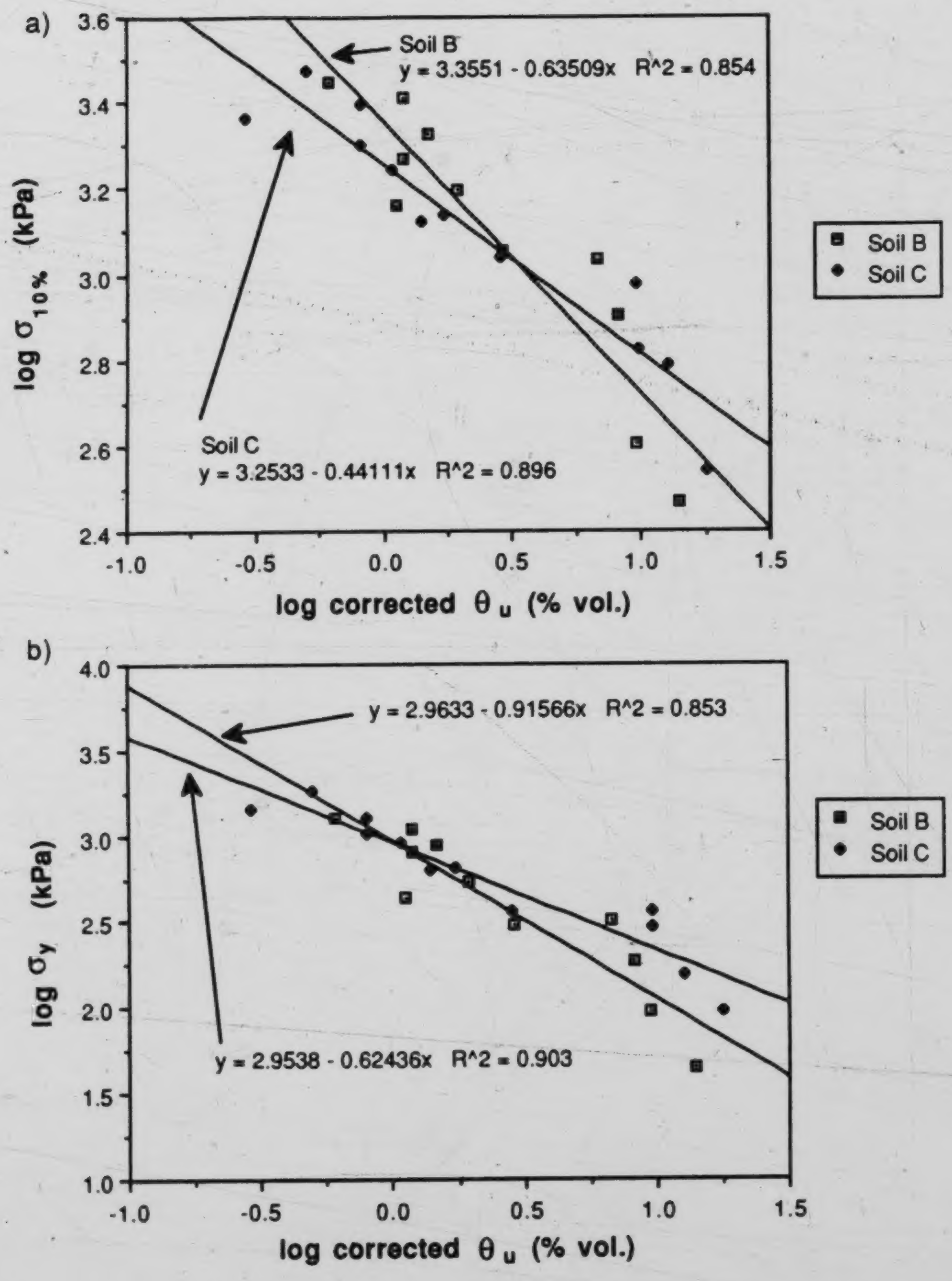

Figure 6.31: Strength vs corrected Unfrozen water content for soils B and C
a) 10% Strength b) Yield Strength

a)

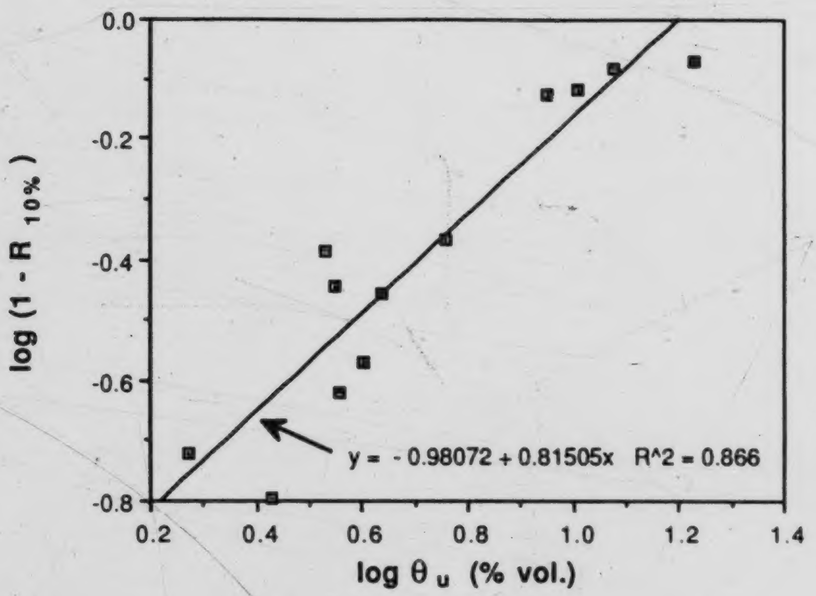

b)

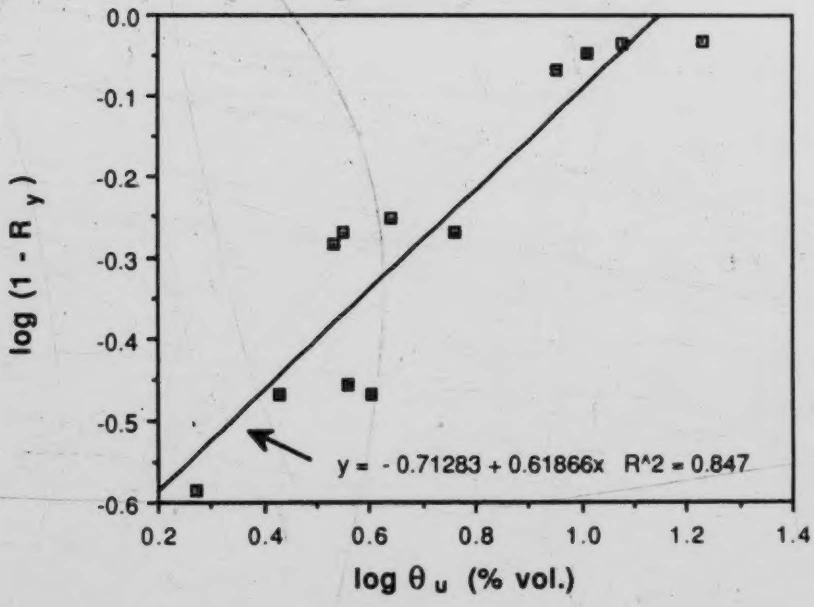

Figure 6.32: a) normalized 10% Strength vs Unfrozen water content for soil B
b) normalized Yield strength vs Unfrozen water content for soil B

a)

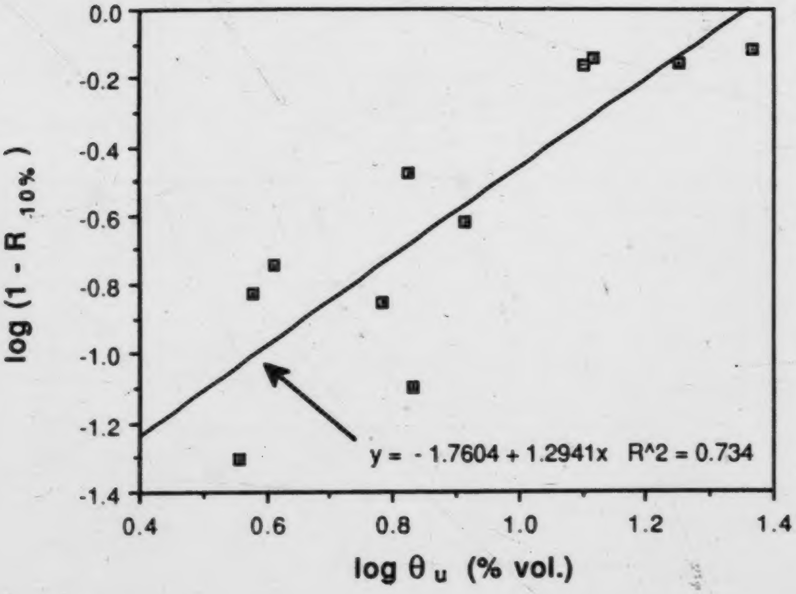

b)

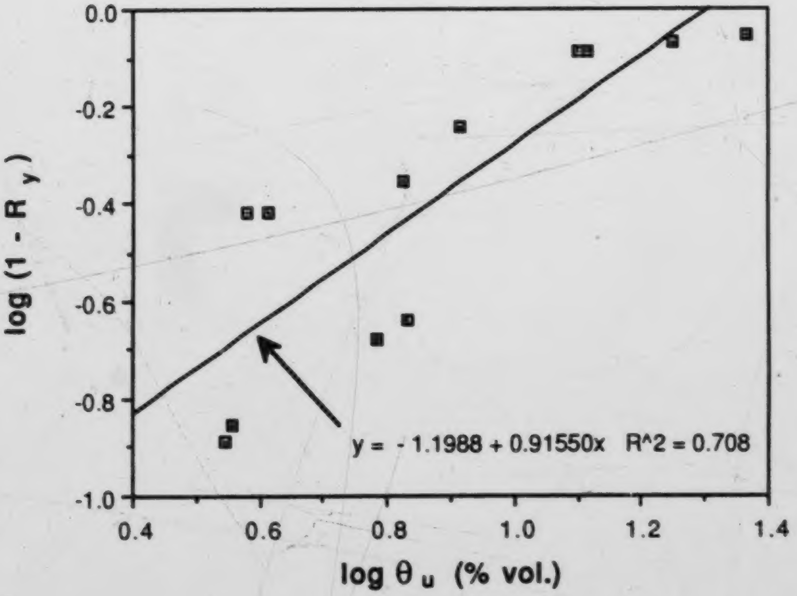

Figure 6.33: a) normalized 10% Strength vs Unfrozen water content for soil C
b) normalized Yield strength vs Unfrozen water content for soil C

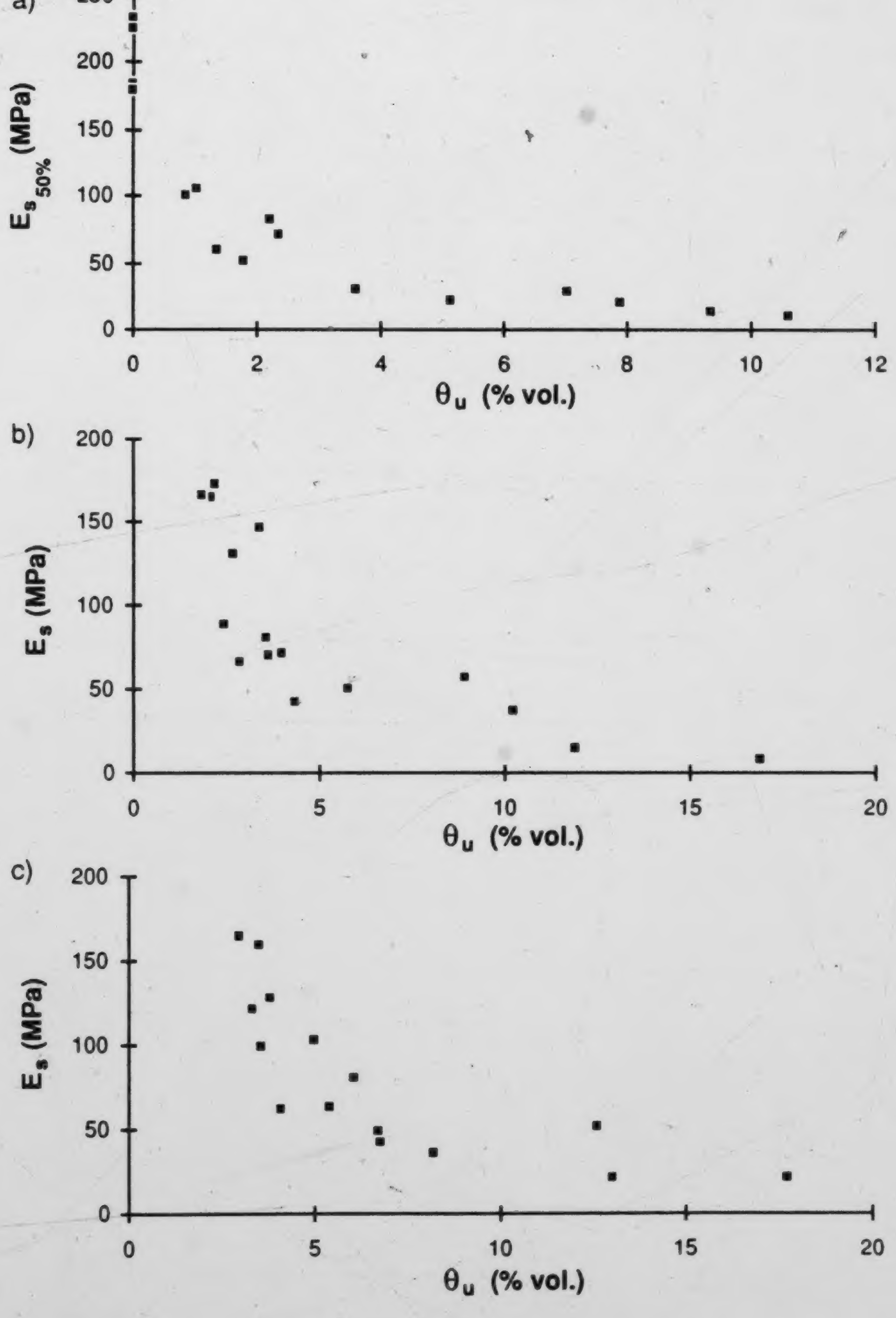

Figure 6.34: Secant modulus vs Unfrozen water content
a) Soil A b) Soil B c) Soil C

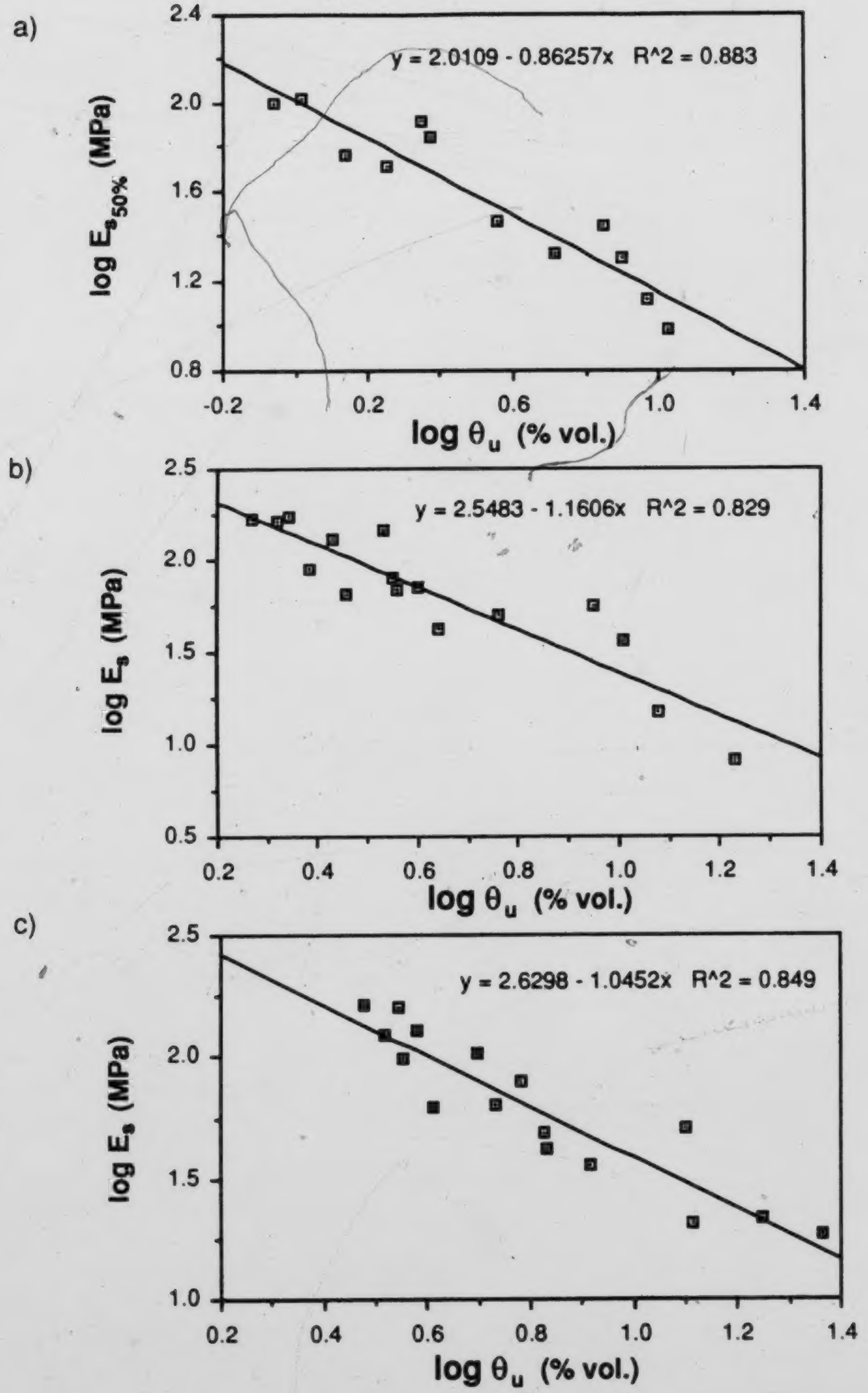

Figure 6.35: Secant modulus vs Unfrozen water content regressions
a) Soil A b) Soil B c) Soil C

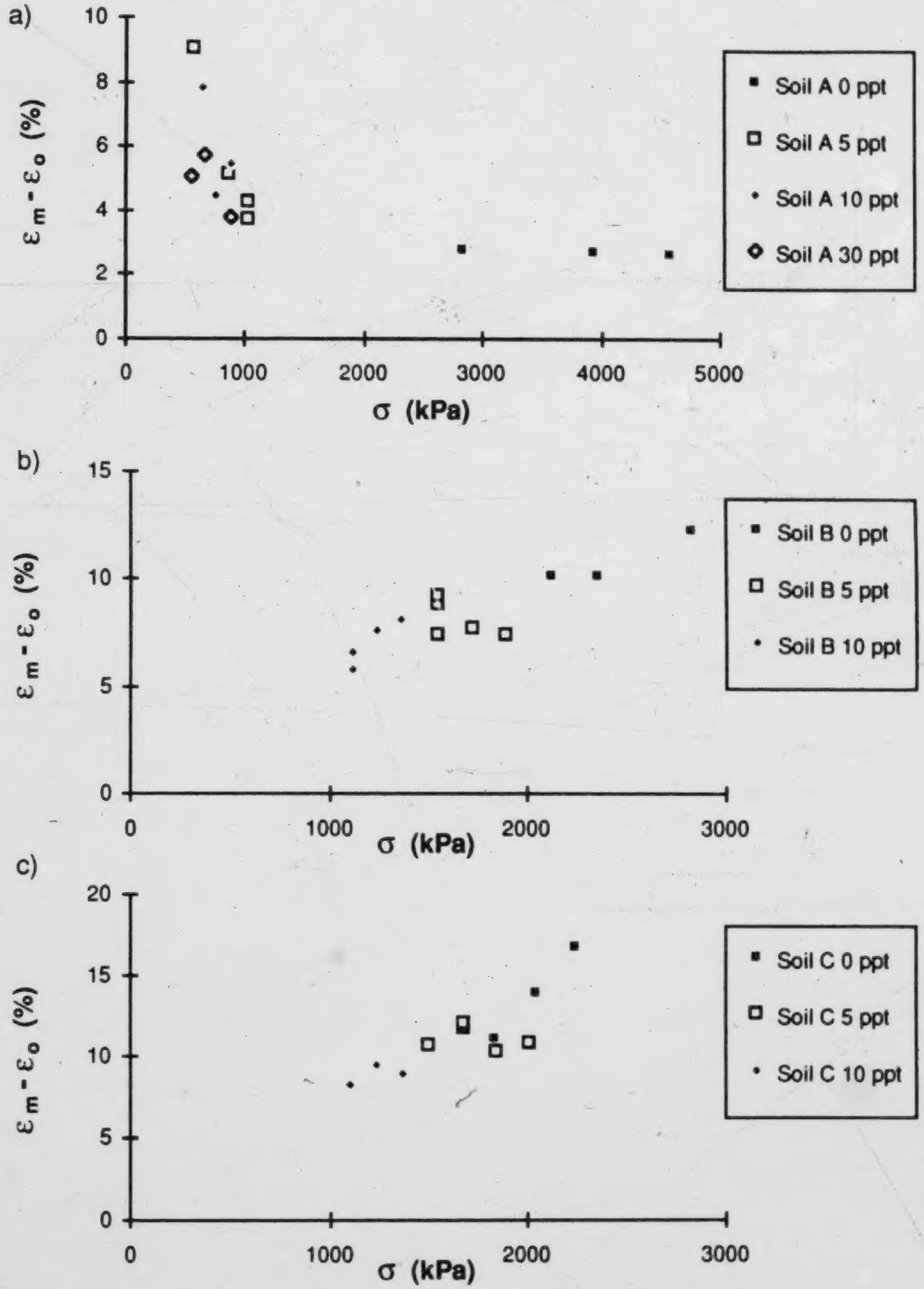

Figure 6.36: Creep strain to failure vs Stress a) Soil A b) Soil B c) Soil C

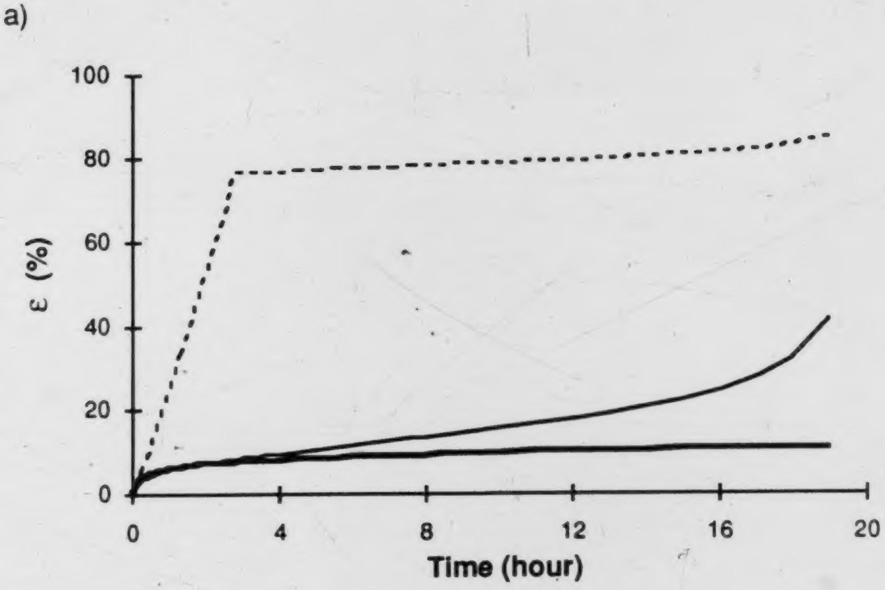

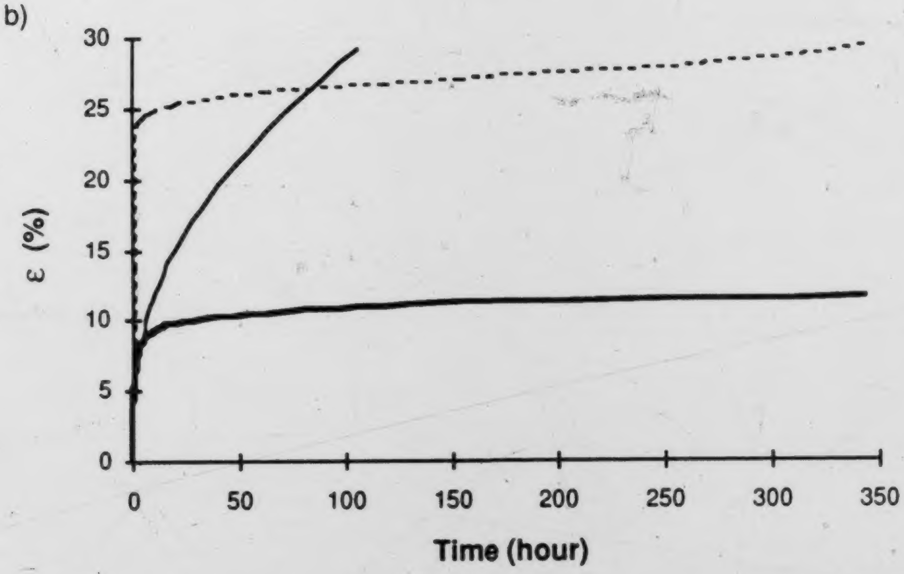

Figure 6.37: Comparison between measured strain and predicted strain using Vyalov bilinear or linear approach
a) Test CR-71 (soil B 0 ppt) b) Test CR-36 (soil C 0 ppt)
— measured strain -- Vyalov-bilinear approach — Vyalov-linear approach

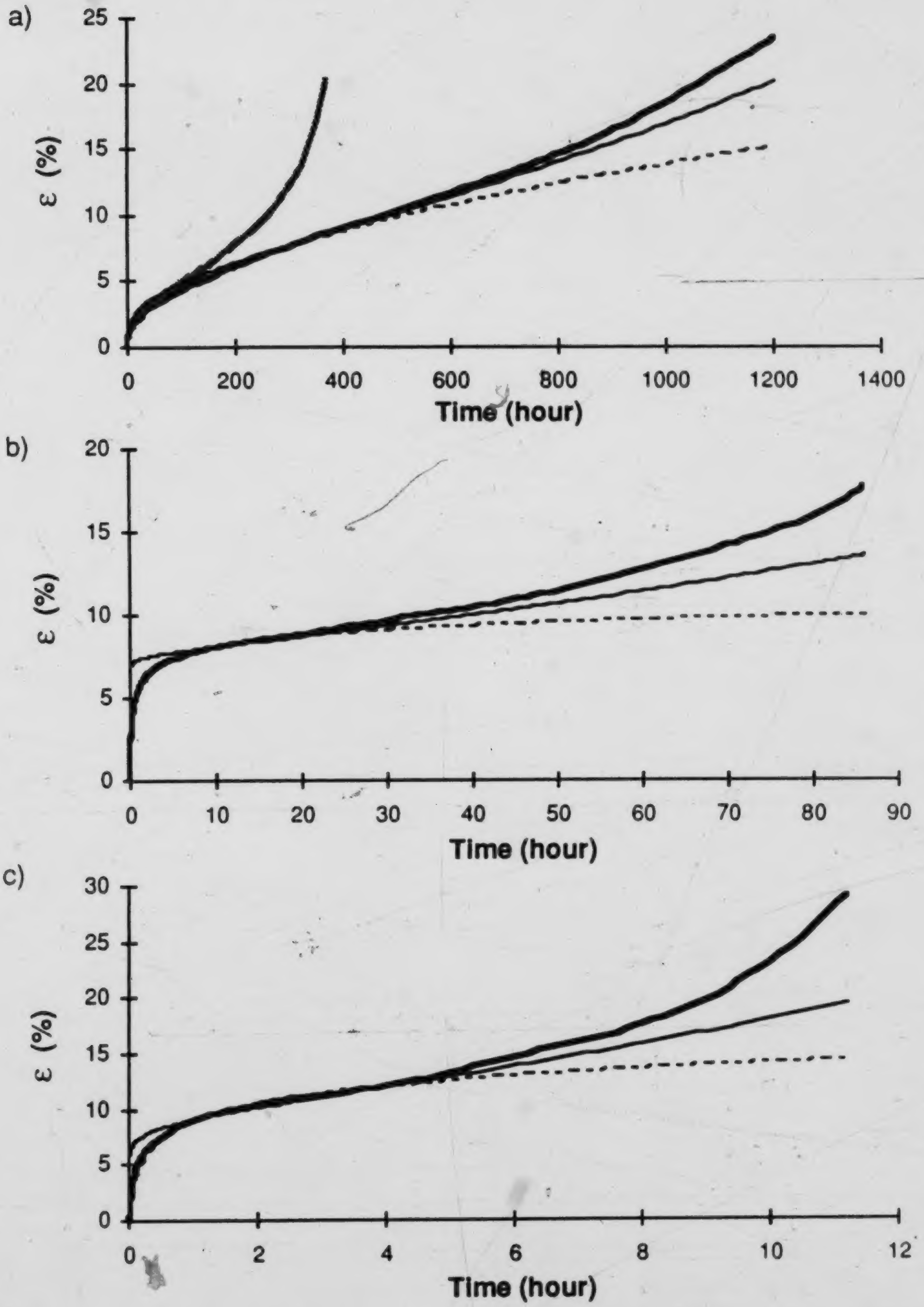

Figure 6.38: Comparison between measured strain and predicted strain for soils A, B, C at 5 ppt a) Test CR-67 b) Test CR-49 c) Test CR-66

▬ measured strain -- Sayles — Vyalov — Gardener

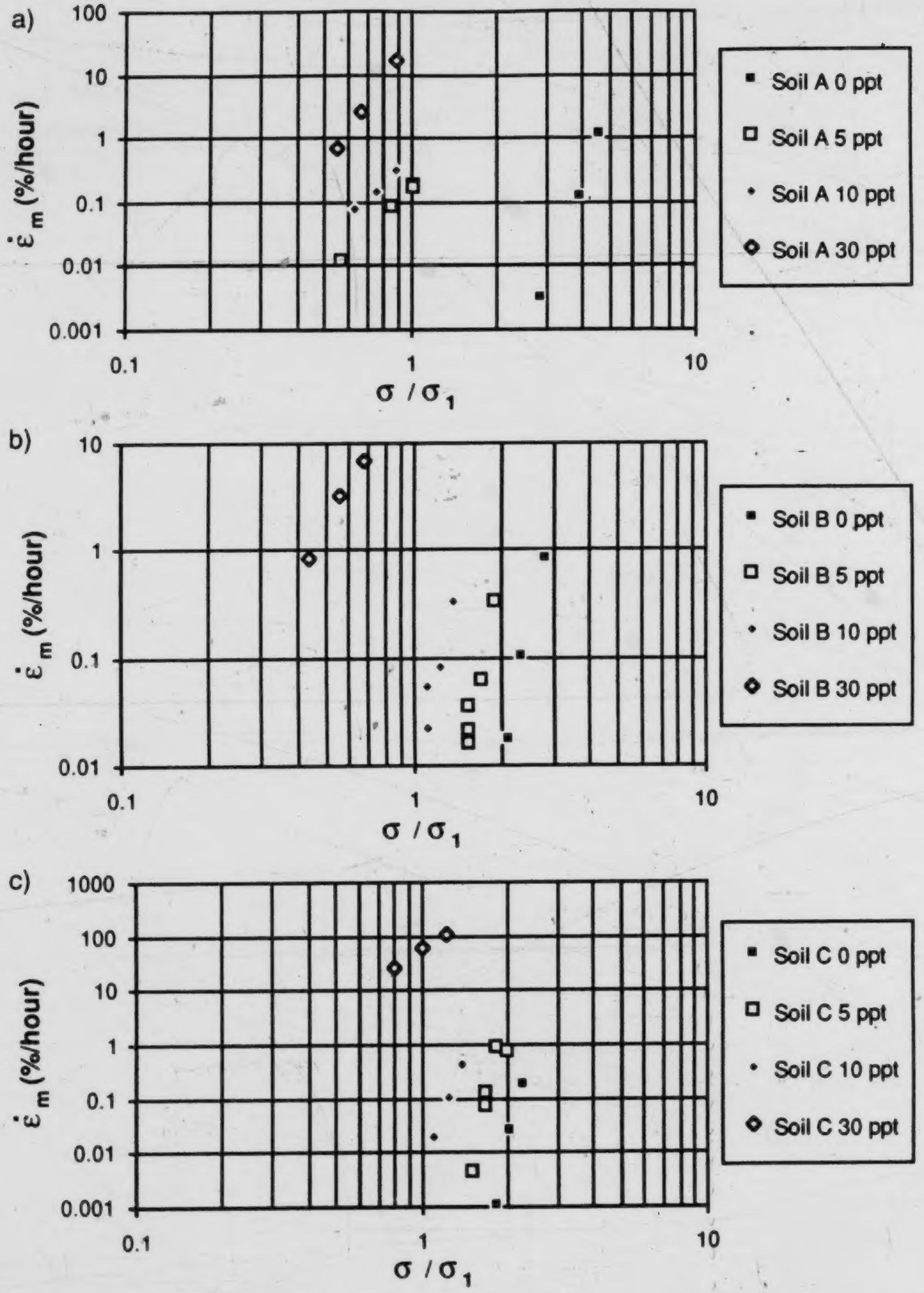

Figure 6.39: Strain rate at failure vs Stress ratio a) Soil A b) Soil B c) Soil C

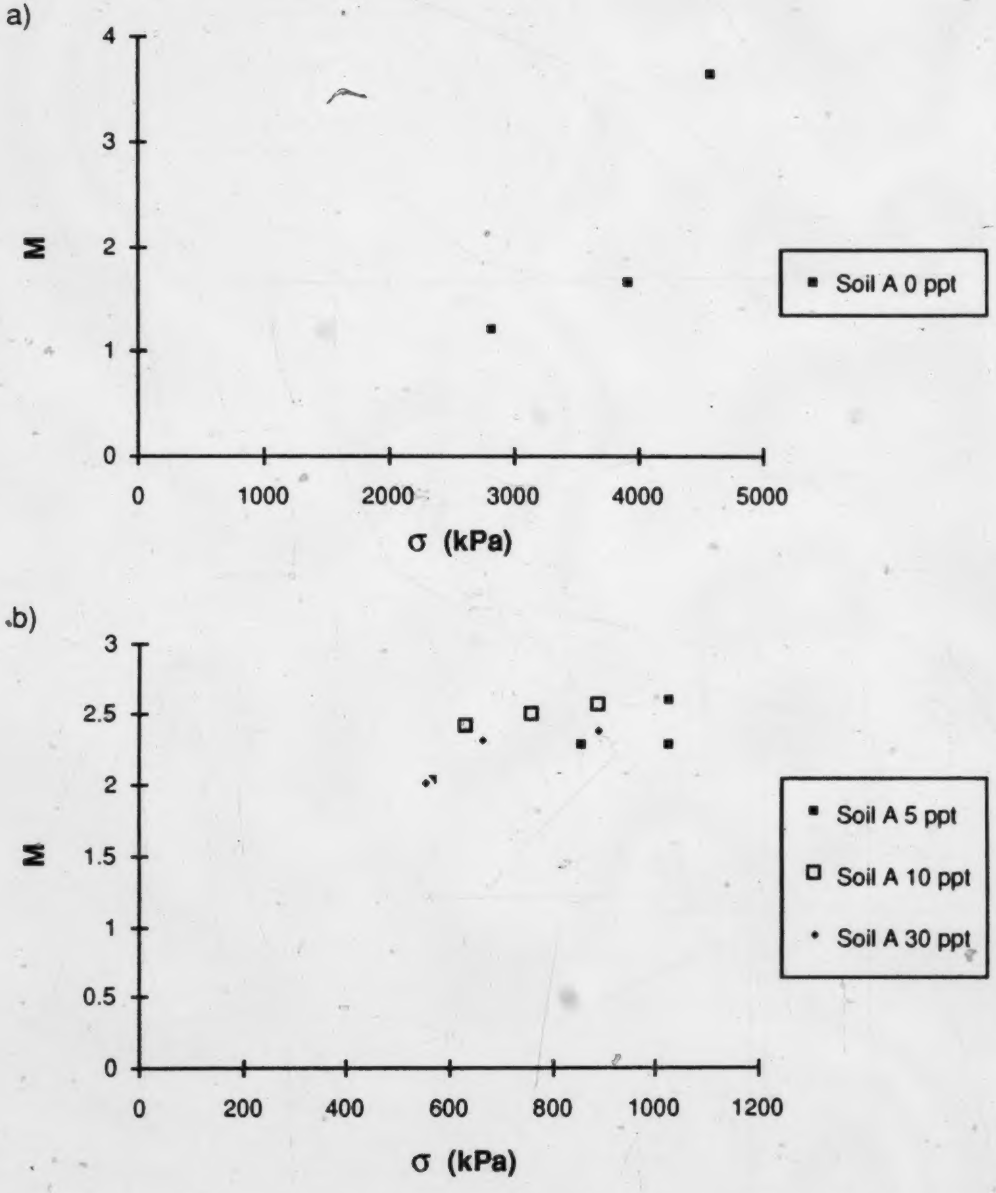

Figure 6.40: Sayles' M creep parameter for soil A a) 0 ppt b) 5, 10 , 30 ppt

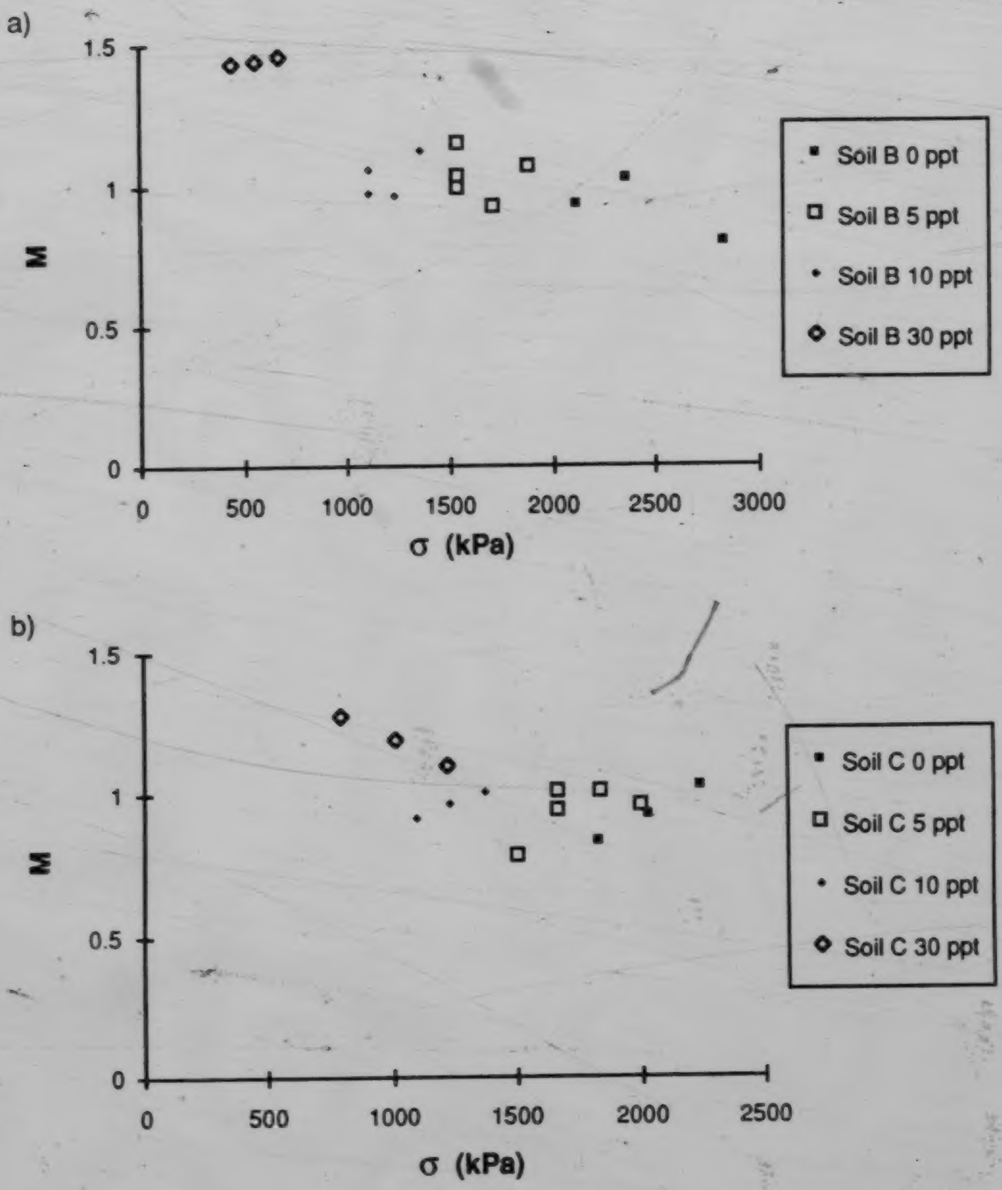

Figure 6.41: Sayles' M creep parameter a) Soil B b) Soil C

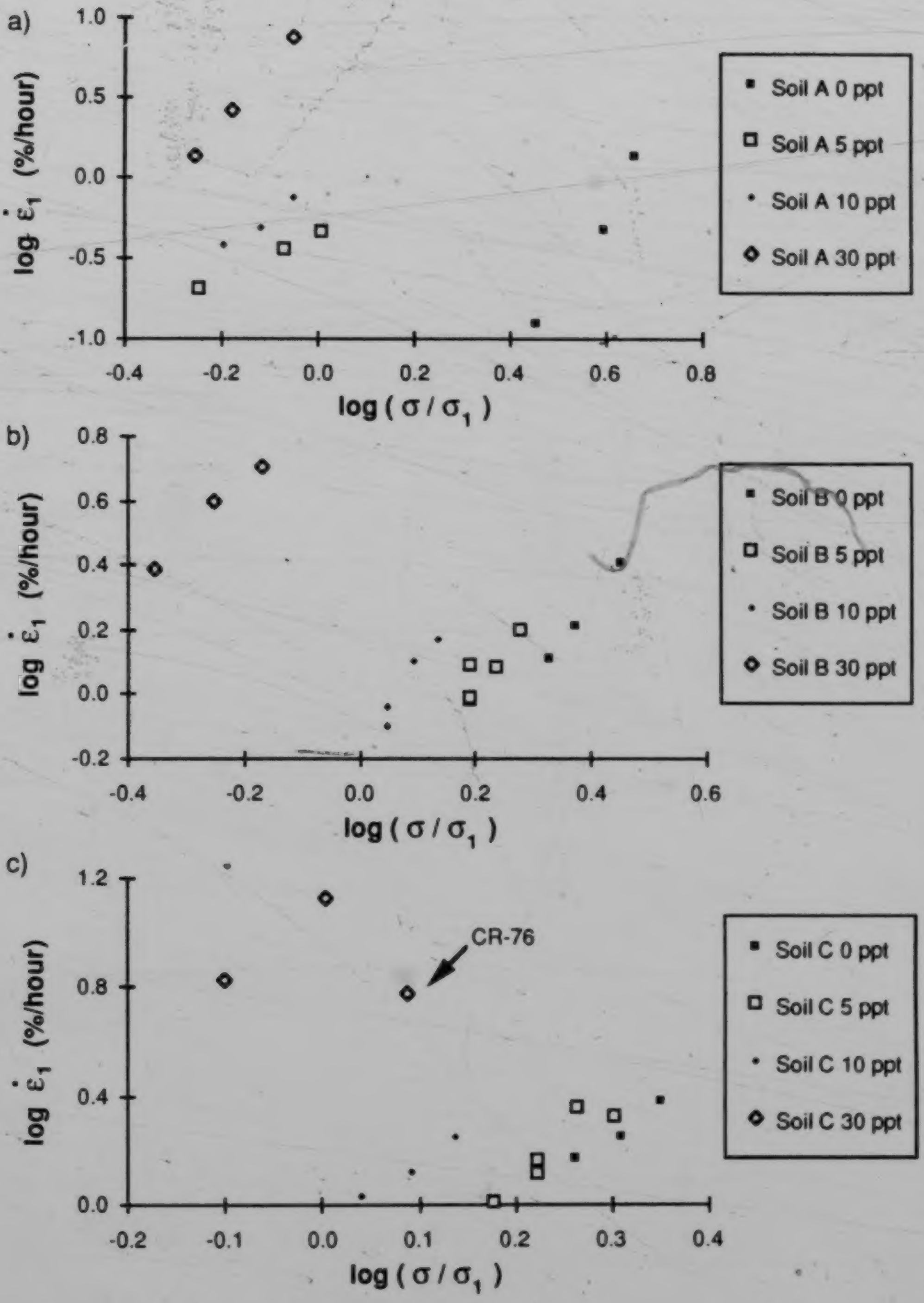

Figure 6.42: Strain rate 1 hour predicted by Sayles' equation vs Stress ratio
a) Soil A b) Soil B c) Soil C

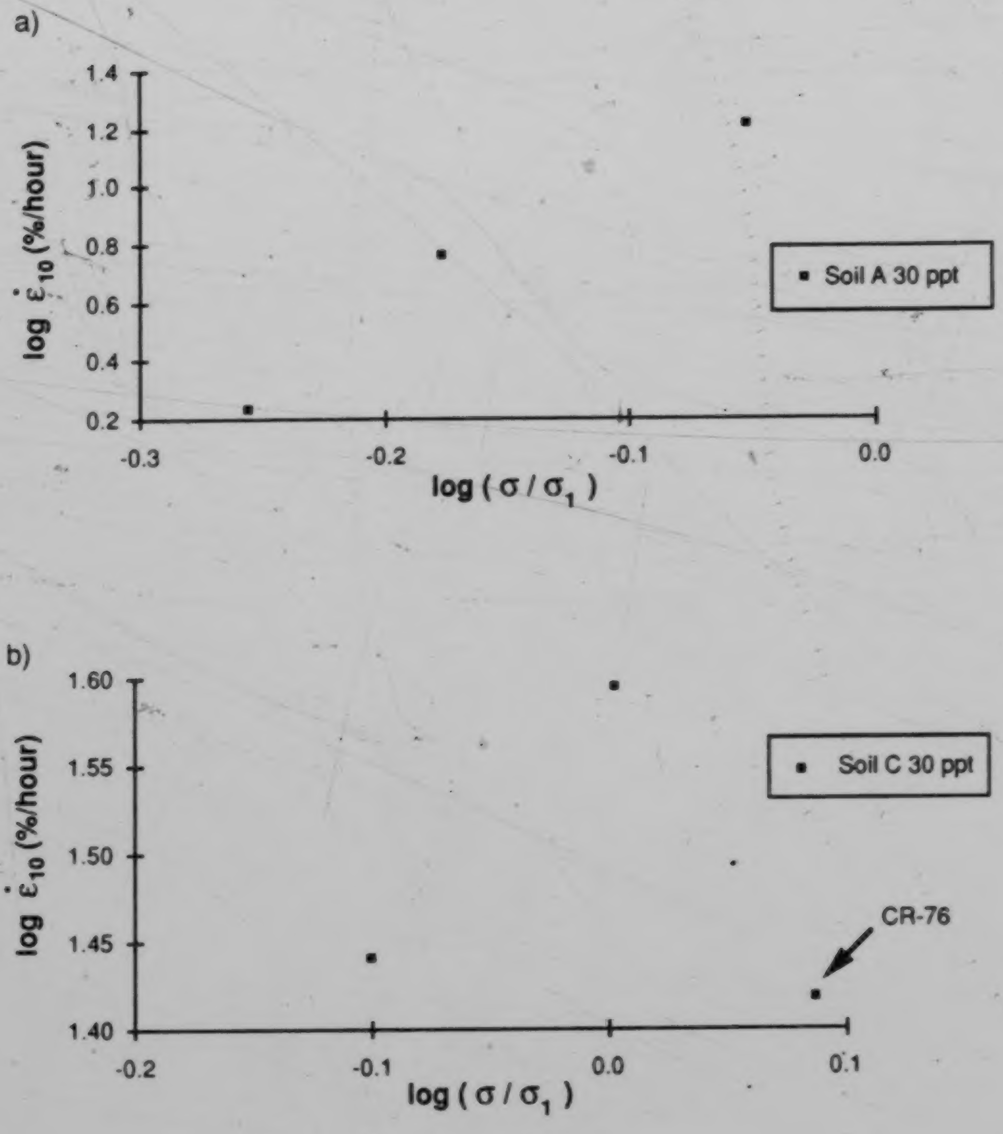

Figure 6.43: Strain rate 10 minute predicted by Sayles' equation vs Stress ratio
a) Soil A 30 ppt b) Soil C 30 ppt

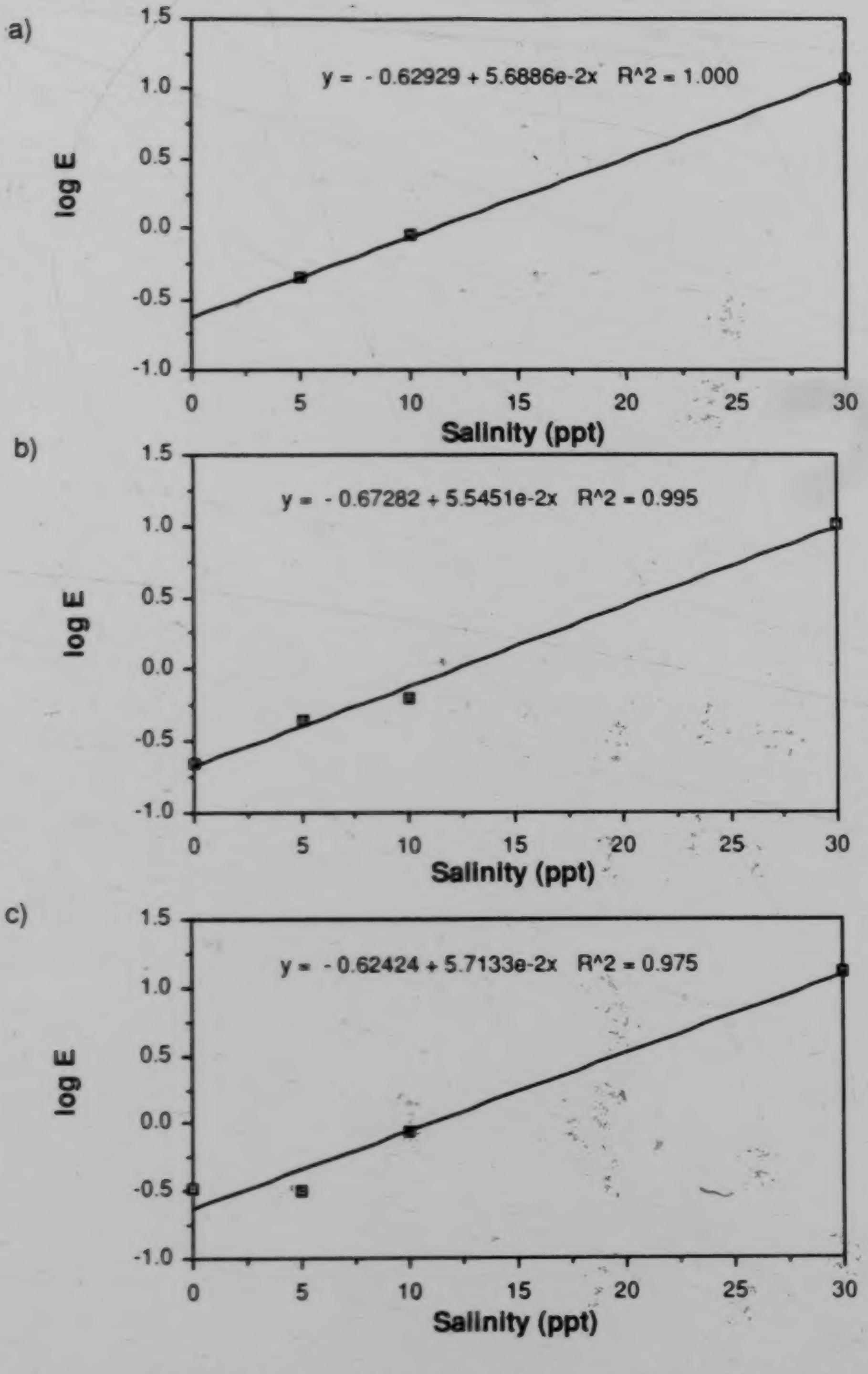

Figure 6.44: E vs Salinity regressions a) Soil A 5, 10, 30 ppt b) Soil B c) Soil C

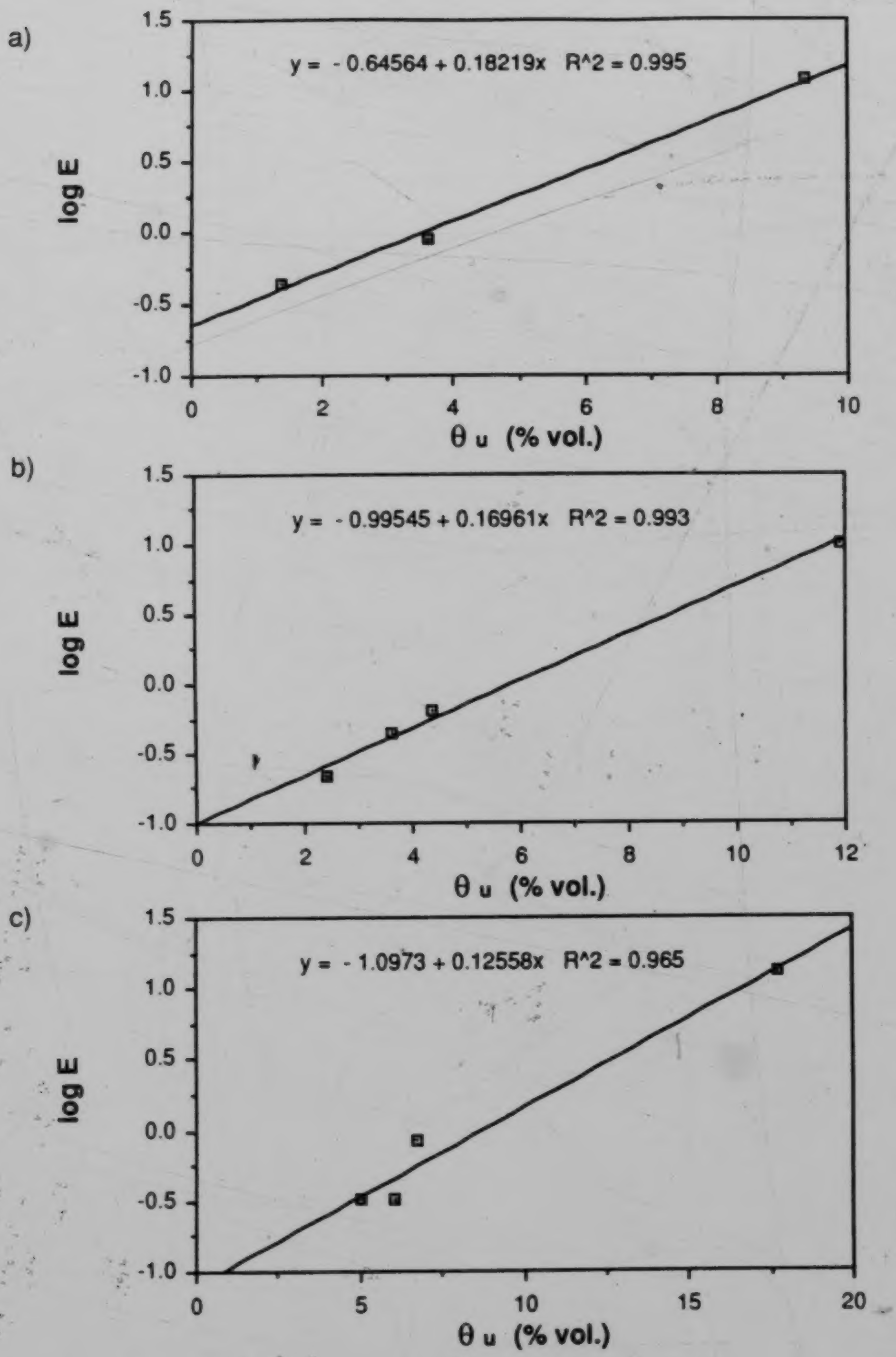

Figure 6.45: E vs UInfrozen water content regressions
a) Soil A 5, 10, 30 ppt b) Soil B c) Soil C

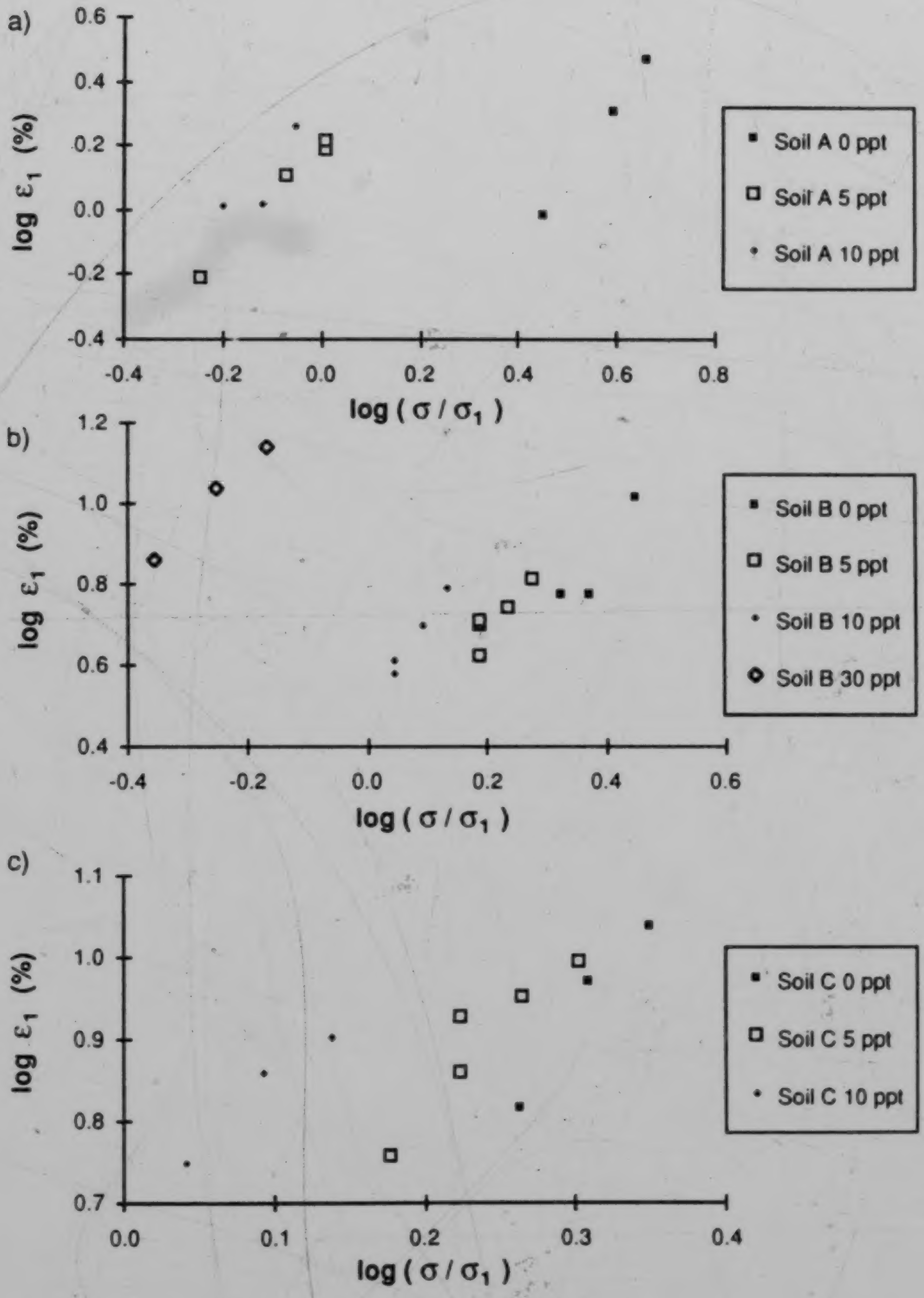

Figure 6.46: Strain 1 hour (measured strain) vs Stress ratio
a) Soil A 0, 5, 10 ppt b) Soil B 0, 5, 10 ,30 ppt c) Soil C 0, 5, 10 ppt

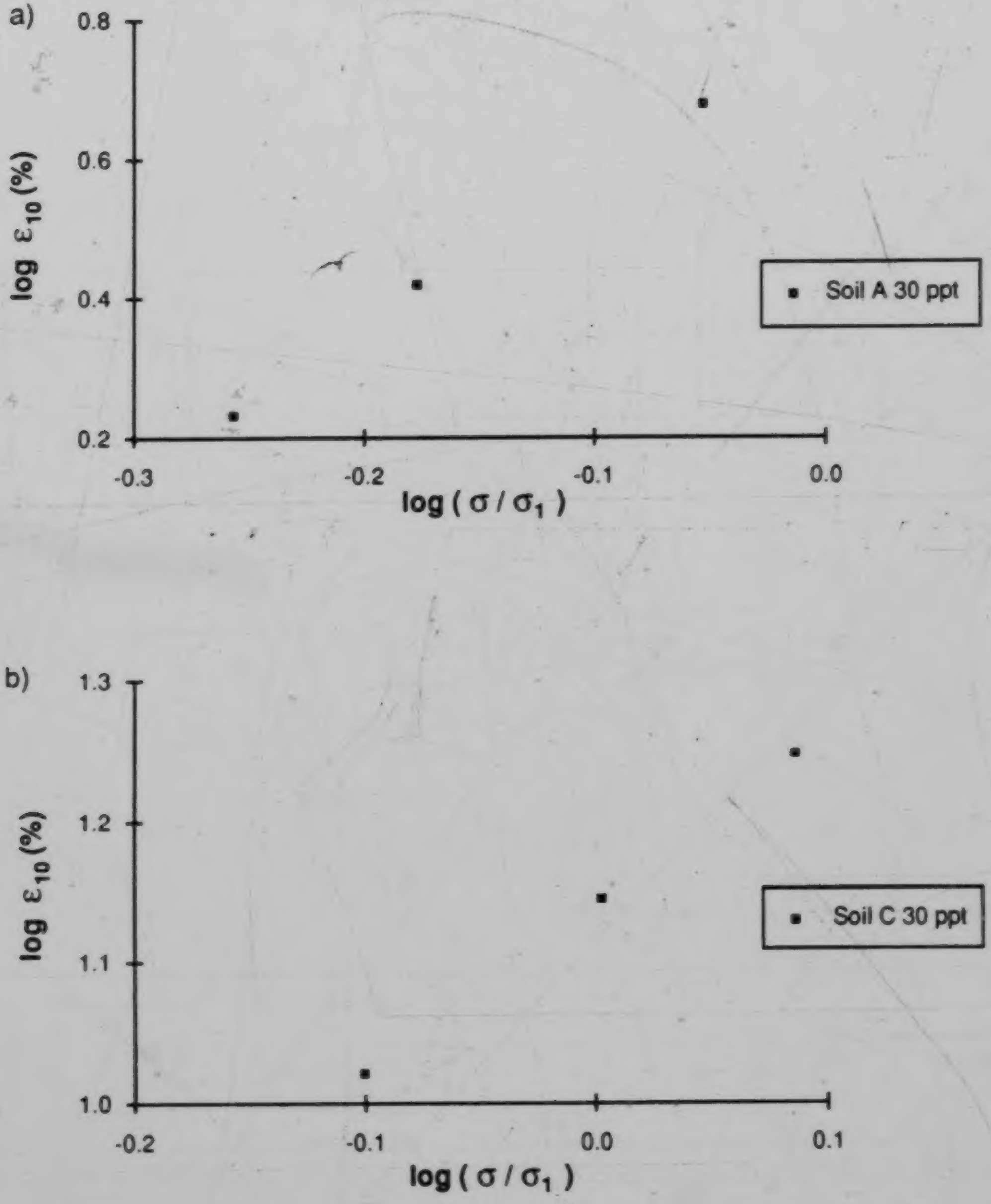

Figure 6.47: Strain 10 minute (measured strain) vs Stress ratio
a) Soil A 30 ppt b) Soil C 30 ppt

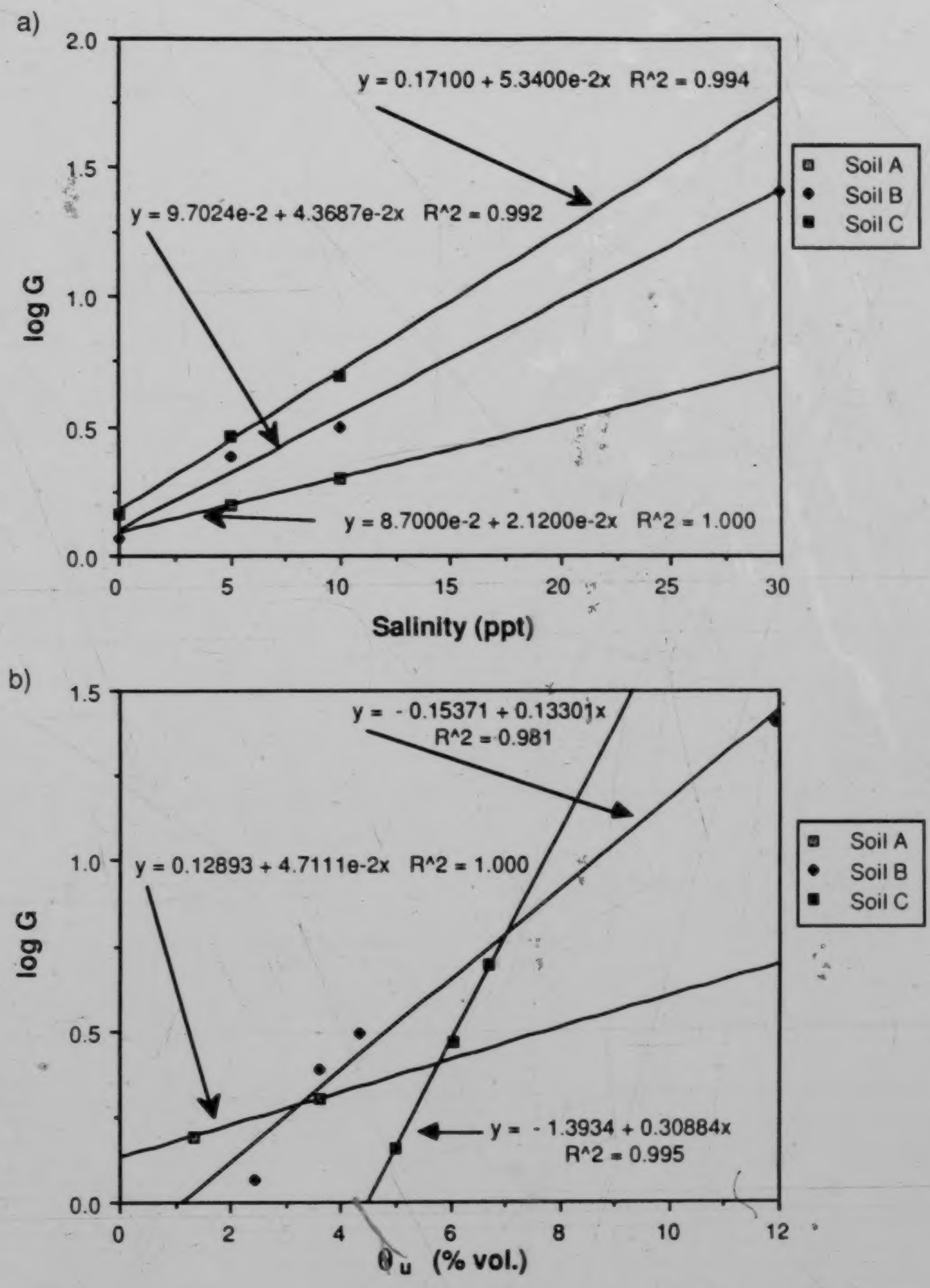

Figure 6.48: a) G vs Salinity for soil A 5, 10 ppt, soil B, soil C 0, 5, 10 ppt
b) G vs Unfrozen water content for soil A 5, 10 ppt, soil B, soil C 0, 5 10 ppt

a)

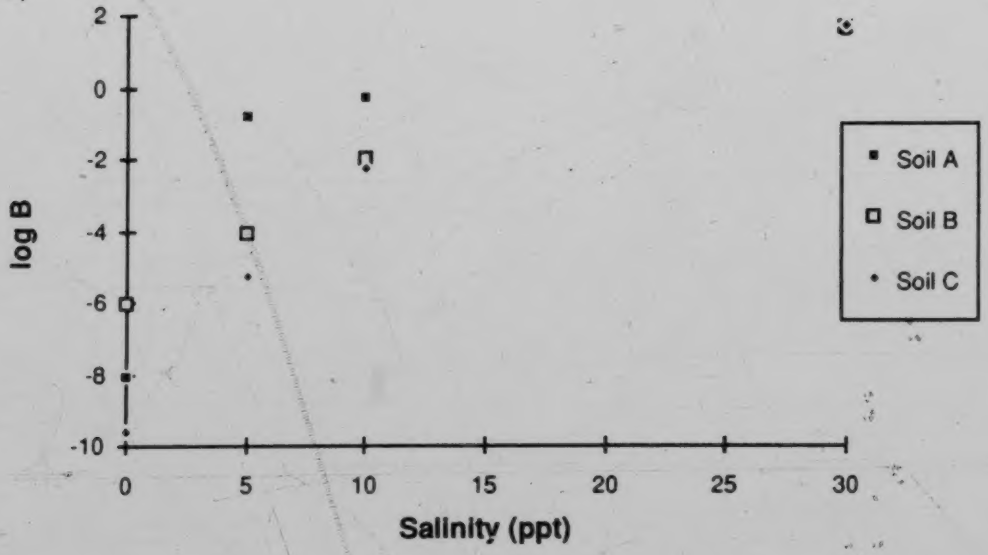

b)

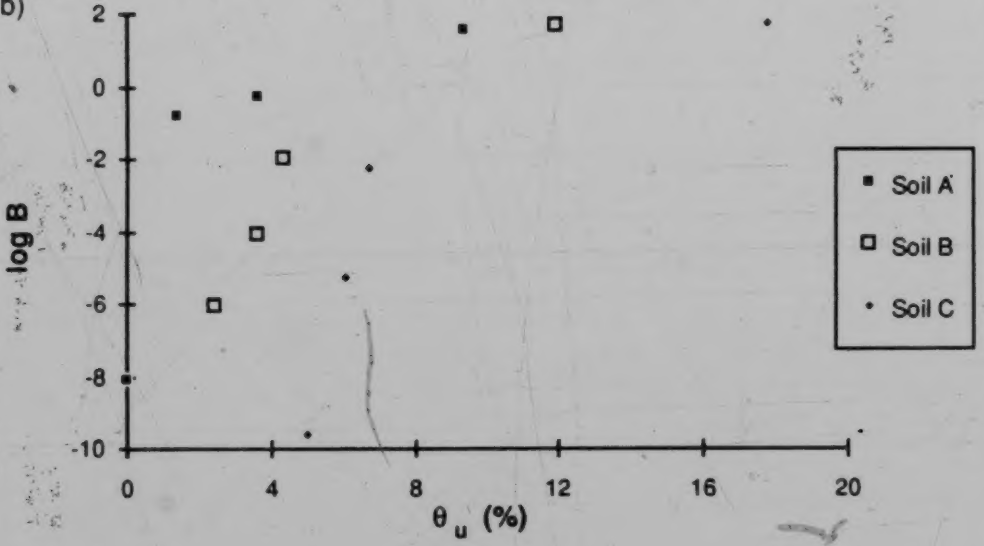

Figure 6.49: a) Flow law parameter B vs Salinity
b) Flow law parameter B vs Unfrozen water content

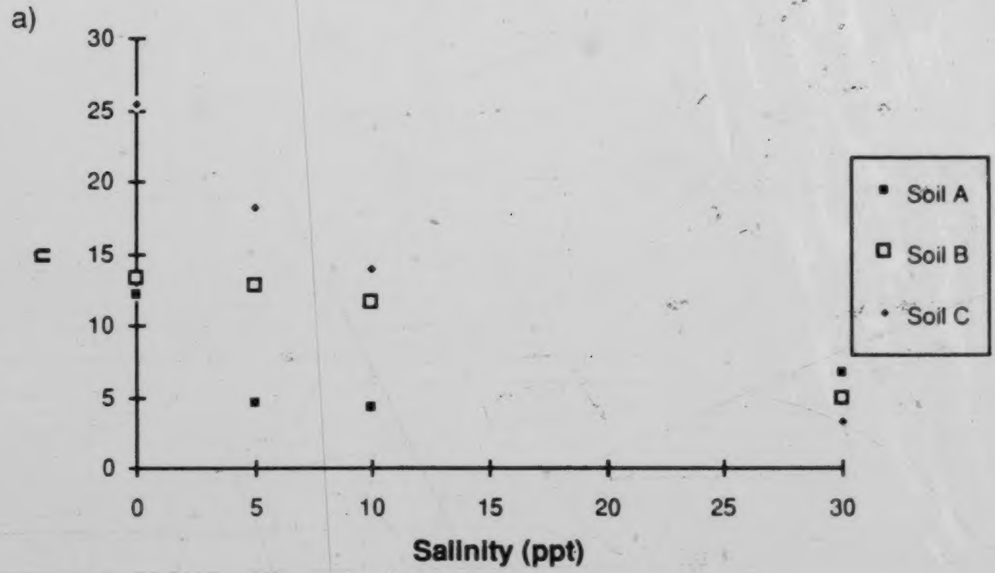

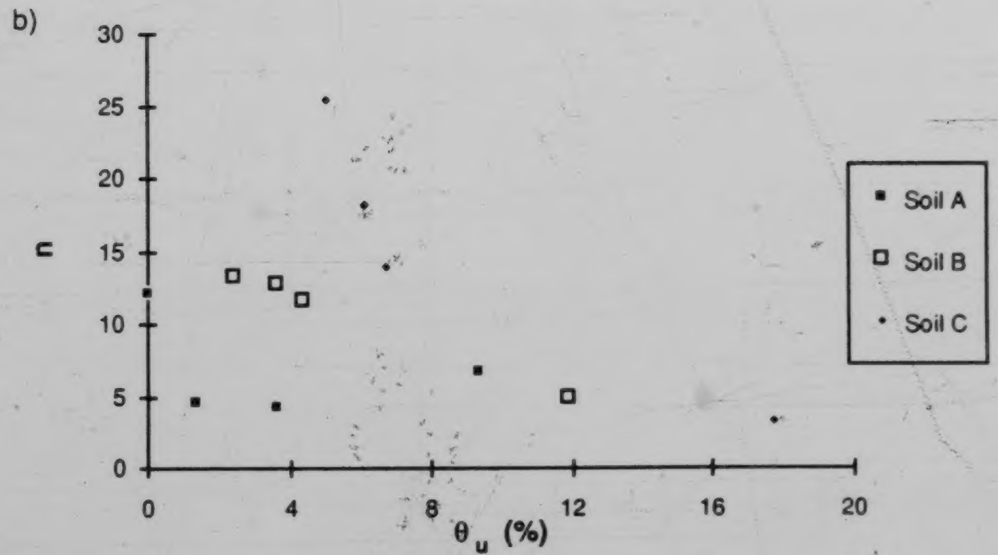

Figure 6.50: a) Flow law parameter n vs Salinity
b) Flow law parameter n vs Unfrozen water content

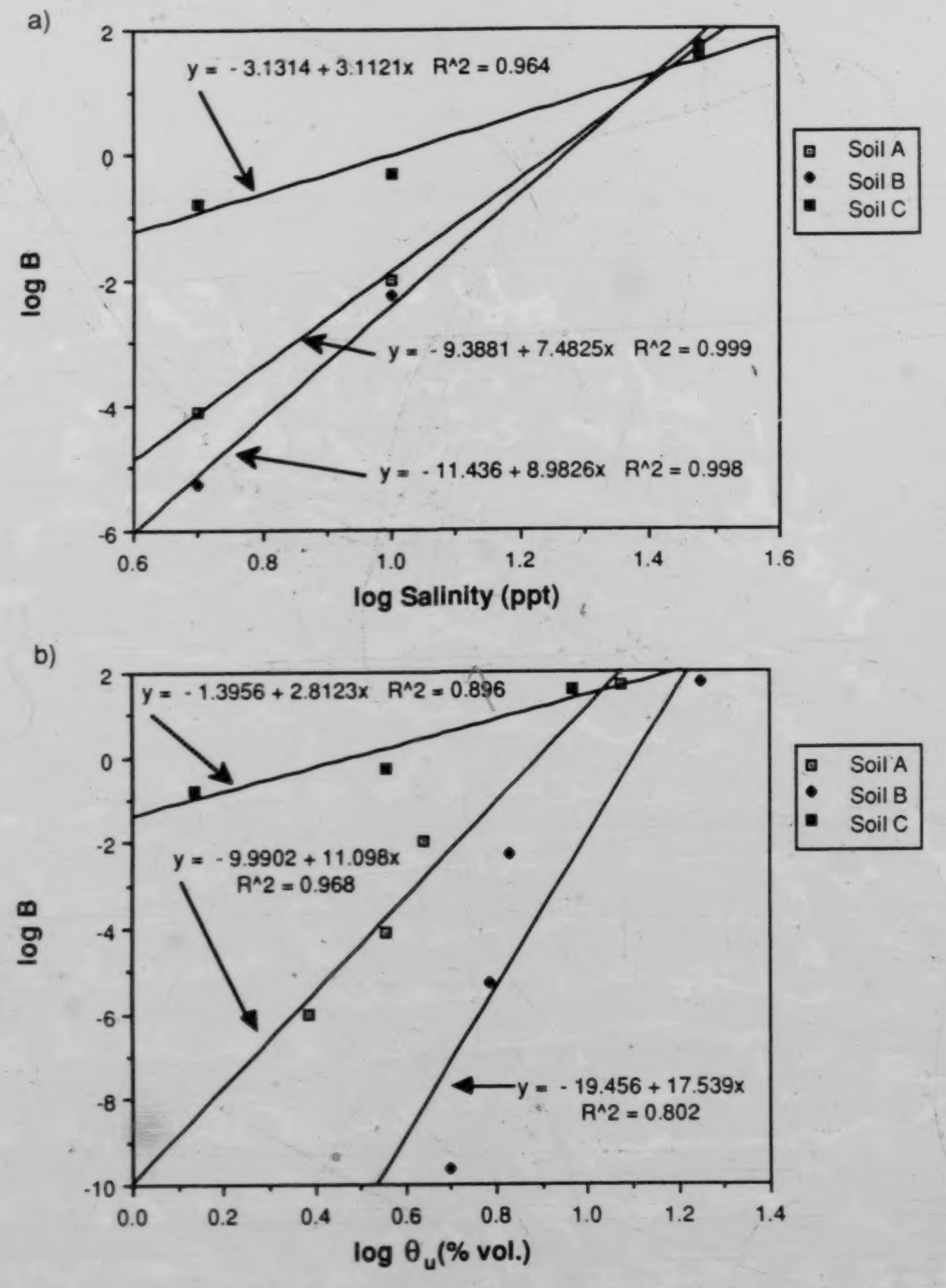

Figure 6.51: a) Flow law parameter B vs Salinity for soils A,B, C
b) Flow law parameter B vs Unfrozen water content for soils A, B, C

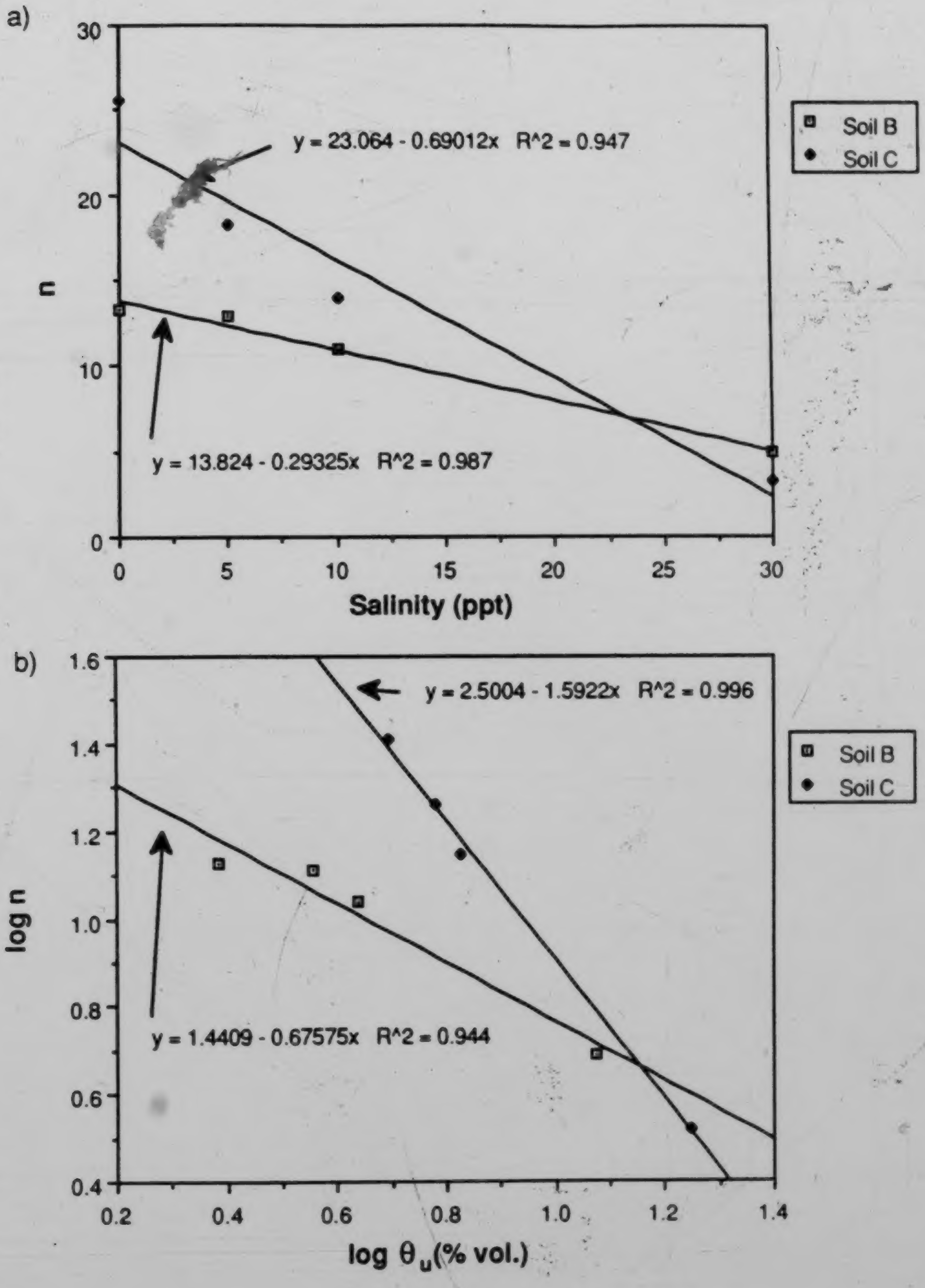

Figure 6.52: a) Flow law parameter n vs Salinity for soils B and C
b) Flow law parameter n vs Unfrozen water content for soils B and C

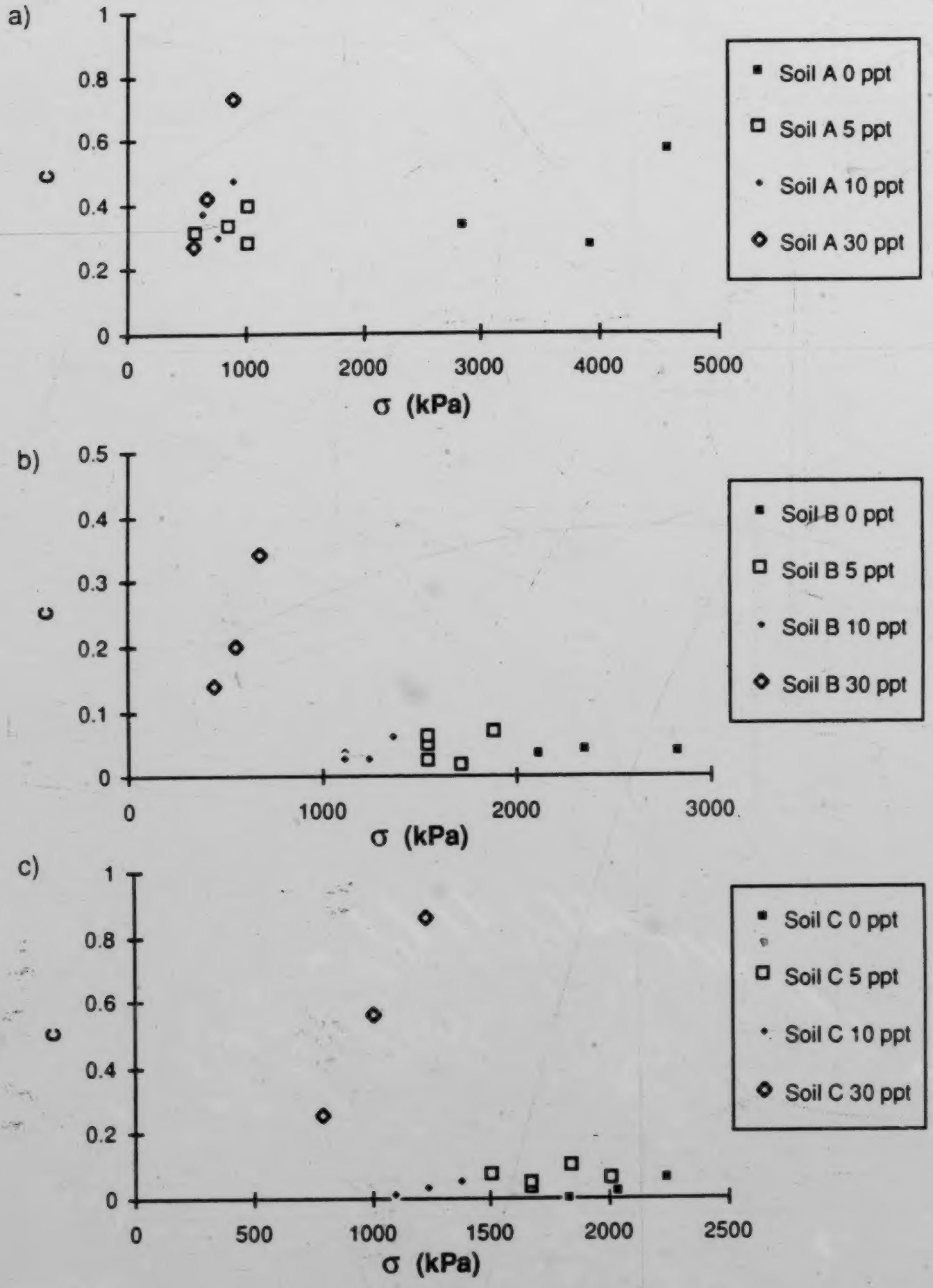

Figure 6.53: Gardener's creep parameter c vs Stress a) Soil A b) Soil B c) Soil C

a)

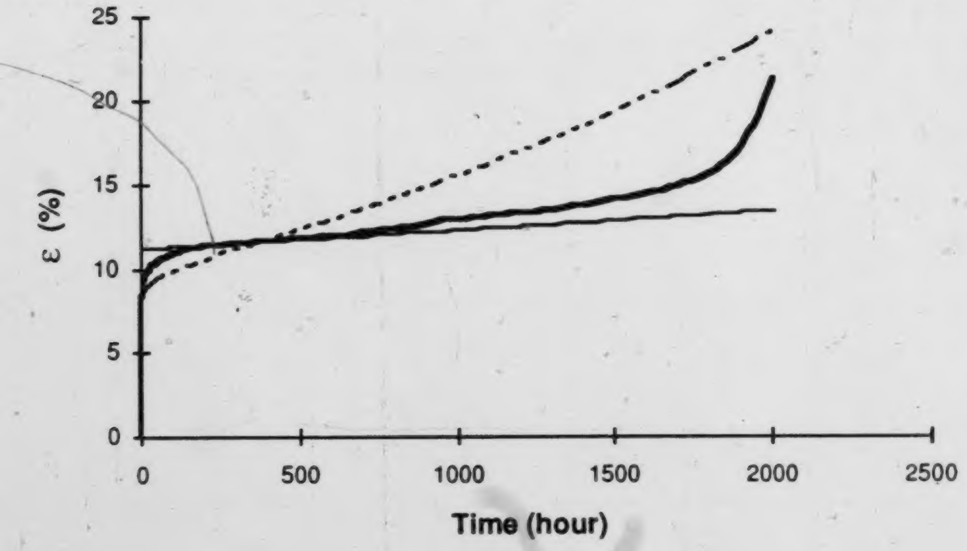

b)

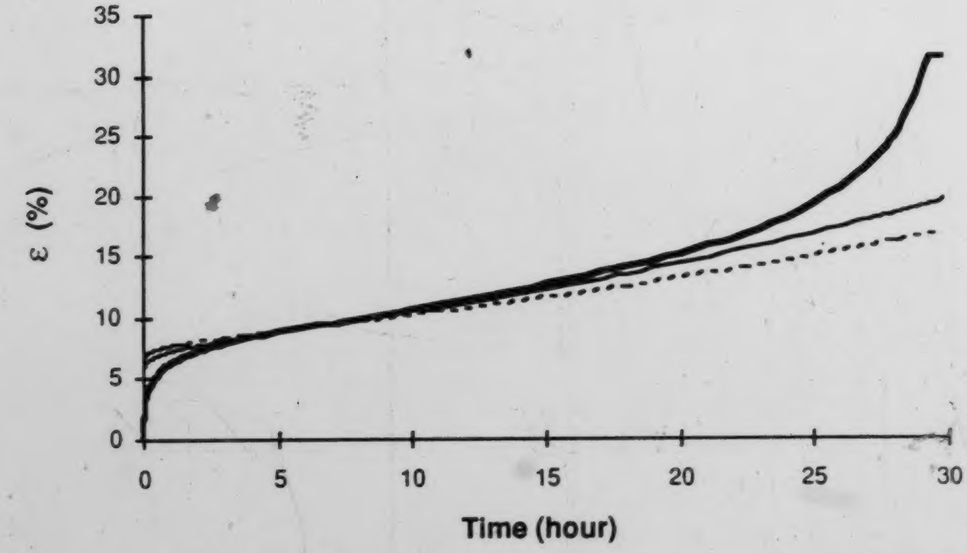

Figure 6.54: Comparison between measured strain and predicted strain using Gardener's approach with the specific c value or the average c value a) Test CR-36 b) Test CR-82

— measured strain — Gardener - - Gardener c-average

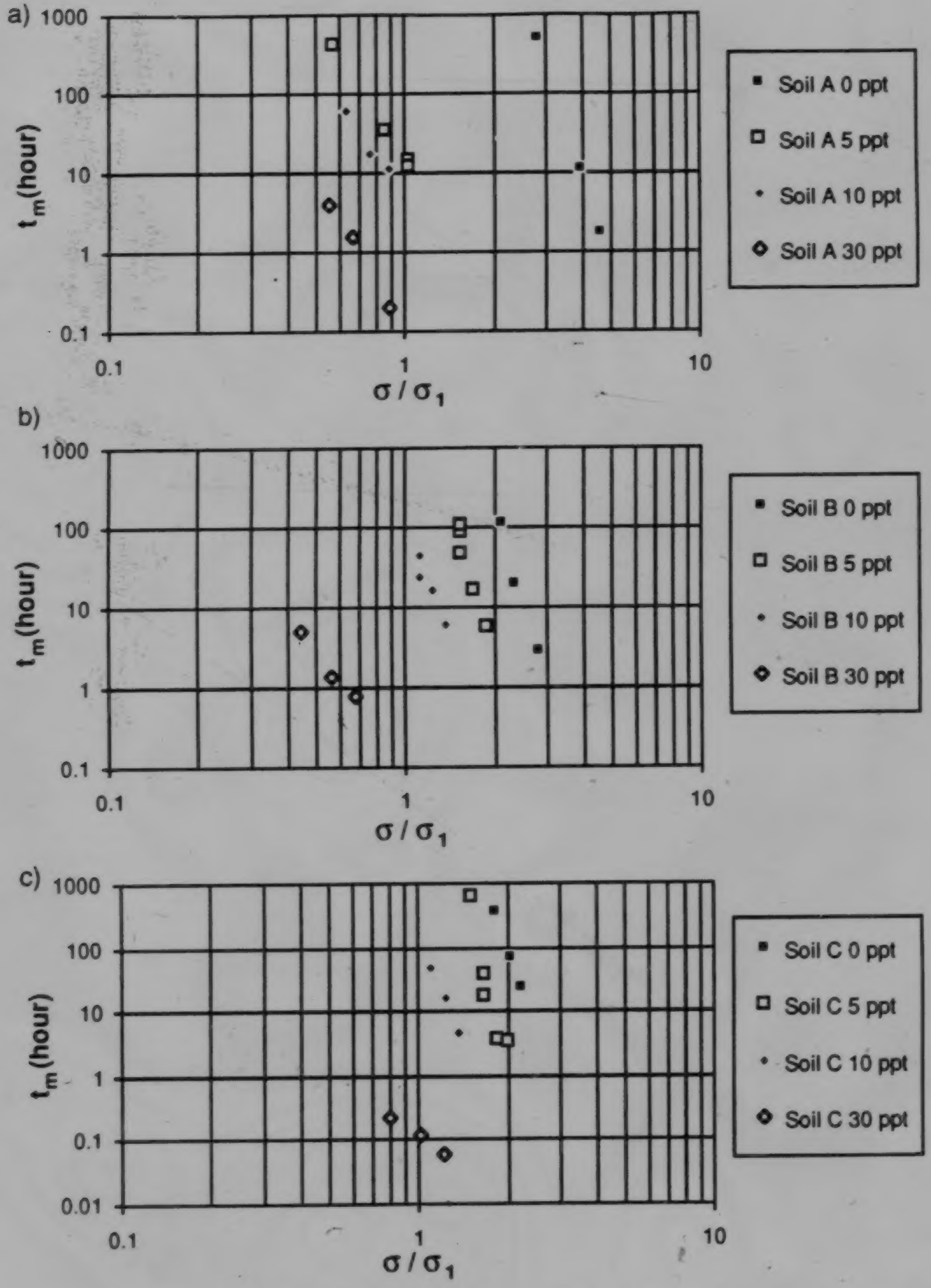

Figure 6.55: Time to failure vs Stress ratio a) Soil A b) Soil B c) Soil C

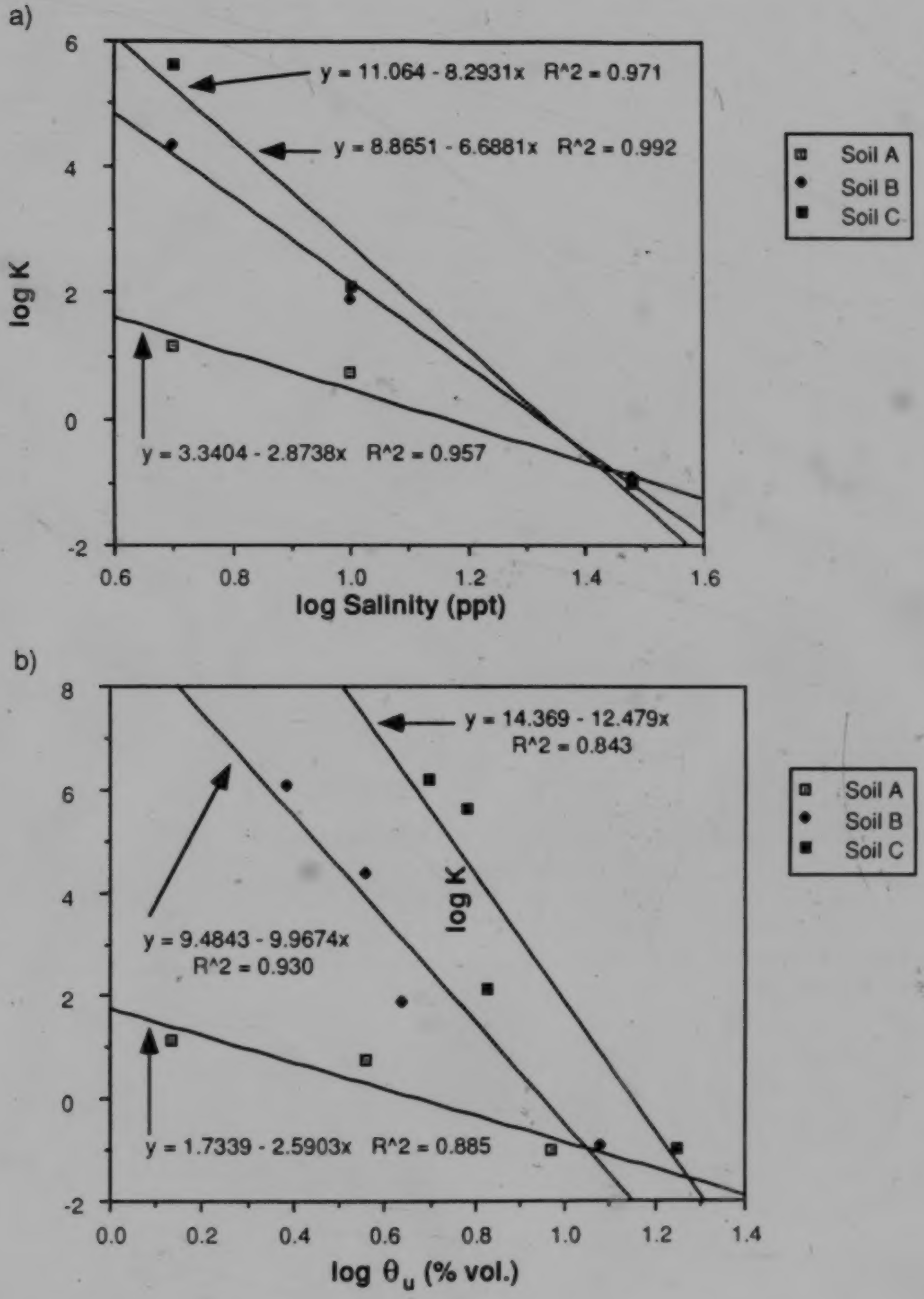

Figure 6.56: a) K vs Salinity for soils A,B, C
b) K vs Unfrozen water content for soils A, B, C

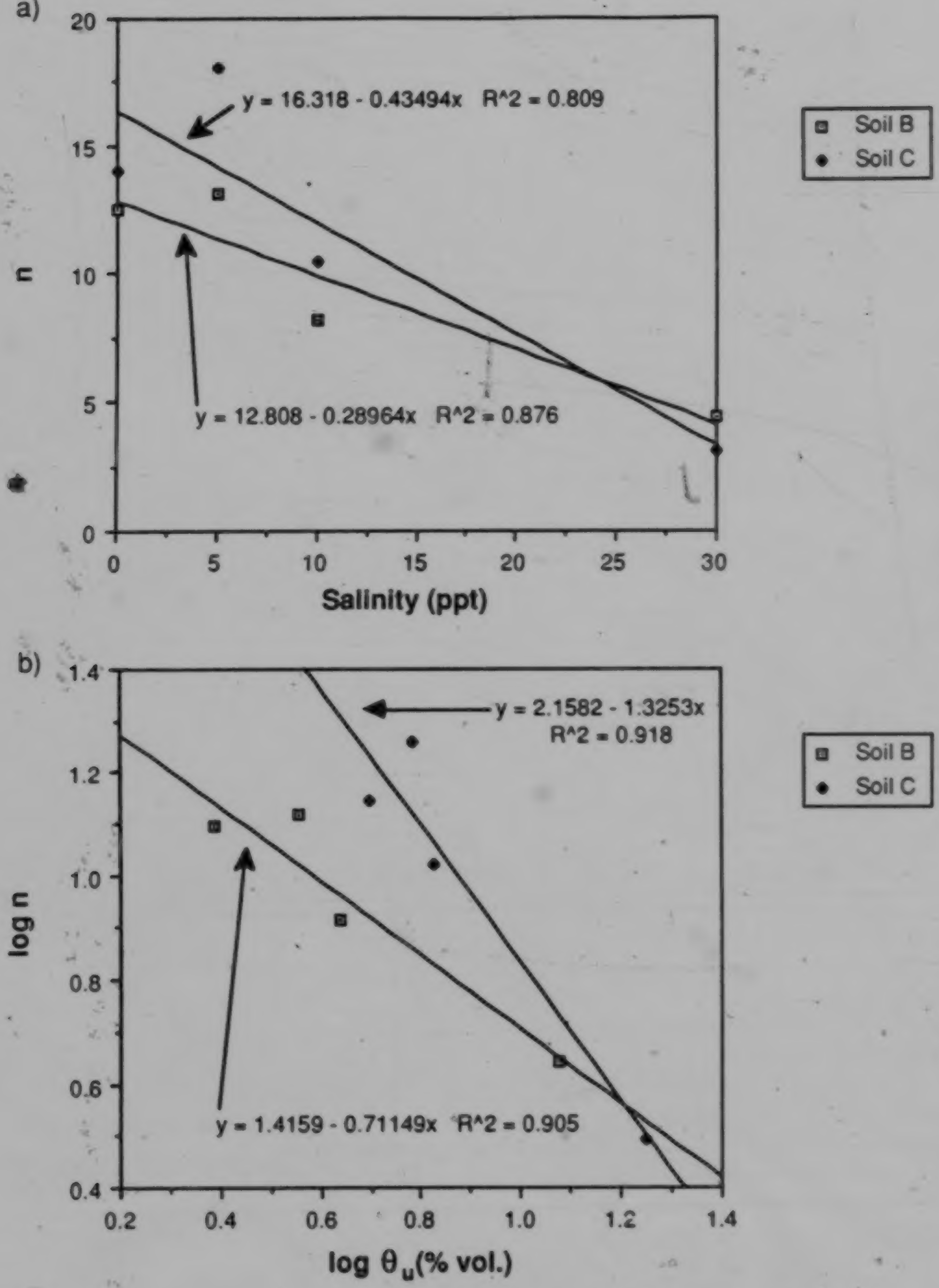

Figure 6.57: a) Parameter n from Gardener vs Salinity for soils B and C
b) Parameter n from Gardener vs Unfrozen water content for soils B and C

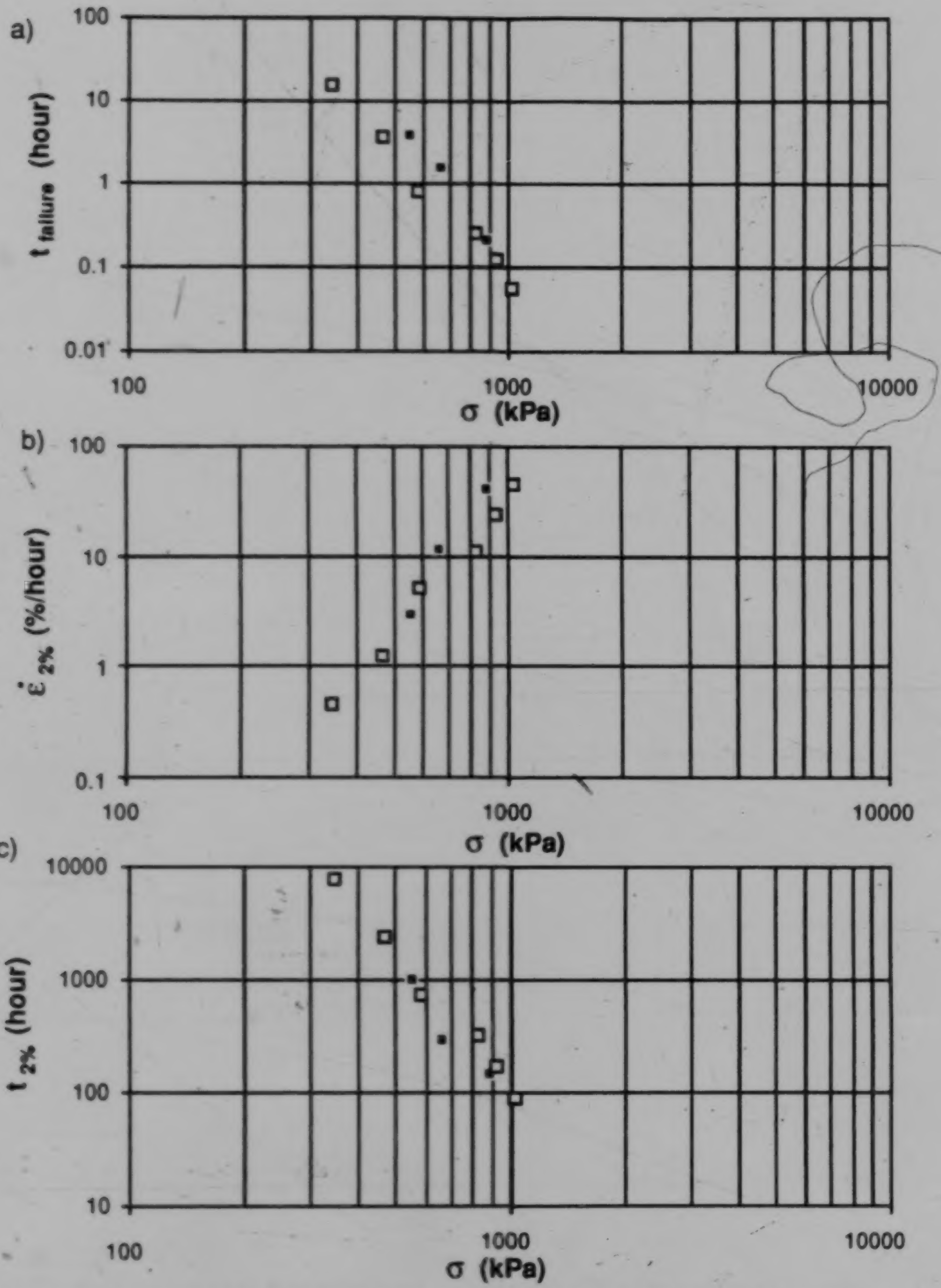

Figure 6.58: Creep results comparison between soil A 30 ppt and Pharr and Godavarti (1987) results a) Time to failure vs Stress b) Strain rate at 2% strain vs Stress c) Time to 2% strain vs Stress

■ Soil A 30 ppt □ Pharr and Godavarti (1987)

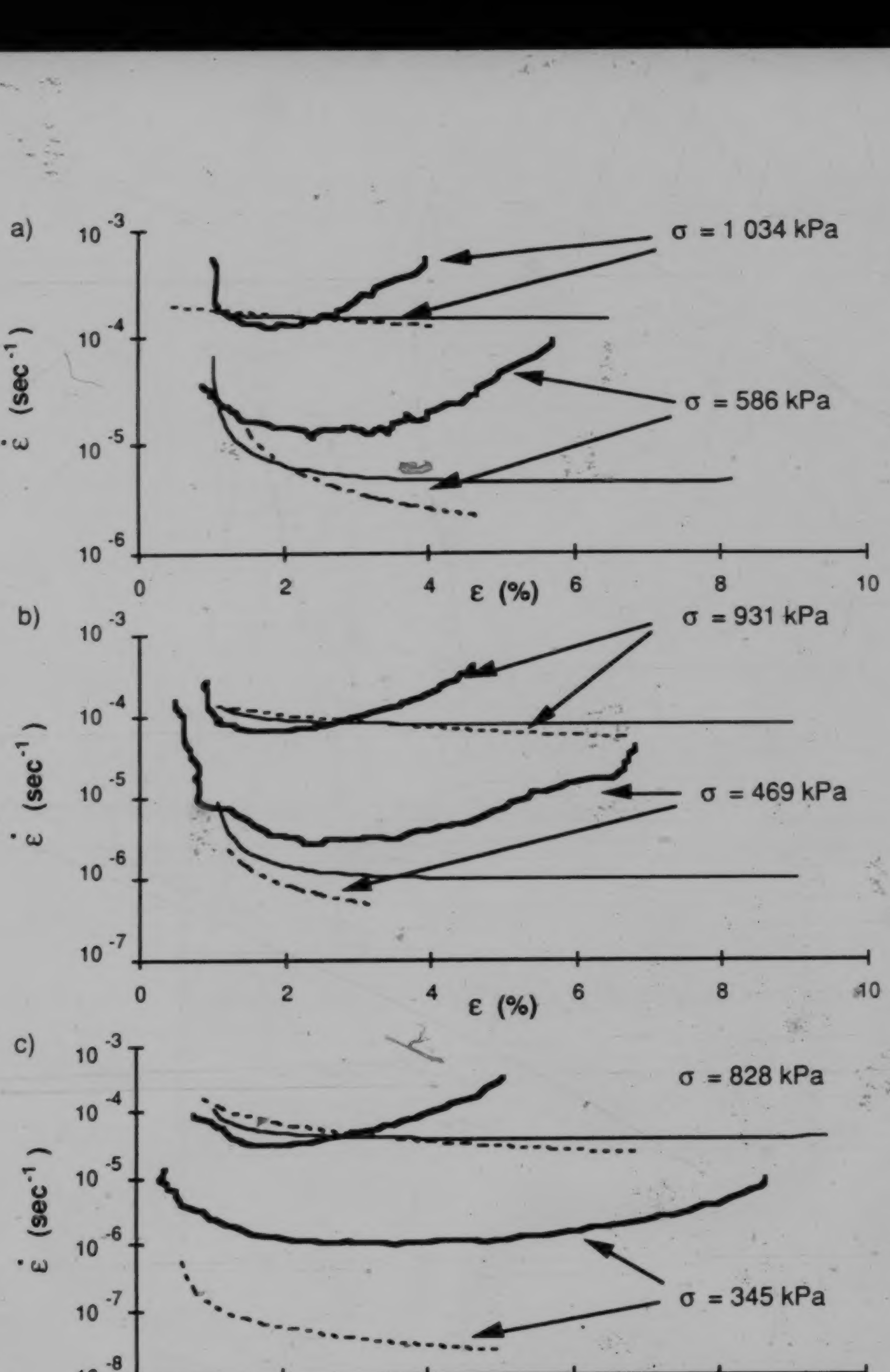

Figure 6.59: Comparison between strain rate vs strain curves from Pharr and Godavarti (1987) and the prediction using the results from this study a) Stresses of 1 034 and 586 kPa b) Stresses of 931 and 469 kPa c) Stresses of 828 and 345 kPa

▬ Pharr and Godavarti (1987) - - Sayles' method — Gardener's method

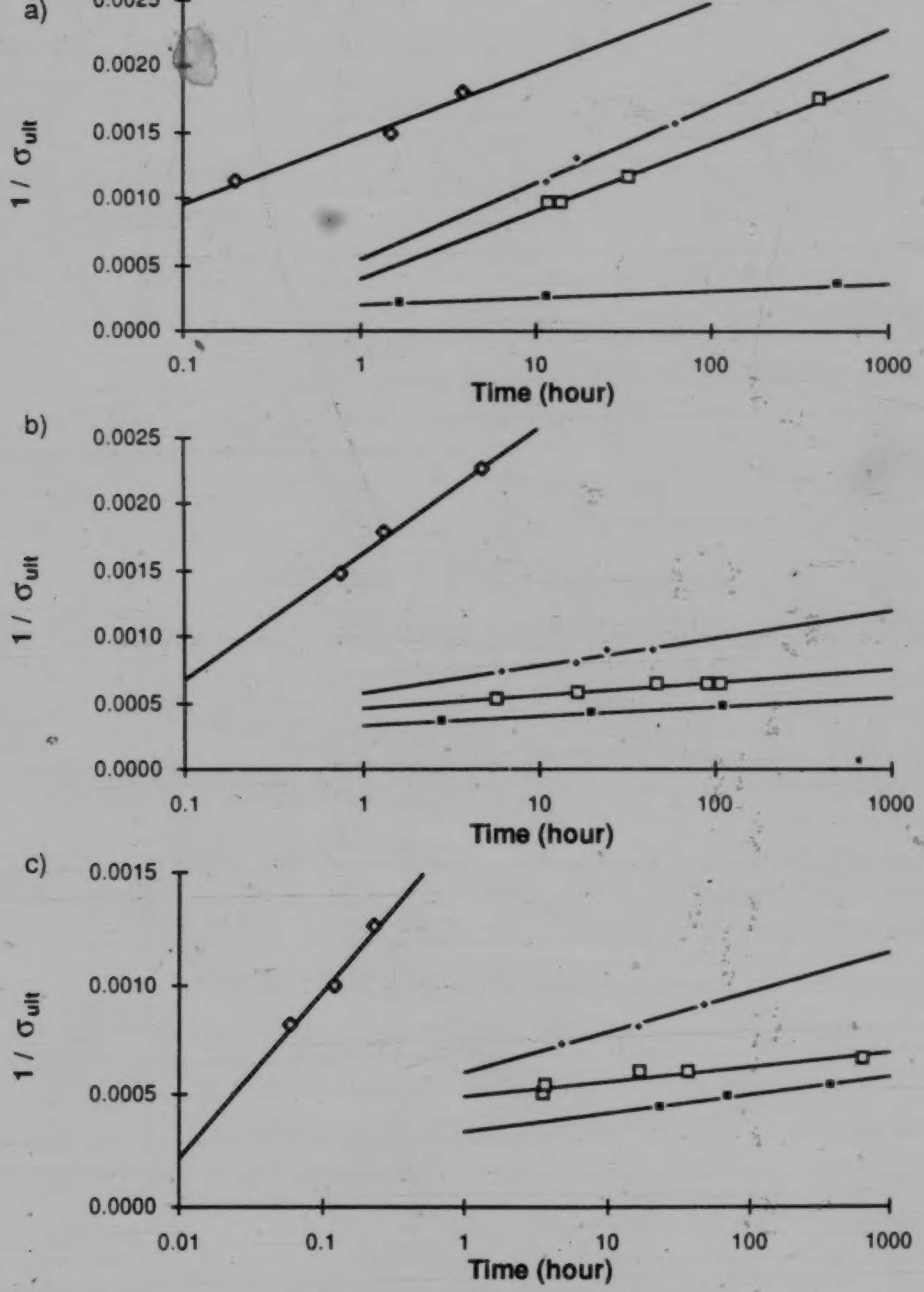

Figure 6.60: 1 / Ultimate Strength vs Time a) Soil A b) Soil B c) Soil C
▪ 0 ppt ☐ 5 ppt • 10 ppt ◆ 30 ppt

7. CONCLUSION AND RECOMMENDATIONS

7.1. CONCLUSION

First, the prediction of unfrozen water content based on the sodium chloride phase diagram has been shown to be valid for coarse-grained soils. However, for soils containing some fines, this prediction is not valid since the fine-grained soil particles influence the unfrozen water content. However, combining the prediction using the phase diagram with a measurement of the unfrozen water content at 0 salinity gives acceptable results when compared to measured values of unfrozen water content. The method of unfrozen water content prediction proposed by Banin and Anderson (1974) and modified by Patterson and Smith appears to be invalid for high soil salinities since the predicted unfrozen water content is much lower than the measured unfrozen water content. The use of time-domain reflectometry shows great promise in the determination of unfrozen water content for saline frozen soils, since it is a simple method which gives reliable values of the unfrozen water content. The problems mentioned in the literature about loss of resolution with an increase in salinity have been circumvented by an appropriate choice of transmission line length of 80 to 100 mm. The author experienced problems with the TDR method only at a temperature of -1°C and salinity of 30 ppt, conditions where the soil is unfrozen. At this point the definition of the reflection point posed problems. For non-plastic soils containing fines, the author believes that the measurement of the unfrozen water content should be conducted using the TDR method.

The deformation behaviour of frozen saline soils w as shown to be influenced drastically by the presence of fines in the soil. The sand, Soil A, behaved like a brittle material showing loss of resistance after reaching peak strength. The presence of fines in the frozen soil modified the stress-strain behaviour. Soils B and C displayed a strain strengthening behaviour with an initial yield point corresponding with the onset of failure of the ice matrix. As stated in Chapter 6, the difference in behaviour between Soil A and

Soils B and C is believed to be caused by a difference in the unfrozen water distribution. In coarse-grained soils, the ice is in direct contact with the soil grains, as opposed to the unfrozen water being in contact with the fine-grained soil grains.

Density had some influence on the strength of Soil B. An increase of 5% in total density caused a 30% increase in the 10% strength . Yield strength appears independent of density for values greater than 2.0 Mg/m^3 or moisture content less than 19%. However, the yield strength increased for high moisture content or low densities. More study is needed to confirm the important influence that density has on the strength.

The influence of temperature on the unconfined compressive strength of frozen saline soils followed a power law. For each soil, a unique equation could be established to model the behaviour for all salinities except 30 ppt. At high salinities, the effect of temperature has more impact on the variation of unfrozen water content with temperature. A new approach to correlate strength and temperature was investigated. The normalized strength, R, defined as the ratio of strength at a given temperature and salinity to the strength at 0 salinity for the same temperature, proved to be nearly constant with respect to temperature for a given soil at a given salinity. R decreased with an increase in salinity. The method of strength prediction for sands proposed by Stuckert and Mahar was shown to overpredict strength for soils with salinities larger than 5 ppt using their equation for ice strength. Their approach appears valid when ice strengths from the literature were used in their model.

The secant modulus is also a function of temperature and salinity. It follows a relationship similar to that developed for strength. The secant modulus was also shown to decrease following a power law with an increase in unfrozen water content despite a wide scatter in the data.

The combined effect of temperature and salinity on strength was investigated by considering the variation of strength with unfrozen water content. The strength was shown to decrease with an increase in unfrozen water content following a power law. For a given soil type, good correlation between strength and unfrozen water content were obtained. However, using the concept of corrected unfrozen water content, it was shown that unfrozen water content is not a unifying parameter for all soils, i.e. the relationship between soil strength and unfrozen water content depends on the soil type. This conclusion seems reasonable since the soil mineralogy, structure and fabric should definitely affect the frozen soil strength if a dense packing is achieved, as it was the case for the studied soils.

The approach proposed by Pharr and Merwin (1985) to predict strength based on ice mechanics was considered by using the ratio R as the strength ratio and measured unfrozen water content as brine content. This comparison showed that the direct relationship between strength and unfrozen water content relationships was better than the relationships proposed by Pharr and Merwin (1985).

The time dependent response of the three soils studied followed the minimum strain rate theory and not the secondary steady-state theory. Three methods of time dependent deformations were investigated as possible tools for predicting the creep behaviour of saline frozen soils. The method proposed by Vyalov (1988) based on the hardening theory was shown to be inappropriate for Soils B and C, and fairly poor for Soil A. Methods by Sayles (1968) and Gardener et al. (1984) predictes the creep strains well at least up to the time of the onset of failure. Using a stress exponent of 3, when applying a flow law similar to that of ice to correlate minimum strain rate and stress, is not valid for the soils studied.

The dependency of the creep parameters from the creep models to salinity or unfrozen water content was then investigated. Sayles' M time exponent was shown to be practically independent of stress (except for Soil A 0 ppt). This difference between Soil A 0 ppt and all the other soils was explained by the complete absence of unfrozen water in Soil A 0 ppt which causes a different mode of deformation. M was also shown to be independent of salinity for low to medium salinities (0 to 10 ppt). For a salinity of 30 ppt, the value of M was higher than the average value for the other salinities The strain rate after 1 hour and the strain after 1 hour were both shown to be functions of stress and salinity (or unfrozen water content) following equation 6.15 and 6.18. The strain rate and strain after 1 hour both increase with an increase in applied stress and an increase in salinity.

The minimum strain rate for a stress of 1 000 kPa, which was given by the parameter B from the ice flow law, was shown to increase with an increase in salinity or unfrozen water content following a power law (Equation 6.19). The stress exponent, n, can be considered constant for the coarse-grained soil, Soil A, and is a function of salinity or unfrozen water content for Soils B and C (Equation 6.21).

Gardener's time exponent c was shown to be practically independent of stress and salinity for low to medium salinities (0 to 10 ppt). The time to failure for a stress of 1 000 kPa, the K value, was shown to decrease with an increase in salinity or unfrozen water content following a power law.

An attempt was made to predict the creep strain rate vs strain relationship found in the literature for Ottawa sand at a salinity of 32 ppt. Two observations were made; first, the investigated models can not predict the development of strains during the tertiary creep period; and secondly, the equations developed have to be used for stresses in the same range as the studied applied stresses. Additional work is needed to try to fit more results using the equations developed in this study. No strain vs time data were available in the literature for comparison.

For the soils studied, correspondence between constant strain rate tests and constant stress tests can not be established. The author believes that the stress path and accumulated strains affect failure in frictional materials.

The ultimate strength predicted by Vyalov's 1963 equation was shown to predict a long-term strength for frozen saline soils which is dependent on salinity. This conflicts with the initial assumption that the long-term strength should be independent on salinity since it is a function of the unfrozen resistance. However, since Vyalov's equation shows a variation of long-term strength with salinity, the equation could be used in practice to predict the 30 year strength as an upper bound on the strength for the stability criteria.

7.2. PRACTICAL IMPLICATIONS OF THE RESULTS

Results from this study will help designers who work in saline permafrost environment or in ground freezing of soils of marine origin. The database presented in Chapter 2 is a valuable source of information for preliminary design, since it provides information about soil salinity for communities of the Canadian Arctic.

The proposed method for the determination of unfrozen water content will significantly reduce the number of required direct measurements of unfrozen water content, since the phase composition of a given soil at any salinity can be deduced from the phase composition curve based on experimental measurements of unfrozen water content of the same non-saline soil.

A prediction of strength, deformation modulus, and time dependent behaviour can be made using a limited number of experimental tests since correlations are presented between the mechanical properties and unfrozen water content for each soil. Such results can be used in analytical or numerical predictions of stresses and deformation required in foundation design or ice loads calculations.

Each method investigated to predict time dependent deformations of saline frozen soils has its particular field of application. Since Sayles' (1968) method was shown to be able to predict the beginning of the strain-time curve, this approach should be used for foundation design where limiting the deformations is the prime concern. Gardener et al.'s (1984) method would be used more efficiently to predict time or strain rate at failure, since it does not predict the initial strains with great accuracy.

Finally, the author believes that the concept of ultimate or long-term strength should be abandoned. Instead a strain to failure criteria should be used, and an acceptable stress level to reach the critical strain within a given time should be calculated. If the long-term strength concept has to be used, the author suggests to use the strength of the unfrozen soil especially for highly saline materials or long design life.

7.3. RECOMMENDATIONS FOR FUTURE WORK

The study of the distribution of salinity and the resulting database should be continuously updated as more information in saline permafrost environment becomes available. As more data are available, the understanding of the origin of saline permafrost will be improved since a better correlation between soil origin and salinity will be possible. The author hopes that a greater effort will be made to measure salinity systematically as part of the standard site investigation procedure in northern regions. Moreover, the ionic composition of the pore fluid should be investigated since the type of salts present greatly influences the freezing point depression and the phase composition curve.

Since it has been shown that mechanical properties can be correlated to unfrozen water content, more research is needed on the development of methods for field determination of unfrozen water content. The time-domain reflectometry method has been used in the field, but more experience is needed to prove its reliability. Also a new piece of equipment called the Variable Frequency Capacitancemeter shows some promise and its use should be investigated from an engineering perspective.

The influence of strain rate and confining pressure were not investigated in this study. Some previous results show a dependence of the strength on strain rate and confining pressure for frozen saline sands. Further investigation should be carried out to understand the influence of these on the strength. Moreover, a strain rate vs strength relationship could be compared to a strain rate vs applied stress from constant stress tests relationship, to further study the correlation between constant strain rate tests and constant stress tests for these materi[illegible]

The creep testing was conducted at only one temperature. Temperature has an important influence on the creep process and should be investigated further . Moreover, extending the temperature range of creep tests will allow for verification of the dependency of the creep parameters on unfrozen water content.

Few field studies on the behaviour of saline permafrost have been presented in the literature. The results from this research should be used to analyze field records of bearing capacity or adfreeze strength. Some research presently underway at the University of Alberta may partially fill this gap in the literature (Biggar, 1991).

An increase in salinity could have one beneficial effect on the behaviour of frozen soils: frost heave. Additional research should be carried out in the possible use of salt injection to improve the behaviour of frost susceptible soils, which can cause serious damage to infrastructures.

Finally, no consideration was given to purely cohesive frozen materials. The influence of their mineralogy on the unfrozen water content has been widely studied in the literature. However, available data on the mechanical behaviour of frozen saline fine-grained soils are very sparse. More work on the mechanical behaviour of these soils will allow confirmation of the dependency of strength and time dependent deformation on the unfrozen water content.

8. BIBILIOGRAPHY

Aas, G., 1980. Laboratory determination of strength properties of frozen salt marine clay. Proceedings, 2nd International Symposium on Ground Freezing, Trondheim, Norway, 144-156.

Akimow, Y.P. et al., 1983. The physicochemical nature of the formation of unfrozen water in frozen soils. Proceedings, 4th International Permafrost Conference, Soviet Contribution, Fairbanks, Alaska,USA, 195-199.

Andersland, O.B. and AlNouri , I., 1970. Time-dependent strength behavior of frozen soils. Journal of Soil Mechanics and Foundation Division, ASCE, **96**, SM4, 1249-1265.

Andersland, O.B., 1963. Physicomechanical properties of frozen soils. Discussion of Session 6, Proceedings, 1st International Permafrost Conference, Lafayette, Indiana, USA, 338-342.

Anderson, D.M., 1967. The interface between ice and silicate surfaces. Journal of Colloid and Interface Science, **25**, 174-191.

Anderson, D.M., 1967. Ice nucleation and the substrate-ice interface. Nature, **216**, 563-566.

Anderson, D.M. and Hoekstra, P., 1965. Migration of inter-lamellar water during freezing and thawing of Wyoming bentonite. Proceedings, Soil Science Society of America, **29**, 498-504.

Anderson, D.M. and Morgenstern, N.R., 1973. Physics, chemistry and mechanics of frozen ground: a review. Proceedings, 2nd International Permafrost Conference, North American Contribution, Yakutsk, USSR, 257-288.

Anderson, D.M. and Tice, A.R., 1980. Low temperature phase changes in montmorillonite and nontronite at high water contents and high salt contents. Cold Regions Science and Technology, **3**, 139-144.

Anderson, D.M. and Tice, A.R., 1973. The unfrozen interfacial phase in frozen soil water systems. Ecological Studies, **4** , 107-124.

Anderson, D.M. and Tice, A.R., 1972. Predicting unfrozen water contents in frozen soils from surface area measurements. Highway Research Record, **393**, 12-18.

Anderson, D.M. and Tice, A.R., 1971. Low-temperature phases of interfacial water in clay-water systems. Proceedings, Soil Science Society of America, **35**, 47-54.

Andrews, J.T., 1989. Quaternary geology of the northeastern Canadian Shield; in Chapter 3 of **Quaternary Geology of Canada and Greenland**, R.J. Fulton (Ed.); Geological Survey of Canada.

Assur, A., 1980. Some promising trends in ice mechanics. in *Physics and Mechanics of Ice*, International Union of Theoretical and Applied Mechanics Symposium, Copenhagen, August 6-10, 1979. P. Tryde (ed.), Springer-Verlag, Berlin and Heidelberg, 1-15.

Assur, A. 1958. Composition of sea ice and its tensile strength. Arctic sea ice. Washington, D.C., National Academy of Sciences-National Research Council Publication no. 598, 106-138.

Assur, A. and Weeks, U.F., 1964. Growth, structure and strength of sea ice. U.S. Army CRREL Research Report 135, 19p.

ASTM, Annual Book of ASTM Standars. © 1986, American Society for Testing and Materials.

Azizi, F., 1989. Primary creep of polycrystalline ice under constant stress. Cold Regions Science and Technology, **16**, 159-165.

Baker, G.C. and Osterkanp, T.E., 1988. Salt Redistribution during laboratory freezing of saline sand columns. Proceedings, 5th International Symposium on Ground Freezing, Nottingham, UK, 29-33.

Baker, T.H.W. and Kurfurst, P.J., 1985 Accoustic and mechanical properties of frozen sand. Proceedings, 4th International Symposium on Ground Freezing, **1**, Sapporo, Japan, 227-234.

Baker, T.H.W. , Jones, S.J. and Parameswaran, V.R., 1981. Confined and unconfined compression tests on frozen sands. Proceedings, 4th Canadian Permafrost Conference, Calgary, Alberta, Canada, 387-393.

Baker, T.H.W., 1979. Strain rate effect on the compressive strength of frozen sand. Engineering Geology, **13**, 223-231.

Banin, A. and Anderson, D.M., 1974. Effects of salt concentration changes during freezing on the unfrozen water content of porous materials. Water Resources Research, **10** (1), 124-128.

Barnes, P., Tabor, D. and Walker, J.C.F., 1971. The friction and creep of polycrystalline ice. Proceedings, Royal Society of London, **324 A**, 127-155.

Berggren, A.-L. and Furuberg, T., 1985. A new Norwegian creep model and creep equipment. Proceedings, 4th International Symposium on Ground Freezing, **1**, Sapporo, Japan, 181-185.

Biggar, K.W., 1991. Adfreeze and grouted piles in saline permafrost. Ph.D. Thesis, University of Alberta, Edmonton, Alberta. (in preparation).

Bishop, A.W. and Henkel, D.J. **The measurement of soil properties in the triaxial test**. © 1962, 2nd edition, Edward Arnold (Publishers) Ltd, London, 228p.

Black, P.B., 1990. Three fucnctions that model empirically measured unfrozen water content data and predict relative hydraulic conductivity. U.S. Army CRREL Report 90-5. 7 p.

Black, P.B., 1989. On the use of the ϕ-variable to describe the state of water in porous media. U.S. Army CRREL Report 89-3. 7 p.

Bottraud, J.-C. and Rhoades, J.D., 1985. Referencing water content effects on soil electrical conductivity-salinity calibrations. Journal of Soil Science Society of America, **49** (6), 1579-1581.

Bouyoucos, G.J. and McCool, M.M., 1916. Further studies on the freezing point lowering of soils. Michigan Agriculture Experimental Station Technical Bulletin, no. 31. 51p.

Cannell, G.H. and Gardner, W.H., 1959. Freezing-point depression in stabilized soil aggregates, synthetic soil and quartz sand. Proceedings, Soil Science Society of America, **23**, 418-422.

Cary, J.W. and Mayland, H.F., 1972. Salt and water movement in unsaturated frozen soil. Proceedings, Soil Science Society of America, **36**, 549-555.

Chamberlain, E.J., 1983. Frost heave of saline soils. Proceedings, 4th International Conference on Permafrost, Fairbanks, Alaska, USA, 121-126.

Chen, C.S. and Nagy, S., 1987. Prediction and correlation of freezing point depression of aqueaous solutions. Transactions ASAE, **30** (4), 1176-1180.

Chen, X.B. et al., 1980. On salt heave of saline soil. Proceedings, 5th International Symposium on Ground Freezing, Nottiongham, UK, 35-39.

Cheung, C.H., 1979. Influence of salt on the unfrozen water inf frozen clays. Ph. D. Thesis McGill University.

Chipman, R.A. **Transmission Lines**. © 1968, Shaum's Outline Series, McGraw-Hill Book Company, 236p.

Colbeck, S., 1981. Introduction to the basic thermodynamics of cold capillary systems. U.S. Army CRREL Report 81-6. 9p.

Colbeck, S., 1982. Configuration of ice in frozen media. Soil Science, **133** (2), 116-123.

Colbeck, S., 1985. A technique for observing freezing fronts. Soil Science, **139** (1), 13-20.

Cole, D.M. , 1983. The relationship between creep and strength behavior of ice at failure. Cold Regions Science and Technology, **8**, 189-197.

Cole, D.M., 1983. The effect of stress application rate on the creep behavior of polycrystalline ice. Journal of Energy Resources Technology, ASME, **105**, 454-459.

Cox, G.F.N. and Weeks, W.F., 1983. Equations for determinig the gas and brine volumes in sea ice samples. Journal of Glaciology, **29** (102), 306-316.

Cox, G.F.N., Richter-Menge, J.A., Weeks, W.F., Bosworth, H. Perron, N., Mellor, M. and Durell, G., 1985. Mechanical properties of multi-year sea ice. Phase II: Test results. U.S. Army CRREL Report 85-16. 81p.

Cruden, D.M. and Thomson, S. Exercises in terrain analysis. © 1987, Pica Pica Press, Edmonton, Alberta, Canada. 185p.

Dalton, F.N. and Van Genuchten , M., 1986. The time-domain reflectometry method for measuring soil water content and salinity. Geoderma, **38**, 237-250.

Dasberg, S. and Dalton, F.N., 1985. Time-domain reflectometry field measurements of soil water content and electrical conductivity. Journal of Soil Science Society of America, **49**, 293-297.

Davis, J.L. and Annan, A.P., 1977. Electromagnetic detection of soil moisture: Progress report I. Canadian Journal of Remote Sensing, **3** (1), 76-86.

Dillon, H.B. and Andersland, O.B., 1966. Predicting unfrozen water contents in frozen soils. Canadian Geotechnical Journal, **3** (2), 53-60.

Domaschuk, K.L., Man, C.S., Shields, D.H. and Yong, E., 1983. Creep behavior of frozen saline silt under istropic compression. Proceedings, 4th International Conferenceon Permafrost, Fairbanks, Alaska, USA, 238-243.

Dubikov, G.I., Ivanova, N.V. and Aksenov, V.I., 1988. Pore solutions of frozen ground and its properties. Proceedings, 5th International Conference on Permafrost, Trondhein, Norway, **1**, 333-338.

Dyke, A.S., and Dredge, L.A., 1989. Quaternary Geology of the northwestern Canadian Shield; in Chapter 3 of **Quaternary Geology of Canada and Greenland**, R.J. Fulton (Ed.); Geological Survey of Canada.

Dyke, A.S., and Prest, V.K., 1987. Late Wisconsin and Holocene history of the Laurentide Ice Sheet, Géographie Physique et Quaternaire, **XLI**, 2, 237 - 263.

Dyke, A.S., Andrews, J.T. and Miller, G.H., 1982. Quaternary geology of Cumberland Peninsula, Baffin Island District of Franklin. Memoir 403, Geological Survey of Canada, Department of Energy, Mines and Resources, Ottawa.

Dyke, A.S., Vincent, J.-S., Andrews, J.T., Dredge, L.A. and Cowan, W.R., 1989. The Laurentide ice sheet and an introduction to the Quaternary geology of the Canadian Shield; in Chapter 3 of **Quaternary Geology of Canada and Greenland**, R.J. Fulton (Ed.); Geological Survey of Canada.

Ersoy, T. and Torgrol, E., 1978. Temperature and strain rate effects on the strength of compacted frozen silty clay. Proceedings, 3rd International Conference on Permafrost, Edmonton, Alberta, Canada, **1**, 642-647.

Farouki, O.T., 1982. Thermal properties of soils relevant to ground freezing. Design techniques for their estimation. 3rd. International Symposium on Ground Freezing, Hanover, New Hampshire, USA, 139-146.

Farouki, O.T., 1981. Thermal properties of soils. U.S. Army CRREl Monograph 91-1, 136 p.

Fish, A.M., 1987. Shape of creep curves in frozen soils and polycrystalline ice. Canadian Geotechnical Journal, **24**, 623-629.

Fish, A.M., 1985. Creep strength, strain rate,temperature and unfrozen water relationship in frozen soil. Proceedings, 4th International Symposium on Ground Freezing, Sapporo, **2**, 29-36.

Fish, A.M., 1984. Thermodynamic model of creep at constant stress and constant strain rate. Cold Regions Science and Technology, **45**, 143-161.

Fish, A.M., 1983. Thermodynamic model of creep at constant stress and constant strain rates. U.S. Army CRREL Report 83-33. 18 p.

Fish, A.M., 1982. Comparative analysis of USSR construction codes and the U.S. Army technical manual for design of foundations on permafrost. U.S. Army CRREL Report 82-14. 20p.

Forbes, D.L., 1980. Late Quaternary sea levels in the Southern Beaufort Sea, in Current Research, Part B, Geological Survey of Canada, Paper 80 - 1B, 75 - 87.

Frolov, A.D. and Gusev, B.V., 1973. Dielectric method of determining the unfrozen water content in frozen sandy-clay soils. Proceedings, 2nd International Conference on Permafrost, Soviet contribution, Yakutsk, USSR, 356-358.

Furuberg, T. and Berggren, A.-L., 1988. Mechanical properties of frozen saline clays. Proceedings,5th International Conference on Permafrost, Trondheim, Norway, **2**, 1078-1084.

Gardner, A.R.,Jones, R.H. and Harris, J.S., 1984. A new creep equation for frozen soils and ice. Cold Regions Science and Technology, **9**, 271-275.

Gardner, A.R., Jones, R.H. and Harris, J.S., 1982. Strength and creep testing of frozen soils. Proceedings, 3rd International Symposium on Ground Freezing, Hanover, New Hampshire, USA, 53-60.

Geological Survey of Canada, 1978. Surficial geology and geomorphology of Fort Simpson, District of Mackenzie, Map 3 - 1978.

Geological Survey of Canada, 1979. Surficial geology of Mackenzie Delta, District of Mackenzie, Map 32 - 1979.

Geological Survey of Canada, 1980. Surficial Geology of Eskimo Point, District of Keewatin, Map 8 - 1980.

Gilpin, R.R., 1980. A model for the prediction of ice lensing and frost heave in soils. Water Resources Research, **16**, 918-930.

Glen, J.W., 1975. The mechanics of ice. U.S. Army CRREL Monograph II-C2 b, 43p.

Glen, J.W., 1955. The creep of polycrystalline ice. Proceedings, Royal Society of London, **228 A**, 519-538.

Golubev, V.N., 1973. Ice structure as a function of salintiy of the freezing water. Proceedings, 2nd International Conference on Permafrost, Soviet contribution, Yakutsk, USSR, 327-330.

Goughnour, R.R. and Andersland, O.B., 1968. Mechanical properties of sand-ice system. Journal Soil Mechanics and Foundation Division, ASCE, **94**, SM 4, 923-950.

Gregersen, O. et al., 1983 Engineering properties and fourndation alternatives in marine Svea Clay, Svalbard. Proceedings, 4th International Conference on Permafrost, Fairbanks, Alaska, USA, 384-388.

Gupta, S.C. and Hanks, R.J., 1972. Influence of water content on electrical conductivity of the soil . Proceedings, Soil Science Society of America, **36** (6), 855-857.

Hallet, B., 1978. Solute redistribution in freezing ground. Proceedings, 3rd International Conference on Permafrost, Edmonton, Alberta, Canada, **1**, 85-91.

Handbook of Chemistry and Physics. 69th edition, © 1988-1989, CRC Press, Boca Raton, Florida.

Hayhoe, H.N. and Balchin, D., 1988. Time-domain reflectometry and electrical conductance measurements during seasonal soil frost. Cold Regions Science and Technology, **15**, 195-200.

Hayhoe, H.N. and Balchin, D., 1986. Electrical determination for soil frost. Canadian Agricultural Engineering, **28** (2), 77-80.

Haynes J.M., 1975. Discussion about the freezing point depression in small pores. Fondation Française d'Etude Nordiques, Actes et Documents, **6**, 234-236.

Hill, P.R., Mudie, P.J., Moran, K. and Blasco, S.M., 1985. A sea - level curve for the Canadian Beaufort shelf. Canadian Journal of Earth Sciences, **22**, 1383 - 1393.

Hoekstra, P., 1969. The physics and chemistry of frozen soils. Higway Research Board Special Report 103, 78-90.

Hoekstra, P. and Delaney, A., 1974. Dielectric properties of soil at UHF and microwave frequencies. Journal of Geophysics Research, **79**, 1699-1708.

Hodgson, D.A. and Haselton, G.M. (1974). Reconnaissance Glacial Geology, Northeast Baffin Island. Paper 74-20, Geological Survey of Canada, Department of Energy, Mines and Ressources.

Horiguchi, K., 1987. An osmotic model for soil freezing. Cold Regions Science and Technology, **14**, 13-22.

Horiguchi, K., 1985. Determination of unfrozen water content by DSC. Proceedings, 4th International Symposium on Ground Freezing, Sapporo, Japan, 33-38.

Hult, J.A.H. **Creep in Engineering Structures.** © 1966, Blaisedell Publishing Company, Waltham, Massachusetts. 115 p.

Inaba, H., 1983. Heat transfer behavior of frozen soils. Transactions ASME, **105**, 680-683.

Iwata, S., 1985. A mechanism for the existence of an unfrozen liquid in the vicinity of a solid surface. Proceedings, 4th International Symposium on Ground Freezing, Sapporo, Japan, 25-31.

Jacka, T.H., 1984. The time and strain required for development of minimum strain rates in ice. Cold Regions Science and Technology, **8**, 261-268.

Jessberger, H.L. and Jordan, P., 1982. Frozen saline sand subjected to dynamic loads. Proceedings, 3rd International Symposium on Ground Freezing, Hanover, New Hampshire, USA, 19-25.

Kay, B.D. and and Groenevelt, P.H., 1983. The redistribution of solutes in freezing soil: Exclusion of solutes. Proceedings, 4th International Conferenceon Permafrost, Fairbanks, Alaska, USA, 584-588.

Kay, B.D. and Groenevelt, P.H., 1974. On the interaction of water and heat transport in frozen and unfrozen soils: I. Basic Theory; the vapor phase. Proceedings, Soil Science Society of America, **38**, 395-400.

Kay, B.D. and Perfect, E., 1988. State of the art: Heat and mass transfer in freezing soils. Proceedings, 5th International Symposium on Ground Freezing, Nottingham, UK, 3-21.

Keune, R. and Hoekstra, P., 1967. Calculating the amount of unfrozen water in frozen ground from moisture characteristic curves. U.S. Army CRREL Special Report 114. 7 p.

Kinosita, S. and Ishizaki, T., 1980. Freezing point depression in moist soil. Proceedings, 2nd International Symposium on Ground Freezing, Trondheim, Norway, 640-646.

Koopmans, R.W.R. and Miller, R.D., 1966. Soil freezing and soil water characteristic curves. Proceedings, Soil Science Society of America, **30**, 680-685.

Ladanyi, B., 1981. Shear-induced stresses in the pore ice in frozen particular materials. Proceedings, Symposium on Free Boundary Problems. Research Notes in Mathematics, no. 78, Pitman Books Ltd. II, 549-560.

Ladanyi, B., 1972. An engineering theory of creep of frozen soils. Canadian Geotechnical Journal, **9**, 63-80.

Ladanyi, B. and Morel, J.-F., 1988. Effect of internal confinement on compression strength of frozen sand. Candadian Geotechnical Journal, **27**, 8-18.

Ladanyi, B. and Arteau, J., 1979. Effect of specimen shape on creep response of frozen sand. Engineering Geology, **13**, 207-222.

Lade, P.V., Jessberger, H.L. and Diekmann, N., 1980. Stress-strain and volumetric behavior of frozen soil. Proceedings, 2nd International Symposium on Ground Freezing, Trondhein, Norway, 48-64.

Lange, G.R. and McKim, H.L., 1963. Saturation, phase composition and freezing-point depression in a rigid soil model. Proceedings, 1st International Conference on Permafrost, Lafayette, Indiana, USA, 187-192.

Lebedenko, Y.P. and Shevchenko, L.V., 1988 Cryogenic deformations in fine-grained soils. Proceedings, 5th International Conference on Permafrost, **1**, Trondhein, Norway, 396-400.

Lee, H.A., 1962. Method of deglaciation, age and submergence, and rate of uplift west and east of Hudson Bay, Canada. Biuletyn Peryglacjalny, **11**, 239-245.

Loch, J.P.G., 1979. Thermodynamic equilibrium between ice and water in porous media. NGI Publication no. 125, 1-4.

Loch, J.P.G. and Kay, B.D., 1978 Water redistribution in partially frozen saturated silt under several temperature gradients and overburden loads. Journal Soil Science Society of America, **42**, 400-406.

Lovell, C.W., 1957. Temperature effects on phase composition and strength of partially-frozen soil. Highway Research Board, Bulletin 168, 74-95.

Low, P.F., Anderson, D.M. and Hoekstra, P., 1968 Some thermodynamic relationships for soils at or below the freezing point: 1. Freezing point depression and heat capacity. Water Resources Research, **4** (2), 379-394.

Low, P.F., Hoekstra, P. and Anderson, D.M., 1967 Some thermodynamic relationships for soils at or below the freezing point: 2. Effects of temperature and pressure on unfrozen soil water. U.S. Army CRREL Research Report 222. 5 p.

Low, P.F. and Lovell, C.W., 1959. The factor of moisture in frost action. Highway Research Board Bulletin, **225**, 23-44.

Lunardini, V.J., 1988. Effect of variable thermal properties on freezing with an unfrozen water content. Proceedings, 5th International Conference on Permafrost, **2**, Trondheim, Norway, 1127-1132.

Mahar, L., Wilson, R. and Vinson, T., 1983 Physical and numerical modeling of uniaxial freezing in a saline gravel. Proceedings, 4th International Conference on Permafrost, Fairbanks, Alaska, USA, 773-778.

Makkonen, L. and Lehmus, E., 1987. Studies on adhesion strength of saline ice. Proceedings, 9th International Conference on Port and Ocean Engineering Under Arctic Conditions, Fairbanks, Alaska, USA, 45-55.

Mayer, E., 1987. Non-freezing water in simple salt solutions. Chemical Physics Letters, **139**, 370-374.

McGaw, R.W. and Tice, A.R., 1976. A simple procedure to calculate the volume of water remaining unfrozen in a freezing soil. Proceedings, 2nd Conference on Soil-Water Problems in Cold Regions, Edmonton, Alberta, Canada, 114-122.

McRoberts, E.C., 1988. Secondary creep interpretations of ice rich permafrost-Secondary creep, Permafrost Soils, Creep of ice. Proceedings, 5th International Conference on Permafrost, **2**, Trondheim, Norway, 1137-1142.

McRoberts, E.C., Law, T.C. and Murray, T.K., 1978. Creep test on undisturbed ice-rich silt. Proceedings, 3rd International Conference on Permafrost, Edmonton, Alberta, Canada, **1**, 539-545.

Mellor, M., 1983. Mechanical behavior of sea ice. U.S. Army CRREL monograph 83-1. 105p.

Mellor, M. and Cole, D.M., 1983. Stress/strain/time relations for ice under uniaxial compression. Cold Regions science and Technology, **6**, 207-230.

Mellor, M. and Cole, D.M., 1982. Deformation and failure of ice under constant stress or constant strain-rate. Cold Regions science and Technology, **5**, 201-219.

Mellor, M., 1979. Mechanical properties of polycrystalline ice; in Physics and Mechanics of Ice, International Union of Theoretical and Applied Mechanics Symposium, Copenhagen, 217-245.

Mel'nichenko, N.A., Mekhaylov, V.I. and Chizhik, V.I., 1979. Studies of the temperature-dependence of the brine content of sea ice by the pulse NMR method. U.S. Army U.S. Army CRREL Draft translation 757. 6 p.

Miller, R.D. Freezing phenomena is soils in **Application of Soil Physics.** © 1980, Daniel Hillel editor, Academic Press. , 254-299.

Miller, R.D., 1980. The adsorbed film controversy. Cold Regions Science and Technology, **3**, 83-86.

Morgenstern, N.R., 1988. Recent observations on the deformation of ice and ice-rich permafrost. J. Ross Mackay Symposium Volume, Edited by M. Church and O. Slaymaker, UBC press, in press. 133-153.

Morgenstern, N.R., Roggensack, W.D. and Weaver, J.S., 1980. The behaviour of friction piles in ice and ice-rich soils. Canadian Geotechnical Journal, **17**, 405-415.

Morland, L.W., 1981. Viscoelastic fluid relation for the deformation of ice. Cold Regions science and Technology, **4**, 255-268.

Morland, L.W., 1979. Constitutive laws for ice. Cold Regions science and Technology, **1**, 101-108.

Murrmann, R.P., 1973. Ionic mobility in permafrost. Proceedings, 2nd International Conference on Permafrost, North American Contribution, Yakutsk, USSR, 352-359.

Nakano, Y., Tice, A.R., Oliphant, J.L. and Jenkins, T.K., 1983. Soil-water diffusivity of unsaturated soils at subzero temperatures. Proceedings, 4th International Conference on Permafrost, Fairbanks, Alaska, USA, 889-893.

Nawwar, A.M., Nadreau, J.P. and Wang, Y.S., 1983. Triaxial compressive strength of saline ice. Proceedings, 7th International Conference on Port and Ocean Engineering under Arctic Conditions, Espoo, Finland, 193-202.

Nerseova, Z.A. and Tsytovich, N.A., 1963. Unfrozen water in frozen soils. Proceedings, 1st International Conferenceon Permafrost, Lafayette, Indiana, USA, 230-234.

Neukirchner, R.J., 1985. Pile Creep Designs for frozen layered profiles. Proceedings, of Conference Arctic 85: Civil Engineering in the Arctic Offshore, San Francisco, California, USA, 1103-1111.

Neukirchner, R.J. and Nyman, K.J., 1985. Creep rate analysis of pile load test data. Proceedings, of Conference Arctic 85: Civil Engineering in the Arctic Offshore, San Francisco, California, USA, 1112-1121.

Nixon, J.F., 1988. Pile load tests in saline permafrost at Clyde River, Northwest Territories. Canadian Geotechnical Journal, **25**, 24-32.

Nixon, J.F., 1978. Foundation design approaches in permafrost areas. Canadian Geotechnical Journal, **15**, 96-112.

Nixon, J.F. and Lem, G., 1984. Creep and strength testing of frozen saline fine-grained soils. Canadian Geotechnical Journal, **21**, 518-529.

Nixon, J.F. and McRoberts, E.C., 1976. A design approach for pile foundations in permafrost. Canadian Geotechnical Journal, 13, 40-57.

Nixon, J.F. and Neukirchner, R.J., 1984. Design of vertical and laterally loaded piles in saline permafrost. Proceedings, Cold Regions Engineering Specialty Conference, Edmonton, Alberta, Canada, 131-144.

Nixon, M.S. and Pharr, G.M. 1984 The effects of temperature, stress and salinity on the creep of frozen saline soil. Transactions of the ASME Journal of Energy Resources Technology, **106**, 344-348.

Odqvist, F.K. **Mathematical Theory of Creep and Creep Rupture.** © 1966, Oxford University Press, London, 168p.

Ogata, N., Yasuda, M. and Kataoka, T., 1983. Effects of salt concentration on strength and creep behaviour of artifically frozen soils. Cold Regions Science and Technology, **8**, 139-153.

Oliphant, J. and Tice, A.R., 1982. Comparison ou unfrozen water contents measured by DSC and NMR. Proceedings, 3rd International Symposium on Ground Freezing, Hanover, New Hampshire, USA, 115-121.

Orth, W., 1988. A creep formula for practical application based on crystal mechanics. Proceedings, 5th International Symposium on Ground Freezing, Nottingham, UK, 205-211.

Orth, W., 1985. Deformation behaviour of frozen sand and its physical interpretation. Proc 4th International Symposium on Ground Freezing, Sapporo, Japan, 245-253.

Orth, W. and Meibner, H., 1982. Long-term creep of frozen soil in uniaxial and triaxial test. Proceedings, 3rd International Symposium on Ground Freezing, Hanover, New Hampshire, USA, 81-87.

Osterkamp, T.E., 1987. Freezing and thawing of soils and permafrost containing unfrozen water or brine. Water Resources Research, **23** (12), 2279-2285.

Pandit, B. I. and King, M.S., 1978. Influence of pore fluid salinity on seismic and electrical properties of rocks at permafrost temperatures. Proceedings, 3rd International Conference on Permafrost, **1**, Lafayette, Indiana, USA, 553-559.

Parameswaran, V.R., 1986. Bearing capacity calculations for piles in permafrost. Proceedings, 4th International Conference on Cold Regions Enginerring, TCCRE, ASCE, Anchorage, Alaska, USA, 751-759.

Parameswaran, V.R., 1980. Deformation behaviour and strength of frozen sand. Canadian Geotechnical Journal, **17**, 74-88.

Patterson, D.E. and Smith, M.W., 1985. Unfrozen water content in saline soils: results using time-domain reflectometry. Canadian Geotechnical Journal, **22**, 95-101.

Patterson, D.E. and Smith, M.W., 1983. Mesasurement of unfrozen water content in saline permafrost using time-domain reflectometry. Proceedings, 4th International Conference on Permafrost, Fairbanks, Alaska, USA, 968-972.

Patterson, D.E. and Smith, M.W., 1981. The measurement of unfrozen water content by time-domain reflectometry: results from laboratory tests. Canadian Geotechnical Journal, **18**, 131-144.

Perkins, T.K. and Ruedrich, R.A., 1974. A study of factors influencing the mechanical properties of deep permafrost. Journal of Petroleum Technology, **26**, 1167-1177.

Pharr, G.M. and Godavarti, P.S., 1987. A comparison of the creep behavior of saline ice and frozen saline Ottawa sand at -8°C. Cold Regions Science and Technology, **14**, 273-279.

Pharr, G.M. and Merwin, J.E., 1985. Effects of brine content on the strength of frozen Ottawa sand. Cold Regions Science and Technology, **11**, 205-212.

Rampton, V.N., 1988. Quaternary geology of the Tuktoyaktuk Coastlands, Northwest Territories. Memoir 423, Geological Survey of Canada, Department of Energy, Mines and Resources, Ottawa.

Rampton, V.N., and Bouchard, M., 1975. Surficial geology of Tuktoyaktuk, District of Mackenzie. Paper 74-53, Geological Survey of Canada, Department of Energy, Mines and Resources, Ottawa.

Rein, R.G., 1985. Correspondence of creep data and constant strain-rate data for frozen silt. Cold Regions Science and Technology, **11**, 187-194.

Rein, R.G. and Hathi, V.V., 1978. The effect of stress on strain at the onset of tertiary creep of frozen soil. Canadian Geotechnical Journal, **15**, 424-426.

Rein, R.G., Hathi, V.V. and Sliepcevich, C.M., 1975. Creep of sand-ice system. Journal of Geotechnical Engineering Division, ASCE, **101** (GT2), 115-128.

Rhoades, J.D., 1982. Soluble salts in Methods of Soil Analysis, Part 2: Chemical and Microbiological Properties, Second Edition, Agronomy no. 9, Part 2, American Society of Agronomy, A.L. Page et al, editors.

Rhoades, J.D., Raats, P.A.C. and Prather, R.J., 1976. Effects of liquid-phase electrical conductivity, water content, and surface conductivity on bulk soil electrical conductivity. Journal of Soil Science Society of America, **40**, 651-655.

Roggensack, W.D. and Morgenstern, N.R., 1978. Direct shear tests on natural fine-grained permafrrost soils. Proceedings, 3rd International Conference on Permafrost, Edmonton, Alberta, Canada, 729-735.

Sadovsky, A.V., Maksimyak, R.V. and Razbegin, V.N., 1988. State of the art: Mechanical properties of frozen soils. Proceedings, 5th International Symposium on Ground Freezing, Nottingham, UK, 443-463.

Sarkisyan, R.M., Nersesova, A.Z., Vyalov, S.S. and Zatsarnaya, A.G., 1973. Handbook on the determination of the physical, thermal and mechanical properties of frozen soils. Technical Translation 245, Division of Building Research, National Research Council of Canada, Ottawa, 1983, 202 p.

Savigny, K.W. and Morgenstern, N.R., 1986. Creep behaviour of undisturbed clay permafrost. Canadian Geotechnical Journal, **23**, 515-527.

Sayles, F.H., 1988. State of the art: Mechanical properties of frozen soil. Proceedings, 5th International Symposium on Ground Freezing, Nottingham, UK, 143-165.

Sayles, F.H. and Haines, D., 1974. Creep of frozen silt and clay. U.S. Army CRREL Technical Report 252. 50p.

Sayles, F.H. 1973. Triaxial and creep tests on frozen Ottawa sand. Proceedings, 2nd International Conference on Permafrost, North American Contribution, Yakutsk, USSR, 384-391.

Sayles, F.H., 1968. Creep of frozen sands. U.S. Army CRREL Technical Report 190. 54 p.

Schwarz, J. and Weeks, W.F., 1977. Engineering properties of sea ice. Journal of Glaciology, **19** (81), 499-531.

Sego, D.C., 1980. Deformation of ice under low stresses. Ph. D. thesis, University of Alberta, Edmonton, Alberta, 429p.

Sego, D.C. and Chernenko, D., 1984. Confining pressure influence on the strength of frozen saline sand. Proceedings, Cold Regions Engineering Specialty Conference, Montreal, Quebec, Canada, 565-578.

Sego, D.C., Schultz, T. and Banasch, R., 1982. Strength and deformation behaviour of frozen saline sand. Proceedings, 3rd International Symposium on Ground Freezing, Hanover, New Hampshire, USA, 11-17.

Sego, D.C. and Morgenstern, N.R., 1985. Punch indentation of polycrystalline ice. Canadian Geotechnical Journal, **22**, 226-233.

Sego, D.C. and Morgenstern, N.R., 1983. Deformation of ice under low stresses. Canadian Geotechnical Journal, **20**, 587-602.

Sheeran, D.E. and Yong, R.N., 1975. Water and salt distribution in freezing soils. Proceedings, 1st Conferenceon Soil-Water Problems in Cold Regions, Calgary, Alberta, Canada, 58-69.

Shibata, T., Adachi, T., Yashima, A., Takahashi, T. and Yoshioka, I., 1985. Time-dependence and volumetric change characteristic of frozen sand under triaxial stress condition. Proceedings, 4th International Symposium on Ground Freezing, Sapporo, Japan, 173-179.

Shields, D.H., Domaschuk, L., Man, C.-S. and Kenyon, R.M., 1985. The deformation properties of warm permafrost. ASTM Special Technical Publication 883, 473-486.

Shussherina, E.P. and Bobkov, Y.P., 1969 Effect of moisture content on frozen ground strength. Technical Translation TT-1918, National Research Council of Canada, 8-19.

Smith, G.D. and Morland, L.W., 1981. Viscous relations for the steady creep of polycrystalline ice. Cold Regions science and Technology, **5**, 141-150.

Smith, M.V. and Patterson, D.E., 1980. The measurement of unfrozen water content by time-domain reflectometry. Proceedings, 2nd International Symposium on Ground Freezing, Trondhein, Norway, 383-399.

Smith, M.V. and Patterson, D.E. 1979. An investigation into the use of TDR to determine the unfrozen water content of freezing soils. Earth Physics Branch Open File no. 79-14, Energy, Mines and Ressources, Canada. 37 p.

Smith, M.V. and Tice, A.R., 1988. Measurement of the unfrozen water content of soils. Comparison of NMR and TDR methods. U.S. Army CRREL Report 88-18, 11 p.

Stuckert, B. and Mahar, L., 1984. Role of ice content in the strength of frozen saline coarse grained soils. Proceedings,of Cold Regions Engineering Specialty Conference, Montreal, Quebec, Canada, 579-587.

Takagi, S., 1963. Theory of freezing-point depression with special reference to soil water. Proceedings, 1st International Conference on Permafrost, Lafayette, Indiana, USA, 216-224.

Takagi, S., 1959. Theory of freezing-point depression of soil water and a note on the extra-thermodynamics of soil moisture. Soil Science, **88**, 25-31.

Thurmond, V.L. and Brass, G.W., 1987. Geochemistry of freezing brines-Low-temperature properties of sodium chloride. U.S. Army CRREL Report 87-13. 11p.

Tice, A.R., Black, P.B. and Berg, R.L., 1988. Unfrozen water contents of undisturbed and remolded Alaskan silt as determined by nuclear magnetic resonance. U.S. Army CRREL Report 88-19. 17p.

Tice, A.R., Anderson, D.M. and Sterrett, K.F., 1980. Unfrozen water contents of submarine permafrost determinded by nuclear magnetic resonance. Proceedings, 2nd International Symposium on Ground Freezing, Trondhein, Norway, 400-412.

Tice, A.R., Burrous, C.M. and Anderson, D.M., 1978. Determination of unfrozen water in frozen soil by pulsed magnetic resonance. Proceedings, 3rd International Conference on Permafrost, **1**, Edmonton, Alberta, Canada, 159-155.

Tice, A.R., Burrous, C.M. and Anderson, D.M., 1978. Phase composition measuremnets on soils at very high water contents by the pulsed magnetic resonance technique. Transportation Research Record, **675**, 11-14.

Tice, A.R., Anderson, D.M. and Banin, A., 1976. The prediction of unfrozen water contents in frozen soils from liquid limit determination. U.S. Army CRREL Report 76-8. 9 p.

Ting, J.M., 1983 (a). Tertiary creep model for frozen sands. Journal of the Geotechnical Engineering Division, ASCE, **109** (7), 932-945.

Ting, J.M., 1983 (b). On the nature of the minimum creep rate - time correlation for soil, ice and frozen soil. Canadian Geotechnical Journal, **20**, 176-182.

Ting, J.M., Martin, R.T. and Ladd, C.C., 1983. Mechanisms of strength for frozen sand. Journal of the Geotechnical Engineering Division, ASCE, **109** (10), 1286-1302.

Ting, J.M. and Martin R.T., 1979. Application of the Andrade equation to creep data for ice and frozen soil. Cold Regions science and Technology, **1**, 29-36.

Topp, G.C. and Davis J.L., 1985. Measurement of soil water content using time-domain reflectometry: a field evaluation. Journal of Soil Science Society of America, **49**, 19-24.

Topp, G.C., Davis, J.L. and Annan, A.P., 1982. Electromagnetic determination of soil water content using time-domain reflectometry: I. Applications to wetting fronts and steep gradients. Journal of Soil Science Society of America, **46**, 672-678.

Topp, G.C., Davis, J.L. and Annan, A.P., 1980. Electromagnetic determination of soil water content: measurement in coaxial transmission lines. Water Resources Research, **16** (3), 574-582.

Tsytovich, N.A. The mechanics of frozen ground. McGraw-Hill Book Company, New York, NY. 426p.

Tsytovich, N.A., Kronik, Y.A., Markin, K.F., Aksenov, V.I. and Samuel'son, M.V., 1973. Physical and mechanical properties of saline soils. Proceedings, 2nd International Conference on Permafrost, USSR Contribution, Yakutsk, USSR, 238-247.

Van Loon, W.K.P., Perfect, E., Groenevelt, P.H. and Kay, B.D., 1990. A new method to measure bulk electrical conductivity in soils with time-domain reflectometry. Canadian Journal of Soil Science, in press.

Van Loon, W.K.P., Perfect, E., Groenevelt, P.H. and Kay, B.D., 1990. Application of dispersion theory to time-domain reflectometry in soils. Transport in porous media, in press.

Velli, Y.Y. and Grishin, P.A., 1982. On the functional dependance of the freezing point of soils on the composition of water soluble salts in an interstitial solution. Technical translation 2070, National Research Council of Canada. 8 p.

Velli, Y.Y. , Lenzniiep, Karpunina, A.A., 1973. Saline permafrost as bearing ground for construction.Proceedings, 2nd International Conferenceon Permafrost, USSR Contribution, Yakutsk, USSR, 545-550.

Vershinin, P.V., Deriagin, B.V. and Kirilenko, N.V., 1960. The non-freezing water in soil. Tranlation no. 30, Arctic Construction and Frost Effects Laboratory, U.S. Army, Corps of Engineers. 1-10.

Vincent, J-S., 1989. Quaternary geology of the northeastern Canadian Shield; in Chapter 2 of **Quaternary Geology of Canada and Greenland**, R.J. Fulton (Ed.); Geological Survey of Canada.

Vinogradov, A.M., 1985. Creep properties of ice: theory and experiment. Proceedings, Conference Arctic 85: Civil Engineering in the Arctic Offshore, San Francisco, California, USA, 447-455.

Vinson, T.S. and Sheldon, L.J., 1985. Latent heat of frozen saline coarse grained soil. Journal of Geotechnical Engineering Division, ASCE, **3** (5), 607-623.

Vinson, T.S., Mahar, L.J. and Wilson, R., 1983. Model study of freezing front penetration in offshore granular fill structures. 7th International Conferenceon Port and Ocean Engineering under Arctic Conditions, Helsinki, Finland, 1025-1034.

Vyalov, S.S., Slepak, M.E., Maximyak, R.V. and Chapayev, A.A., 1988 (a). Frozen soil deformation and failure under different loading. Proceedings, 5th International Symposium on Ground Freezing, Nottingham, UK, 465-471.

Vyalov, S.S., Maximyak, R.V. Razbegin, V.N., Slepak, M.E. and Chapayev, A.A., 1988 (b). Stress-strain behaviour of frozen soils. Proceedings, 5th International Conference on Permafrost, Trondheim, Norway, 1186-1191.

Vyalov, S.S., 1963. Rheology of frozen soils. Proceedings, 1st International Conference on Permafrost, Lafayette, Indiana, USA, 332-337.

Vyalov, S.S. and Tsytovich, N.A., 1955. Creep and long-term strength of frozen soils. Dok. Akak. Nauk , **104**, 850-853.

Weaver, J.S. and Morgenstern, N.R., 1981. Simple shear creep tests on frozen soils. Canadian Geotechnical Journal, **18**, 217-229.

Weeks, W.F. and Ackley, S.F., 1982. Growth, structure and properties of sea ice. U.S. Army CRREL Monograph 82-1. 130p.

Weeks, W.F. and Assur A., 1967. The mechanical properties of sea ice . U.S. Army CRREL Monograph II-B3. 80p.

Weeks, W.F. and Lofgren, G., 1967. The effective solute distribution coefficient during the freezing on NaCl solutions. Proceedings, 1st International Conference on Low Temperature Science, **1**, part 1, 579-597.

Williams, P.J., 1988. Thermodynamic and mechanical conditions within frozen soils and their effects. Proceedings, 5th International Conference on Permafrost, Trondhein, Norway, 493-498.

Williams, P.J., 1964. Specific heat and apparent specific heat of frozen soils. Geotechnique, **14**, 133-142.

Williams, P.J., 1963. Suction and its effects in unfrozen water of frozen soil. Proceedings, 1st International Conference on Permafrost, Lafayette, Indiana, USA, 225-229.

Wilson, R. and Vinson, T.S., 1983. Solute redistribution and freezing rates in a coarse-grained soil with saline porewater. Transportation Research Report 83-15, Transportation Research Institue, Oregon State University, Corvallis, Oregon. 212 p.

Wong, T.T. and Sego, D.C., 1989. Design requirements for ice forces. Canadian Geotechnical Journal, **26**, 524-535.

Wu, T.H., 1964. A nuclear magnetic resonance study of water in clay. Journal of Geophysicics Research, **69**, 1083-1091.

Xiangsheng, C., 1988. Mechanical characteristics of artificially frozen clays under triaxial stress condition. Proceedings, 5th International Symposium on Ground Freezing, Nottingham, UK, 173-179.

Yen, Y.C., 1981. Review of thermal properties of snow, ice and sea ice. U.S. Army CRREL Report 81-10. 27 p.

Yong, R.N., Cheung, C.H. and Sheeran, D.E., 1979. Prediction of salt influence on unfrozen water content in frozen soils. Engineering Geology, **13**, 137-155.

Youssef, H., 1987. Compressibility of sand-ice system. Proceedings, 9th International Conference on Port and Ocean Engineering under Arctic Conditions, Fairbanks, Alaska, USA, 497-506.

Zhu, Yuanlin and Carbee, D.L., 1987. Creep and strength behavior of frozen silt in unizxial compression. U.S. Army CRREL Report 87-10. 67 p.

Zhu, Yuanlin, Zhang, Jiayi and Wu, Siwang, 1982. Elastic and compressive deformation of frozen soils. Proceedings, 3rd International Symposium on Ground Freezing, Hanover, New Hampshire, USA, 65-77.

APPENDIX A

DATABASE of SALINITY MEASUREMENTS from the NORTHWEST TERRITORIES

COMMUNITY	PROJECT	LOCATION	GEOLOGICAL UNIT	TERRAIN TYPE	HOLE	DATE	SOIL CLASSIFICATION (USCS)	DEPTH(m)	TEMP (°C)	DENSITY (Mg/m3)	M.C. (%)	SALINITY (ppt)	CONSULTANT	COMMENTS
ARCTIC BAY	School Extension	N73°02' W85°11'	I-a	R	4	83/09/30	Dolomitic Shale + Slate	0.2			9	1	Lupien,Rosenberg,Journeaux	Drilling by
ARCTIC BAY	School Extension	N73°02' W85°11'	I-a	R	4	83/09/30	Dolomitic Shale + Slate	0.8			12	2	and Ass. Inc.	percussion
ARCTIC BAY	School Extension	N73°02' W85°11'	I-a	R	4	83/09/30	Dolomitic Shale + Slate	1.4			12	3	Lupien,Rosenberg,Journeaux	drilling rig
ARCTIC BAY	School Extension	N73°02' W85°11'	I-a	R	4	83/09/30	Dolomitic Shale + Slate	2			10	3	and Ass. Inc.	on air drill
ARCTIC BAY	School Extension	N73°02' W85°11'	I-a	R	4	83/09/30	Dolomitic Shale + Slate	2.6			11	4	Lupien,Rosenberg,Journeaux	PF thickness
ARCTIC BAY	School Extension	N73°02' W85°11'	I-a	R	4	83/09/30	Slate + Limestone	3.4			14	8	and Ass. Inc.	>300m
ARCTIC BAY	School Extension	N73°02' W85°11'	I-a	R	4	83/09/30	Dolomitic Limestone	4.5			19	22	Lupien,Rosenberg,Journeaux	Active layer:
ARCTIC BAY	School Extension	N73°02' W85°11'	I-a	R	4	83/09/30	Dolomitic Limestone	5.8			11	24	and Ass. Inc.	0.75-1.5m
ARCTIC BAY	School Extension	N73°02' W85°11'	I-a	R	4	83/09/30	Calcareous Shale+Mudstone	7			13	27	Lupien,Rosenberg,Journeaux	File # : 3786
ARCTIC BAY	School Extension	N73°02' W85°11'	I-a	R	4	83/09/30	Calcareous Shale+Mudstone	7.6			12	29	and Ass. Inc.	
ARCTIC BAY	School Extension	N73°02' W85°11'	I-a	R	4	83/09/30	Calcareous Shale+Mudstone	8.2			14	24	Lupien,Rosenberg,Journeaux	
ARCTIC BAY	School Extension	N73°02' W85°11'	I-a	R	4	83/09/30	Calcareous Shale+Mudstone	8.9			15	22	and Ass. Inc.	
ARCTIC BAY	School Extension	N73°02' W85°11'	I-a	R	4	83/09/30	Calcareous Shale+Mudstone	9.4			15	20	Lupien,Rosenberg,Journeaux	
ARCTIC BAY	School Extension	N73°02' W85°11'	I-a	R	4	83/09/30	Calcareous Shale+Mudstone	10			16	9	and Ass. Inc.	
ARCTIC BAY	School Extension	N73°02' W85°11'	I-a	R	4	83/09/30	Calcareous Shale+Mudstone	10.7			33	3	Lupien,Rosenberg,Journeaux	
ARCTIC BAY	School Extension	N73°02' W85°11'	I-a	R	10	83/09/30	Dolomitic Shale + Slate	1			7	3	and Ass. Inc.	
ARCTIC BAY	School Extension	N73°02' W85°11'	I-a	R	10	83/09/30	Dolomitic Shale + Slate	2			9	3	Lupien,Rosenberg,Journeaux	
ARCTIC BAY	School Extension	N73°02' W85°11'	I-a	R	10	83/09/30	Dolomitic Shale + Slate	3			10	5	and Ass. Inc.	
ARCTIC BAY	School Extension	N73°02' W85°11'	I-a	R	10	83/09/30	Dolomitic Shale + Slate	4			9	7	Lupien,Rosenberg,Journeaux	
ARCTIC BAY	School Extension	N73°02' W85°11'	I-a	R	10	83/09/30	Dolomitic Shale + Slate	5			9	8	and Ass. Inc.	
ARCTIC BAY	School Extension	N73°02' W85°11'	I-a	R	10	83/09/30	Dolomitic Shale + Slate	6			10	8	Lupien,Rosenberg,Journeaux	
ARCTIC BAY	School Extension	N73°02' W85°11'	I-a	R	10	83/09/30	Dolomitic Shale + Slate	7			11	8	and Ass. Inc.	
ARCTIC BAY	School Extension	N73°02' W85°11'	I-a	R	10	83/09/30	Dolomitic Shale + Slate	8			9	12	Lupien,Rosenberg,Journeaux	
ARCTIC BAY	School Extension	N73°02' W85°11'	I-a	R	10	83/09/30	Dolomitic Shale + Slate	9			12	13	and Ass. Inc.	
ARCTIC BAY	School Extension	N73°02' W85°11'	I-a	R	10	83/09/30	Dolomitic Shale + Slate	10			16	16	Lupien,Rosenberg,Journeaux	
ARCTIC BAY	School Extension	N73°02' W85°11'	I-a	R	10	83/09/30	Dolomitic Shale + Slate	11			13	32	and Ass. Inc.	
ARCTIC BAY	School Extension	N73°02' W85°11'	I-a		GRID 18 6W	85/10/05		0.75	-2				Lupien,Rosenberg,Journeaux	
ARCTIC BAY	School Extension	N73°02' W85°11'	I-a		GRID 18 6W	85/10/05		1.5	-2.7				and Ass. Inc.	
ARCTIC BAY	School Extension	N73°02' W85°11'	I-a		GRID 18 6W	85/10/05		2.25	-4				Lupien,Rosenberg,Journeaux	
ARCTIC BAY	School Extension	N73°02' W85°11'	I-a		GRID 18 6W	85/10/05		3.75	-6.8				and Ass. Inc.	
ARCTIC BAY	School Extension	N73°02' W85°11'	I-a		GRID 18 6W	85/10/05		5.25	-8.6				Lupien,Rosenberg,Journeaux	
ARCTIC BAY	School Extension	N73°02' W85°11'	I-a		GRID 18 6W	85/10/05		6.75	-10.6				and Ass. Inc.	
ARCTIC BAY	School Extension	N73°02' W85°11'	I-a		GRID 18 6W	85/10/05		8.25	-11.6				Lupien,Rosenberg,Journeaux	
ARCTIC BAY	School Extension	N73°02' W85°11'	I-a		GRID 18 6W	85/10/05		9.75	-12				and Ass. Inc.	
ARCTIC BAY	School Extension	N73°02' W85°11'	I-a		GRID 18 6W	85/10/05		11.25	-12.2				Lupien,Rosenberg,Journeaux	
ARCTIC BAY	School Extension	N73°02' W85°11'	I-a		GRID 18 6W	85/11/24		0.75	-11.3				and Ass. Inc.	
ARCTIC BAY	School Extension	N73°02' W85°11'	I-a		GRID 18 6W	85/11/24		1.5	-10.6				Lupien,Rosenberg,Journeaux	
ARCTIC BAY	School Extension	N73°02' W85°11'	I-a		GRID 18 6W	85/11/24		2.25	-9.4				and Ass. Inc.	
ARCTIC BAY	School Extension	N73°02' W85°11'	I-a		GRID 18 6W	85/11/24		3.75	-8.3				Lupien,Rosenberg,Journeaux	
ARCTIC BAY	School Extension	N73°02' W85°11'	I-a		GRID 18 6W	85/11/24		5.25	-9				and Ass. Inc.	
ARCTIC BAY	School Extension	N73°02' W85°11'	I-a		GRID 18 6W	85/11/24		6.75	-10.2				Lupien,Rosenberg,Journeaux	
ARCTIC BAY	School Extension	N73°02' W85°11'	I-a		GRID 18 6W	85/11/24		8.25	-11.3				and Ass. Inc.	
ARCTIC BAY	School Extension	N73°02' W85°11'	I-a		GRID 18 6W	85/11/24		9.75	-11.4				Lupien,Rosenberg,Journeaux	
ARCTIC BAY	School Extension	N73°02' W85°11'	I-a		GRID 18 6W	85/11/24		11.25	-12				and Ass. Inc.	
ARCTIC RED RIVER	Fire Hall	N67°27' W133°45'	III-a		86-3	86/10/16		6	-3.1				Thurber Cons. Ltd.	File 15-22-78
ARCTIC RED RIVER	Fire Hall	N67°27' W133°45'	III-a	M	86-1	86/10/14	CL	3.3			35	1.8	Thurber Cons. Ltd.	Active layer:
ARCTIC RED RIVER	Fire Hall	N67°27' W133°45'	III-a	M	86-2	86/10/14	CI	3.8			17	3.7	Thurber Cons. Ltd.	0.7-0.8m
ARCTIC RED RIVER	Fire Hall	N67°27' W133°45'	III-a	M	86-2	86/10/14	CI	3.3			18	3.7	Thurber Cons. Ltd.	High ice content
ARCTIC RED RIVER	Fire Hall	N67°27' W133°45'	III-a	M	86-3	86/10/14	CI	3.8			20	14	Thurber Cons. Ltd.	in top 3.0 to 5.0 m
ARCTIC RED RIVER	Fire Hall	N67°27' W133°45'	III-a	M	86-3	86/10/14	CI	3.3			19	14.4	Thurber Cons. Ltd.	Salinity determination
ARCTIC RED RIVER	Fire Hall	N67°27' W133°45'	III-a	M	86-3	86/10/14							Thurber Cons. Ltd.	by method 3
ARCTIC RED RIVER	Gymnasium	N67°27' W133°45'	III-a	M	86-1	86/10/14	CI	3			16	3.1	Thurber Cons. Ltd.	File 15-22-77
ARCTIC RED RIVER	Gymnasium	N67°27' W133°45'	III-a	M	86-1	86/10/14	CI	3.3			15	4	Thurber Cons. Ltd.	Salinity determination
ARCTIC RED RIVER	Gymnasium	N67°27' W133°45'	III-a	M	86-2	86/10/14	CI	3.8			19	3.9	Thurber Cons. Ltd.	by method 3
ARCTIC RED RIVER	Gymnasium	N67°27' W133°45'	III-a		86-2	86/10/16		6	-3.6				Thurber Cons. Ltd.	
ARCTIC RED RIVER	Gymnasium	N67°27' W133°45'	III-a	M	86-3	86/10/14	CI	3.3			14	4.4	Thurber Cons. Ltd.	
ARCTIC RED RIVER	Two Lake water	N67°27' W133°45'	III-a	Ms	87-7	87/02/10	CL-ML	1.4			35	1.2	Thurber Cons. Ltd.	File 17-337-27
ARCTIC RED RIVER	intake pumphouse	N67°27' W133°45'	III-a	Ms	87-7	87/02/10	CL-ML	2.9			18	16.3	Thurber Cons. Ltd.	Continuous pf
ARCTIC RED RIVER	facility	N67°27' W133°45'	III-a	R	87-7	87/02/10	shale	4.5			11	9.5	Thurber Cons. Ltd.	Salinity determination
ARCTIC RED RIVER	[illegible] facility	N67°27' W133°45'	III-a	R	87-7	87/02/10	shale	7.6			3	8.2	Thurber Cons. Ltd.	by method 3
ARCTIC RED RIVER	[illegible] facility	N67°27' W133°45'	III-a	R	87-7	87/02/10	shale	9.1			3	9.7	Thurber Cons. Ltd.	
ARCTIC RED RIVER	[illegible] facility	N67°27' W133°45'	III-a	Ms	87-8	87/02/10	CI	2.2			20	12.7	Thurber Cons. Ltd.	
ARCTIC RED RIVER	[illegible] facility	N67°27' W133°45'	III-a	Ms	87-8	87/02/10	CI	3.7			12	9.8	Thurber Cons. Ltd.	
ARCTIC RED RIVER	[illegible] facility	N67°27' W133°45'	III-a	Ms	87-8	87/02/10	CI	5.3			10	33.5	Thurber Cons. Ltd.	
ARCTIC RED RIVER	[illegible] facility	N67°27' W133°45'	III-a	Ms	87-8	87/02/10	CL	6.8			14	5	Thurber Cons. Ltd.	
ARCTIC RED RIVER	[illegible] facility	N67°27' W133°45'	III-a	PO' (3)	87-8	87/02/10	SC	9.8			9	24.8	Thurber Cons. Ltd.	
ARCTIC RED RIVER	[illegible] facility	N67°27' W133°45'	III-a	PO' (3)	87-8	87/02/10	SM-SC	11.2			7	41.3	Thurber Cons. Ltd.	
ARCTIC RED RIVER	[illegible] facility	N67°27' W133°45'	III-a	PO' (3)	87-8	87/02/10	SM-SC	12.5			4	70.4	Thurber Cons. Ltd.	

COMMUNITY	PROJECT	LOCATION	GEOLOGICAL UNIT	TERRAIN TYPE	HOLE	DATE	SOIL CLASSIFICATION (USCS)	DEPTH(m)	TEMP (°C)	DENSITY (Mg/m3)	M.C. (%)	SALINITY (ppt)	CONSULTANT	COMMENTS
BAKER LAKE	Adfreeze test piles	N64°18' W 96°05'	II-a		86-3	87/10/24	(no soil type)	0-1.5			0.18	19.4	Thurber Cons. Ltd.	File 15-22-90
BAKER LAKE	Adfreeze test piles	N64°18' W 96°05'	II-a		86-3	87/10/24	(no soil type)	1.5-3.0			3.7	4.9	Thurber Cons. Ltd.	Additional salinity
BAKER LAKE	Adfreeze test piles	N64°18' W 96°05'	II-a		86-3	87/10/24	(no soil type)	3.0-4.5			4.5	16.3	Thurber Cons. Ltd.	tests done using
BAKER LAKE	Adfreeze test piles	N64°18' W 96°05'	II-a		86-3	87/10/24	(no soil type)	4.5-6.1			1.6	30	Thurber Cons. Ltd.	[illegible]
BAKER LAKE	Adfreeze test piles	N64°18' W 96°05'	II-a		86-4	87/10/24	(no soil type)	0-1.5			1.5	4.1	Thurber Cons. Ltd.	(no sample type)
BAKER LAKE	Adfreeze test piles	N64°18' W 96°05'	II-a		86-4	87/10/24	(no soil type)	1.5-3.0			1.1	8.9	Thurber Cons. Ltd.	
BAKER LAKE	Adfreeze test piles	N64°18' W 96°05'	II-a		86-4	87/10/24	(no soil type)	3.0-4.5			6.6	7.2	Thurber Cons. Ltd.	Salinity determination
BAKER LAKE	Adfreeze test piles	N64°18' W 96°05'	II-a		86-4	87/10/24	(no soil type)	4.5-6.1			1.4	12.1	Thurber Cons. Ltd.	by method 3
BAKER LAKE	Housing	N64°18' W 96°05'	II-a			84/04/16			M.A.G.T. = -7°C				Thurber Cons. Ltd.	File 15-34-86
BAKER LAKE	Housing	N64°18' W 96°05'	II-a	M	84-2	84/04/16	ML	3.3			9	0.08	Thurber Cons. Ltd.	Very low salinity
BAKER LAKE	Housing	N64°18' W 96°05'	II-a											Salinity determination
														by method 3
BROUGHTON ISLAND	School	N67°33' W64°02'	I-b		1	87/08/07		1	0.7				Hardy BBT	Air track drilling
BROUGHTON ISLAND	School	N67°33' W64°02'	I-b		1	87/08/07		4	-7.2				Hardy BBT	Active layer
BROUGHTON ISLAND	School	N67°33' W64°02'	I-b		1	87/08/07		5	-8.4				Hardy BBT	up to app. 1.5m
BROUGHTON ISLAND	School	N67°33' W64°02'	I-b		1	87/08/07		6	-9.1				Hardy BBT	Salinity determination
BROUGHTON ISLAND	School	N67°33' W64°02'	I-b		1	87/08/07		7	-9.2				Hardy BBT	probably method 3
BROUGHTON ISLAND	School	N67°33' W64°02'	I-b		1	87/08/07		8	-9				Hardy BBT	
BROUGHTON ISLAND	School	N67°33' W64°02'	I-b		1	87/08/07		9	-8.7				Hardy BBT	
BROUGHTON ISLAND	School	N67°33' W64°02'	I-b	V (U)	1	87/08/06	SP	2.5			7	2.7	Hardy BBT	
BROUGHTON ISLAND	School	N67°33' W64°02'	I-b	V (U)	1	87/08/06	ML	5.4			11	22	Hardy BBT	
BROUGHTON ISLAND	School	N67°33' W64°02'	I-b	V (U)	1	87/08/06	ML	8.4			13	15.7	Hardy BBT	
BROUGHTON ISLAND	School	N67°33' W64°02'	I-b	V (U)	1	87/08/06	ML	9.6			11	15.1	Hardy BBT	
BROUGHTON ISLAND	School	N67°33' W64°02'	I-b	V (U)	2	87/08/06	SM	1.8			9	9.7	Hardy BBT	
BROUGHTON ISLAND	School	N67°33' W64°02'	I-b	V (U)	2	87/08/06	ML	4.4			16	6.2	Hardy BBT	
BROUGHTON ISLAND	School	N67°33' W64°02'	I-b	V (U)	2	87/08/06	SP	5.4			12	12.2	Hardy BBT	
BROUGHTON ISLAND	School	N67°33' W64°02'	I-b	V (U)	3	87/08/06	ML	2.5			18	18.1	Hardy BBT	
BROUGHTON ISLAND	School	N67°33' W64°02'	I-b	V (U)	3	87/08/06	SM	4.5			9	5.6	Hardy BBT	
BROUGHTON ISLAND	School	N67°33' W64°02'	I-b	V (U)	4	87/08/06	SM	1.3			12	0.6	Hardy BBT	
BROUGHTON ISLAND	School	N67°33' W64°02'	I-b	V (U)	4	87/08/06	SP	4.2			11	6.3	Hardy BBT	
BROUGHTON ISLAND	School	N67°33' W64°02'	I-b	V (U)	4	87/08/06	SM-SP	4.3			11	12.4	Hardy BBT	
BROUGHTON ISLAND	School	N67°33' W64°02'	I-b	V (U)	4	87/08/06	SM-SP	7.7			13	13.8	Hardy BBT	
BROUGHTON ISLAND	School	N67°33' W64°02'	I-b	V (U)	4	87/08/06	SM-SP	10.5			12	10.9	Hardy BBT	
BROUGHTON ISLAND	School	N67°33' W64°02'	I-b	V (U)	5	87/08/06	SP	1.5			14	0.6	Hardy BBT	
BROUGHTON ISLAND	School	N67°33' W64°02'	I-b	V (U)	5	87/08/06	SP	2.7			16	3.4	Hardy BBT	
BROUGHTON ISLAND	School	N67°33' W64°02'	I-b	V (U)	5	87/08/06	SP-GP	4.3			11	3.1	Hardy BBT	
BROUGHTON ISLAND	School	N67°33' W64°02'	I-b	V (U)	5	87/08/06	SP-GP	7.5			11	10.8	Hardy BBT	
BROUGHTON ISLAND	School	N67°33' W64°02'	I-b	V (U)	5	87/08/06	SP-GP	8.5			9	11.6	Hardy BBT	
BROUGHTON ISLAND	School	N67°33' W64°02'	I-b	V (U)	6	87/08/06	SP	1.8			9	2.3	Hardy BBT	
BROUGHTON ISLAND	School	N67°33' W64°02'	I-b	V (U)	6	87/08/06	SP	3.2			11	13.7	Hardy BBT	
BROUGHTON ISLAND	School	N67°33' W64°02'	I-b	V (U)	6	87/08/06	SM	6.2			9	13.1	Hardy BBT	
BROUGHTON ISLAND	School	N67°33' W64°02'	I-b	V (U)	6	87/08/06	SM	7.4			11	18.2	Hardy BBT	
BROUGHTON ISLAND	School	N67°33' W64°02'	I-b	V (U)	6	87/08/06	SM	9.6			9	12.4	Hardy BBT	
BROUGHTON ISLAND	School	N67°33' W64°02'	I-b	W (U)	7	87/08/06	SM	1.8			21	2.5	Hardy BBT	
BROUGHTON ISLAND	School	N67°33' W64°02'	I-b	V (U)	7	87/08/06	SM	4			11	10.8	Hardy BBT	
BROUGHTON ISLAND	School	N67°33' W64°02'	I-b	V (U)	7	87/08/06	SM	5.8			9	19.3	Hardy BBT	
BROUGHTON ISLAND	School	N67°33' W64°02'	I-b	V (U)	7	87/08/06	SM	7.5			13	18.3	Hardy BBT	
BROUGHTON ISLAND	School	N67°33' W64°02'	I-b	V (U)	8	87/08/07	SP	2.7			18	6.9	Hardy BBT	
BROUGHTON ISLAND	School	N67°33' W64°02'	I-b	V (U)	8	87/08/07	SM	5			9	6.7	Hardy BBT	
CAPE DORSET	Recreational Complex	N64°14' W76°32'	I-b	Bn	86-1	86/12/05	bedrock	3.8			2	9.5	Thurber Cons. Ltd.	File 15-22-82
CAPE DORSET	Recreational Complex	N64°14' W76°32'	I-b		86-1	86/12/05		5.1	-3				Thurber Cons. Ltd.	Salinity determination
CAPE DORSET	Recreational Complex	N64°14' W76°32'	I-b	C (U)	86-2	86/12/05	ML	2.1			15	2	Thurber Cons. Ltd.	by method 3
CAPE DORSET	Recreational Complex	N64°14' W76°32'	I-b	C (U)	86-3	86/12/05	ML	2.3			10	2.1	Thurber Cons. Ltd.	
CAPE DORSET	Recreational Complex	N64°14' W76°32'	I-b	C (U)	86-4	86/12/05	ML	2.1			10	1.1	Thurber Cons. Ltd.	
CAPE DORSET	Recreational Complex	N64°14' W76°32'	I-b	C (U)	86-5	86/12/05	GP	3.8			6	12.3	Thurber Cons. Ltd.	
CAPE DORSET	Recreational Complex	N64°14' W76°32'	I-b	C (U)	86-5	86/12/05	GP	5.5			5	25.2	Thurber Cons. Ltd.	
CAPE DORSET	Recreational Complex	N64°14' W76°32'	I-b		86-5	86/12/08		5.7	-3.4				Thurber Cons. Ltd.	
CAPE DORSET	Recreational Complex	N64°14' W76°32'	I-b	C (U)	86-6	86/12/07	GP	5.5			8	15.5	Thurber Cons. Ltd.	
CAPE DORSET	Recreational Complex	N64°14' W76°32'	I-b		86-6	86/12/08		5.9	-3.9				Thurber Cons. Ltd.	
CAPE DORSET	Recreational Complex	N64°14' W76°32'	I-b	R	86-6	86/12/07	bedrock	7			2	23	Thurber Cons. Ltd.	
CAPE DORSET	Recreational Complex	N64°14' W76°32'	I-b	C (U)	86-7	86/12/07	GP	5.4			4	19.6	Thurber Cons. Ltd.	
CAPE DORSET	Recreational Complex	N64°14' W76°32'	I-b	C (U)	86-8	86/12/07	GP	3.8			8	12.7	Thurber Cons. Ltd.	
CAPE DORSET	Recreational Complex	N64°14' W76°32'	I-b	C (U)	86-9	86/12/07	ML	2.3			12	5.2	Thurber Cons. Ltd.	
CAPE DORSET	Recreational Complex	N64°14' W76°32'	I-b	C (U)	86-10	86/12/07	GP	3.8			7	11.4	Thurber Cons. Ltd.	
CAPE DORSET	Recreational Complex	N64°14' W76°32'	I-b	C (U)	86-11	86/12/07	ML	2.3			12	6	Thurber Cons. Ltd.	
CAPE DORSET	Recreational Complex	N64°14' W76°32'	I-b	C (U)	86-11	86/12/07	GP	3.8			9	13.9	Thurber Cons. Ltd.	
CAPE DORSET	Recreational Complex	N64°14' W76°32'	I-b	C (U)	86-12	86/12/07	ML	2.3			13	4.4	Thurber Cons. Ltd.	
CAPE DORSET	School	N64°14' W76°32'	I-b		87-6	87/08/04		6.1	-3.6				Thurber Cons. Ltd.	File 15-22-89

COMMUNITY	PROJECT	LOCATION	GEOLOGICAL UNIT	TERRAIN TYPE	HOLE	DATE	SOIL CLASSIFICATION (USCS)	DEPTH(m)	TEMP (°C)	DENSITY (Mg/m3)	M.C. (%)	SALINITY (ppt)	CONSULTANT	COMMENTS
CAPE DORSET	School	N64°14' W76°32'	I-b	Wv	87-1	87/08/03	GM-SM	3.3			9	0.5	Thurber Cons. Ltd.	Continuous PF
CAPE DORSET	School	N64°14' W76°32'	I-b	Wv	87-2	87/08/03	SP-GP	1.6			4	0.4	Thurber Cons. Ltd.	Active layer app. 1.5m
CAPE DORSET	School	N64°14' W76°32'	I-b	Wv	87-3	87/08/04	SP-GP	2			2	0.9	Thurber Cons. Ltd.	Very low salinity
CAPE DORSET	School	N64°14' W76°32'	I-b											Salinity determination
														by method 3
CLYDE RIVER	[illegible] School	N70°27' W68°33'	I-b						M.A.G.T. = -10°c				Paper by J.F.D Nixon, [illegible]	
CLYDE RIVER	[illegible] School	N70°27' W68°33'	I-b			82/09/30		0.1	-3.4				Paper by J.F.D Nixon, [illegible]	
CLYDE RIVER	[illegible] School	N70°27' W68°33'	I-b			82/09/30		0.6	-0.5				Paper by J.F.D Nixon, [illegible]	
CLYDE RIVER	[illegible] School	N70°27' W68°33'	I-b			82/09/30		3	-4.8				Paper by J.F.D Nixon, [illegible]	
CLYDE RIVER	[illegible] School	N70°27' W68°33'	I-b			82/09/30		7	-9.6				Paper by J.F.D Nixon, [illegible]	
CLYDE RIVER	[illegible] School	N70°27' W68°33'	I-b			82/09/30		8.6	-9.9				Paper by J.F.D Nixon, [illegible]	
CLYDE RIVER	[illegible] School	N70°27' W68°33'	I-b			82/10/02		0.1	-3.3				Paper by J.F.D Nixon, [illegible]	
CLYDE RIVER	[illegible] School	N70°27' W68°33'	I-b			82/10/02		0.6	-0.5				Paper by J.F.D Nixon, [illegible]	
CLYDE RIVER	[illegible] School	N70°27' W68°33'	I-b			82/10/02		3	-4.8				Paper by J.F.D Nixon, [illegible]	
CLYDE RIVER	[illegible] School	N70°27' W68°33'	I-b			82/10/02		7	-9.5				Paper by J.F.D Nixon, [illegible]	
CLYDE RIVER	[illegible] School	N70°27' W68°33'	I-b			82/10/02		8.6	-9.9				Paper by J.F.D Nixon, [illegible]	
CLYDE RIVER	[illegible] School	N70°27' W68°33'	I-b			82/10/17		0.1	-2				Paper by J.F.D Nixon, [illegible]	
CLYDE RIVER	[illegible] School	N70°27' W68°33'	I-b			82/10/17		0.6	-1.5				Paper by J.F.D Nixon, [illegible]	
CLYDE RIVER	[illegible] School	N70°27' W68°33'	I-b			82/10/17		3	-4.2				Paper by J.F.D Nixon, [illegible]	
CLYDE RIVER	[illegible] School	N70°27' W68°33'	I-b			82/10/17		7	-9.3				Paper by J.F.D Nixon, [illegible]	
CLYDE RIVER	[illegible] School	N70°27' W68°33'	I-b			82/10/17		8.6	-9.7				Paper by J.F.D Nixon, [illegible]	
CLYDE RIVER	[illegible] School	N70°27' W68°33'	I-b			82/10/26		0.1	-6				Paper by J.F.D Nixon, [illegible]	
CLYDE RIVER	[illegible] School	N70°27' W68°33'	I-b			82/10/26		0.6	-3.1				Paper by J.F.D Nixon, [illegible]	
CLYDE RIVER	[illegible] School	N70°27' W68°33'	I-b			82/10/26		3	-4.1				Paper by J.F.D Nixon, [illegible]	
CLYDE RIVER	[illegible] School	N70°27' W68°33'	I-b			82/10/26		7	-9.3				Paper by J.F.D Nixon, [illegible]	
CLYDE RIVER	[illegible] School	N70°27' W68°33'	I-b			82/10/26		8.6	-9.7				Paper by J.F.D Nixon, [illegible]	
CLYDE RIVER	[illegible] School	N70°27' W68°33'	I-b	W'O'	NRC-1	83/10	SM	0.75			7.7	3.1	Paper by J.F.D Nixon, [illegible]	NRC holes:
CLYDE RIVER	[illegible] School	N70°27' W68°33'	I-b	W'O'	NRC-1	83/10	SM	1.5			5.2	3.7	Paper by J.F.D Nixon, [illegible]	samples tested at NRC
CLYDE RIVER	[illegible] School	N70°27' W68°33'	I-b	W'O'	NRC-1	83/10	SM	2.25			6.7	6.8	Paper by J.F.D Nixon, [illegible]	in 1983
CLYDE RIVER	[illegible] School	N70°27' W68°33'	I-b	W'O'	NRC-1	83/10	SM	3			6.4	12.9	Paper by J.F.D Nixon, [illegible]	Salinity determination
CLYDE RIVER	[illegible] School	N70°27' W68°33'	I-b	W'O'	NRC-1	83/10	SM	3.75			10.1	19.1	Paper by J.F.D Nixon, [illegible]	by method 3
CLYDE RIVER	[illegible] School	N70°27' W68°33'	I-b	W'O'	NRC-1	83/10	SM	4.5			16.9	34	Paper by J.F.D Nixon, [illegible]	Some massive ground
CLYDE RIVER	[illegible] School	N70°27' W68°33'	I-b	W'O'	NRC-1	83/10	SM	5.25			24	36.5	Paper by J.F.D Nixon, [illegible]	ice locally
CLYDE RIVER	[illegible] School	N70°27' W68°33'	I-b	W'O'	NRC-1	83/10	SM	6			17.6	44.5	Paper by J.F.D Nixon, [illegible]	
CLYDE RIVER	[illegible] School	N70°27' W68°33'	I-b	W'O'	NRC-2	83/10	SM	0.75			8.6	0.8	Paper by J.F.D Nixon, [illegible]	
CLYDE RIVER	[illegible] School	N70°27' W68°33'	I-b	W'O'	NRC-2	83/10	SM	1.5			10.1	2.4	Paper by J.F.D Nixon, [illegible]	
CLYDE RIVER	[illegible] School	N70°27' W68°33'	I-b	W'O'	NRC-2	83/10	SM	2.25			9.4	6.9	Paper by J.F.D Nixon, [illegible]	
CLYDE RIVER	[illegible] School	N70°27' W68°33'	I-b	W'O'	NRC-2	83/10	SM	3			9.4	13.5	Paper by J.F.D Nixon, [illegible]	
CLYDE RIVER	[illegible] School	N70°27' W68°33'	I-b	W'O'	NRC-2	83/10	SM	3.75			11.2	13.5	Paper by J.F.D Nixon, [illegible]	
CLYDE RIVER	[illegible] School	N70°27' W68°33'	I-b	W'O'	NRC-2	83/10	SM	4.5			9.2	17.5	Paper by J.F.D Nixon, [illegible]	
CLYDE RIVER	[illegible] School	N70°27' W68°33'	I-b	W'O'	NRC-2	83/10	SM	5.25			9.5	15.5	Paper by J.F.D Nixon, [illegible]	
CLYDE RIVER	[illegible] School	N70°27' W68°33'	I-b	W'O'	NRC-2	83/10	SM	6			11.5	26.9	Paper by J.F.D Nixon, [illegible]	
CLYDE RIVER	[illegible] School	N70°27' W68°33'	I-b	W'O'	NRC-3	83/10	SM	0.75			7.1	8.6	Paper by J.F.D Nixon, [illegible]	
CLYDE RIVER	[illegible] School	N70°27' W68°33'	I-b	W'O'	NRC-3	83/10	SM	1.5			12.6	1.4	Paper by J.F.D Nixon, [illegible]	
CLYDE RIVER	[illegible] School	N70°27' W68°33'	I-b	W'O'	NRC-3	83/10	SM	2.25			5.6	4.9	Paper by J.F.D Nixon, [illegible]	
CLYDE RIVER	[illegible] School	N70°27' W68°33'	I-b	W'O'	NRC-3	83/10	SM	3			7.5	8.8	Paper by J.F.D Nixon, [illegible]	
CLYDE RIVER	[illegible] School	N70°27' W68°33'	I-b	W'O'	NRC-3	83/10	SM	3.75			8.9	10.5	Paper by J.F.D Nixon, [illegible]	
CLYDE RIVER	[illegible] School	N70°27' W68°33'	I-b	W'O'	NRC-3	83/10	SM	4.5			10.6	12.7	Paper by J.F.D Nixon, [illegible]	
CLYDE RIVER	[illegible] School	N70°27' W68°33'	I-b	W'O'	NRC-3	83/10	SM	5.25			10.8	15	Paper by J.F.D Nixon, [illegible]	
CLYDE RIVER	[illegible] School	N70°27' W68°33'	I-b	W'O'	NRC-3	83/10	SM	6			10.5	20.5	Paper by J.F.D Nixon, [illegible]	
CLYDE RIVER	[illegible] School	N70°27' W68°33'	I-b	W'O'	NRC-4	83/10	SM	0.75			8.8	1.4	Paper by J.F.D Nixon, [illegible]	
CLYDE RIVER	[illegible] School	N70°27' W68°33'	I-b	W'O'	NRC-4	83/10	SM	1.5			13.7	1.2	Paper by J.F.D Nixon, [illegible]	
CLYDE RIVER	[illegible] School	N70°27' W68°33'	I-b	W'O'	NRC-4	83/10	SM	2.25			7.4	4.1	Paper by J.F.D Nixon, [illegible]	
CLYDE RIVER	[illegible] School	N70°27' W68°33'	I-b	W'O'	NRC-4	83/10	SM	3			6	8.5	Paper by J.F.D Nixon, [illegible]	
CLYDE RIVER	[illegible] School	N70°27' W68°33'	I-b	W'O'	NRC-4	83/10	SM	3.75			6.3	11.5	Paper by J.F.D Nixon, [illegible]	
CLYDE RIVER	[illegible] School	N70°27' W68°33'	I-b	W'O'	NRC-4	83/10	SM	4.5			9.6	15.3	Paper by J.F.D Nixon, [illegible]	
CLYDE RIVER	[illegible] School	N70°27' W68°33'	I-b	W'O'	NRC-4	83/10	SM	5.25			7.8	17.8	Paper by J.F.D Nixon, [illegible]	
CLYDE RIVER	[illegible] School	N70°27' W68°33'	I-b	W'O'	NRC-4	83/10	SM	6			8.8	23.9	Paper by J.F.D Nixon, [illegible]	
CLYDE RIVER	[illegible] School	N70°27' W68°33'	I-b	W'O'	NRC-5	83/10	SM	0.75			4.1	6.5	Paper by J.F.D Nixon, [illegible]	
CLYDE RIVER	[illegible] School	N70°27' W68°33'	I-b	W'O'	NRC-5	83/10	SM	1.5			10.8	4.2	Paper by J.F.D Nixon, [illegible]	
CLYDE RIVER	[illegible] School	N70°27' W68°33'	I-b	W'O'	NRC-5	83/10	SM	2.25			9.4	7	Paper by J.F.D Nixon, [illegible]	
CLYDE RIVER	[illegible] School	N70°27' W68°33'	I-b	W'O'	NRC-5	83/10	SM	3			12.5	14.4	Paper by J.F.D Nixon, [illegible]	
CLYDE RIVER	[illegible] School	N70°27' W68°33'	I-b	W'O'	NRC-5	83/10	SM	3.75			10.9	13.8	Paper by J.F.D Nixon, [illegible]	
CLYDE RIVER	[illegible] School	N70°27' W68°33'	I-b	W'O'	NRC-5	83/10	SM	4.5			6.9	37.3	Paper by J.F.D Nixon, [illegible]	
CLYDE RIVER	[illegible] School	N70°27' W68°33'	I-b	W'O'	NRC-5	83/10	SM	5.25			10.9	18.1	Paper by J.F.D Nixon, [illegible]	
CLYDE RIVER	[illegible] School	N70°27' W68°33'	I-b	W'O'	NRC-5	83/10	SM	6			10.8	33.4	Paper by J.F.D Nixon, [illegible]	
CLYDE RIVER	[illegible] School	N70°27' W68°33'	I-b	W'O'	NRC-6	83/10	SM	0.75			17.1	3.4	Paper by J.F.D Nixon, [illegible]	
CLYDE RIVER	[illegible] School	N70°27' W68°33'	I-b	W'O'	NRC-6	83/10	SM	1.5			8.2	2	Paper by J.F.D Nixon, [illegible]	
CLYDE RIVER	[illegible] School	N70°27' W68°33'	I-b	W'O'	NRC-6	83/10	SM	2.25			5.6	5.8	Paper by J.F.D Nixon, [illegible]	

COMMUNITY	PROJECT	LOCATION	GEOLOGICAL UNIT	TERRAIN TYPE	HOLE	DATE	SOIL CLASSIFICATION (USCS)	DEPTH(m)	TEMP (°C)	DENSITY (Mg/m3)	M.C. (%)	SALINITY (ppt)	CONSULTANT	COMMENTS
CLYDE RIVER	[illegible]	N70°27' W68°35'	I-b	W'G'	NRC-6	85/10	SM	3			9.7	9.9	Paper by J.F.D Nixon, 1988	
CLYDE RIVER	[illegible]	N70°27' W68°35'	I-b	W'G'	NRC-6	85/10	SM	3.75			11.4	18.3	Paper by J.F.D Nixon, 1988	
CLYDE RIVER	[illegible]	N70°27' W68°35'	I-b	W'G'	NRC-6	85/10	SM	4.5			11.1	40.2	Paper by J.F.D Nixon, 1988	
CLYDE RIVER	[illegible]	N70°27' W68°35'	I-b	W'G'	NRC-6	85/10	SM	5.25			12.4	40.9	Paper by J.F.D Nixon, 1988	
CLYDE RIVER	[illegible]	N70°27' W68°35'	I-b	W'G'	NRC-6	85/10	SM	6			13.1	44.2	Paper by J.F.D Nixon, 1988	
CLYDE RIVER	[illegible]	N70°27' W68°35'	I-b	W'G'	H-2	85/02	SM	1.52			13.1	1.2	Paper by J.F.D Nixon, 1988	Holes done by
CLYDE RIVER	[illegible]	N70°27' W68°35'	I-b	W'G'	H-2	85/02	SM	3.05			8.8	8.4	Paper by J.F.D Nixon, 1988	Hagan Engineering
CLYDE RIVER	[illegible]	N70°27' W68°35'	I-b	W'G'	H-2	85/02	SM	3.81			12.4	5.2	Paper by J.F.D Nixon, 1988	& Testing Ltd.
CLYDE RIVER	[illegible]	N70°27' W68°35'	I-b	W'G'	H-2	85/02	SM	4.57			9.1	8.1	Paper by J.F.D Nixon, 1988	
CLYDE RIVER	[illegible]	N70°27' W68°35'	I-b	W'G'	H-2	85/02	SM	5.33			9.1	7	Paper by J.F.D Nixon, 1988	
CLYDE RIVER	[illegible]	N70°27' W68°35'	I-b	W'G'	H-2	85/02	SM	6.1			12.5	12.2	Paper by J.F.D Nixon, 1988	
CLYDE RIVER	[illegible]	N70°27' W68°35'	I-b	W'G'	H-3	85/02	SM	1.52			14.1	6.9	Paper by J.F.D Nixon, 1988	
CLYDE RIVER	[illegible]	N70°27' W68°35'	I-b	W'G'	H-3	85/02	SM	3.05			7.5	7.2	Paper by J.F.D Nixon, 1988	
CLYDE RIVER	[illegible]	N70°27' W68°35'	I-b	W'G'	H-3	85/02	SM	3.81			9.9	6.3	Paper by J.F.D Nixon, 1988	
CLYDE RIVER	[illegible]	N70°27' W68°35'	I-b	W'G'	H-3	85/02	SM	4.57			8.8	8.4	Paper by J.F.D Nixon, 1988	
CLYDE RIVER	[illegible]	N70°27' W68°35'	I-b	W'G'	H-3	85/02	SM	5.33			11.7	8.9	Paper by J.F.D Nixon, 1988	
CLYDE RIVER	[illegible]	N70°27' W68°35'	I-b	W'G'	H-3	85/02	SM	6.1			9.9	12.1	Paper by J.F.D Nixon, 1988	
CORAL HARBOUR	Adfreeze Pile Tests	N64°08' W83°10'	II-c		87-1	87/10/26	(no soil type)	0-1.5			0.08	7.5	Thurber Cons. Ltd.	File 15-22-90
CORAL HARBOUR	Adfreeze Pile Tests	N64°08' W83°10'	II-c		87-1	87/10/26	(no soil type)	1.5-3			8.2	1.3	Thurber Cons. Ltd.	Salinity determination
CORAL HARBOUR	Adfreeze Pile Tests	N64°08' W83°10'	II-c		87-1	87/10/26	(no soil type)	3-4.5			5.4	2.9	Thurber Cons. Ltd.	by method 3
CORAL HARBOUR	Adfreeze Pile Tests	N64°08' W83°10'	II-c		87-1	87/10/26	(no soil type)	4.5-6			12.3	1.6	Thurber Cons. Ltd.	
ESKIMO POINT	School	N61°07' W94°03'	II-a			85/10/29			M.A.G.T. = -5°C				Thurber Cons. Ltd.	File 15-22-68
ESKIMO POINT	School	N61°07' W94°03'	II-a	W (U)	85-3	85/10/29	SM-ML	3.8			≈10	11.2	Thurber Cons. Ltd.	Continuous pf
ESKIMO POINT	School	N61°07' W94°03'	II-a	W (U)	85-5	85/10/29	SM-ML	3.8			≈10	5.1	Thurber Cons. Ltd.	Active layer:1-3m
ESKIMO POINT	School	N61°07' W94°03'	II-a	W (U)	85-7	85/10/29	GM-SM	3.8			≈10	3.8	Thurber Cons. Ltd.	Salinity determination
ESKIMO POINT	School	N61°07' W94°03'	II-a	W (U)	85-10	85/10/29	SM	3.8			≈10	14.2	Thurber Cons. Ltd.	by method 3
ESKIMO POINT	Water Supply	N61°07' W94°03'	II-a		3-A	66/05	unknown sand	28-30 ft			10 to 15	2.8 - 4.2	Strong, Lamb and Nelson	Salinity given as
ESKIMO POINT	Water Supply	N61°07' W94°03'	II-a		4-A	66/05	unknown sand	30-32 ft			10 to 15	0.8-1.2	Strong, Lamb and Nelson	chloride content
ESKIMO POINT	Adfreeze pile Tests	N61°07' W94°03'	II-a		Lot 467	87/10/23	(no soil type)	0-1.5			8	2.5	Thurber Cons. Ltd.	File 15-22-90
ESKIMO POINT	Adfreeze pile Tests	N61°07' W94°03'	II-a		Lot 467	87/10/23	(no soil type)	1.5-3			9.1	1.4	Thurber Cons. Ltd.	Salinity determination
ESKIMO POINT	Adfreeze pile Tests	N61°07' W94°03'	II-a		Lot 467	87/10/23	(no soil type)	3-4.5			6	11.2	Thurber Cons. Ltd.	by method 3
ESKIMO POINT	Adfreeze pile Tests	N61°07' W94°03'	II-a		Lot 467	87/10/23	(no soil type)	4.5-6.1			6.3	38.3	Thurber Cons. Ltd.	
ESKIMO POINT	Subdivision	N61°07' W94°03'	II-a	W (U)	85-1	85/10/30	SM	3.8			8	1.4	Thurber Cons. Ltd.	File 15-23-58
ESKIMO POINT	Subdivision	N61°07' W94°03'	II-a	W (U)	85-3	85/10/30	SM	3.9			9	2.1	Thurber Cons. Ltd.	Salinity determination
ESKIMO POINT	Subdivision	N61°07' W94°03'	II-a	W (U)	85-5	85/10/30	SM-ML	3.8			6	2.2	Thurber Cons. Ltd.	by method 3
ESKIMO POINT	Subdivision	N61°07' W94°03'	II-a		85-4	85/10/30		0.4	-0.9				Thurber Cons. Ltd.	
ESKIMO POINT	Subdivision	N61°07' W94°03'	II-a		85-4	85/10/30		1.4	1.9				Thurber Cons. Ltd.	
ESKIMO POINT	Subdivision	N61°07' W94°03'	II-a		85-4	85/10/30		2	2.1				Thurber Cons. Ltd.	
ESKIMO POINT	Subdivision	N61°07' W94°03'	II-a		85-4	85/10/30		2.9	3.6				Thurber Cons. Ltd.	
ESKIMO POINT	Subdivision	N61°07' W94°03'	II-a		85-4	85/10/30		3.5	3.9				Thurber Cons. Ltd.	
ESKIMO POINT	Subdivision	N61°07' W94°03'	II-a		85-5	85/10/30		0.2	-3.6				Thurber Cons. Ltd.	
ESKIMO POINT	Subdivision	N61°07' W94°03'	II-a		85-5	85/10/30		0.5	-1				Thurber Cons. Ltd.	
ESKIMO POINT	Subdivision	N61°07' W94°03'	II-a		85-5	85/10/30		0.8	0.6				Thurber Cons. Ltd.	
ESKIMO POINT	Subdivision	N61°07' W94°03'	II-a		85-5	85/10/30		1.1	0.8				Thurber Cons. Ltd.	
ESKIMO POINT	Subdivision	N61°07' W94°03'	II-a		85-5	85/10/30		1.4	0.8				Thurber Cons. Ltd.	
ESKIMO POINT	Subdivision	N61°07' W94°03'	II-a		85-5	85/10/30		1.7	0.8				Thurber Cons. Ltd.	
ESKIMO POINT	Subdivision	N61°07' W94°03'	II-a		85-5	85/10/30		2.3	0.8				Thurber Cons. Ltd.	
ESKIMO POINT	Subdivision	N61°07' W94°03'	II-a		85-5	85/10/30		3.9	-1.8				Thurber Cons. Ltd.	
ESKIMO POINT	Subdivision	N61°07' W94°03'	II-a		85-5	85/10/30		3.4	-3.7				Thurber Cons. Ltd.	
FORT GOOD HOPE	Recreational Facility	N66°15' W128°38'	III-a		PR 87-4	87/10/01	SM-ML	1.1			18	0.7	Thurber Cons. Ltd.	File 15-22-93
FORT GOOD HOPE	Recreational Facility	N66°15' W128°38'	III-a	M	PR 87-5	87/10/01	CI	2.1			--	2.6	Thurber Cons. Ltd.	Salinity determination
FORT GOOD HOPE	Recreational Facility	N66°15' W128°38'	III-a	M	PR 87-5	87/10/01	CI	2.8			19	2.4	Thurber Cons. Ltd.	by method 3
FORT McPHERSON		N67°27' W134°53'	III-a			1984							Aas. Engineering Services Ltd.	Groundwater taken
FORT McPHERSON		N67°27' W134°53'	III-a			1984	Fill organics clay and silt						Aas. Engineering Services Ltd.	from sub permafrost
FORT McPHERSON		N67°27' W134°53'	III-a			1984	Bedrock shale weathered						Aas. Engineering Services Ltd.	depths (≥100 ft) in the
FORT McPHERSON		N67°27' W134°53'	III-a			1984							Aas. Engineering Services Ltd.	Mackenzie valley is
FORT McPHERSON		N67°27' W134°53'	III-a			1984							Aas. Engineering Services Ltd.	often very saline as a
FORT McPHERSON		N67°27' W134°53'	III-a			1984							Aas. Engineering Services Ltd.	result of ancient sub-
FORT McPHERSON		N67°27' W134°53'	III-a										Aas. Engineering Services Ltd.	mergence of the region
FORT McPHERSON		N67°27' W134°53'	III-a										Aas. Engineering Services Ltd.	under the Arctic Ocean
FORT McPHERSON		N67°27' W134°53'	III-a										Aas. Engineering Services Ltd.	embayment
FORT McPHERSON		N67°27' W134°53'	III-a										Aas. Engineering Services Ltd.	Continuous pf
FORT McPHERSON	Recreational Complex	N67°27' W134°53'	III-a	M	86-1	86/10/13	CL-ML	2.4			36	0.7	Thurber Cons. Ltd.	Thurber's File 15-22-7
FORT McPHERSON	Recreational Complex	N67°27' W134°53'	III-a	M	86-2	86/10/13	shale (non-weathered)	5.4			5	12.2	Thurber Cons. Ltd.	Salinity determination
FORT McPHERSON	Recreational Complex	N67°27' W134°53'	III-a		86-2	86/10/15		6	-3.4				Thurber Cons. Ltd.	by method 3
FORT McPHERSON	Recreational Complex	N67°27' W134°53'	III-a	M	86-3	86/10/13	CL-CI	2.3			16	22.7	Thurber Cons. Ltd.	

COMMUNITY	PROJECT	LOCATION	GEOLOGICAL UNIT	TERRAIN TYPE	HOLE	DATE	SOIL CLASSIFICATION (USCS)	DEPTH(m)	TEMP (°C)	DENSITY (Mg/m3)	M.C. (%)	SALINITY (ppt)	CONSULTANT	COMMENTS
FORT McPHERSON	Recreational Complex	N67°27'W134°53'	III-a	M	86-3	86/10/15	CL-CI	6	-4.2				Thurber Cons. Ltd.	
FORT McPHERSON	Recreational Complex	N67°27'W134°53'	III-a	R	86-4	86/10/13	shale	5.4			9	5.6	Thurber Cons. Ltd.	
FORT McPHERSON	Recreational Complex	N67°27'W134°53'	III-a	R	86-6	86/10/15	shale	6	-3.6		-10		Thurber Cons. Ltd.	
FORT McPHERSON	Sewage System Improvements	N67°27'W134°53'	III-a	M	PS 86-2	86/10/07	CL	1.2			35	0.4	Thurber Cons. Ltd.	File 17-357-28
FORT McPHERSON	Sewage System Improvements	N67°27'W134°53'	III-a	M	PS 86-2	86/10/15	CL	1.2	-1				Thurber Cons. Ltd.	Salinity determination
FORT McPHERSON	Sewage System Improvements	N67°27'W134°53'	III-a	M	PS 86-5	86/10/07	CL-ML	1.2			22	1.8	Thurber Cons. Ltd.	by method 3
FORT McPHERSON	Sewage System Improvements	N67°27'W134°53'	III-a	R	86-1	86/10/15	Shale	3.9			12	4.2	Thurber Cons. Ltd.	
FORT McPHERSON	Sewage System Improvements	N67°27'W134°53'	III-a	R	86-3	86/10/15	Shale	3.9			9	13	Thurber Cons. Ltd.	
FORT NORMAN	Recreation Complex	N64°54'W125°34'	III-a	M	88-1	88/03/21	ML	5			28	0.4	Thurber Cons. Ltd.	File 15-22-101
FORT NORMAN	Recreation Complex	N64°54'W125°34'	III-a		88-1	88/03/21		6.1	-0.3				Thurber Cons. Ltd.	Discontinuous pf
FORT NORMAN	Recreation Complex	N64°54'W125°34'	III-a	M	88-5	88/03/21	ML	5.4			28	0.8	Thurber Cons. Ltd.	A lot of groundwater
FORT NORMAN	Recreation Complex	N64°54'W125°34'	III-a	M	88-6	88/03/21	ML	3.8			36	0.4	Thurber Cons. Ltd.	in boreholes
FORT NORMAN	Recreation Complex	N64°54'W125°34'	III-a		88-6	88/03/21		6.1	-0.5				Thurber Cons. Ltd.	Drilling stopped
FORT NORMAN	Recreation Complex	N64°54'W125°34'	III-a	M	88-7	88/03/21	ML	3.6			32	0.6	Thurber Cons. Ltd.	at water table
FORT NORMAN	Recreation Complex	N64°54'W125°34'	III-a		88-7	88/03/21		6.1	-0.8				Thurber Cons. Ltd.	Active layer : 0.5m
FORT NORMAN	Recreation Complex	N64°54'W125°34'	III-a										Thurber Cons. Ltd.	where no vegetation
FORT NORMAN	Recreation Complex	N64°54'W125°34'	III-a											disturbance
FORT NORMAN	Recreation Complex		III-a										Thurber Cons. Ltd.	Active layer: 3.0m
FORT NORMAN	Recreation Complex	N64°54'W125°34'	III-a										Thurber Cons. Ltd.	where vegetation
FORT NORMAN	Recreation Complex	N64°54'W125°34'	III-a										Thurber Cons. Ltd.	disturbance
FORT NORMAN	Recreation Complex	N64°54'W125°34'	III-a										Thurber Cons. Ltd.	Salinity method 3
			III-a											
FORT SIMPSON	Nahanni Lee Duplex	N61°52'W121°23'	III-a	F	87-1	87/03/09	SM-SP	7			23	0.5	Thurber Cons. Ltd.	File 19-248-4
FORT SIMPSON	Nahanni Lee Duplex	N61°52'W121°23'	III-a		87-1	87/03/12		7	-0.2				Thurber Cons. Ltd.	Salinity : method 3
FORT SIMPSON	Nahanni Lee Duplex	N61°52'W121°23'	III-a		87-1	87/03/13		7	-0.1				Thurber Cons. Ltd.	
FORT SIMPSON	Nahanni Lee Duplex	N61°52'W121°23'	III-a	F	87-2	87/03/09	SM-SP	7			25	0.8	Thurber Cons. Ltd.	
FORT SIMPSON	Nahanni Lee Duplex	N61°52'W121°23'	III-a		87-2	87/03/12		7	0.1				Thurber Cons. Ltd.	
FORT SIMPSON	Nahanni Lee Duplex	N61°52'W121°23'	III-a		87-2	87/03/13		7	-0.1				Thurber Cons. Ltd.	
FORT SIMPSON	Nahanni Lee Duplex	N61°52'W121°23'	III-a	F	87-4	87/03/09	SM-ML	6.1			35	0.7	Thurber Cons. Ltd.	
FORT SIMPSON	Nahanni Lee Duplex	N61°52'W121°23'	III-a	F	87-7	87/03/09	SP-SM	7			18	0.8	Thurber Cons. Ltd.	
FORT SIMPSON	Nahanni Lee Duplex	N61°52'W121°23'	III-a	F	87-10	87/03/09	SP-SM	7			23	0.6	Thurber Cons. Ltd.	
FORT SIMPSON	Nahanni Lee Duplex	N61°52'W121°23'	III-a	F (?)	87-13	87/03/09	ML	4.7			29	0.9	Thurber Cons. Ltd.	
GJOA HAVEN	Residential Housing and	N68°38' W95°53'	II-b	W	84-4	84/04/12	SM	2			18	0.19	Thurber Cons. Ltd.	File 15-34-5
GJOA HAVEN	Warehouse	N68°38' W95°53'	II-b										Thurber Cons. Ltd.	Airtrack drill
GJOA HAVEN	Res. Housing and Warehouse	N68°38' W95°53'	II-b										Thurber Cons. Ltd.	Active layer 0.5-1.5 m
GJOA HAVEN	Res. Housing and Warehouse	N68°38' W95°53'	II-b										Thurber Cons. Ltd.	Continuous permafrost
GJOA HAVEN	Res. Housing and Warehouse	N68°38' W95°53'	II-b										Thurber Cons. Ltd.	Salinity : method 3
HOLMAN	Hamlet Office	N70°43'W117°43'	III-d	W	85-1	85/11/14	GM-SM	2.4			11	3.02	Thurber Cons. Ltd.	File 15-22-64
HOLMAN	Hamlet Office	N70°43'W117°43'	III-d	W	85-2	85/11/14	GM-SM	3			10	3.68	Thurber Cons. Ltd.	Salinity determination
HOLMAN	Hamlet Office	N70°43'W117°43'	III-d	W	85-3	85/11/14	GM-SP	4			7	4.38	Thurber Cons. Ltd.	by method 3
HOLMAN	Hamlet Office	N70°43'W117°43'	III-d	W	85-4	85/11/15	GM-SM	2.7			13	4.02	Thurber Cons. Ltd.	
IQALUIT	Arctic College	N63°44' W68°31'	I-b	M	86-1	86/10	GP	3.8			8	0.1	Thurber Cons. Ltd.	File 15-22-71
IQALUIT	Pile Installation	N63°44' W68°31'	I-b	M	86-2	86/10	SM	3.7			6	1.5	Thurber Cons. Ltd.	Salinity determination
IQALUIT	Pile Installation	N63°44' W68°31'	I-b	M	86-4	86/10	GP-GM	3.8			6	1.3	Thurber Cons. Ltd.	by method 3
IQALUIT	Pile Installation	N63°44' W68°31'	I-b	M	86-4	86/10	GP-GM	5.1			3	3.3	Thurber Cons. Ltd.	
IQALUIT	Pile Installation	N63°44' W68°31'	I-b	M	86-5	86/10	GM	4				1.4	Thurber Cons. Ltd.	
IQALUIT	Pile Installation	N63°44' W68°31'	I-b	M	86-5	86/10	GM	5.2				1.1	Thurber Cons. Ltd.	
IQALUIT	Pile Installation	N63°44' W68°31'	I-b		86-5	86/10/12		6.1	-1.6				Thurber Cons. Ltd.	
IQALUIT	Pile Installation	N63°44' W68°31'	I-b	M	86-6	86/10	GP	5.3			10	0.8	Thurber Cons. Ltd.	
IQALUIT	Pile Installation	N63°44' W68°31'	I-b	M	86-6	86/10	GP	6.9			5	1.1	Thurber Cons. Ltd.	
IQALUIT	Pile Installation	N63°44' W68°31'	I-b	M	86-7	86/10	GP	3.8			3	0.9	Thurber Cons. Ltd.	
IQALUIT	Pile Installation	N63°44' W68°31'	I-b	M	86-7	86/10	GP	5.1			6	1.4	Thurber Cons. Ltd.	
IQALUIT	Pile Installation	N63°44' W68°31'	I-b		86-7	86/10/13		4.6	0.7				Thurber Cons. Ltd.	
IQALUIT	Pile Installation	N63°44' W68°31'	I-b		86-7	86/11/26			-2.3				Thurber Cons. Ltd.	
IQALUIT	Pile Installation	N63°44' W68°31'	I-b		86-8	86/10/13		6.1	0.6				Thurber Cons. Ltd.	
IQALUIT	Pile Installation	N63°44' W68°31'	I-b		86-8	86/10/30		6.1	-1.4				Thurber Cons. Ltd.	
IQALUIT	Pile Installation	N63°44' W68°31'	I-b		86-8	86/11/26		6.1	-2.7				Thurber Cons. Ltd.	
IQALUIT	Pile Installation	N63°44' W68°31'	I-b	M	86-12	86/10	SM	2.4			8	0.1	Thurber Cons. Ltd.	
IQALUIT	Pile Installation	N63°44' W68°31'	I-b	Bm	86-13	86/10	bedrock (granite)	4			3	0.3	Thurber Cons. Ltd.	
IQALUIT	Pile Installation	N63°44' W68°31'	I-b		86-13	86/11/26		3.7	-2.3				Thurber Cons. Ltd.	
IQALUIT	Pile Installation	N63°44' W68°31'	I-b	M	86-15	86/10	SM	3.6			11	0.2	Thurber Cons. Ltd.	
IQALUIT	Pile Installation	N63°44' W68°31'	I-b	Bm	86-16	86/10	bedrock or boulders	3.8			6	0.5	Thurber Cons. Ltd.	Some excess ice
IQALUIT	Pile Installation	N63°44' W68°31'	I-b	M	86-17	86/10	SM	3.8			15	0.4	Thurber Cons. Ltd.	
IQALUIT	Pile Installation	N63°44' W68°31'	I-b	Bm	86-19	86/10	bedrock (granite)	3.6			2	2	Thurber Cons. Ltd.	
IQALUIT	Pile Installation	N63°44' W68°31'	I-b	Bm	86-23	86/10	bedrock (granite)	3			3	1.9	Thurber Cons. Ltd.	

COMMUNITY	PROJECT	LOCATION	GEOLOGICAL UNIT	TERRAIN TYPE	HOLE	DATE	SOIL CLASSIFICATION (USCS)	DEPTH(m)	TEMP (°C)	DENSITY (Mg/m3)	M.C. (%)	SALINITY (ppt)	CONSULTANT	COMMENTS
IQALUIT	Pile Installation	N63°44' W68°31'	I-b	M	86-24	86/10	GP	2.5			7	0.2	Thurber Cons. Ltd.	
IQALUIT	Pile Installation	N63°44' W68°31'	I-b	Rm	86-25	86/10	bedrock (granite)	3.7			6	0.6	Thurber Cons. Ltd.	
IQALUIT	Pile Installation	N63°44' W68°31'	I-b		86-26	86/10	SM	3.3			5	0.8	Thurber Cons. Ltd.	
IQALUIT	Pile Installation	N63°44' W68°31'	I-b	M	86-27	86/10	SM	3.9			11	0.1	Thurber Cons. Ltd.	
IQALUIT	Young Offenders Home	N63°44' W68°31'	I-b	M	87-1	87/11/18	GW-GM	0.7			3	0.7	Thurber Cons. Ltd.	File 15-22-92
IQALUIT	Facility	N63°44' W68°31'	I-b	M	87-1	87/11/18	GW-SW	2.2			3	1.2	Thurber Cons. Ltd.	Salinity determination
IQALUIT	[illegible] Facility	N63°44' W68°31'	I-b	M	87-1	87/11/18	GW-SW	3.8			4	1.4	Thurber Cons. Ltd.	by method 3
IQALUIT	[illegible] Facility	N63°44' W68°31'	I-b	M	87-1	87/11/18	GW	5.3			5	1.3	Thurber Cons. Ltd.	
IQALUIT	[illegible] Facility	N63°44' W68°31'	I-b	M	87-1	87/11/18	GW	6.9			6	1.6	Thurber Cons. Ltd.	
IQALUIT	[illegible] Facility	N63°44' W68°31'	I-b	M	87-2	87/11/18	SP	3.8			11	1.5	Thurber Cons. Ltd.	
IQALUIT	[illegible] Facility	N63°44' W68°31'	I-b	M	87-2	87/11/18	GP-SP	5.3			9	2.3	Thurber Cons. Ltd.	
IQALUIT	[illegible] Facility	N63°44' W68°31'	I-b	M	87-3	87/11/18	SP	3.8			8	1.6	Thurber Cons. Ltd.	
IQALUIT	[illegible] Facility	N63°44' W68°31'	I-b	M	87-3	87/11/18	GP-SP	5.3			9	2.9	Thurber Cons. Ltd.	
IQALUIT	[illegible] Facility	N63°44' W68°31'	I-b		87-3	87/11/24		6.2	-3				Thurber Cons. Ltd.	
IQALUIT	[illegible] Facility	N63°44' W68°31'	I-b	M	87-4	87/11/18	GM-GP	2.3			7	0.8	Thurber Cons. Ltd.	
IQALUIT	[illegible] Facility	N63°44' W68°31'	I-b	M	87-4	87/11/18	SP	3.8			9	1.7	Thurber Cons. Ltd.	
IQALUIT	[illegible] Facility	N63°44' W68°31'	I-b	M	87-4	87/11/18	SP	5.3			12	1.1	Thurber Cons. Ltd.	
IQALUIT	[illegible] Facility	N63°44' W68°31'	I-b	M	87-4	87/11/18	SP	6.9			12	1.2	Thurber Cons. Ltd.	
IQALUIT	[illegible] Facility	N63°44' W68°31'	I-b	M	87-5	87/11/18	GP-SP	2.3			11	0.6	Thurber Cons. Ltd.	
IQALUIT	[illegible] Facility	N63°44' W68°31'	I-b	M	87-5	87/11/18	GW-SW	3.8			8	1.4	Thurber Cons. Ltd.	
IQALUIT	[illegible] Facility	N63°44' W68°31'	I-b	M	87-5	87/11/18	GW-SW	5.3			9	1.1	Thurber Cons. Ltd.	
IQALUIT	[illegible] Facility	N63°44' W68°31'	I-b	M	87-5	87/11/18	GW-SW	6.9			8	1.3	Thurber Cons. Ltd.	
IQALUIT	[illegible] Facility	N63°44' W68°31'	I-b	M	87-6	87/11/18	SM	3.8			13	0.5	Thurber Cons. Ltd.	
IQALUIT	[illegible] Facility	N63°44' W68°31'	I-b	M	87-6	87/11/18	GM-SM	5.3			8	0.9	Thurber Cons. Ltd.	
IQALUIT	[illegible] Facility	N63°44' W68°31'	I-b	M	87-7	87/11/18	SP	3.8			11	1.2	Thurber Cons. Ltd.	
IQALUIT	[illegible] Facility	N63°44' W68°31'	I-b	M	87-7	87/11/18	GW-SW	5.3			13	1.1	Thurber Cons. Ltd.	
IQALUIT	[illegible] Facility	N63°44' W68°31'	I-b		87-7	87/11/24		6.2	-3				Thurber Cons. Ltd.	
IQALUIT	[illegible] Facility	N63°44' W68°31'	I-b	M	87-8	87/11/18	SP	3.9			10	2.1	Thurber Cons. Ltd.	
IQALUIT	[illegible] Facility	N63°44' W68°31'	I-b	M	87-8	87/11/18	SP	5.3			10	2	Thurber Cons. Ltd.	
IQALUIT	[illegible] Facility	N63°44' W68°31'	I-b	M	87-9	87/11/18	GM	3.9			3	1.6	Thurber Cons. Ltd.	
IQALUIT	[illegible] Facility	N63°44' W68°31'	I-b	M	87-9	87/11/18	GM-GP	5.3			9	1.1	Thurber Cons. Ltd.	
IQALUIT	[illegible] Facility	N63°44' W68°31'	I-b		87-9	87/11/24		6.2	-2.9				Thurber Cons. Ltd.	
IQALUIT	[illegible] Facility	N63°44' W68°31'	I-b	M	87-10	87/11/18	GP	3.9			8	1.5	Thurber Cons. Ltd.	
IQALUIT	[illegible] Facility	N63°44' W68°31'	I-b	M	87-10	87/11/18	GP	5.3			3	3.1	Thurber Cons. Ltd.	
IQALUIT	[illegible] Facility	N63°44' W68°31'	I-b	M	87-11	87/11/18	SP	2.3			10	1	Thurber Cons. Ltd.	
IQALUIT	[illegible] Facility	N63°44' W68°31'	I-b	M	87-11	87/11/18	GP	3.9			7	1.6	Thurber Cons. Ltd.	
IQALUIT	[illegible] Facility	N63°44' W68°31'	I-b	M	87-11	87/11/18	GP	5.3			8	1.8	Thurber Cons. Ltd.	
IQALUIT	[illegible] Facility	N63°44' W68°31'	I-b	M	87-11	87/11/18	SP	7.1			9	1.8	Thurber Cons. Ltd.	
IQALUIT	[illegible] Facility	N63°44' W68°31'	I-b	M	87-12	87/11/18	GM-SM	3.9			9	1.1	Thurber Cons. Ltd.	
IQALUIT	[illegible] Facility	N63°44' W68°31'	I-b	M	87-12	87/11/18	GM-GP	5.3			8	1.9	Thurber Cons. Ltd.	
IQALUIT	[illegible] House	N63°44' W68°31'	I-b	M	87-1	87/05	SP	4.5			6	2.2	Thurber Cons. Ltd.	File 19-321-0
IQALUIT	[illegible] House	N63°44' W68°31'	I-b	M	87-1	87/05	SP	6.2			8	0.8	Thurber Cons. Ltd.	Salinity determination
IQALUIT	[illegible] House	N63°44' W68°31'	I-b	M	87-1	87/05	SP	7.8			8	0.8	Thurber Cons. Ltd.	by method 3
IQALUIT	[illegible] House	N63°44' W68°31'	I-b	M	87-2	87/05	SP	4.5			17	1.6	Thurber Cons. Ltd.	
IQALUIT	[illegible] House	N63°44' W68°31'	I-b	M	87-2	87/05	SP	6.2			4	4.9	Thurber Cons. Ltd.	
IQALUIT	[illegible] House	N63°44' W68°31'	I-b	M	87-2	87/05	SP	7.8			12	2.1	Thurber Cons. Ltd.	
IQALUIT	[illegible] House	N63°44' W68°31'	I-b	M	87-3	87/05	SP	2.9			16	0.4	Thurber Cons. Ltd.	
IQALUIT	[illegible] House	N63°44' W68°31'	I-b	M	87-3	87/05	SP	4.5			18	0.4	Thurber Cons. Ltd.	
IQALUIT	[illegible] House	N63°44' W68°31'	I-b	M	87-3	87/05	SP	6.2			18	2.5	Thurber Cons. Ltd.	
IQALUIT	[illegible] House	N63°44' W68°31'	I-b	M	87-3	87/05	SP	7.8			18	3.1	Thurber Cons. Ltd.	
IQALUIT	[illegible] House	N63°44' W68°31'	I-b	M	87-4	87/05	SP	4.5			6	3.6	Thurber Cons. Ltd.	
IQALUIT	[illegible] House	N63°44' W68°31'	I-b	M	87-4	87/05	SP	6.2			6	1.6	Thurber Cons. Ltd.	
IQALUIT	[illegible] House	N63°44' W68°31'	I-b	M	87-4	87/05	SP	7.8			4	2.5	Thurber Cons. Ltd.	
IQALUIT	Discovery Lodge Expansion	N63°44' W68°31'	I-b	M	87-1	87/07/15	ML	2.4			25	5.5	Thurber Cons. Ltd.	File 19-477-01
IQALUIT	Discovery Lodge Expansion	N63°44' W68°31'	I-b	M	87-1	87/07/15	ML	3.7			9	7.9	Thurber Cons. Ltd.	Salinity determination
IQALUIT	Discovery Lodge Expansion	N63°44' W68°31'	I-b	M	87-1	87/07/15	ML	5.3			8	14.1	Thurber Cons. Ltd.	by method 3
IQALUIT	Discovery Lodge Expansion	N63°44' W68°31'	I-b	M	87-2	87/07/15	CL-ML	2.4			10	5	Thurber Cons. Ltd.	
IQALUIT	Discovery Lodge Expansion	N63°44' W68°31'	I-b	M	87-2	87/07/15	CL-ML	3.7			19	7.6	Thurber Cons. Ltd.	
IQALUIT	Discovery Lodge Expansion	N63°44' W68°31'	I-b	M	87-2	87/07/15	SM-ML	5.3			9	14.8	Thurber Cons. Ltd.	
IQALUIT	U of A Pile Test	N63°44' W68°31'	I-b	M	1 - 3	88/06	CL-ML	2.4			9.9	8	University of Alberta	Salinity determination
IQALUIT	U of A Pile Test	N63°44' W68°31'	I-b	M	1 - 3	88/06	CL-ML	3.4			6	16	University of Alberta	by method 1
IQALUIT	U of A Pile Test	N63°44' W68°31'	I-b	M	1 - 3	88/06	CL-ML	4.6			7.3	19	University of Alberta	
IQALUIT	U of A Pile Test	N63°44' W68°31'	I-b	M	1 - 3	88/06	CL-ML	5.5			7.1	20	University of Alberta	
IQALUIT	U of A Pile Test	N63°44' W68°31'	I-b	M	1 - 3	88/06	CL-ML	6.4			6.5	24	University of Alberta	
IQALUIT	U of A Pile Test	N63°44' W68°31'	I-b	M	1 - 12	88/06	CL-ML	5.1			5.6	15	University of Alberta	
IQALUIT	U of A Pile Test	N63°44' W68°31'	I-b	M	1 - 12	88/06	CL-ML	4.6			7	19	University of Alberta	
IQALUIT	U of A Pile Test	N63°44' W68°31'	I-b	M	1 - 12	88/06	CL-ML	6.1			6.8	21	University of Alberta	
IQALUIT	U of A Pile Test	N63°44' W68°31'	I-b	M	1 - 12	88/06	CL-ML	7.6			8.2	22	University of Alberta	
IQALUIT	U of A Pile Test	N63°44' W68°31'	I-b	M	1 - 14	88/06	CL-ML	4.6			7.9	7	University of Alberta	
IQALUIT	U of A Pile Test	N63°44' W68°31'	I-b	M	1 - 14	88/06	CL-ML	6.1			9.6	16	University of Alberta	

COMMUNITY	PROJECT	LOCATION	GEOLOGICAL UNIT	TERRAIN TYPE	HOLE	DATE	SOIL CLASSIFICATION (USCS)	DEPTH(m)	TEMP (°C)	DENSITY (Mg/m3)	M.C. (%)	SALINITY (ppt)	CONSULTANT	COMMENTS
IQALUIT	U of A Pile Test	N63°44' W68°31'	I-b	M	1 - 14	88/06	CL-ML	7.6			8.4	15	University of Alberta	
INUVIK	Forward Operating Location	N68°21' W133°43'								Bulk Density			Thurber Cons. Ltd.	File 17-550-31
INUVIK	Forward Operating Location	N68°21' W133°43'								(kN/m3)			Thurber Cons. Ltd.	Salinity determination
INUVIK	Forward Operating Location	N68°21' W133°43'	III-a	M	88-11	88/11/09	CI	4.1		19.2	21.2	11	Thurber Cons. Ltd.	by method 3
INUVIK	Forward Operating Location	N68°21' W133°43'	III-a	M or R	88-14	88/11/09	CH	1.3		16.4	27.8	1.4	Thurber Cons. Ltd.	
INUVIK	Forward Operating Location	N68°21' W133°43'	III-a	M or R	88-14	88/11/09	CH	2.7		17.4	37.8	4.7	Thurber Cons. Ltd.	
INUVIK	Forward Operating Location	N68°21' W133°43'	III-a	M	88-14	88/11/09	CH	3.7			13.8	9.4	Thurber Cons. Ltd.	
INUVIK	Forward Operating Location	N68°21' W133°43'	III-a	M	88-14	88/11/09	CH	7			15	8.6	Thurber Cons. Ltd.	
INUVIK	Forward Operating Location	N68°21' W133°43'	III-a	M	88-31	88/11/15	CI	3.6		20.1	21.2	10.5	Thurber Cons. Ltd.	
INUVIK	Forward Operating Location	N68°21' W133°43'	III-a	M	88-31	88/11/18		5.4	-3.1				Thurber Cons. Ltd.	
INUVIK	Forward Operating Location	N68°21' W133°43'	III-a	M	88-34A	88/11/11	CL-ML	1.2			38.8	2.3	Thurber Cons. Ltd.	
INUVIK	Forward Operating Location	N68°21' W133°43'	III-a	M	88-34A	88/11/11	CI	2.6			31.2	8.3	Thurber Cons. Ltd.	
INUVIK	Forward Operating Location	N68°21' W133°43'	III-a	M	88-34A	88/11/11	CI	4.2			21.8	10	Thurber Cons. Ltd.	
INUVIK	Forward Operating Location	N68°21' W133°43'	III-a	M	88-34A	88/11/11	CI	5.7			16.7	10.4	Thurber Cons. Ltd.	
INUVIK	Forward Operating Location	N68°21' W133°43'	III-a	M	88-34A	88/11/11	CI	7			17.3	11.3	Thurber Cons. Ltd.	
INUVIK	Forward Operating Location	N68°21' W133°43'	III-a	M	88-34A	88/11/11	CI	8.3			18	12.1	Thurber Cons. Ltd.	
INUVIK	Forward Operating Location	N68°21' W133°43'	III-a	M	88-34A	88/11/11	CH	10.4			18.2	23.5	Thurber Cons. Ltd.	
INUVIK	Forward Operating Location	N68°21' W133°43'	III-a	M	88-34A	88/11/11	CH	11.9			19.9	25.6	Thurber Cons. Ltd.	
INUVIK	Forward Operating Location	N68°21' W133°43'	III-a	M	88-34A	88/11/11	CH	13			13.6	39.2	Thurber Cons. Ltd.	
INUVIK	Forward Operating Location	N68°21' W133°43'	III-a	M	88-34A	88/11/11	CH	14.8			14	41	Thurber Cons. Ltd.	
INUVIK	Forward Operating Location	N68°21' W133°43'	III-a	M	88-42	88/11/10	ML	2.1		20.8	43	1.2	Thurber Cons. Ltd.	
JEAN MARIE CREEK	Norman Wells Pipeline	N61°11.4' W120°42.2'	III-a		85-12B T3	85/04/17		1	-3.41				Hardy Associates Ltd. (1978)	Thermistor installed
JEAN MARIE CREEK	Norman Wells Pipeline	N61°11.4' W120°42.2'	III-a		85-12B T3	85/04/17		2	-2.81				Hardy Associates Ltd. (1978)	and monitored
JEAN MARIE CREEK	Norman Wells Pipeline	N61°11.4' W120°42.2'	III-a		85-12B T3	85/04/17		3	-1.66				Hardy Associates Ltd. (1978)	for EMR
JEAN MARIE CREEK	Norman Wells Pipeline	N61°11.4' W120°42.2'	III-a		85-12B T3	85/04/17		4	-0.64				Hardy Associates Ltd. (1978)	
JEAN MARIE CREEK	Norman Wells Pipeline	N61°11.4' W120°42.2'	III-a		85-12B T3	85/04/17		6	0.1				Hardy Associates Ltd. (1978)	
JEAN MARIE CREEK	Norman Wells Pipeline	N61°11.4' W120°42.2'	III-a		85-12B T3	85/04/17		8	0.23				Hardy Associates Ltd. (1978)	
JEAN MARIE CREEK	Norman Wells Pipeline	N61°11.4' W120°42.2'	III-a		85-12B T3	85/04/17		10	0.34				Hardy Associates Ltd. (1978)	
JEAN MARIE CREEK	Norman Wells Pipeline	N61°11.4' W120°42.2'	III-a		85-12B T3	85/04/17		12.3	0.33				Hardy Associates Ltd. (1978)	
JEAN MARIE CREEK	Norman Wells Pipeline	N61°11.4' W120°42.2'	III-a		85-12B T3	85/04/17		17.2	0.78				Hardy Associates Ltd. (1978)	
JEAN MARIE CREEK	Norman Wells Pipeline	N61°11.4' W120°42.2'	III-a		85-12B T3	87/10/04		1	-0.5				Hardy Associates Ltd. (1978)	
JEAN MARIE CREEK	Norman Wells Pipeline	N61°11.4' W120°42.2'	III-a		85-12B T3	87/10/04		2	-0.21				Hardy Associates Ltd. (1978)	
JEAN MARIE CREEK	Norman Wells Pipeline	N61°11.4' W120°42.2'	III-a		85-12B T3	87/10/04		3	-0.27				Hardy Associates Ltd. (1978)	
JEAN MARIE CREEK	Norman Wells Pipeline	N61°11.4' W120°42.2'	III-a		85-12B T3	87/10/04		4	-0.24				Hardy Associates Ltd. (1978)	
JEAN MARIE CREEK	Norman Wells Pipeline	N61°11.4' W120°42.2'	III-a		85-12B T3	87/10/04		6	0.02				Hardy Associates Ltd. (1978)	
JEAN MARIE CREEK	Norman Wells Pipeline	N61°11.4' W120°42.2'	III-a		85-12B T3	87/10/04		8	0.18				Hardy Associates Ltd. (1978)	
JEAN MARIE CREEK	Norman Wells Pipeline	N61°11.4' W120°42.2'	III-a		85-12B T3	87/10/04		10	0.13				Hardy Associates Ltd. (1978)	
JEAN MARIE CREEK	Norman Wells Pipeline	N61°11.4' W120°42.2'	III-a		85-12B T3	87/10/04		12.5	0.47				Hardy Associates Ltd. (1978)	
JEAN MARIE CREEK	Norman Wells Pipeline	N61°11.4' W120°42.2'	III-a		85-12B T3	87/10/04		17.2	0.77				Hardy Associates Ltd. (1978)	
JEAN MARIE CREEK	Norman Wells Pipeline	N61°11.4' W120°42.2'	III-a	M (?)	85-12B O1	85/03/07	ML	3 to 7.3			~ 40	~ 0.18	Hardy Associates Ltd. (1978)	Salinity testing done
JEAN MARIE CREEK	Norman Wells Pipeline	N61°11.4' W120°42.2'	III-a		85-12B O1	85/03/07							Hardy Associates Ltd. (1978)	at Carleton Univ.
JEAN MARIE CREEK	Norman Wells Pipeline	N61°11.4' W120°42.2'	III-a		85-12B O1	85/03/07							Hardy Associates Ltd. (1978)	for EMR
JEAN MARIE CREEK	Norman Wells Pipeline	N61°11.4' W120°42.2'	III-a		85-12B O1	85/03/07							Hardy Associates Ltd. (1978)	Salinity determination
JEAN MARIE CREEK	Norman Wells Pipeline	N61°11.4' W120°42.2'	III-a		85-12B O1	85/03/07							Hardy Associates Ltd. (1978)	by method 2
MANNERS CREEK	Norman Wells Pipeline	N61°56.7' W121°5.6'	III-a		85-8A T3	85/03/08		1	-3.67				Hardy Associates Ltd. (1978)	Thermistor installed
MANNERS CREEK	Norman Wells Pipeline	N61°56.7' W121°5.6'	III-a		85-8A T3	85/03/08		2	-3.28				Hardy Associates Ltd. (1978)	and monitored
MANNERS CREEK	Norman Wells Pipeline	N61°56.7' W121°5.6'	III-a		85-8A T3	85/03/08		3	-1.75				Hardy Associates Ltd. (1978)	for EMR
MANNERS CREEK	Norman Wells Pipeline	N61°56.7' W121°5.6'	III-a		85-8A T3	85/03/08		4	-0.85				Hardy Associates Ltd. (1978)	
MANNERS CREEK	Norman Wells Pipeline	N61°56.7' W121°5.6'	III-a		85-8A T3	85/03/08		6	-0.38				Hardy Associates Ltd. (1978)	
MANNERS CREEK	Norman Wells Pipeline	N61°56.7' W121°5.6'	III-a		85-8A T3	85/03/08		8	-0.29				Hardy Associates Ltd. (1978)	
MANNERS CREEK	Norman Wells Pipeline	N61°56.7' W121°5.6'	III-a		85-8A T3	85/03/08		10	-0.22				Hardy Associates Ltd. (1978)	
MANNERS CREEK	Norman Wells Pipeline	N61°56.7' W121°5.6'	III-a		85-8A T3	85/03/08		12	-0.01				Hardy Associates Ltd. (1978)	
MANNERS CREEK	Norman Wells Pipeline	N61°56.7' W121°5.6'	III-a		85-8A T3	85/03/08		14	-0.07				Hardy Associates Ltd. (1978)	
MANNERS CREEK	Norman Wells Pipeline	N61°56.7' W121°5.6'	III-a		85-8A T3	85/03/08		17	0.27				Hardy Associates Ltd. (1978)	
MANNERS CREEK	Norman Wells Pipeline	N61°56.7' W121°5.6'	III-a		85-8A T3	87/10/05		1	0.45				Hardy Associates Ltd. (1978)	
MANNERS CREEK	Norman Wells Pipeline	N61°56.7' W121°5.6'	III-a		85-8A T3	87/10/05		2	-0.12				Hardy Associates Ltd. (1978)	
MANNERS CREEK	Norman Wells Pipeline	N61°56.7' W121°5.6'	III-a		85-8A T3	87/10/05		3	-0.19				Hardy Associates Ltd. (1978)	
MANNERS CREEK	Norman Wells Pipeline	N61°56.7' W121°5.6'	III-a		85-8A T3	87/10/05		4	-0.36				Hardy Associates Ltd. (1978)	
MANNERS CREEK	Norman Wells Pipeline	N61°56.7' W121°5.6'	III-a		85-8A T3	87/10/05		6	-0.35				Hardy Associates Ltd. (1978)	
MANNERS CREEK	Norman Wells Pipeline	N61°56.7' W121°5.6'	III-a		85-8A T3	87/10/05		8	-0.5				Hardy Associates Ltd. (1978)	
MANNERS CREEK	Norman Wells Pipeline	N61°56.7' W121°5.6'	III-a		85-8A T3	87/10/05		10	-0.27				Hardy Associates Ltd. (1978)	
MANNERS CREEK	Norman Wells Pipeline	N61°56.7' W121°5.6'	III-a		85-8A T3	87/10/05		12	-0.12				Hardy Associates Ltd. (1978)	
MANNERS CREEK	Norman Wells Pipeline	N61°56.7' W121°5.6'	III-a		85-8A T3	87/10/05		14	0				Hardy Associates Ltd. (1978)	
MANNERS CREEK	Norman Wells Pipeline	N61°56.7' W121°5.6'	III-a		85-8A T3	87/10/05		17	0.35				Hardy Associates Ltd. (1978)	
MANNERS CREEK	Norman Wells Pipeline	N61°56.7' W121°5.6'	III-a		85-8A T3	87/10/05		20	0.6				Hardy Associates Ltd. (1978)	
MANNERS CREEK	Norman Wells Pipeline	N61°56.7' W121°5.6'	III-a							Dry density			Hardy Associates Ltd. (1978)	
MANNERS CREEK	Norman Wells Pipeline	N61°56.7' W121°5.6'	III-a	M (?)	85-8A O1	85/03/05	SM-ML	8.5		1337	29.1	0.02	Hardy Associates Ltd. (1978)	Salinity testing done

COMMUNITY	PROJECT	LOCATION	GEOLOGICAL UNIT	TERRAIN TYPE	HOLE	DATE	SOIL CLASSIFICATION (USCS)	DEPTH(m)	TEMP (°C)	DENSITY (Mg/m3)	M.C. (%)	SALINITY (ppt)	CONSULTANT	COMMENTS
MANNERS CREEK	Norman Wells Pipeline	N61°26.7' W121°5.6'	III-a	M (U)	85-8A G1	[illegible]	SM-ML	1.15		1465	26	0.02	Hardy Associates Ltd. (1978)	at Carleton Univ.
MANNERS CREEK	Norman Wells Pipeline	N61°26.7' W121°5.6'	III-a	M (U)	85-8A G1	[illegible]	SP	1.8		1433	25	0.05	Hardy Associates Ltd. (1978)	for EMR
MANNERS CREEK	Norman Wells Pipeline	N61°26.7' W121°5.6'	III-a	M (U)	85-8A G1	[illegible]	SP	2.35		1329	24.9	0.02	Hardy Associates Ltd. (1978)	Salinity determination
MANNERS CREEK	Norman Wells Pipeline	N61°26.7' W121°5.6'	III-a	M (U)	85-8A G1	[illegible]	SM-ML	2.85		1454	24.6	0.06	Hardy Associates Ltd. (1978)	by method 2
MANNERS CREEK	Norman Wells Pipeline	N61°26.7' W121°5.6'	III-a	M (U)	85-8A G1	[illegible]	SM-ML	3.5		1421	26.2	0.09	Hardy Associates Ltd. (1978)	
MANNERS CREEK	Norman Wells Pipeline	N61°26.7' W121°5.6'	III-a	M (U)	85-8A G1	[illegible]	ML-SM	4.3		1490	28.8	0.06	Hardy Associates Ltd. (1978)	
MANNERS CREEK	Norman Wells Pipeline	N61°26.7' W121°5.6'	III-a	M (U)	85-8A G1	[illegible]	SP-CL	5.15		1341	31.8	0.08	Hardy Associates Ltd. (1978)	
MANNERS CREEK	Norman Wells Pipeline	N61°26.7' W121°5.6'	III-a	M (U)	85-8A G1	[illegible]	CI	5.85		1507	30.7	0.06	Hardy Associates Ltd. (1978)	
MANNERS CREEK	Norman Wells Pipeline	N61°26.7' W121°5.6'	III-a	M (U)	85-8A G1	[illegible]	ML-CI	6.5		1635	23.6	0.09	Hardy Associates Ltd. (1978)	
MANNERS CREEK	Norman Wells Pipeline	N61°26.7' W121°5.6'	III-a	M (U)	85-8A G1	[illegible]	CI	7.25		1176	41.1	0.07	Hardy Associates Ltd. (1978)	
MANNERS CREEK	Norman Wells Pipeline	N61°26.7' W121°5.6'	III-a	M (U)	85-8A G1	[illegible]	CI	8.05		1198	43.6	0.09	Hardy Associates Ltd. (1978)	
MANNERS CREEK	Norman Wells Pipeline	N61°26.7' W121°5.5'	III-a		85-8C T3	[illegible]		1	-0.94				Hardy Associates Ltd. (1978)	Thermistor installed
MANNERS CREEK	Norman Wells Pipeline	N61°26.7' W121°5.5'	III-a		85-8C T3	[illegible]		2	-0.15				Hardy Associates Ltd. (1978)	and monitored
MANNERS CREEK	Norman Wells Pipeline	N61°26.7' W121°5.5'	III-a		85-8C T3	[illegible]		3	-0.14				Hardy Associates Ltd. (1978)	for EMR
MANNERS CREEK	Norman Wells Pipeline	N61°26.7' W121°5.5'	III-a		85-8C T3	[illegible]		4	-0.03				Hardy Associates Ltd. (1978)	
MANNERS CREEK	Norman Wells Pipeline	N61°26.7' W121°5.5'	III-a		85-8C T3	[illegible]		6	-0.05				Hardy Associates Ltd. (1978)	
MANNERS CREEK	Norman Wells Pipeline	N61°26.7' W121°5.5'	III-a		85-8C T3	[illegible]		8	-0.02				Hardy Associates Ltd. (1978)	
MANNERS CREEK	Norman Wells Pipeline	N61°26.7' W121°5.5'	III-a		85-8C T3	[illegible]		10	0.52				Hardy Associates Ltd. (1978)	
MANNERS CREEK	Norman Wells Pipeline	N61°26.7' W121°5.5'	III-a		85-8C T3	[illegible]		12	0.63				Hardy Associates Ltd. (1978)	
MANNERS CREEK	Norman Wells Pipeline	N61°26.7' W121°5.5'	III-a		85-8C T3	[illegible]		14	0.61				Hardy Associates Ltd. (1978)	
MANNERS CREEK	Norman Wells Pipeline	N61°26.7' W121°5.5'	III-a		85-8C T3	[illegible]		17	1.04				Hardy Associates Ltd. (1978)	
MANNERS CREEK	Norman Wells Pipeline	N61°26.7' W121°5.5'	III-a		85-8C T3	[illegible]		20	1.47				Hardy Associates Ltd. (1978)	
MANNERS CREEK	Norman Wells Pipeline	N61°26.7' W121°5.5'	III-a		85-8C T3	17/10/85		1	0.06				Hardy Associates Ltd. (1978)	
MANNERS CREEK	Norman Wells Pipeline	N61°26.7' W121°5.5'	III-a		85-8C T3	17/10/85		2	-0.12				Hardy Associates Ltd. (1978)	
MANNERS CREEK	Norman Wells Pipeline	N61°26.7' W121°5.5'	III-a		85-8C T3	17/10/85		3	-0.15				Hardy Associates Ltd. (1978)	
MANNERS CREEK	Norman Wells Pipeline	N61°26.7' W121°5.5'	III-a		85-8C T3	17/10/85		4	-0.1				Hardy Associates Ltd. (1978)	
MANNERS CREEK	Norman Wells Pipeline	N61°26.7' W121°5.5'	III-a		85-8C T3	17/10/85		6	0.09				Hardy Associates Ltd. (1978)	
MANNERS CREEK	Norman Wells Pipeline	N61°26.7' W121°5.5'	III-a		85-8C T3	17/10/85		8	0.32				Hardy Associates Ltd. (1978)	
MANNERS CREEK	Norman Wells Pipeline	N61°26.7' W121°5.5'	III-a		85-8C T3	17/10/85		10	0.58				Hardy Associates Ltd. (1978)	
MANNERS CREEK	Norman Wells Pipeline	N61°26.7' W121°5.5'	III-a		85-8C T3	17/10/85		12	0.74				Hardy Associates Ltd. (1978)	
MANNERS CREEK	Norman Wells Pipeline	N61°26.7' W121°5.5'	III-a		85-8C T3	17/10/85		14	0.96				Hardy Associates Ltd. (1978)	
MANNERS CREEK	Norman Wells Pipeline	N61°26.7' W121°5.5'	III-a		85-8C T3	17/10/85		17	1.37				Hardy Associates Ltd. (1978)	
MANNERS CREEK	Norman Wells Pipeline	N61°26.7' W121°5.5'	III-a		85-8C T3	17/10/85		20	1.67				Hardy Associates Ltd. (1978)	
MANNERS CREEK	Norman Wells Pipeline	N61°26.7' W121°5.5'	III-a	M (U)	85-8C G1	[illegible]	ML	1.85		1097	34.9	0.22	Hardy Associates Ltd. (1978)	Salinity testing done
MANNERS CREEK	Norman Wells Pipeline	N61°26.7' W121°5.5'	III-a	M (U)	85-8C G1	[illegible]	ML	2.07		1038	79	0.25	Hardy Associates Ltd. (1978)	at Carleton Univ.
MANNERS CREEK	Norman Wells Pipeline	N61°26.7' W121°5.5'	III-a	M (U)	85-8C G1	[illegible]	ML	2.12		926	132.9	0.22	Hardy Associates Ltd. (1978)	for EMR
MANNERS CREEK	Norman Wells Pipeline	N61°26.7' W121°5.5'	III-a	M (U)	85-8C G1	[illegible]	ML	2.67		1111	56.7	0.22	Hardy Associates Ltd. (1978)	Salinity determination
MANNERS CREEK	Norman Wells Pipeline	N61°26.7' W121°5.5'	III-a										Hardy Associates Ltd. (1978)	by method 2
PANGNIRTUNG	[illegible]	N66°08' W65°43'	I-b	M	86-1	86/11/29	CL	3.9			20	16.6	Thurber Cons. Ltd.	File 15-22-72
PANGNIRTUNG	[illegible]	N66°08' W65°43'	I-b	M	86-1	86/11/29	CL	4.8			20	25.1	Thurber Cons. Ltd.	Airtrack drill
PANGNIRTUNG	[illegible]	N66°08' W65°43'	I-b		86-1	86/11/30			-4.6				Thurber Cons. Ltd.	Active layer = 1.5m
PANGNIRTUNG	[illegible]	N66°08' W65°43'	I-b		86-1	86/12/02			-5.6				Thurber Cons. Ltd.	Salinity determination
PANGNIRTUNG	[illegible]	N66°08' W65°43'	I-b	M	86-2	86/11/29	CL	3.8			7	8.2	Thurber Cons. Ltd.	by method 3
PANGNIRTUNG	[illegible]	N66°08' W65°43'	I-b	M	86-2	86/11/29	SM	5.3			7	7.6	Thurber Cons. Ltd.	
PANGNIRTUNG	[illegible]	N66°08' W65°43'	I-b	M	86-3	86/11/30	SM-ML	3.8			10	5	Thurber Cons. Ltd.	
PANGNIRTUNG	[illegible]	N66°08' W65°43'	I-b	M	86-3	86/11/30	SM-ML	5.3			13	11.7	Thurber Cons. Ltd.	
PANGNIRTUNG	[illegible]	N66°08' W65°43'	I-b		86-3	86/12/02		6	-4.4				Thurber Cons. Ltd.	
PANGNIRTUNG	[illegible]	N66°08' W65°43'	I-b	M	86-4	86/11/30	ML	3.8			19	11.7	Thurber Cons. Ltd.	
PANGNIRTUNG	[illegible]	N66°08' W65°43'	I-b	M	86-4	86/11/30	SM	5.3			6	9.3	Thurber Cons. Ltd.	
PANGNIRTUNG	[illegible]	N66°08' W65°43'	I-b	M	86-5	86/11/30	ML	3.8			17	19.1	Thurber Cons. Ltd.	
PANGNIRTUNG	[illegible]	N66°08' W65°43'	I-b	M	86-5	86/11/30	ML	5.3			10	25.6	Thurber Cons. Ltd.	
PANGNIRTUNG	[illegible]	N66°08' W65°43'	I-b	M	86-6	86/11/30	ML	3.8			16	12.4	Thurber Cons. Ltd.	
PANGNIRTUNG	[illegible]	N66°08' W65°43'	I-b	M	86-7	86/12/01	CL	3.8			25	16.6	Thurber Cons. Ltd.	
PANGNIRTUNG	[illegible]	N66°08' W65°43'	I-b	M	86-7	86/12/01	CL	4.9			22	21.5	Thurber Cons. Ltd.	
PANGNIRTUNG	[illegible]	N66°08' W65°43'	I-b		86-7	86/12/02			-4.8				Thurber Cons. Ltd.	
PANGNIRTUNG	[illegible]	N66°08' W65°43'	I-b	M	86-8	86/12/01	ML	3.2			16	14.6	Thurber Cons. Ltd.	
PANGNIRTUNG	[illegible]	N66°08' W65°43'	I-b	M	86-8	86/12/01	ML	4.1			16	31.3	Thurber Cons. Ltd.	
PANGNIRTUNG	[illegible]	N66°08' W65°43'	I-b	M	86-8	86/12/01	CL	3.3			19	17.5	Thurber Cons. Ltd.	
PANGNIRTUNG	Recreation Complex	N66°08' W65°43'	I-b	M	86-1	86/12/03	SM	2.3			5	4.7	Thurber Cons. Ltd.	File 15-22-81
PANGNIRTUNG	Recreation Complex	N66°08' W65°43'	I-b	M	86-1	86/12/03	SP-SM	3.8			6	19.9	Thurber Cons. Ltd.	Salinity determination
PANGNIRTUNG	Recreation Complex	N66°08' W65°43'	I-b	M	86-1	86/12/03	SP-SM	5.3			6	28.8	Thurber Cons. Ltd.	by method 3
PANGNIRTUNG	Recreation Complex	N66°08' W65°43'	I-b		86-1	86/12/04		6.1	-4.3				Thurber Cons. Ltd.	
PANGNIRTUNG	Recreation Complex	N66°08' W65°43'	I-b	M	86-2	86/12/03	SM	0.8			16	8.1	Thurber Cons. Ltd.	
PANGNIRTUNG	Recreation Complex	N66°08' W65°43'	I-b	M	86-3	86/12/03	SM	0.8			11	8.2	Thurber Cons. Ltd.	
PANGNIRTUNG	Recreation Complex	N66°08' W65°43'	I-b	M	86-4	86/12/03	SM	2.3			16	7.8	Thurber Cons. Ltd.	
PANGNIRTUNG	Recreation Complex	N66°08' W65°43'	I-b	M	86-4	86/12/03	SM	3.8			10	13.3	Thurber Cons. Ltd.	
PANGNIRTUNG	Recreation Complex	N66°08' W65°43'	I-b	M	86-4	86/12/03	SM	5.3			10	23.9	Thurber Cons. Ltd.	
PANGNIRTUNG	Adfreeze pile Test	N66°08' W65°43'	I-b		Lot 2 Pile 9	1986	(no soil type)				0.12	89.2	Thurber Cons. Ltd.	File 15-22-90
PANGNIRTUNG	Adfreeze pile Test	N66°08' W65°43'	I-b		Lot 2 Pile 30	1986	(no soil type)				0.06	166.3	Thurber Cons. Ltd.	Salinity determination

COMMUNITY	PROJECT	LOCATION	GEOLOGICAL UNIT	TERRAIN TYPE	HOLE	DATE	SOIL CLASSIFICATION (USCS)	DEPTH(m)	TEMP (°C)	DENSITY (Mg/m3)	M.C. (%)	SALINITY (ppt)	CONSULTANT	COMMENTS
PANGNIRTUNG	Adfreeze pile Test	N66°08' W65°43'	I-b		Lot 3 Pile 4	1986	(no soil type)				0.08	133.4	Thurber Cons. Ltd.	by method 3
PANGNIRTUNG	Adfreeze pile Test	N66°08' W65°43'	I-b		Lot 4 Pile 21	1987	(no soil type)				0.07	208	Thurber Cons. Ltd.	
PANGNIRTUNG		N66°08' W65°43'	I-b											
PELLY BAY	Adfreeze pile Test	N68°32' W89°48'	II-b			87/10/24	(no soil type)	0-1.5			5.7	12	Thurber Cons. Ltd.	Thurber's
PELLY BAY	Adfreeze pile Test	N68°32' W89°48'	II-b			87/10/24	(no soil type)	1.5-3			29.9	14.5	Thurber Cons. Ltd.	Salinity determination
PELLY BAY	Adfreeze pile Test	N68°32' W89°48'	II-b			87/10/24	(no soil type)	3-4.5			12.4	29.8	Thurber Cons. Ltd.	by method 3
PELLY BAY	Adfreeze pile Test	N68°32' W89°48'	II-b			87/10/24	(no soil type)	4.5-6.1			23.1	33.7	Thurber Cons. Ltd.	
POND INLET	Primary School	N72°41' W78°00'	I-a	M	86-1	86/08/25	SP	3.8			13	6.8	Thurber Cons. Ltd.	File 15-22-73
POND INLET	Primary School	N72°41' W78°00'	I-a		86-1	86/08/26		5	-5				Thurber Cons. Ltd.	Active layer maximum
POND INLET	Primary School	N72°41' W78°00'	I-a	M	86-2	86/08/25	SM	3.8			7	13.7	Thurber Cons. Ltd.	depth 1.5m
POND INLET	Primary School	N72°41' W78°00'	I-a	M	86-2	86/08/25	SM	5.3			6	23.4	Thurber Cons. Ltd.	Salinity determination
POND INLET	Primary School	N72°41' W78°00'	I-a	M	86-3	86/08/25	SM	3.8			7	21.1	Thurber Cons. Ltd.	by method 3
POND INLET	Primary School	N72°41' W78°00'	I-a		86-3	86/08/26		6.1	-9.2				Thurber Cons. Ltd.	
POND INLET	Primary School	N72°41' W78°00'	I-a	M	86-4	86/08/25	SM	3.8			16	8.9	Thurber Cons. Ltd.	
POND INLET	Primary School	N72°41' W78°00'	I-a	M	86-4	86/08/25	SM	6.9			11	21.2	Thurber Cons. Ltd.	
POND INLET	Primary School	N72°41' W78°00'	I-a		86-5	86/08/26		2.9	-5				Thurber Cons. Ltd.	
POND INLET	Primary School	N72°41' W78°00'	I-a	M	86-5	86/08/25	SP	3.8			13	3.5	Thurber Cons. Ltd.	
POND INLET	Primary School	N72°41' W78°00'	I-a	M	86-5	86/08/25	SP-SM	5.3			16	4.6	Thurber Cons. Ltd.	
POND INLET	Proposed subdivision	N72°41' W78°00'	I-a	M	87-3	87/05/06	Boulders	2			12	2.6	Thurber Cons. Ltd.	File 15-23-43
POND INLET	Proposed subdivision	N72°41' W78°00'	I-a		87-6	87/06/10		1	-2.8				Thurber Cons. Ltd.	Salinity determination
POND INLET	Proposed subdivision	N72°41' W78°00'	I-a		87-7	87/06/15		6.4	-14.3				Thurber Cons. Ltd.	by method 3
POND INLET	Proposed subdivision	N72°41' W78°00'	I-a	M	87-9	87/06/11	SM	0.7			9	1.3	Thurber Cons. Ltd.	
POND INLET	Proposed subdivision	N72°41' W78°00'	I-a	M	87-9	87/06/11	SM	2.4			15	1.5	Thurber Cons. Ltd.	
POND INLET	Proposed subdivision	N72°41' W78°00'	I-a	M	87-9	87/06/11	CI	4			13	7.7	Thurber Cons. Ltd.	
POND INLET	Proposed subdivision	N72°41' W78°00'	I-a	M	87-9	87/06/11	SC-CL	5.2			12	11.4	Thurber Cons. Ltd.	
POND INLET	Proposed subdivision	N72°41' W78°00'	I-a	M	87-12	87/06/11	SM	3.9			12	0.7	Thurber Cons. Ltd.	
POND INLET	Proposed subdivision	N72°41' W78°00'	I-a		87-12	87/06/11		6.1	-14				Thurber Cons. Ltd.	
POND INLET	Proposed subdivision	N72°41' W78°00'	I-a	M	87-12	87/06/11	SP-SM	6.9			9	1.6	Thurber Cons. Ltd.	
POND INLET	Proposed subdivision	N72°41' W78°00'	I-a	M	87-13	87/06/11	SM-SP	0.9			4	1.2	Thurber Cons. Ltd.	
POND INLET	Proposed subdivision	N72°41' W78°00'	I-a	M	87-13	87/06/11	SM-SP	2.3			5	1.6	Thurber Cons. Ltd.	
POND INLET	Proposed subdivision	N72°41' W78°00'	I-a	M	87-13	87/06/11	GM	3.9			6	0.5	Thurber Cons. Ltd.	
POND INLET	Proposed subdivision	N72°41' W78°00'	I-a	M	87-13	87/06/11	SM	5.5			4	12.3	Thurber Cons. Ltd.	
POND INLET	Proposed subdivision	N72°41' W78°00'	I-a	M	87-20	87/06/13	SP-SM	2.3			8	2	Thurber Cons. Ltd.	
POND INLET	Proposed subdivision	N72°41' W78°00'	I-a	M	87-20	87/06/13	SP	3.8			6	4	Thurber Cons. Ltd.	
POND INLET	Proposed subdivision	N72°41' W78°00'	I-a	M	87-20	87/06/13	SP	5.4			6	17.7	Thurber Cons. Ltd.	
POND INLET	Proposed subdivision	N72°41' W78°00'	I-a	M	87-21	87/06/13	SC	0.8			17	1	Thurber Cons. Ltd.	
POND INLET	Proposed subdivision	N72°41' W78°00'	I-a	M	87-21	87/06/13	SM	2.3			15	4	Thurber Cons. Ltd.	
POND INLET	Proposed subdivision	N72°41' W78°00'	I-a	M	87-21	87/06/13	GM	4.3			12	5.9	Thurber Cons. Ltd.	
POND INLET	Proposed subdivision	N72°41' W78°00'	I-a	M	87-21	87/06/13	SM	5.5			6	9.4	Thurber Cons. Ltd.	
POND INLET	Proposed subdivision	N72°41' W78°00'	I-a		87-23	87/06/15		6.1	-13.1				Thurber Cons. Ltd.	
POND INLET	Water Supply	N72°41' W78°00'	I-a	M	87-1A	87/06/12	SM	3.8			8	5.5	Thurber Cons. Ltd.	File 17-397-023
POND INLET	Water Supply	N72°41' W78°00'	I-a	M	87-1A	87/06/12	SM	5.3			12	1.8	Thurber Cons. Ltd.	Salinity determination
POND INLET	Water Supply	N72°41' W78°00'	I-a		87-1A	87/06/14		6	-2.6				Thurber Cons. Ltd.	by method 3
POND INLET	Water Supply	N72°41' W78°00'	I-a		87-1A	87/06/15		6	-3.7				Thurber Cons. Ltd.	
POND INLET	Water Supply	N72°41' W78°00'	I-a	M	87-1A	87/06/12	SM	6.9			18	0.4	Thurber Cons. Ltd.	
POND INLET	Water Supply	N72°41' W78°00'	I-a	M	87-2A	87/06/12	SP	3.7			12	0.2	Thurber Cons. Ltd.	
POND INLET	Water Supply	N72°41' W78°00'	I-a	M	87-2A	87/06/12	SP	5.3			11	0.2	Thurber Cons. Ltd.	
POND INLET	Water Supply	N72°41' W78°00'	I-a	M	87-2A	87/06/14		6	-9.3				Thurber Cons. Ltd.	
POND INLET	Water Supply	N72°41' W78°00'	I-a		87-2A	87/06/15		6	-10				Thurber Cons. Ltd.	
POND INLET	Water Supply	N72°41' W78°00'	I-a	M	87-2A	87/06/12	SP	7			9	0.3	Thurber Cons. Ltd.	
POND INLET	Water Supply	N72°41' W78°00'	I-a		87-3A	87/06/14		6	-4.1				Thurber Cons. Ltd.	
POND INLET	Water Supply	N72°41' W78°00'	I-a		87-3A	87/06/15		6	-3.5				Thurber Cons. Ltd.	
POND INLET	Water Supply	N72°41' W78°00'	I-a		87-4A	87/06/14		6	-4.1				Thurber Cons. Ltd.	
POND INLET	Water Supply	N72°41' W78°00'	I-a		87-4A	87/06/15		6	-4.1				Thurber Cons. Ltd.	
RANKINS INLET	Education Center	N62°49' W92°05'	II-a	M	86-1	86/07/30	SM-ML	3.7			3	2.6	Thurber Cons. Ltd.	File 15-22-70
RANKINS INLET	Education Center	N62°49' W92°05'	II-a	M	86-2	86/07/30	SM	2.4			6	3	Thurber Cons. Ltd.	Active layer +/- 1m
RANKINS INLET	Education Center	N62°49' W92°05'	II-a	M	86-3	86/07/30	SM-ML	2.3			6	3.9	Thurber Cons. Ltd.	Salinity determination
RANKINS INLET	Education Center	N62°49' W92°05'	II-a	M	86-4	86/07/30	SM	2.7			7	4.1	Thurber Cons. Ltd.	by method 3
RANKINS INLET	Education Center	N62°49' W92°05'	II-a	M	86-5	86/07/30	SM	2.4			11	4.3	Thurber Cons. Ltd.	
RANKINS INLET	Education Center	N62°49' W92°05'	II-a	M	86-6	86/07/30	SM-ML	3.8			6	4.3	Thurber Cons. Ltd.	
RANKINS INLET	Education Center	N62°49' W92°05'	II-a	M	86-7	86/07/30	SM-ML	6.8			7	4.5	Thurber Cons. Ltd.	
RANKINS INLET	Education Center	N62°49' W92°05'	II-a	M	86-15	86/07/31	SM-ML	3.8			9	3.4	Thurber Cons. Ltd.	
RANKINS INLET	Education Center	N62°49' W92°05'	II-a	M	86-16	86/07/31	SM-ML	4.8			5	5.4	Thurber Cons. Ltd.	
RANKINS INLET	Education Center	N62°49' W92°05'	II-a		86-3	86/08/01		0.35	3.7				Thurber Cons. Ltd.	
RANKINS INLET	Education Center	N62°49' W92°05'	II-a		86-3	86/08/01		0.66	1.8				Thurber Cons. Ltd.	
RANKINS INLET	Education Center	N62°49' W92°05'	II-a		86-3	86/08/01		0.96	-0.2				Thurber Cons. Ltd.	
RANKINS INLET	Education Center	N62°49' W92°05'	II-a		86-3	86/08/01		1.76	-2.2				Thurber Cons. Ltd.	

COMMUNITY	PROJECT	LOCATION	GEOLOGICAL UNIT	TERRAIN TYPE	HOLE	DATE	SOIL CLASSIFICATION (USCS)	DEPTH(m)	TEMP (°C)	DENSITY (Mg/m3)	M.C. (%)	SALINITY (ppt)	CONSULTANT	COMMENTS
RANKINE INLET	Education Center	N62°49' W92°05'	II-a		86-3	86/08/01		2.49	-3.8				Thurber Cons. Ltd.	
RANKINE INLET	Education Center	N62°49' W92°05'	II-a		86-3	86/08/01		4.01	-3.7				Thurber Cons. Ltd.	
RANKINE INLET	Education Center	N62°49' W92°05'	II-a		86-3	86/08/01		3.54	-7				Thurber Cons. Ltd.	
RANKINE INLET	Education Center	N62°49' W92°05'	II-a		86-5	86/07/31		0.25	7.7				Thurber Cons. Ltd.	
RANKINE INLET	Education Center	N62°49' W92°05'	II-a		86-5	86/07/31		0.55	1.5				Thurber Cons. Ltd.	
RANKINE INLET	Education Center	N62°49' W92°05'	II-a		86-5	86/07/31		0.86	-8.5				Thurber Cons. Ltd.	
RANKINE INLET	Education Center	N62°49' W92°05'	II-a		86-5	86/07/31		1.16	-1.8				Thurber Cons. Ltd.	
RANKINE INLET	Education Center	N62°49' W92°05'	II-a		86-5	86/07/31		1.77	-3.5				Thurber Cons. Ltd.	
RANKINE INLET	Education Center	N62°49' W92°05'	II-a		86-5	86/07/31		2.69	-5.3				Thurber Cons. Ltd.	
RANKINE INLET	Education Center	N62°49' W92°05'	II-a		86-5	86/07/31		4.21	-7.7				Thurber Cons. Ltd.	
RANKINE INLET	Education Center	N62°49' W92°05'	II-a		86-5	86/07/31		5.74	-8.2				Thurber Cons. Ltd.	
RANKINE INLET	Education Center	N62°49' W92°05'	II-a		86-13	86/08/01		6.1	-7.7				Thurber Cons. Ltd.	
RANKINE INLET	Education Center	N62°49' W92°05'	II-a		86-22	86/08/01		4.6	-7.7				Thurber Cons. Ltd.	
RANKINE INLET	Fish Processing Plant	N62°49' W92°05'	II-a	M	87-1	87/05/08	GM-SM	3			8	6.6	Thurber Cons. Ltd.	File 15-41-0
RANKINE INLET	Fish Processing Plant	N62°49' W92°05'	II-a	M	87-1	87/05/08	GM-SM	4.6			5	6.5	Thurber Cons. Ltd.	Salinity determination
RANKINE INLET	Fish Processing Plant	N62°49' W92°05'	II-a	M	87-1	87/05/08	GM-SM	6.1			9	13.8	Thurber Cons. Ltd.	by method 3
RANKINE INLET	Fish Processing Plant	N62°49' W92°05'	II-a		87-1	87/05/09		6	-7.7				Thurber Cons. Ltd.	
RANKINE INLET	Fish Processing Plant	N62°49' W92°05'	II-a	M	87-2	87/05/08	ML	3			21	15.2	Thurber Cons. Ltd.	
RANKINE INLET	Fish Processing Plant	N62°49' W92°05'	II-a	M	87-2	87/05/08	GM	4.6			7	16.3	Thurber Cons. Ltd.	
RANKINE INLET	Fish Processing Plant	N62°49' W92°05'	II-a	M	87-2	87/05/08	GM	6.1			5	23	Thurber Cons. Ltd.	
RANKINE INLET	Fish Processing Plant	N62°49' W92°05'	II-a		87-2	87/05/09		6	-4.5				Thurber Cons. Ltd.	
RANKINE INLET	Fish Processing Plant	N62°49' W92°05'	II-a	M	87-3	87/05/08	GM	3			8	22.7	Thurber Cons. Ltd.	
RANKINE INLET	Fish Processing Plant	N62°49' W92°05'	II-a	M	87-3	87/05/08	GM	4.6			9	19.6	Thurber Cons. Ltd.	
RANKINE INLET	Fish Processing Plant	N62°49' W92°05'	II-a	M	87-3	87/05/08	GM	6.1			7	19.6	Thurber Cons. Ltd.	
RANKINE INLET	Fish Processing Plant	N62°49' W92°05'	II-a		87-3	87/05/09		6	-5				Thurber Cons. Ltd.	
RANKINE INLET	Fish Processing Plant	N62°49' W92°05'	II-a	M	87-4	87/05/08	ML	3			19	21.3	Thurber Cons. Ltd.	
RANKINE INLET	Fish Processing Plant	N62°49' W92°05'	II-a	M	87-4	87/05/08	GM	4.6			7	25.6	Thurber Cons. Ltd.	
RANKINE INLET	Fish Processing Plant	N62°49' W92°05'	II-a	M	87-4	87/05/08	GM	6.1			2	30.6	Thurber Cons. Ltd.	
RANKINE INLET	Fish Processing Plant	N62°49' W92°05'	II-a		87-4	87/05/09		6	-8				Thurber Cons. Ltd.	
RANKINE INLET	Fish Processing Plant	N62°49' W92°05'	II-a	M	87-5	87/05/08	ML	3			23	17.8	Thurber Cons. Ltd.	
RANKINE INLET	Fish Processing Plant	N62°49' W92°05'	II-a	M	87-5	87/05/08	GM-SM	4.6			8	21	Thurber Cons. Ltd.	
RANKINE INLET	Fish Processing Plant	N62°49' W92°05'	II-a	M	87-5	87/05/08	SM	6.1			5	14.6	Thurber Cons. Ltd.	
RANKINE INLET	Fish Processing Plant	N62°49' W92°05'	II-a	M	87-6	87/05/08	GM-SM	3			8	8.6	Thurber Cons. Ltd.	
RANKINE INLET	Fish Processing Plant	N62°49' W92°05'	II-a	M	87-6	87/05/08	GM-SM	4.6			6	15.9	Thurber Cons. Ltd.	
REPULSE BAY	Proposed New School	N66°32' W86°15'	II-a	Rn	87-1	87/11/12	Bedrock (granite)	2.6			3	1.6	Thurber Cons. Ltd.	File 15-22-96
REPULSE BAY	Proposed New School	N66°32' W86°15'	II-a		87-1	87/11/13		2.75	-4.2				Thurber Cons. Ltd.	Temperature at 10:00
REPULSE BAY	Proposed New School	N66°32' W86°15'	II-a		87-1	87/11/13		2.75	-5.1				Thurber Cons. Ltd.	Temperature at 14:00
REPULSE BAY	Proposed New School	N66°32' W86°15'	II-a	W	87-2	87/11/12	SP-SM	1.4			12	0.9	Thurber Cons. Ltd.	Salinity determination
REPULSE BAY	Proposed New School	N66°32' W86°15'	II-a	Rn	87-2	87/11/12	Bedrock (granite)	2.6			4	2.8	Thurber Cons. Ltd.	by method 3
REPULSE BAY	Proposed New School	N66°32' W86°15'	II-a	Rn	87-2	87/11/12	Bedrock (granite)	3.7			3	2.8	Thurber Cons. Ltd.	
REPULSE BAY	Proposed New School	N66°32' W86°15'	II-a	W	87-3	87/11/12	SP-SM	1.4			9	2.3	Thurber Cons. Ltd.	
REPULSE BAY	Proposed New School	N66°32' W86°15'	II-a	W	87-3	87/11/12	SM-ML	4			11	10.4	Thurber Cons. Ltd.	
REPULSE BAY	Proposed New School	N66°32' W86°15'	II-a		87-3	87/11/13		4.27	-5.3				Thurber Cons. Ltd.	Temperature at 10:00
REPULSE BAY	Proposed New School	N66°32' W86°15'	II-a		87-3	87/11/13		4.27	-6.4				Thurber Cons. Ltd.	Temperature at 14:00
REPULSE BAY	Proposed New School	N66°32' W86°15'	II-a	W	87-5	87/11/12	GM-GP	1.4			11	1.1	Thurber Cons. Ltd.	
REPULSE BAY	Proposed New School	N66°32' W86°15'	II-a		87-5	87/11/13		3.05	-5.2				Thurber Cons. Ltd.	Temperature at 10:00
REPULSE BAY	Proposed New School	N66°32' W86°15'	II-a		87-5	87/11/13		3.05	-6.3				Thurber Cons. Ltd.	Temperature at 14:00
REPULSE BAY	Proposed New School	N66°32' W86°15'	II-a	Rn	87-6	87/11/13	Bedrock (granite)	2.7			3	3.2	Thurber Cons. Ltd.	
REPULSE BAY	Adfreeze Pile Test	N66°32' W86°15'	II-a		87-1	87/10/26	(no soil type)	0-1.5			12.5	0.56	Thurber Cons. Ltd.	File 15-22-90
REPULSE BAY	Adfreeze Pile Test	N66°32' W86°15'	II-a		87-1	87/10/26	(no soil type)	1.5-3			18.6	0.48	Thurber Cons. Ltd.	Salinity determination
REPULSE BAY	Adfreeze Pile Test	N66°32' W86°15'	II-a		87-1	87/10/26	(no soil type)	3-4.5			5.3	2.2	Thurber Cons. Ltd.	by method 3
REPULSE BAY	Adfreeze Pile Test	N66°32' W86°15'	II-a		87-1	87/10/26	(no soil type)	4.5-6			18.8	0.9	Thurber Cons. Ltd.	
RICHARDS ISLAND	[illegible] Area Drilling	W134°22.5' to 134°45'	III-c							Bulk density			Hardy Associates Ltd. (1978)	Continuous permafrost
RICHARDS ISLAND	[illegible] Area Drilling	N69°25' to 69°32.5'	III-c	F	HA83-D1	83/05	ML-OL	0.5			99	1	Hardy Associates Ltd. (1978)	in Uplands
RICHARDS ISLAND	[illegible] Area Drilling	W134°22.5' to 134°45'	III-c	F	HA83-D1	83/05	ML-OL	0.9		1139	138	1.2	Hardy Associates Ltd. (1978)	Discontinuous pf
RICHARDS ISLAND	[illegible] Area Drilling	N69°25' to 69°32.5'	III-c	F	HA83-D1	83/05	ML	2.2			33	0.9	Hardy Associates Ltd. (1978)	in modern delta
RICHARDS ISLAND	[illegible] Area Drilling	W134°22.5' to 134°45'	III-c	F	HA83-D1	83/05	ML	3.3		1505	33	2.4	Hardy Associates Ltd. (1978)	Salinity determination
RICHARDS ISLAND	[illegible] Area Drilling	N69°25' to 69°32.5'	III-c	F	HA83-D1	83/05	ML	4.3			77	0.7	Hardy Associates Ltd. (1978)	probably by method 3
RICHARDS ISLAND	[illegible] Area Drilling	W134°22.5' to 134°45'	III-c	F	HA83-D1	83/05	CL	5			43	1.8	Hardy Associates Ltd. (1978)	
RICHARDS ISLAND	[illegible] Area Drilling	N69°25' to 69°32.5'	III-c	F	HA83-D1	83/05	ML	6.3		1819	32	2.3	Hardy Associates Ltd. (1978)	
RICHARDS ISLAND	[illegible] Area Drilling	W134°22.5' to 134°45'	III-c	M or W"O"	HA83-D1	83/05	CL	7.4		2082	16	4.5	Hardy Associates Ltd. (1978)	
RICHARDS ISLAND	[illegible] Area Drilling	N69°25' to 69°32.5'	III-c	M or W"O"	HA83-D1	83/05	CL	8.2			18	2.5	Hardy Associates Ltd. (1978)	
RICHARDS ISLAND	[illegible] Area Drilling	W134°22.5' to 134°45'	III-c	M or W"O"	HA83-D1	83/05	CL	9.2			19	2.1	Hardy Associates Ltd. (1978)	
RICHARDS ISLAND	[illegible] Area Drilling	N69°25' to 69°32.5'	III-c	M or W"O"	HA83-D1	83/05	CL	9.8		2073	18	3.3	Hardy Associates Ltd. (1978)	
RICHARDS ISLAND	[illegible] Area Drilling	W134°22.5' to 134°45'	III-c	F"O"	HA83-D1	83/05	SM	16.1			28	1.2	Hardy Associates Ltd. (1978)	
RICHARDS ISLAND	[illegible] Area Drilling	N69°25' to 69°32.5'	III-c	F"O"	HA83-D1	83/05	SM	20.8		1912	26	1.8	Hardy Associates Ltd. (1978)	
RICHARDS ISLAND	[illegible] Area Drilling	W134°22.5' to 134°45'	III-c	F"O"	HA83-D1	83/05	SM	25.2			19	3	Hardy Associates Ltd. (1978)	
RICHARDS ISLAND	[illegible] Area Drilling	N69°25' to 69°32.5'	III-c	F"O"	HA83-D1	83/05	SM	30.1		2045	20	3.3	Hardy Associates Ltd. (1978)	

COMMUNITY	PROJECT	LOCATION	GEOLOGICAL UNIT	TERRAIN TYPE	HOLE	DATE	SOIL CLASSIFICATION (USCS)	DEPTH(m)	TEMP (°C)	DENSITY (Mg/m3)	M.C. (%)	SALINITY (ppt)	CONSULTANT	COMMENTS
RICHARDS ISLAND	Illisarvik Area Drilling	W134°22.5' to 134°45'	III-c	F"O"	HA83-D1	83/03	SM	33.3		1816	32	8.7	Hardy Associates Ltd. (1978)	
RICHARDS ISLAND	Illisarvik Area Drilling	N69°25' to 69°32.5'	III-c	F"O"	HA83-D1	83/03	SM	50.1		2006	23	7.3	Hardy Associates Ltd. (1978)	
RICHARDS ISLAND	Illisarvik Area Drilling	W134°22.5' to 134°45'	III-c	F"O"	HA83-D1	83/03	SP	60.9		1854	31	1.9	Hardy Associates Ltd. (1978)	
RICHARDS ISLAND	Illisarvik Area Drilling	N69°25' to 69°32.5'	III-c		HA83-D1	83/03	OL-OH	70.8		1663	40	15.8	Hardy Associates Ltd. (1978)	
RICHARDS ISLAND	Illisarvik Area Drilling	W134°22.5' to 134°45'	III-c		HA83-D1	83/03/19		2	-12				Hardy Associates Ltd. (1978)	
RICHARDS ISLAND	Illisarvik Area Drilling	N69°25' to 69°32.5'	III-c		HA83-D1	83/03/19		6	-7				Hardy Associates Ltd. (1978)	
RICHARDS ISLAND	Illisarvik Area Drilling	W134°22.5' to 134°45'	III-c		HA83-D1	83/03/19		9	-5				Hardy Associates Ltd. (1978)	
RICHARDS ISLAND	Illisarvik Area Drilling	N69°25' to 69°32.5'	III-c		HA83-D1	83/03/19		12	-4.8				Hardy Associates Ltd. (1978)	
RICHARDS ISLAND	Illisarvik Area Drilling	W134°22.5' to 134°45'	III-c		HA83-D1	83/03/19		17	-5				Hardy Associates Ltd. (1978)	
RICHARDS ISLAND	Illisarvik Area Drilling	N69°25' to 69°32.5'	III-c		HA83-D1	83/03/19		30	-5				Hardy Associates Ltd. (1978)	
RICHARDS ISLAND	Illisarvik Area Drilling	W134°22.5' to 134°45'	III-c		HA83-D1	83/03/19		50	-5				Hardy Associates Ltd. (1978)	
RICHARDS ISLAND	Illisarvik Area Drilling	N69°25' to 69°32.5'	III-c		HA83-D2	83/03	OL	0.6		1271	115	0.9	Hardy Associates Ltd. (1978)	
RICHARDS ISLAND	Illisarvik Area Drilling	W134°22.5' to 134°45'	III-c	F or L	HA83-D2	83/03	ML	0.9			43	1.4	Hardy Associates Ltd. (1978)	
RICHARDS ISLAND	Illisarvik Area Drilling	N69°25' to 69°32.5'	III-c	F or L	HA83-D2	83/03	CL	1.7		1937	24	1.9	Hardy Associates Ltd. (1978)	
RICHARDS ISLAND	Illisarvik Area Drilling	W134°22.5' to 134°45'	III-c	F or L	HA83-D2	83/03	CL	2.2		1640	47	3.1	Hardy Associates Ltd. (1978)	
RICHARDS ISLAND	Illisarvik Area Drilling	N69°25' to 69°32.5'	III-c	F or L	HA83-D2	83/03	ML + ICE	2.8			1758	0.5	Hardy Associates Ltd. (1978)	
RICHARDS ISLAND	Illisarvik Area Drilling	W134°22.5' to 134°45'	III-c	F or L	HA83-D2	83/03	CL-ML	3.4		1600	35	2.9	Hardy Associates Ltd. (1978)	
RICHARDS ISLAND	Illisarvik Area Drilling	N69°25' to 69°32.5'	III-c	F or L	HA83-D2	83/03	CL-ML	4.1		1498	62	1.2	Hardy Associates Ltd. (1978)	
RICHARDS ISLAND	Illisarvik Area Drilling	W134°22.5' to 134°45'	III-c	F or L	HA83-D2	83/03	CL-ML	4.9			67	2.5	Hardy Associates Ltd. (1978)	
RICHARDS ISLAND	Illisarvik Area Drilling	N69°25' to 69°32.5'	III-c	F"O"	HA83-D2	83/03	SM	10.7		1874	27	6.3	Hardy Associates Ltd. (1978)	
RICHARDS ISLAND	Illisarvik Area Drilling	W134°22.5' to 134°45'	III-c	F"O"	HA83-D2	83/03	SM	20.1		2041	20	8	Hardy Associates Ltd. (1978)	
RICHARDS ISLAND	Illisarvik Area Drilling	N69°25' to 69°32.5'	III-c	F"O"	HA83-D2	83/03	CL	20.9			30	15	Hardy Associates Ltd. (1978)	
RICHARDS ISLAND	Illisarvik Area Drilling	W134°22.5' to 134°45'	III-c	F"O"	HA83-D2	83/03	SM	30.9		1945	25	1.2	Hardy Associates Ltd. (1978)	
RICHARDS ISLAND	Illisarvik Area Drilling	N69°25' to 69°32.5'	III-c	F"O"	HA83-D2	83/03	SM	40.2		2047	21	1.1	Hardy Associates Ltd. (1978)	
RICHARDS ISLAND	Illisarvik Area Drilling	W134°22.5' to 134°45'	III-c	F"O"	HA83-D2	83/03	SP	50.8		1959	24	8.5	Hardy Associates Ltd. (1978)	
RICHARDS ISLAND	Illisarvik Area Drilling	N69°25' to 69°32.5'	III-c		HA83-D2	83/03/19		3	-0.5				Hardy Associates Ltd. (1978)	
RICHARDS ISLAND	Illisarvik Area Drilling	W134°22.5' to 134°45'	III-c		HA83-D2	83/03/19		10	-1				Hardy Associates Ltd. (1978)	
RICHARDS ISLAND	Illisarvik Area Drilling	N69°25' to 69°32.5'	III-c		HA83-D2	83/03/19		20	-1				Hardy Associates Ltd. (1978)	
RICHARDS ISLAND	Illisarvik Area Drilling	W134°22.5' to 134°45'	III-c		HA83-D2	83/03/19		30	-1.3				Hardy Associates Ltd. (1978)	
RICHARDS ISLAND	Illisarvik Area Drilling	N69°25' to 69°32.5'	III-c		HA83-D2	83/03/19		40	-1.3				Hardy Associates Ltd. (1978)	
RICHARDS ISLAND	Illisarvik Area Drilling	W134°22.5' to 134°45'	III-c		HA83-D2	83/03/19		50	-2.3				Hardy Associates Ltd. (1978)	
RICHARDS ISLAND	Illisarvik Area Drilling	N69°25' to 69°32.5'	III-c		HA83-D2	83/03/19		55	-1.4				Hardy Associates Ltd. (1978)	
RICHARDS ISLAND	Illisarvik Area Drilling	W134°22.5' to 134°45'	III-c		HA83-D2	83/03/19		60	-2				Hardy Associates Ltd. (1978)	
RICHARDS ISLAND	Illisarvik Area Drilling	N69°25' to 69°32.5'	III-c		HA83-D2	83/03/19		70	-1.6				Hardy Associates Ltd. (1978)	
RICHARDS ISLAND	Illisarvik Area Drilling	W134°22.5' to 134°45'	III-c	F	HA83-M1	83/03	OL	0.1			42	0.9	Hardy Associates Ltd. (1978)	
RICHARDS ISLAND	Illisarvik Area Drilling	N69°25' to 69°32.5'	III-c	F	HA83-M1	83/03	ML	0.4			48	1.1	Hardy Associates Ltd. (1978)	
RICHARDS ISLAND	Illisarvik Area Drilling	W134°22.5' to 134°45'	III-c	M or W"O"	HA83-M1	83/03	CL	3.4			38	2	Hardy Associates Ltd. (1978)	
RICHARDS ISLAND	Illisarvik Area Drilling	N69°25' to 69°32.5'	III-c	M or W"O"	HA83-M1	83/03	CL	5.7		1625	30	3.1	Hardy Associates Ltd. (1978)	
RICHARDS ISLAND	Illisarvik Area Drilling	W134°22.5' to 134°45'	III-c	F"O"	HA83-M1	83/03	SM	10.6		1860	27	1.2	Hardy Associates Ltd. (1978)	
RICHARDS ISLAND	Illisarvik Area Drilling	N69°25' to 69°32.5'	III-c	F"O"	HA83-M1	83/03	SM	15.5			21	3.3	Hardy Associates Ltd. (1978)	
RICHARDS ISLAND	Illisarvik Area Drilling	W134°22.5' to 134°45'	III-c	F"O"	HA83-M1	83/03	SM + ICE	20.2			316	0.6	Hardy Associates Ltd. (1978)	
RICHARDS ISLAND	Illisarvik Area Drilling	N69°25' to 69°32.5'	III-c	F"O"	HA83-M1	83/03	SM	20.9		1902	25	3.5	Hardy Associates Ltd. (1978)	
RICHARDS ISLAND	Illisarvik Area Drilling	W134°22.5' to 134°45'	III-c	F	HA83-M2	83/03	ML	0.5		1640	48	1.5	Hardy Associates Ltd. (1978)	
RICHARDS ISLAND	Illisarvik Area Drilling	N69°25' to 69°32.5'	III-c	F	HA83-M2	83/03	ML	1.1			49	2.3	Hardy Associates Ltd. (1978)	
RICHARDS ISLAND	Illisarvik Area Drilling	W134°22.5' to 134°45'	III-c	F	HA83-M2	83/03	MH	1.4		1738	35	4.9	Hardy Associates Ltd. (1978)	
RICHARDS ISLAND	Illisarvik Area Drilling	N69°25' to 69°32.5'	III-c	M or W"O"	HA83-M2	83/03	CI	3.2			21	4	Hardy Associates Ltd. (1978)	
RICHARDS ISLAND	Illisarvik Area Drilling	W134°22.5' to 134°45'	III-c	M or W"O"	HA83-M2	83/03	CI	5.8		1986	22	3	Hardy Associates Ltd. (1978)	
RICHARDS ISLAND	Illisarvik Area Drilling	N69°25' to 69°32.5'	III-c	F"O"	HA83-M2	83/03	SM	10.4			28	1.1	Hardy Associates Ltd. (1978)	
RICHARDS ISLAND	Illisarvik Area Drilling	W134°22.5' to 134°45'	III-c	F"O"	HA83-M2	83/03	SM	10.7		1941	25	1.4	Hardy Associates Ltd. (1978)	
RICHARDS ISLAND	Illisarvik Area Drilling	N69°25' to 69°32.5'	III-c	F	HA83-M2A	83/03	ML	3			29	2.5	Hardy Associates Ltd. (1978)	
RICHARDS ISLAND	Illisarvik Area Drilling	W134°22.5' to 134°45'	III-c	M or W"O"	HA83-M2A	83/03	CI	5.1			22	22.1	Hardy Associates Ltd. (1978)	
RICHARDS ISLAND	Illisarvik Area Drilling	N69°25' to 69°32.5'	III-c	F"O"	HA83-M2A	83/03	SM	10.2		1999	26	1.4	Hardy Associates Ltd. (1978)	
RICHARDS ISLAND	Illisarvik Area Drilling	W134°22.5' to 134°45'	III-c	V	HA83-M4	83/03	ML-OL	12.1			46	10	Hardy Associates Ltd. (1978)	
RICHARDS ISLAND	Illisarvik Area Drilling	N69°25' to 69°32.5'	III-c	V	HA83-M4	83/03	MH	15.5			44	3.3	Hardy Associates Ltd. (1978)	
RICHARDS ISLAND	Illisarvik Area Drilling	W134°22.5' to 134°45'	III-c	V	HA83-M4	83/03	CL	22.1			24	3	Hardy Associates Ltd. (1978)	
RICHARDS ISLAND	Illisarvik Area Drilling	N69°25' to 69°32.5'	III-c	V (U)	[illegible]	83/03	SC	1.4			22	2.2	Hardy Associates Ltd. (1978)	
RICHARDS ISLAND	Illisarvik Area Drilling	W134°22.5' to 134°45'	III-c	V (U)	[illegible]	83/03	SC	3.4		1937	24	3.4	Hardy Associates Ltd. (1978)	
RICHARDS ISLAND	Illisarvik Area Drilling	N69°25' to 69°32.5'	III-c	V (U)	[illegible]	83/03	SC	10.3			22	3.3	Hardy Associates Ltd. (1978)	
RICHARDS ISLAND	Illisarvik Area Drilling	W134°22.5' to 134°45'	III-c	V (U)	[illegible]	83/03	CI	15.1			30	15.4	Hardy Associates Ltd. (1978)	
RICHARDS ISLAND	Illisarvik Area Drilling	N69°25' to 69°32.5'	III-c	V (U)	[illegible]	83/03	SP	15.3			25	11.4	Hardy Associates Ltd. (1978)	
RICHARDS ISLAND	Illisarvik Area Drilling	W134°22.5' to 134°45'	III-c	V (U)	[illegible]	83/03	CL	15.6		1847	32	9.6	Hardy Associates Ltd. (1978)	
RICHARDS ISLAND	Illisarvik Area Drilling	N69°25' to 69°32.5'	III-c	V (U)	[illegible]	83/03	SM	20.6		1997	28	3.3	Hardy Associates Ltd. (1978)	
RICHARDS ISLAND	GSC Near Shore Investigation	W134°22.5' to 134°45'	III-c							Dry Density			Dallimore et al. ([illegible])	Salinity determination
RICHARDS ISLAND	GSC Near Shore Investigation	N69°25' to 69°32.5'	III-c	F	87-1	Summer 87	SM	1.88		1540	33.6	0.58	Dallimore et al. ([illegible])	by method 4
RICHARDS ISLAND	GSC Near Shore Investigation	W134°22.5' to 134°45'	III-c		87-1	Summer 87	ICE	1.95		25	3374	0.3	Dallimore et al. ([illegible])	Hole 87-1:
RICHARDS ISLAND	GSC Near Shore Investigation	N69°25' to 69°32.5'	III-c		87-1	Summer 87	ICE	2.36				0.14	Dallimore et al. ([illegible])	[illegible]
RICHARDS ISLAND	GSC Near Shore Investigation	W134°22.5' to 134°45'	III-c		87-1	Summer 87	ICE	2.83				0.12	Dallimore et al. ([illegible])	
RICHARDS ISLAND	GSC Near Shore Investigation	N69°25' to 69°32.5'	III-c		87-1	Summer 87	ICE	3.1		1	75448	0.13	Dallimore et al. ([illegible])	
RICHARDS ISLAND	GSC Near Shore Investigation	W134°22.5' to 134°45'	III-c		87-1	Summer 87	ICE	3.48				0.1	Dallimore et al. ([illegible])	
RICHARDS ISLAND	GSC Near Shore Investigation	N69°25' to 69°32.5'	III-c		87-1	Summer 87	ICE	3.86				0.05	Dallimore et al. ([illegible])	

COMMUNITY	PROJECT	LOCATION	GEOLOGICAL UNIT	TERRAIN TYPE	HOLE	DATE	SOIL CLASSIFICATION (USCS)	DEPTH(m)	TEMP (°C)	DENSITY (Mg/m3)	M.C. (%)	SALINITY (ppt)	CONSULTANT	COMMENTS
RICHARDS ISLAND	GSC Near-Shore Investigation	W134°22.5' to 134°45'	III-c		87-1	Summer 87	ICE	4.32				0.14	Dallimore et al. (1988)	
RICHARDS ISLAND	GSC Near-Shore Investigation	N69°25' to 69°32.5'	III-c		87-1	Summer 87	ICE	4.68		21	4188	0.4	Dallimore et al. (1988)	
RICHARDS ISLAND	GSC Near-Shore Investigation	W134°22.5' to 134°45'	III-c		87-1	Summer 87	ICE	4.95				0.16	Dallimore et al. (1988)	
RICHARDS ISLAND	GSC Near-Shore Investigation	N69°25' to 69°32.5'	III-c		87-1	Summer 87	ICE	5.3				0.17	Dallimore et al. (1988)	
RICHARDS ISLAND	GSC Near-Shore Investigation	W134°22.5' to 134°45'	III-c		87-1	Summer 87	ICE	5.75				0.19	Dallimore et al. (1988)	
RICHARDS ISLAND	GSC Near-Shore Investigation	N69°25' to 69°32.5'	III-c	F"O"(I)	87-1	Summer 87	SM	6.86		1519	26.57	4.34	Dallimore et al. (1988)	
RICHARDS ISLAND	GSC Near-Shore Investigation	W134°22.5' to 134°45'	III-c	F"O"(I)	87-1	Summer 87	SM	7.28		1503	22.06	3.19	Dallimore et al. (1988)	
RICHARDS ISLAND	GSC Near-Shore Investigation	N69°25' to 69°32.5'	III-c	F"O"(I)	87-1	Summer 87	SM	7.86		1472	27.39	3.41	Dallimore et al. (1988)	
RICHARDS ISLAND	GSC Near-Shore Investigation	W134°22.5' to 134°45'	III-c	F"O"(I)	87-1	Summer 87	SM	8.01		1540	25.6	4.59	Dallimore et al. (1988)	
RICHARDS ISLAND	GSC Near-Shore Investigation	N69°25' to 69°32.5'	III-c	F"O"(I)	87-1	Summer 87	SM	8.99		1475	22.47	3.66	Dallimore et al. (1988)	
RICHARDS ISLAND	GSC Near-Shore Investigation	W134°22.5' to 134°45'	III-c	F"O"(I)	87-1	Summer 87	SM	9.77		1514	24.95	4.34	Dallimore et al. (1988)	
RICHARDS ISLAND	GSC Near-Shore Investigation	N69°25' to 69°32.5'	III-c	F"O"(I)	87-1	Summer 87	SM	10.68		1545	27.84	3.01	Dallimore et al. (1988)	
RICHARDS ISLAND	GSC Near-Shore Investigation	W134°22.5' to 134°45'	III-c	F"O"(I)	87-1	Summer 87	SM	11.32		1508	25.7	3.61	Dallimore et al. (1988)	
RICHARDS ISLAND	GSC Near-Shore Investigation	N69°25' to 69°32.5'	III-c	F"O"(I)	87-1	Summer 87	SM	11.84		1502	24.49	3.19	Dallimore et al. (1988)	
RICHARDS ISLAND	GSC Near-Shore Investigation	W134°22.5' to 134°45'	III-c	F"O"(I)	87-1	Summer 87	SM	14.65		1641	21.84	1.39	Dallimore et al. (1988)	
RICHARDS ISLAND	GSC Near-Shore Investigation	N69°25' to 69°32.5'	III-c	F"O"(I)	87-1	Summer 87	SM	15.17		1464	25.59	2.96	Dallimore et al. (1988)	
RICHARDS ISLAND	GSC Near-Shore Investigation	W134°22.5' to 134°45'	III-c	F"O"(I)	87-1	Summer 87	SM	17.1		1535	20.07	3.44	Dallimore et al. (1988)	
RICHARDS ISLAND	GSC Near-Shore Investigation	N69°25' to 69°32.5'	III-c	F"O"(I)	87-1	Summer 87	SM	18.5		1739	12.67	3.85	Dallimore et al. (1988)	
RICHARDS ISLAND	GSC Near-Shore Investigation	W134°22.5' to 134°45'	III-c	F"O"(I)	87-1	Summer 87	SM	19.98		1663	20.49	6.04	Dallimore et al. (1988)	
RICHARDS ISLAND	GSC Near-Shore Investigation	N69°25' to 69°32.5'	III-c	F"O"(I)	87-1	Summer 87	SM	20.67		1699	19.41	7.88	Dallimore et al. (1988)	
RICHARDS ISLAND	GSC Near-Shore Investigation	W134°22.5' to 134°45'	III-c	F"O"(I)	87-1	Summer 87	SM	21.56		1538	24.59	6.3	Dallimore et al. (1988)	
RICHARDS ISLAND	GSC Near-Shore Investigation	N69°25' to 69°32.5'	III-c	F"O"(I)	87-1	Summer 87	SM	23.07		1693	20.64	10	Dallimore et al. (1988)	
RICHARDS ISLAND	GSC Near-Shore Investigation	W134°22.5' to 134°45'	III-c	F"O"(I)	87-1	Summer 87	SM	23.94		1683	19.88	6.04	Dallimore et al. (1988)	
RICHARDS ISLAND	GSC Near-Shore Investigation	N69°25' to 69°32.5'	III-c	F"O"(I)	87-1	Summer 87	SM	25.68		1544	28.77	6.04	Dallimore et al. (1988)	
RICHARDS ISLAND	GSC Near-Shore Investigation	W134°22.5' to 134°45'	III-c	F"O"(I)	87-1	Summer 87	SM	26.58		1470	25.95	3.16	Dallimore et al. (1988)	
RICHARDS ISLAND	GSC Near-Shore Investigation	N69°25' to 69°32.5'	III-c	F"O"(I)	87-1	Summer 87	SM	27.11		1475	26.75	1.39	Dallimore et al. (1988)	
RICHARDS ISLAND	GSC Near-Shore Investigation	W134°22.5' to 134°45'	III-c	F"O"(I)	87-1	Summer 87	SM	27.71		1254	34.12	0.45	Dallimore et al. (1988)	
RICHARDS ISLAND	GSC Near-Shore Investigation	N69°25' to 69°32.5'	III-c	F"O"(I)	87-1	Summer 87	SM	28.53		1508	22.98	0.32	Dallimore et al. (1988)	
RICHARDS ISLAND	GSC Near-Shore Investigation	W134°22.5' to 134°45'	III-c	F"O"(I)	87-1	Summer 87	SM	29.24		1698	20.29	0.37	Dallimore et al. (1988)	Hole 87-2 :
RICHARDS ISLAND	GSC Near-Shore Investigation	N69°25' to 69°32.5'	III-c		87-2	Summer 87	ICE	2.1			3293	0.31	Dallimore et al. (1988)	near shore hole
RICHARDS ISLAND	GSC Near-Shore Investigation	W134°22.5' to 134°45'	III-c		87-2	Summer 87	ICE	2.3		151	506	0.61	Dallimore et al. (1988)	
RICHARDS ISLAND	GSC Near-Shore Investigation	N69°25' to 69°32.5'	III-c	F"O"(I)	87-2	Summer 87	SM	7.76		1566	21.21	3.1	Dallimore et al. (1988)	
RICHARDS ISLAND	GSC Near-Shore Investigation	W134°22.5' to 134°45'	III-c	F"O"(I)	87-2	Summer 87	SM	8.34		1084	56.31	0.13	Dallimore et al. (1988)	
RICHARDS ISLAND	GSC Near-Shore Investigation	N69°25' to 69°32.5'	III-c	F"O"(I)	87-2	Summer 87	SM	15.58		1747	18.54	3.16	Dallimore et al. (1988)	
RICHARDS ISLAND	GSC Near-Shore Investigation	W134°22.5' to 134°45'	III-c	F"O"(I)	87-2	Summer 87	SM	17.66			24.53	1.08	Dallimore et al. (1988)	
RICHARDS ISLAND	GSC Near-Shore Investigation	N69°25' to 69°32.5'	III-c	F"O"(I)	87-2	Summer 87	SM	18.35		1640	17.87	3.58	Dallimore et al. (1988)	
RICHARDS ISLAND	GSC Near-Shore Investigation	W134°22.5' to 134°45'	III-c	F"O"(I)	87-2	Summer 87	SM	21.88		1554	24.96	3.91	Dallimore et al. (1988)	
RICHARDS ISLAND	GSC Near-Shore Investigation	N69°25' to 69°32.5'	III-c	F"O"(I)	87-2	Summer 87	SM	23.23		1725	19.6	4.08	Dallimore et al. (1988)	
RICHARDS ISLAND	GSC Near-Shore Investigation	W134°22.5' to 134°45'	III-c	F"O"(I)	87-2	Summer 87	SM	25.05		1596	24.245	3.25	Dallimore et al. (1988)	
RICHARDS ISLAND	GSC Near-Shore Investigation	N69°25' to 69°32.5'	III-c	F"O"(I)	87-2	Summer 87	SM	26.86			24.78	2.18	Dallimore et al. (1988)	
RICHARDS ISLAND	GSC Near-Shore Investigation	W134°22.5' to 134°45'	III-c	F"O"(I)	87-2	Summer 87	SM	27.3		1062	46.7	1.54	Dallimore et al. (1988)	
RICHARDS ISLAND	GSC Near-Shore Investigation	N69°25' to 69°32.5'	III-c	F"O"(I)	87-2	Summer 87	SM	27.95		1588	29.5	0.26	Dallimore et al. (1988)	
RICHARDS ISLAND	GSC Near-Shore Investigation	W134°22.5' to 134°45'	III-c	F"O"(I)	87-2	Summer 87	SM	29.31		1595	25.1	0.14	Dallimore et al. (1988)	
RICHARDS ISLAND	GSC Near-Shore Investigation	N69°25' to 69°32.5'	III-c	F"O"(I)	87-3	Summer 87	SM	4.6		1791	19.59	3.61	Dallimore et al. (1988)	Hole 87-3 :
RICHARDS ISLAND	GSC Near-Shore Investigation	W134°22.5' to 134°45'	III-c	F"O"(I)	87-3	Summer 87	SM	6.09			21.24	10.9	Dallimore et al. (1988)	near shore hole
RICHARDS ISLAND	GSC Near-Shore Investigation	N69°25' to 69°32.5'	III-c	F"O"(I)	87-3	Summer 87	SM	7.63		1702	18.84	6.83	Dallimore et al. (1988)	
RICHARDS ISLAND	GSC Near-Shore Investigation	W134°22.5' to 134°45'	III-c	F"O"(I)	87-3	Summer 87	SM	15.37		1588	23.91	1.17	Dallimore et al. (1988)	
RICHARDS ISLAND	GSC Near-Shore Investigation	N69°25' to 69°32.5'	III-c	F"O"(I)	87-3	Summer 87	SM	16.3		1632	28.7	2.14	Dallimore et al. (1988)	
RICHARDS ISLAND	GSC Near-Shore Investigation	W134°22.5' to 134°45'	III-c	F"O"(I)	87-3	Summer 87	SM	16.88			24.87	1.31	Dallimore et al. (1988)	
RICHARDS ISLAND	GSC Near-Shore Investigation	N69°25' to 69°32.5'	III-c	F"O"(I)	87-3	Summer 87	SM	17.63			24.48	3.53	Dallimore et al. (1988)	
RICHARDS ISLAND	GSC Near-Shore Investigation	W134°22.5' to 134°45'	III-c	F"O"(I)	87-3	Summer 87	SM	18			18.78	2.59	Dallimore et al. (1988)	
RICHARDS ISLAND	GSC Near-Shore Investigation	N69°25' to 69°32.5'	III-c	F"O"(I)	87-3	Summer 87	SM	19.2		1640	22.76	2.02	Dallimore et al. (1988)	
RICHARDS ISLAND	GSC Near-Shore Investigation	W134°22.5' to 134°45'	III-c	F"O"(I)	87-3	Summer 87	SM	21.2		1591	23.95	3.41	Dallimore et al. (1988)	
RICHARDS ISLAND	GSC Near-Shore Investigation	N69°25' to 69°32.5'	III-c	F"O"(I)	87-3	Summer 87	SM	22.73			24.96	2.18	Dallimore et al. (1988)	
RICHARDS ISLAND	GSC Near-Shore Investigation	W134°22.5' to 134°45'	III-c	F"O"(I)	87-3	Summer 87	SM	23.98		986	28.54	1.04	Dallimore et al. (1988)	
RICHARDS ISLAND	GSC Near-Shore Investigation	N69°25' to 69°32.5'	III-c	F"O"(I)	87-3	Summer 87	SM	24.3			27.54	0.45	Dallimore et al. (1988)	
RICHARDS ISLAND	GSC Near-Shore Investigation	W134°22.5' to 134°45'	III-c	F"O"(I)	87-3	Summer 87	SM	24.53			27.39	3.41	Dallimore et al. (1988)	
RICHARDS ISLAND	GSC Near-Shore Investigation	N69°25' to 69°32.5'	III-c	F"O"(I)	87-3	Summer 87	SM	24.73			26.16	2.74	Dallimore et al. (1988)	
RICHARDS ISLAND	GSC Near-Shore Investigation	W134°22.5' to 134°45'	III-c	F"O"(I)	87-3	Summer 87	SM	25.7			34.23	1.4	Dallimore et al. (1988)	
RICHARDS ISLAND	GSC Near-Shore Investigation	N69°25' to 69°32.5'	III-c	F"O"(I)	87-3	Summer 87	SM	26.42		1246	40.32	2.1	Dallimore et al. (1988)	
RICHARDS ISLAND	GSC Near-Shore Investigation	W134°22.5' to 134°45'	III-c	F"O"(I)	87-4	Summer 87	SM	2.49		1310	23.64	10.43	Dallimore et al. (1988)	Hole 87-4 :
RICHARDS ISLAND	GSC Near-Shore Investigation	N69°25' to 69°32.5'	III-c	F"O"(I)	87-4	Summer 87	SM	4.73			4.34	22.19	Dallimore et al. (1988)	near shore hole
RICHARDS ISLAND	GSC Near-Shore Investigation	W134°22.5' to 134°45'	III-c	F"O"(I)	87-4	Summer 87	SM	6.42		1803	14.18	3.1	Dallimore et al. (1988)	
RICHARDS ISLAND	GSC Near-Shore Investigation	N69°25' to 69°32.5'	III-c	F"O"(I)	87-4	Summer 87	SM	7.98		1628	28.14	3.26	Dallimore et al. (1988)	
RICHARDS ISLAND	GSC Near-Shore Investigation	W134°22.5' to 134°45'	III-c	F"O"(I)	87-4	Summer 87	SM	8.88			21.1	6.48	Dallimore et al. (1988)	
RICHARDS ISLAND	GSC Near-Shore Investigation	N69°25' to 69°32.5'	III-c	F"O"(I)	87-4	Summer 87	SM	9.73			21.38	3.61	Dallimore et al. (1988)	
RICHARDS ISLAND	GSC Near-Shore Investigation	W134°22.5' to 134°45'	III-c	F"O"(I)	87-4	Summer 87	SM	11.79			38.61	2.96	Dallimore et al. (1988)	
RICHARDS ISLAND	GSC Near-Shore Investigation	N69°25' to 69°32.5'	III-c	F"O"(I)	87-4	Summer 87	SM	12.96		1763	23.6	3.91	Dallimore et al. (1988)	
RICHARDS ISLAND	GSC Near-Shore Investigation	W134°22.5' to 134°45'	III-c	F"O"(I)	87-4	Summer 87	SM	13.68			22.98	1.95	Dallimore et al. (1988)	
RICHARDS ISLAND	GSC Near-Shore Investigation	N69°25' to 69°32.5'	III-c	F"O"(I)	87-4	Summer 87	SM	18.31		1630	21.66	1.94	Dallimore et al. (1988)	

COMMUNITY	PROJECT	LOCATION	GEOLOGICAL UNIT	TERRAIN TYPE	HOLE	DATE	SOIL CLASSIFICATION (USCS)	DEPTH(m)	TEMP (°C)	DENSITY (Mg/m3)	M.C. (%)	SALINITY (ppt)	CONSULTANT	COMMENTS
RICHARDS ISLAND	GSC Near-Shore Investigation	W134°22.5' to 134°45'	III-c	L (U)	87-5	Summer 87	CL	0.09		811	78.61	0.59	Dallimore et al. (1988)	Hole 87-5 :
RICHARDS ISLAND	GSC Near-Shore Investigation	N69°25' to 69°32.5'	III-c	L (U)	87-5	Summer 87	CL	0.55		481	161.01	0.44	Dallimore et al. (1988)	on shore hole
RICHARDS ISLAND	GSC Near-Shore Investigation	W134°22.5' to 134°45'	III-c	L (U)	87-5	Summer 87	SM	1.32		1335	31.72	1.39	Dallimore et al. (1988)	
RICHARDS ISLAND	GSC Near-Shore Investigation	N69°25' to 69°32.5'	III-c	L (U)	87-5	Summer 87	SM	1.72		1295	35.03	3.12	Dallimore et al. (1988)	
RICHARDS ISLAND	GSC Near-Shore Investigation	W134°22.5' to 134°45'	III-c	L (U)	87-5	Summer 87	SM	2.42			468	0.45	Dallimore et al. (1988)	
RICHARDS ISLAND	GSC Near-Shore Investigation	N69°25' to 69°32.5'	III-c	L (U)	87-5	Summer 87	SM	2.55			76.91	0.75	Dallimore et al. (1988)	
RICHARDS ISLAND	GSC Near-Shore Investigation	W134°22.5' to 134°45'	III-c	F"O" (U)	87-5	Summer 87	SM	3.33		1433	48.27	2.92	Dallimore et al. (1988)	
RICHARDS ISLAND	GSC Near-Shore Investigation	N69°25' to 69°32.5'	III-c	F"O" (U)	87-5	Summer 87	SM	3.89		1260	92.43	1.43	Dallimore et al. (1988)	
RICHARDS ISLAND	GSC Near-Shore Investigation	W134°22.5' to 134°45'	III-c	F"O" (U)	87-5	Summer 87	SM	4.36		1697	39.04	6.3	Dallimore et al. (1988)	
RICHARDS ISLAND	GSC Near-Shore Investigation	N69°25' to 69°32.5'	III-c	F"O" (U)	87-5	Summer 87	SM	5.25		1760	42.68	6.56	Dallimore et al. (1988)	
RICHARDS ISLAND	GSC Near-Shore Investigation	W134°22.5' to 134°45'	III-c	F"O" (U)	87-5	Summer 87	SM	5.92		1795	40.38	5.53	Dallimore et al. (1988)	
RICHARDS ISLAND	GSC Near-Shore Investigation	N69°25' to 69°32.5'	III-c	F"O" (U)	87-5	Summer 87	SM	6.57		1648	48.7	6.39	Dallimore et al. (1988)	
RICHARDS ISLAND	GSC Near-Shore Investigation	W134°22.5' to 134°45'	III-c	F"O" (U)	87-5	Summer 87	SM	7.51		1754	39.08	7.61	Dallimore et al. (1988)	
RICHARDS ISLAND	GSC Near-Shore Investigation	N69°25' to 69°32.5'	III-c	F"O" (U)	87-5	Summer 87	SM	7.78		1727	38.45	9.74	Dallimore et al. (1988)	
RICHARDS ISLAND	GSC Near-Shore Investigation	W134°22.5' to 134°45'	III-c	F"O" (U)	87-5	Summer 87	SM	7.92		1664	49.59	5.58	Dallimore et al. (1988)	
RICHARDS ISLAND	GSC Near-Shore Investigation	N69°25' to 69°32.5'	III-c	F"O" (U)	87-5	Summer 87	SM	8.62		2047	24.74	9.83	Dallimore et al. (1988)	
RICHARDS ISLAND	GSC Near-Shore Investigation	W134°22.5' to 134°45'	III-c	F"O" (U)	87-5	Summer 87	SM	9		1964	24.72	11.26	Dallimore et al. (1988)	
RICHARDS ISLAND	GSC Near-Shore Investigation	N69°25' to 69°32.5'	III-c	F"O" (U)	87-5	Summer 87	SM	10.64		2037	30.8	1.58	Dallimore et al. (1988)	
RICHARDS ISLAND	GSC Near-Shore Investigation	W134°22.5' to 134°45'	III-c	F"O" (U)	87-5	Summer 87	SM	13.97		1834	27.49	23.89	Dallimore et al. (1988)	
RICHARDS ISLAND	GSC Near-Shore Investigation	N69°25' to 69°32.5'	III-c	F"O" (U)	87-5	Summer 87	SM	15.8		1348	31.57	11.8	Dallimore et al. (1988)	
RICHARDS ISLAND	GSC Near-Shore Investigation	W134°22.5' to 134°45'	III-c	F"O" (U)	87-5	Summer 87	SM	16.04		1592	32.4	30.17	Dallimore et al. (1988)	
RICHARDS ISLAND	GSC Near-Shore Investigation	N69°25' to 69°32.5'	III-c	F"O" (U)	87-5	Summer 87	SM	17		1004	45.56	2.33	Dallimore et al. (1988)	
RICHARDS ISLAND	GSC Near-Shore Investigation	W134°22.5' to 134°45'	III-c	F"O" (U)	87-5	Summer 87	SM	17.32			239.98	1.27	Dallimore et al. (1988)	
RICHARDS ISLAND	GSC Near-Shore Investigation	N69°25' to 69°32.5'	III-c		87-5	Summer 87	ICE	18.08		0		1	Dallimore et al. (1988)	
RICHARDS ISLAND	GSC Near-Shore Investigation	W134°22.5' to 134°45'	III-c		87-5	Summer 87	ICE	18.5		0		0.15	Dallimore et al. (1988)	
RICHARDS ISLAND	GSC Near-Shore Investigation	N69°25' to 69°32.5'	III-c		87-5	Summer 87	ICE	19.54		0		0.11	Dallimore et al. (1988)	
RICHARDS ISLAND	GSC Near-Shore Investigation	W134°22.5' to 134°45'	III-c		87-5	Summer 87	ICE	20.96		0		0.03	Dallimore et al. (1988)	
RICHARDS ISLAND	GSC Near-Shore Investigation	N69°25' to 69°32.5'	III-c		87-5	Summer 87	ICE	21.41		0		0.005	Dallimore et al. (1988)	
RICHARDS ISLAND	GSC Near-Shore Investigation	W134°22.5' to 134°45'	III-c		87-5	Summer 87	ICE	22.28		0		0.11	Dallimore et al. (1988)	
RICHARDS ISLAND	GSC Near-Shore Investigation	N69°25' to 69°32.5'	III-c		87-5	Summer 87	ICE	23.07		0		0.14	Dallimore et al. (1988)	
RICHARDS ISLAND	GSC Near-Shore Investigation	W134°22.5' to 134°45'	III-c		87-5	Summer 87	ICE	23.63		0		0.16	Dallimore et al. (1988)	
RICHARDS ISLAND	GSC Near-Shore Investigation	N69°25' to 69°32.5'	III-c	F"O" (U)	87-5	Summer 87	SM	24.78			33.71	0.12	Dallimore et al. (1988)	
RICHARDS ISLAND	GSC Near-Shore Investigation	W134°22.5' to 134°45'	III-c		87-5	Summer 87	ICE	25.52				0.32	Dallimore et al. (1988)	
RICHARDS ISLAND	GSC Near-Shore Investigation	N69°25' to 69°32.5'	III-c	F"O" (U)	87-5	Summer 87	SM	26.94		783	80.69	0.39	Dallimore et al. (1988)	
RICHARDS ISLAND	GSC Near-Shore Investigation	W134°22.5' to 134°45'	III-c	F"O" (U)	87-5	Summer 87	SM	27.54			21.37	0.56	Dallimore et al. (1988)	
RICHARDS ISLAND	GSC Near-Shore Investigation	N69°25' to 69°32.5'	III-c	F"O" (U)	87-5	Summer 87	SM	28.41		1072	25.79	0.57	Dallimore et al. (1988)	
RICHARDS ISLAND	GSC Near-Shore Investigation	W134°22.5' to 134°45'	III-c	F"O" (U)	87-5	Summer 87	CL-ML	29.37			34.52	0.75	Dallimore et al. (1988)	
RICHARDS ISLAND	GSC Near-Shore Investigation	N69°25' to 69°32.5'	III-c	L (U)	87-6	Summer 87	CL-ML	0.39		1435	27.08	0.51	Dallimore et al. (1988)	Hole 87-6:
RICHARDS ISLAND	GSC Near-Shore Investigation	W134°22.5' to 134°45'	III-c	L (U)	87-6	Summer 87	CL-ML	0.57		1189	45.89	0.37	Dallimore et al. (1988)	on shore hole
RICHARDS ISLAND	GSC Near-Shore Investigation	N69°25' to 69°32.5'	III-c	L (U)	87-6	Summer 87	CL-ML	1.56		1264	30.3	2.31	Dallimore et al. (1988)	
RICHARDS ISLAND	GSC Near-Shore Investigation	W134°22.5' to 134°45'	III-c	F"O" (U)	87-6	Summer 87	SM	2.78		1012	38.61	2.82	Dallimore et al. (1988)	
RICHARDS ISLAND	GSC Near-Shore Investigation	N69°25' to 69°32.5'	III-c	F"O" (U)	87-6	Summer 87	SM	3.85		1311	38.99	4.25	Dallimore et al. (1988)	
RICHARDS ISLAND	GSC Near-Shore Investigation	W134°22.5' to 134°45'	III-c	F"O" (U)	87-6	Summer 87	SM	4.67		1356	18.14	18.9	Dallimore et al. (1988)	
RICHARDS ISLAND	GSC Near-Shore Investigation	N69°25' to 69°32.5'	III-c	F"O" (U)	87-6	Summer 87	SM	4.9			171.84	0.39	Dallimore et al. (1988)	
RICHARDS ISLAND	GSC Near-Shore Investigation	W134°22.5' to 134°45'	III-c	F"O" (U)	87-6	Summer 87	SM	5.2			4081	0.05	Dallimore et al. (1988)	
RICHARDS ISLAND	GSC Near-Shore Investigation	N69°25' to 69°32.5'	III-c	F"O" (U)	87-6	Summer 87	SM	5.4			108.7	0.48	Dallimore et al. (1988)	
RICHARDS ISLAND	GSC Near-Shore Investigation	W134°22.5' to 134°45'	III-c	F"O" (U)	87-6	Summer 87	SM	5.45			2150	0.1	Dallimore et al. (1988)	
RICHARDS ISLAND	GSC Near-Shore Investigation	N69°25' to 69°32.5'	III-c	F"O" (U)	87-6	Summer 87	ICE	5.75				0.05	Dallimore et al. (1988)	
RICHARDS ISLAND	GSC Near-Shore Investigation	W134°22.5' to 134°45'	III-c	F"O" (U)	87-6	Summer 87	SM	6.05			1026	0.18	Dallimore et al. (1988)	
RICHARDS ISLAND	GSC Near-Shore Investigation	N69°25' to 69°32.5'	III-c	F"O" (U)	87-6	Summer 87	SM	6.2			39564	0.14	Dallimore et al. (1988)	
RICHARDS ISLAND	GSC Near-Shore Investigation	W134°22.5' to 134°45'	III-c	F"O" (U)	87-6	Summer 87	SM	6.4			27655	0.1	Dallimore et al. (1988)	
RICHARDS ISLAND	GSC Near-Shore Investigation	N69°25' to 69°32.5'	III-c	F"O" (U)	87-6	Summer 87	SM	6.6			117.25	0.75	Dallimore et al. (1988)	
RICHARDS ISLAND	GSC Near-Shore Investigation	W134°22.5' to 134°45'	III-c	F"O" (U)	87-6	Summer 87	SM	6.8			5026	0.63	Dallimore et al. (1988)	
RICHARDS ISLAND	GSC Near-Shore Investigation	N69°25' to 69°32.5'	III-c	F"O" (U)	87-6	Summer 87	SM	7.08		1684	22.44	7.35	Dallimore et al. (1988)	
RICHARDS ISLAND	GSC Near-Shore Investigation	W134°22.5' to 134°45'	III-c	F"O" (U)	87-6	Summer 87	SM	7.67		626	111.78	0.95	Dallimore et al. (1988)	
RICHARDS ISLAND	GSC Near-Shore Investigation	N69°25' to 69°32.5'	III-c	F"O" (U)	87-6	Summer 87	SM	7.82		1449	29.95	4.5	Dallimore et al. (1988)	
RICHARDS ISLAND	GSC Near-Shore Investigation	W134°22.5' to 134°45'	III-c	F"O" (U)	87-6	Summer 87	SM	11.94		1840	16.84	27.87	Dallimore et al. (1988)	
RICHARDS ISLAND	GSC Near-Shore Investigation	N69°25' to 69°32.5'	III-c	F"O" (U)	87-6	Summer 87	SM	27.92		1617	21.69	4.42	Dallimore et al. (1988)	
RICHARDS ISLAND	GSC Near-Shore Investigation	W134°22.5' to 134°45'	III-c	F"O" (U)	87-7	Summer 87	SM	13.54		14	6161	0.11	Dallimore et al. (1988)	Hole 87-7:
RICHARDS ISLAND	GSC Near-Shore Investigation	N69°25' to 69°32.5'	III-c	F"O" (U)	87-7	Summer 87	SM	18.54		1435	26.64	4.42	Dallimore et al. (1988)	near shore hole
RICHARDS ISLAND	GSC Near-Shore Investigation	W134°22.5' to 134°45'	III-c	F"O" (U)	87-7	Summer 87	SM	24.02		1411	22.84	0.3	Dallimore et al. (1988)	
RICHARDS ISLAND	GSC Near-Shore Investigation	N69°25' to 69°32.5'	III-c	F"O" (U)	87-8	Summer 87	SM	5.43		1514	22.46	14.82	Dallimore et al. (1988)	Hole 87-8:
RICHARDS ISLAND	GSC Near-Shore Investigation	W134°22.5' to 134°45'	III-c	F"O" (U)	87-8	Summer 87	SM	11.05		1478	19.3	6.84	Dallimore et al. (1988)	near shore hole
RICHARDS ISLAND	GSC Near-Shore Investigation	N69°25' to 69°32.5'	III-c	F"O" (U)	87-8	Summer 87	SM	24.6		1642	37.17	4.5	Dallimore et al. (1988)	
RICHARDS ISLAND	GSC Near-Shore Investigation	W134°22.5' to 134°45'	III-c	F"O" (U)	87-10	Summer 87	SM	9.05		1388	21.33	8.67	Dallimore et al. (1988)	Hole 87-10:
RICHARDS ISLAND	GSC Near-Shore Investigation	N69°25' to 69°32.5'	III-c	F"O" (U)	87-10	Summer 87	SM	12.99		1511	22.9	11.39	Dallimore et al. (1988)	offshore hole
RICHARDS ISLAND	GSC Near-Shore Investigation	W134°22.5' to 134°45'	III-c	F"O" (U)	87-10	Summer 87	SM	16.18		1544	22.7	11.82	Dallimore et al. (1988)	Soil is uniform.
RICHARDS ISLAND	GSC Near-Shore Investigation	N69°25' to 69°32.5'	III-c	F"O" (U)	87-11	Summer 87	SM	8.91			21.69	6.91	Dallimore et al. (1988)	Hole 87-11:
RICHARDS ISLAND	GSC Near-Shore Investigation	W134°22.5' to 134°45'	III-c	F"O" (U)	87-11	Summer 87	SM	13.02			23.83	2.96	Dallimore et al. (1988)	offshore hole
RICHARDS ISLAND	GSC Near-Shore Investigation	N69°25' to 69°32.5'	III-c	F"O" (U)	87-11	Summer 87	SM	13.48			23.1	8.67	Dallimore et al. (1988)	Soil is uniform.

COMMUNITY	PROJECT	LOCATION	GEOLOGICAL UNIT	TERRAIN TYPE	HOLE	DATE	SOIL CLASSIFICATION (USCS)	DEPTH(m)	TEMP (°C)	DENSITY (Mg/m3)	M.C. (%)	SALINITY (ppt)	CONSULTANT	COMMENTS
RICHARDS ISLAND	GSC Near-Shore Investigation	W134°22.5' to 134°43'	III-c	F"O" (U)	87-11	Summer 87	SM	15			22.07	6.91	Dallimore et al. (1988)	
RICHARDS ISLAND	GSC Near-Shore Investigation	N69°25' to 69°32.5'	III-c	F"O" (U)	87-11	Summer 87	SM	16.23			24.64	4.34	Dallimore et al. (1988)	
RICHARDS ISLAND	GSC Near-Shore Investigation	W134°22.5' to 134°43'	III-c	F"O" (U)	87-11	Summer 87	SM	22.63			28.84	6.39	Dallimore et al. (1988)	
RICHARDS ISLAND	GSC Near-Shore Investigation	N69°25' to 69°32.5'	III-c	F"O" (U)	87-11	Summer 87	SM	28.73			21.83	13.42	Dallimore et al. (1988)	
RICHARDS ISLAND	GSC Near-Shore Investigation	W134°22.5' to 134°43'	III-c	F"O" (U)	87-12	Summer 87	SM	3.35			15.89	5.27	Dallimore et al. (1988)	Hole 87-12:
RICHARDS ISLAND	GSC Near-Shore Investigation	N69°25' to 69°32.5'	III-c	F"O" (U)	87-12	Summer 87	SM	5.73			22.02	6.83	Dallimore et al. (1988)	offshore hole
RICHARDS ISLAND	GSC Near-Shore Investigation	W134°22.5' to 134°43'	III-c	F"O" (U)	87-12	Summer 87	SM	10.3		1399	21.84	10.89	Dallimore et al. (1988)	Soil is unfrozen.
RICHARDS ISLAND	GSC Near-Shore Investigation	N69°25' to 69°32.5'	III-c	F"O" (U)	87-12	Summer 87	SM	12.6			21.88	7.09	Dallimore et al. (1988)	
RICHARDS ISLAND	GSC Near-Shore Investigation	W134°22.5' to 134°43'	III-c	F"O" (U)	87-12	Summer 87	SM	20.94			19.39	13.25	Dallimore et al. (1988)	
RICHARDS ISLAND	GSC Near-Shore Investigation	N69°25' to 69°32.5'	III-c	F"O" (U)	87-12	Summer 87	SM	23.98		1254	23.38	1.86	Dallimore et al. (1988)	
RICHARDS ISLAND	GSC Near-Shore Investigation	W134°22.5' to 134°43'	III-c	F"O" (U)	87-12	Summer 87	SM	25.26			23.74	4.42	Dallimore et al. (1988)	
RICHARDS ISLAND	GSC Near-Shore Investigation	N69°25' to 69°32.5'	III-c	W (U)	87-13	Summer 87	CL-ML	0.99			30.08	4.93	Dallimore et al. (1988)	
RICHARDS ISLAND	GSC Near-Shore Investigation	W134°22.5' to 134°43'	III-c	F"O" (U)	87-13	Summer 87	SM	20.83			23.07	6.22	Dallimore et al. (1988)	
RICHARDS ISLAND	GSC Near-Shore Investigation	N69°25' to 69°32.5'	III-c	F"O" (U)	87-13	Summer 87	SM	22.31		1392	23.01	7.26	Dallimore et al. (1988)	
RICHARDS ISLAND	GSC Near-Shore Investigation	W134°22.5' to 134°43'	III-c	F"O" (U)	87-13	Summer 87	SM	23.80			21.23	12.71	Dallimore et al. (1988)	
RICHARDS ISLAND	GSC Near-Shore Investigation	N69°25' to 69°32.5'	III-c	F"O" (U)	87-13	Summer 87	SM	25.38		1322	21.32	18.23	Dallimore et al. (1988)	
RICHARDS ISLAND	GSC Near-Shore Investigation	W134°22.5' to 134°43'	III-c	F"O" (U)	87-13	Summer 87	SM	27.28			27.39	3.87	Dallimore et al. (1988)	
RICHARDS ISLAND	GSC Near-Shore Investigation	N69°25' to 69°32.5'	III-c	F"O" (U)	87-13	Summer 87	SM	28.42			40.12	18.36	Dallimore et al. (1988)	
RICHARDS ISLAND	GSC Near-Shore Investigation	W134°35' N69°28'	III-c	F"O" (U)	87-13	Summer 87	SM	29.98		1336	32.7	29.59	Dallimore et al. (1988)	
SPENCE BAY	Recreation Complex	N69°32'W93°32'	II-b	M	82-P1	86/07/07	ML	0.45			12	0.02	Geocon	Many glacial advances
SPENCE BAY	Recreation Complex	N69°32'W93°32'	II-b	M	82-P1	86/07/07			M.A.A.T. = -12 °C				Geocon	Active layer ~1m
TABLE MOUNTAIN	Norman Wells Pipeline	N65°26.5'W125°38.5'	III-a		85-7A T3	85/04/10		1	-3.37				Hardy Associates Ltd. (1978)	Thermistor installed
TABLE MOUNTAIN	Norman Wells Pipeline	N65°26.5'W125°38.5'	III-a		85-7A T3	85/04/10		2	-2.26				Hardy Associates Ltd. (1978)	and monitored
TABLE MOUNTAIN	Norman Wells Pipeline	N65°26.5'W125°38.5'	III-a		85-7A T3	85/04/10		3	-1.38				Hardy Associates Ltd. (1978)	for EMR
TABLE MOUNTAIN	Norman Wells Pipeline	N65°26.5'W125°38.5'	III-a		85-7A T3	85/04/10		4	-0.83				Hardy Associates Ltd. (1978)	
TABLE MOUNTAIN	Norman Wells Pipeline	N65°26.5'W125°38.5'	III-a		85-7A T3	85/04/10		6	-0.75				Hardy Associates Ltd. (1978)	
TABLE MOUNTAIN	Norman Wells Pipeline	N65°26.5'W125°38.5'	III-a		85-7A T3	85/04/10		8	-0.74				Hardy Associates Ltd. (1978)	
TABLE MOUNTAIN	Norman Wells Pipeline	N65°26.5'W125°38.5'	III-a		85-7A T3	85/04/10		10	-0.83				Hardy Associates Ltd. (1978)	
TABLE MOUNTAIN	Norman Wells Pipeline	N65°26.5'W125°38.5'	III-a		85-7A T3	85/04/10		12	-0.73				Hardy Associates Ltd. (1978)	
TABLE MOUNTAIN	Norman Wells Pipeline	N65°26.5'W125°38.5'	III-a		85-7A T3	85/04/10		14	-0.78				Hardy Associates Ltd. (1978)	
TABLE MOUNTAIN	Norman Wells Pipeline	N65°26.5'W125°38.5'	III-a		85-7A T3	85/04/10		17	-0.73				Hardy Associates Ltd. (1978)	
TABLE MOUNTAIN	Norman Wells Pipeline	N65°26.5'W125°38.5'	III-a		85-7A T3	85/04/10		20	-0.79				Hardy Associates Ltd. (1978)	
TABLE MOUNTAIN	Norman Wells Pipeline	N65°26.5'W125°38.5'	III-a		85-7A T3	87/10/06		1	0.18				Hardy Associates Ltd. (1978)	
TABLE MOUNTAIN	Norman Wells Pipeline	N65°26.5'W125°38.5'	III-a		85-7A T3	87/10/06		2	-0.28				Hardy Associates Ltd. (1978)	
TABLE MOUNTAIN	Norman Wells Pipeline	N65°26.5'W125°38.5'	III-a		85-7A T3	87/10/06		3	-0.4				Hardy Associates Ltd. (1978)	
TABLE MOUNTAIN	Norman Wells Pipeline	N65°26.5'W125°38.5'	III-a		85-7A T3	87/10/06		4	-0.63				Hardy Associates Ltd. (1978)	
TABLE MOUNTAIN	Norman Wells Pipeline	N65°26.5'W125°38.5'	III-a		85-7A T3	87/10/06		6	-0.57				Hardy Associates Ltd. (1978)	
TABLE MOUNTAIN	Norman Wells Pipeline	N65°26.5'W125°38.5'	III-a		85-7A T3	87/10/06		8	-0.66				Hardy Associates Ltd. (1978)	
TABLE MOUNTAIN	Norman Wells Pipeline	N65°26.5'W125°38.5'	III-a		85-7A T3	87/10/06		10	-0.7				Hardy Associates Ltd. (1978)	
TABLE MOUNTAIN	Norman Wells Pipeline	N65°26.5'W125°38.5'	III-a		85-7A T3	87/10/06		12	-0.74				Hardy Associates Ltd. (1978)	
TABLE MOUNTAIN	Norman Wells Pipeline	N65°26.5'W125°38.5'	III-a		85-7A T3	87/10/06		14	-0.73				Hardy Associates Ltd. (1978)	
TABLE MOUNTAIN	Norman Wells Pipeline	N65°26.5'W125°38.5'	III-a		85-7A T3	87/10/06		17	-0.6				Hardy Associates Ltd. (1978)	Salinity determination
TABLE MOUNTAIN	Norman Wells Pipeline	N65°26.5'W125°38.5'	III-a		85-7A T3	87/10/06		20	-0.55				Hardy Associates Ltd. (1978)	by method 3
TABLE MOUNTAIN	Norman Wells Pipeline	N65°26.5'W125°38.5'	III-a	M	85-7A O1	85/02/27				Dry density			Hardy Associates Ltd. (1978)	Salinity testing done
TABLE MOUNTAIN	Norman Wells Pipeline	N65°26.5'W125°38.5'	III-a	M	85-7A O1	85/02/27	ML	1.35		1229	24.3	0.24	Hardy Associates Ltd. (1978)	at Carleton Univ.
TABLE MOUNTAIN	Norman Wells Pipeline	N65°26.5'W125°38.5'	III-a	M	85-7A O1	85/02/27	ML	1.84		1568	24	0.24	Hardy Associates Ltd. (1978)	for EMR
TABLE MOUNTAIN	Norman Wells Pipeline	N65°26.5'W125°38.5'	III-a	M	85-7A O1	85/02/27	ML	2.34		1430	25.7	0.41	Hardy Associates Ltd. (1978)	Salinity determination
TABLE MOUNTAIN	Norman Wells Pipeline	N65°26.5'W125°38.5'	III-a	M	85-7A O1	85/02/27	ML	2.55		1380	27.8	0.88	Hardy Associates Ltd. (1978)	by method 2
TABLE MOUNTAIN	Norman Wells Pipeline	N65°26.5'W125°38.5'	III-a	M	85-7A O1	85/02/27	ML-MH	3.18		1496	25.3	1.02	Hardy Associates Ltd. (1978)	
TABLE MOUNTAIN	Norman Wells Pipeline	N65°26.5'W125°38.5'	III-a	M	85-7A O1	85/02/27	ML-MH	3.61		1622	25.4	1.28	Hardy Associates Ltd. (1978)	
TABLE MOUNTAIN	Norman Wells Pipeline	N65°26.5'W125°38.5'	III-a	M	85-7A O1	85/02/27	ML-MH	4.3		1637	24.5	1.13	Hardy Associates Ltd. (1978)	
TABLE MOUNTAIN	Norman Wells Pipeline	N65°26.5'W125°38.5'	III-a	M	85-7A O1	85/02/27	ML-MH	4.97		1454	27.4	1.28	Hardy Associates Ltd. (1978)	
TABLE MOUNTAIN	Norman Wells Pipeline	N65°26.5'W125°38.5'	III-a	M	85-7A O1	85/02/27	ML-MH	5.48		1616	24.1	0.9	Hardy Associates Ltd. (1978)	
TABLE MOUNTAIN	Norman Wells Pipeline	N65°26.5'W125°38.5'	III-a	M	85-7A O1	85/02/27	ML-MH	6.02		1362	24.6	1.05	Hardy Associates Ltd. (1978)	
TABLE MOUNTAIN	Norman Wells Pipeline	N65°26.5'W125°38.5'	III-a	M	85-7A O1	85/02/27	CI-CH	6.67		1085	32.7	0.6	Hardy Associates Ltd. (1978)	
TABLE MOUNTAIN	Norman Wells Pipeline	N65°26.5'W125°38.5'	III-a	M	85-7A O1	85/02/27	CI-CH	7.17		1181	32.5	0.83	Hardy Associates Ltd. (1978)	
TABLE MOUNTAIN	Norman Wells Pipeline	N65°26.5'W125°38.5'	III-a	M	85-7A O1	85/02/27	ML-MH	7.51		1582	26.9	0.86	Hardy Associates Ltd. (1978)	
TABLE MOUNTAIN	Norman Wells Pipeline	N65°26.5'W125°38.5'	III-a	M	85-7A O1	85/02/27	ML-MH	8		1674	23.7	1.21	Hardy Associates Ltd. (1978)	
TABLE MOUNTAIN	Norman Wells Pipeline	N65°26.5'W125°38.5'	III-a	M	85-7A O1	85/02/27	CI-CH	8.05		1610	27.2	0.75	Hardy Associates Ltd. (1978)	
TABLE MOUNTAIN	Norman Wells Pipeline	N65°26.5'W125°38.5'	III-a	M	85-7A O1	85/02/27	CI-CH	10		1614	22.3	0.75	Hardy Associates Ltd. (1978)	
TABLE MOUNTAIN	Norman Wells Pipeline	N65°26.5'W125°38.5'	III-a	M	85-7A O1	85/02/27	ML-MH	10.33		1587	23.2	0.83	Hardy Associates Ltd. (1978)	
TABLE MOUNTAIN	Norman Wells Pipeline	N65°26.5'W125°38.5'	III-a	M	85-7A O1	85/02/27	CI-CH	10.44		1527	26.4	1.13	Hardy Associates Ltd. (1978)	
TABLE MOUNTAIN	Norman Wells Pipeline	N65°26.5'W125°38.5'	III-a	M	85-7A O1	85/02/27	CI-CH	12.22		1488	28.9	0.68	Hardy Associates Ltd. (1978)	
TABLE MOUNTAIN	Norman Wells Pipeline	N65°26.5'W125°38.5'	III-a	M	85-7A O1	85/02/27	ML-MH	13.54		1491	28.2	1.05	Hardy Associates Ltd. (1978)	
TABLE MOUNTAIN	Norman Wells Pipeline	N65°26.5'W125°38.5'	III-a	M	85-7A O1	85/02/27	ML-MH	14.31		1477	29.6	0.98	Hardy Associates Ltd. (1978)	
TABLE MOUNTAIN	Norman Wells Pipeline	N65°26.5'W125°38.5'	III-a	M	85-7A O1	85/02/27	ML	14.98		1581	24.5	0.86	Hardy Associates Ltd. (1978)	
TABLE MOUNTAIN	Norman Wells Pipeline	N65°26.5'W125°38.5'	III-a	M	85-7A O1	85/02/27	ML	15.54		1553	23.9	0.83	Hardy Associates Ltd. (1978)	
TABLE MOUNTAIN	Norman Wells Pipeline	N65°26.5'W125°38.5'	III-a	M	85-7A O1	85/02/27	ML	16.23		1572	23.1	1.13	Hardy Associates Ltd. (1978)	

COMMUNITY	PROJECT	LOCATION	GEOLOGICAL UNIT	TERRAIN TYPE	HOLE	DATE	SOIL CLASSIFICATION (USCS)	DEPTH(m)	TEMP (°C)	DENSITY (Mg/m3)	M.C. (%)	SALINITY (ppt)	CONSULTANT	COMMENTS
TABLE MOUNTAIN	Norman Wells Pipeline	N63°34.9'W125°38.8'	III-a	M	85-7A G1	85/02/27	CI	16.72		1564	27	1.13	Hardy Associates Ltd. (1978)	
TABLE MOUNTAIN	Norman Wells Pipeline	[illegible]	III-a	M	85-7A G1	85/02/27	CI	16.87		1571	25.8	0.98	Hardy Associates Ltd. (1978)	
TABLE MOUNTAIN	Norman Wells Pipeline	[illegible]	III-a	M	85-7A G1	85/02/27	ML	17.42		1630	23.7	0.75	Hardy Associates Ltd. (1978)	
TABLE MOUNTAIN	Norman Wells Pipeline	[illegible]	III-a	M	85-7A G1	85/02/27	CI	18.44		1604	23.4	0.85	Hardy Associates Ltd. (1978)	
TABLE MOUNTAIN	Norman Wells Pipeline	[illegible]	III-a		85-7B T3	85/03/06	ML	19.6		1631	22.7	1.28	Hardy Associates Ltd. (1978)	Thermistor installed
TABLE MOUNTAIN	Norman Wells Pipeline	[illegible]	III-a		85-7B T3	85/03/06		1	-7.84				Hardy Associates Ltd. (1978)	and monitored
TABLE MOUNTAIN	Norman Wells Pipeline	[illegible]	III-a		85-7B T3	85/03/06		2	-2.06				Hardy Associates Ltd. (1978)	for EMR
TABLE MOUNTAIN	Norman Wells Pipeline	[illegible]	III-a		85-7B T3	85/03/06		3	-0.48				Hardy Associates Ltd. (1978)	
TABLE MOUNTAIN	Norman Wells Pipeline	[illegible]	III-a		85-7B T3	85/03/06		4	-0.59				Hardy Associates Ltd. (1978)	
TABLE MOUNTAIN	Norman Wells Pipeline	[illegible]	III-a		85-7B T3	85/03/06		6	-0.85				Hardy Associates Ltd. (1978)	
TABLE MOUNTAIN	Norman Wells Pipeline	[illegible]	III-a		85-7B T3	85/03/06		8	-0.93				Hardy Associates Ltd. (1978)	
TABLE MOUNTAIN	Norman Wells Pipeline	[illegible]	III-a		85-7B T3	85/03/06		10	-1.03				Hardy Associates Ltd. (1978)	
TABLE MOUNTAIN	Norman Wells Pipeline	[illegible]	III-a		85-7B T3	85/03/06		12	-1.13				Hardy Associates Ltd. (1978)	
TABLE MOUNTAIN	Norman Wells Pipeline	[illegible]	III-a		85-7B T3	85/03/06		14	-1.11				Hardy Associates Ltd. (1978)	
TABLE MOUNTAIN	Norman Wells Pipeline	[illegible]	III-a		85-7B T3	85/03/06		17	-1.17				Hardy Associates Ltd. (1978)	
TABLE MOUNTAIN	Norman Wells Pipeline	[illegible]	III-a		85-7B T3	87/10/86		20	-1.07				Hardy Associates Ltd. (1978)	
TABLE MOUNTAIN	Norman Wells Pipeline	[illegible]	III-a		85-7B T3	87/10/86		1	1.86				Hardy Associates Ltd. (1978)	
TABLE MOUNTAIN	Norman Wells Pipeline	[illegible]	III-a		85-7B T3	87/10/86		2	0.77				Hardy Associates Ltd. (1978)	
TABLE MOUNTAIN	Norman Wells Pipeline	[illegible]	III-a		85-7B T3	87/10/86		3	-0.58				Hardy Associates Ltd. (1978)	
TABLE MOUNTAIN	Norman Wells Pipeline	[illegible]	III-a		85-7B T3	87/10/86		4	-0.53				Hardy Associates Ltd. (1978)	
TABLE MOUNTAIN	Norman Wells Pipeline	[illegible]	III-a		85-7B T3	87/10/86		6	-0.81				Hardy Associates Ltd. (1978)	
TABLE MOUNTAIN	Norman Wells Pipeline	[illegible]	III-a		85-7B T3	87/10/86		8	-0.92				Hardy Associates Ltd. (1978)	
TABLE MOUNTAIN	Norman Wells Pipeline	[illegible]	III-a		85-7B T3	87/10/86		10	-1.02				Hardy Associates Ltd. (1978)	
TABLE MOUNTAIN	Norman Wells Pipeline	[illegible]	III-a		85-7B T3	87/10/86		12	-1.13				Hardy Associates Ltd. (1978)	
TABLE MOUNTAIN	Norman Wells Pipeline	[illegible]	III-a		85-7B T3	87/10/86		14	-1.09				Hardy Associates Ltd. (1978)	
TABLE MOUNTAIN	Norman Wells Pipeline	[illegible]	III-a		85-7B T3	87/10/86		17	-1.15				Hardy Associates Ltd. (1978)	
TABLE MOUNTAIN	Norman Wells Pipeline	[illegible]	III-a					20	-1.04				Hardy Associates Ltd. (1978)	
TABLE MOUNTAIN	Norman Wells Pipeline	[illegible]	III-a	M	85-7B G1	85/02/16				Dry density			Hardy Associates Ltd. (1978)	Salinity testing done at
TABLE MOUNTAIN	Norman Wells Pipeline	[illegible]	III-a	M	85-7B G1	85/02/16	CI	1		1295	29.7	0.3	Hardy Associates Ltd. (1978)	Carleton Univ.
TABLE MOUNTAIN	Norman Wells Pipeline	[illegible]	III-a	M	85-7B G1	85/02/16	CI	1.43		1182	36.7	0.25	Hardy Associates Ltd. (1978)	for EMR
TABLE MOUNTAIN	Norman Wells Pipeline	[illegible]	III-a	M	85-7B G1	85/02/16	CI	1.9		1494	25.3	0.45	Hardy Associates Ltd. (1978)	Salinity determination
TABLE MOUNTAIN	Norman Wells Pipeline	[illegible]	III-a	M	85-7B G1	85/02/16	ML	2.6		1555	21.2	0.75	Hardy Associates Ltd. (1978)	by method 2
TABLE MOUNTAIN	Norman Wells Pipeline	[illegible]	III-a	M	85-7B G1	85/02/16	CI-CH	3.4		1645	22.4	1.6	Hardy Associates Ltd. (1978)	
TABLE MOUNTAIN	Norman Wells Pipeline	[illegible]	III-a	M	85-7B G1	85/02/16	MH	4.6		1611	22.7	1.2	Hardy Associates Ltd. (1978)	
TABLE MOUNTAIN	Norman Wells Pipeline	[illegible]	III-a	M	85-7B G1	85/02/16	CI-CL	4.85		1707	19.2	1.7	Hardy Associates Ltd. (1978)	
TABLE MOUNTAIN	Norman Wells Pipeline	[illegible]	III-a	M	85-7B G1	85/02/16	CI-CL	5.95		1539	22.6	1.4	Hardy Associates Ltd. (1978)	
TABLE MOUNTAIN	Norman Wells Pipeline	[illegible]	III-a	M	85-7B G1	85/02/16	CI-CL	6.4		1728	17.7	1.4	Hardy Associates Ltd. (1978)	
TABLE MOUNTAIN	Norman Wells Pipeline	[illegible]	III-a	M	85-7B G1	85/02/16	CI	7.4		1539	22.5	1.2	Hardy Associates Ltd. (1978)	
TABLE MOUNTAIN	Norman Wells Pipeline	[illegible]	III-a	M	85-7B G1	85/02/16	MH	7.9		1640	21.6	0.55	Hardy Associates Ltd. (1978)	
TABLE MOUNTAIN	Norman Wells Pipeline	[illegible]	III-a	M	85-7B G1	85/02/16	CI-CL	8.63		1489	28.6	0.55	Hardy Associates Ltd. (1978)	
TABLE MOUNTAIN	Norman Wells Pipeline	[illegible]	III-a	M	85-7B G1	85/02/16	CI-CL	10.		1319	33.2	0.45	Hardy Associates Ltd. (1978)	
TABLE MOUNTAIN	Norman Wells Pipeline	[illegible]	III-a	M	85-7B G1	85/02/16	ML-CI	10.2		1188	38.1	0.55	Hardy Associates Ltd. (1978)	
TABLE MOUNTAIN	Norman Wells Pipeline	[illegible]	III-a	M	85-7B G1	85/02/16	ML-CI	10.5		1623	23.4	0.4	Hardy Associates Ltd. (1978)	
TABLE MOUNTAIN	Norman Wells Pipeline	[illegible]	III-a	M	85-7B G1	85/02/16	ML-CI	11.75		1749	18.7	0.45	Hardy Associates Ltd. (1978)	
TABLE MOUNTAIN	Norman Wells Pipeline	[illegible]	III-a	M	85-7B G1	85/02/16	ML-CI	12.45		1768	14.5	0.4	Hardy Associates Ltd. (1978)	
TABLE MOUNTAIN	Norman Wells Pipeline	[illegible]	III-a	M	85-7B G1	85/02/16	ML-CI	13.45		1576	20.4	0.5	Hardy Associates Ltd. (1978)	
TABLE MOUNTAIN	Norman Wells Pipeline	[illegible]	III-a	M	85-7B G1	85/02/16	ML-CI	14.05		1632	19.3	0.5	Hardy Associates Ltd. (1978)	
TABLE MOUNTAIN	Norman Wells Pipeline	[illegible]	III-a		85-7C T3	85/03/10	ML-CI	14.65		1681	20.1	0.4	Hardy Associates Ltd. (1978)	
TABLE MOUNTAIN	Norman Wells Pipeline	[illegible]	III-a		85-7C T3	85/03/10		1	-7.44				Hardy Associates Ltd. (1978)	
TABLE MOUNTAIN	Norman Wells Pipeline	[illegible]	III-a		85-7C T3	85/03/10		2	-4.96				Hardy Associates Ltd. (1978)	
TABLE MOUNTAIN	Norman Wells Pipeline	[illegible]	III-a		85-7C T3	85/03/10		3	-4.12				Hardy Associates Ltd. (1978)	
TABLE MOUNTAIN	Norman Wells Pipeline	[illegible]	III-a		85-7C T3	85/03/10		4	-2.57				Hardy Associates Ltd. (1978)	
TABLE MOUNTAIN	Norman Wells Pipeline	[illegible]	III-a		85-7C T3	85/03/10		6	-1.45				Hardy Associates Ltd. (1978)	
TABLE MOUNTAIN	Norman Wells Pipeline	[illegible]	III-a		85-7C T3	85/03/10		8	-1.28				Hardy Associates Ltd. (1978)	
TABLE MOUNTAIN	Norman Wells Pipeline	[illegible]	III-a		85-7C T3	85/03/10		10	-1.17				Hardy Associates Ltd. (1978)	
TABLE MOUNTAIN	Norman Wells Pipeline	[illegible]	III-a		85-7C T3	85/03/10		12	-1.08				Hardy Associates Ltd. (1978)	
TABLE MOUNTAIN	Norman Wells Pipeline	[illegible]	III-a		85-7C T3	85/03/10		14	-1.06				Hardy Associates Ltd. (1978)	
TABLE MOUNTAIN	Norman Wells Pipeline	[illegible]	III-a		85-7C T3	85/03/10		17	-0.95				Hardy Associates Ltd. (1978)	
TABLE MOUNTAIN	Norman Wells Pipeline	[illegible]	III-a		85-7C T3	87/10/86		20	-0.80				Hardy Associates Ltd. (1978)	
TABLE MOUNTAIN	Norman Wells Pipeline	[illegible]	III-a		85-7C T3	87/10/86		1	0.75				Hardy Associates Ltd. (1978)	
TABLE MOUNTAIN	Norman Wells Pipeline	[illegible]	III-a		85-7C T3	87/10/86		2	-0.45				Hardy Associates Ltd. (1978)	
TABLE MOUNTAIN	Norman Wells Pipeline	[illegible]	III-a		85-7C T3	87/10/86		3	-0.86				Hardy Associates Ltd. (1978)	
TABLE MOUNTAIN	Norman Wells Pipeline	[illegible]	III-a		85-7C T3	87/10/86		4	-1.04				Hardy Associates Ltd. (1978)	
TABLE MOUNTAIN	Norman Wells Pipeline	[illegible]	III-a		85-7C T3	87/10/86		6	-1.21				Hardy Associates Ltd. (1978)	
TABLE MOUNTAIN	Norman Wells Pipeline	[illegible]	III-a		85-7C T3	87/10/86		8	-1.21				Hardy Associates Ltd. (1978)	
TABLE MOUNTAIN	Norman Wells Pipeline	[illegible]	III-a		85-7C T3	87/10/86		10	-1.16				Hardy Associates Ltd. (1978)	
TABLE MOUNTAIN	Norman Wells Pipeline	[illegible]	III-a		85-7C T3	87/10/86		12	-1.09				Hardy Associates Ltd. (1978)	
TABLE MOUNTAIN	Norman Wells Pipeline	[illegible]	III-a		85-7C T3	87/10/86		14	-1.09				Hardy Associates Ltd. (1978)	
TABLE MOUNTAIN	Norman Wells Pipeline	[illegible]	III-a		85-7C T3	87/10/86		17	-0.96				Hardy Associates Ltd. (1978)	
TABLE MOUNTAIN	Norman Wells Pipeline	[illegible]	III-a					20	-0.88				Hardy Associates Ltd. (1978)	

COMMUNITY	PROJECT	LOCATION	GEOLOGICAL UNIT	TERRAIN TYPE	HOLE	DATE	SOIL CLASSIFICATION (USCS)	DEPTH(m)	TEMP (°C)	DENSITY (Mg/m3)	M.C. (%)	SALINITY (ppt)	CONSULTANT	COMMENTS
TABLE MOUNTAIN	Norman Wells Pipeline	N63°26.4'W123°38.8'	III-a	M	85-7C 01	85/02/26				Dry density			Hardy Associates Ltd. (1978)	
TABLE MOUNTAIN	Norman Wells Pipeline	N63°26.4'W123°38.8'	III-a	M	85-7C 01	85/02/26	ML	0.12		1509	24.2	0.25	Hardy Associates Ltd. (1978)	
TABLE MOUNTAIN	Norman Wells Pipeline	N63°26.4'W123°38.8'	III-a	M	85-7C 01	85/02/26	ML	1.09		1591	24	0.31	Hardy Associates Ltd. (1978)	
TABLE MOUNTAIN	Norman Wells Pipeline	N63°26.4'W123°38.8'	III-a	M	85-7C 01	85/02/26	CI	1.63		1528	26.4	0.33	Hardy Associates Ltd. (1978)	
TABLE MOUNTAIN	Norman Wells Pipeline	N63°26.4'W123°38.8'	III-a	M	85-7C 01	85/02/26	ML	2.43		1559	26.1	0.45	Hardy Associates Ltd. (1978)	
TABLE MOUNTAIN	Norman Wells Pipeline	N63°26.4'W123°38.8'	III-a	M	85-7C 01	85/02/26	ML	3.48		1679	23.8	0.94	Hardy Associates Ltd. (1978)	
TABLE MOUNTAIN	Norman Wells Pipeline	N63°26.4'W123°38.8'	III-a	M	85-7C 01	85/02/26	ML	4.18		1545	25.8	1.13	Hardy Associates Ltd. (1978)	
TABLE MOUNTAIN	Norman Wells Pipeline	N63°26.4'W123°38.8'	III-a	M	85-7C 01	85/02/26	ML	4.68		1734	19.4	0.68	Hardy Associates Ltd. (1978)	
TABLE MOUNTAIN	Norman Wells Pipeline	N63°26.4'W123°38.8'	III-a	M	85-7C 01	85/02/26	ML	5.47		1662	18.8	0.75	Hardy Associates Ltd. (1978)	
TABLE MOUNTAIN	Norman Wells Pipeline	N63°26.4'W123°38.8'	III-a	M	85-7C 01	85/02/26	ML-MH	6.25		1643	22.2	1.28	Hardy Associates Ltd. (1978)	
TABLE MOUNTAIN	Norman Wells Pipeline	N63°26.4'W123°38.8'	III-a	M	85-7C 01	85/02/26	CI-CH	7.01		1724	18.9	0.71	Hardy Associates Ltd. (1978)	
TABLE MOUNTAIN	Norman Wells Pipeline	N63°26.4'W123°38.8'	III-a	M	85-7C 01	85/02/26	ML-MH	10.8		1968	19.5	0.68	Hardy Associates Ltd. (1978)	
TABLE MOUNTAIN	Norman Wells Pipeline	N63°26.4'W123°38.8'	III-a	M	85-7C 01	85/02/26	CI-CH	12.75		1529	29	0.6	Hardy Associates Ltd. (1978)	
TABLE MOUNTAIN	Norman Wells Pipeline	N63°26.4'W123°38.8'	III-a	M	85-7C 01	85/02/26	ML-MH	12.95		1232	26.4	0.64	Hardy Associates Ltd. (1978)	
TABLE MOUNTAIN	Norman Wells Pipeline	N63°26.4'W123°38.8'	III-a	M	85-7C 01	85/02/26	ML-MH	13.21		1578	24.4	0.75	Hardy Associates Ltd. (1978)	
TABLE MOUNTAIN	Norman Wells Pipeline	N63°26.4'W123°38.8'	III-a	M	85-7C 01	85/02/26	ML-MH	13.67		1535	27.9	0.85	Hardy Associates Ltd. (1978)	
TABLE MOUNTAIN	Norman Wells Pipeline	N63°26.4'W123°38.8'	III-a	M	85-7C 01	85/02/26	ML	13.98		1316	25.7	0.75	Hardy Associates Ltd. (1978)	
TABLE MOUNTAIN	Norman Wells Pipeline	N63°26.4'W123°38.8'	III-a	M	85-7C 01	85/02/26	ML-MH	15.65		1722	21	1.02	Hardy Associates Ltd. (1978)	
TABLE MOUNTAIN	Norman Wells Pipeline	N63°26.4'W123°38.8'	III-a	M	85-7C 01	85/02/26	ML-MH	15.15		1388	24.2	0.98	Hardy Associates Ltd. (1978)	
TABLE MOUNTAIN	Norman Wells Pipeline	N63°26.4'W123°38.8'	III-a	M	85-7C 01	85/02/26	SM	16.89		1614	21.2	0.75		
TUKTOYAKTUK	Proposed Garage	N69°27' W133°02'	III-b						M.A.G.T. = -3°C		(		Geocon, 1986	Continuous permafrost
TUKTOYAKTUK	Proposed Garage	N69°27' W133°02'	III-b	P'O' (?)	1	85/11/20	SM	0.9			16	1.55	Geocon, 1986	Salinity: NaCl content
TUKTOYAKTUK	Arena	N69°27' W133°02'	III-b	P'O' (?)	A-2	85/02/24	SW-SM	1.1			37	0.0246	Geocon, 1985	Salinity: NaCl content
TUKTOYAKTUK	Arena	N69°27' W133°02'	III-b	P'O' (?)	A-3	85/02/24	SM	1.3			42	0.00022	Geocon, 1985	
TUKTOYAKTUK	Arena	N69°27' W133°02'	III-b	P'O' (?)	A-4	85/02/24	SP-SM	3			22	0.00006	Geocon, 1985	
TUKTOYAKTUK	Granular Management Plan	N69°27' W133°02'	III-b	P'O'	155N-02	87/03/16	GP	0.9-1.5			3	2.3	Hardy BBT	Salinity determination
TUKTOYAKTUK	Granular Management Plan	N69°27' W133°02'	III-b	P'O'	155N-16	87/03/18	SP-SM	0.5-1.5			3	1.3	Hardy BBT	probably by method 3
TUKTOYAKTUK	Granular Management Plan	N69°27' W133°02'	III-b	P'O'	155N-18	87/03/18	GW/GP	0.6-1.8			11	1.1	Hardy BBT	
TUKTOYAKTUK	Granular Management Plan	N69°27' W133°02'	III-b	P'O'	155N-19	87/03/18	GW/GP	1.2-2.1			12	1.6	Hardy BBT	
TUKTOYAKTUK	Granular Management Plan	N69°27' W133°02'	III-b	P'O'	155N-35	87/03/23	SP-SM	0.6-1.8			10	1.5	Hardy BBT	
TUKTOYAKTUK	Granular Management Plan	N69°27' W133°02'	III-b	P'O'	155S-08	87/03/20	GW/GP	0.2-1.1			6	2.3	Hardy BBT	
TUKTOYAKTUK	Granular Management Plan	N69°27' W133°02'	III-b	P'O'	155S-11	87/03/20	GW/GP	0.5-1.5			8	1.7	Hardy BBT	
TUKTOYAKTUK	Granular Management Plan	N69°27' W133°02'	III-b	P'O'	155S-17	87/03/21	GW/GP	0.6-2.1			3	2.6	Hardy BBT	
TUKTOYAKTUK	Granular Management Plan	N69°27' W133°02'	III-b	P'O'	155S-21	87/03/21	SP-SM	2.1-2.4			18	9.1	Hardy BBT	
TUKTOYAKTUK	Sewage Facility	N69°27' W133°02'	III-b		87-1	87/02/04	SP + ICE	6.1			77	0.1	Thurber Cons. Ltd.	File 16-04-38
TUKTOYAKTUK	Sewage Facility	N69°27' W133°02'	III-b		87-1	87/02/11		6	-3.1				Thurber Cons. Ltd.	Salinity determination
TUKTOYAKTUK	Sewage Facility	N69°27' W133°02'	III-b		87-1	87/02/04	SM	5.8			41	0	Thurber Cons. Ltd.	by method 3
TUKTOYAKTUK	Sewage Facility	N69°27' W133°02'	III-b		87-2	87/02/05	SP-SM + ICE	4.2			118	0	Thurber Cons. Ltd.	
TUKTOYAKTUK	Sewage Facility	N69°27' W133°02'	III-b	F (?)	87-2	87/02/11		6.5	-4.2				Thurber Cons. Ltd.	
TUKTOYAKTUK	Sewage Facility	N69°27' W133°02'	III-b	P'O'	87-2	87/02/05	SP	7.5			30	0.3	Thurber Cons. Ltd.	
TUKTOYAKTUK	Sewage Facility	N69°27' W133°02'	III-b		87-3	87/02/02	GM	3.8			8	2.7	Thurber Cons. Ltd.	
TUKTOYAKTUK	Sewage Facility	N69°27' W133°02'	III-b		87-3	87/02/02	ICE	5.1			200	0.1	Thurber Cons. Ltd.	
TUKTOYAKTUK	Sewage Facility	N69°27' W133°02'	III-b		87-3	87/02/02	SM + ICE	8			31	0.1	Thurber Cons. Ltd.	
TUKTOYAKTUK	Sewage Facility	N69°27' W133°02'	III-b		87-4	87/02/04	ICE + SM	4			200	0	Thurber Cons. Ltd.	
TUKTOYAKTUK	Sewage Facility	N69°27' W133°02'	III-b		87-4	87/02/04	ICE + SM	8.8			76	0	Thurber Cons. Ltd.	
TUKTOYAKTUK	Sewage Facility	N69°27' W133°02'	III-b	P'O' (?)	87-5	87/02/05	SM	2.8			18	1	Thurber Cons. Ltd.	
TUKTOYAKTUK	Sewage Facility	N69°27' W133°02'	III-b		87-5	87/02/05	ICE + SM	5.5			32	0.2	Thurber Cons. Ltd.	
TUKTOYAKTUK	Sewage Facility	N69°27' W133°02'	III-b		87-5	87/02/11		6	-3.5				Thurber Cons. Ltd.	
TUKTOYAKTUK	Sewage Facility	N69°27' W133°02'	III-b	F (?)	87-5	87/02/05	SP-SM	9.5			29	0.6	Thurber Cons. Ltd.	
TUKTOYAKTUK	Sewage Facility	N69°27' W133°02'	III-b	F (?)	87-6	87/02/05	SP-SM	7			28	0	Thurber Cons. Ltd.	
TUKTOYAKTUK	Sewage Facility	N69°27' W133°02'	III-b	F (?)	87-6	87/02/05	SP-SM	9.7			25	0.4	Thurber Cons. Ltd.	
TUKTOYAKTUK	Sewage Facility	N69°27' W133°02'	III-b		87-7	87/02/04	ICE + SM	3.9			138	0	Thurber Cons. Ltd.	
TUKTOYAKTUK	Sewage Facility	N69°27' W133°02'	III-b		87-7	87/02/11		6	-4.3				Thurber Cons. Ltd.	
TUKTOYAKTUK	Sewage Facility	N69°27' W133°02'	III-b	F (?)	87-7	87/02/04	SP-SM	7.6			26	0.1	Thurber Cons. Ltd.	
TUKTOYAKTUK	Sewage Facility	N69°27' W133°02'	III-b	F (?)	87-7	87/02/04	SP-SM	9.4			25	0.2	Thurber Cons. Ltd.	
TUKTOYAKTUK	Sewage Facility	N69°27' W133°02'	III-b		87-8	87/02/05	ICE + SP-SM	7.7			82	0.1	Thurber Cons. Ltd.	
TUKTOYAKTUK	Sewage Facility	N69°27' W133°02'	III-b		87-8	87/02/05	ICE + SP-SM	10			45	0.3	Thurber Cons. Ltd.	
WHALE COVE	Proposed Powerhouse	N62°11' W92°36'	II-a	W or M	Pit 87-1	87/09/17	ML + ICE	1.2			21	0.3	Thurber Cons. Ltd.	File 15-37-01
WHALE COVE	Proposed Powerhouse	N62°11' W92°36'	II-a	W or M	Pit 87-5	87/09/17	GP	0.9			9	0.9	Thurber Cons. Ltd.	Salinity determination
WHALE COVE	Proposed Powerhouse	N62°11' W92°36'	II-a	W or M	Pit 87-6	87/09/17	GW-GM	1.2			4	1.1	Thurber Cons. Ltd.	by method 3
WHALE COVE	Proposed Powerhouse	N62°11' W92°36'	II-a	W or M	Pit 87-10	87/09/18	SM-ML	1			5	0.5	Thurber Cons. Ltd.	
WHALE COVE	Multi-Purpose Hall	N62°11' W92°36'	II-a	W or M	85-1	85/05/01	SM	0.7			12	0.45	Thurber Cons. Ltd.	File 15-22-31
WHALE COVE	Multi-Purpose Hall	N62°11' W92°36'	II-a	W or M	85-2	85/05/01	SW	1.3			14	0.42	Thurber Cons. Ltd.	Salinity determination
WHALE COVE	Multi-Purpose Hall	N62°11' W92°36'	II-a	W or M	85-3	85/05/02	SM	2.3			9	0.47	Thurber Cons. Ltd.	by method 3
WRIGLEY	Water Well Program '74	N63°16' W123°37'	III-a	M (?)	82-74	74/09	GP	48				0.61	Hydrogeological Cons. Ltd., 1975	Salinity as total
WRIGLEY	Water Well Program '74	N63°16' W123°37'	III-a										Hydrogeological Cons. Ltd., 1975	dissolved salts
WRIGLEY	Water Well Program '74	N63°16' W123°37'	III-a										Hydrogeological Cons. Ltd., 1975	Drilling mud was used

APPENDIX B

RESULTS of the UNCONFINED CONSTANT STRAIN RATE COMPRESSION TESTS

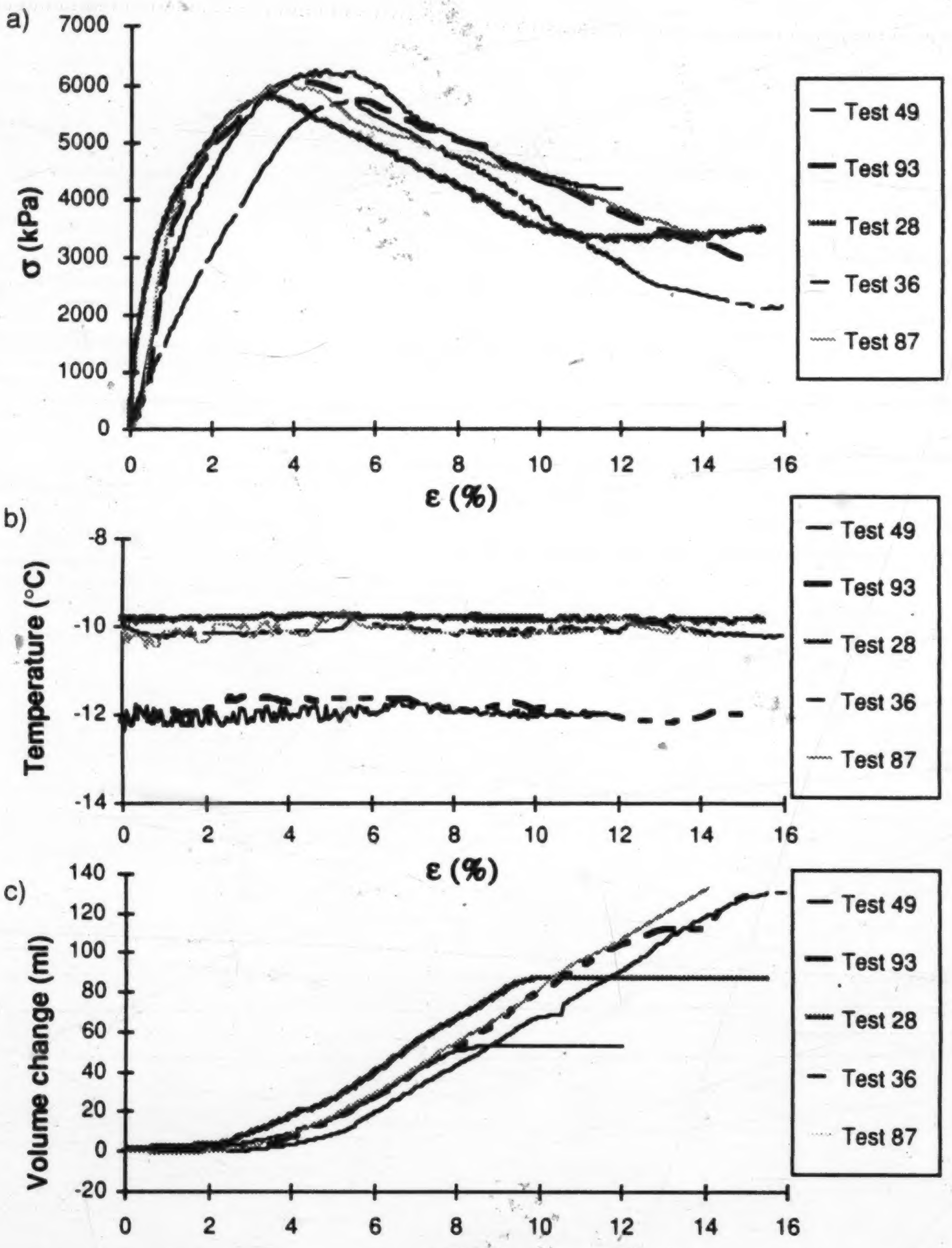

Figure B.1: Compression results soil A 0 ppt T = -12°C and -10°C
a) stress-strain curve b) temperature vs strain
c) volume change vs strain

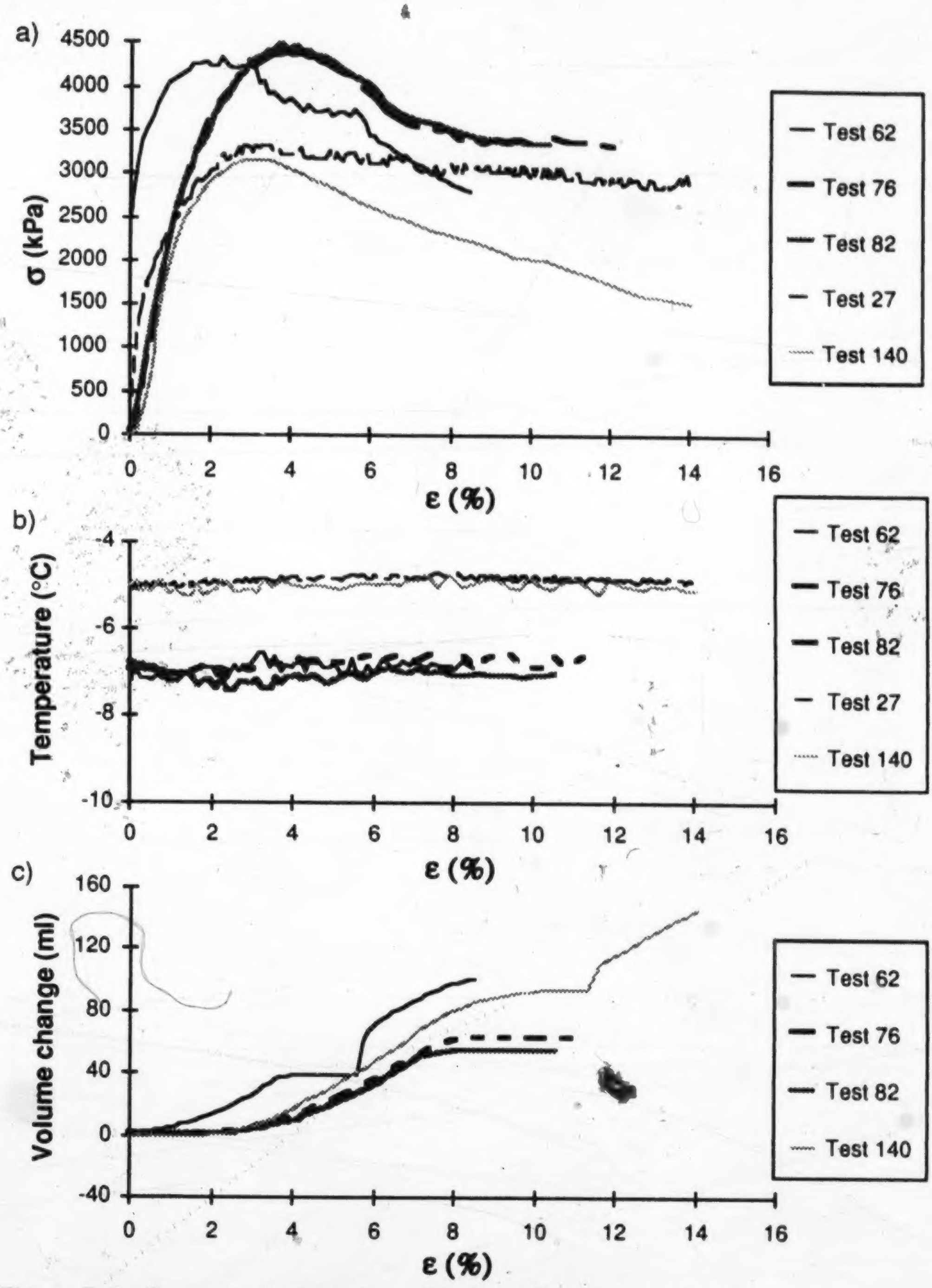

Figure B.2: Compression results soil A 0 ppt T = -7°C and -5°C
a) stress-strain curve b) temperature vs strain
c) volume change vs strain

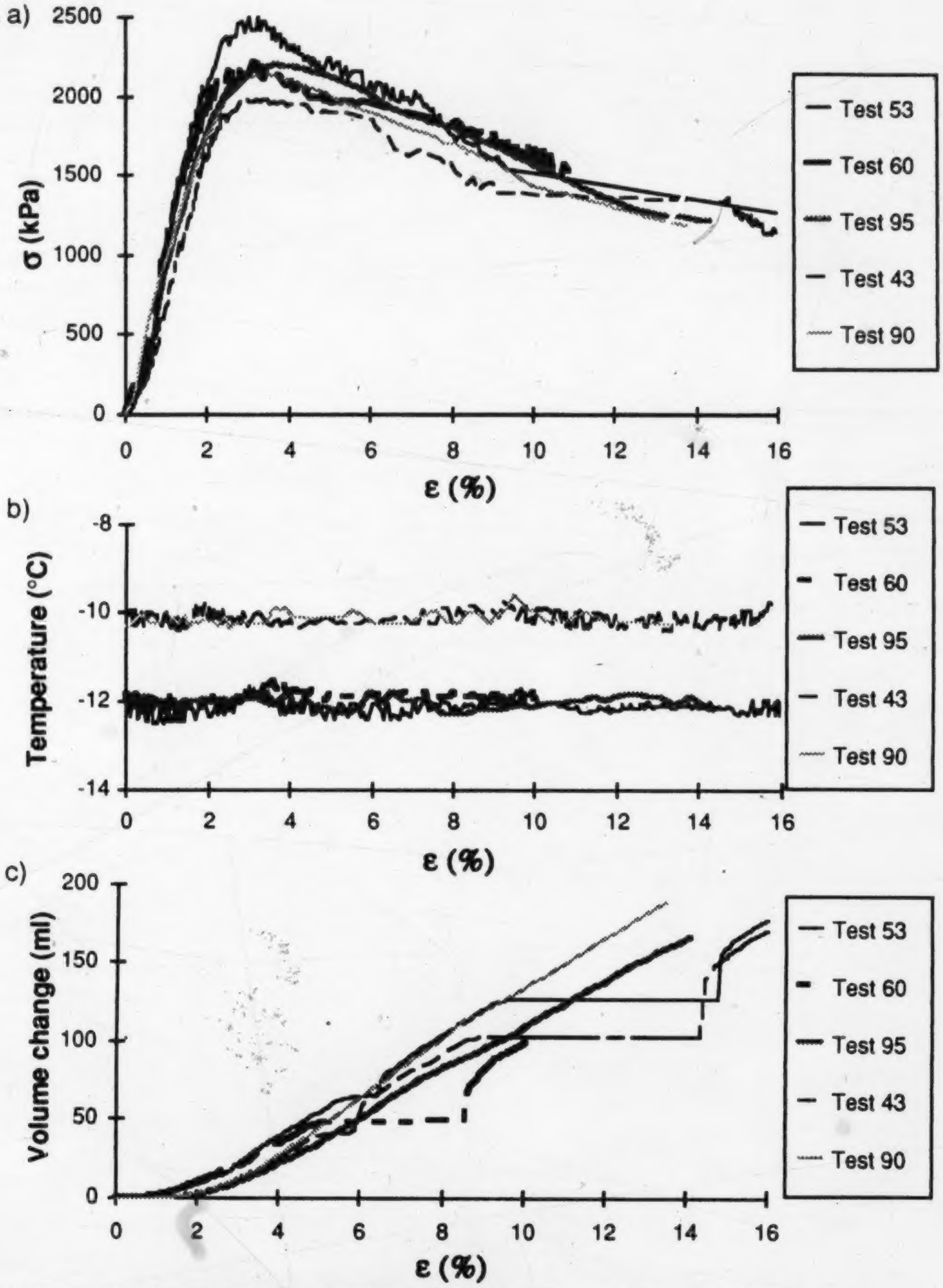

Figure B.3: Compression results soil A 5 ppt T = -12°C and -10°C
a) stress-strain curve b) temperature vs strain
c) volume change vs strain

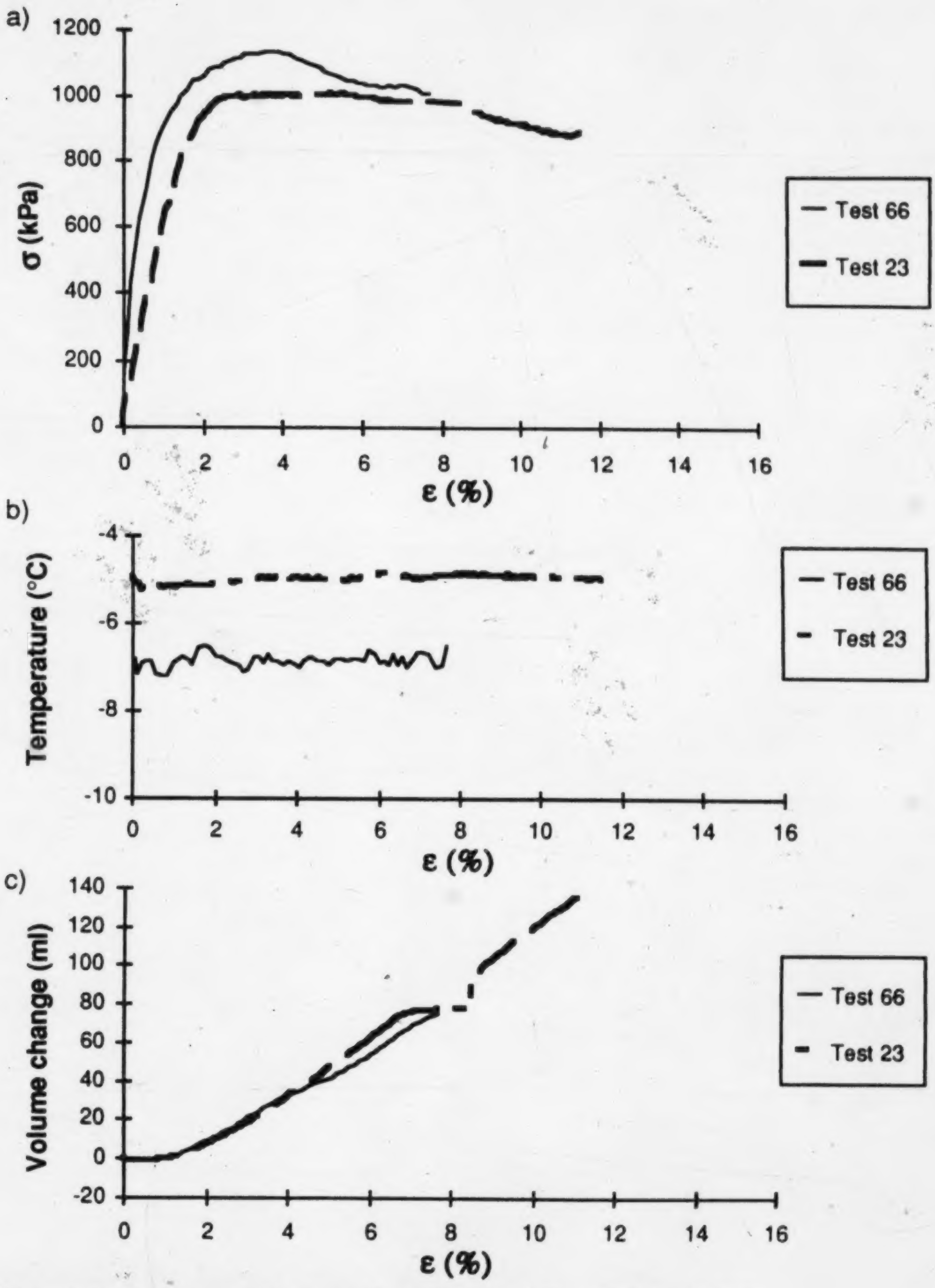

Figure B.4: Compression results soil A 5 ppt T = -7°C and -5°C
a) stress-strain curve b) temperature vs strain
c) volume change vs strain

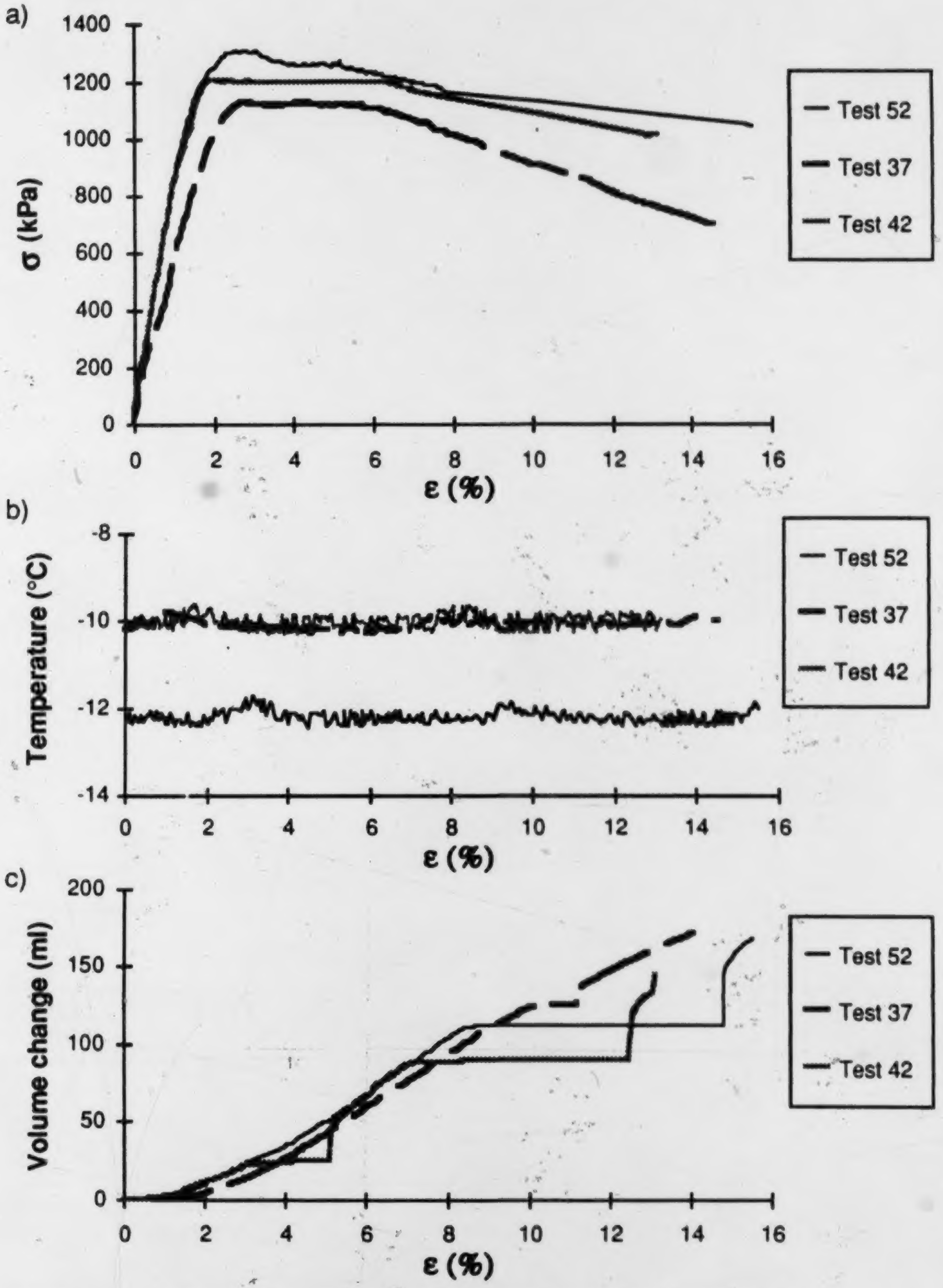

Figure B.5: Compression results soil A 10 ppt T = -12°C and -10°C
a) stress-strain curve b) temperature vs strain
c) volume change vs strain

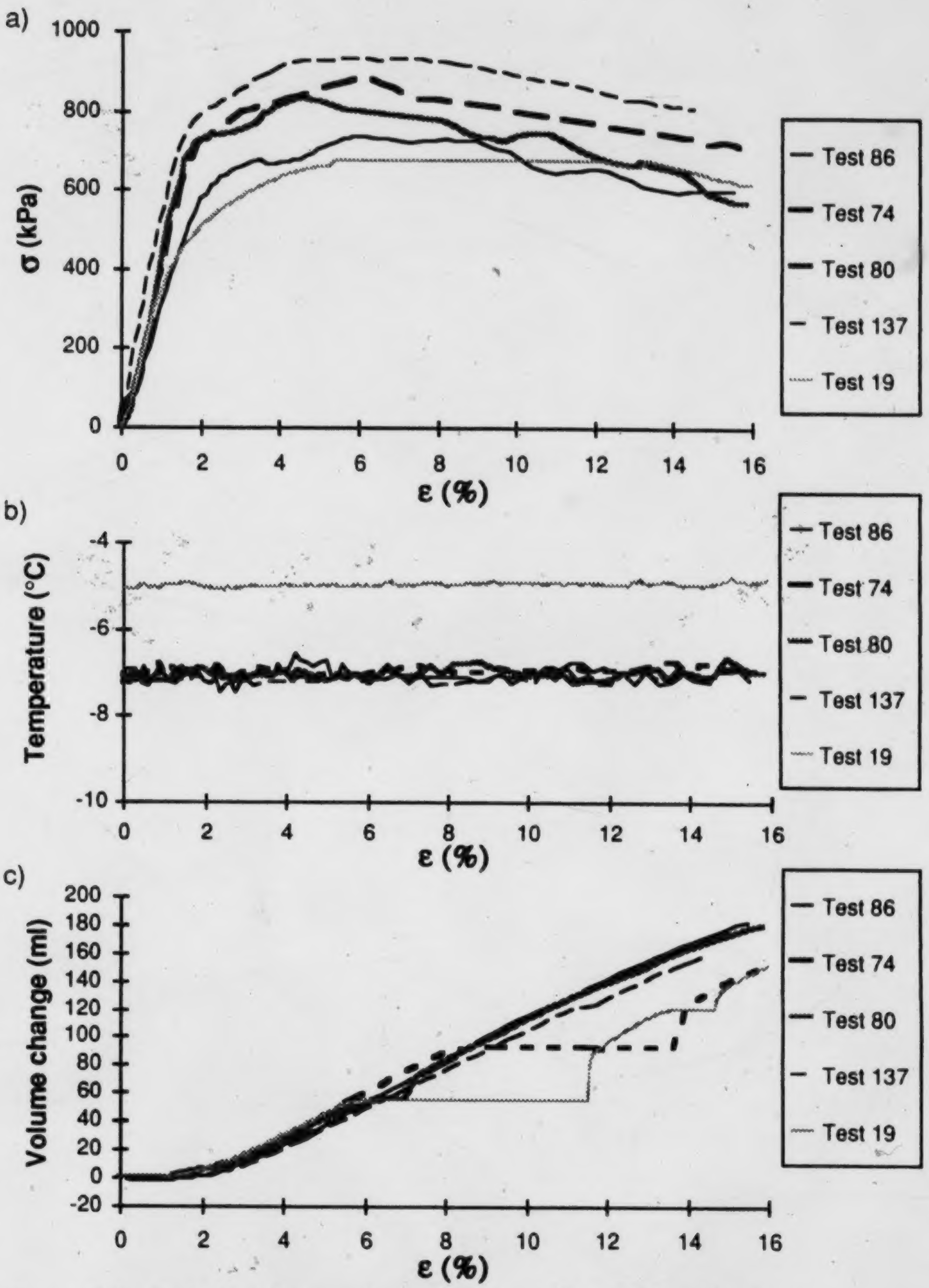

Figure B.6: Compression results soil A 10 ppt T = -7°C and -5°C
a) stress-strain curve b) temperature vs strain
c) volume change vs strain

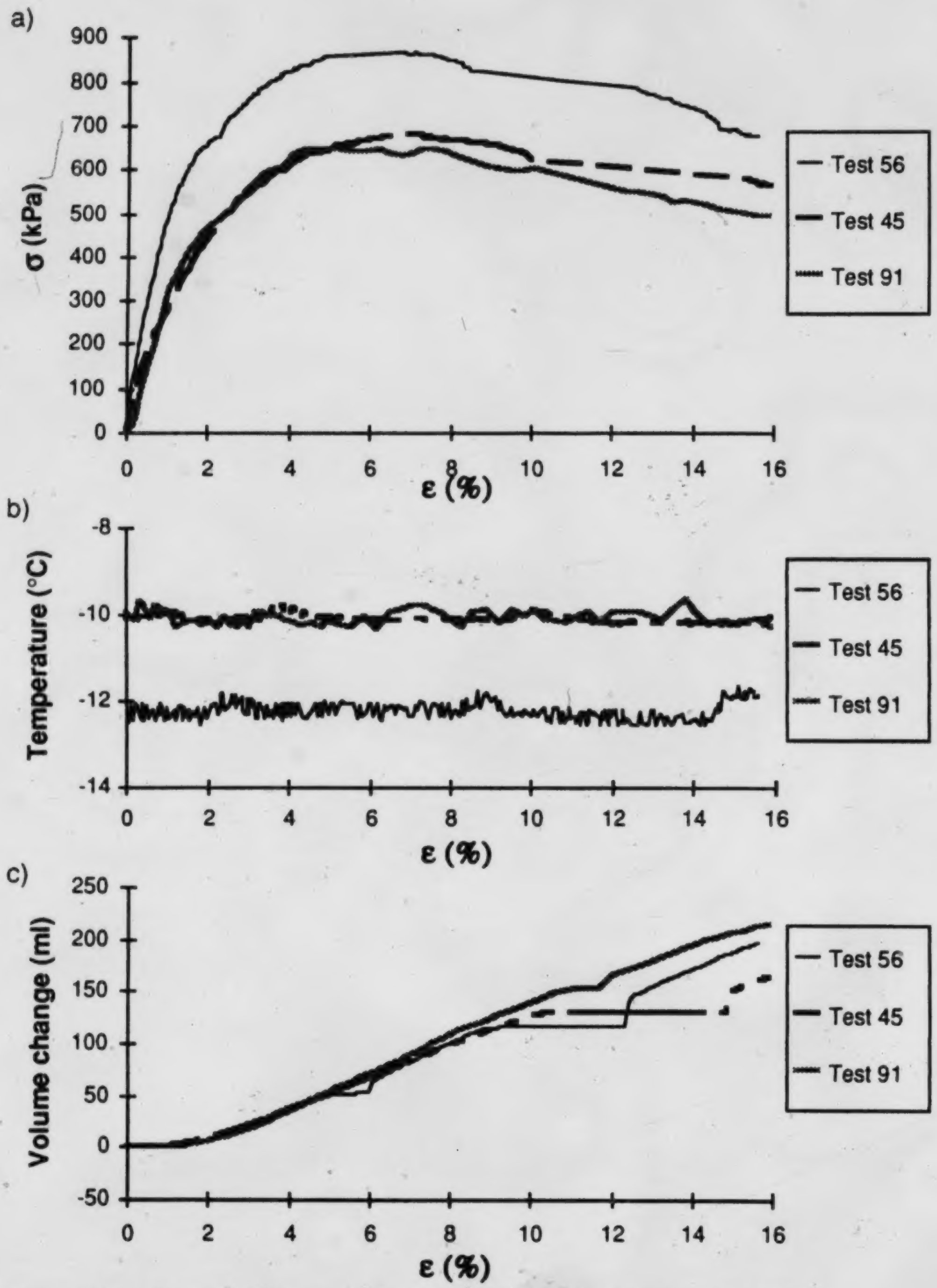

Figure B.7: Compression results soil A 30 ppt T = -12°C and -10°C
a) stress-strain curve b) temperature vs strain
c) volume change vs strain

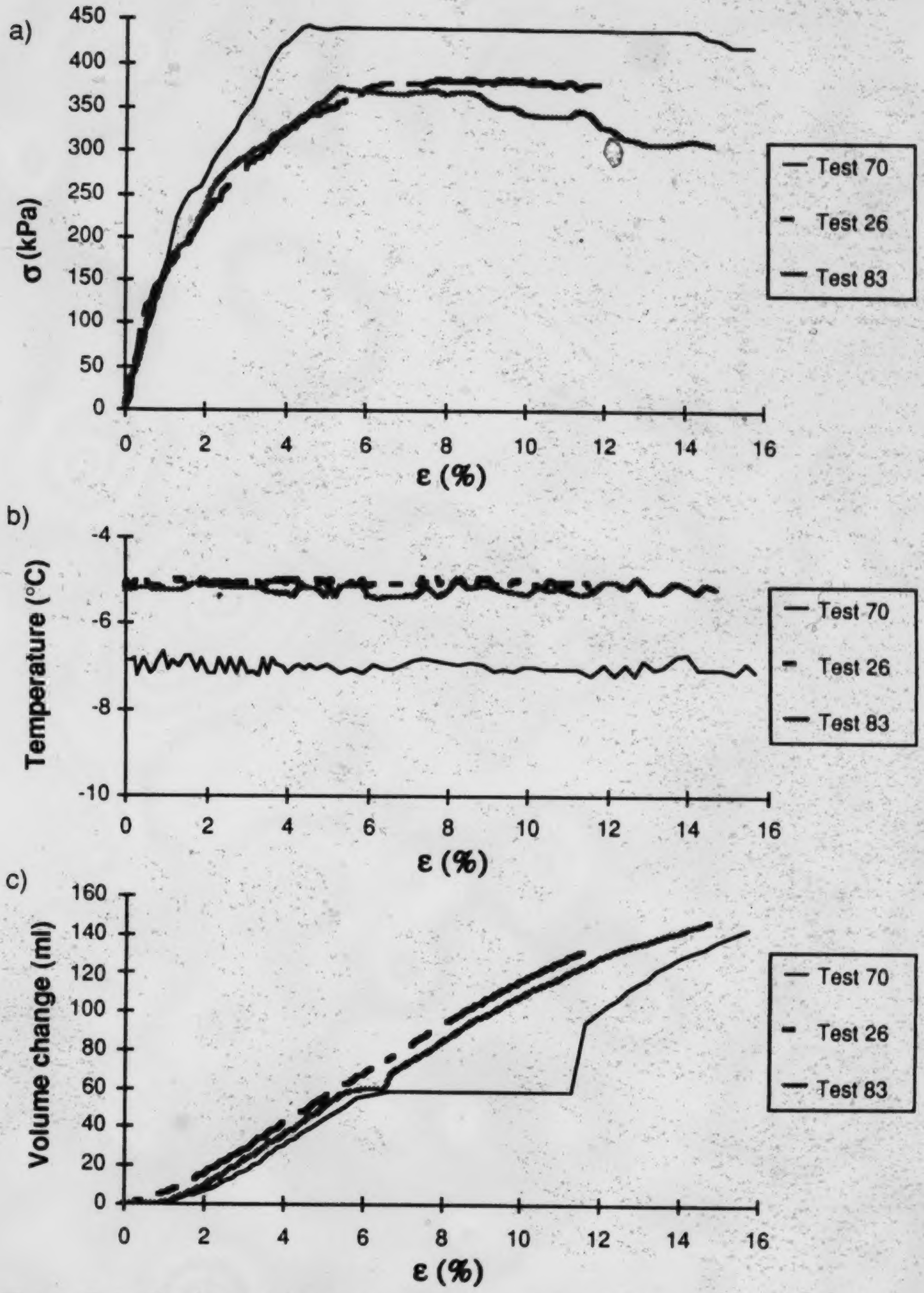

Figure B.8: Compression results soil A 30 ppt T = -7°C and -5°C
a) stress-strain curve b) temperature vs strain
c) volume change vs strain

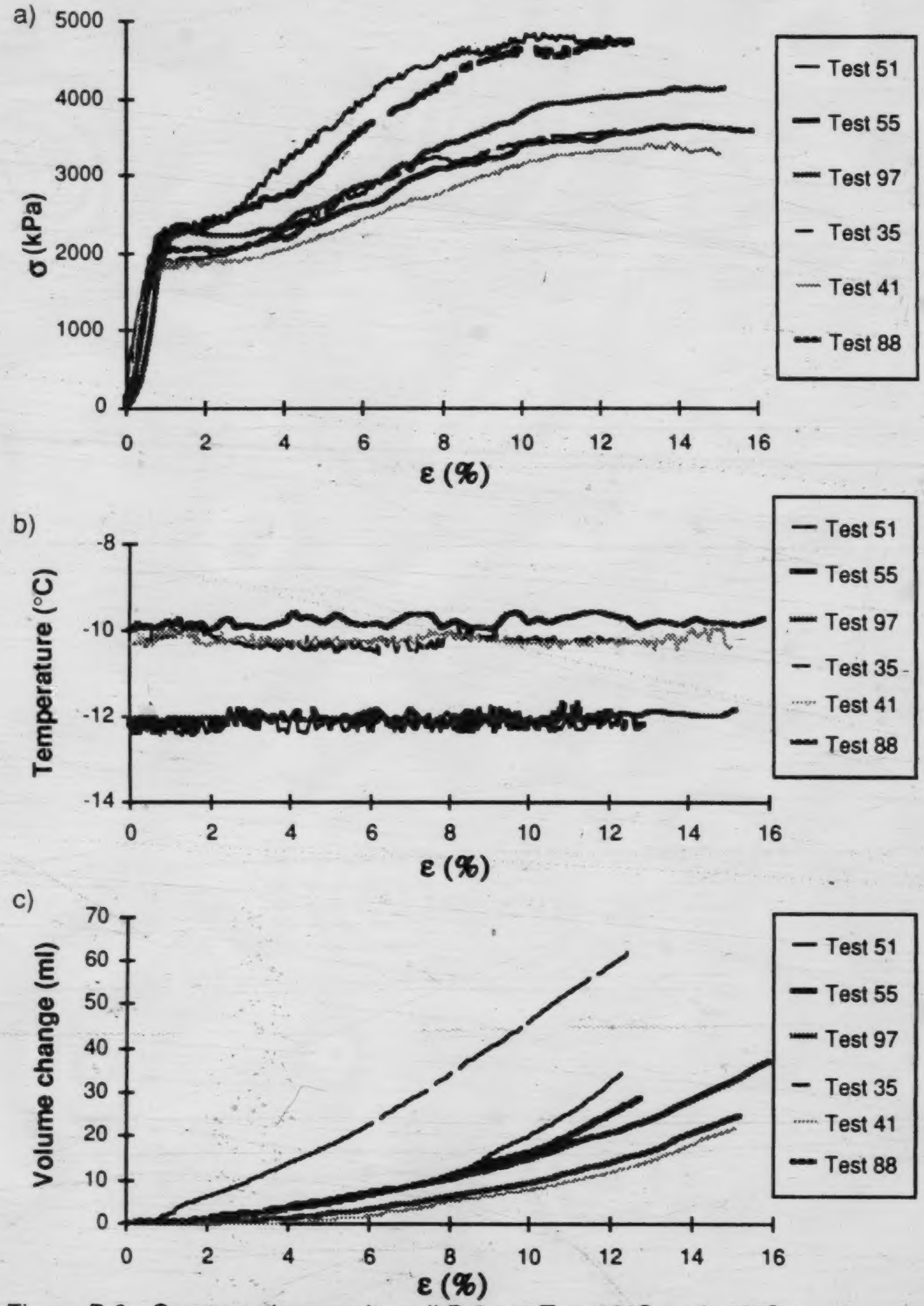

Figure B.9: Compression results soil B 0 ppt T = -12°C and -10°C
a) stress-strain curve b) temperature vs strain
c) volume change vs strain

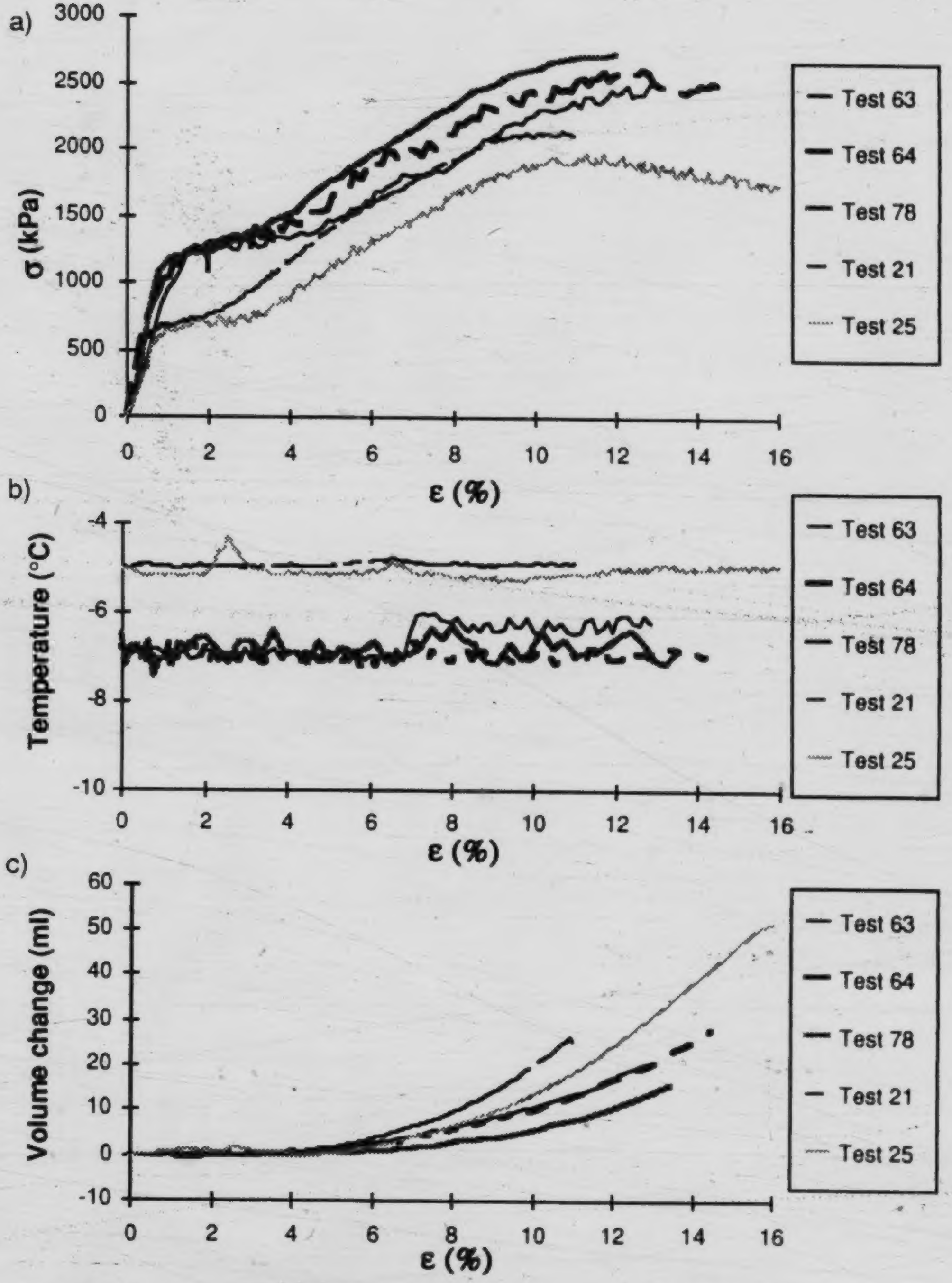

Figure B.10: Compression results soil B 0 ppt T = -7°C and -5°C
a) stress-strain curve b) temperature vs strain
c) volume change vs strain

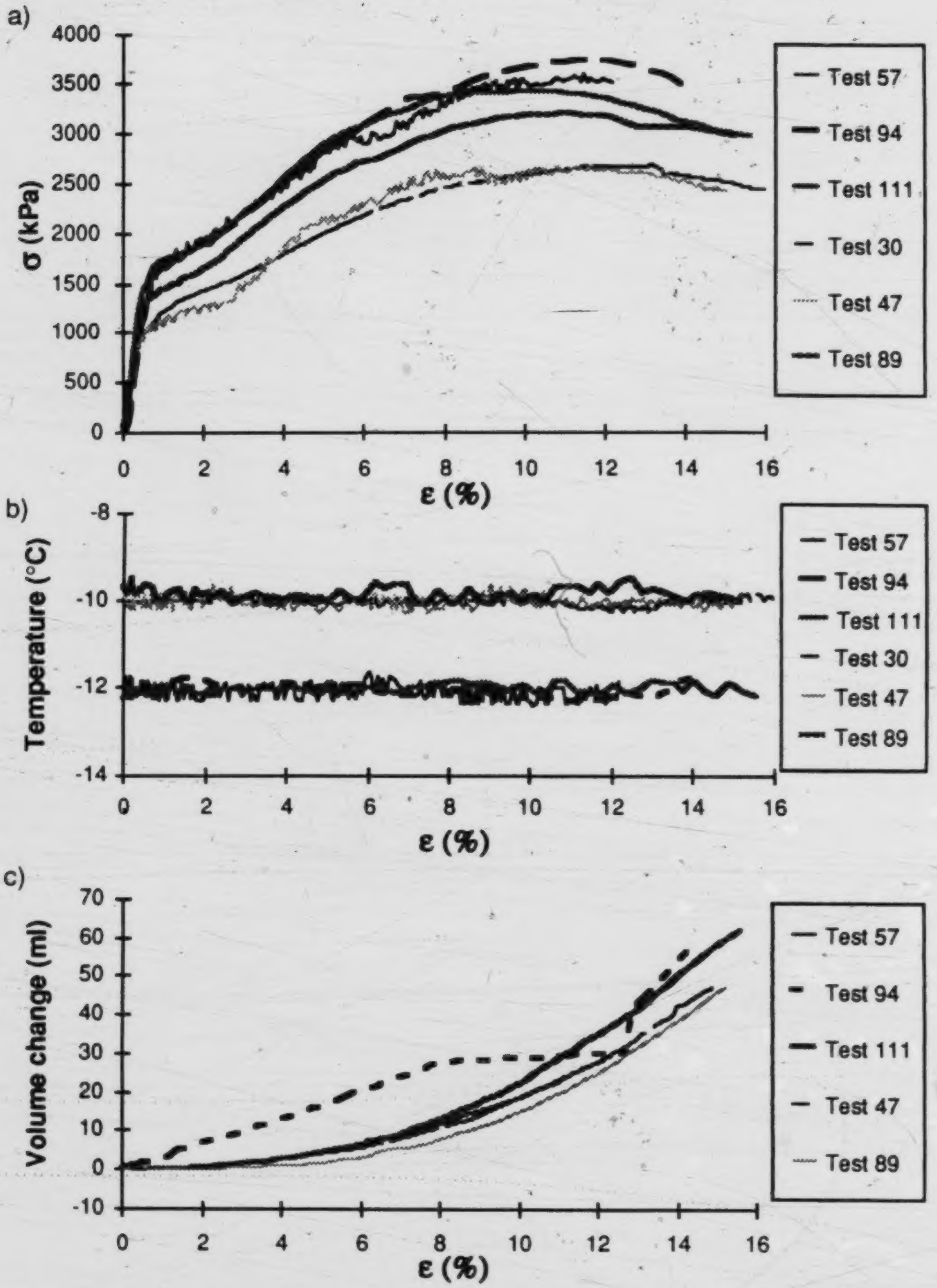

Figure B.11: Compression results soil B 5 ppt T = -12°C and -10°C
a) stress-strain curve b) temperature vs strain
c) volume change vs strain

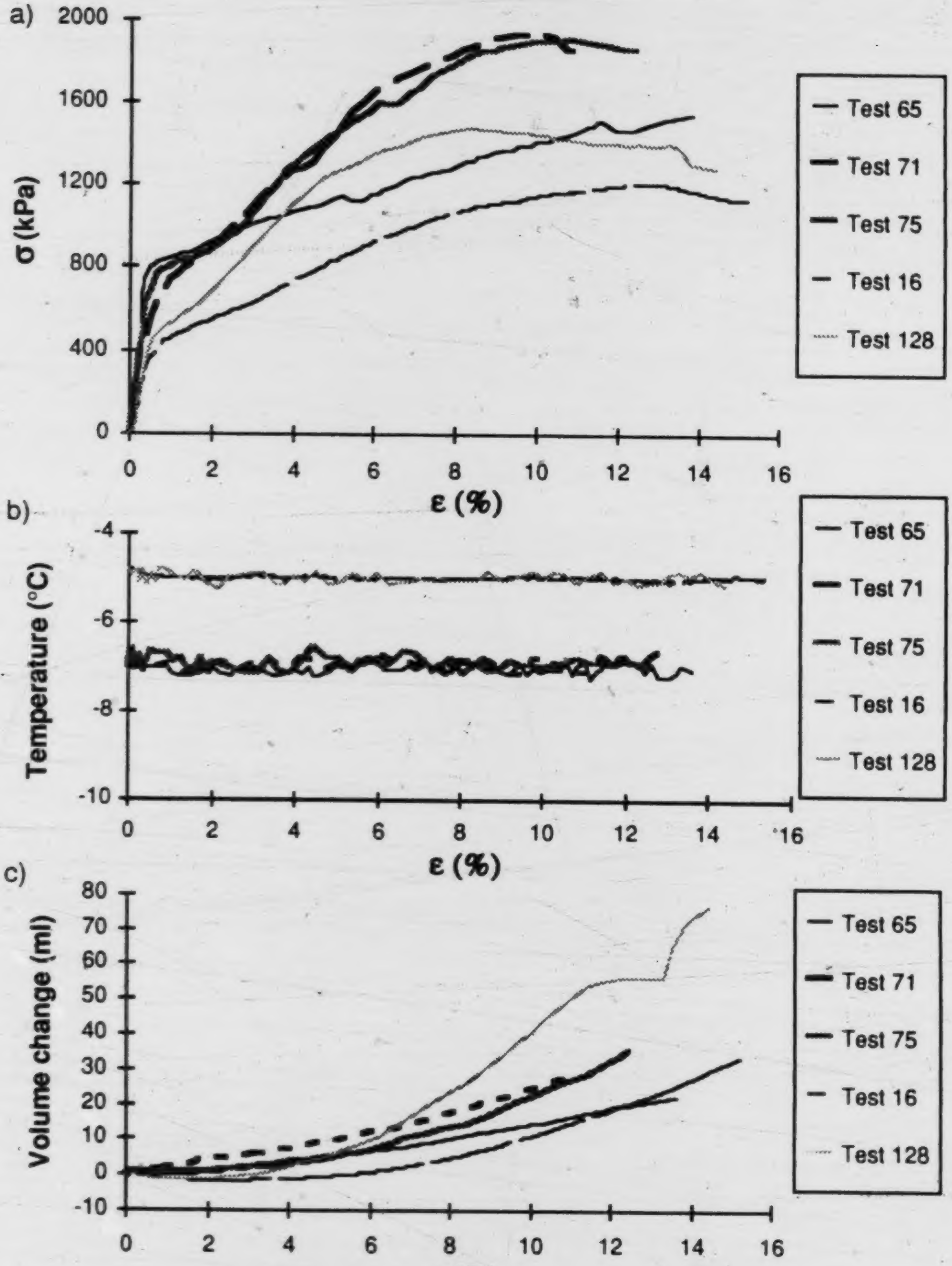

Figure B.12: Compression results soil B 5 ppt T = -7°C and -5°C
a) stress-strain curve b) temperature vs strain
c) volume change vs strain

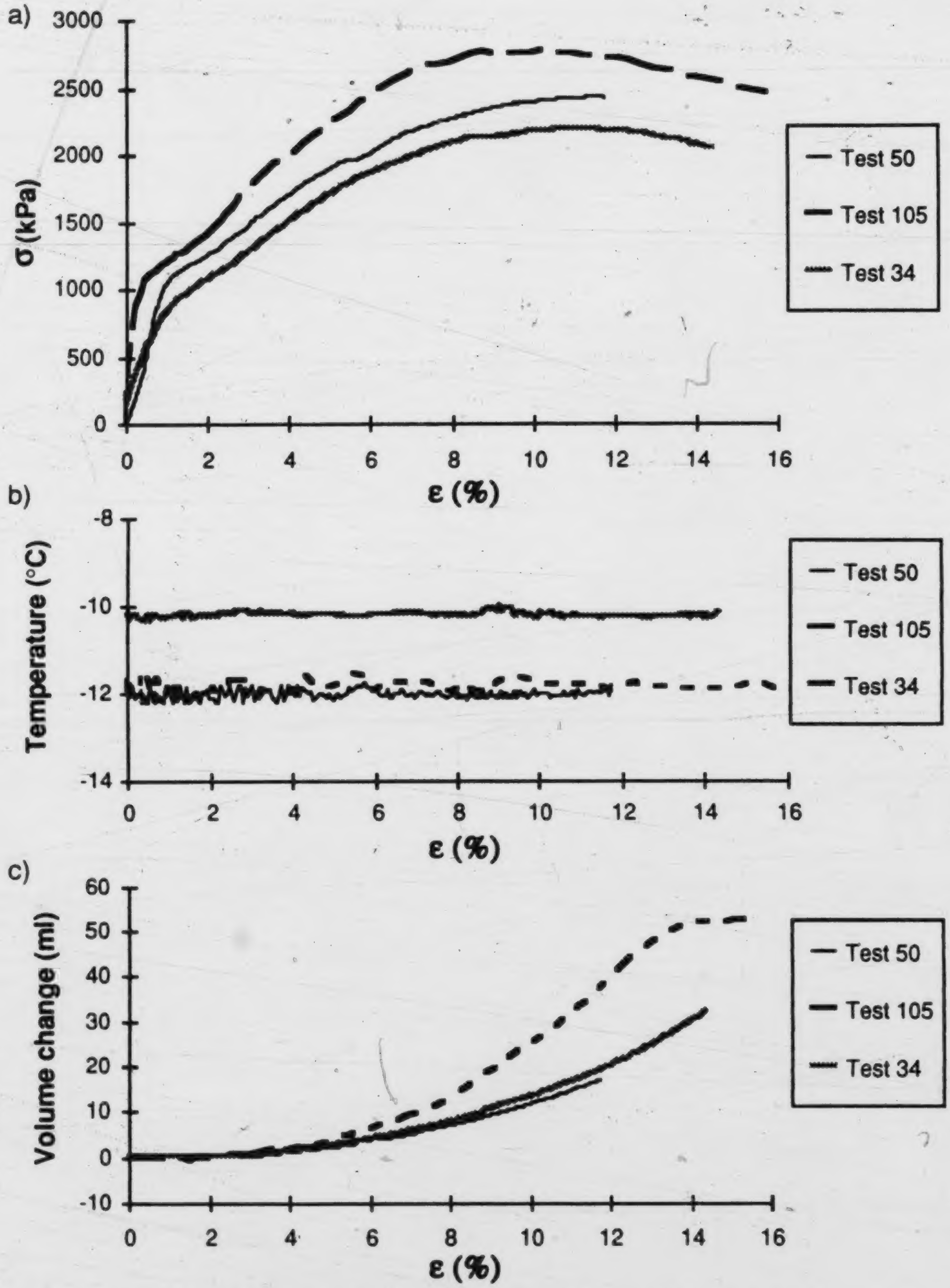

Figure B.13: Compression results soil B 10 ppt T = -12°C and -10°C
a) stress-strain curve b) temperature vs strain
c) volume change vs strain

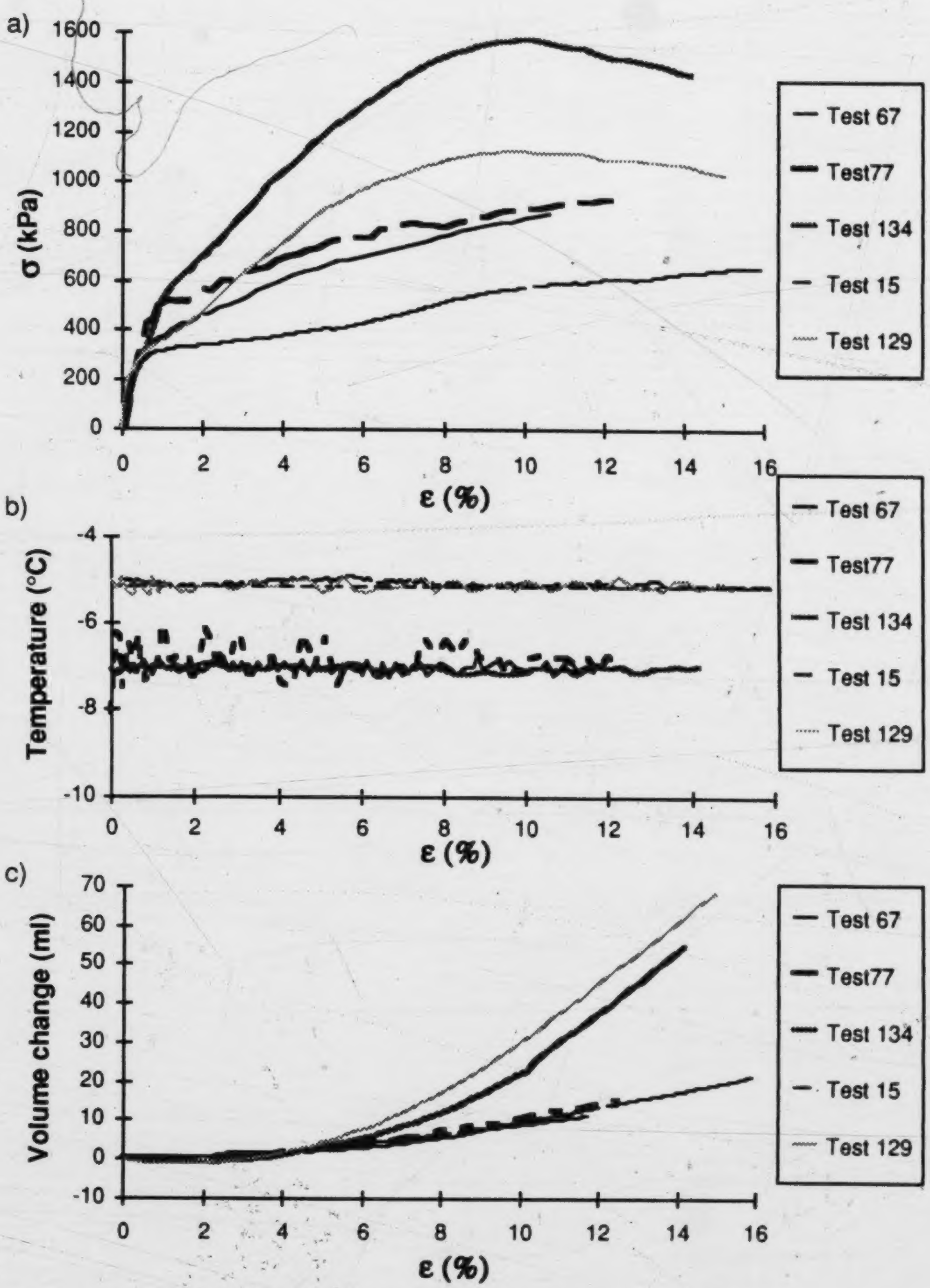

Figure B.14: Compression results soil B 10 ppt T = -7°C and -5°C
a) stress-strain curve b) temperature vs strain
c) volume change vs strain

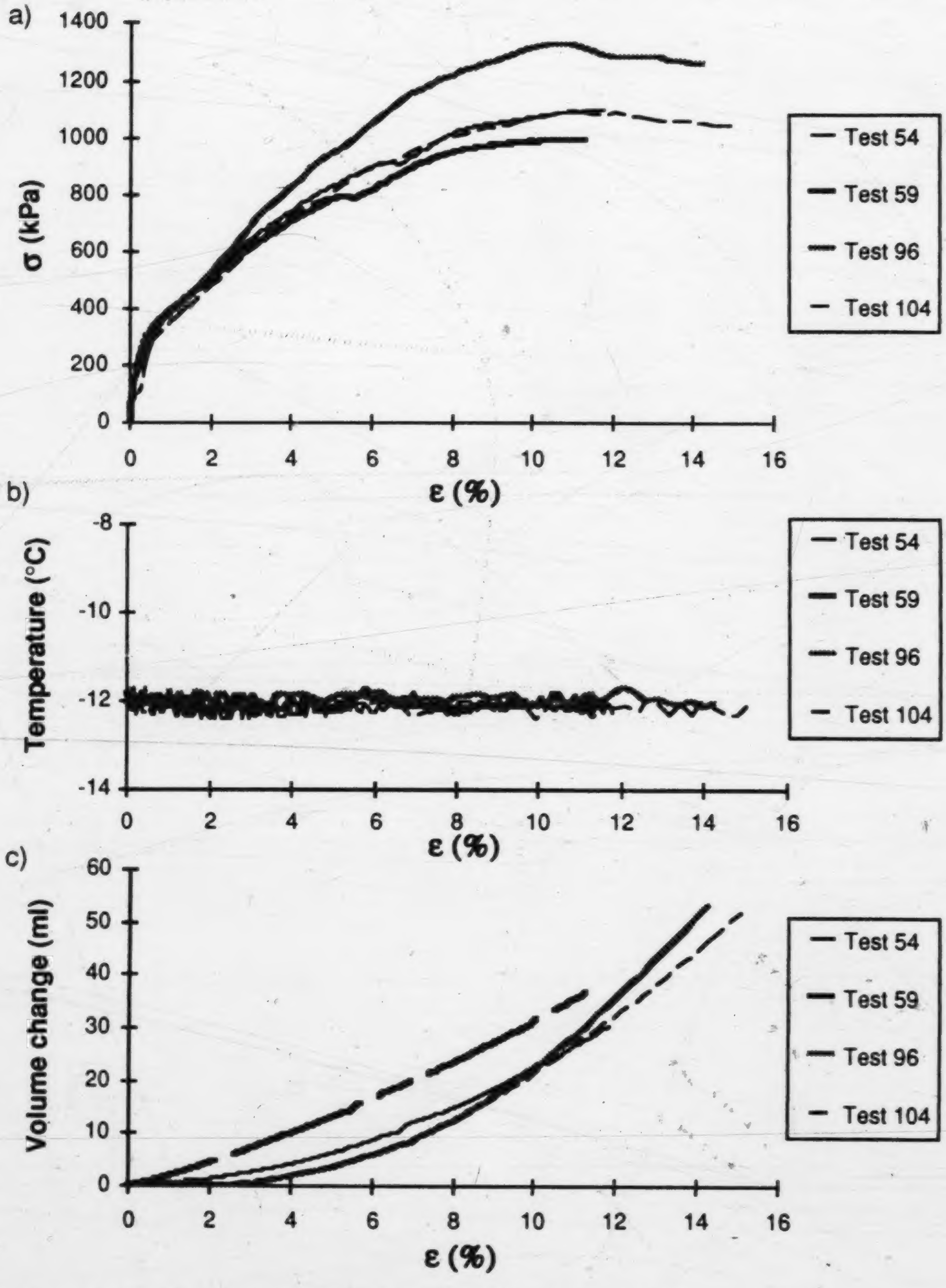

Figure B.15: Compression results soil B 30 ppt T = -12°C
a) stress-strain curve b) temperature vs strain
c) volume change vs strain

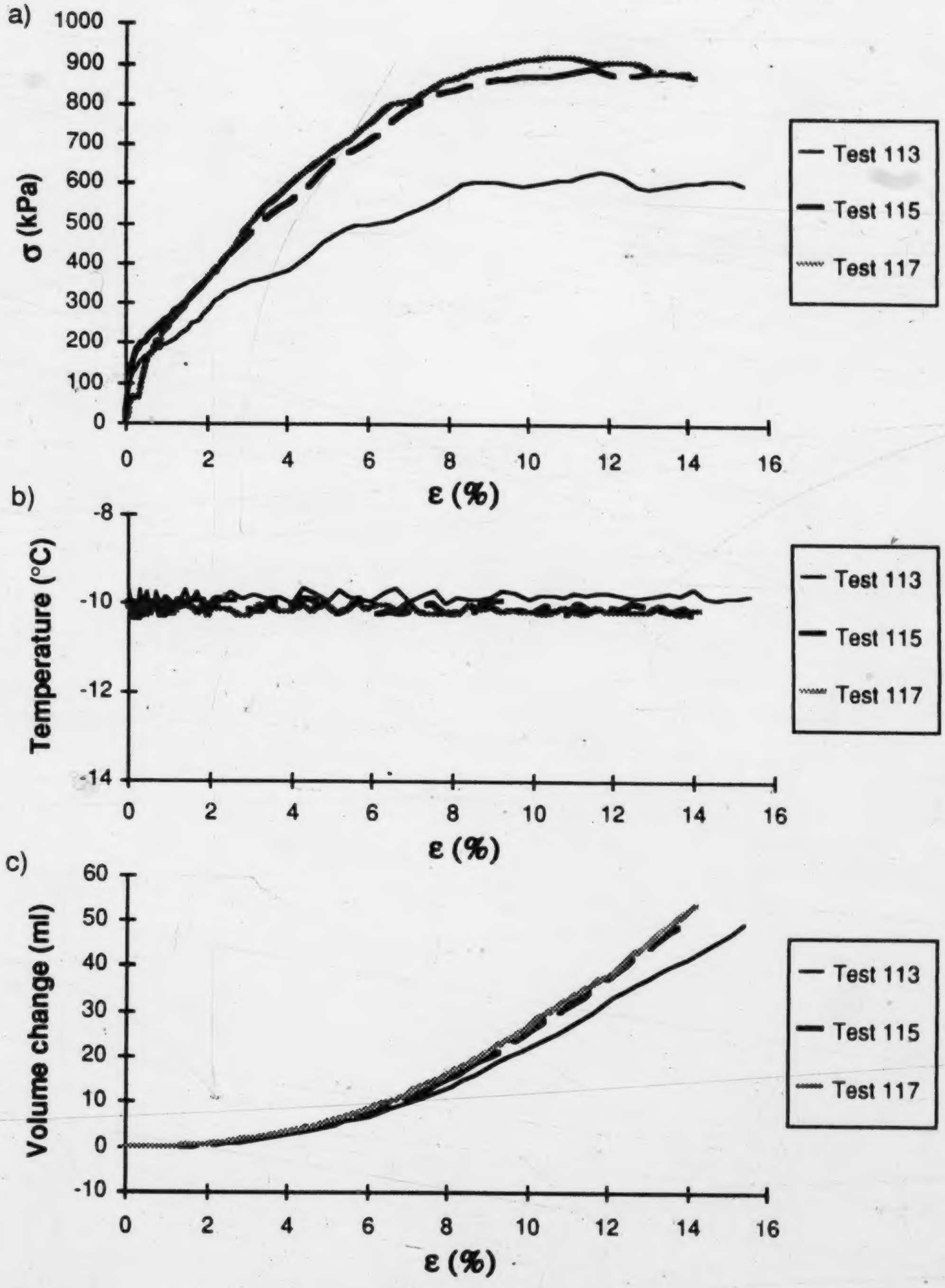

Figure B.16: Compression results soil B 30 ppt T = -10°C
a) stress-strain curve b) temperature vs strain
c) volume change vs strain

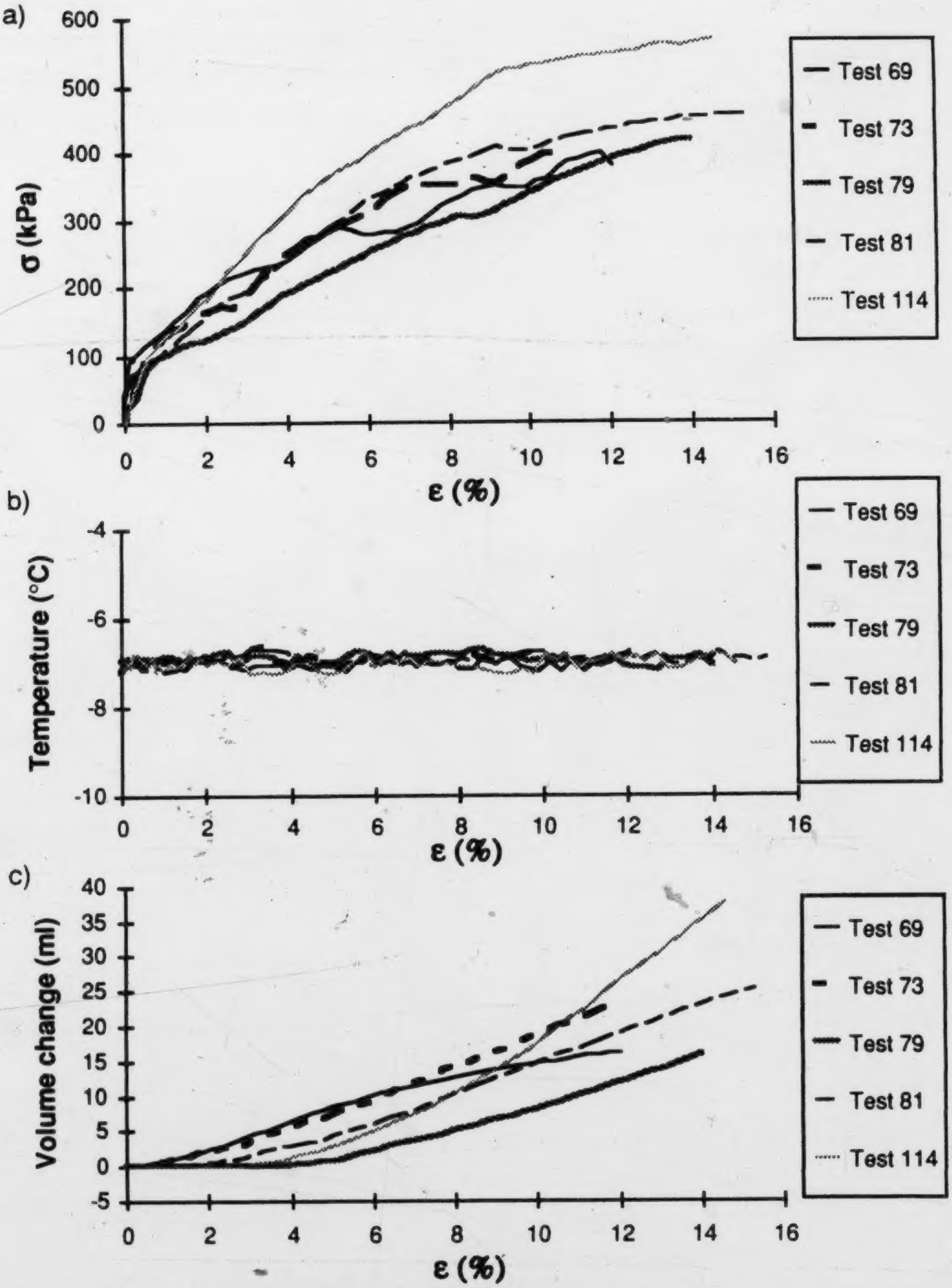

Figure B.17: Compression results soil B 30 ppt T = -7 °C
a) stress-strain curve b) temperature vs strain
c) volume change vs strain

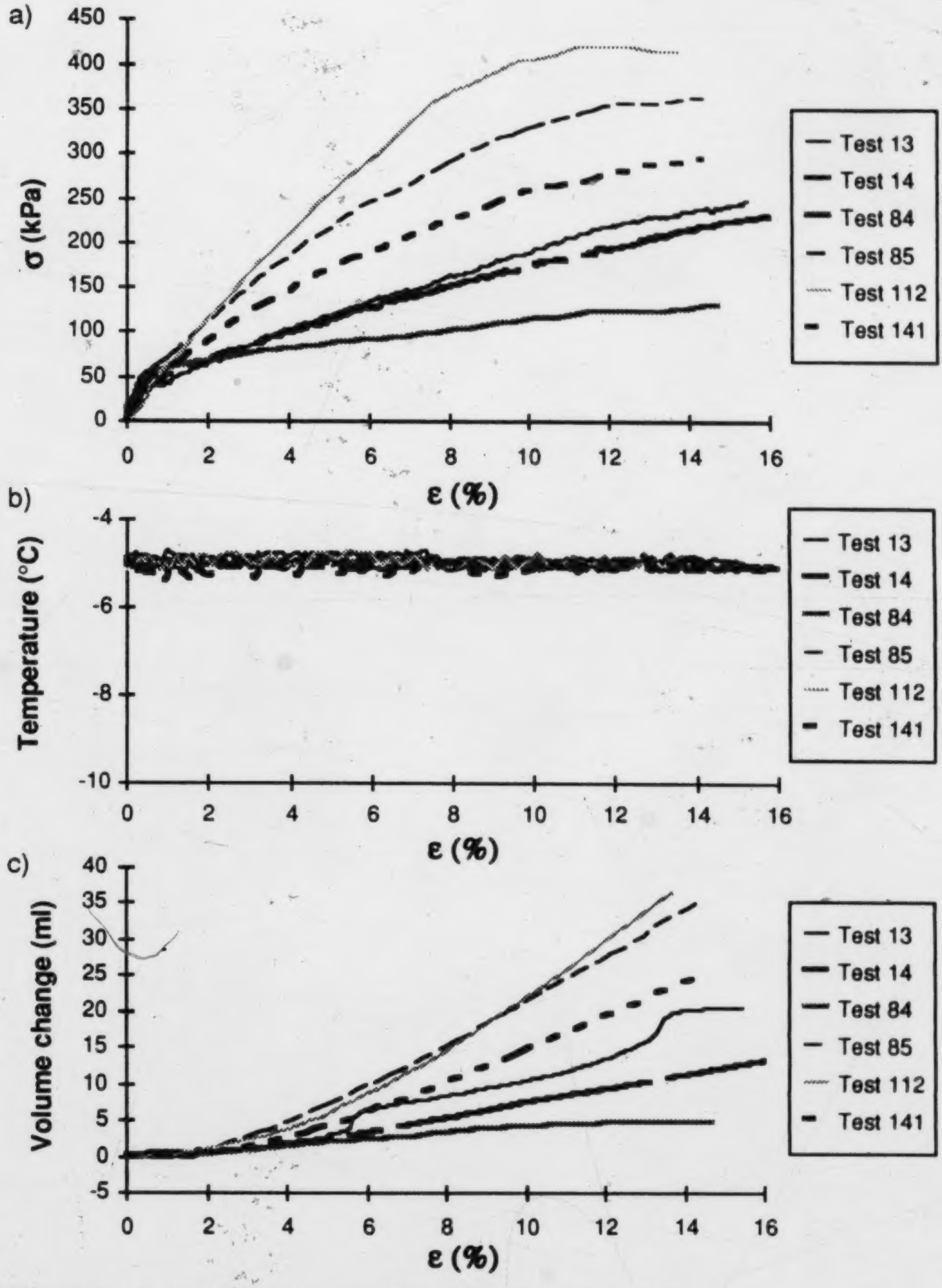

Figure B.18: Compression results soil B 30 ppt T = -5°C
a) stress-strain curve b) temperature vs strain
c) volume change vs strain

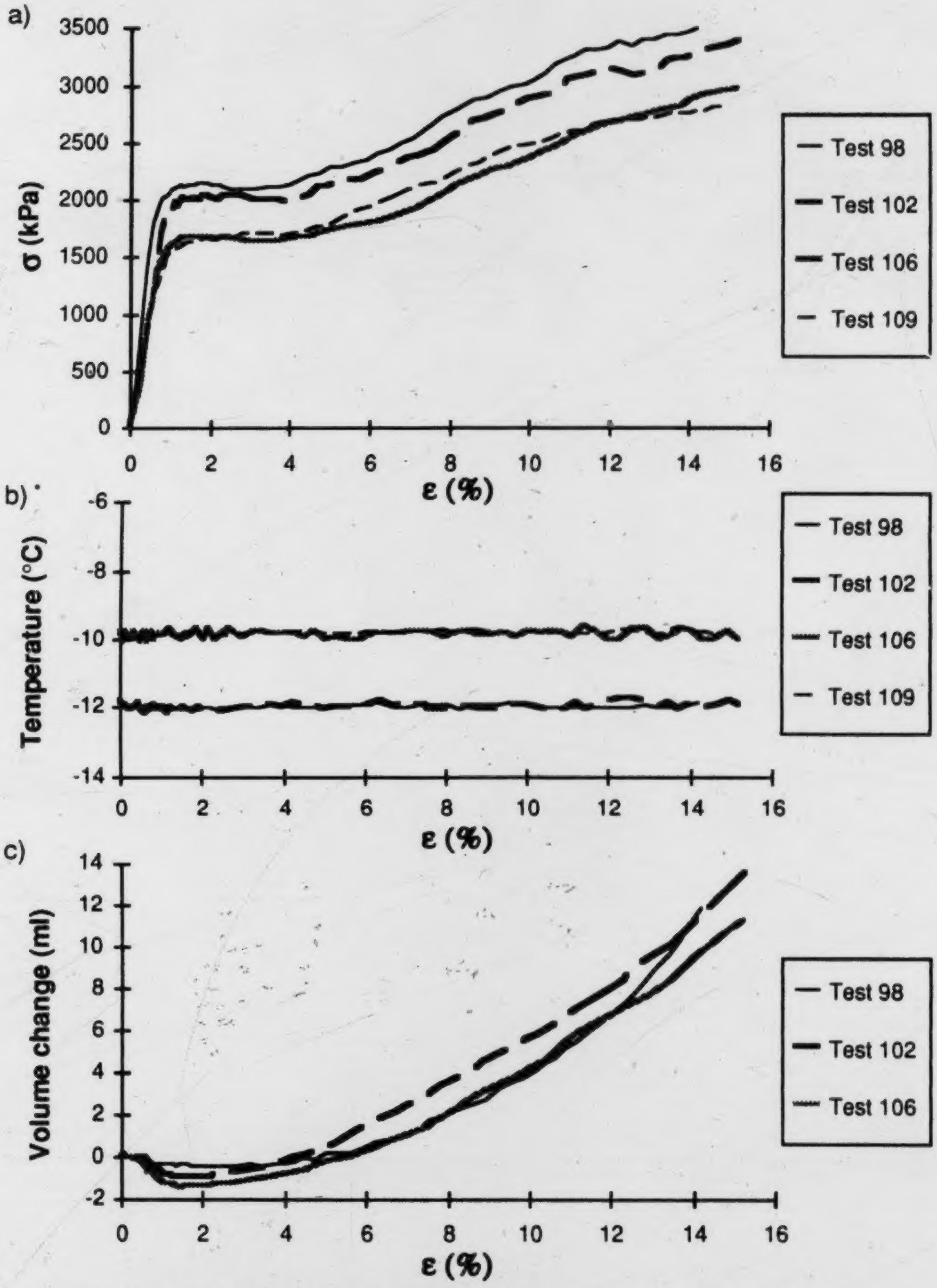

Figure B.19: Compression results soil C 0 ppt T = -12°C and -10°C
a) stress-strain curve b) temperature vs strain
c) volume change vs strain

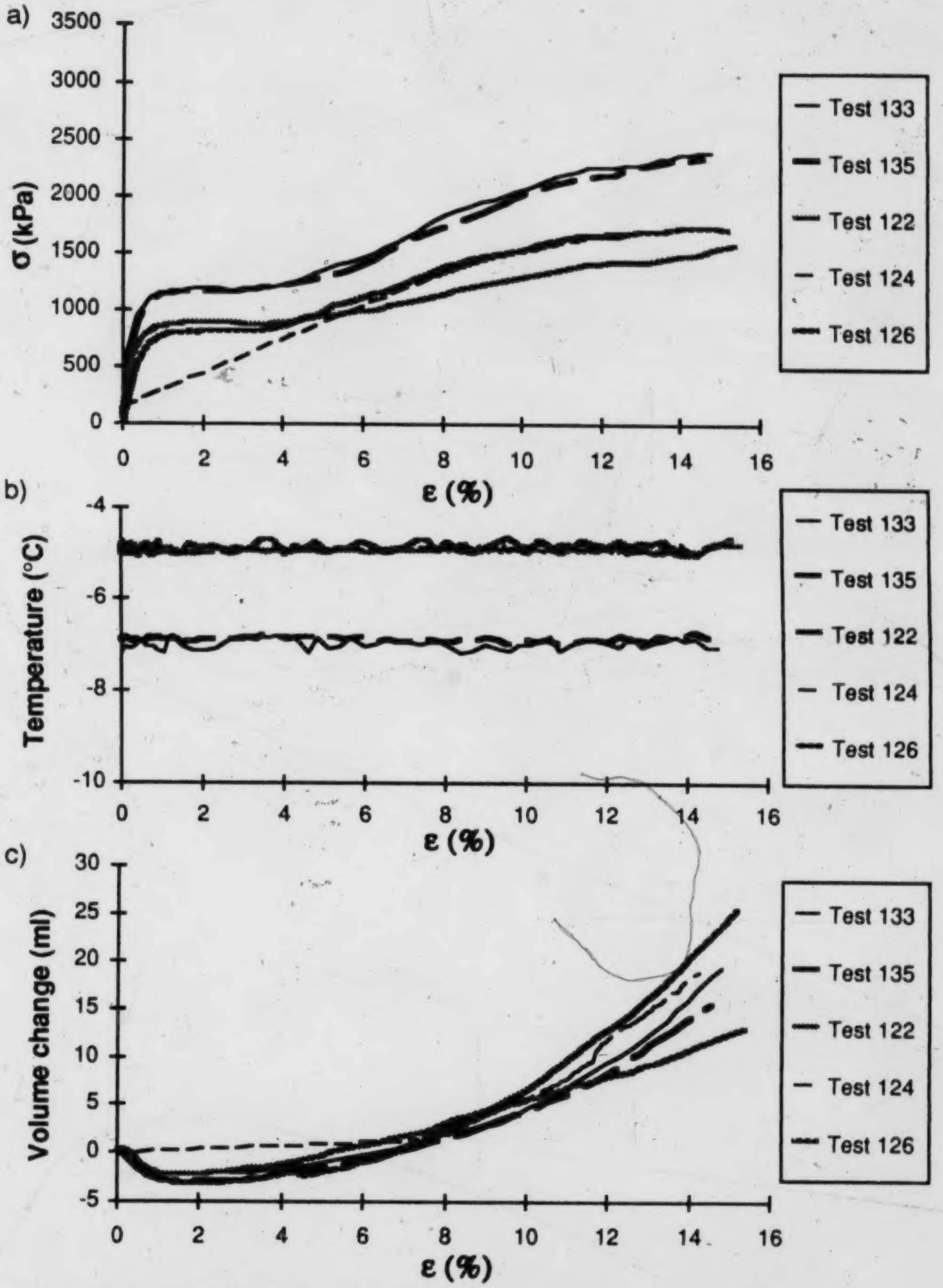

Figure B.20: Compression results soil C 0 ppt T = -7°C and -5°C
a) stress-strain curve b) temperature vs strain
c) volume change vs strain

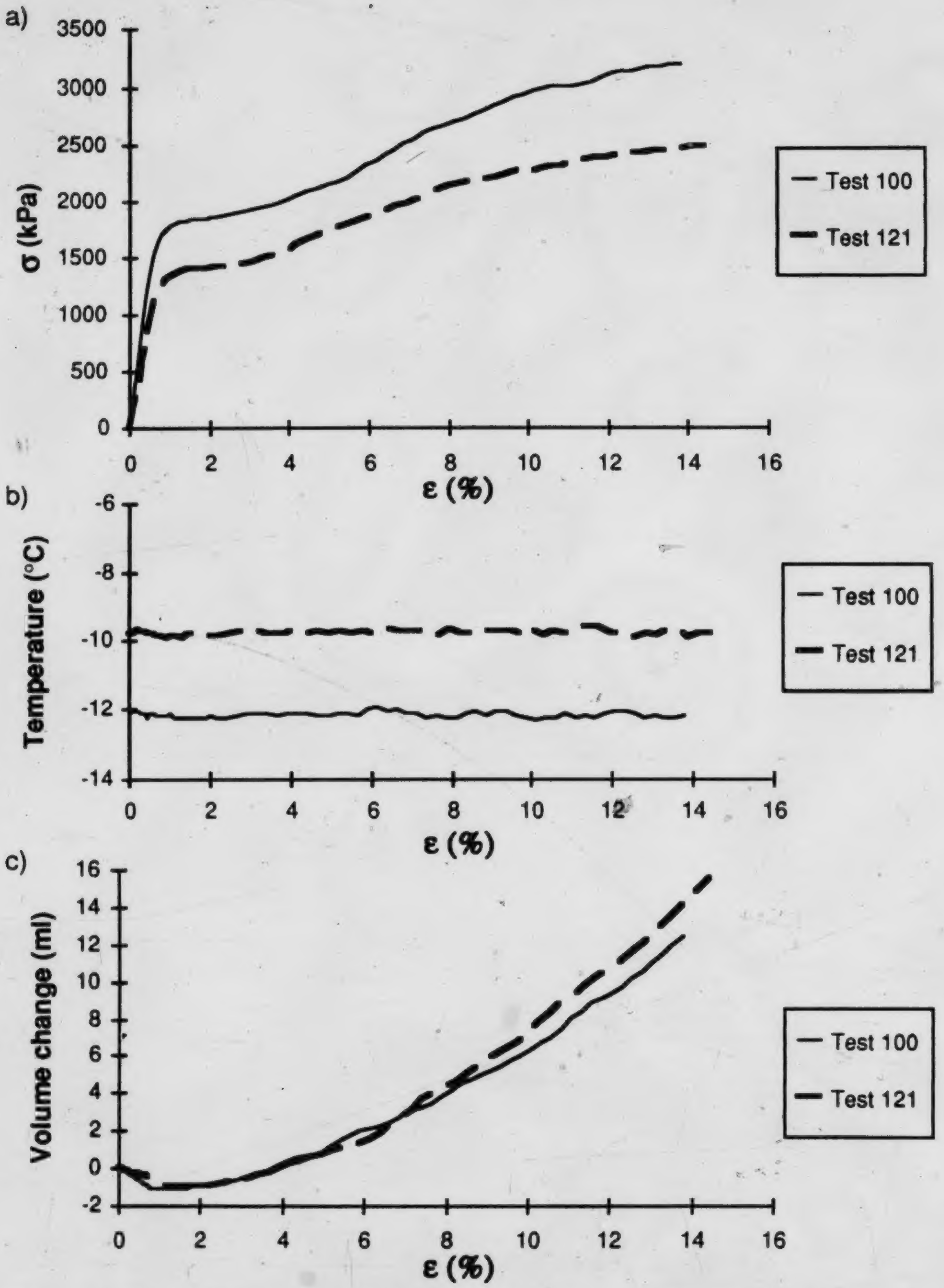

Figure B.21: Compression results soil C 5 ppt T = -12°C and -10°C
a) stress-strain curve b) temperature vs strain
c) volume change vs strain

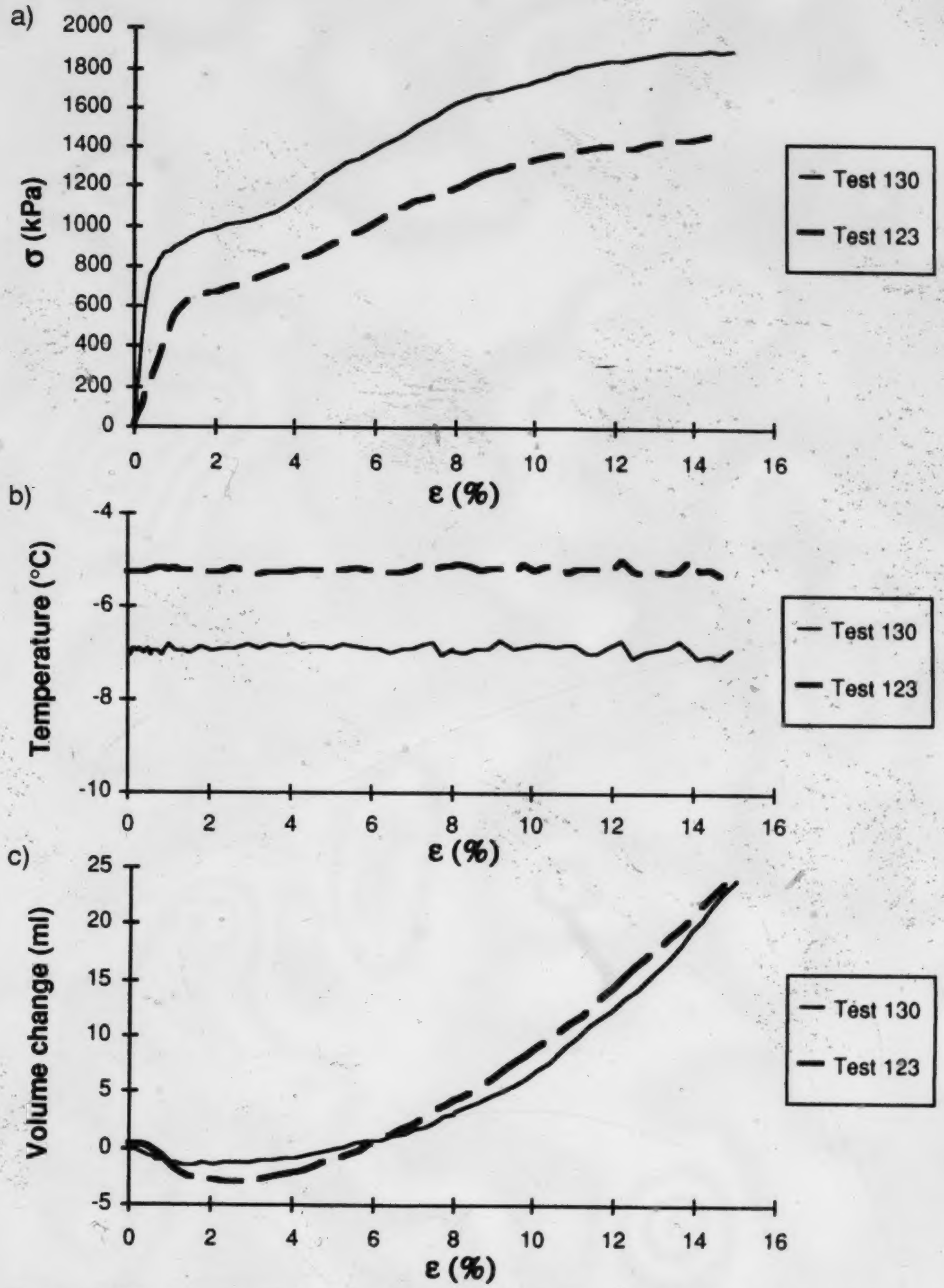

Figure B.22: Compression results soil C 5 ppt T = -7°C and -5°C
a) stress-strain curve b) temperature vs strain
c) volume change vs strain

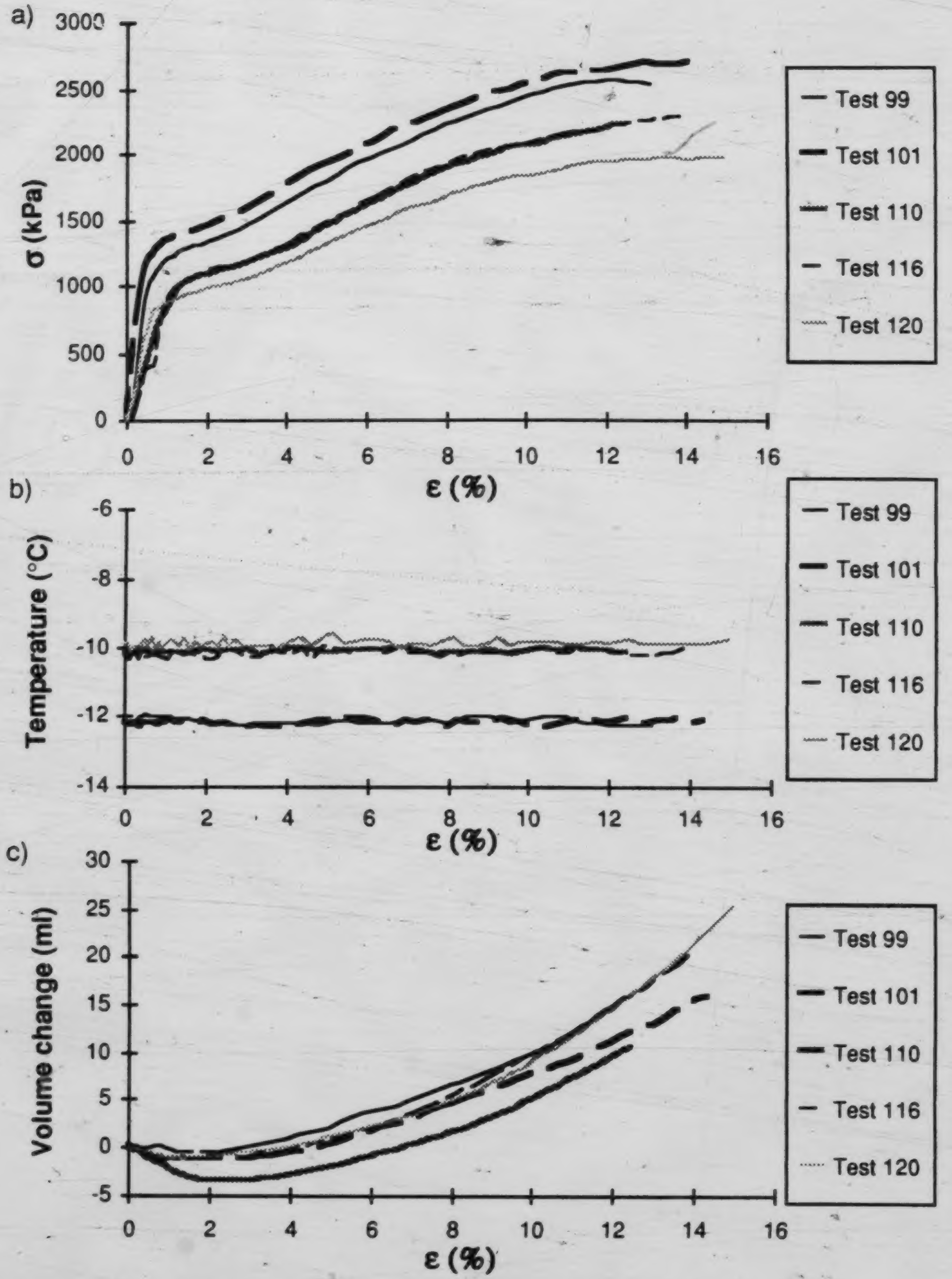

Figure B.23: Compression results soil C 10 ppt T = -12°C and -10°C
a) stress-strain curve b) temperature vs strain
c) volume change vs strain

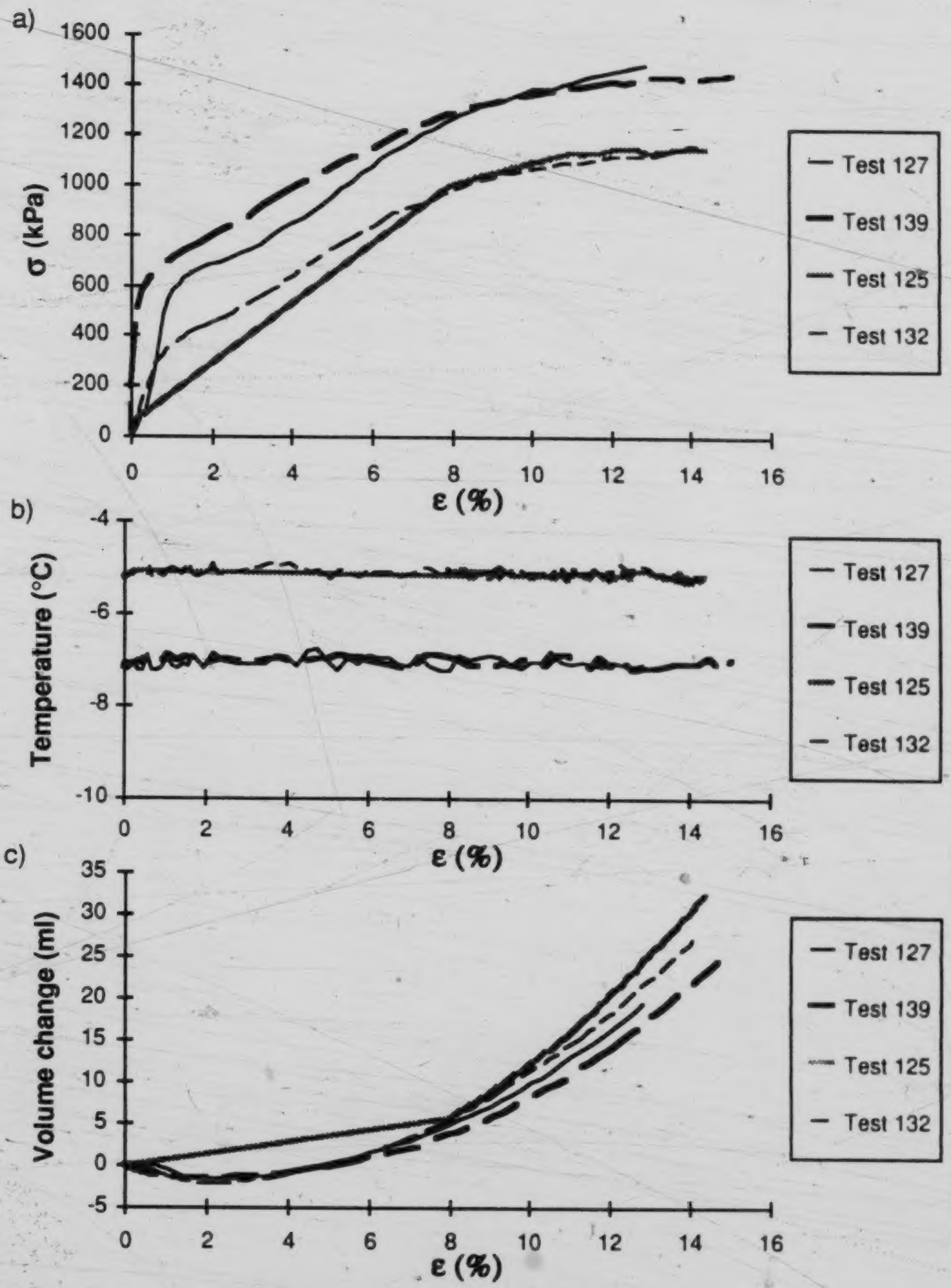

Figure B.24: Compression results soil C 10 ppt T = -7°C and -5°C
a) stress-strain curve b) temperature vs strain
c) volume change vs strain

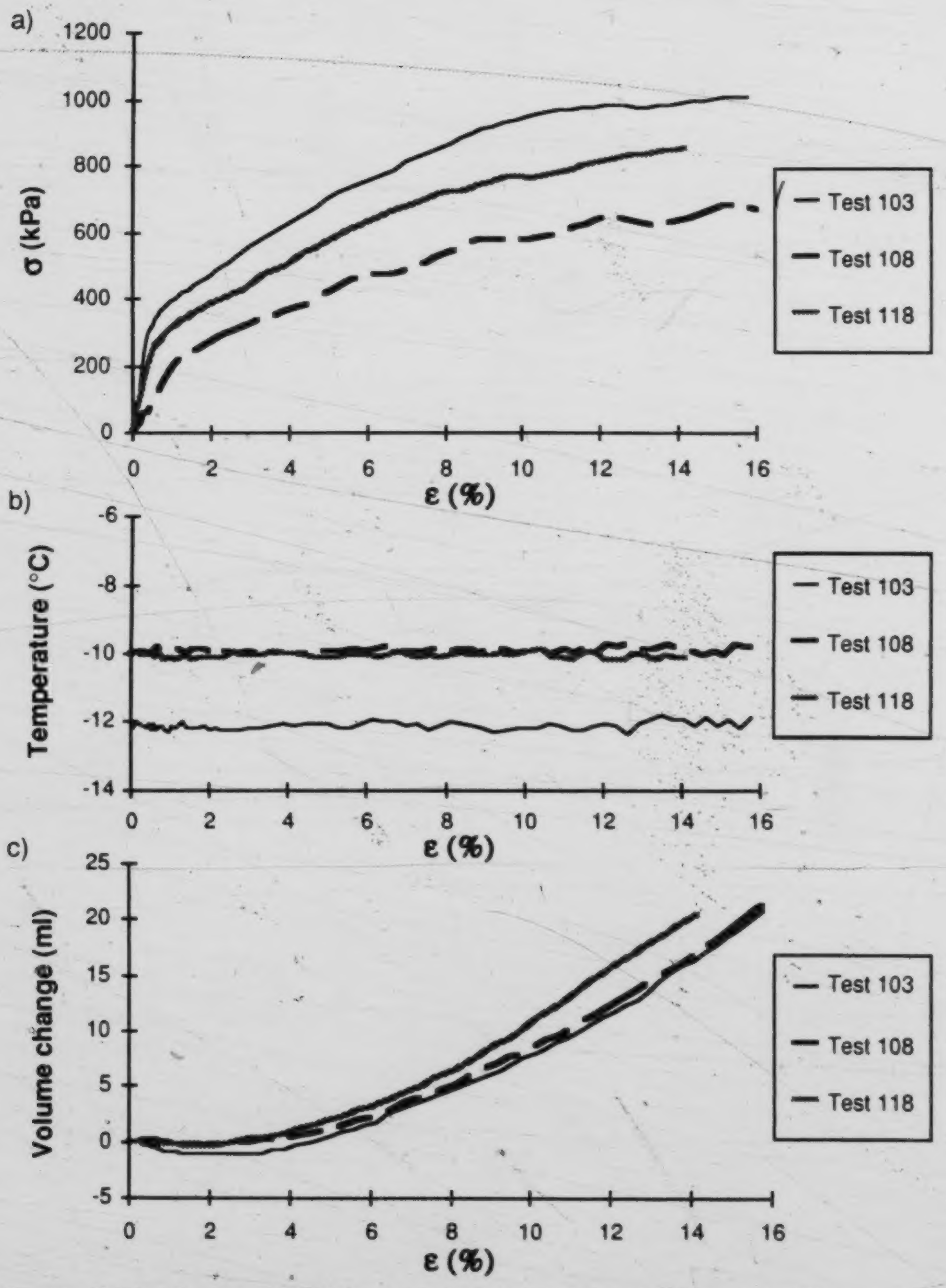

Figure B.25: Compression results soil C 30 ppt T = -12°C and -10°C
a) stress-strain curve b) temperature vs strain
c) volume change vs strain

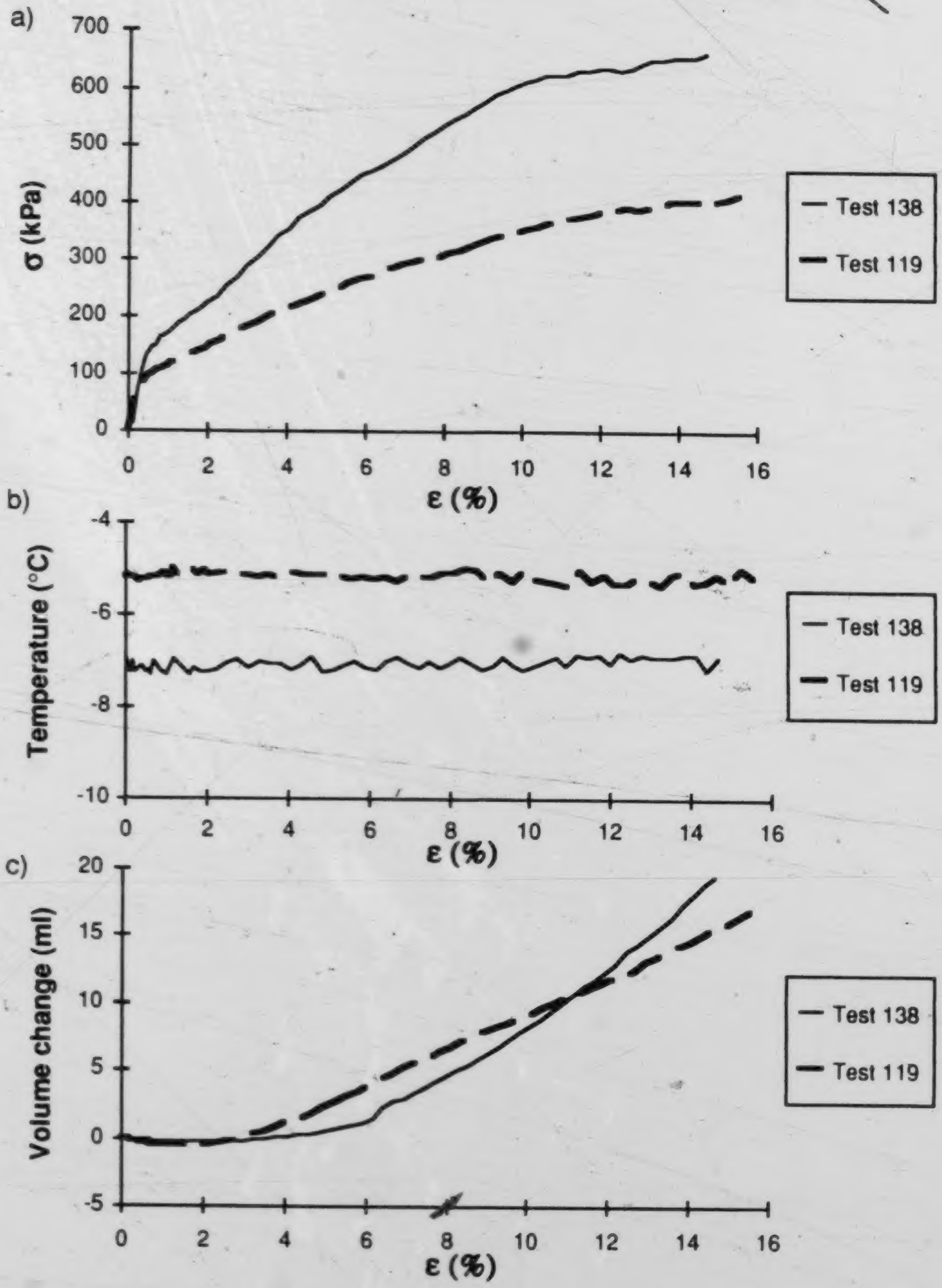

Figure B.26: Compression results soil C 30 ppt T = -7°C and -5°C
a) stress-strain curve b) temperature vs strain
c) volume change vs strain

APPENDIX C

RESULTS of the CONSTANT STRESS (CREEP) COMPRESSION TESTS

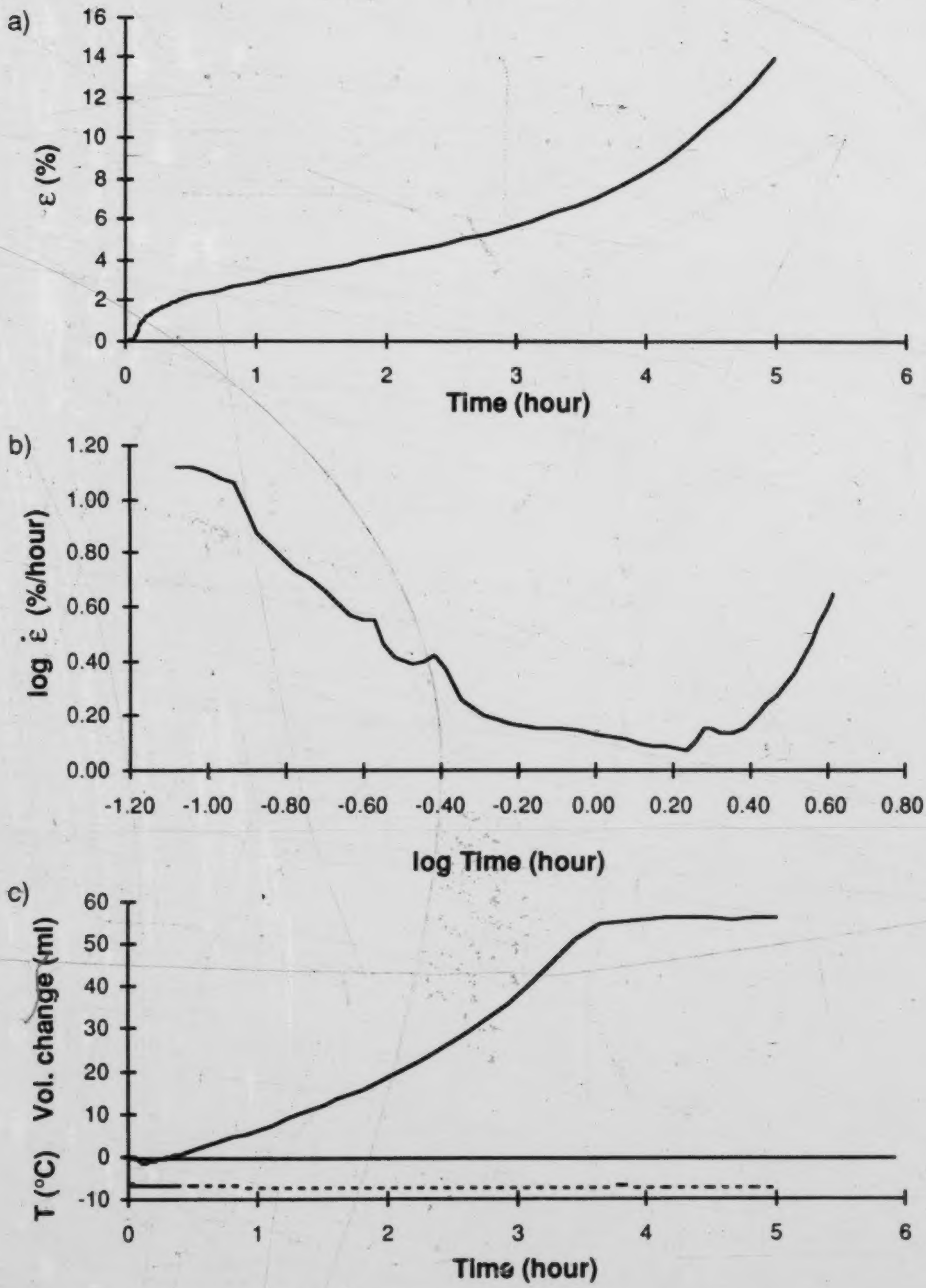

Figure C.1: Creep results test CR-45 soil A 0 ppt at σ=4581 kPa
a) strain vs time b) log strain rate vs log time
c) volume change and temperature vs time

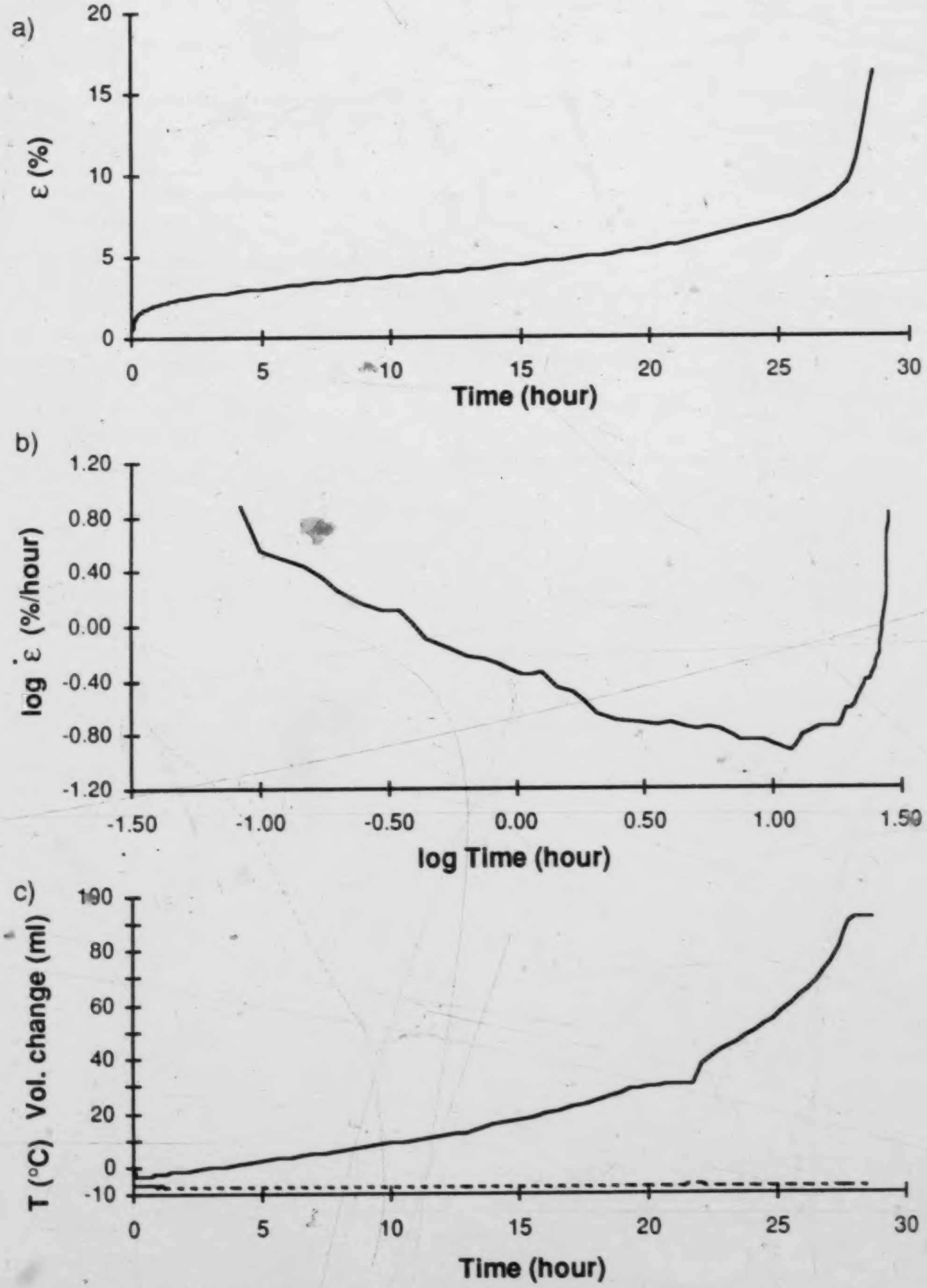

Figure C.2: Creep results test CR-92 soil A 0 ppt at σ=3927 kPa
a) strain vs time b) log strain rate vs log time
c) volume change and temperature vs time

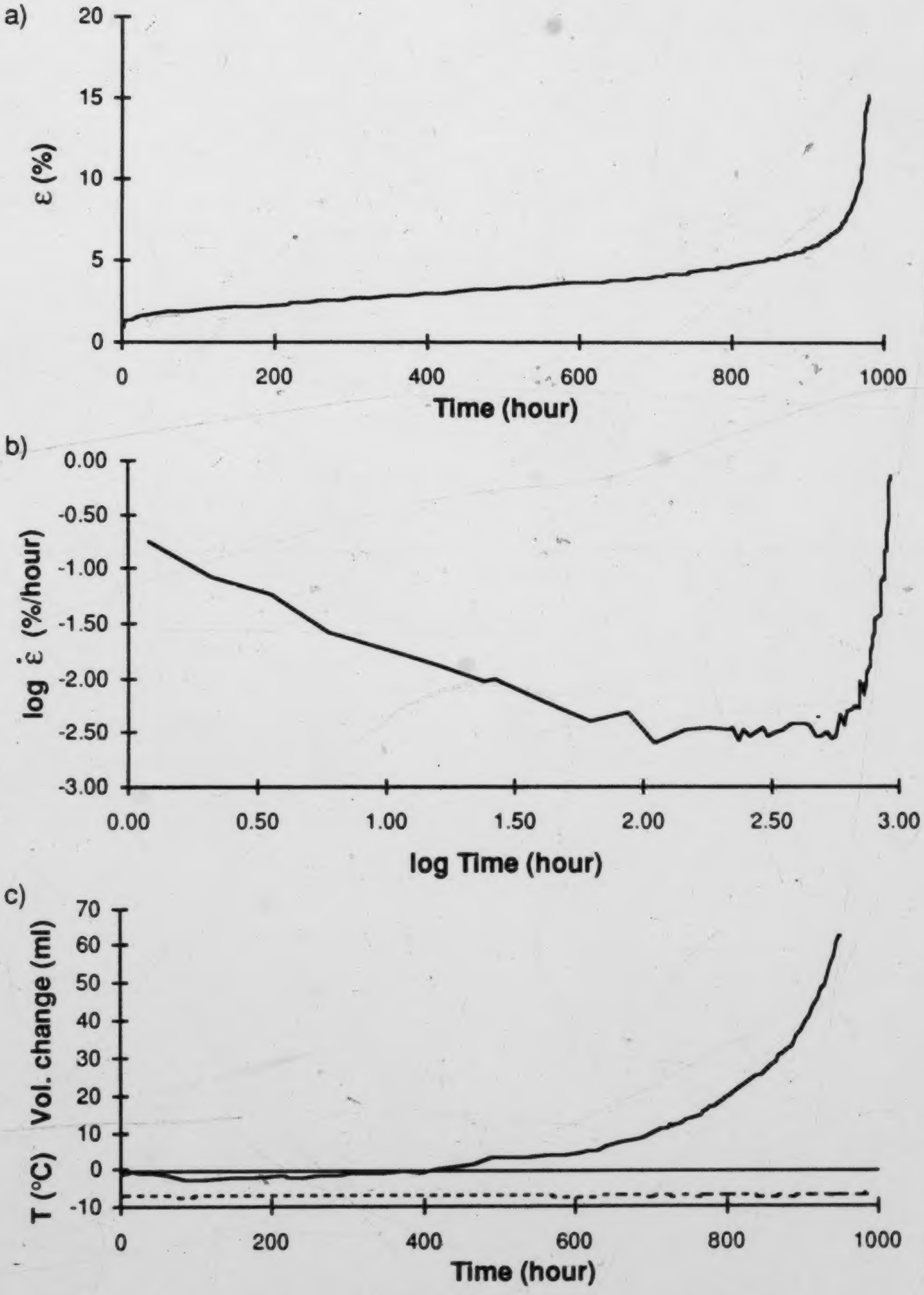

Figure C.3: Creep results test CR-95 soil A 0 ppt at σ=2836 kPa
a) strain vs time b) log strain rate vs log time
c) volume change and temperature vs time

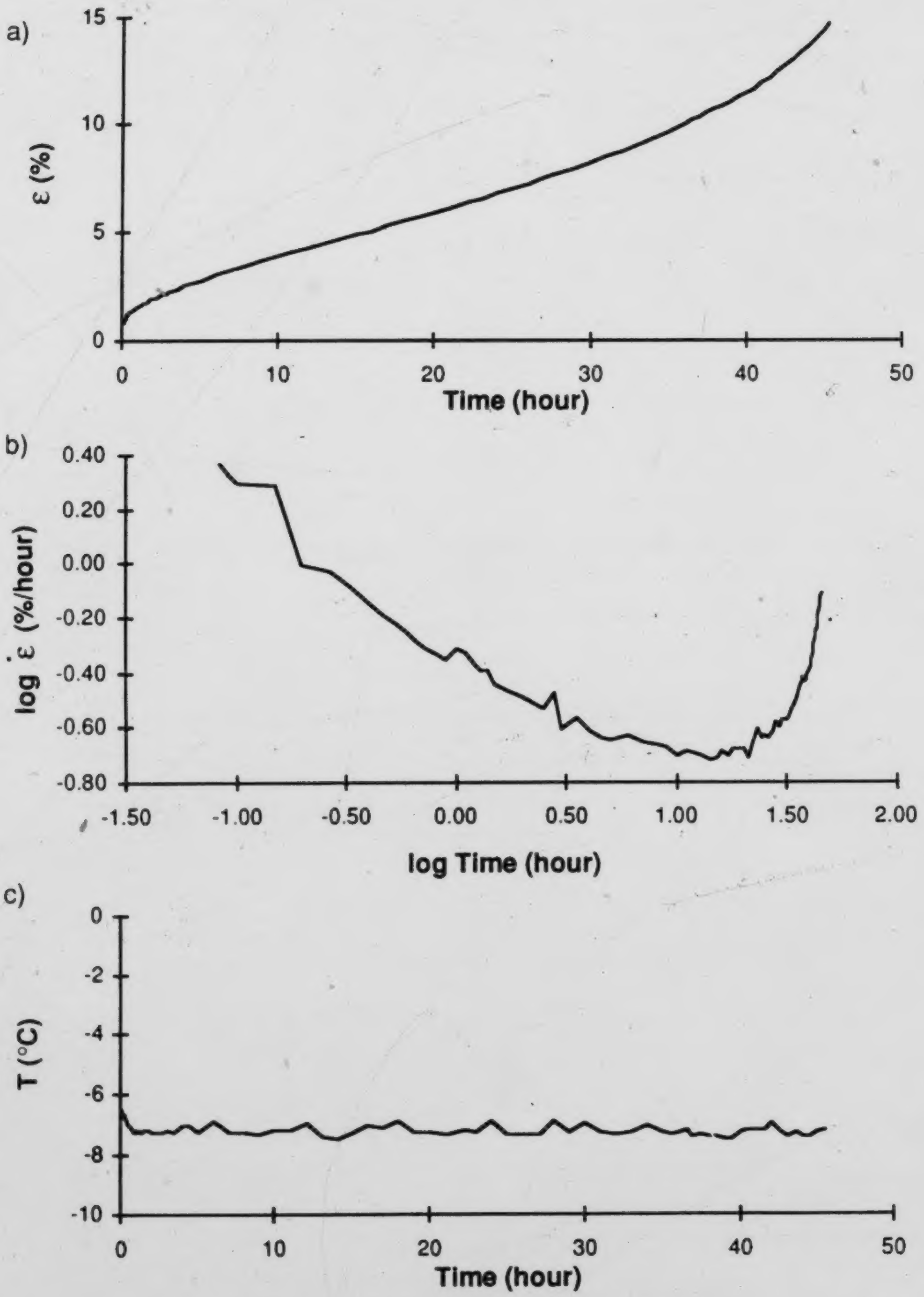

Figure C.4: Creep results test CR-59 soil A 5 ppt at σ=1026 kPa
a) strain vs time b) log strain rate vs log time
c) temperature vs time

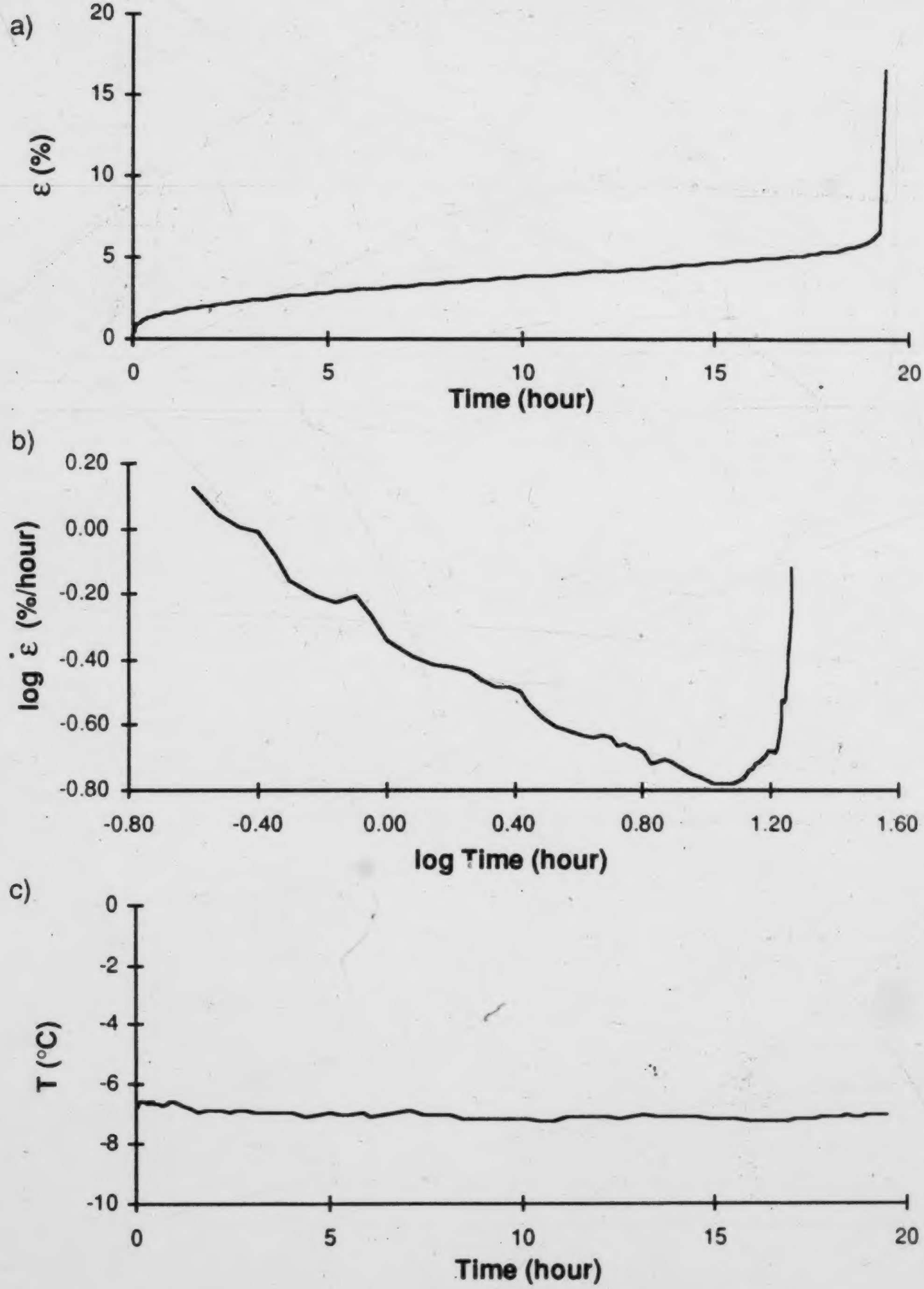

Figure C.5: Creep results test CR-51 soil A 5 ppt at σ=1026 kPa
a) strain vs time b) log strain rate vs log time
c) temperature vs time

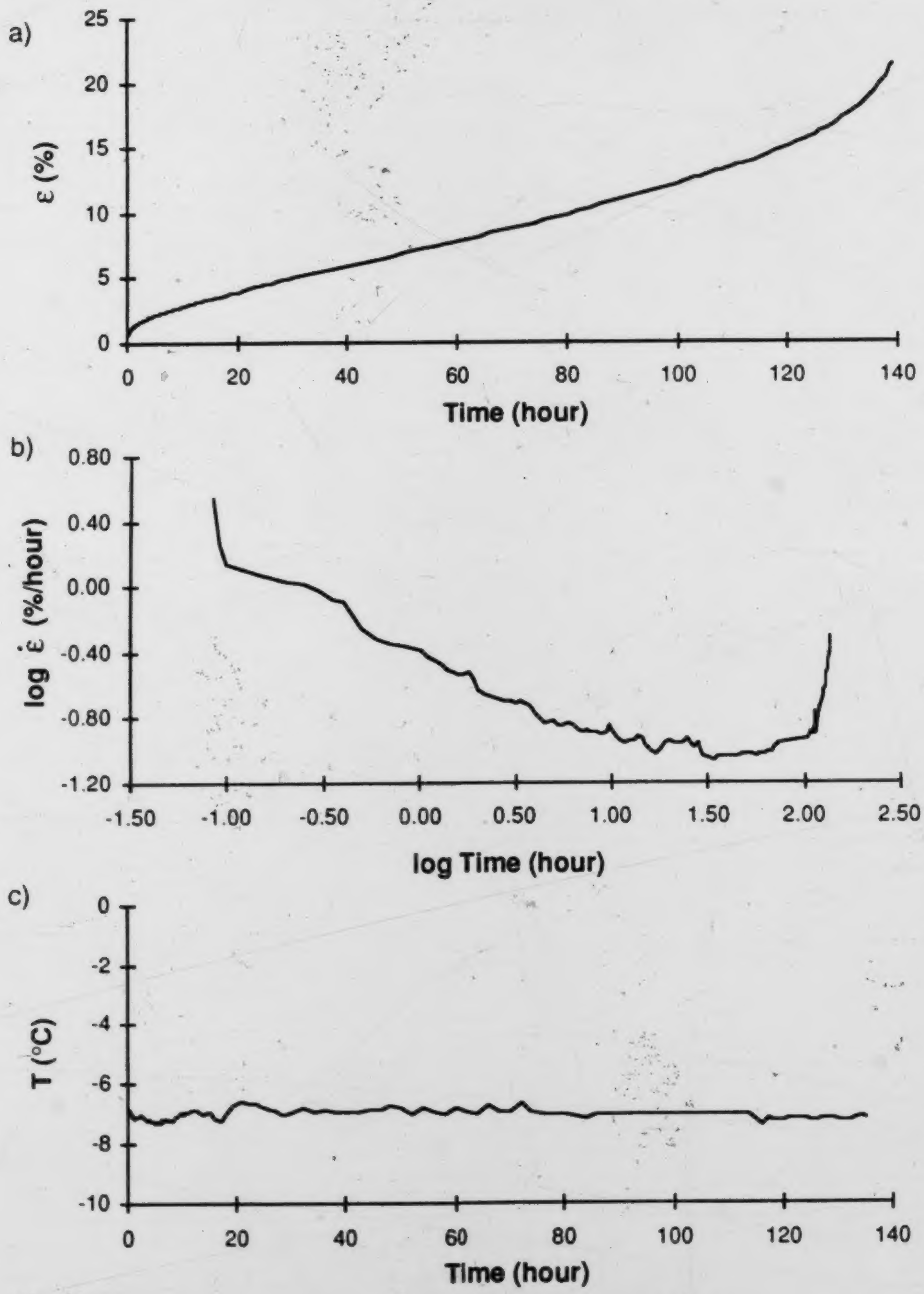

Figure C.6: Creep results test CR-60 soil A 5 ppt at σ=855 kPa
a) strain vs time b) log strain rate vs log time
c) temperature vs time

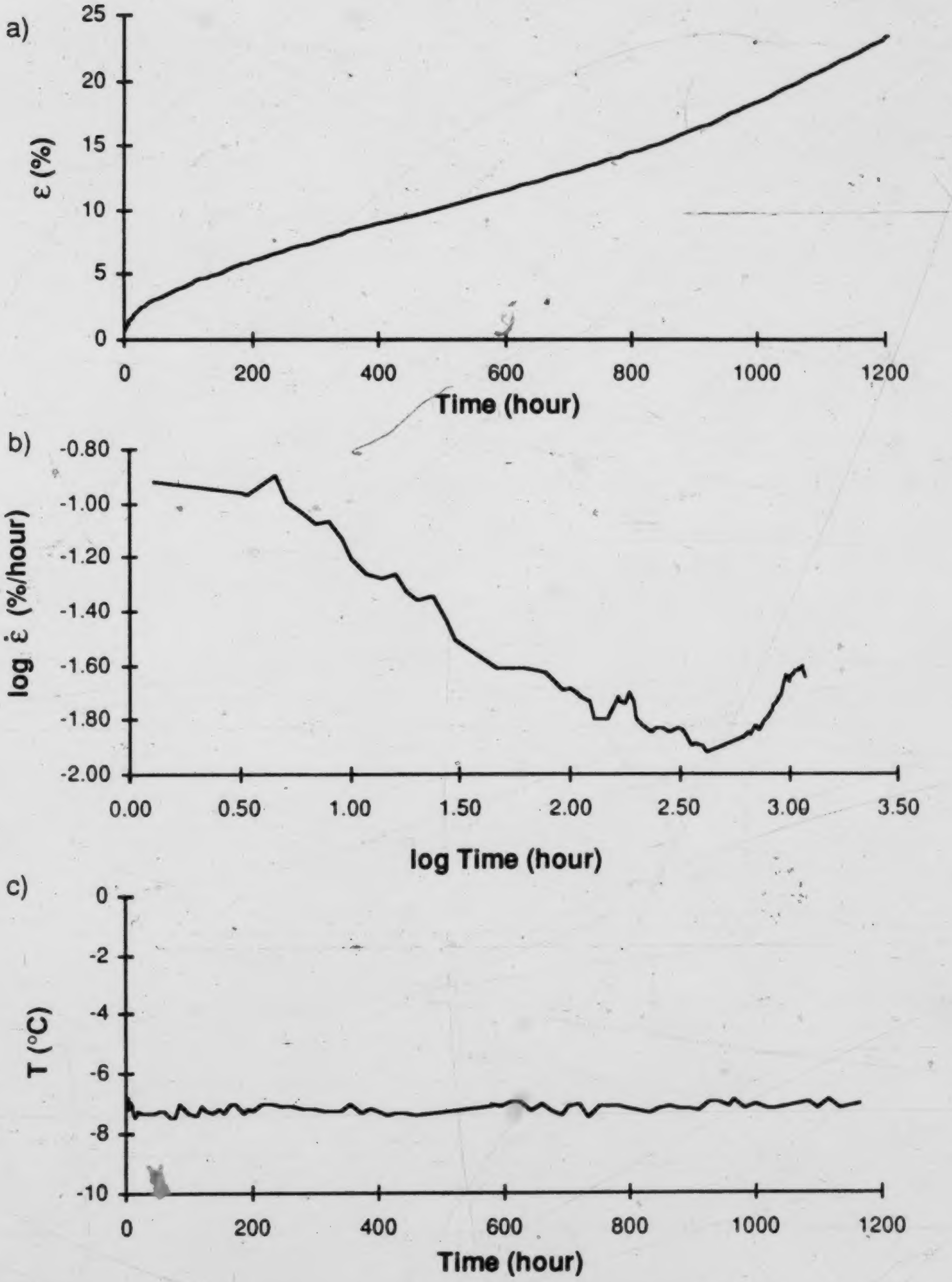

Figure C.7: Creep results test CR-67 soil A 5 ppt at σ=570 kPa
a) strain vs time b) log strain rate vs log time
c) temperature vs time

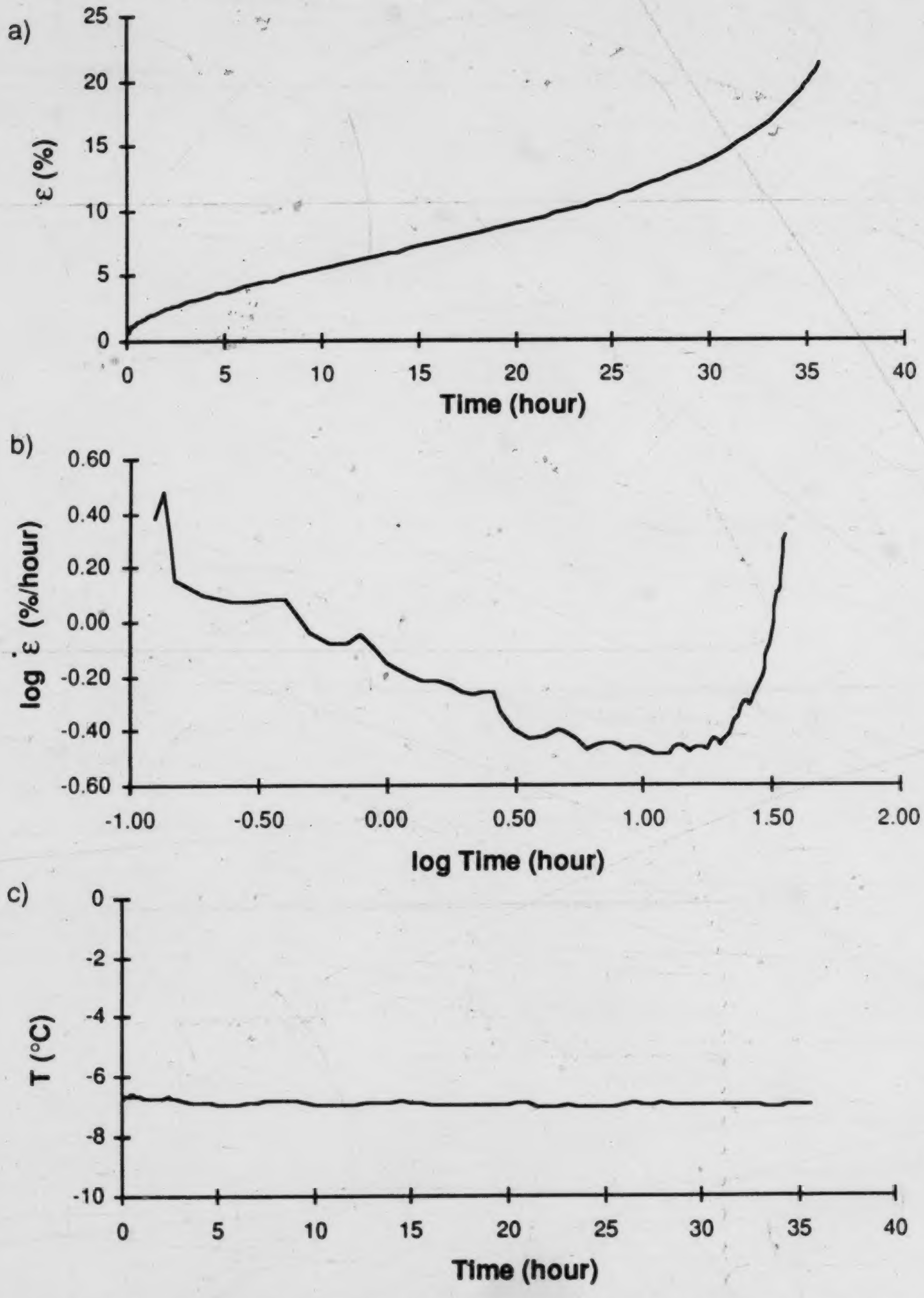

Figure C.8: Creep results test CR-86 soil A 10 ppt at σ=887 kPa
a) strain vs time b) log strain rate vs log time
c) temperature vs time

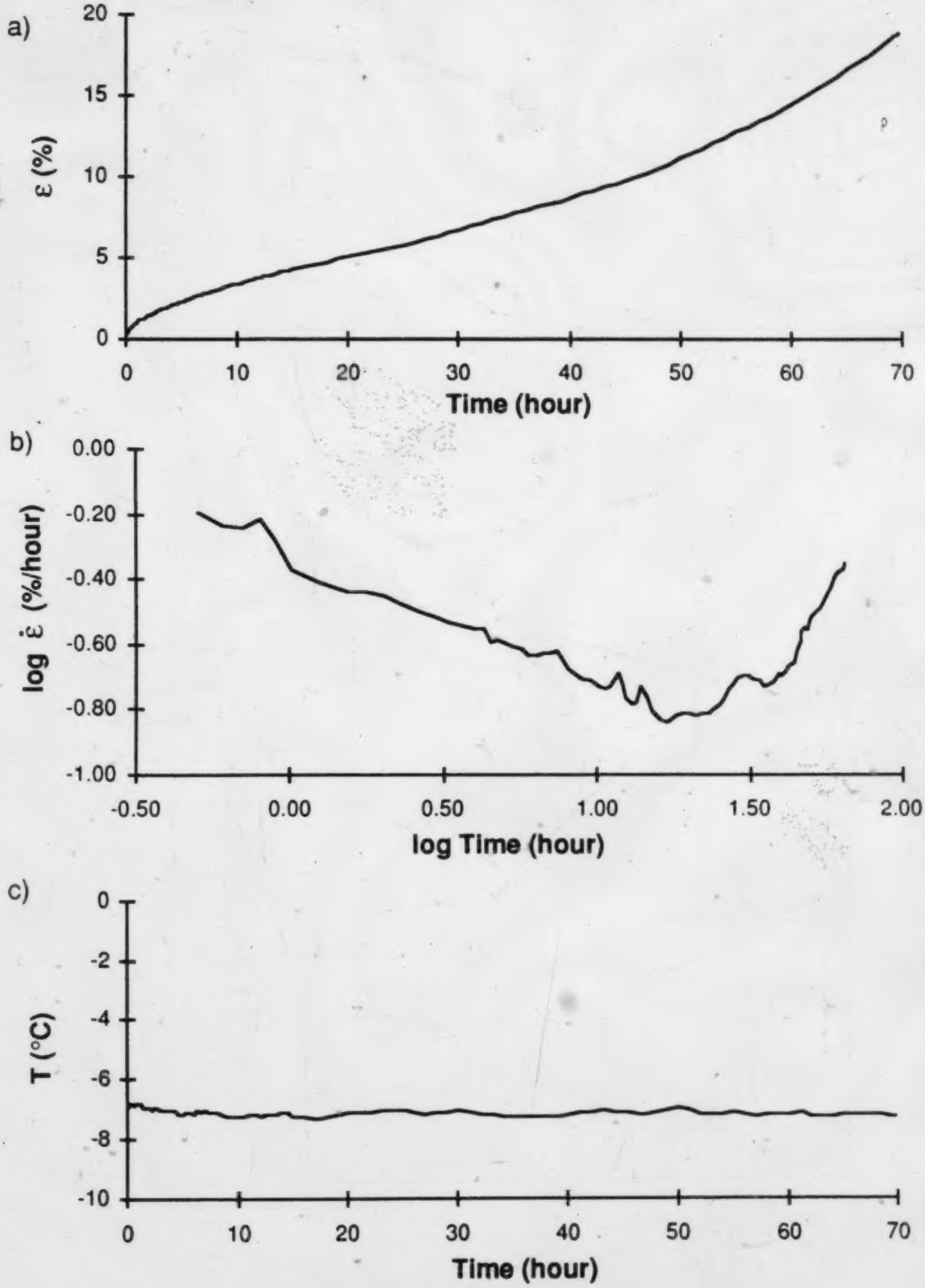

Figure C.9: Creep results test CR-47 soil A 10 ppt at σ=761 kPa
a) strain vs time b) log strain rate vs log time
c) temperature vs time

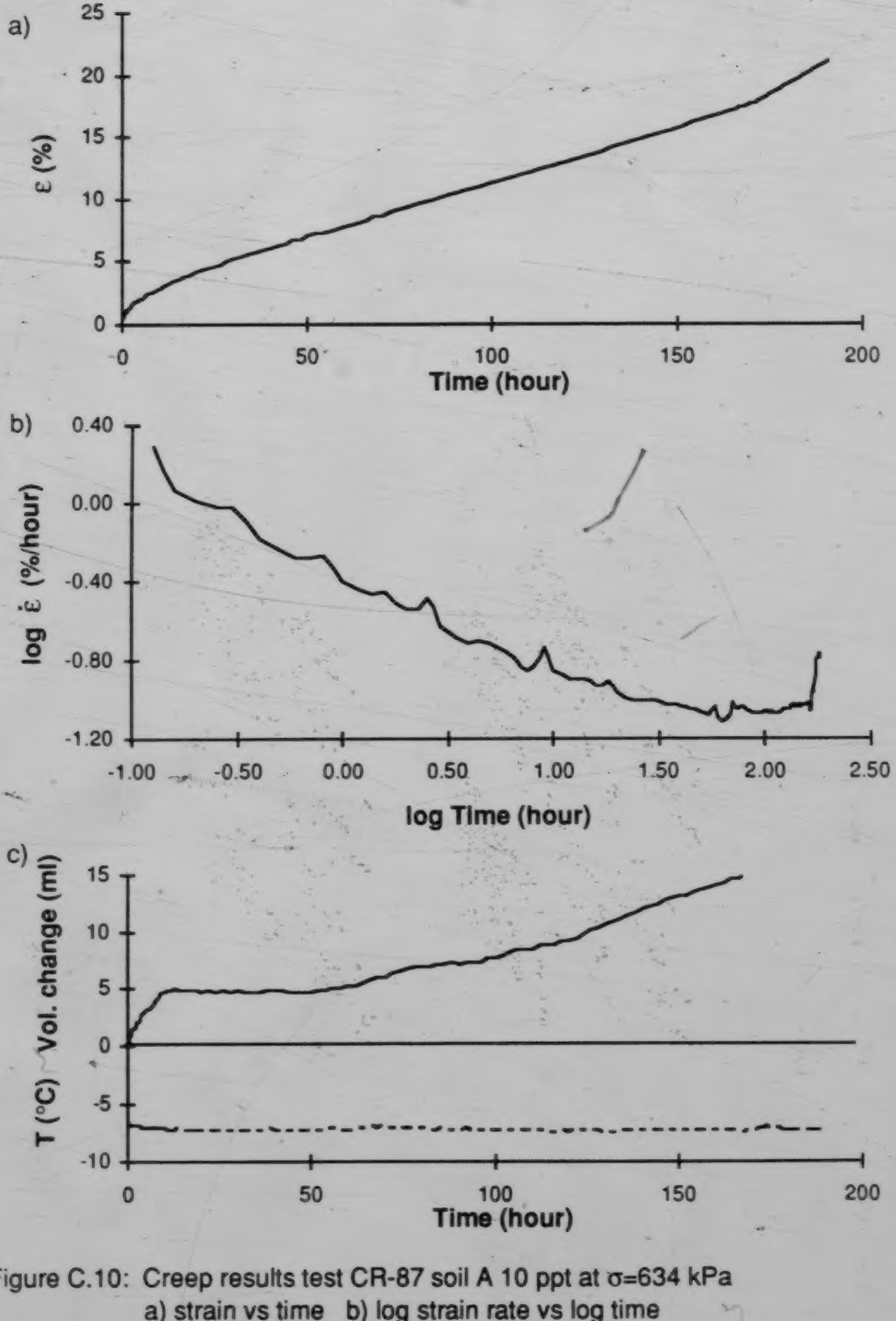

Figure C.10: Creep results test CR-87 soil A 10 ppt at σ=634 kPa
a) strain vs time b) log strain rate vs log time
c) volume change and temperature vs time

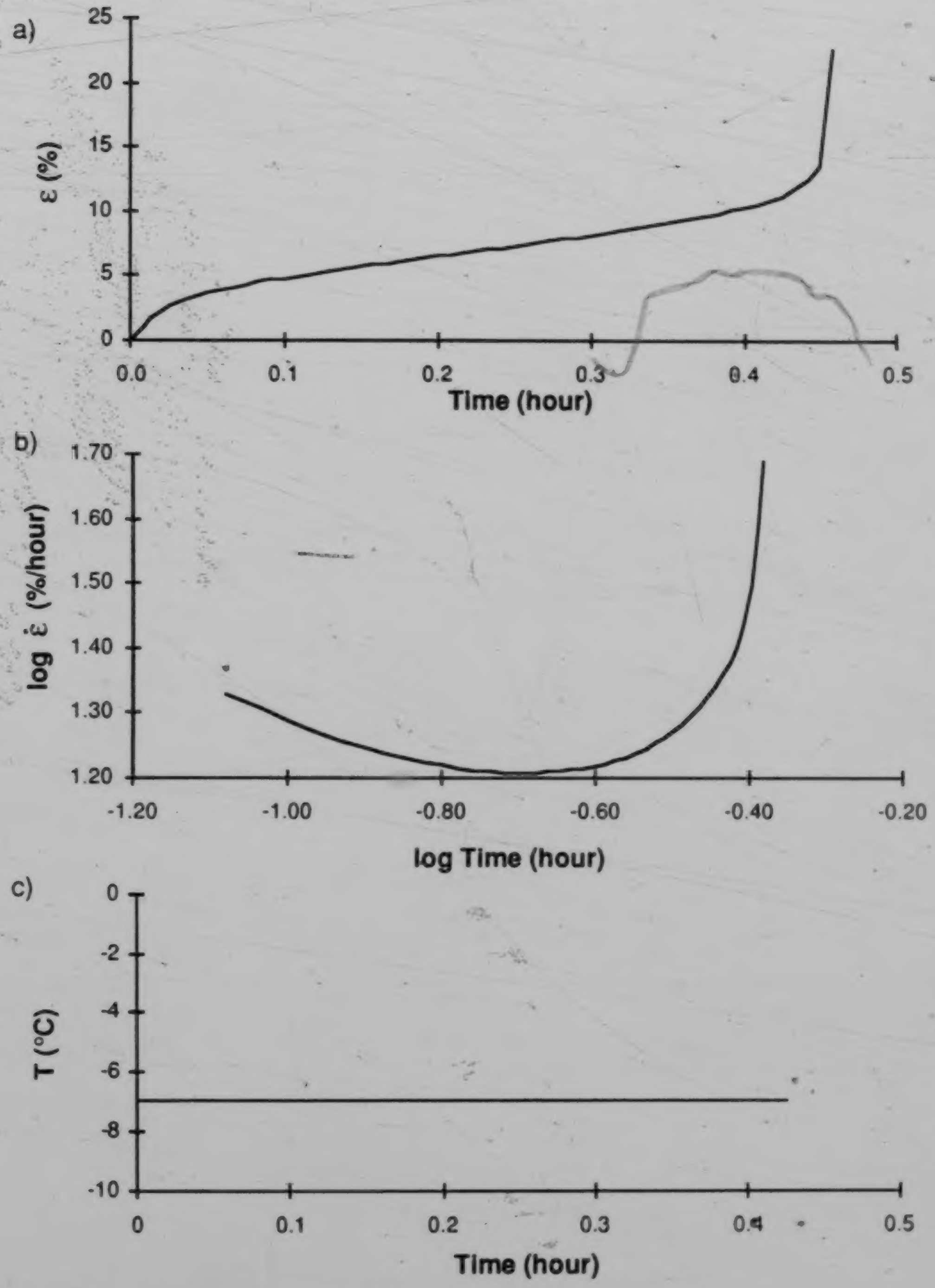

Figure C.11: Creep results test CR-64 soil A 30 ppt at σ=888 kPa
a) strain vs time b) log strain rate vs log time
c) temperature vs time

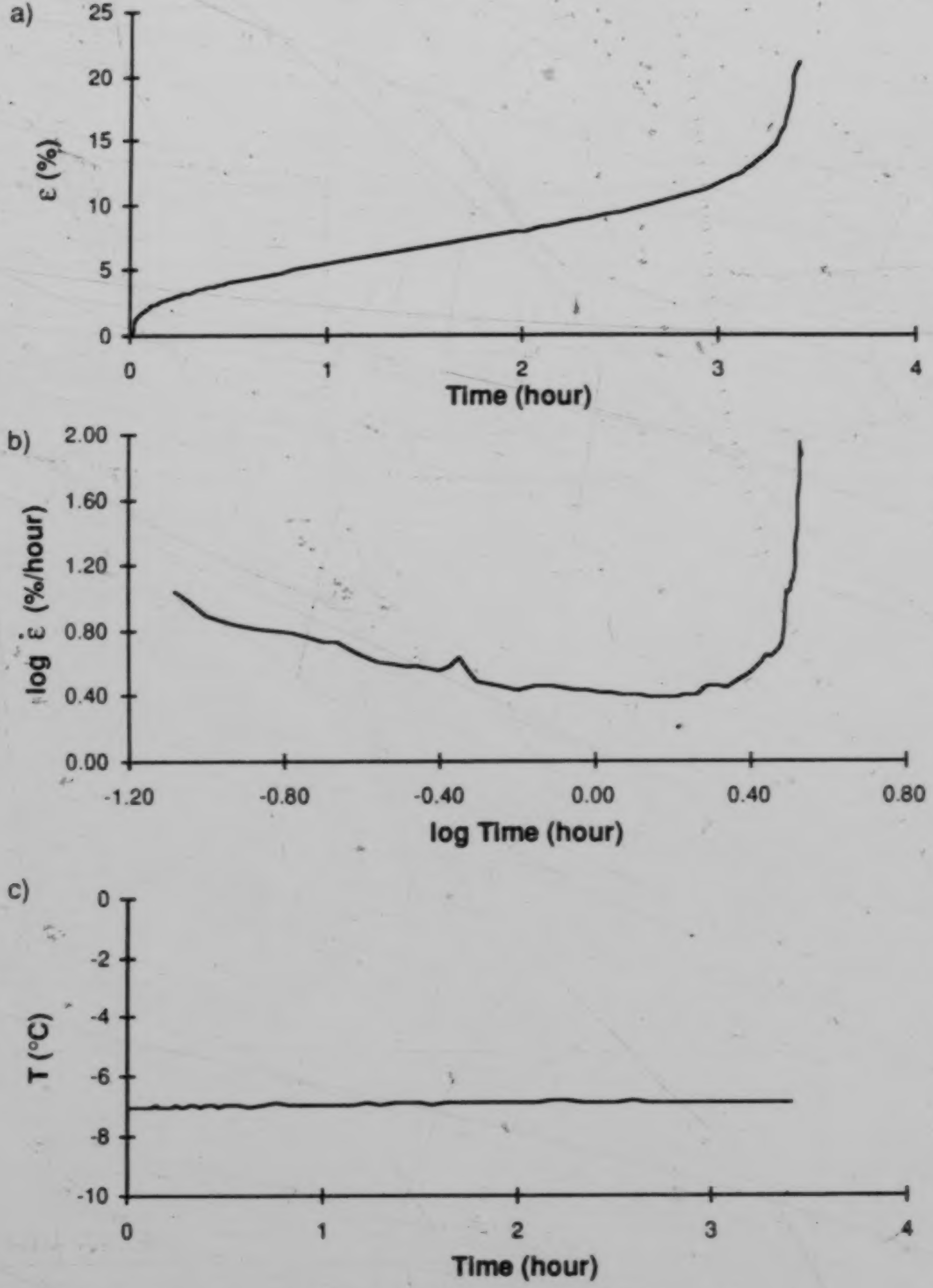

Figure C.12: Creep results test CR-70 soil A 30 ppt at σ=666 kPa
a) strain vs time b) log strain rate vs log time
c) temperature vs time

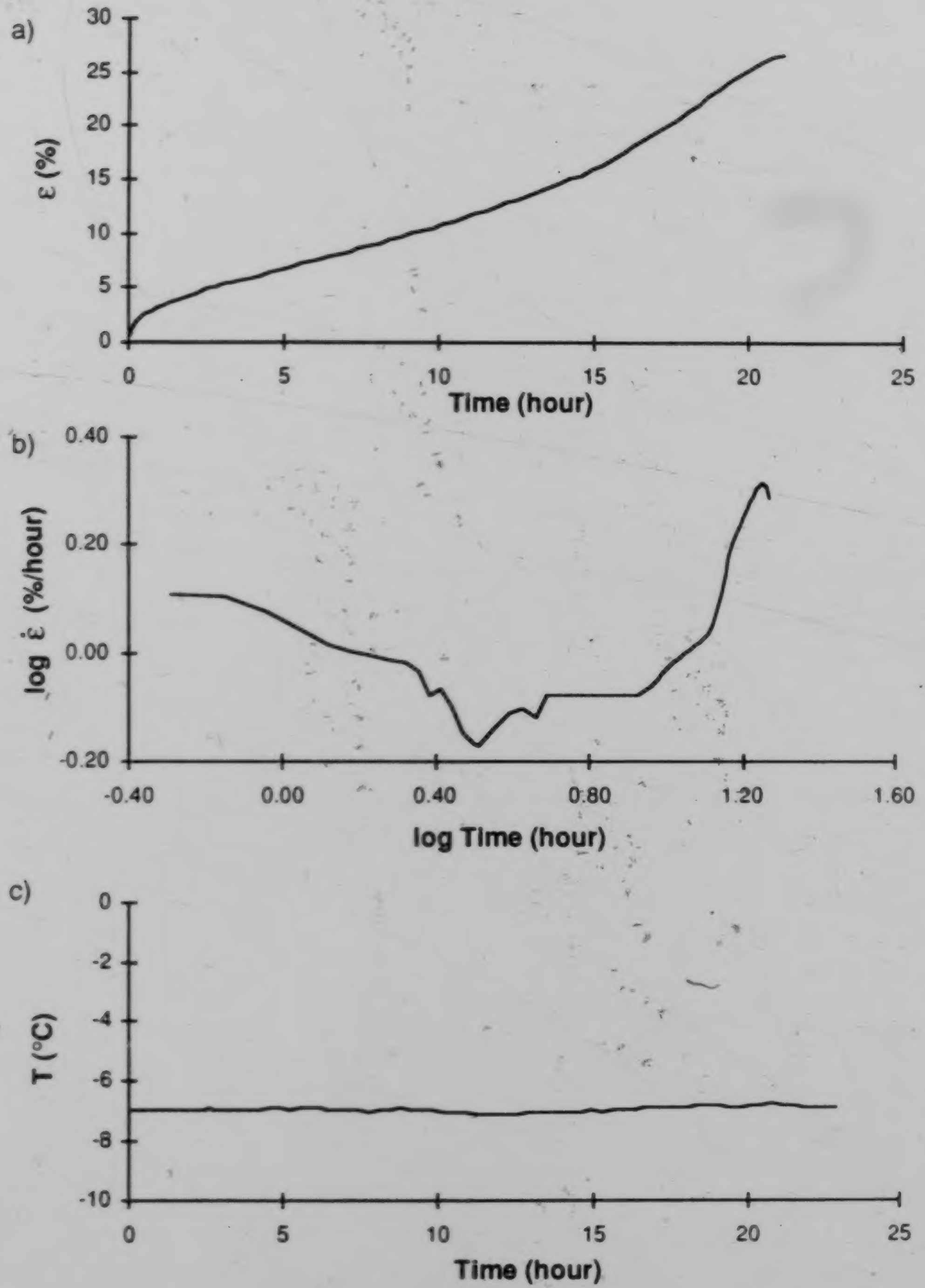

Figure C.13: Creep results test CR-72 soil A 30 ppt at σ=555 kPa
a) strain vs time b) log strain rate vs log time
c) temperature vs time

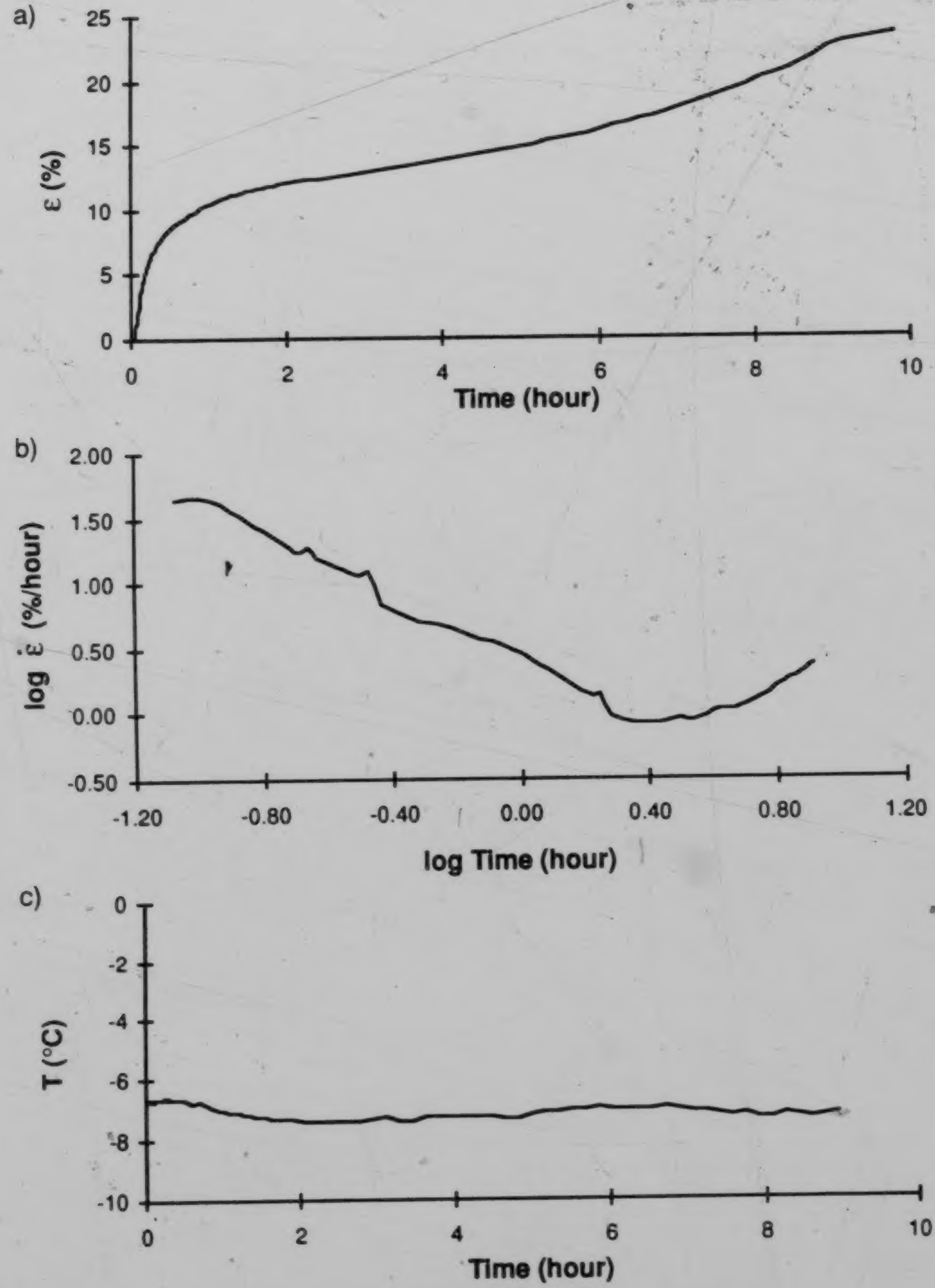

Figure C.14: Creep results test CR-83 soil B 0 ppt at σ=2825 kPa
a) strain vs time b) log strain rate vs log time
c) temperature vs time

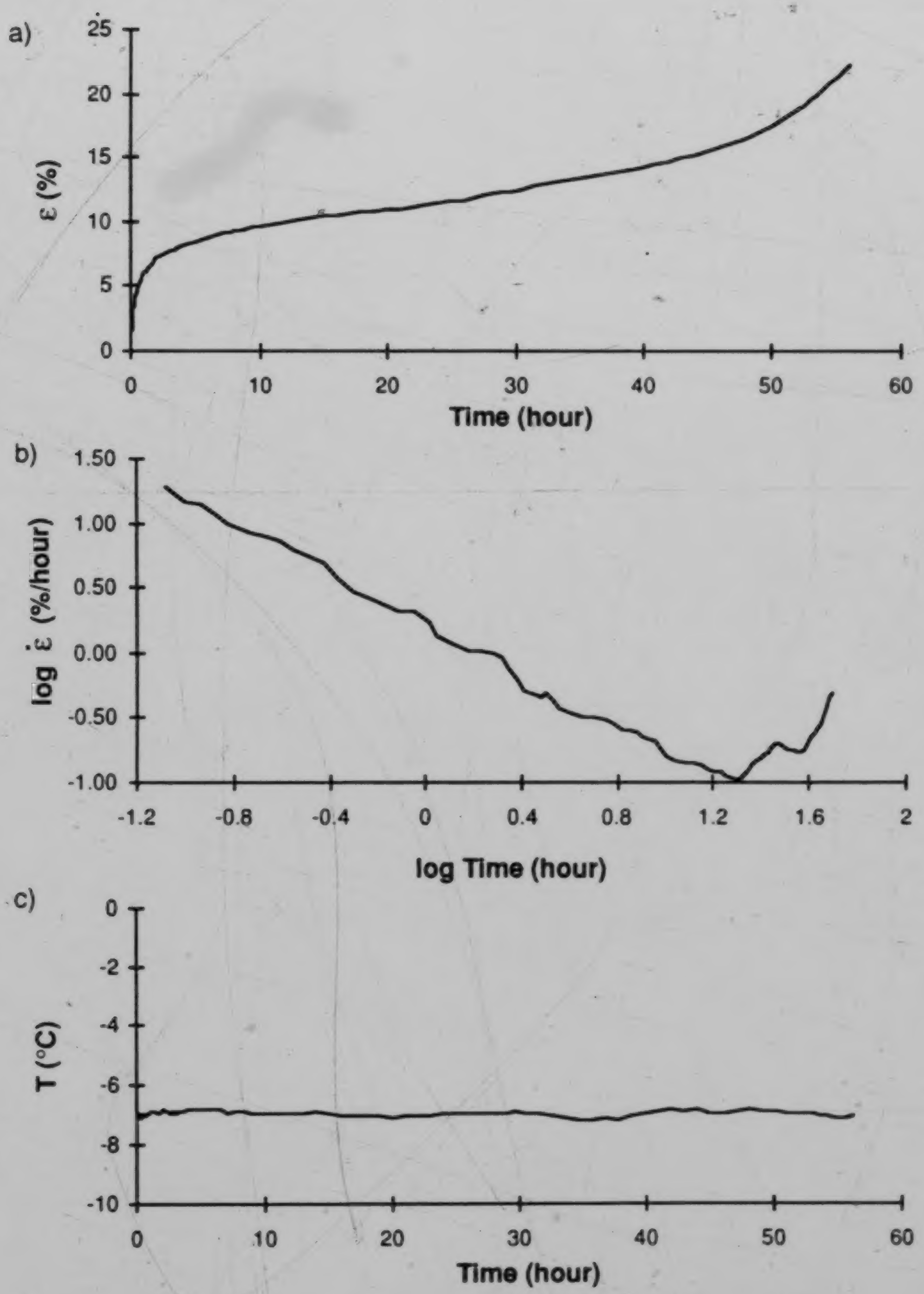

Figure C.15: Creep results test CR-71 soil B 0 ppt at σ=2354 kPa
a) strain vs time b) log strain rate vs log time
c) temperature vs time

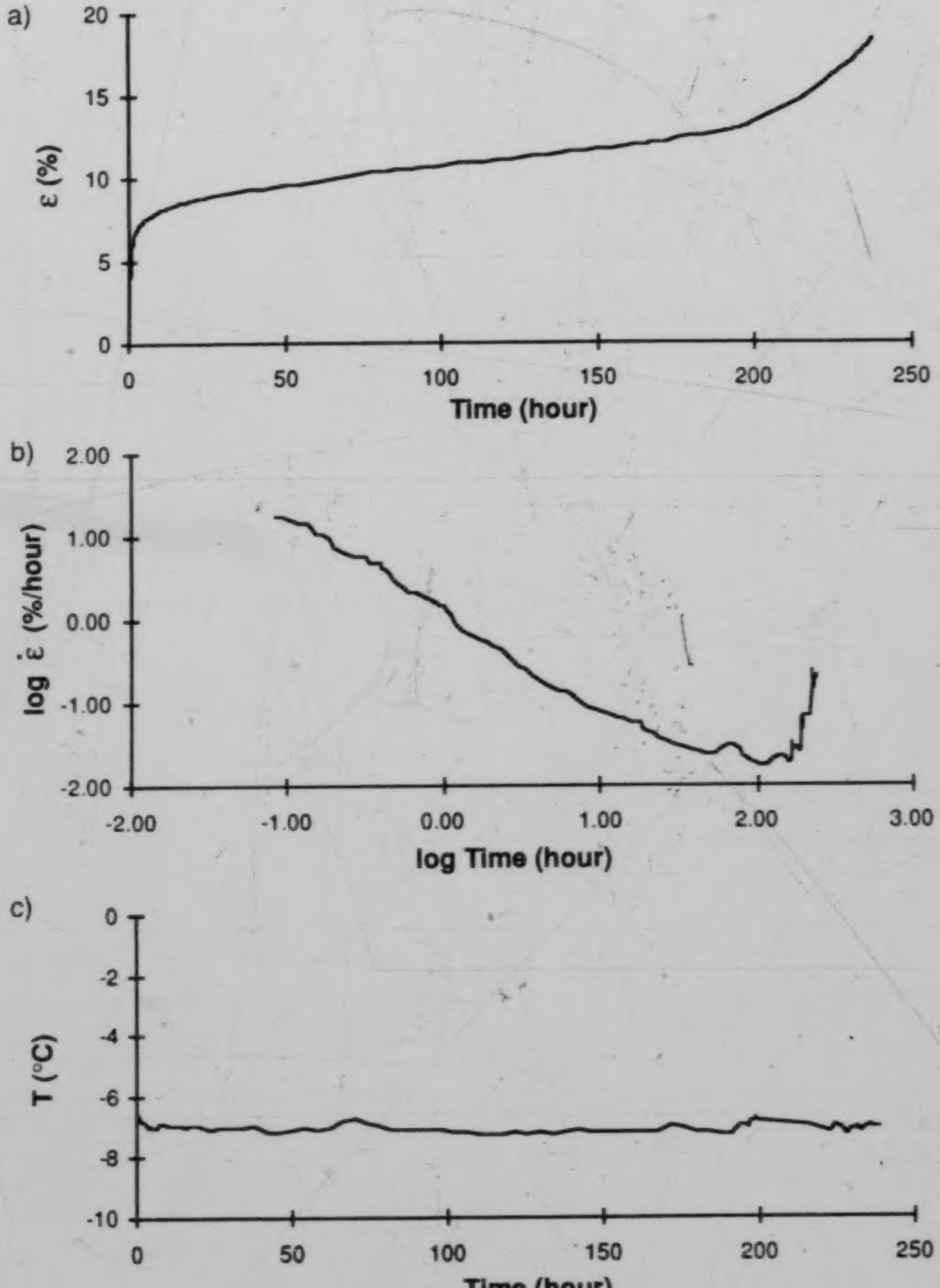

Figure C.16: Creep results test CR-81 soil B 0 ppt at σ=2119 kPa
a) strain vs time b) log strain rate vs log time
c) temperature vs time

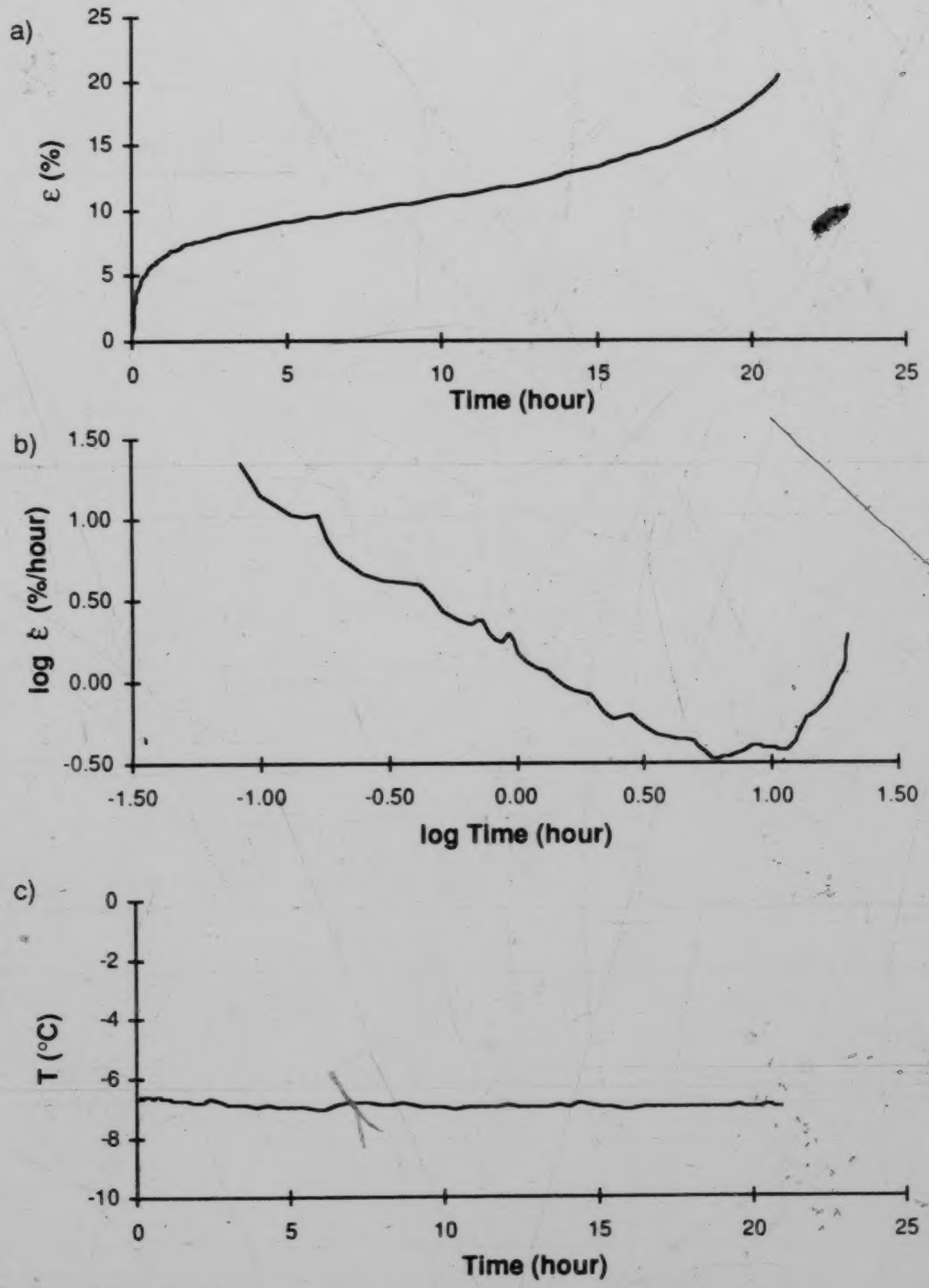

Figure C.17: Creep results test CR-84 soil B 5 ppt at σ=1890 kPa
a) strain vs time b) log strain rate vs log time
c) temperature vs time

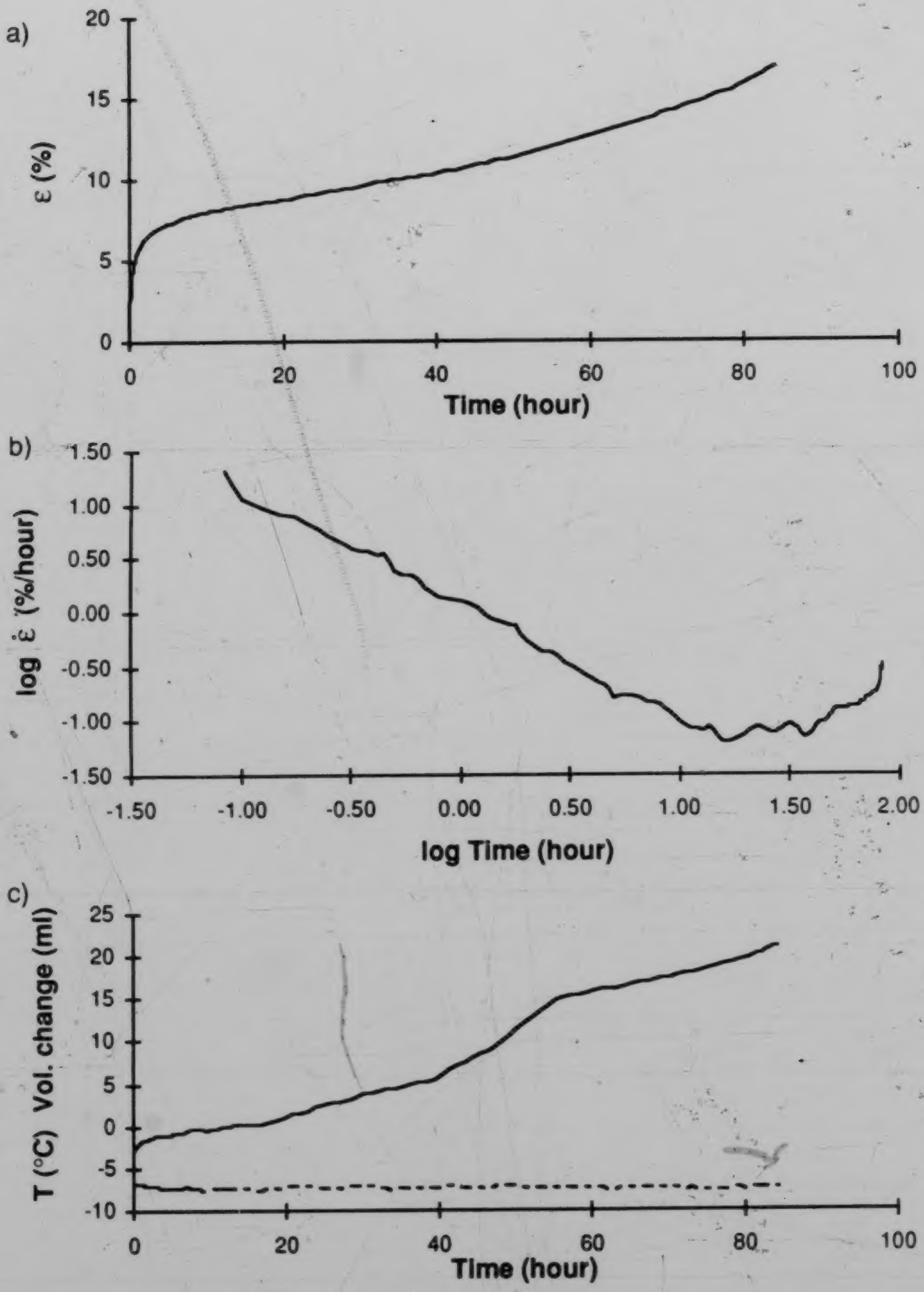

Figure C.18: Creep results test CR-49 soil B 5ppt at σ=1718 kPa
a) strain vs time b) log strain rate vs log time
c) volume change and temperature vs time

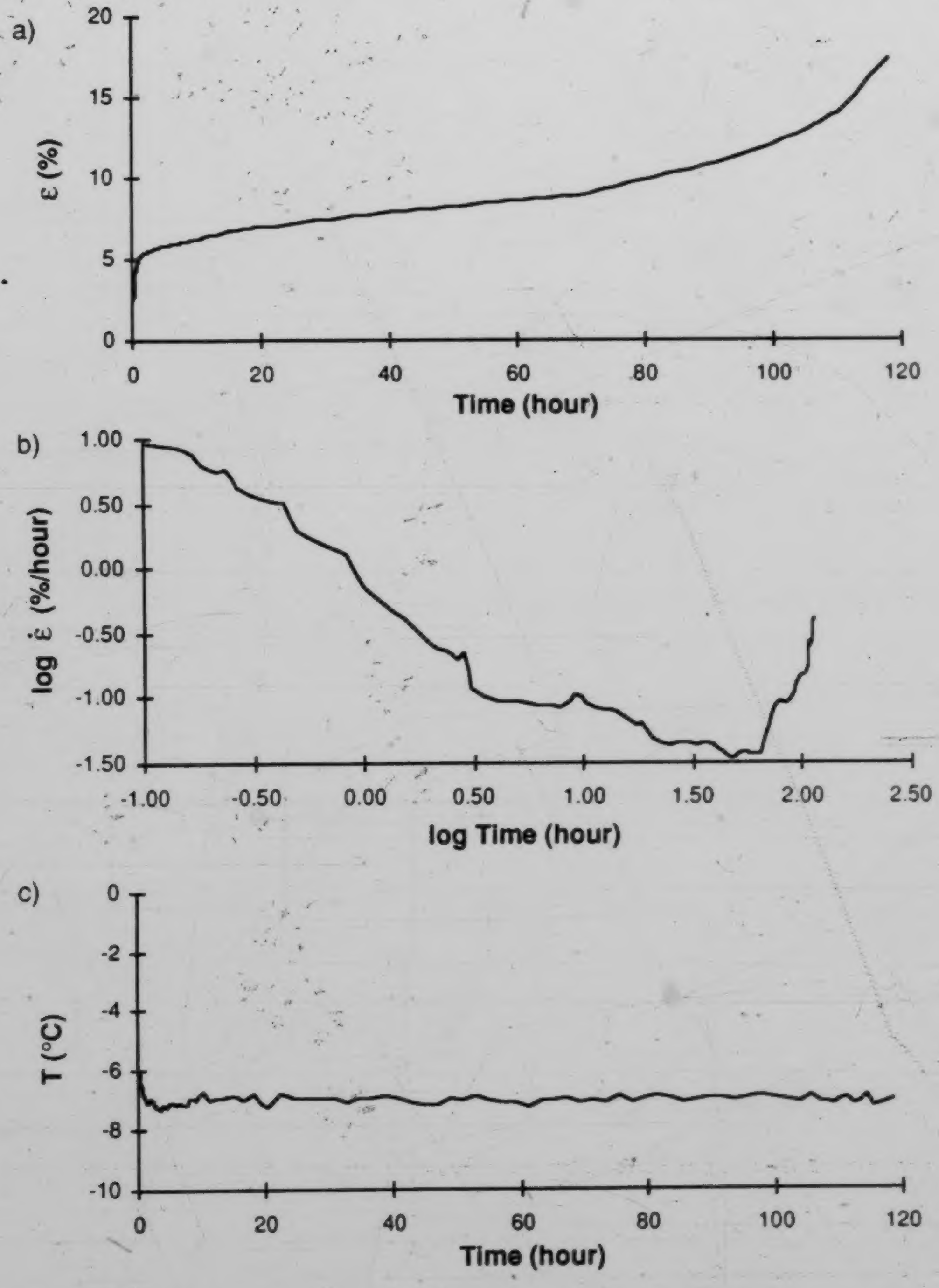

Figure C.19: Creep results test CR-9 soil B 5 ppt at σ=1546 kPa
a) strain vs time b) log strain rate vs log time
c) temperature vs time

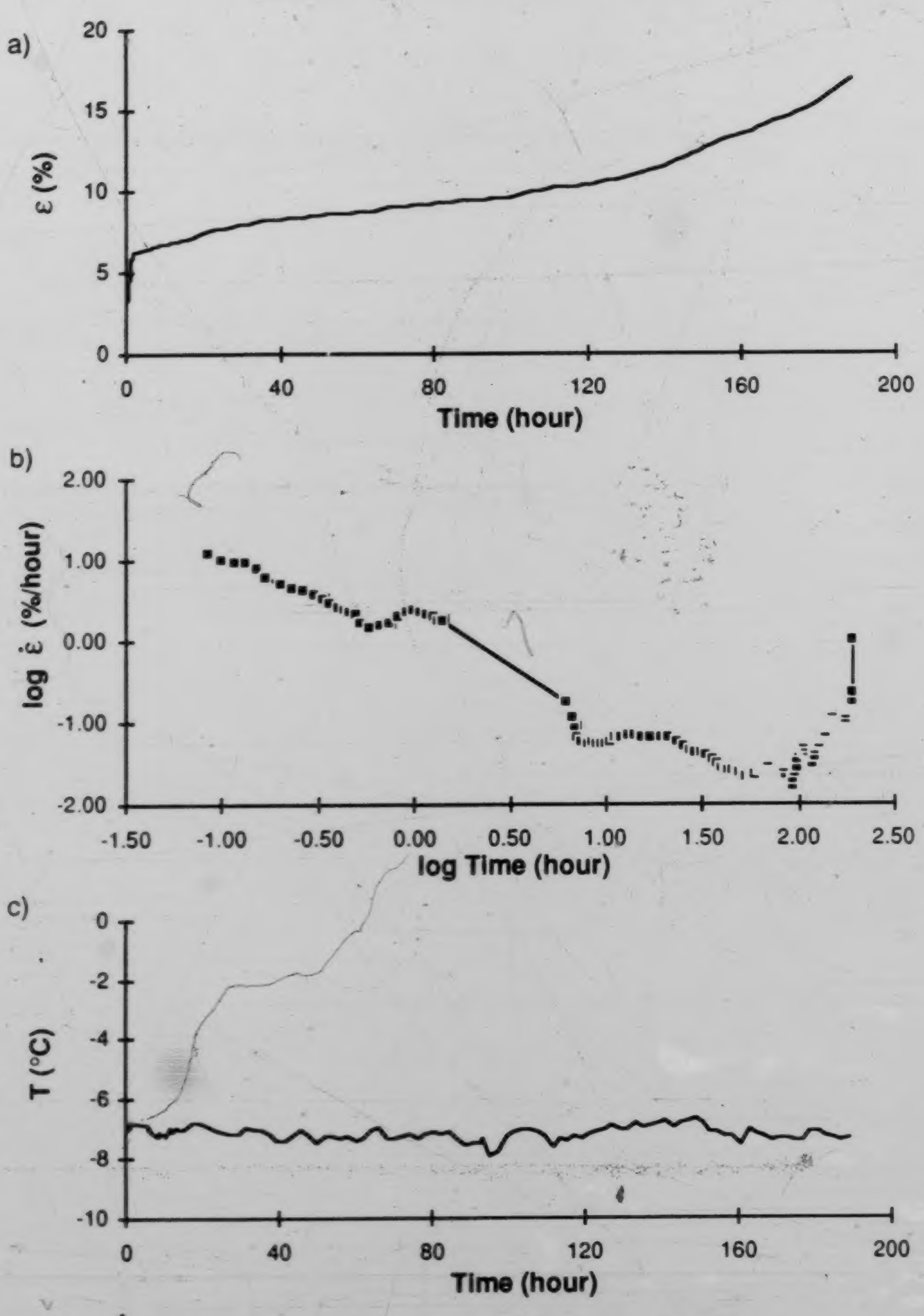

Figure C.20: Creep results test CR-17 soil B 5 ppt at σ=1546 kPa
a) strain vs time b) log strain rate vs log time
c) temperature vs time

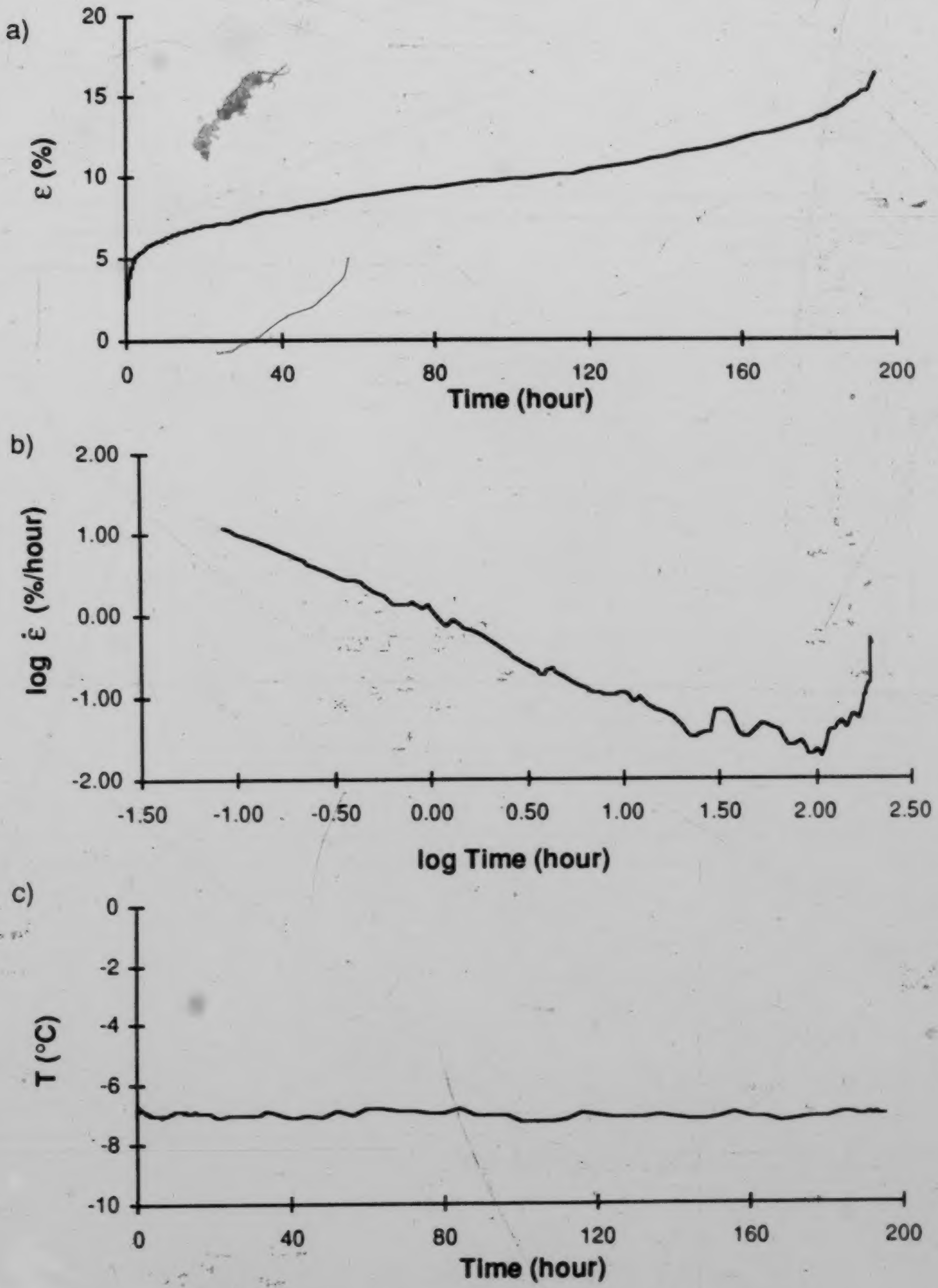

Figure C.21: Creep results test CR-32 soil B 5 ppt at σ=1546 kPa
a) strain vs time b) log strain rate vs log time
c) temperature vs time

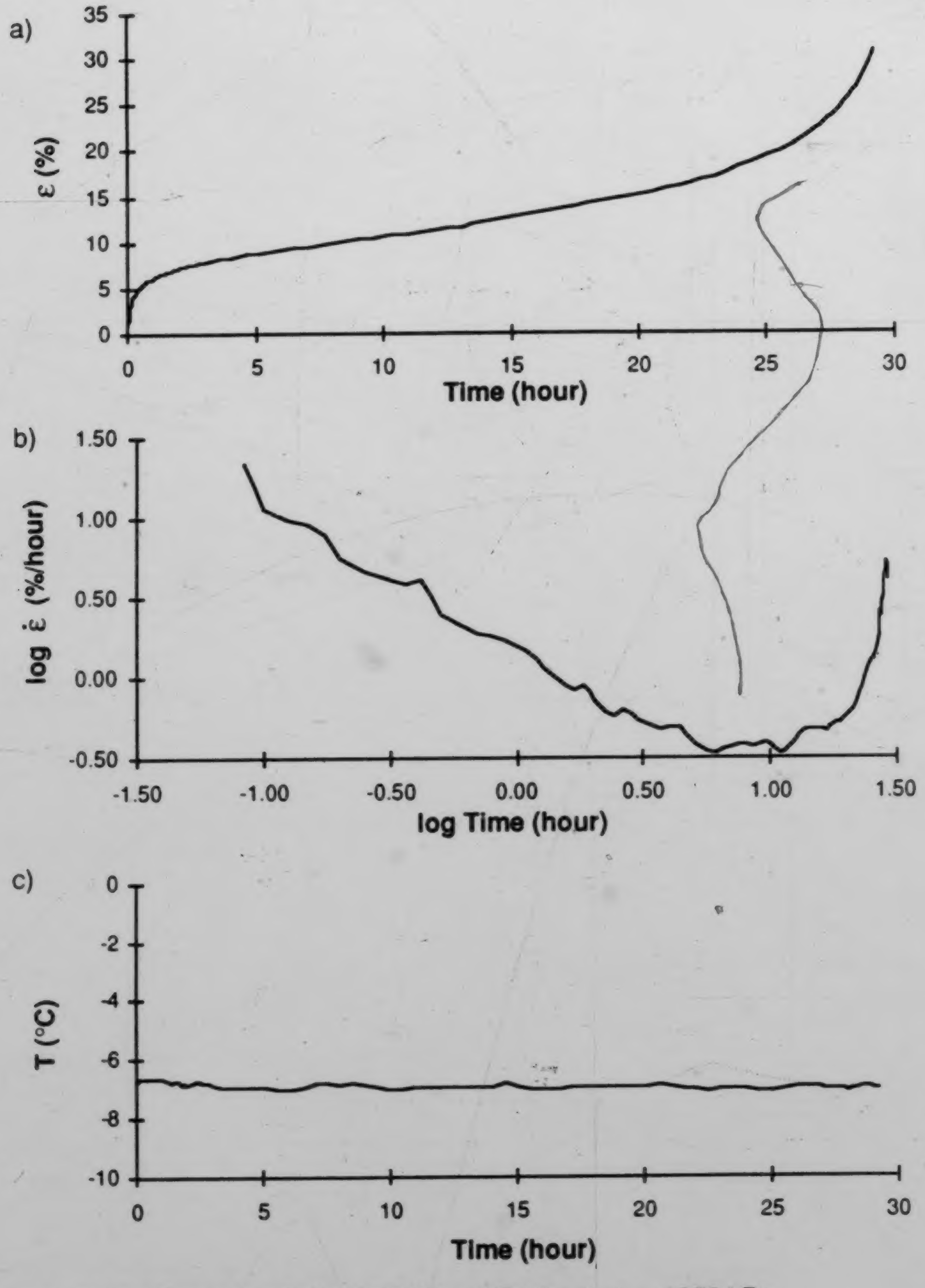

Figure C.22: Creep results test CR-82 soil B 10 ppt at σ=1359 kPa
a) strain vs time b) log strain rate vs log time
c) temperature vs time

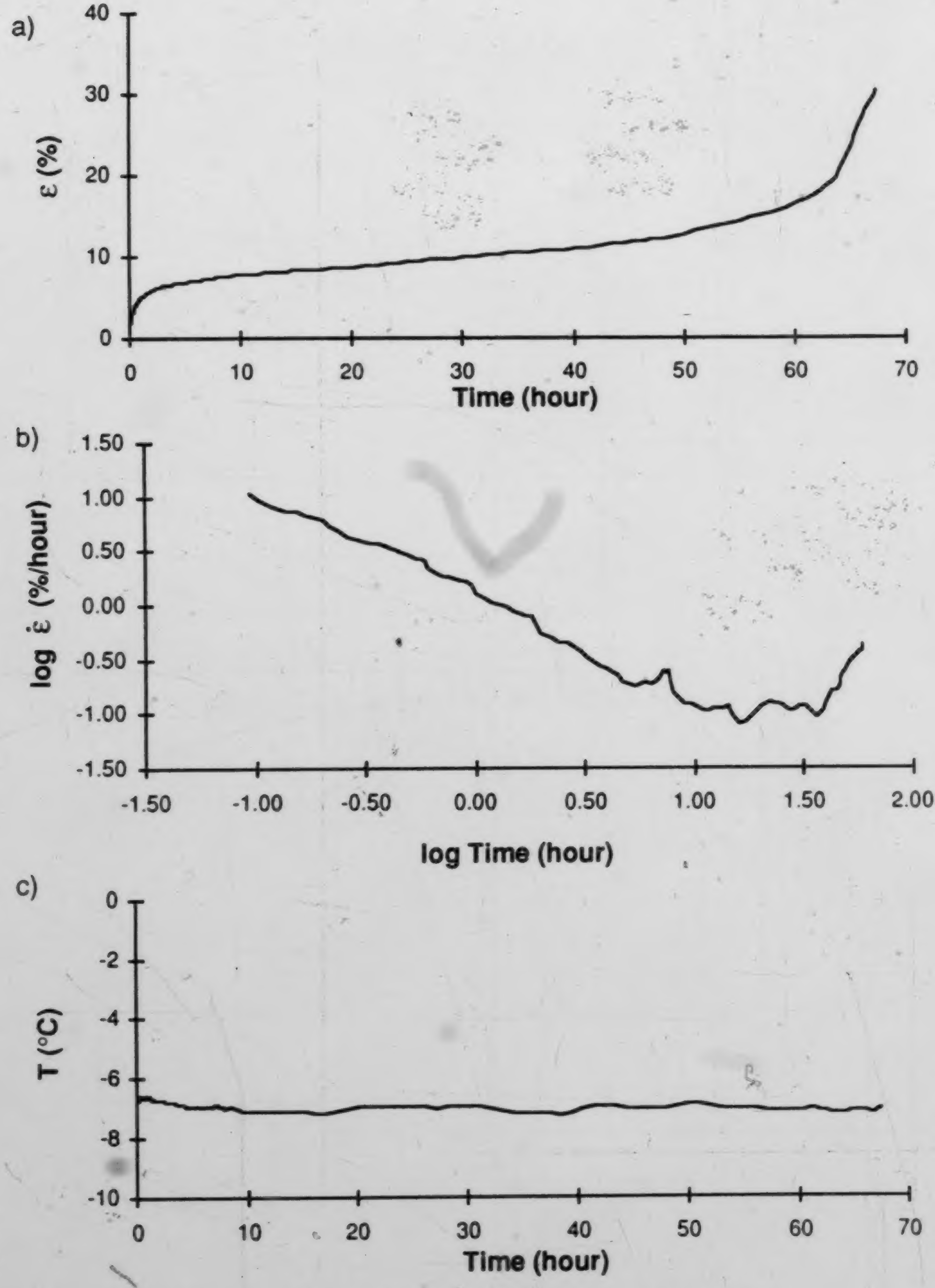

Figure C.23: Creep results test CR-50 soil B 10 ppt at σ=1235 kPa
a) strain vs time b) log strain rate vs log time
c) temperature vs time

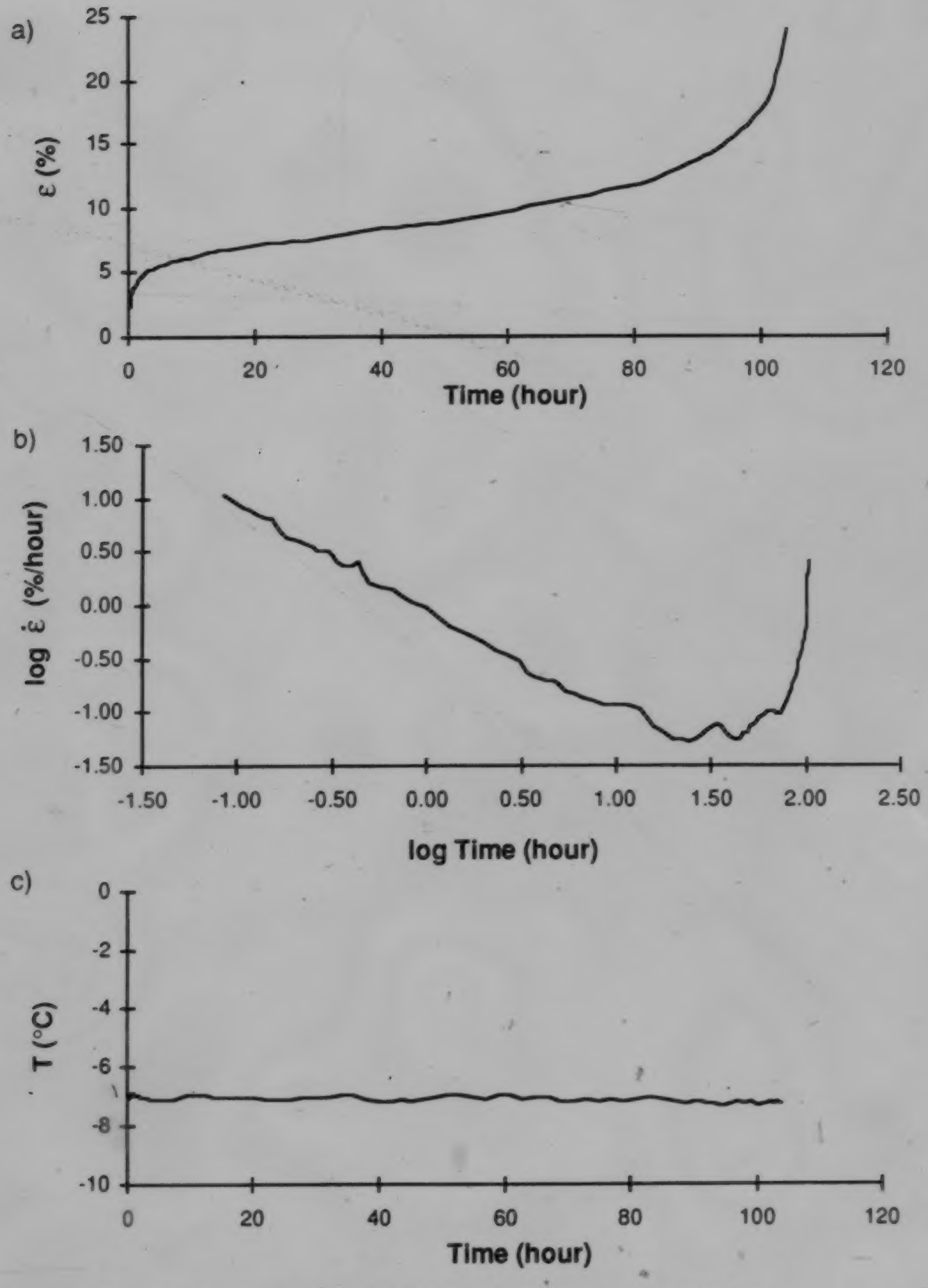

Figure C.24: Creep results test CR-33 soil B 10 ppt at σ=1112 kPa
a) strain vs time b) log strain rate vs log time
c) temperature vs time

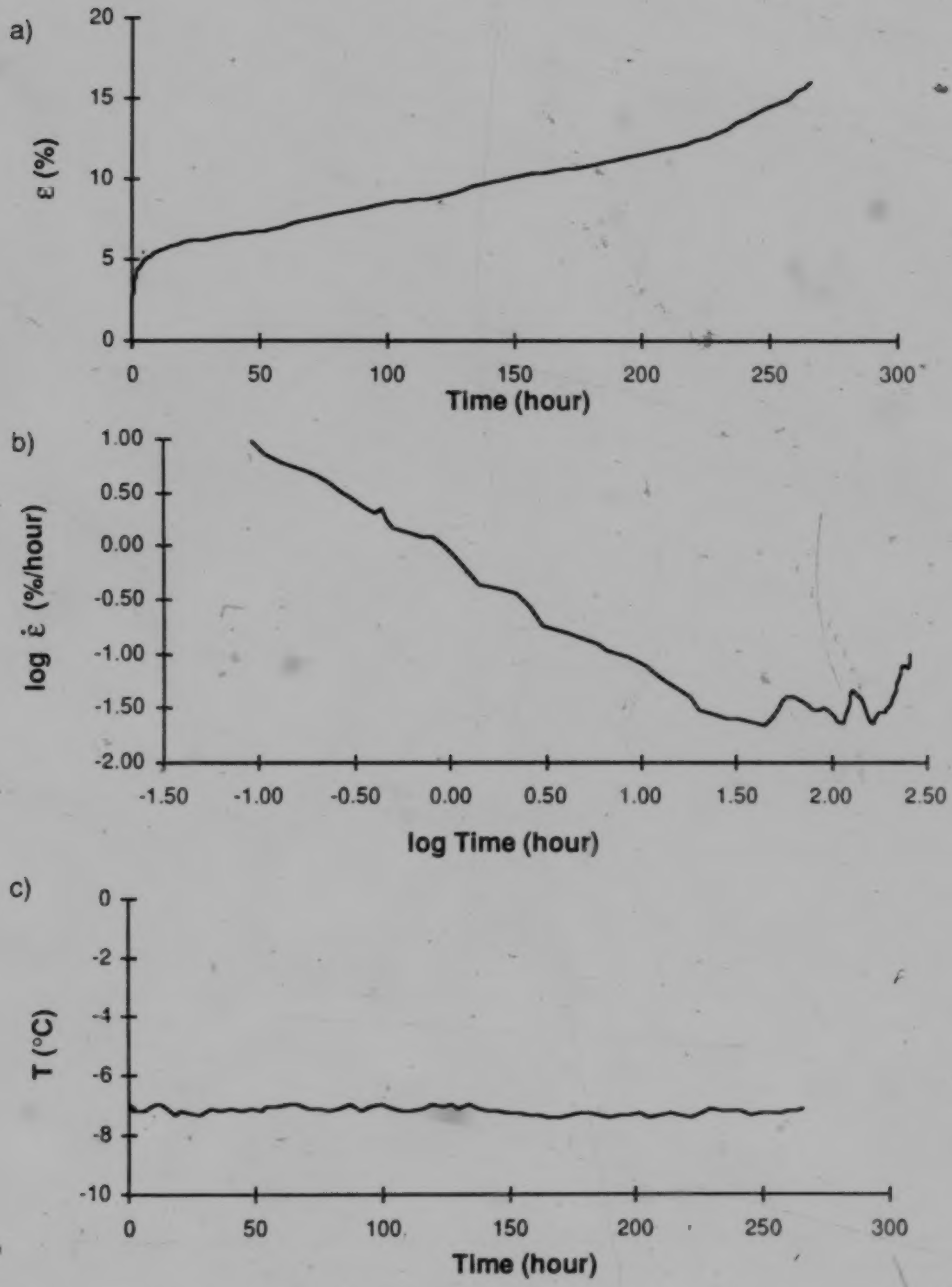

Figure C.25: Creep results test CR-38 soil B 10 ppt at σ=1112 kPa
a) strain vs time b) log strain rate vs log time
c) temperature vs time

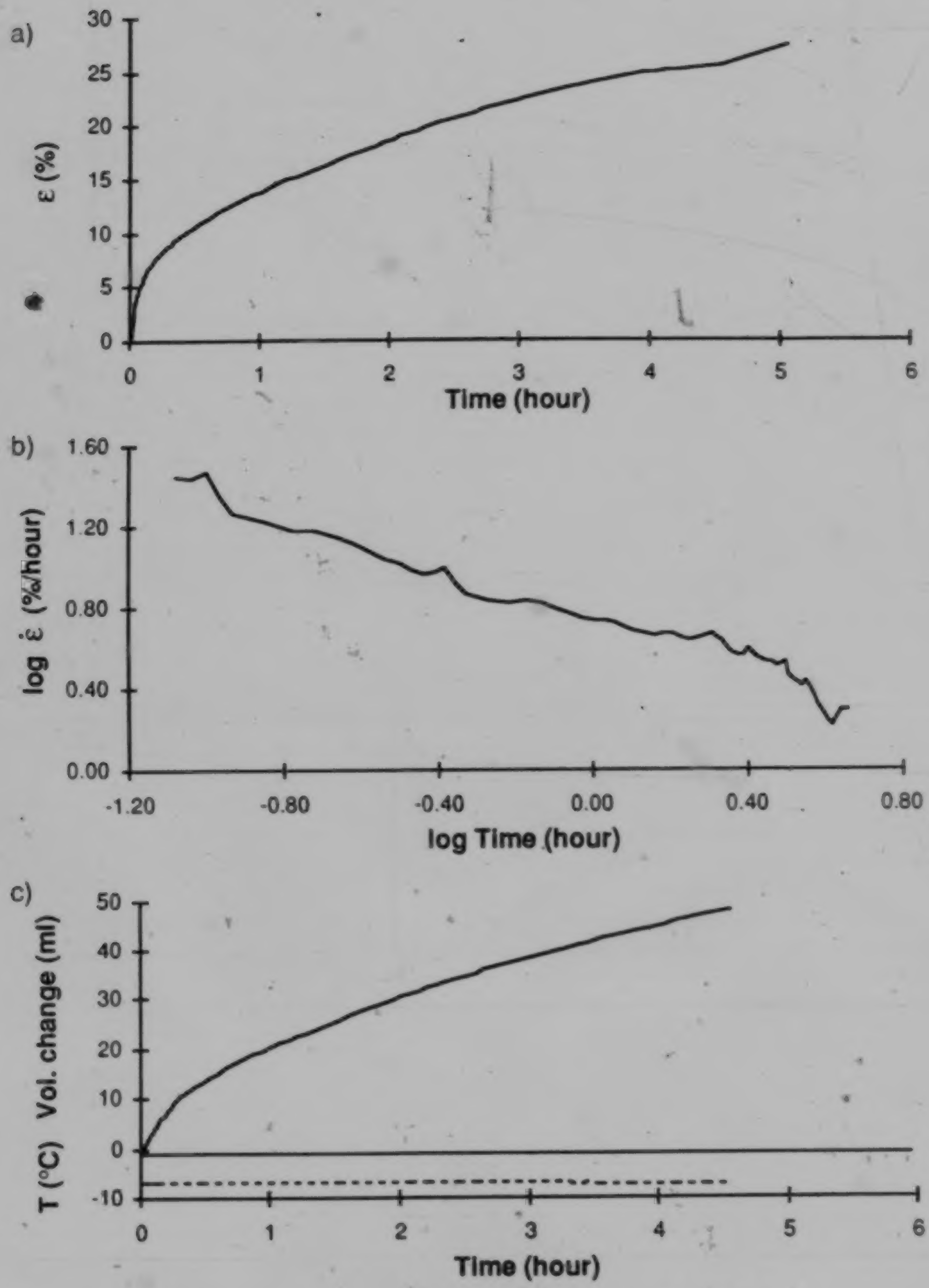

Figure C.26: Creep results test CR-75 soil B 30 ppt at σ=678 kPa
a) strain vs time b) log strain rate vs log time
c) volume change and temperature vs time

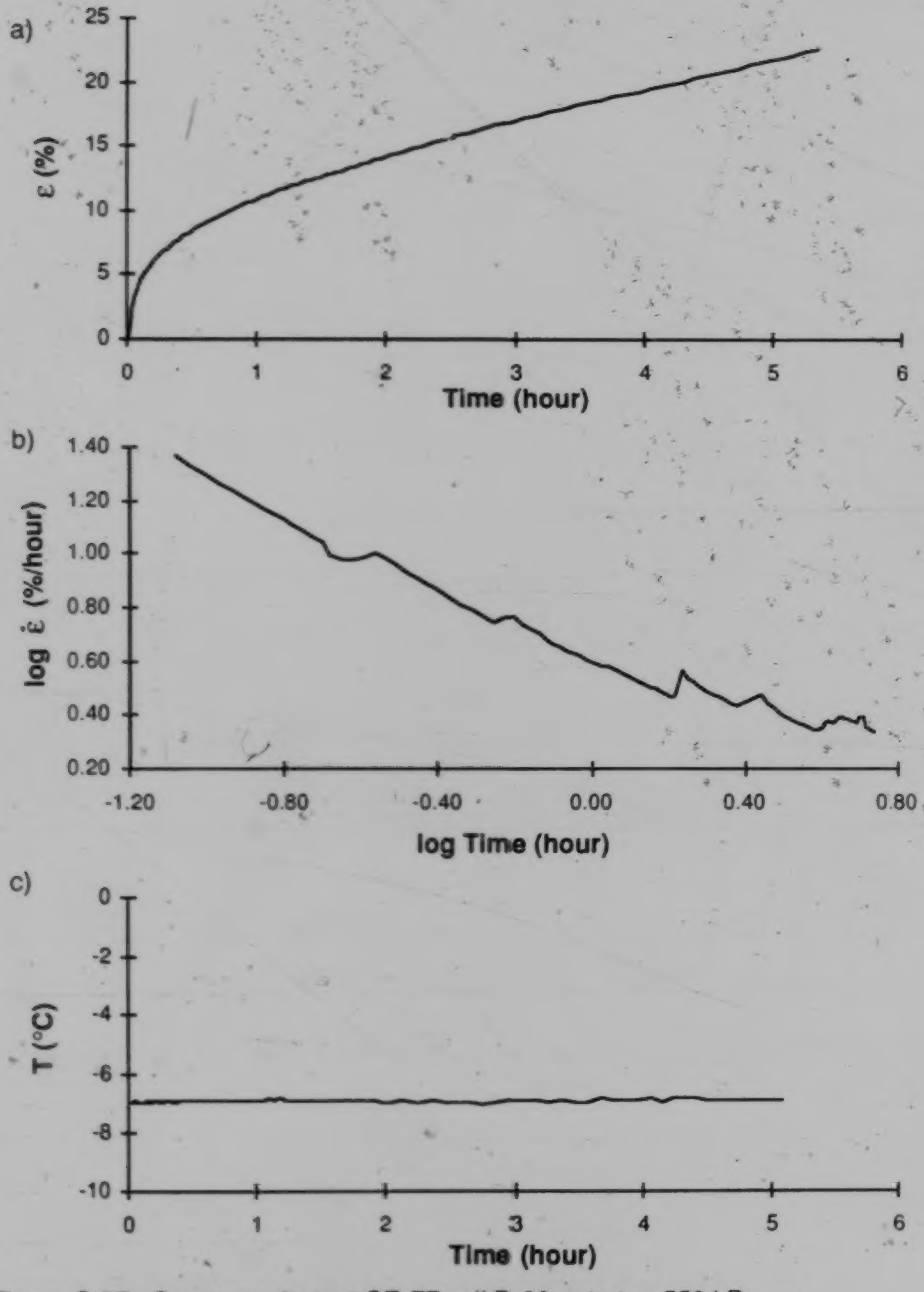

Figure C.27: Creep results test CR-77 soil B 30 ppt at σ=559 kPa.
a) strain vs time b) log strain rate vs log time
c) temperature vs time

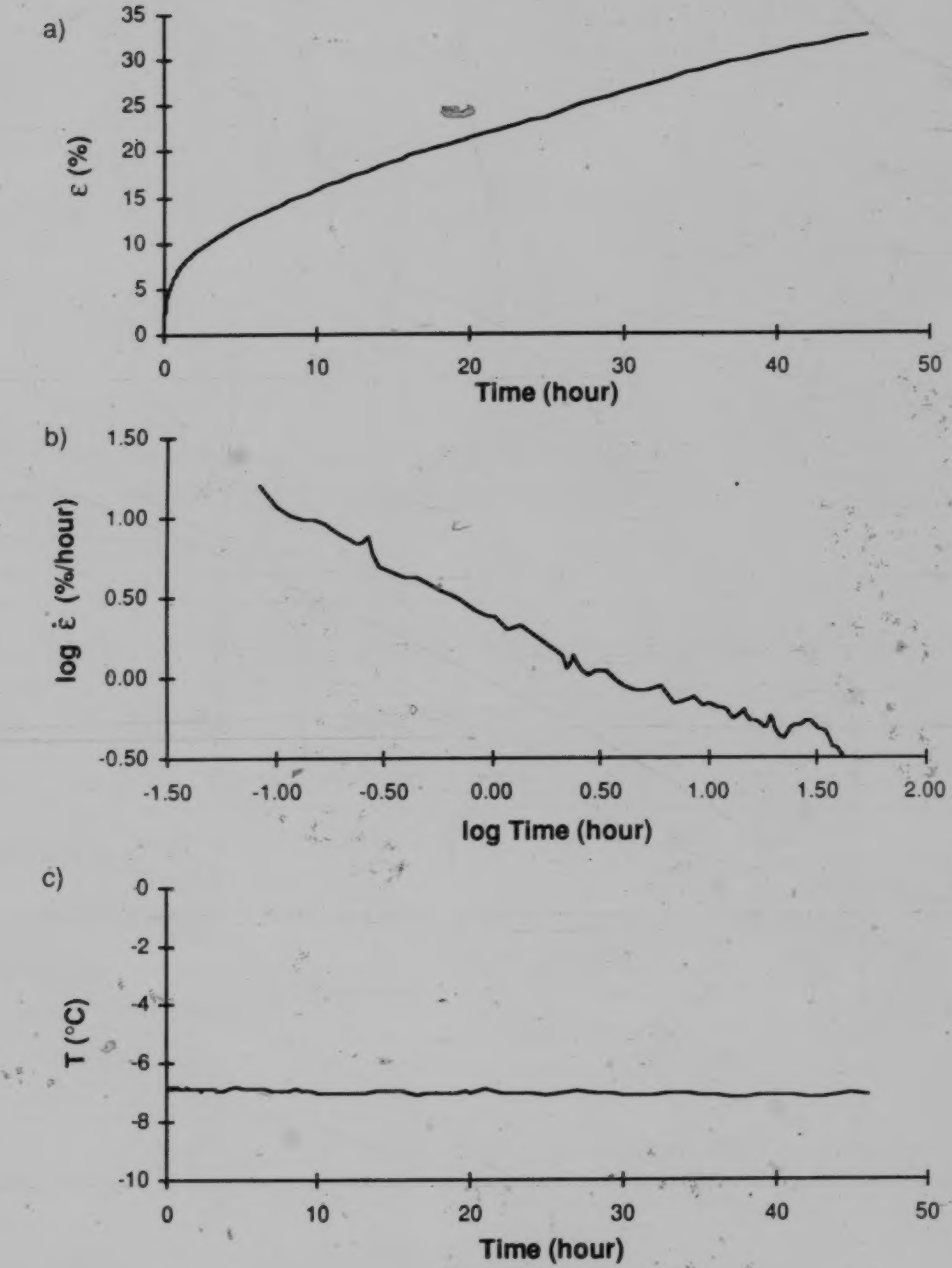

Figure C.28: Creep results test CR-88 soil B 30 ppt at σ=442 kPa
a) strain vs time b) log strain rate vs log time
c) temperature vs time

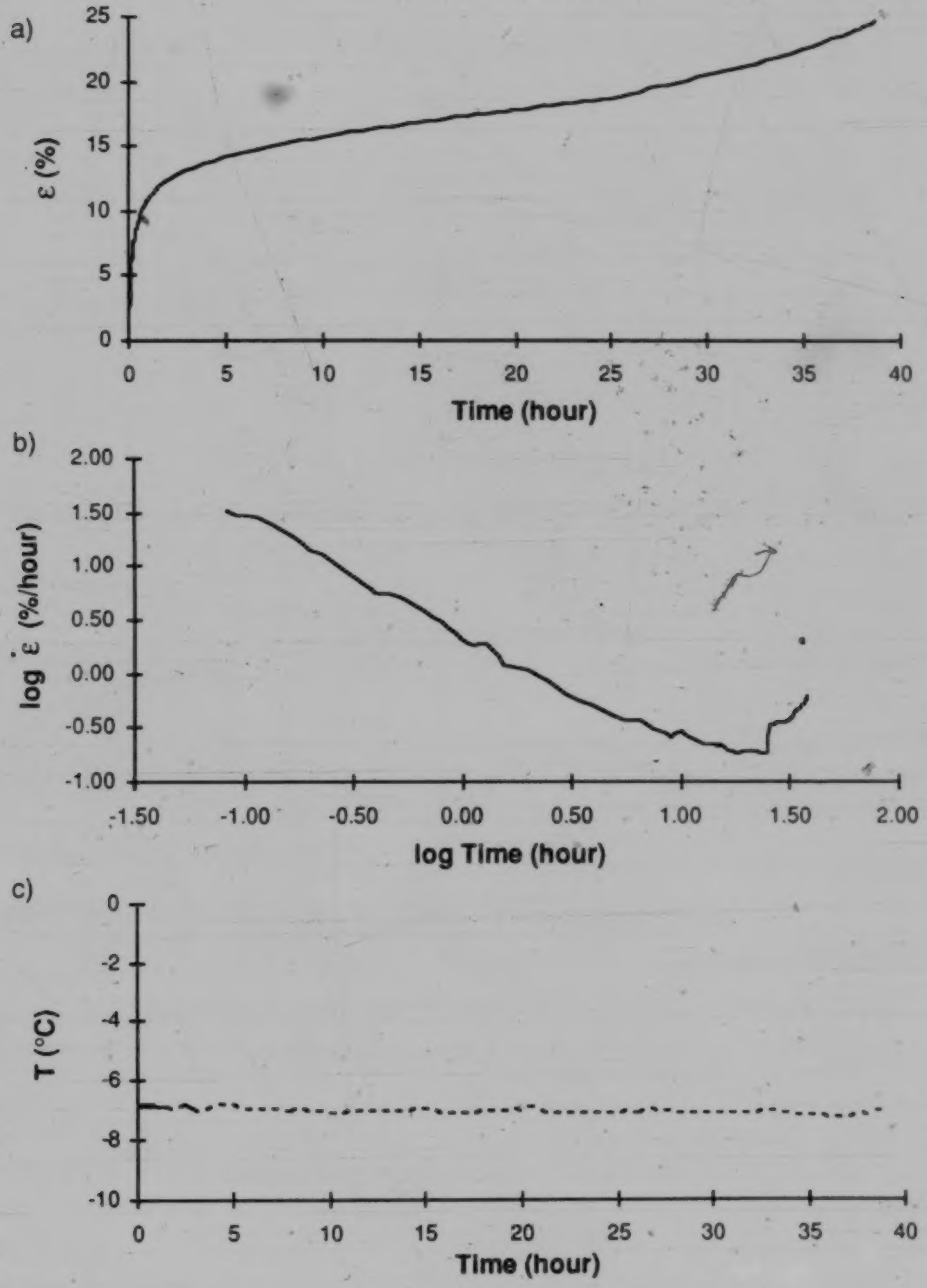

Figure C.29: Creep results test CR-79 soil C 0 ppt at σ=2240 kPa
a) strain vs time b) log strain rate vs log time
c) temperature vs time

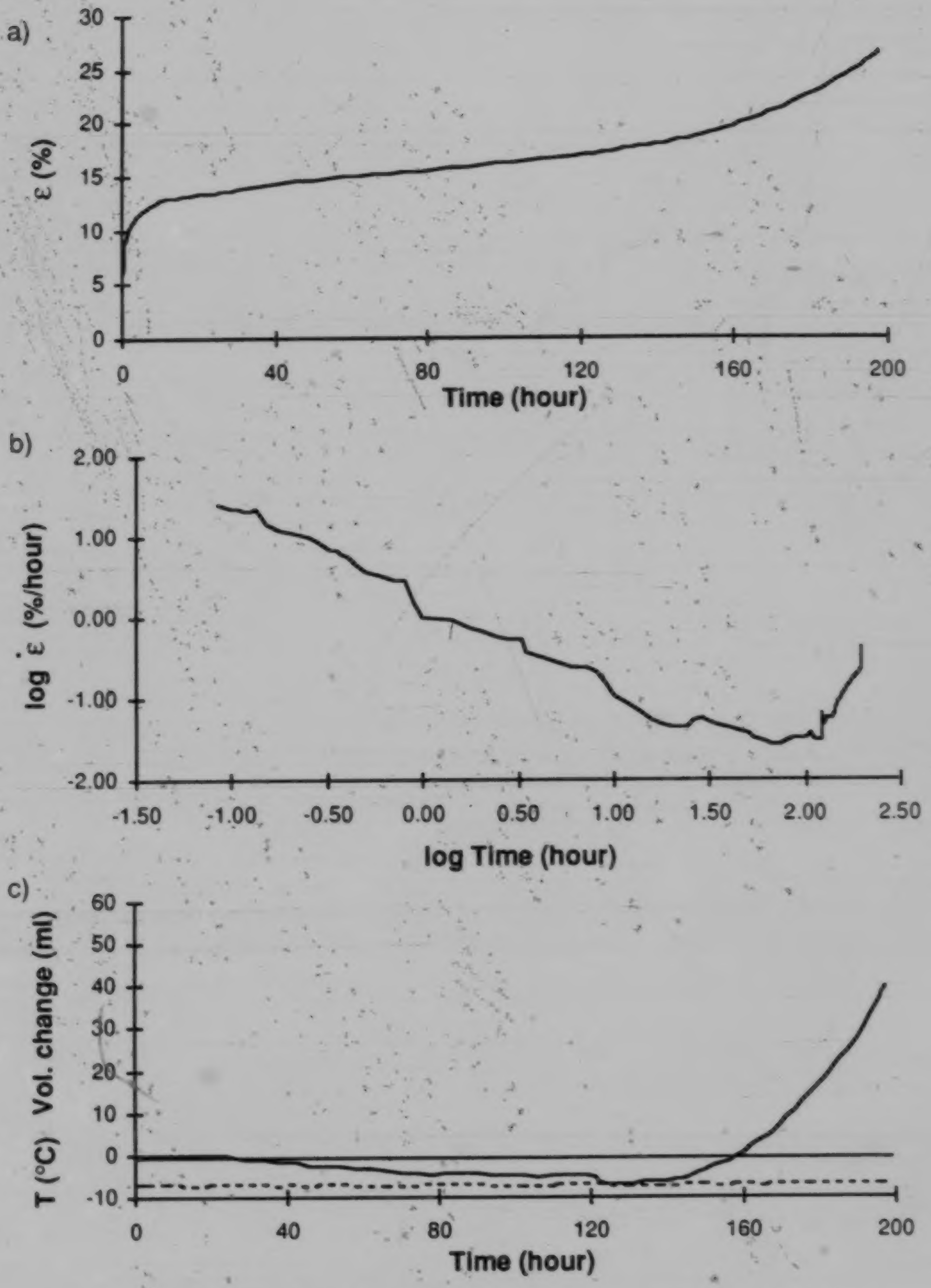

Figure C.30: Creep results test CR-65 soil C 0 ppt at σ=2036 kPa
a) strain vs time b) log strain rate vs log time
c) volume change and temperature vs time

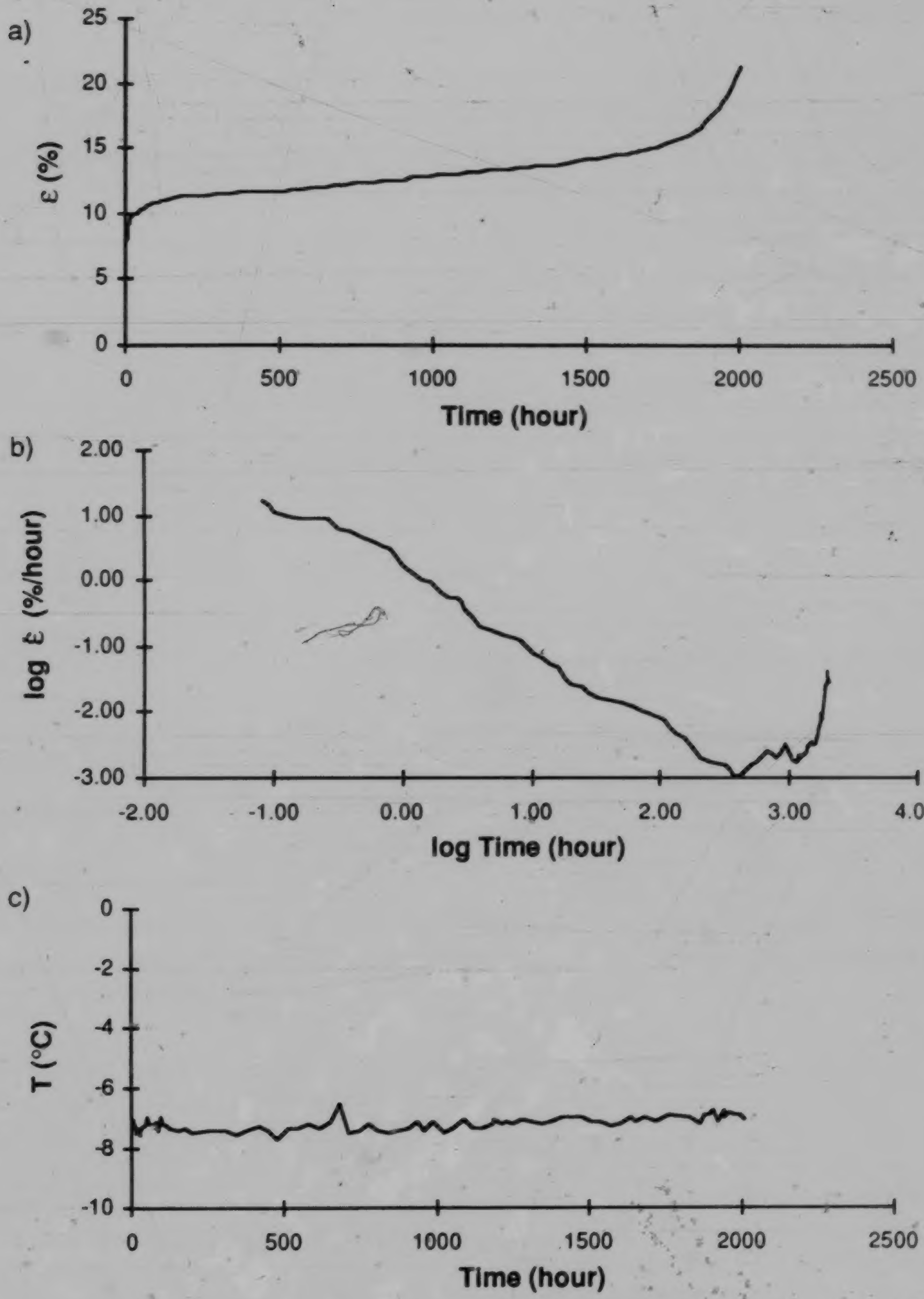

Figure C.31: Creep results test CR-36 soil C 0 ppt at σ=1832 kPa
a) strain vs time b) log strain rate vs log time
c) temperature vs time

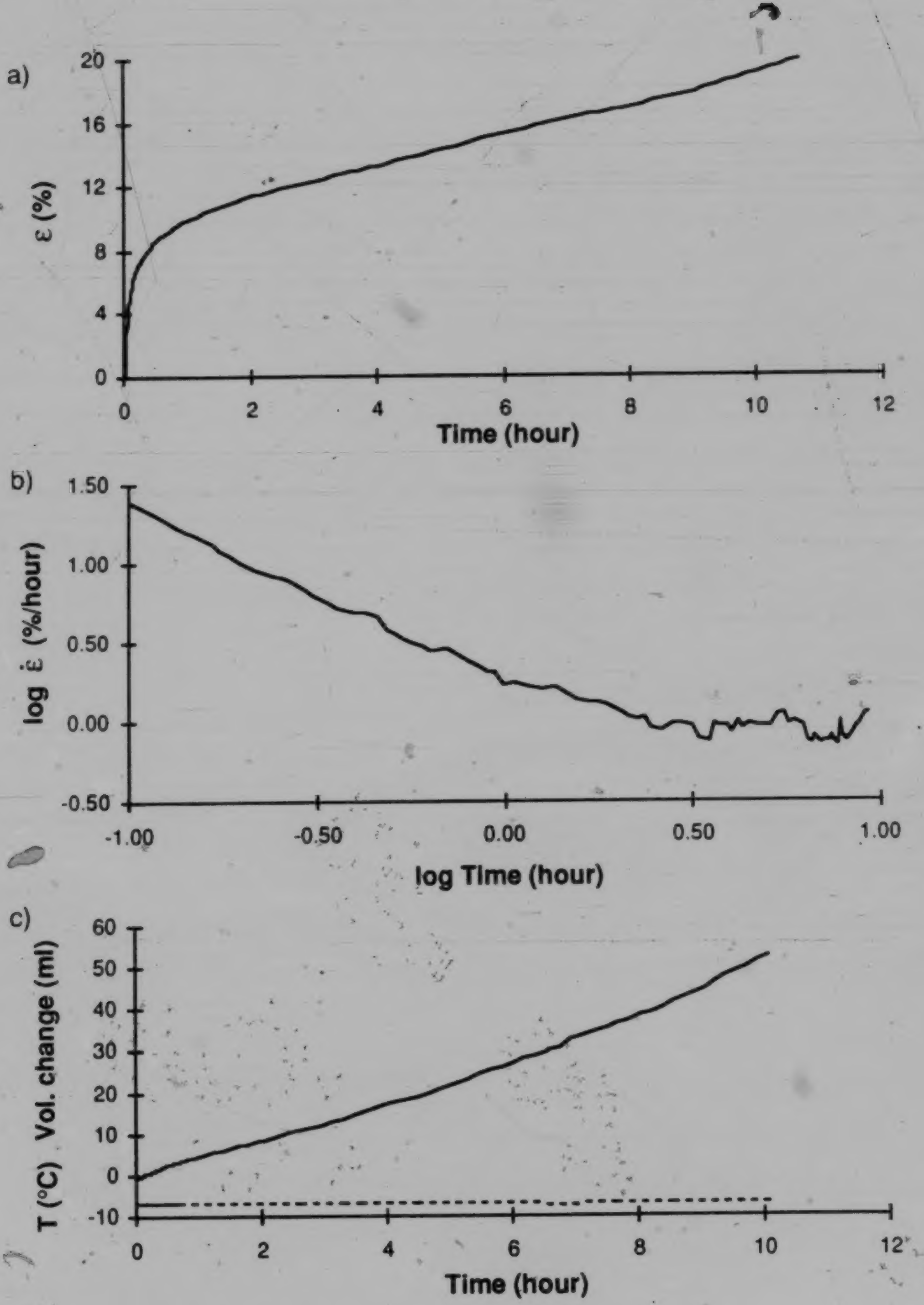

Figure C.32: Creep results test CR-96 soil C 5 ppt at σ=2006 kPa
a) strain vs time b) log strain rate vs log time
c) volume change and temperature vs time

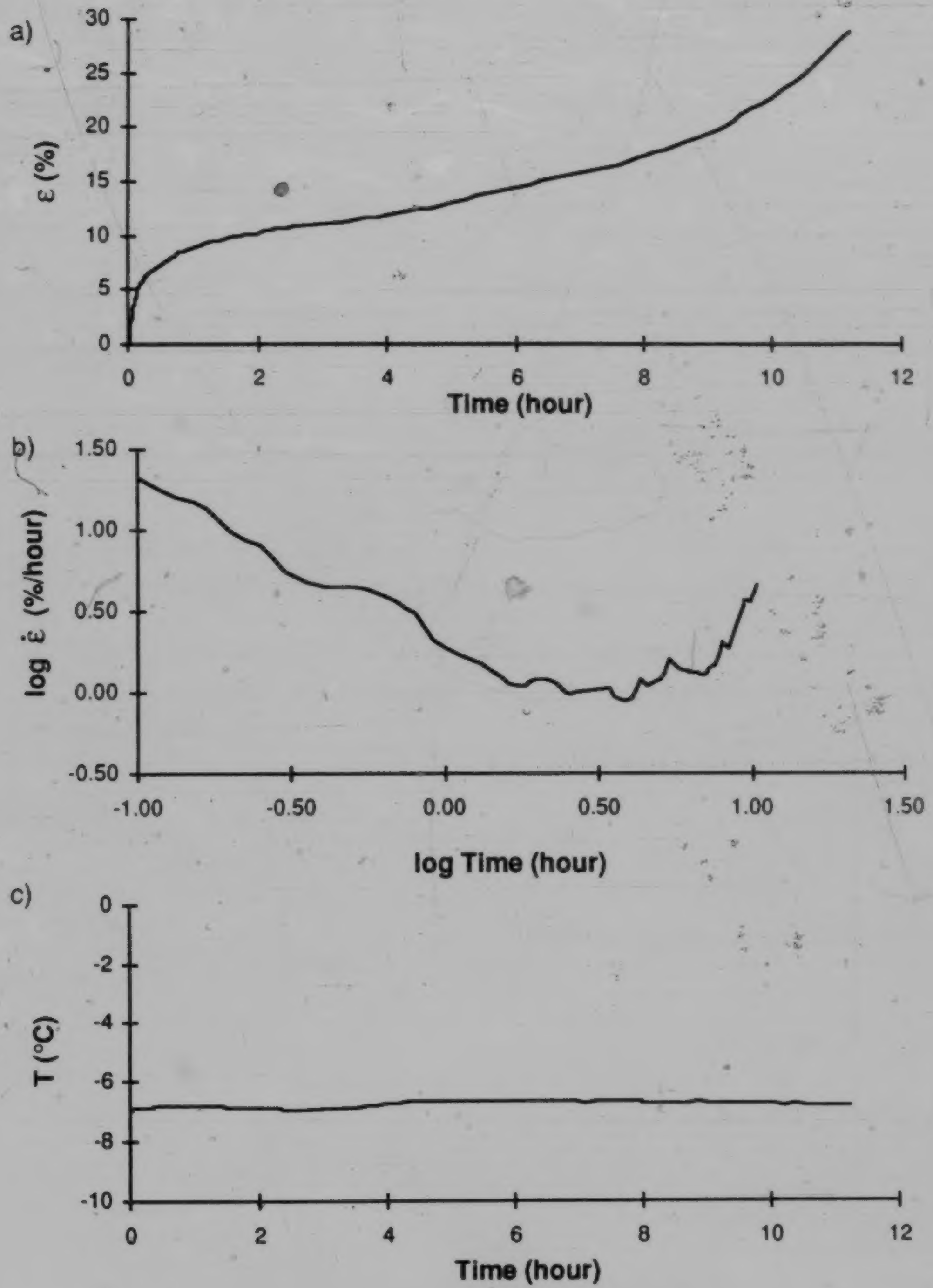

Figure C.33: Creep results test CR-66 soil C 5 ppt at σ=1839 kPa
a) strain vs time b) log strain rate vs log time
c) temperature vs time

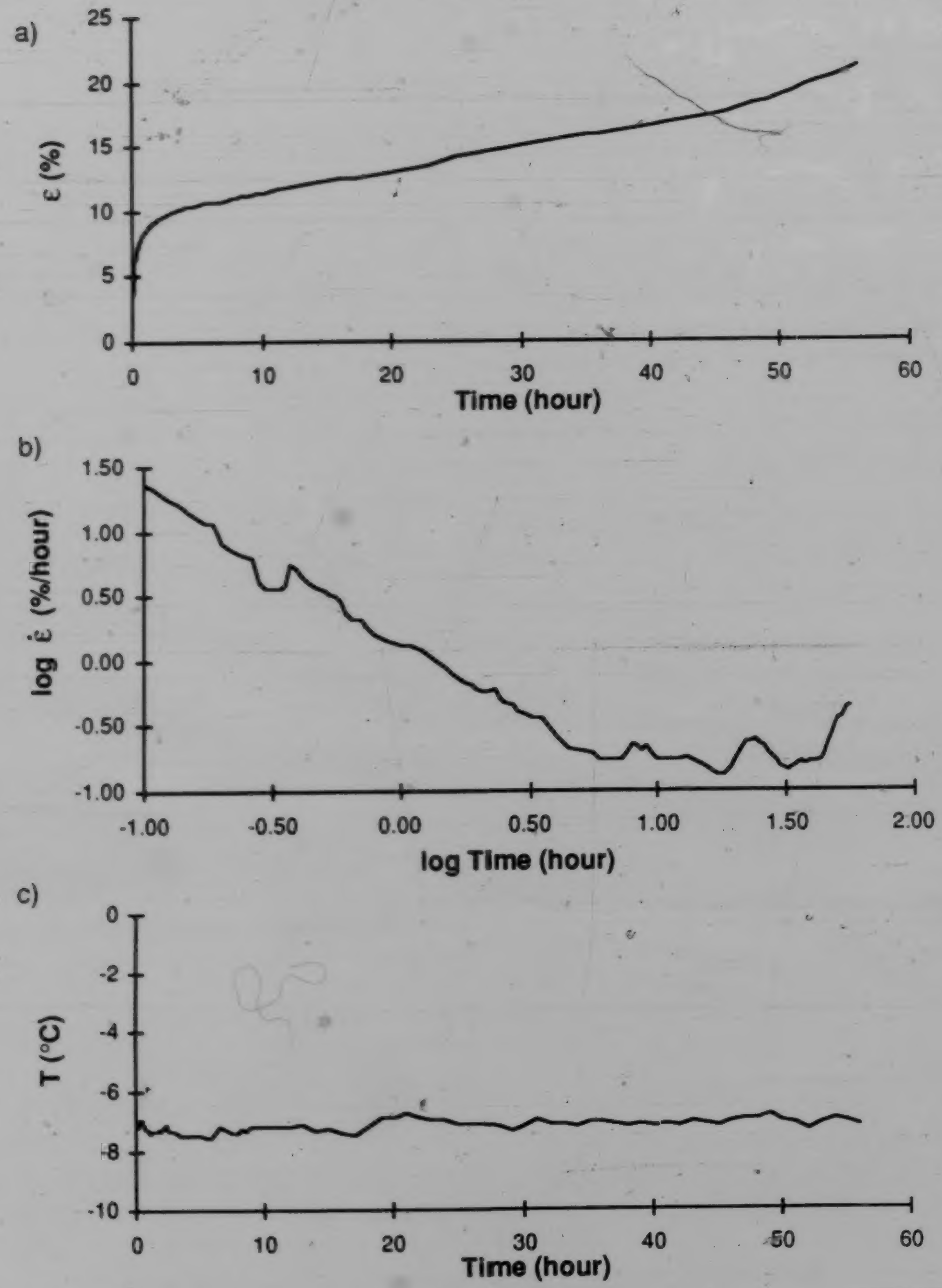

Figure C.34: Creep results test CR-62 soil C 5 ppt at σ=1672 kPa
a) strain vs time b) log strain rate vs log time
c) temperature vs time

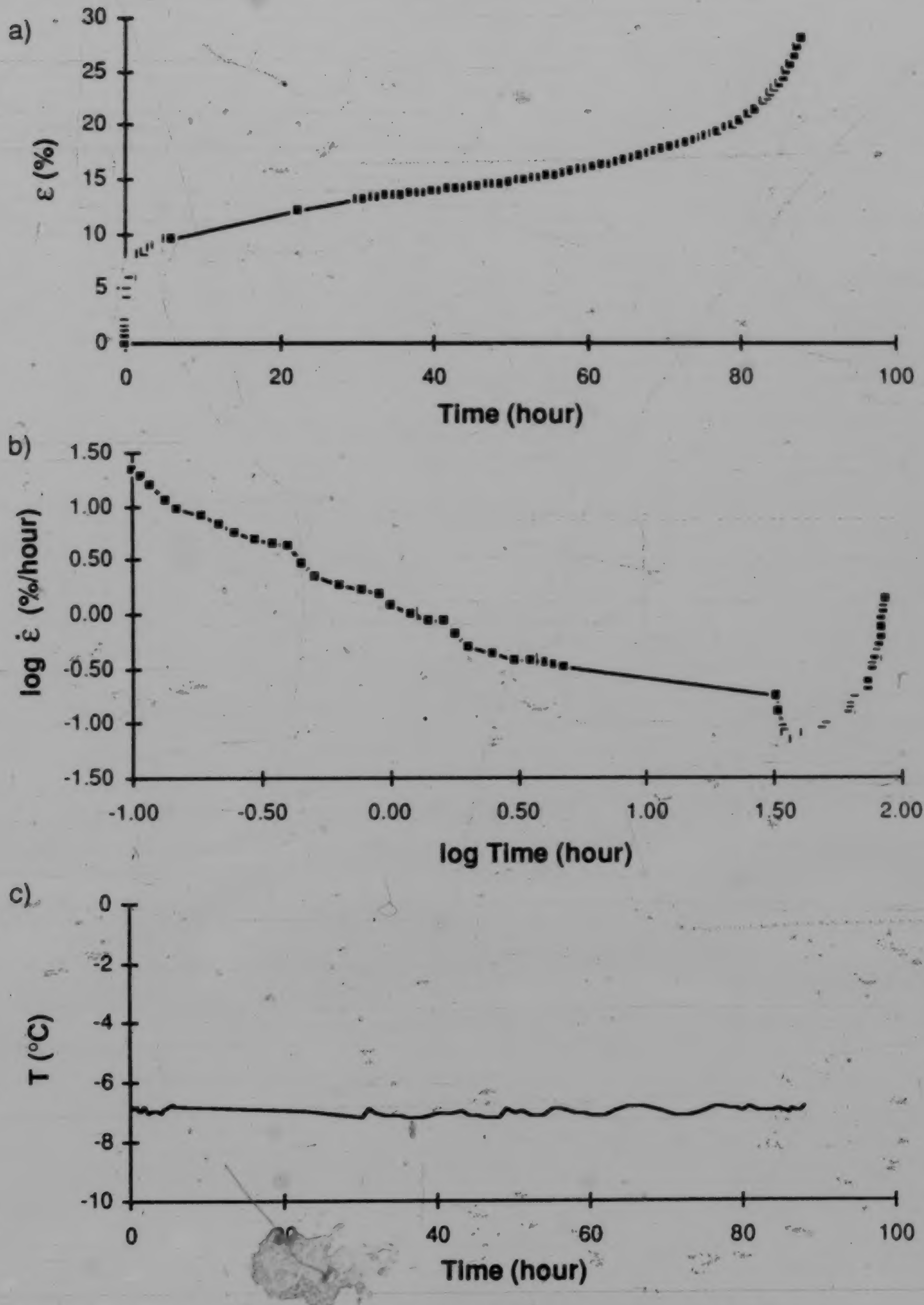

Figure C.35: Creep results test CR-89 soil C 5 ppt at σ=1672 kPa
a) strain vs time b) log strain rate vs log time
c) temperature vs time

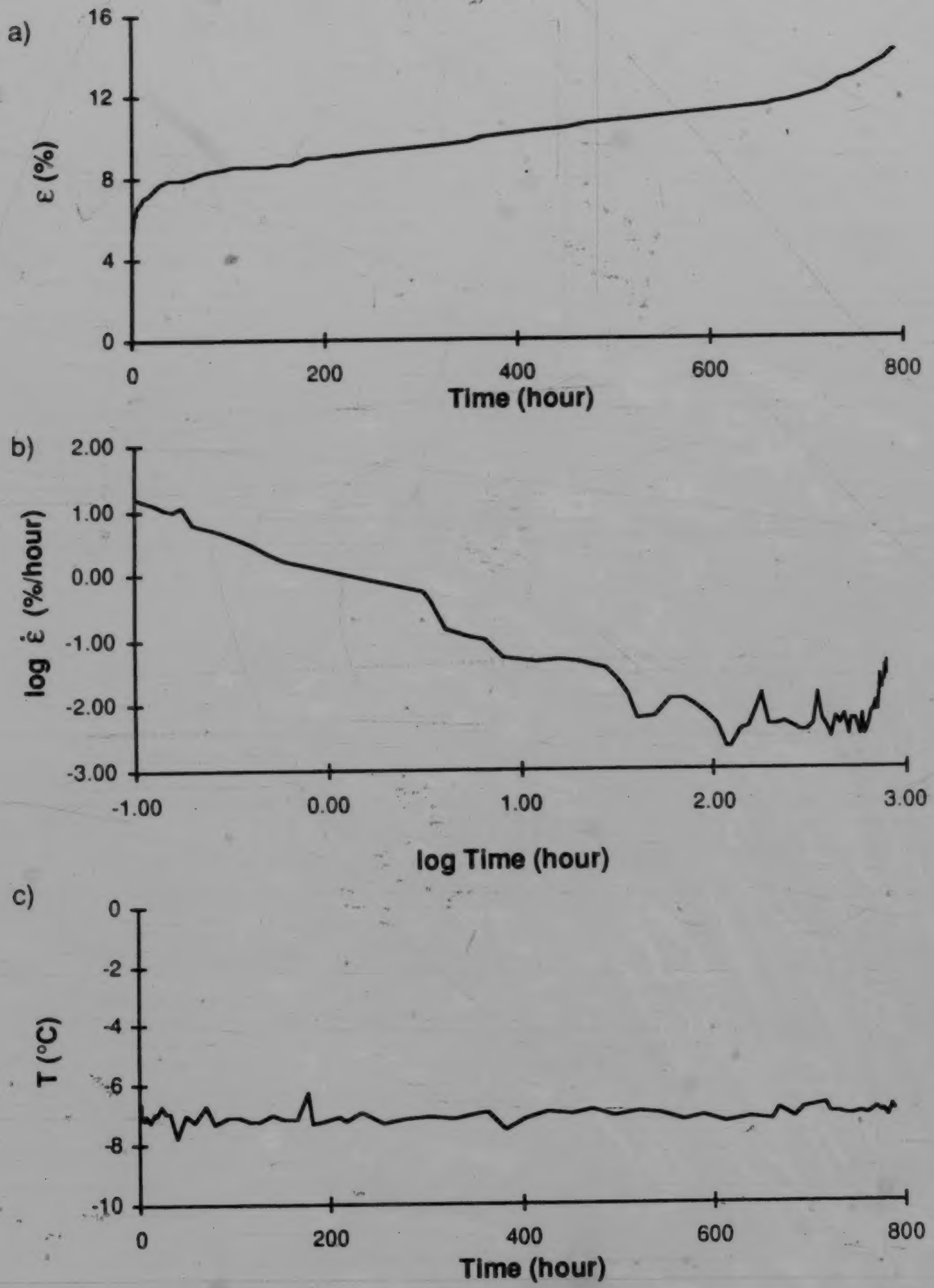

Figure C.36: Creep results test CR-94 soil C 5 ppt at σ=1504 kPa
a) strain vs time b) log strain rate vs log time
c) temperature vs time

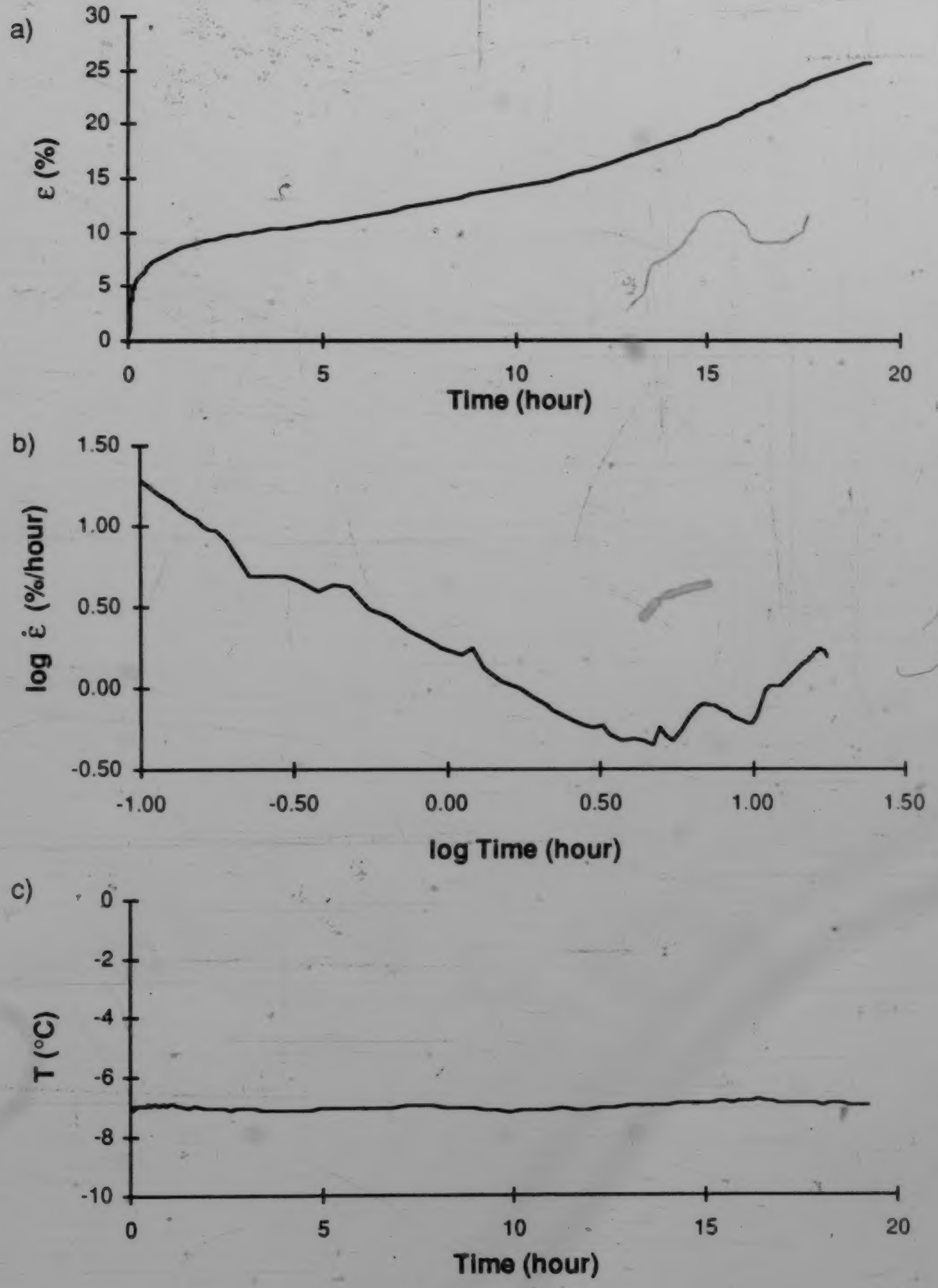

Figure C.37: Creep results test CR-55 soil C 10 ppt at σ=1372 kPa
a) strain vs time b) log strain rate vs log time
c) temperature vs time

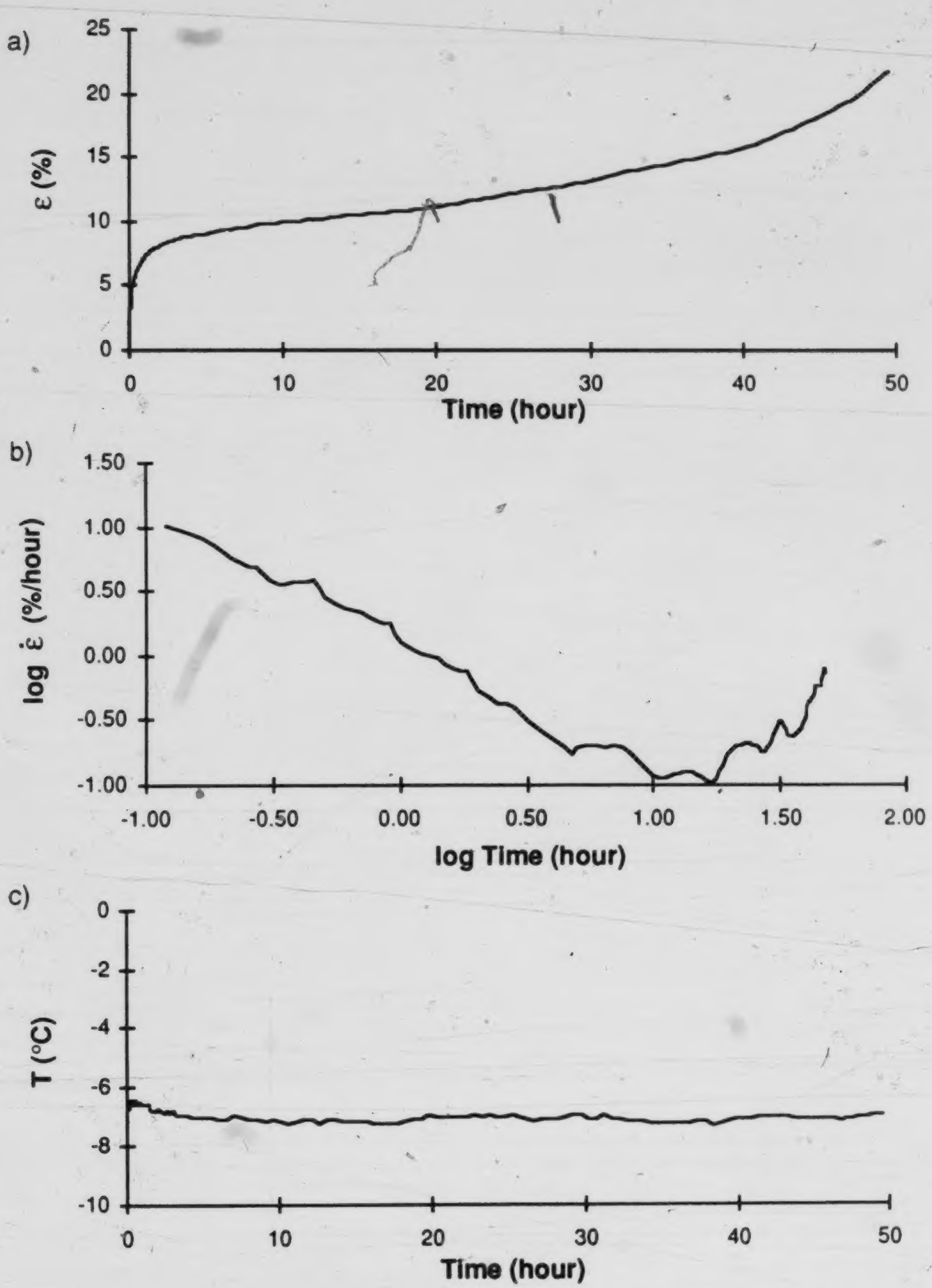

Figure C.38: Creep results test CR-52 soil C 10 ppt at σ=1235 kPa
a) strain vs time b) log strain rate vs log time
c) temperature vs time

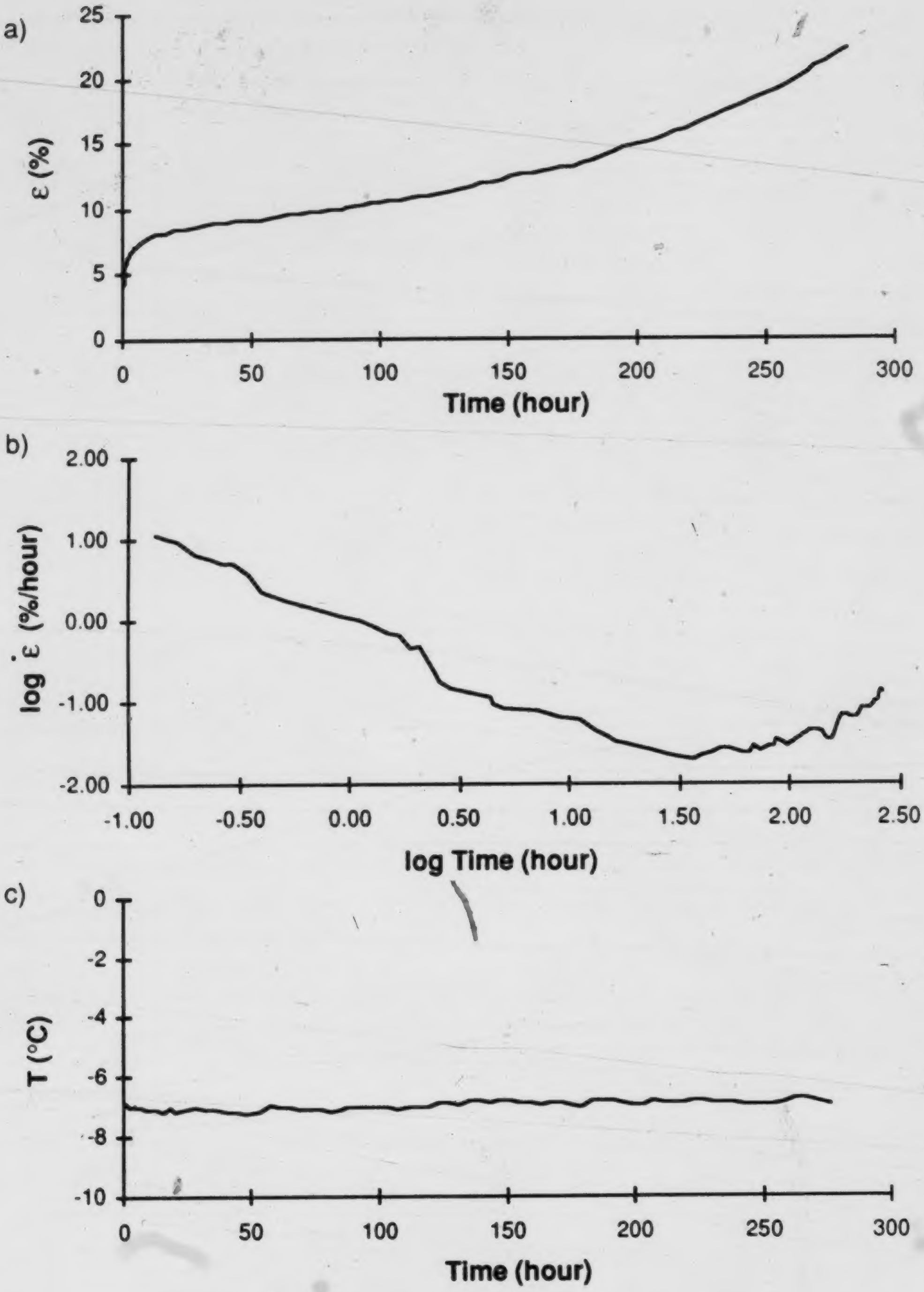

Figure C.39: Creep results test CR-68 soil C 10 ppt at σ=1098 kPa
a) strain vs time b) log strain rate vs log time
c) temperature vs time

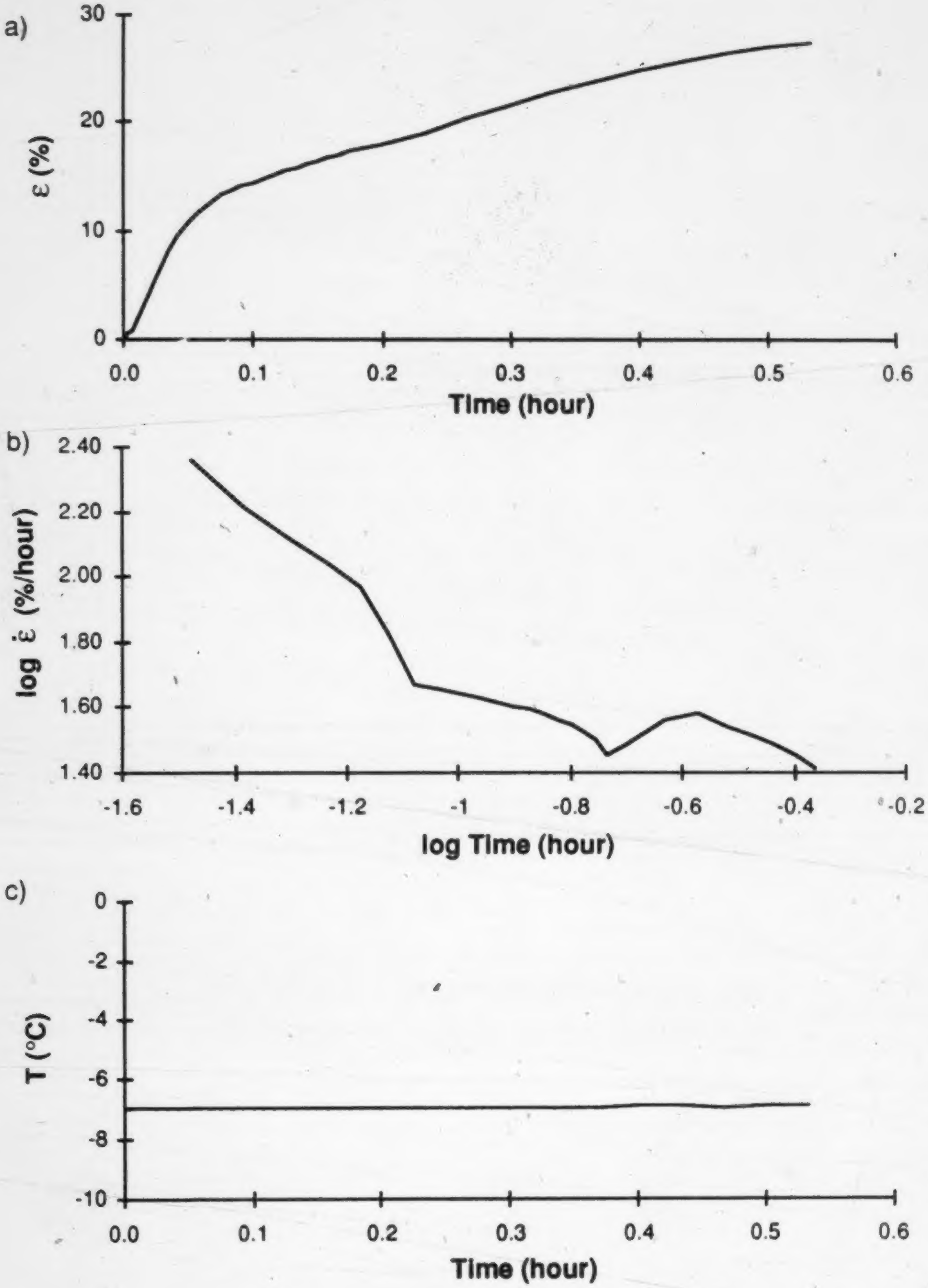

Figure C.40: Creep results test CR-76 soil C 30 ppt at σ=1222 kPa
a) strain vs time b) log strain rate vs log time
c) temperature vs time

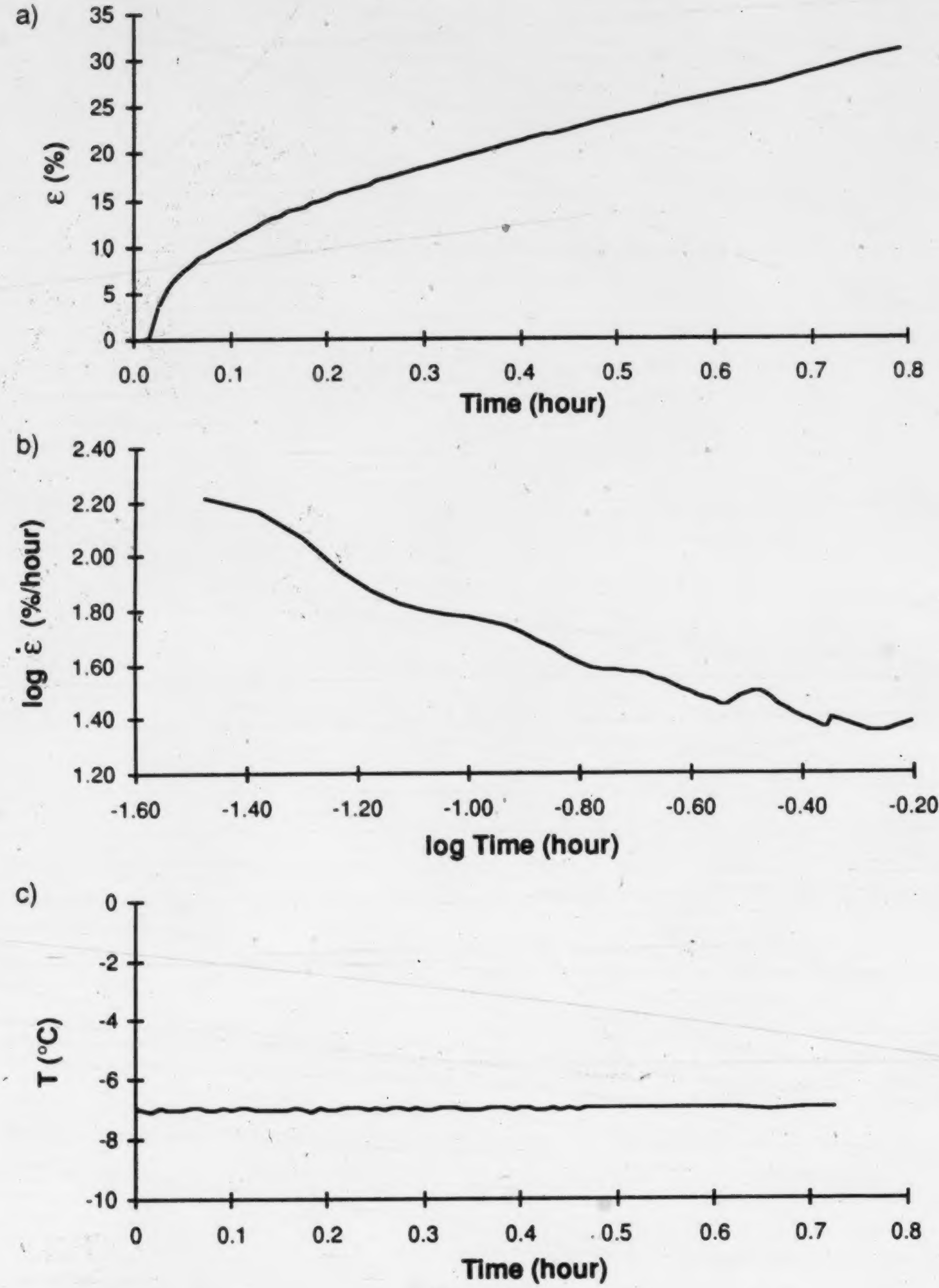

Figure C.41: Creep results test CR-78 soil C 30 ppt at σ=1008 kPa
a) strain vs time b) log strain rate vs log time
c) temperature vs time

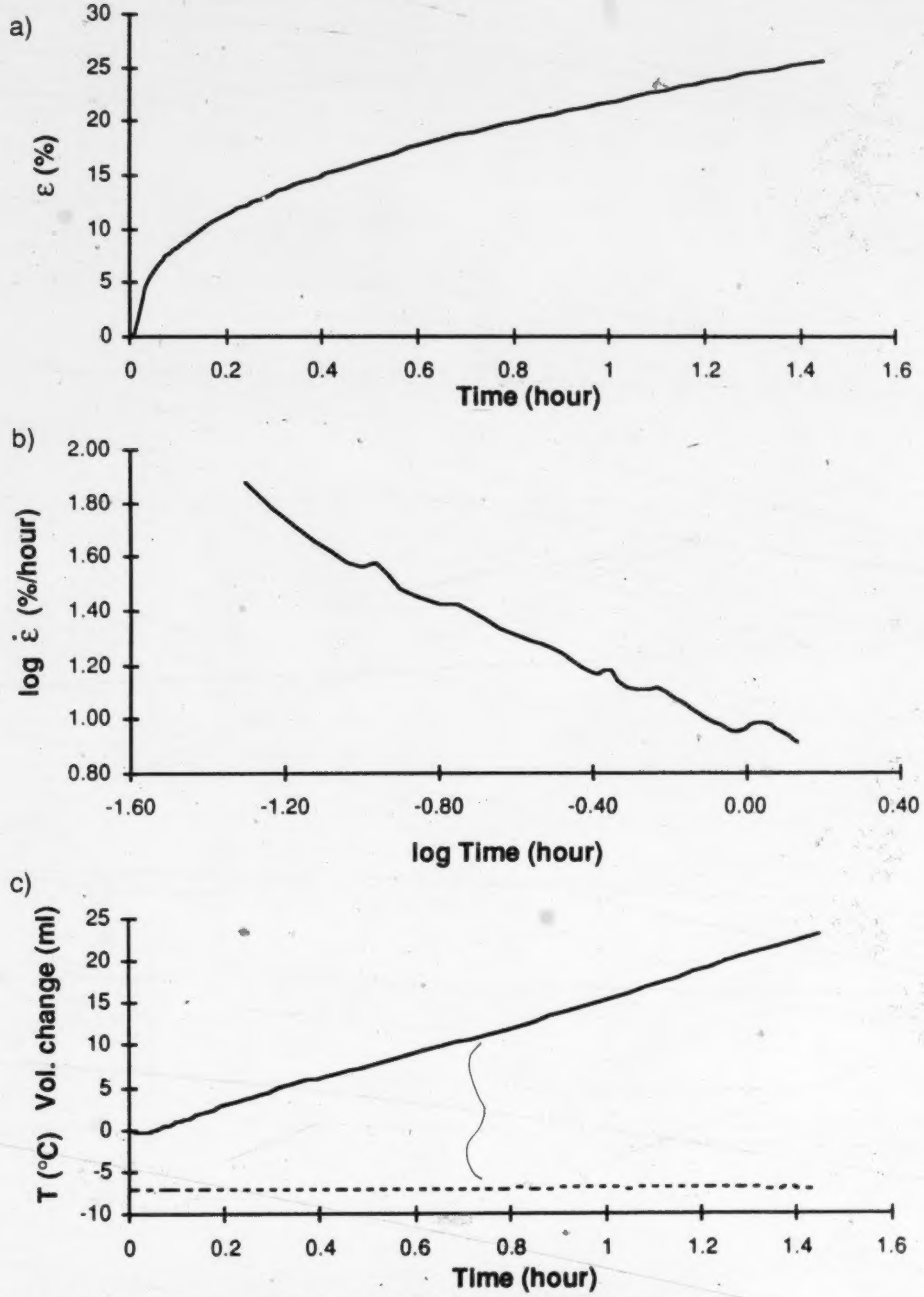

Figure C.42: Creep results test CR-91 soil C 30 ppt at σ=794 kPa
a) strain vs time b) log strain rate vs log time
c) volume change and temperature vs time

APPENDIX D

CONSTANT-STRESS TEST ANALYSIS

D.0. Introduction to examples of strain-time calculations

One example for each method of strain vs time prediction will be presented. The evaluation of the values of the slopes and intercepts were all done using a polynomial regression of degree 1 using the program Cricket Graph, © Cricket Software Inc. The predicted strains are always given in % and the times are in hours.

D.1. Example of calculation of Sayles' (1968) strain-time prediction

Referring to figure D.15, the value of M and -Mlog $\dot{\varepsilon}_{1\ \mathrm{hour}}$ for creep test CR-71, soil B 5 ppt, can be evaluated.

$M = 1.025$

$-M\log \dot{\varepsilon}_{1\ \mathrm{hour}} = -0.218$

The calculated value of $\dot{\varepsilon}_{1\ \mathrm{hour}}$ can now be estimated.

$\dot{\varepsilon}_{1\ \mathrm{hour}} = 1.63$ %/hour

The value of strain after 1 hour of testing was obtained from the measured strain vs time curve. The measured value of $\varepsilon_{1\ \mathrm{hour}}$ is 5.96%.

Knowing all these values, equation 3.57 b) can be applied to predict the strain vs time.

$$\varepsilon = 5.96 + 1.63\left(\frac{1.02}{1.02-1}\right)\left(t^{(1.02-1)/1.02} - 1\right)$$

The strain vs time relationship predicted from the above equation is shown in figure E.5 b).

D.2. Example of calculation of Vyalov et al.'s (1988) strain-time prediction

D.2.1. Soil A

Referring to figure D.8, the values of the slope and the intercept of the $\log\dot{\varepsilon}t^2$ vs $\log\varepsilon$ for creep test CR-86, soil A 10 ppt, can be evaluated.

Slope: $1+1/\alpha = 3.562$

Intercept: $\log(\alpha / a^{1/\alpha}) = -1.087$

The creep parameters α and a can then be calculated.

$\alpha = 0.39$ $\quad a = 1.84$

From figure C.8, the time to failure or time to minimum strain rate was estimated as being $t_f = 11.6$ hour. Using the above values of α, a and t_f, equation 3.55 a) can be used to calculate the strain vs time.

$$\varepsilon = 1.84\left(\frac{t}{1 - t/11.6}\right)^{0.39}$$

The strain vs time relationship predicted from the above equation is shown in figure E.3 a).

D.2.1. Soil B

This example shows how the prediction of Vyalov's equation was done for tests CR-71, soil B 0 ppt or CR-36, soil C 0 ppt. The results of test CR-71 will be used in the following example. The first prediction will be done using two values of α and a, since the plot of logεt^2 vs logε seem to follow a bilinear relationship. The second prediction will be done using an average value of α and a.

a) Bilinear approach

Referring to figure D.15 b), the values of the slopes and intercepts for the dotted lines in the logεt^2 vs logε can be evaluated.

Slope of 1st line: $1 + 1/\alpha_1 = 2.03$ Slope of 2nd line: $1 + 1/\alpha_2 = 7.25$

Intercept of 1st line: $\log (\alpha_1 / a_1^{1/\alpha_1}) = -1.45$

Intercept of 2nd line: $\log (\alpha_2 / a_2^{1/\alpha_2}) = -3.82$

The values of α_1, α_2, a_1 and a_2 can now be calculated.

$\alpha_1 = 0.97$ $a_1 = 24.3$

$\alpha_2 = 0.16$ $a_2 = 6.36$

The first line predict the behaviour up to a measured strain of approximately 7.5% which corresponds to a time of 2.5 hours in the measured strain vs time curve. Therefore the values of α_1 and a_1 will be used up to a time of t=2.5 hr and thereafter the values of α_2 and a_2 will be used. The value of the time to failure was estimated from figure C.15 and is equal to $t_f = 20$ hours.

$$\text{For } t = 0 \text{ to } 2.5\text{ hr} \qquad \varepsilon = 24.3\left(\frac{t}{1 - t/20.0}\right)^{0.97}$$

The predicted strain after 2.5 hours is 67.3%. Therefore, the strain for times greater than 2.5 hours is given by the following equation;

$$\text{For } t > 2.5\text{ hr} \qquad \varepsilon = 67.3 + 6.4\left(\frac{t}{1 - t/20.0}\right)^{0.16}$$

The predicted strain vs time relationship obtained from this equation is shown in figure 6.37.

b) Linear approach

A linear regression was done through all the points on figure D.15 b). The correlation is very poor. The values of slope and intercept for the line are;

Slope: $1 + 1/\alpha = 4.02$

Intercept: $\log(\alpha / a^{1/\alpha}) = -2.77$

Therefore, the values of α and a can be calculated;

$\alpha = 0.33$ $a = 5.75$

The time to failure is the same as for part a), ie $t_f = 20.0$ hours.

The strain vs time can be predicted using the following equation;

$$\varepsilon = 5.75\left(\frac{t}{1 - t / 20.0}\right)^{0.33}$$

The predicted strain vs time relationship is shown in figure 6.37.

D.3. Example of calculation of Gardener et al.'s (1984) strain-time prediction

The minimum strain rate, time to failure (or minimum strain rate) and strain to minimum strain rate are all required to use Gardener's equation. These parameters can be evaluated using the results from the measured constant stress tests shown in Appendix C. For test CR-71, the values of these parameters are;

$\dot{\varepsilon}_m = 0.104\%/\text{hour}$

$t_m = 20.0$ hours

$\varepsilon_m = 10.9\%$

Moreover, the value of the instantaneous strain, ε_o, is required for this method. As explained in section 6.3.2., the instantaneous strain was obtained by taking the measured strain after 120 seconds of stress application minus the strain measured after 30 seconds of stress application. For test CR-71, the instantaneous strain, ε_o, was 0.73%.

Using the above values, the creep parameter c can be evaluated using equation 3.43;

$$c = \left(\frac{0.104 \times 20.0}{10.9 - 0.73}\right)^2$$

Equation 3.42 gives the creep strain as a function of time. To obtain the total strain, the value of the instantaneous strain has to be added to the creep strain. The total strain using Gardener's equation is then given by;

$$\varepsilon = 0.73 + (10.9 - 0.73)\left(\frac{t}{20.0}\right)^c \exp\left[(c^{1/2} - c)\left(\frac{t}{20.0} - 1\right)\right]$$

The strain vs time prediction using the above equation is shown in figure E.5 b).

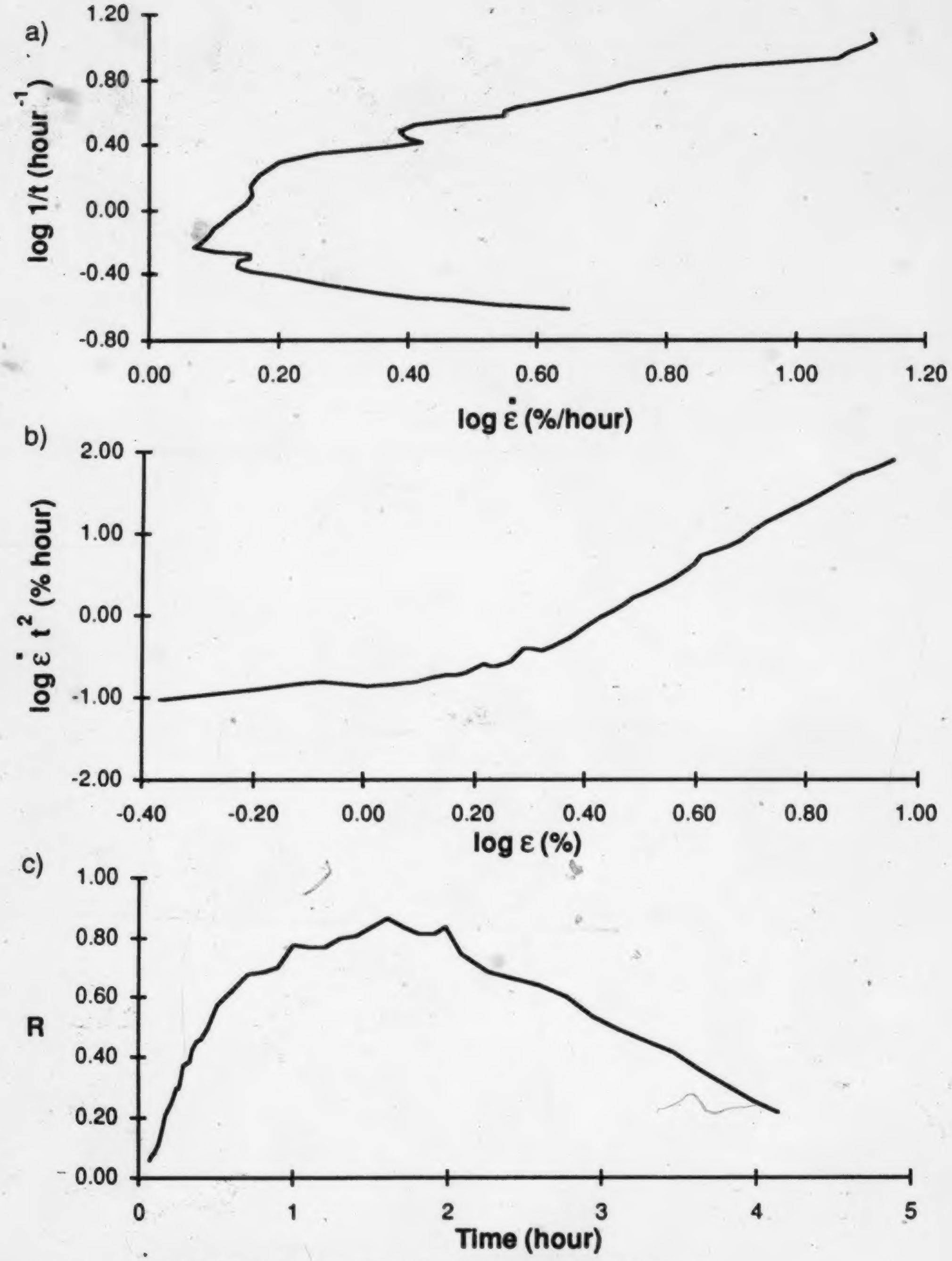

Figure D.1: Creep test CR-45 soil A 0 ppt at σ=4581 kPa
a) log 1/t vs log strain rate (Sayles, 1968)
b) log strain rate time^2 vs log strain (Vyalov, 1988)
c) R = dε / dt vs time (Berggren and Furuberg, 1985)

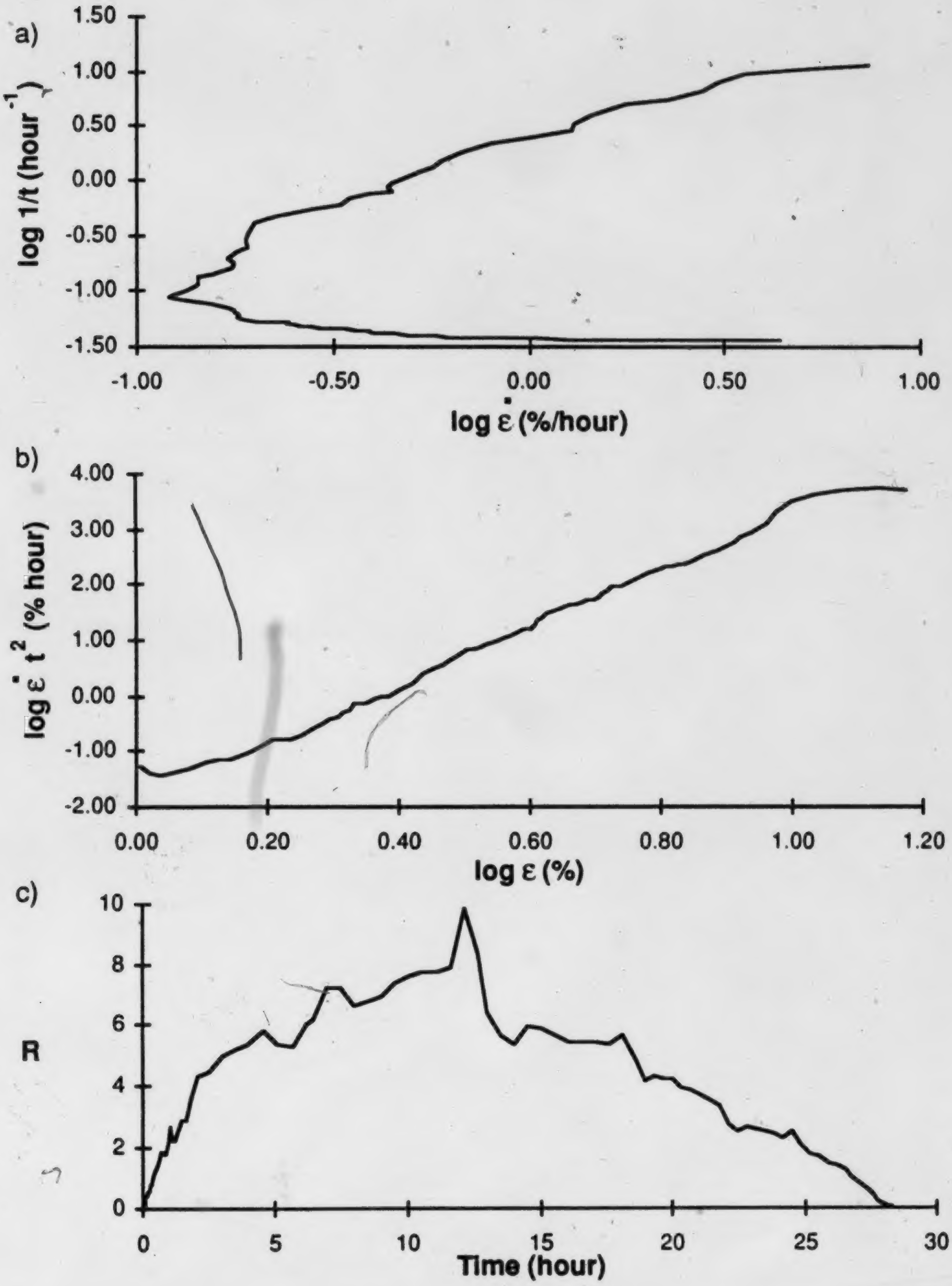

Figure D.2: Creep test CR-92 soil A 0 ppt at σ=3927 kPa
a) log 1/t vs log strain rate (Sayles, 1968)
b) log strain rate time^2 vs log strain (Vyalov, 1988)
c) R = dε / dt vs time (Berggren and Furuberg, 1985)

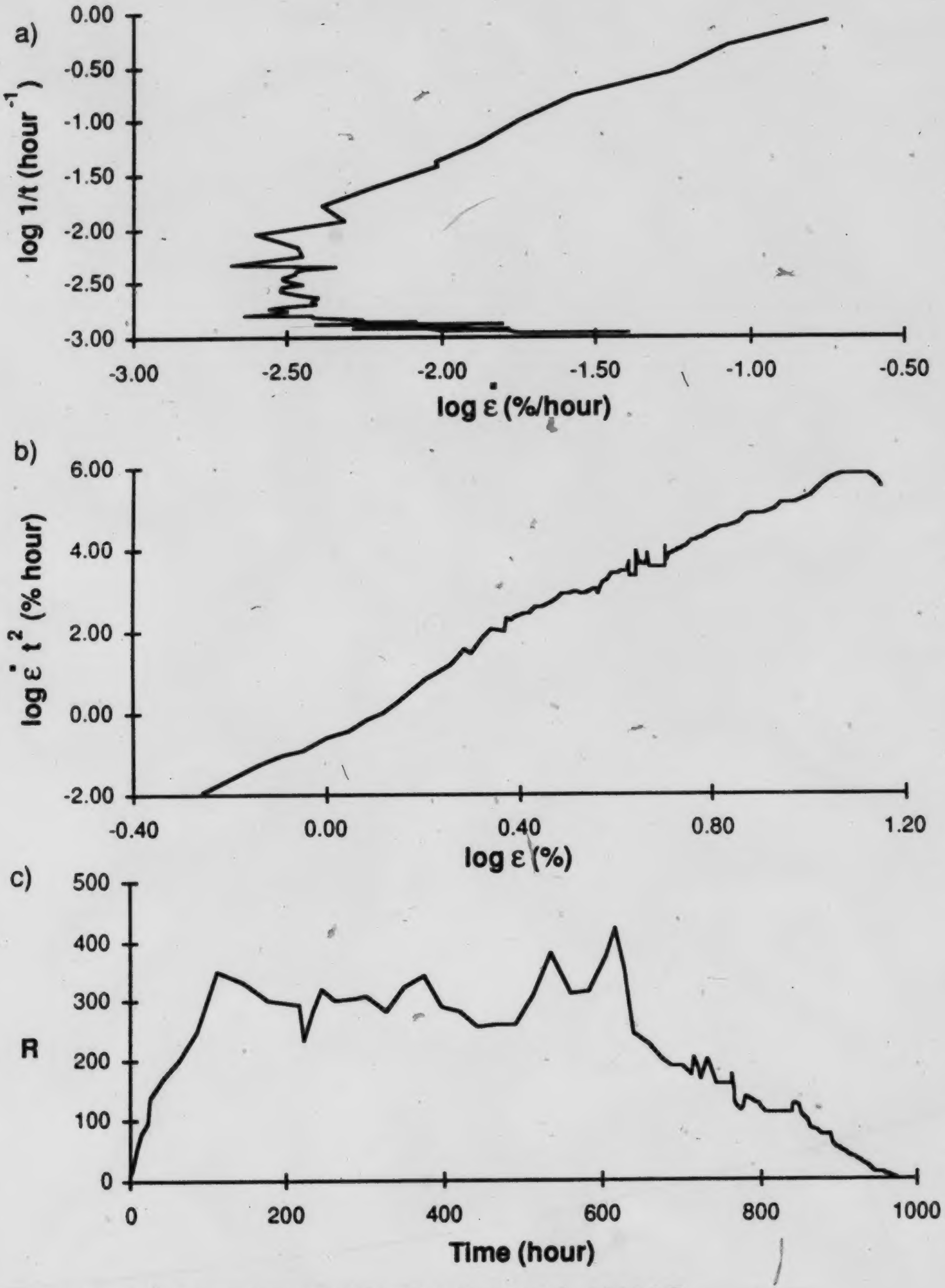

Figure D.3: Creep test CR-95 soil A 0 ppt at σ=2826 kPa
a) log 1/t vs log strain rate (Sayles, 1968)
b) log strain rate time^2 vs log strain (Vyalov, 1988)
c) R = dε / dt vs time (Berggren and Furuberg, 1985)

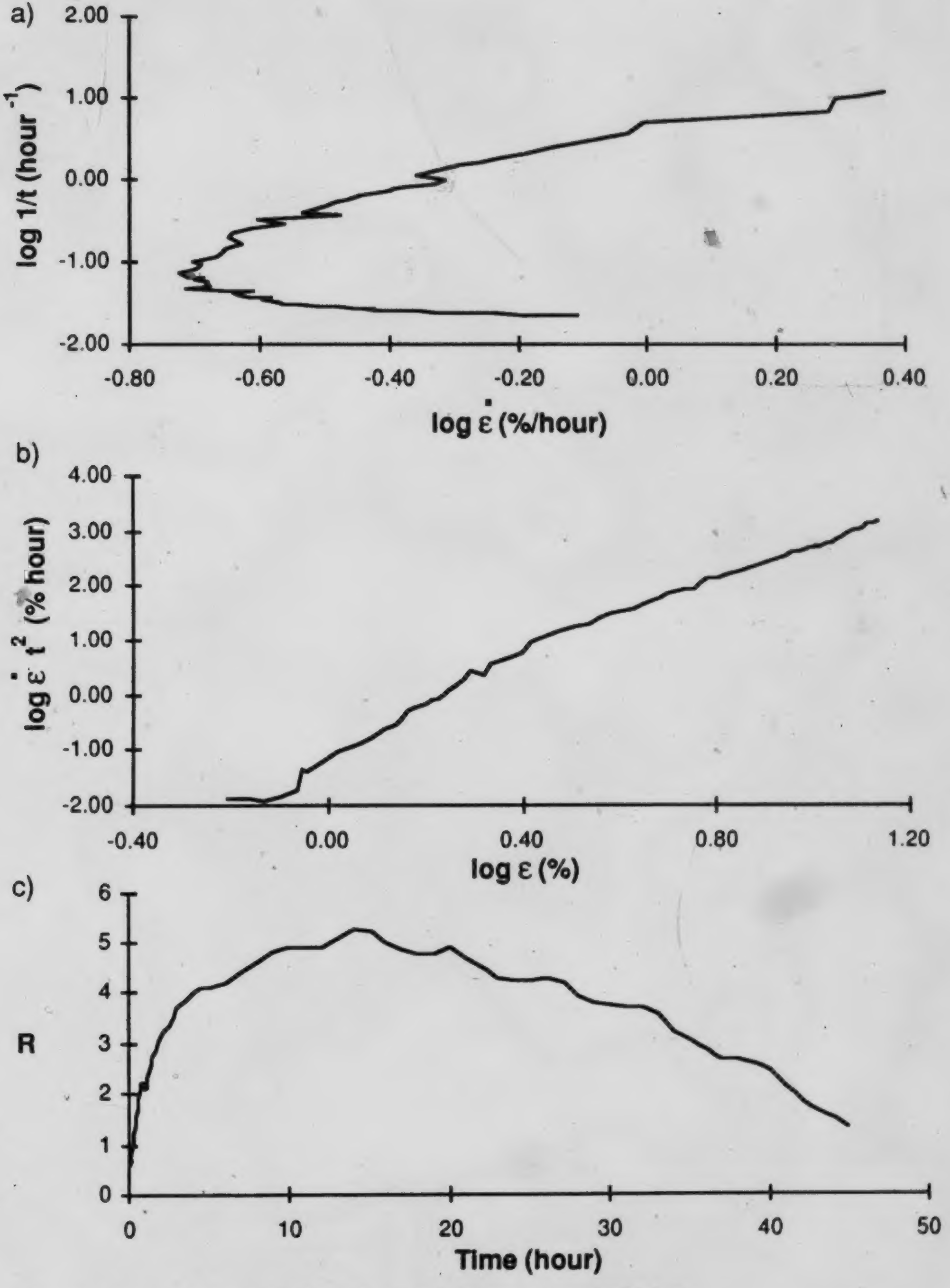

Figure D.4: Creep test CR-59 soil A 5 ppt at σ=1026 kPa
a) log 1/t vs log strain rate (Sayles, 1968)
b) log strain rate time^2 vs log strain (Vyalov, 1988)
c) R = dε / dt vs time (Berggren and Furuberg, 1985)

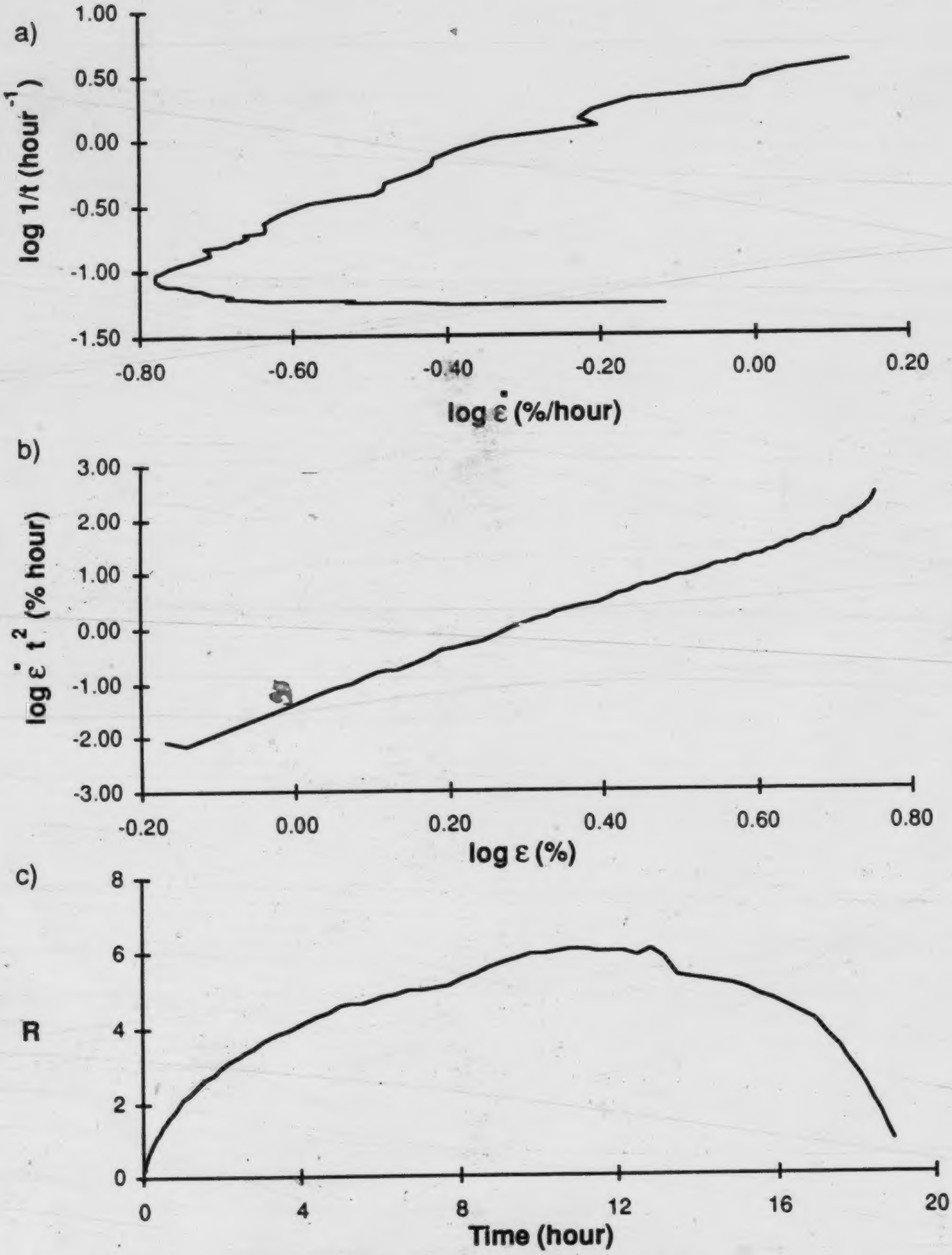

Figure D.5: Creep test CR-51 soil A 5 ppt at σ=1026 kPa
a) log 1/t vs log strain rate (Sayles, 1968)
b) log strain rate time^2 vs log strain (Vyalov, 1988)
c) R = dε / dt vs time (Berggren and Furuberg, 1985)

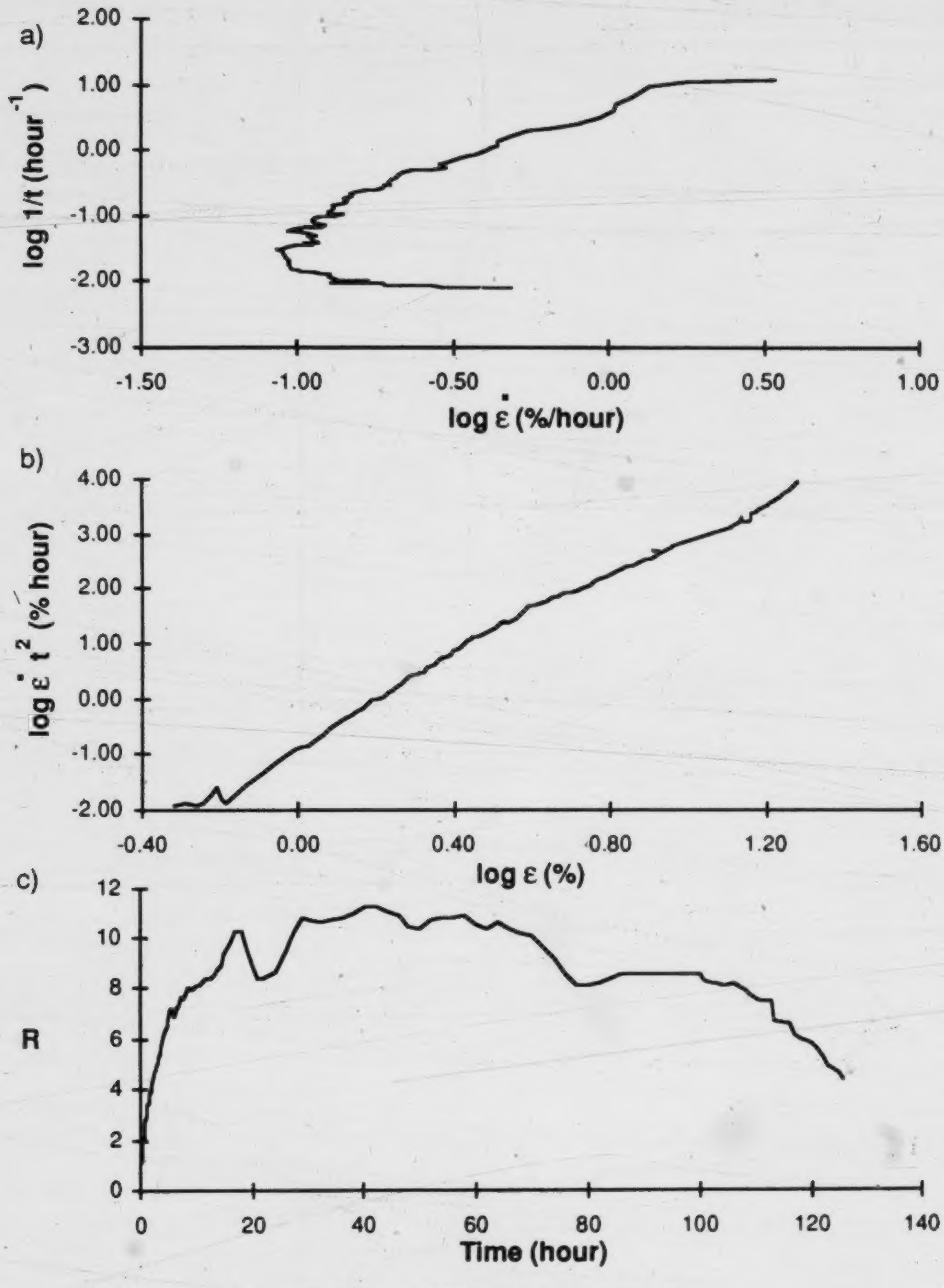

Figure D.6: Creep test CR-60 soil A 5 ppt at σ=855 kPa
a) log 1/t vs log strain rate (Sayles, 1968)
b) log strain rate time^2 vs log strain (Vyalov, 1988)
c) R = dε / dt vs time (Berggren and Furuberg, 1985)

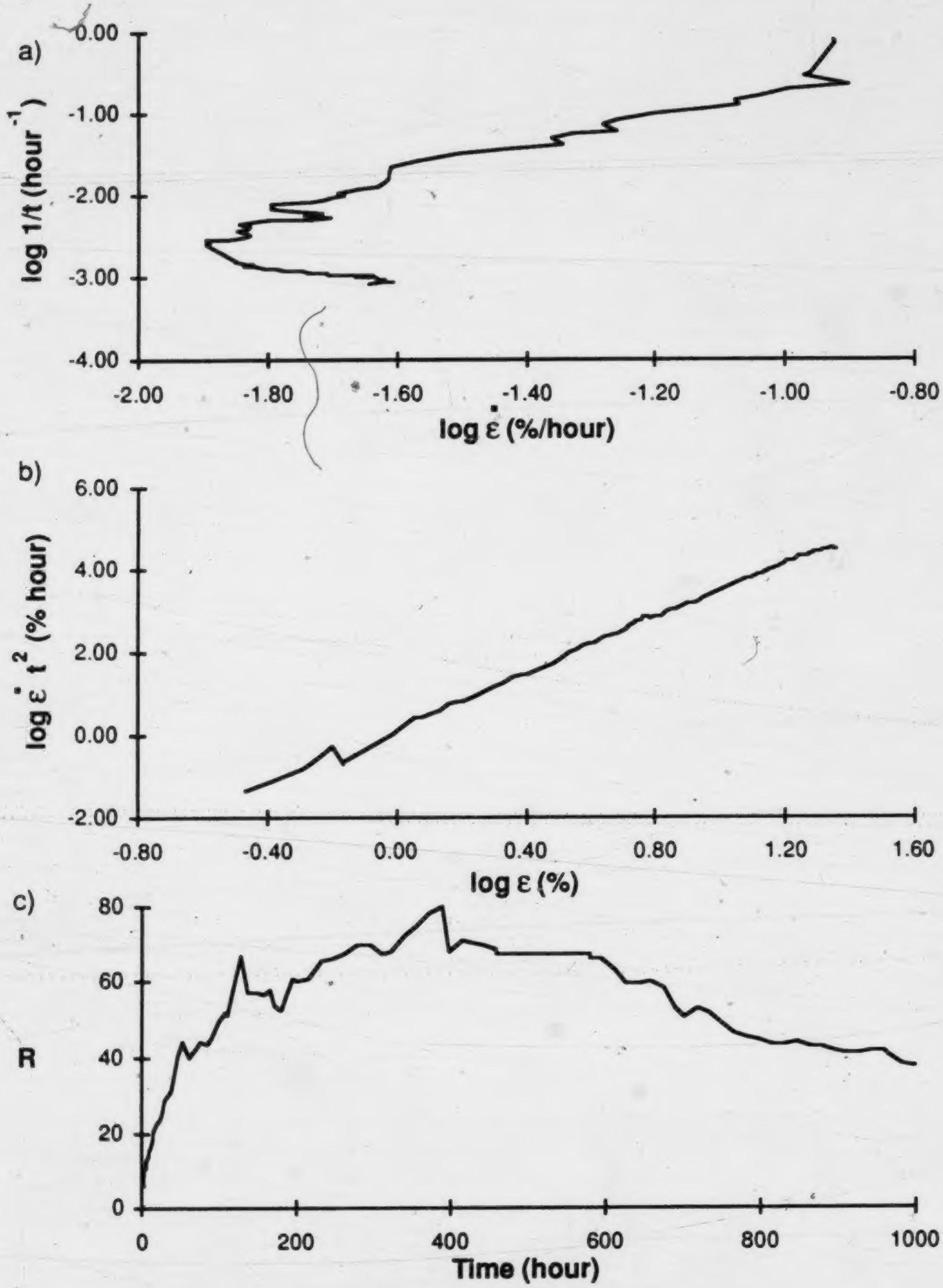

Figure D.7: Creep test CR-67 soil A 5 ppt at σ=570 kPa
a) log 1/t vs log strain rate (Sayles, 1968)
b) log strain rate time^2 vs log strain (Vyalov, 1988)
c) R = dε / dt vs time (Berggren and Furuberg, 1985)

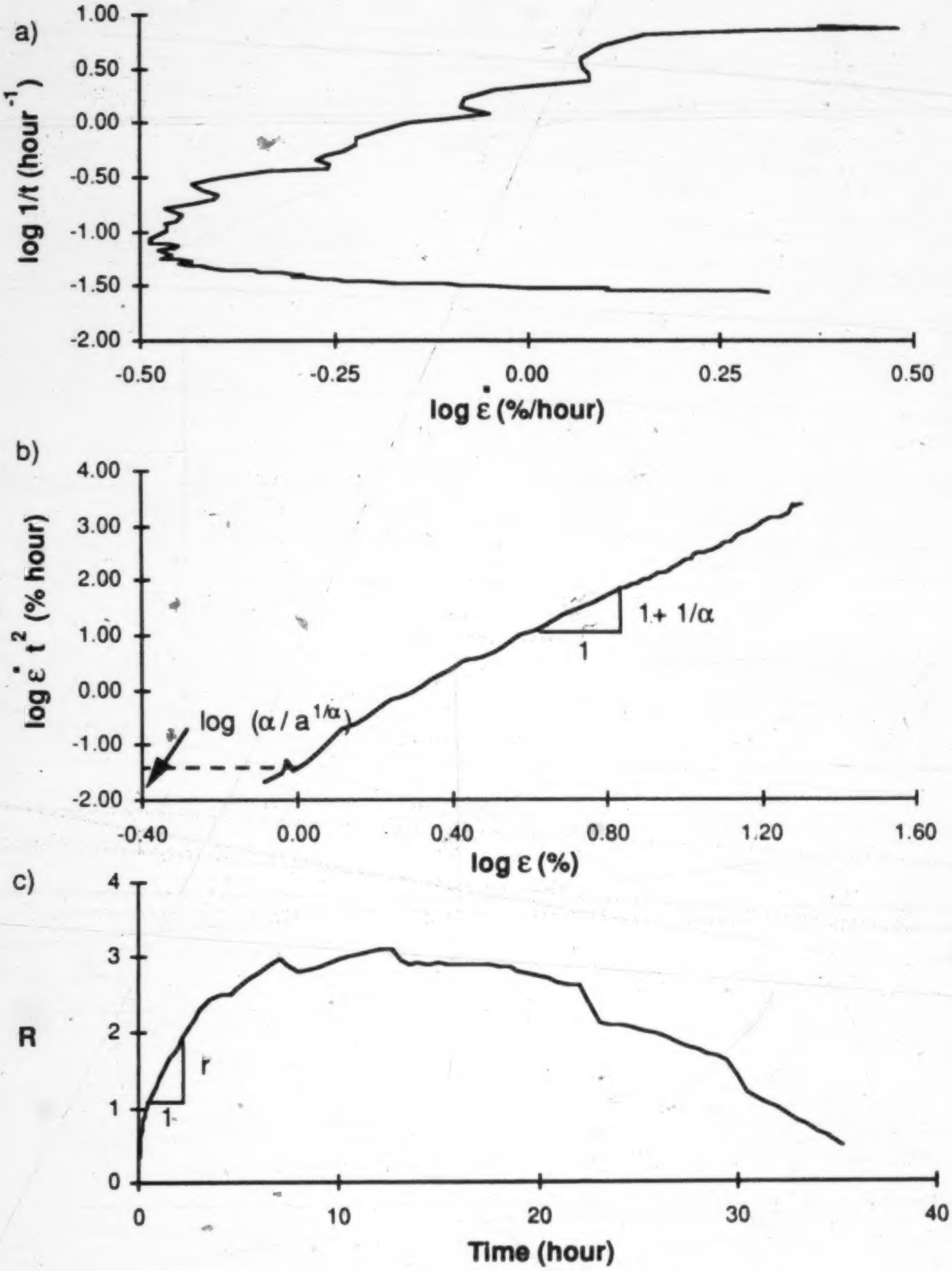

Figure D.8: Creep test CR-86 soil A 10 ppt at σ=887 kPa
a) log 1/t vs log strain rate (Sayles, 1968)
b) log strain rate time^2 vs log strain (Vyalov, 1988)
c) R = dε / dt vs time (Berggren and Furuberg, 1985)

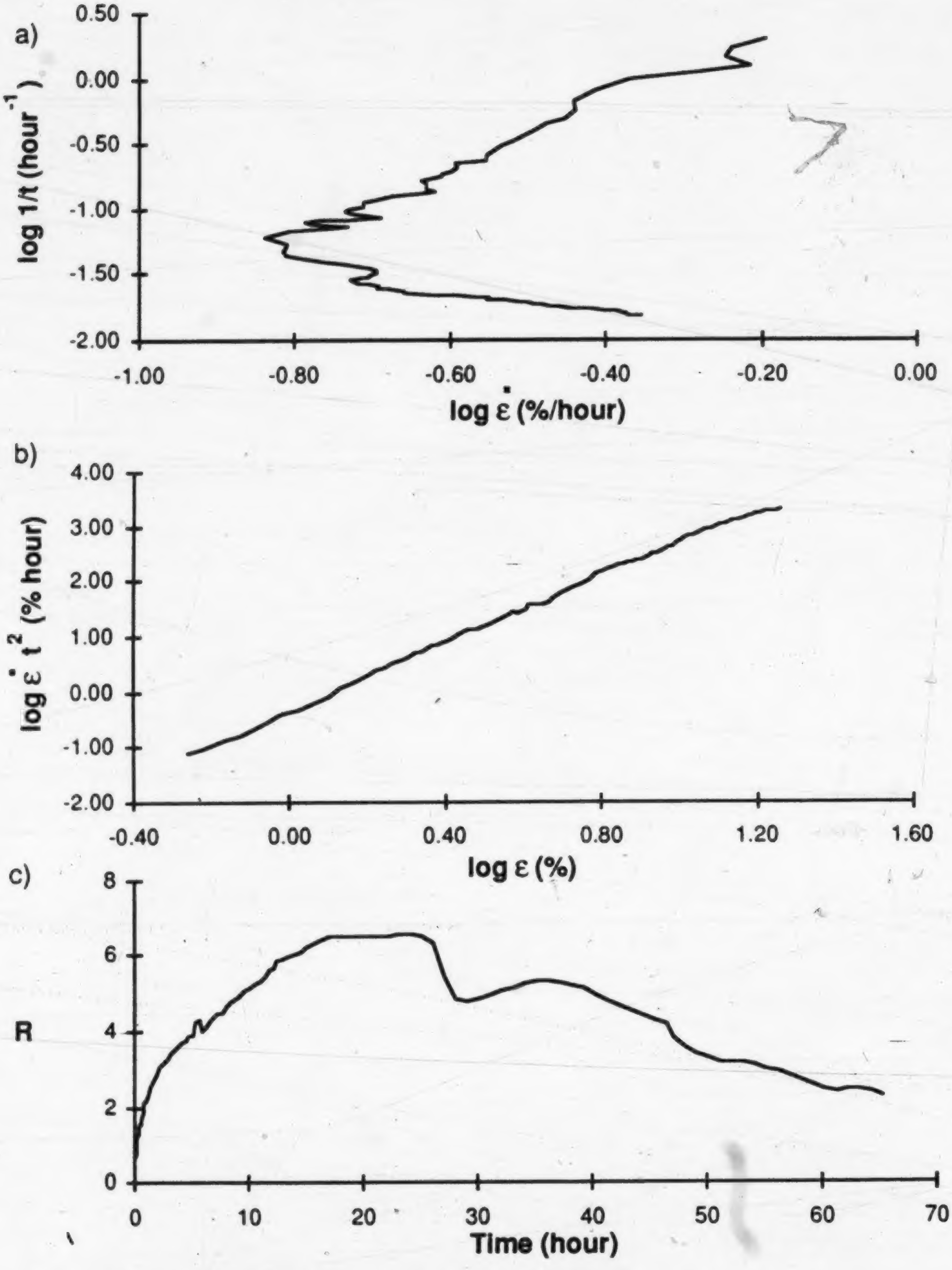

Figure D.9: Creep test CR-47 soil A 10 ppt at σ=761 kPa
a) log 1/t vs log strain rate (Sayles, 1968)
b) log strain rate time^2 vs log strain (Vyalov, 1988)
c) R = dε / dt vs time (Berggren and Furuberg, 1985)

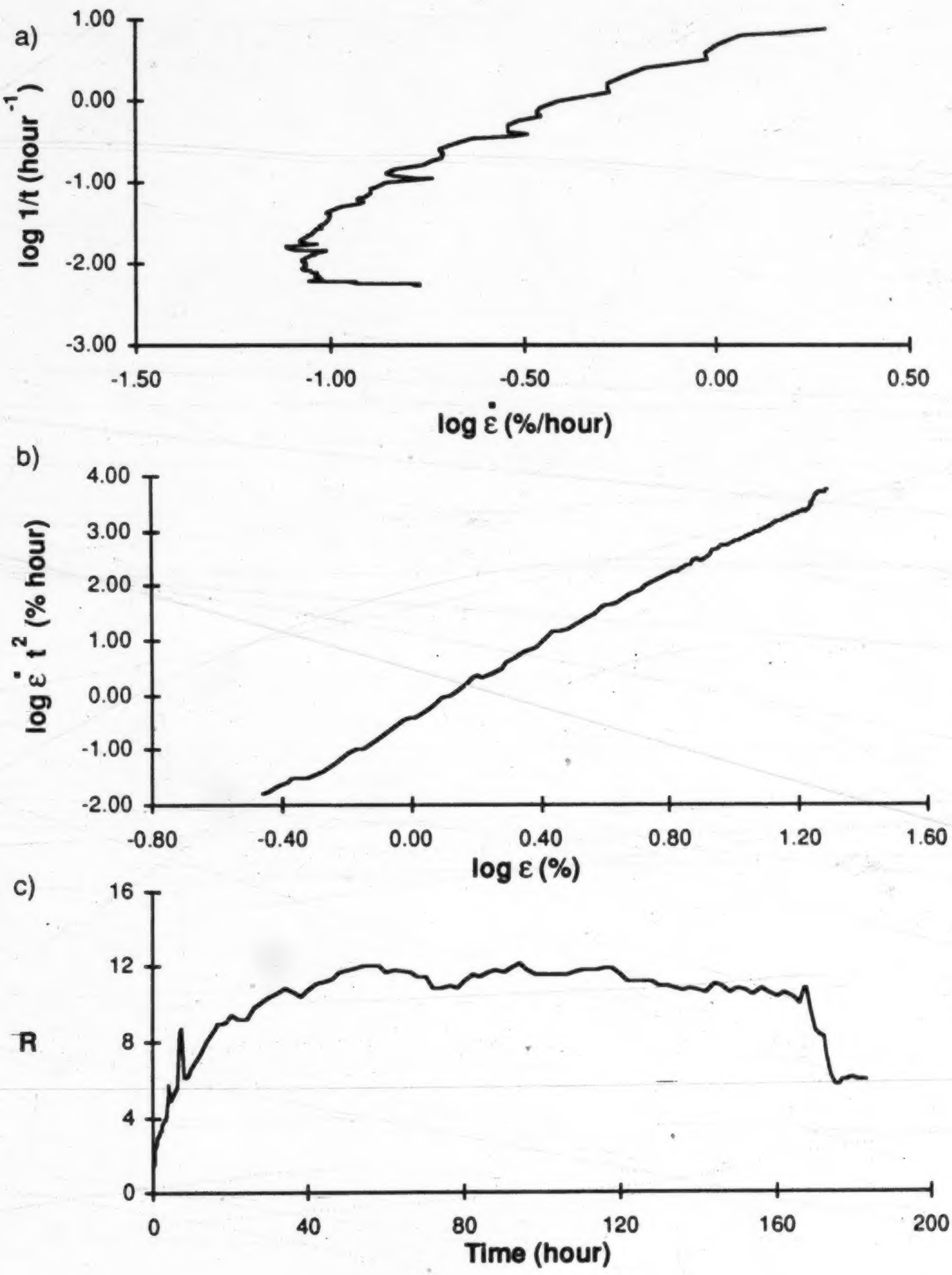

Figure D.10: Creep test CR-87 soil A 10 ppt at σ=634 kPa
a) log 1/t vs log strain rate (Sayles, 1968)
b) log strain rate time^2 vs log strain (Vyalov, 1988)
c) R = dε / dt vs time (Berggren and Furuberg, 1985)

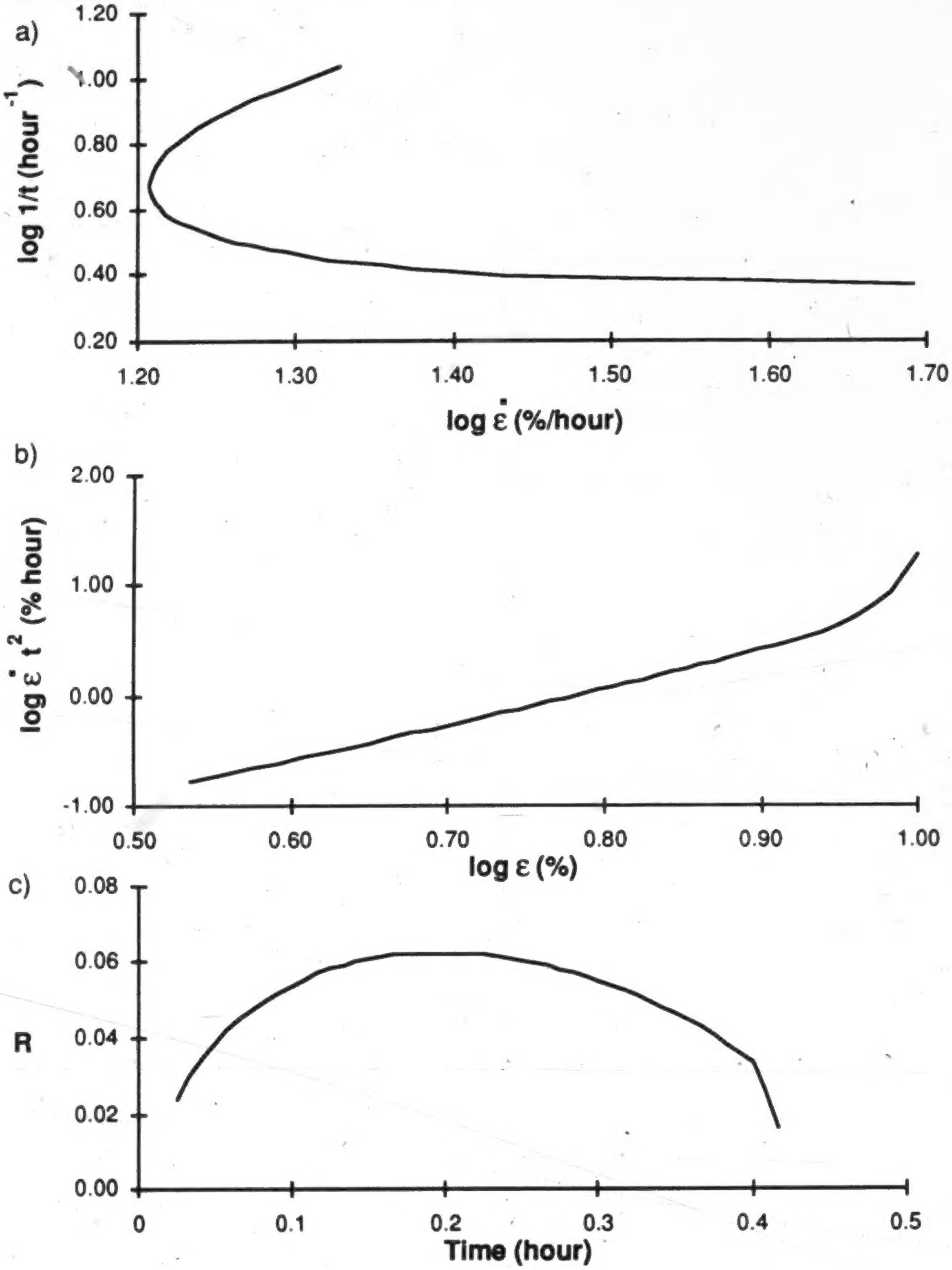

Figure D.11: Creep test CR-64 soil A 30 ppt at σ=888 kPa
a) log 1/t vs log strain rate (Sayles, 1968)
b) log strain rate time^2 vs log strain (Vyalov, 1988)
c) R = dε / dt vs time (Berggren and Furuberg, 1985)

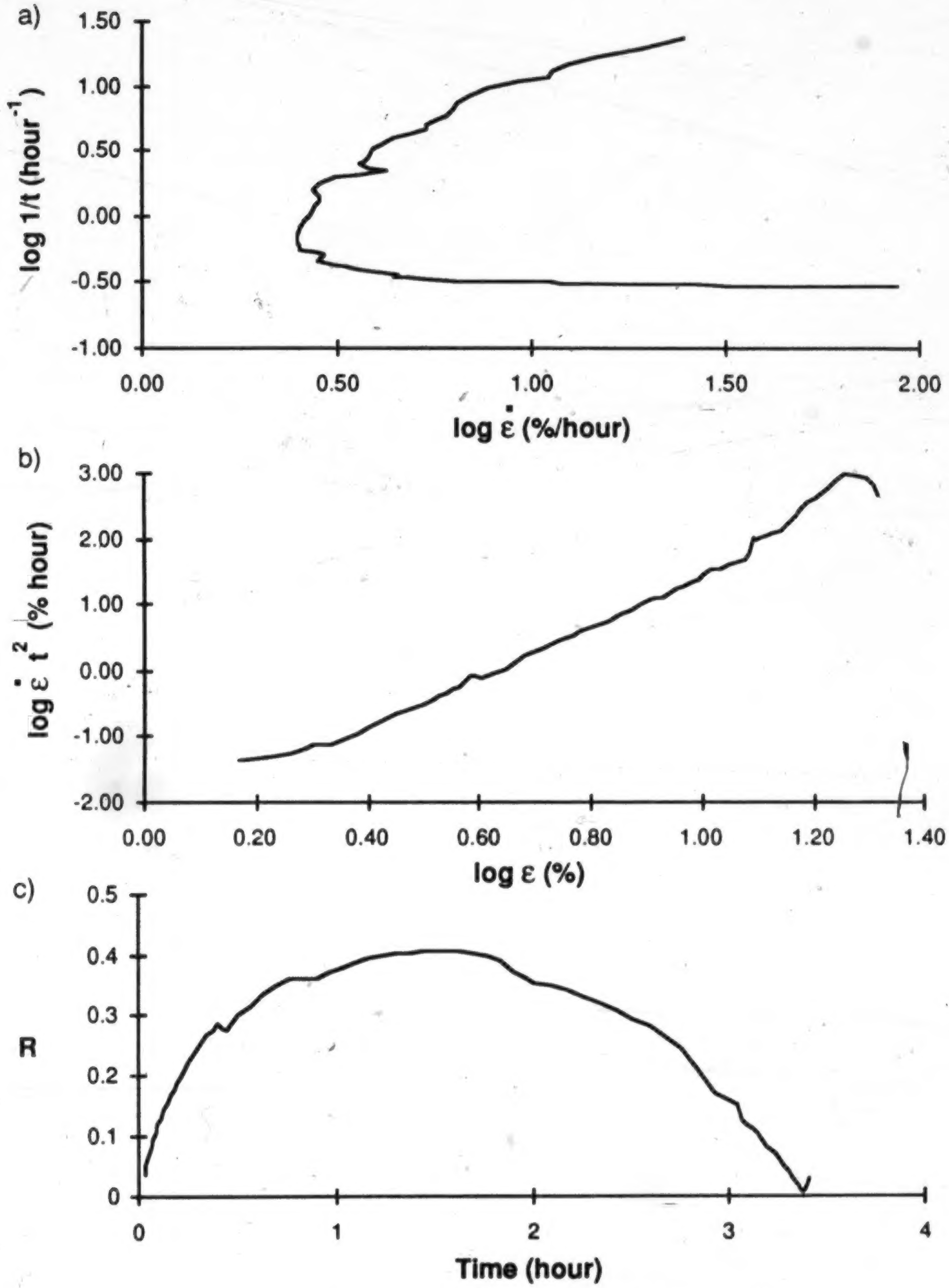

Figure D:12: Creep test CR-70 soil A 0 ppt at σ=666 kPa
a) log 1/t vs log strain rate (Sayles, 1968)
b) log strain rate time^2 vs log strain (Vyalov, 1988)
c) R = dε / dt vs time (Berggren and Furuberg, 1985)

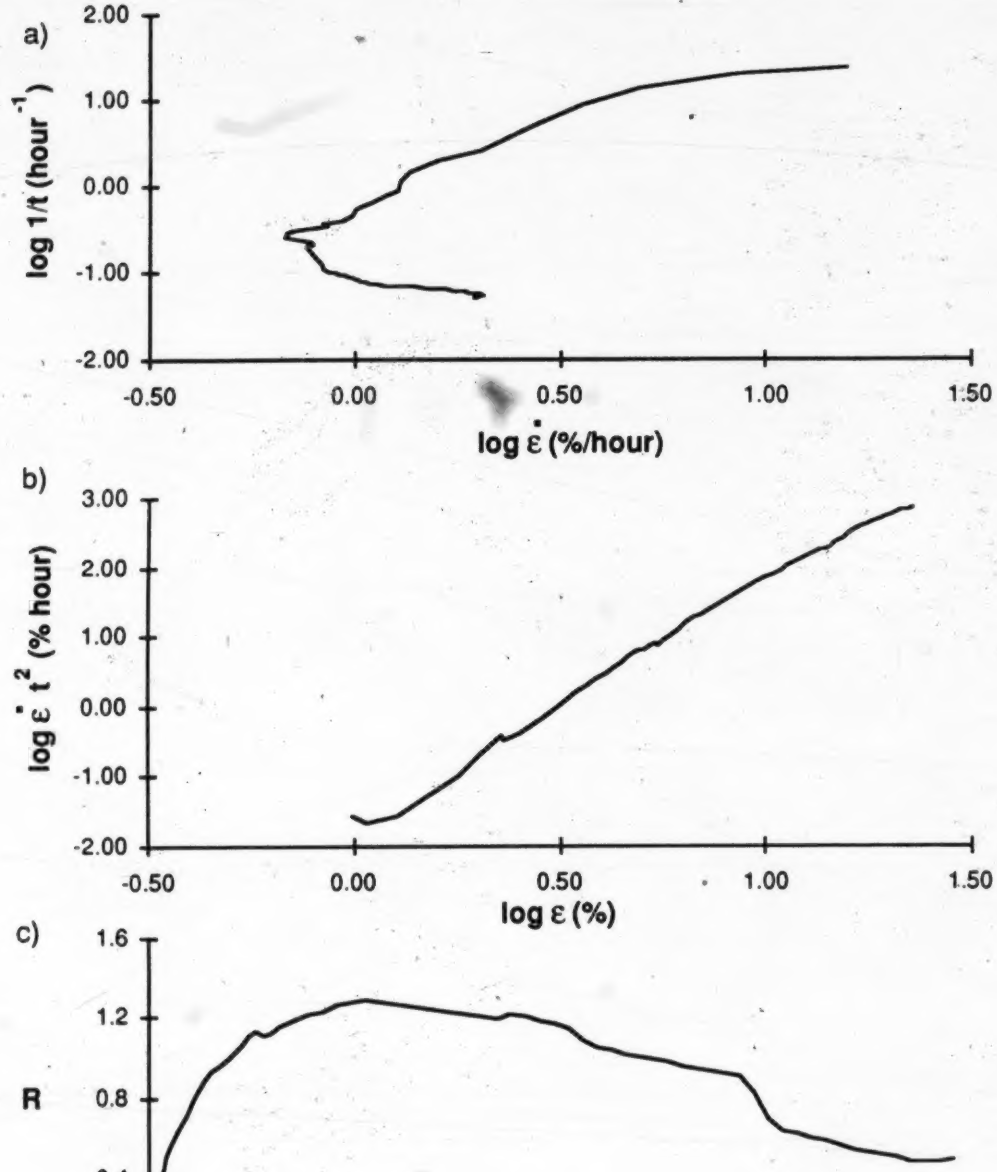

Figure D.13: Creep test CR-72 soil A 30 ppt at σ=555 kPa
a) log 1/t vs log strain rate (Sayles, 1968)
b) log strain rate time^2 vs log strain (Vyalov, 1988)
c) R = dε / dt vs time (Berggren and Furuberg, 1985)

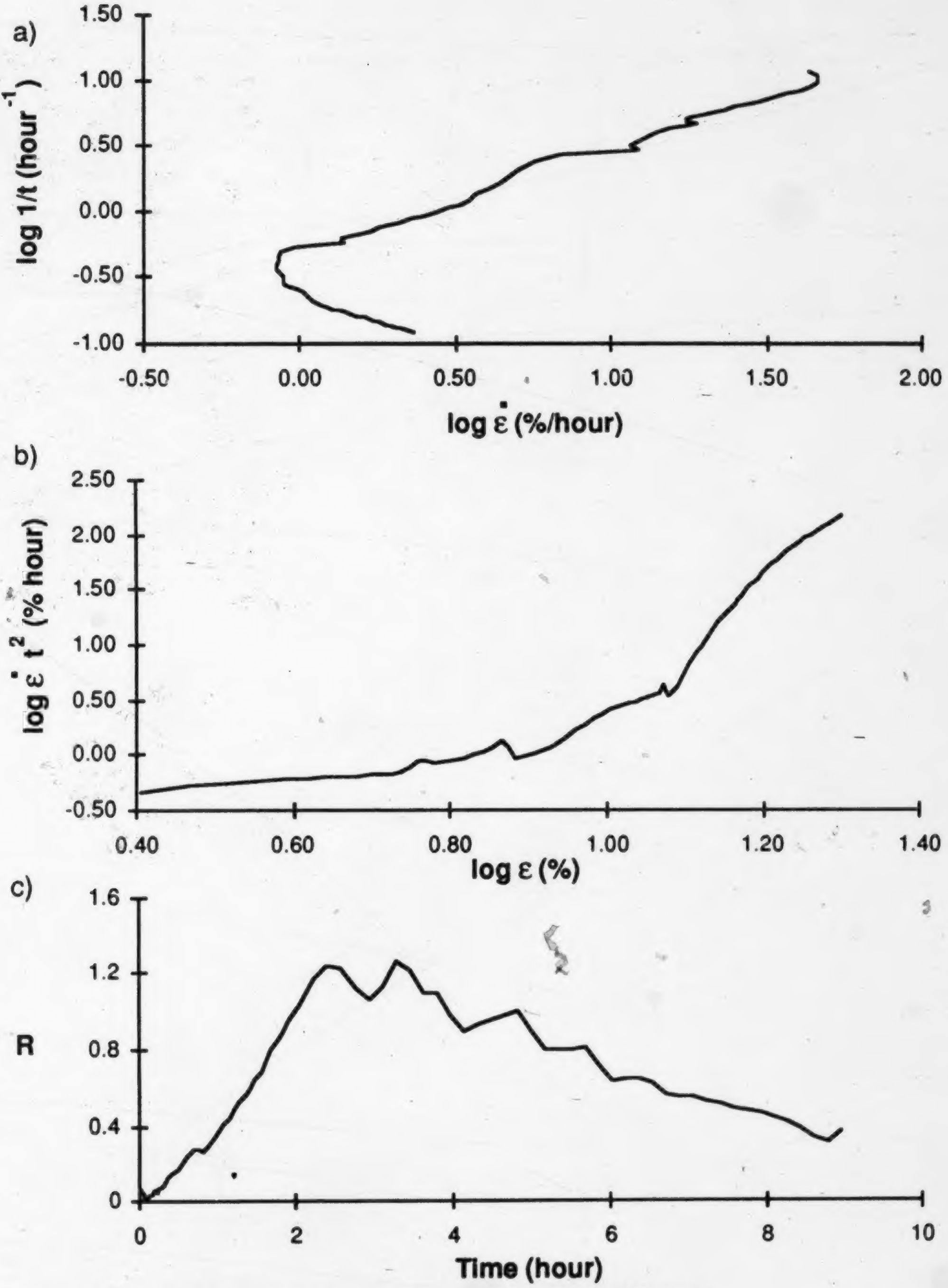

Figure D.14: Creep test CR-83 soil B 0 ppt at σ=2825 kPa
a) log 1/t vs log strain rate (Sayles, 1968)
b) log strain rate time^2 vs log strain (Vyalov, 1988)
c) R = dε / dt vs time (Berggren and Furuberg, 1985)

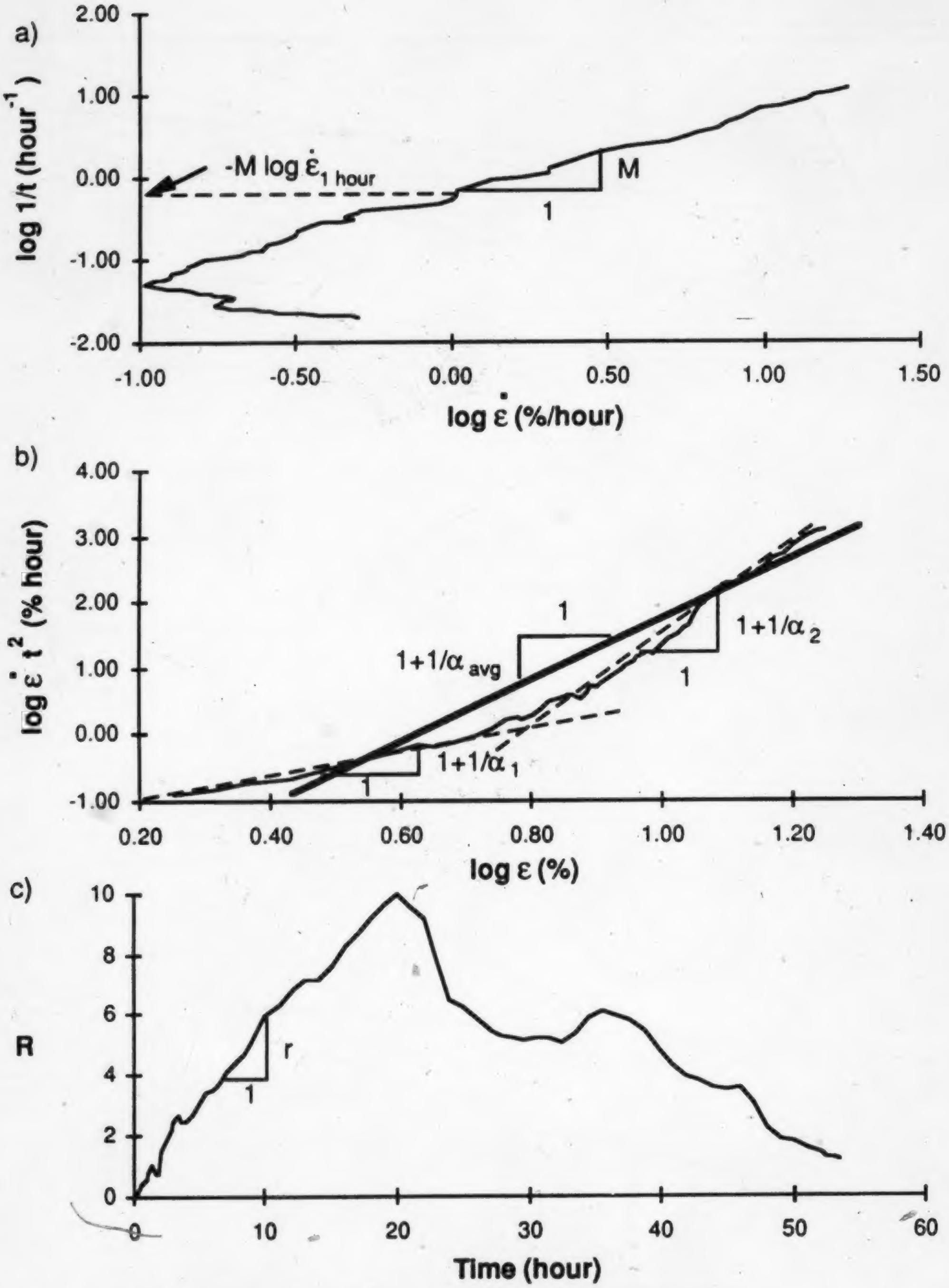

Figure D.15: Creep test CR-71 soil B 0 ppt at σ=2354 kPa
a) log 1/t vs log strain rate (Sayles, 1968)
b) log strain rate time^2 vs log strain (Vyalov, 1988)
c) R = dε / dt vs time (Berggren and Furuberg, 1985)

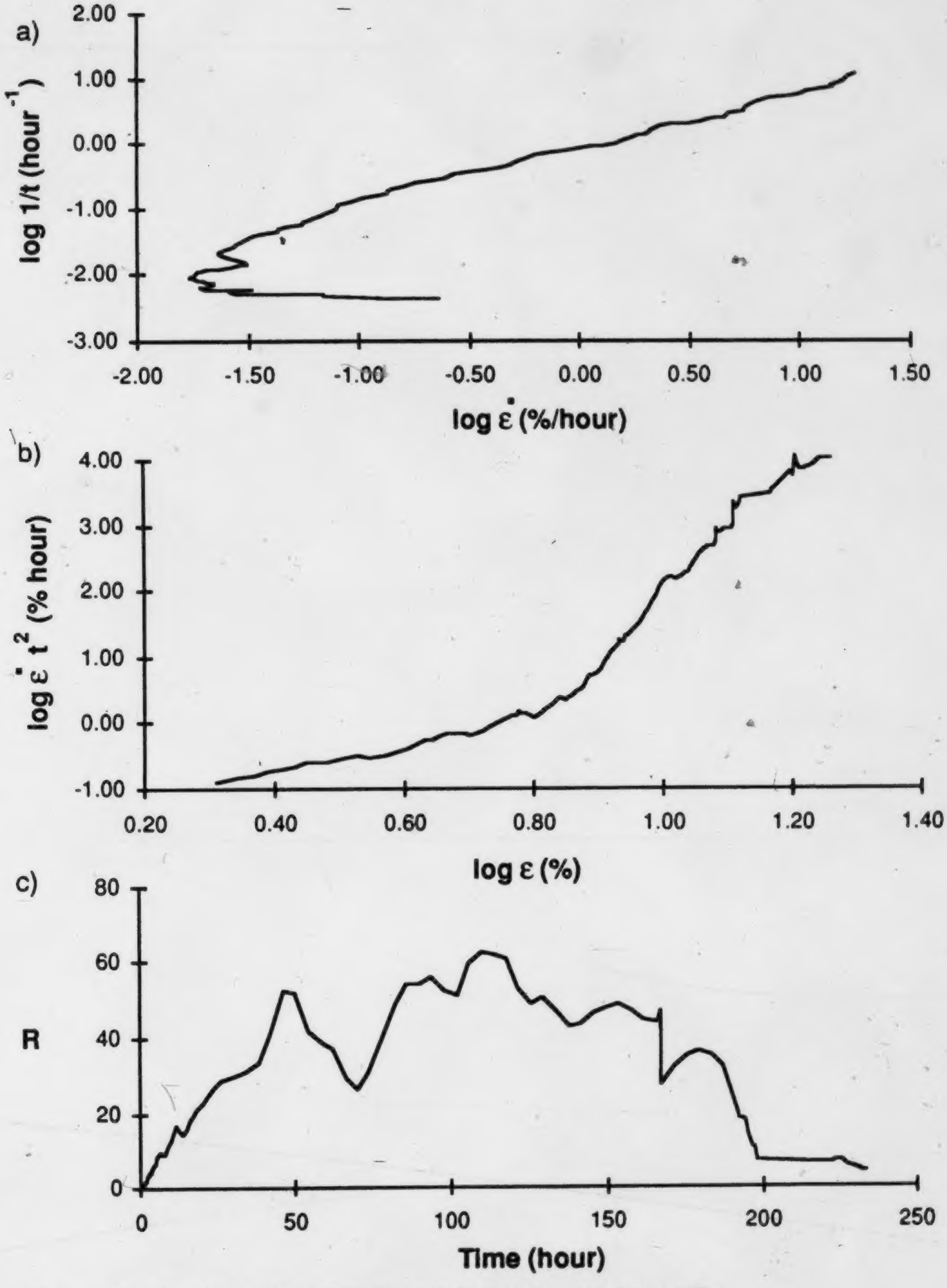

Figure D.16: Creep test CR-81 soil B 0 ppt at σ=2119 kPa
a) log 1/t vs log strain rate (Sayles, 1968)
b) log strain rate time^2 vs log strain (Vyalov, 1988)
c) R = dε / dt vs time (Berggren and Furuberg, 1985)

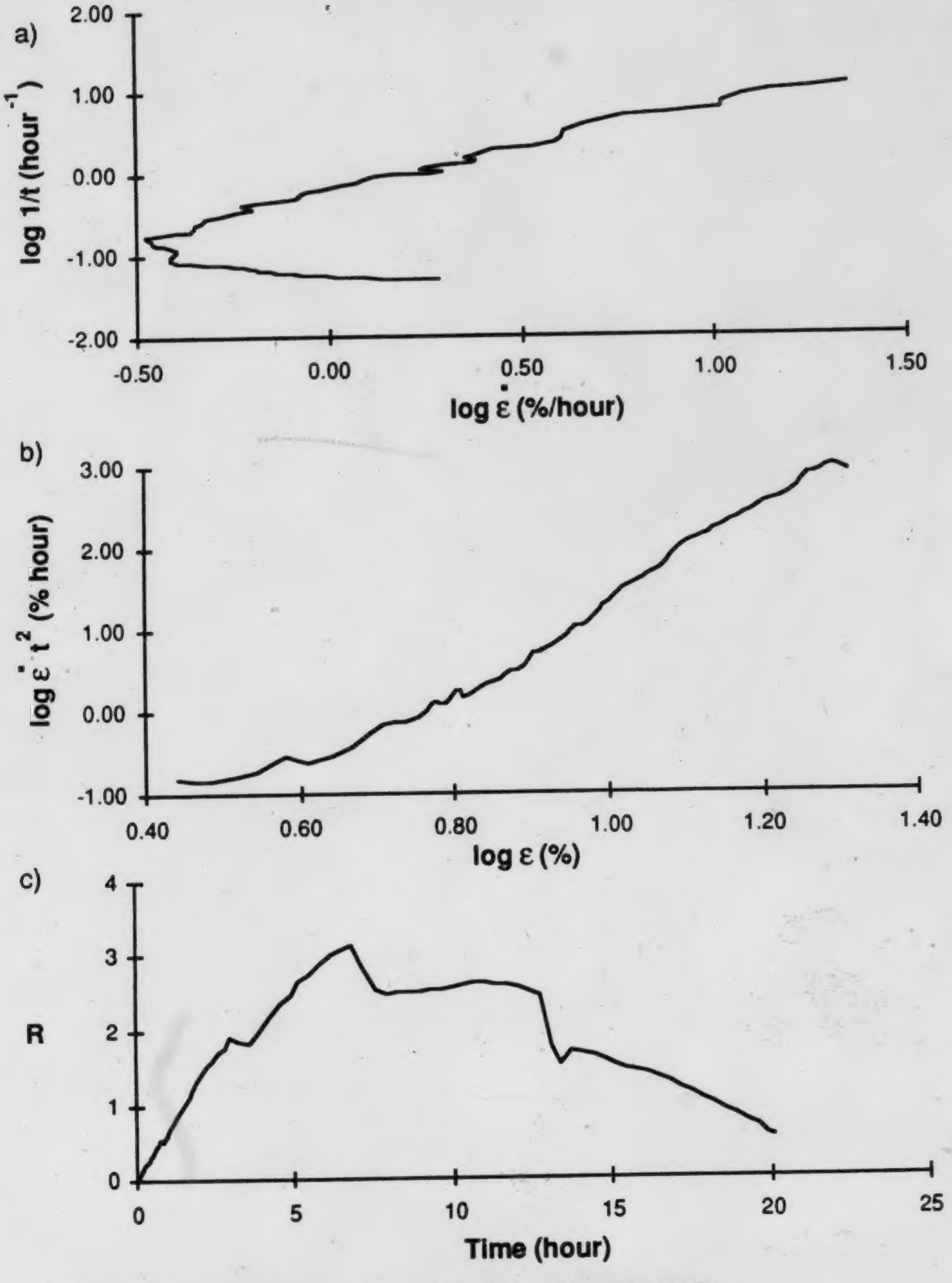

Figure D.17: Creep test CR-84 soil B 5 ppt at σ=1890 kPa
a) log 1/t vs log strain rate (Sayles, 1968)
b) log strain rate time^2 vs log strain (Vyalov, 1988)
c) R = dε / dt vs time (Berggren and Furuberg, 1985)

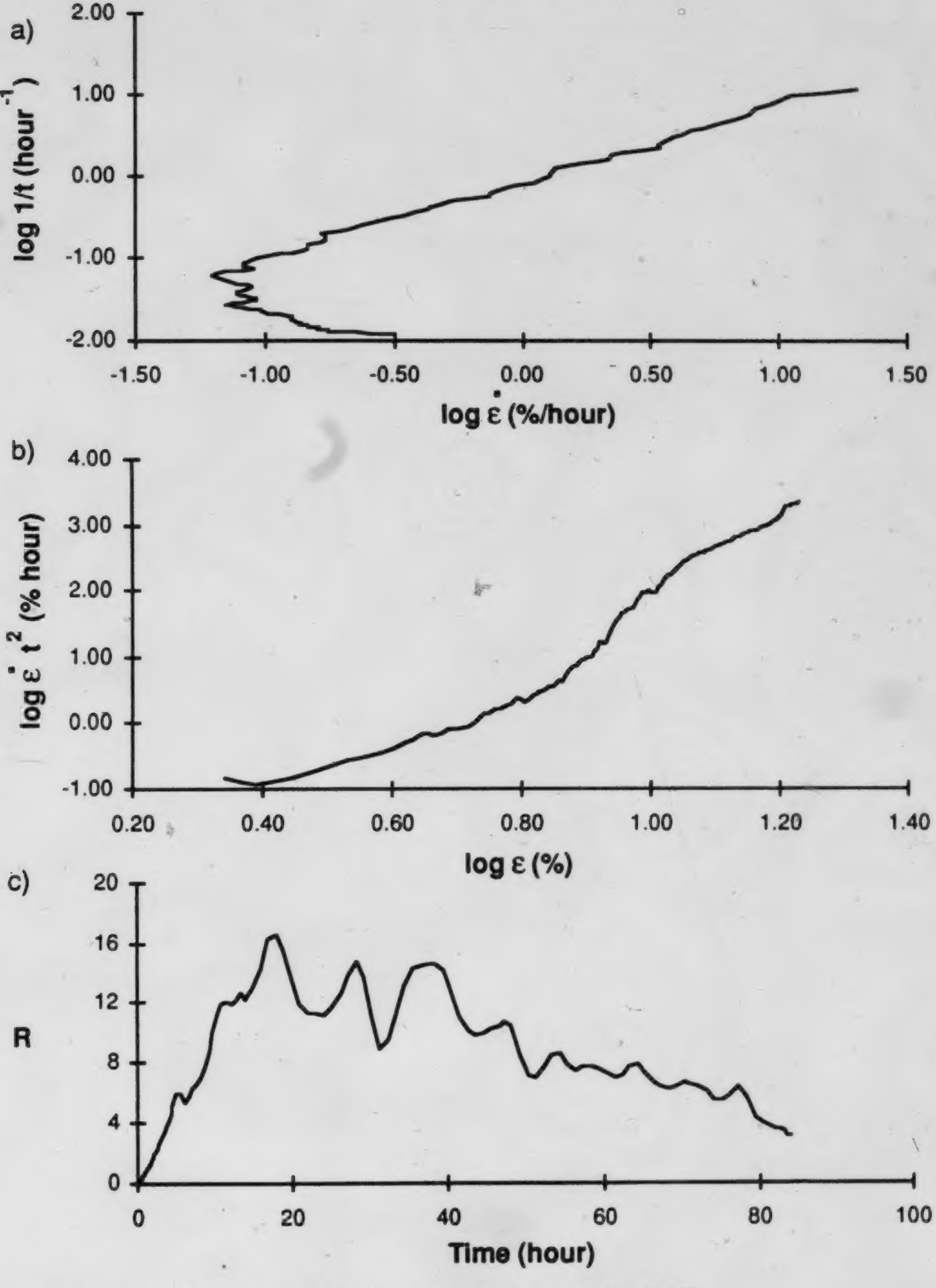

Figure D.18: Creep test CR-49 soil B 5 ppt at σ=1718 kPa
a) log 1/t vs log strain rate (Sayles, 1968)
b) log strain rate time^2 vs log strain (Vyalov, 1988)
c) R = dε / dt vs time (Berggren and Furuberg, 1985)

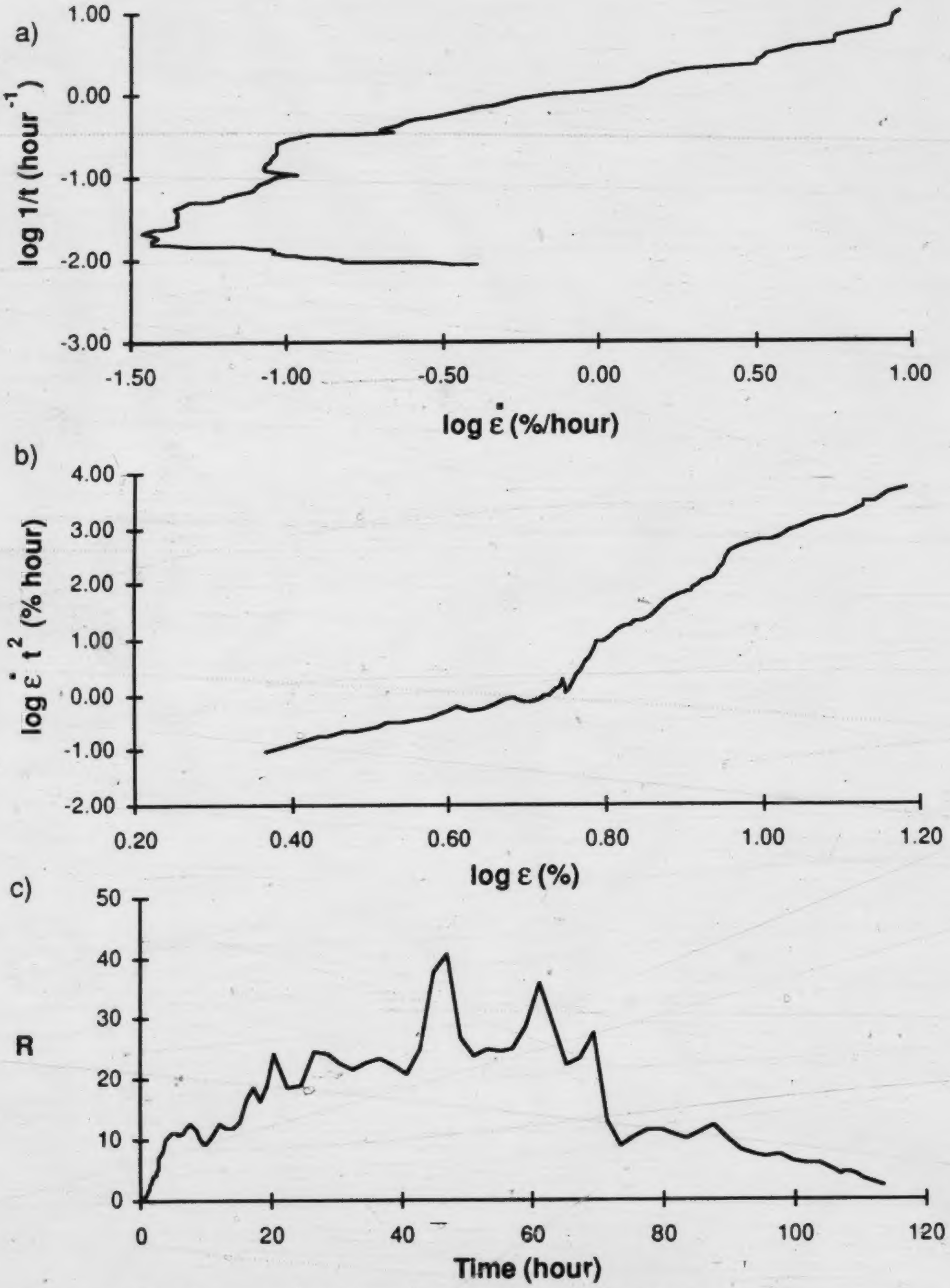

Figure D.19: Creep test CR-9 soil B 5 ppt at σ=1546 kPa
a) log 1/t vs log strain rate (Sayles, 1968)
b) log strain rate time^2 vs log strain (Vyalov, 1988)
c) R = dε / dt vs time (Berggren and Furuberg, 1985)

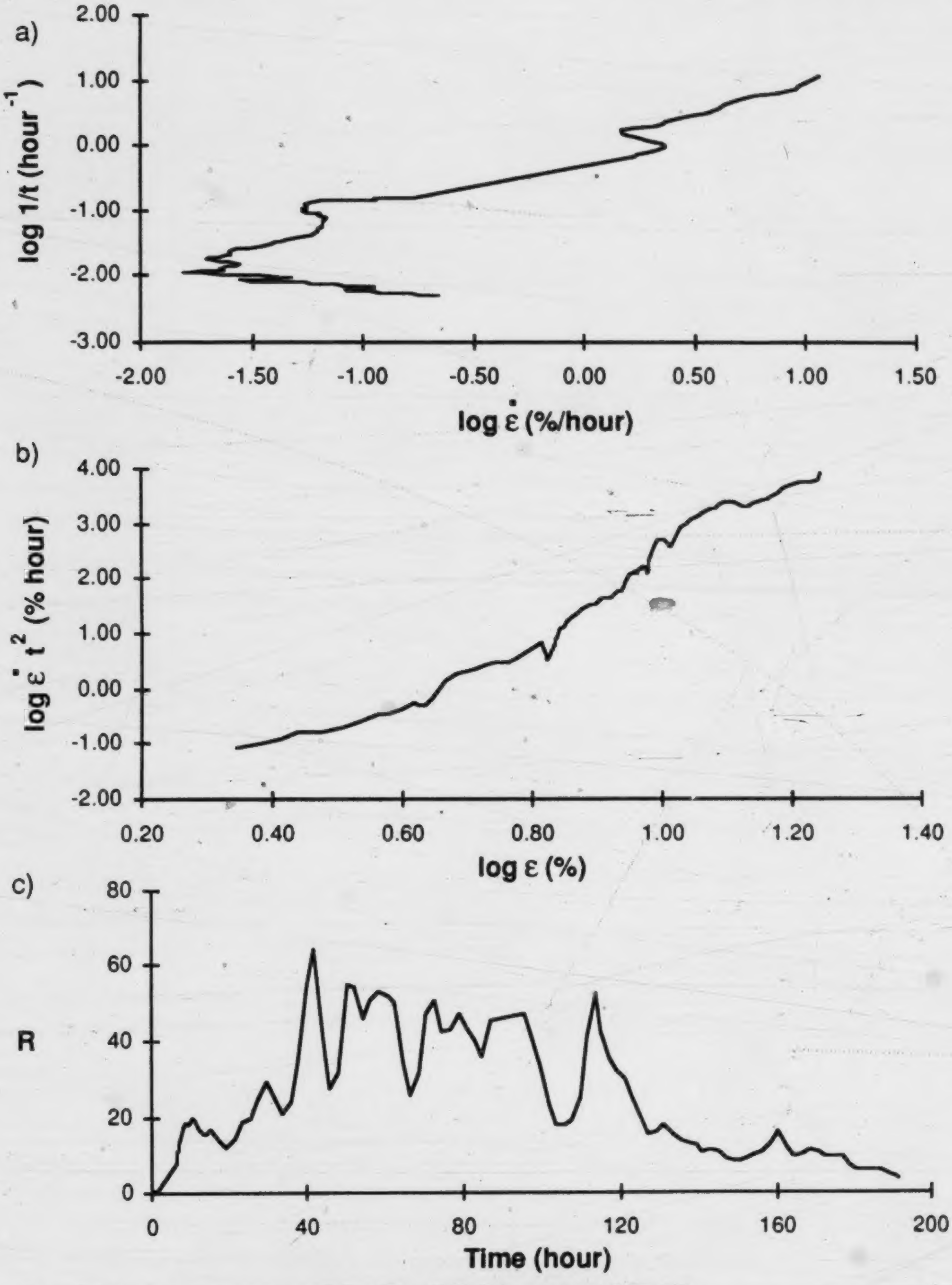

Figure D.20: Creep test CR-17 soil B 5 ppt at σ1546 kPa
a) log 1/t vs log strain rate (Sayles, 1968)
b) log strain rate time^2 vs log strain (Vyalov, 1988)
c) R = dε / dt vs time (Berggren and Furuberg, 1985)

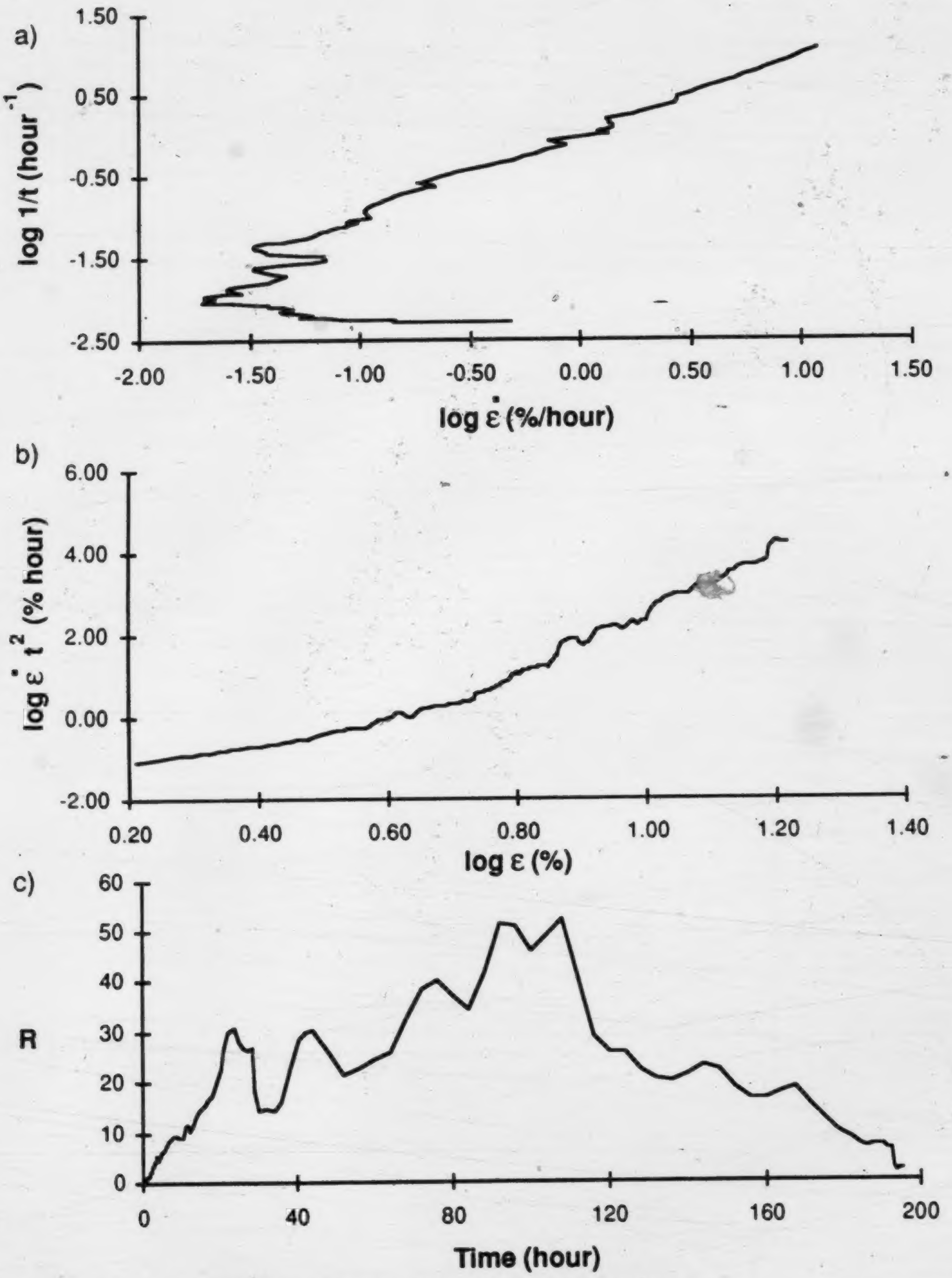

Figure D.21: Creep test CR-32 soil B 5 ppt at σ=1546 kPa
a) log 1/t vs log strain rate (Sayles, 1968)
b) log strain rate time^2 vs log strain (Vyalov, 1988)
c) R = dε / dt vs time (Berggren and Furuberg, 1985)

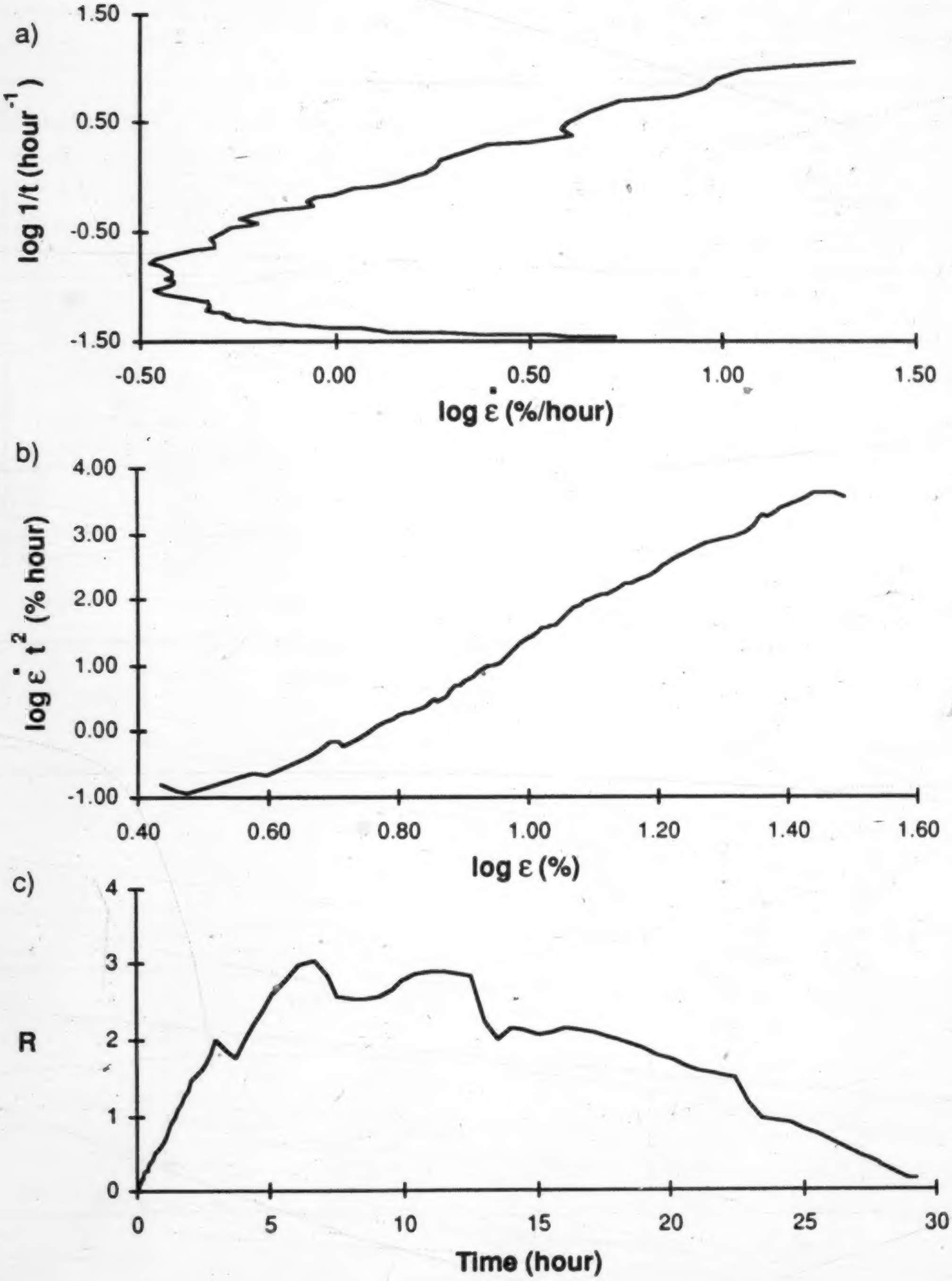

Figure D.22: Creep test CR-82 soil B 10 ppt at σ=1359 kPa
a) log 1/t vs log strain rate (Sayles, 1968)
b) log strain rate time^2 vs log strain (Vyalov, 1988)
c) R = dε / dt vs time (Berggren and Furuberg, 1985)

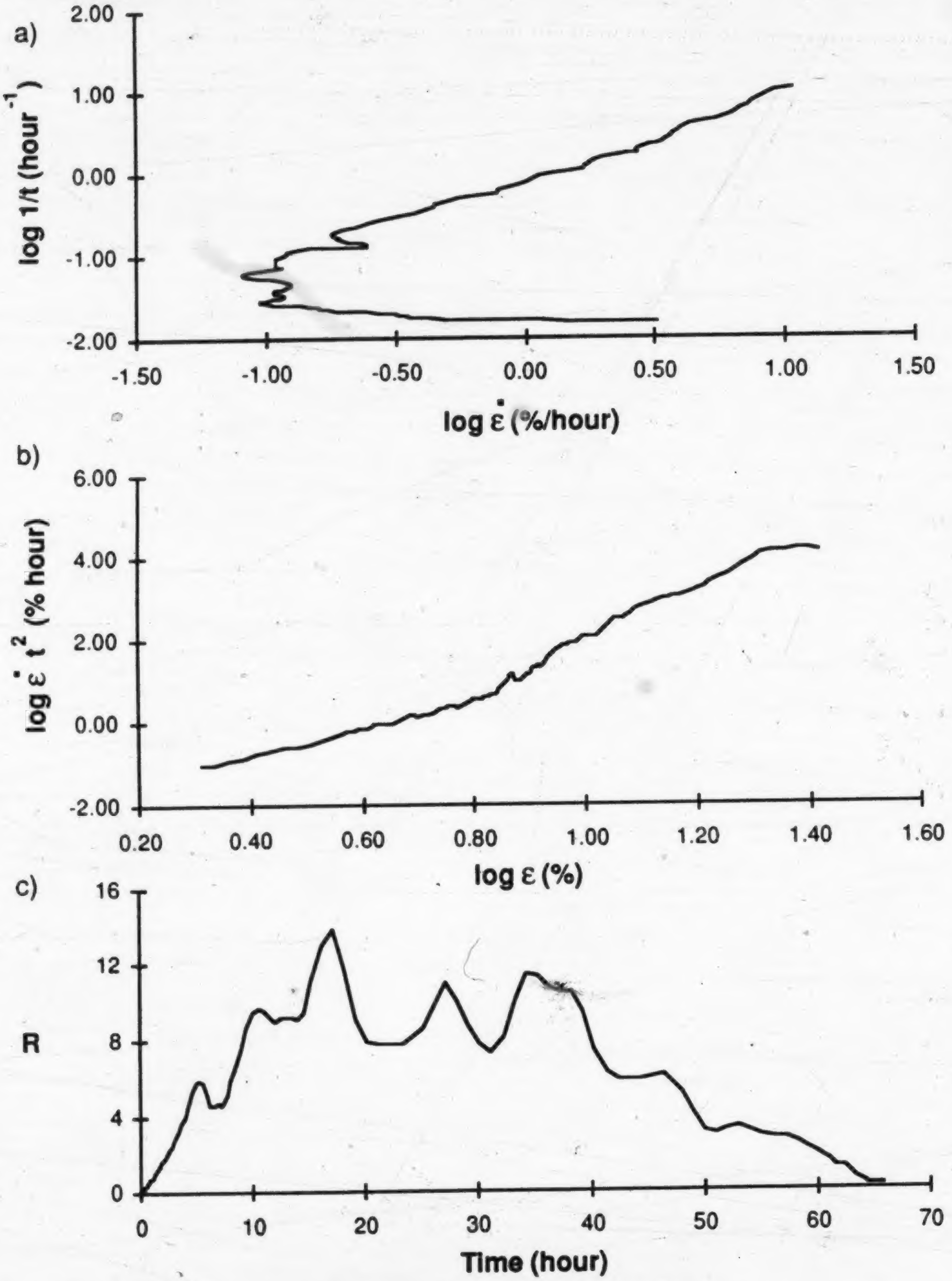

Figure D.23: Creep test CR-50 soil B 10 ppt at σ=1235 kPa
a) log 1/t vs log strain rate (Sayles, 1968)
b) log strain rate time^{2} vs log strain (Vyalov, 1988)
c) R = dε / dt vs time (Berggren and Furuberg, 1985)

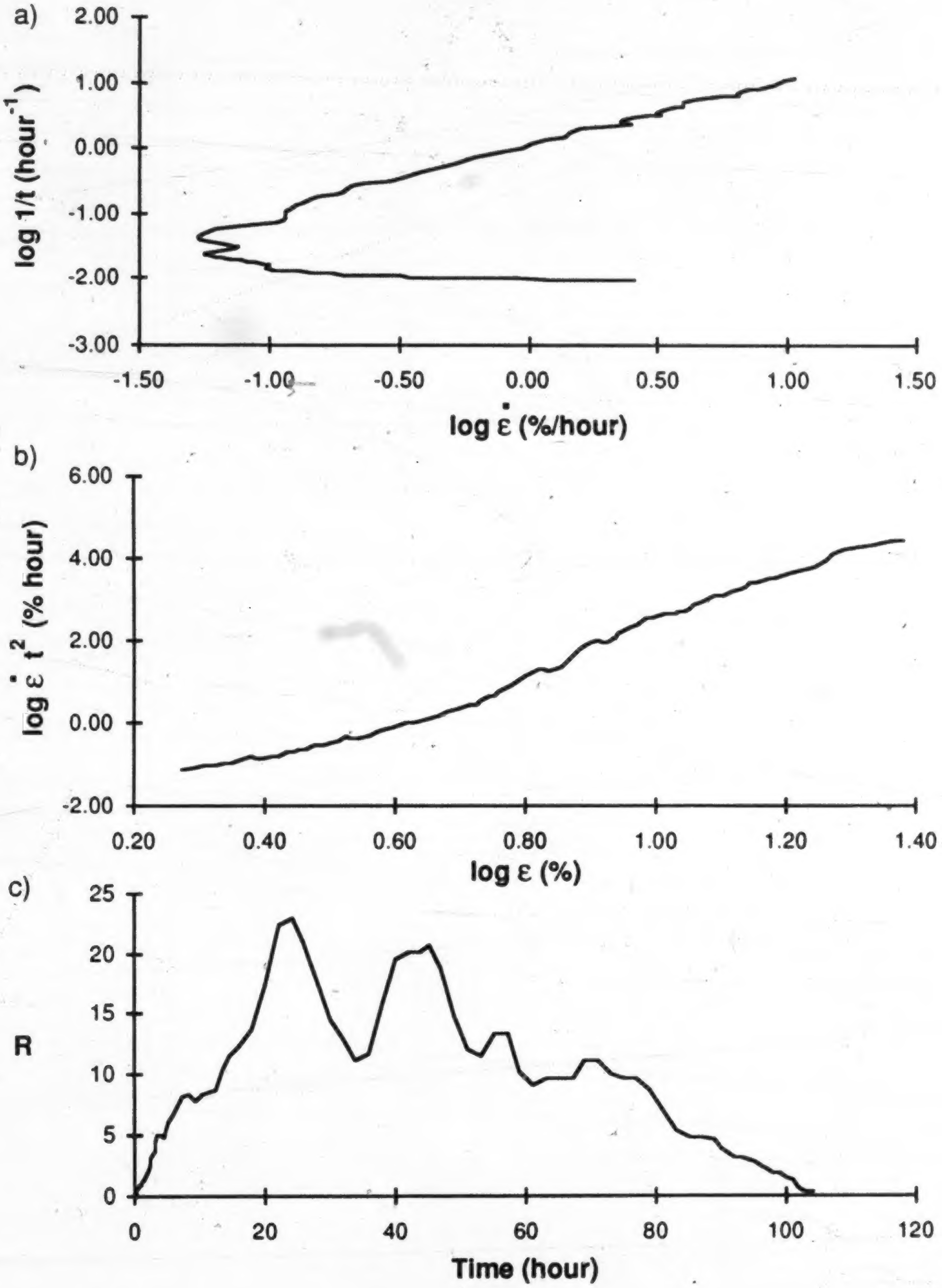

Figure D:24: Creep test CR-33 soil B 30 ppt at σ=1112 kPa
a) log 1/t vs log strain rate (Sayles, 1968)
b) log strain rate time^2 vs log strain (Vyalov, 1988)
c) R = dε / dt vs time (Berggren and Furuberg, 1985)

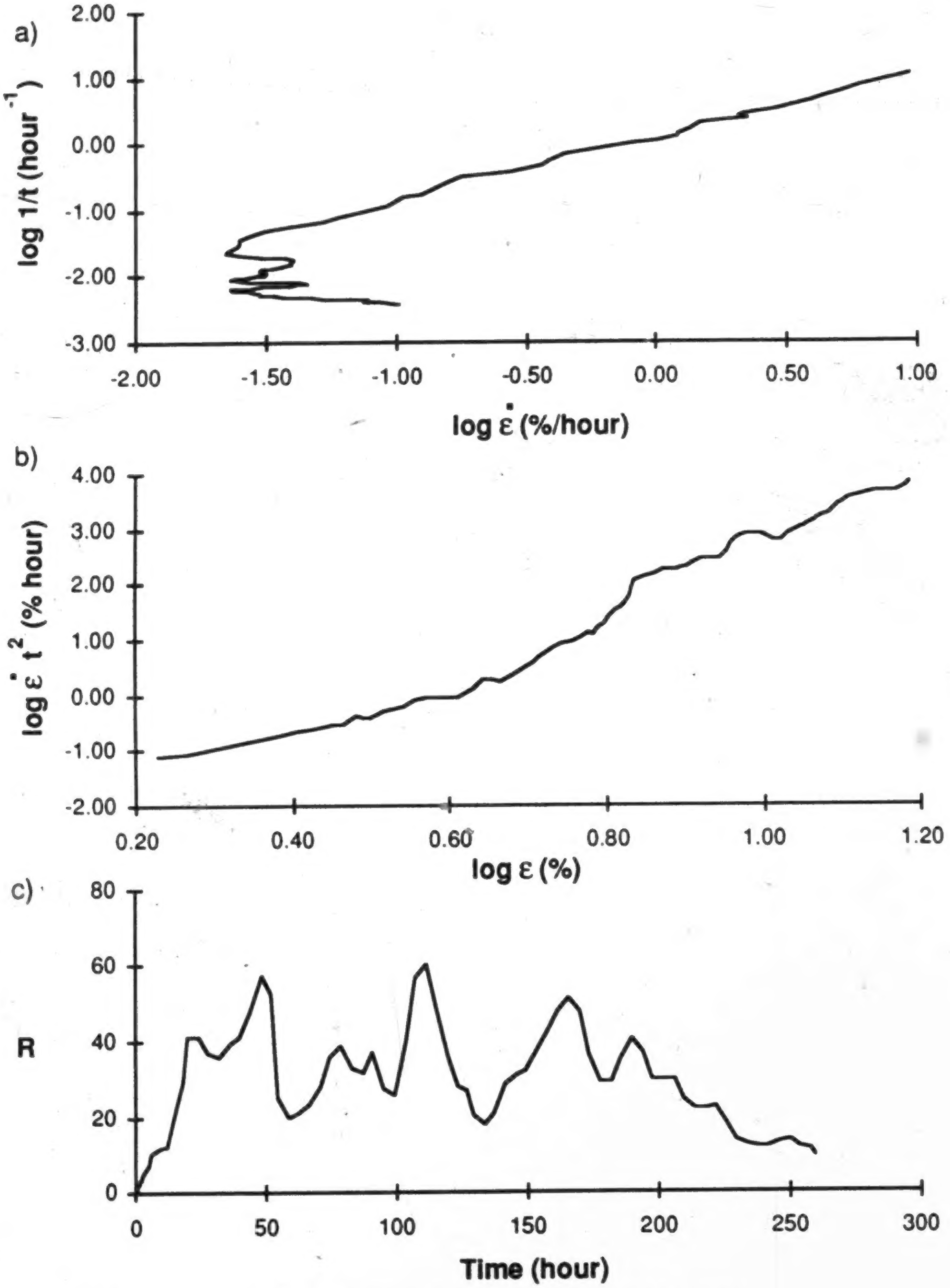

Figure D.25: Creep test CR-38 soil B 10 ppt at σ=1112 kPa
a) log 1/t vs log strain rate (Sayles, 1968)
b) log strain rate time^2 vs log strain (Vyalov, 1988)
c) R = dε / dt vs time (Berggren and Furuberg, 1985)

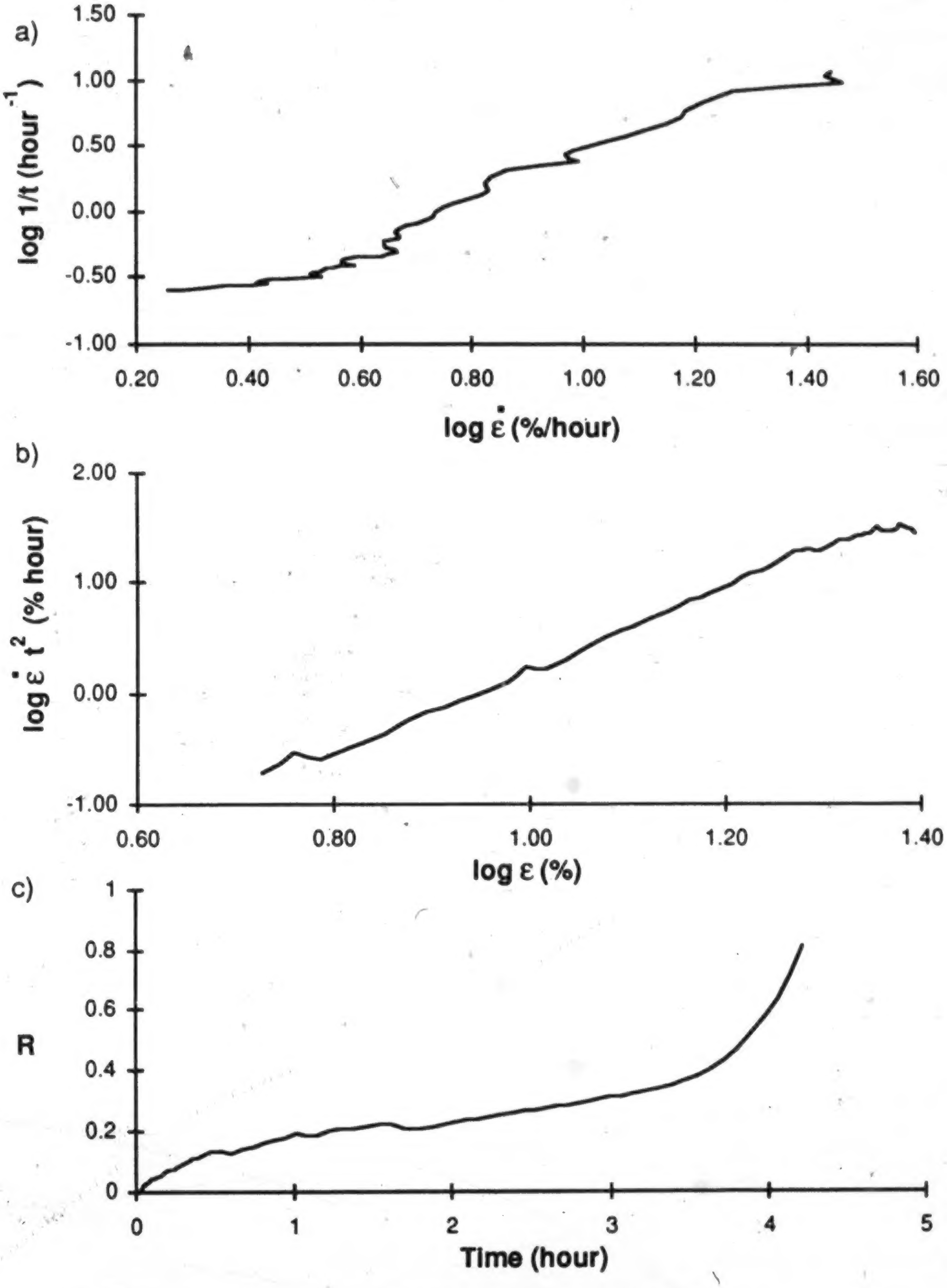

Figure D.26: Creep test CR-75 soil B 30 ppt at σ=678 kPa
a) log 1/t vs log strain rate (Sayles, 1968)
b) log strain rate time^2 vs log strain (Vyalov, 1988)
c) R = dε / dt vs time (Berggren and Furuberg, 1985)

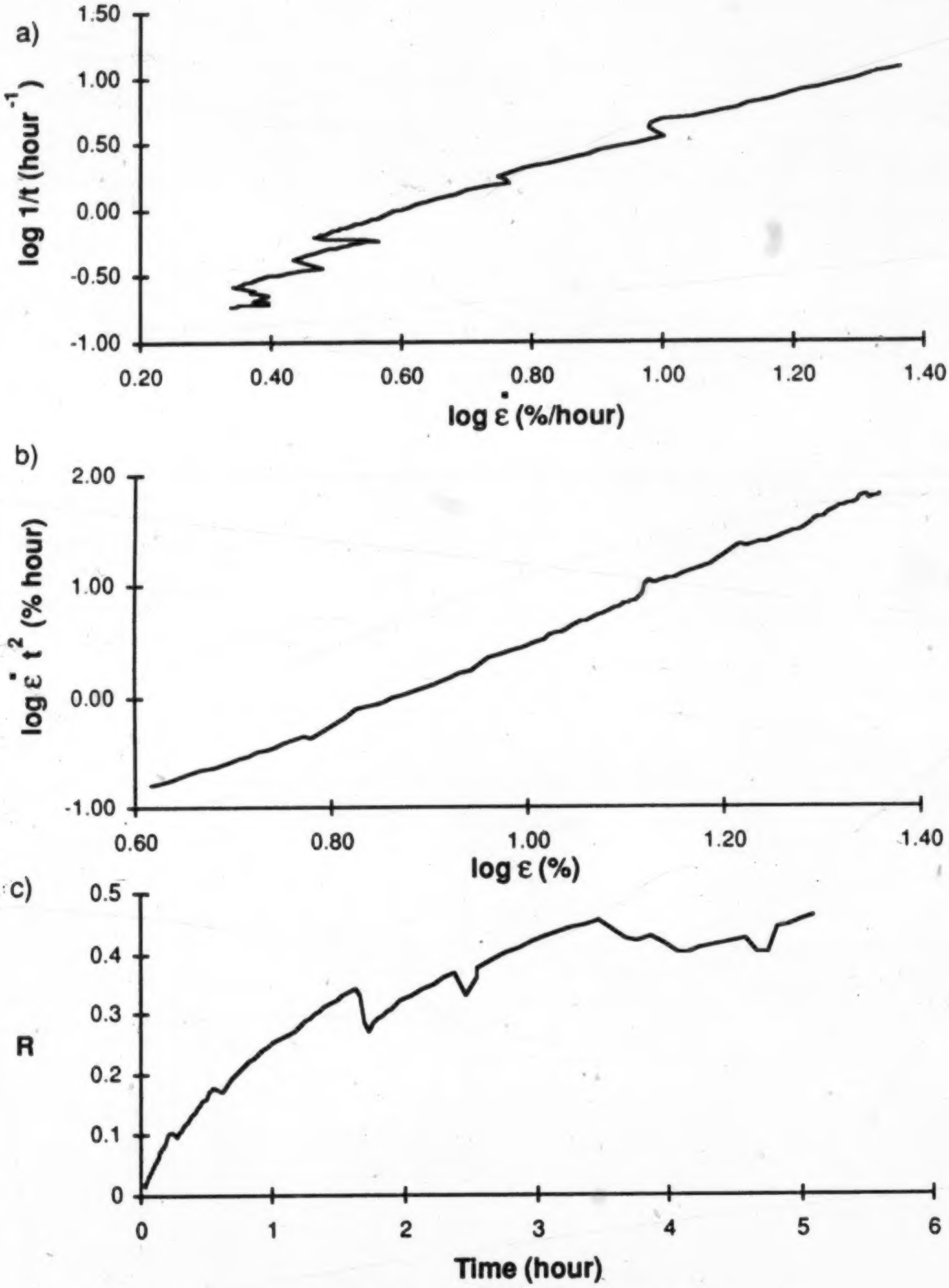

Figure D.27: Creep test CR-77 soil B 30 ppt at σ=559 kPa
a) log 1/t vs log strain rate (Sayles, 1968)
b) log strain rate time^2 vs log strain (Vyalov, 1988)
c) R = dε / dt vs time (Berggren and Furuberg, 1985)

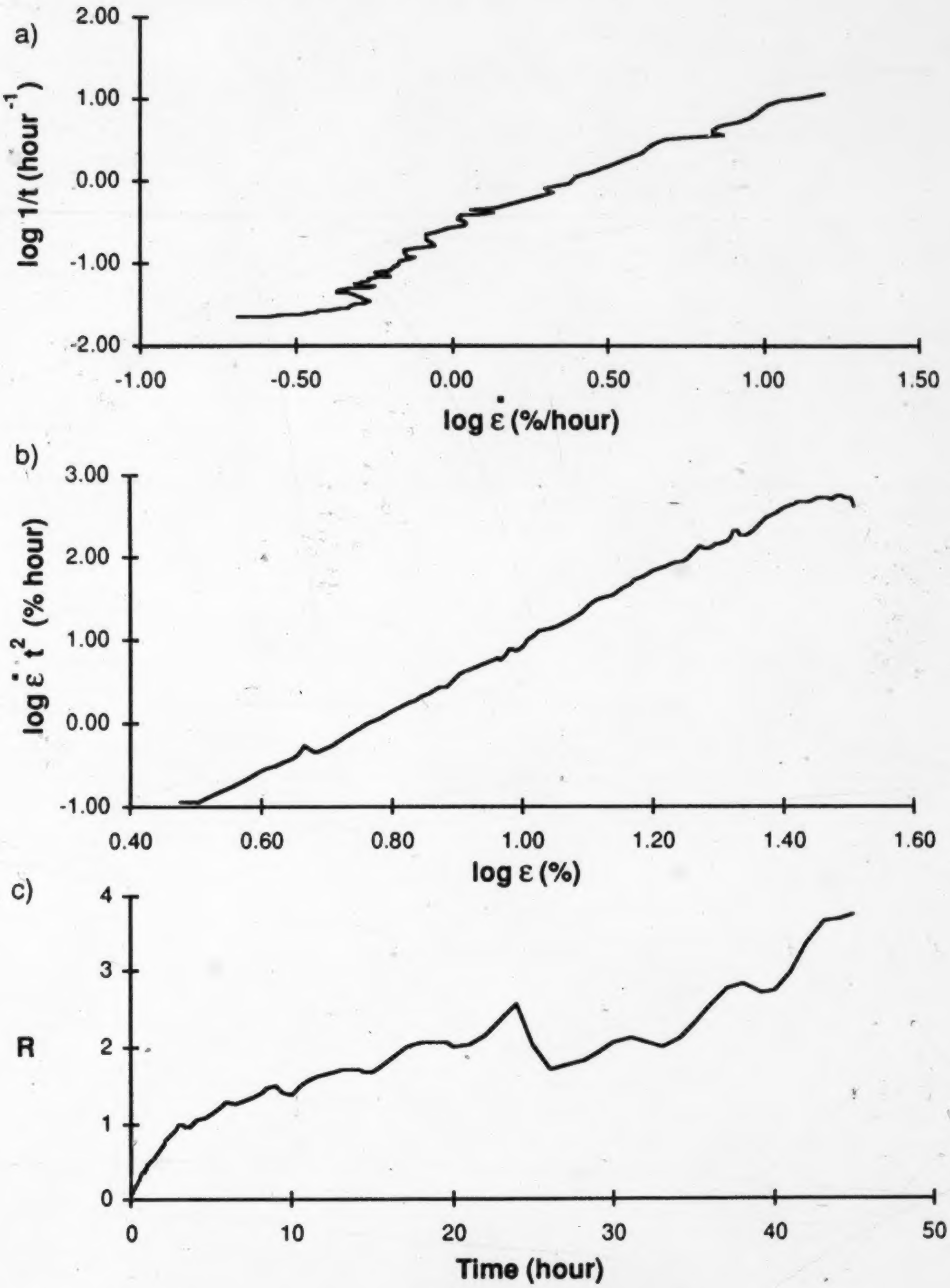

Figure D.28: Creep test CR-88 soil B 30 ppt at σ=442 kPa
a) log 1/t vs log strain rate (Sayles, 1968)
b) log strain rate time^2 vs log strain (Vyalov, 1988)
c) R = dε / dt vs time (Berggren and Furuberg, 1985)

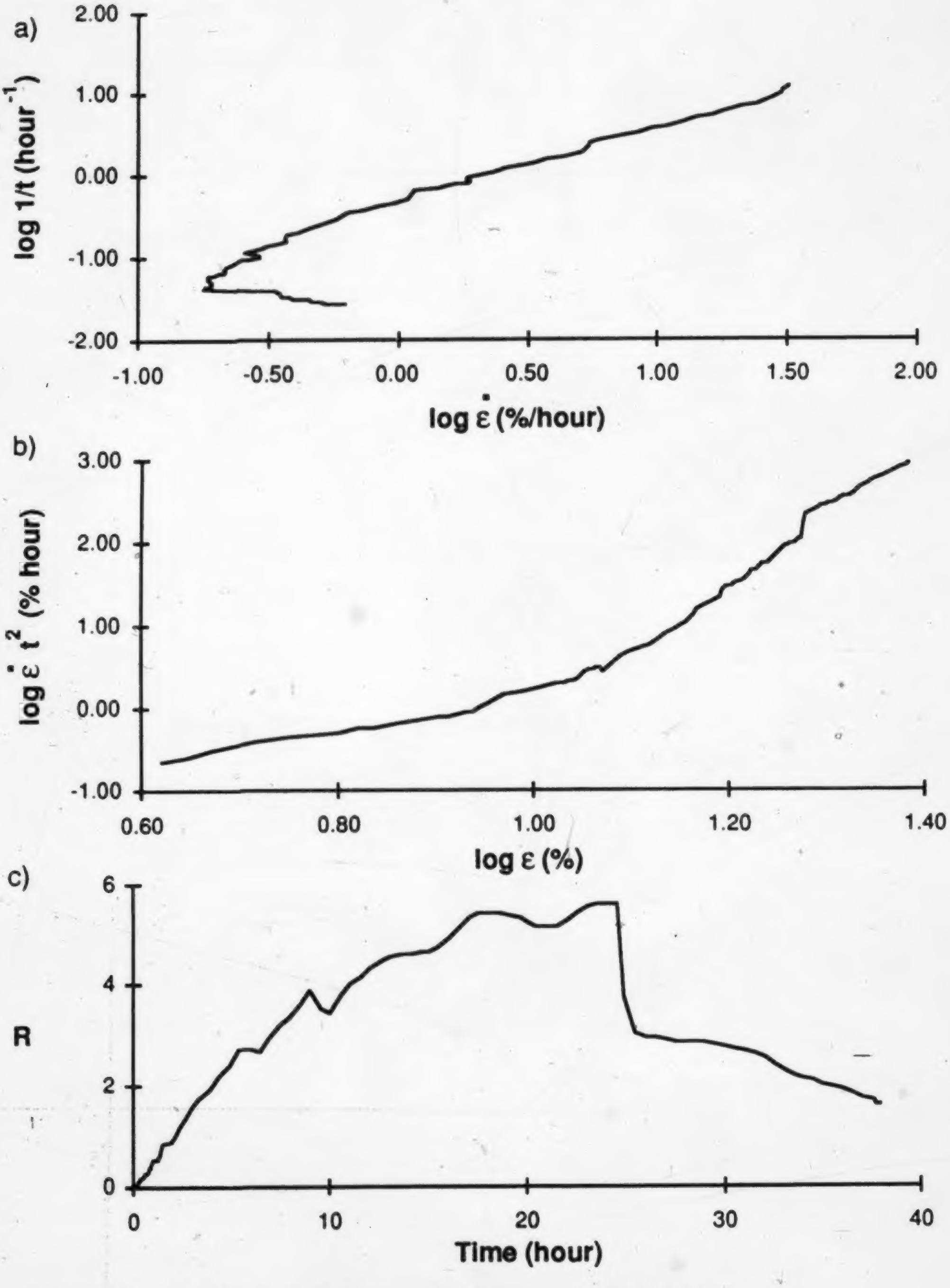

Figure D.29: Creep test CR-79 soil C 0 ppt at σ=2240 kPa
a) log 1/t vs log strain rate (Sayles, 1968)
b) log strain rate time^2 vs log strain (Vyalov, 1988)
c) R = dε / dt vs time (Berggren and Furuberg, 1985)

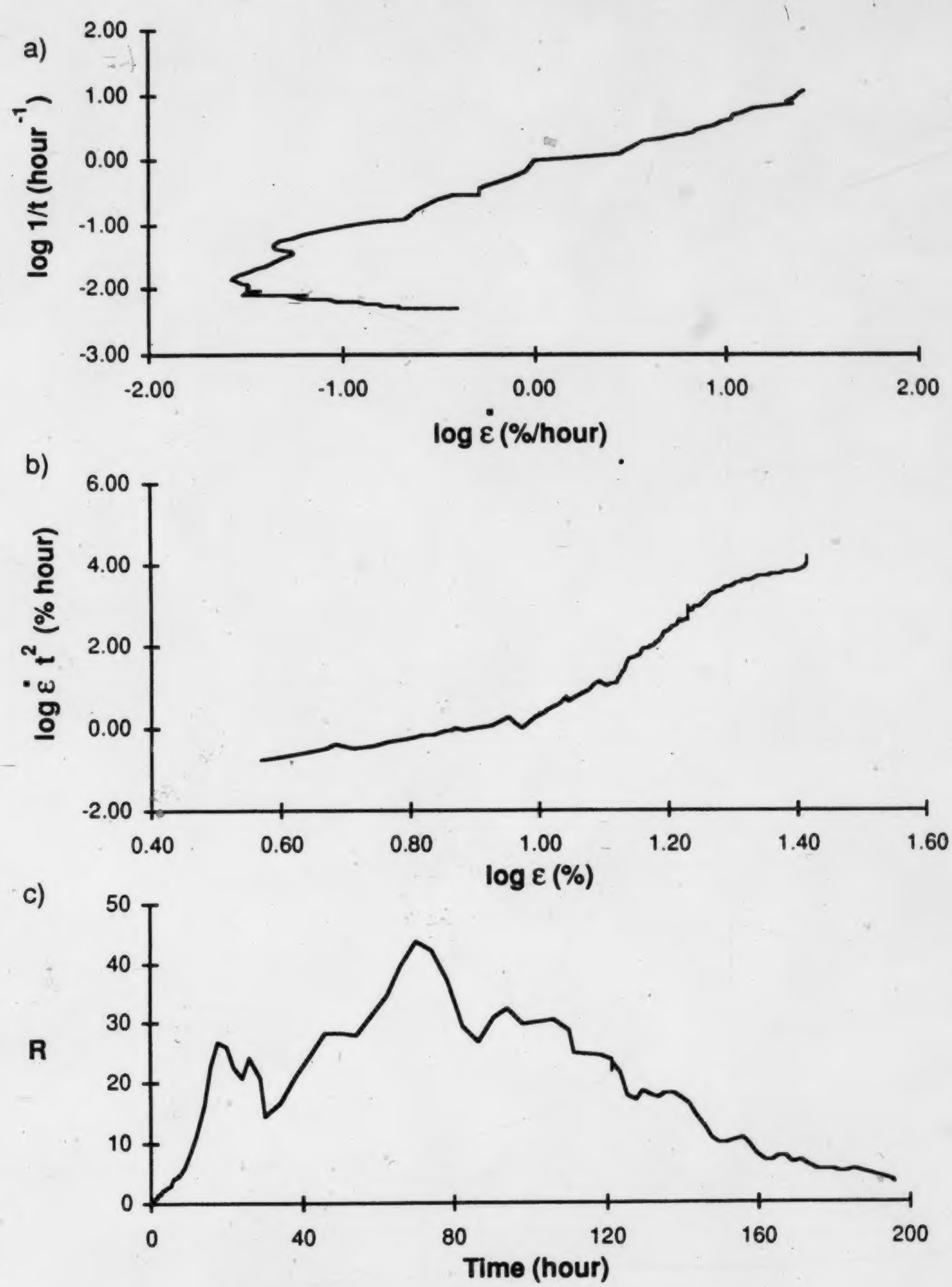

Figure D.30: Creep test CR-65 soil C 0 ppt at σ=2036 kPa
a) log 1/t vs log strain rate (Sayles, 1968)
b) log strain rate time^2 vs log strain (Vyalov, 1988)
c) R = dε / dt vs time (Berggren and Furuberg, 1985)

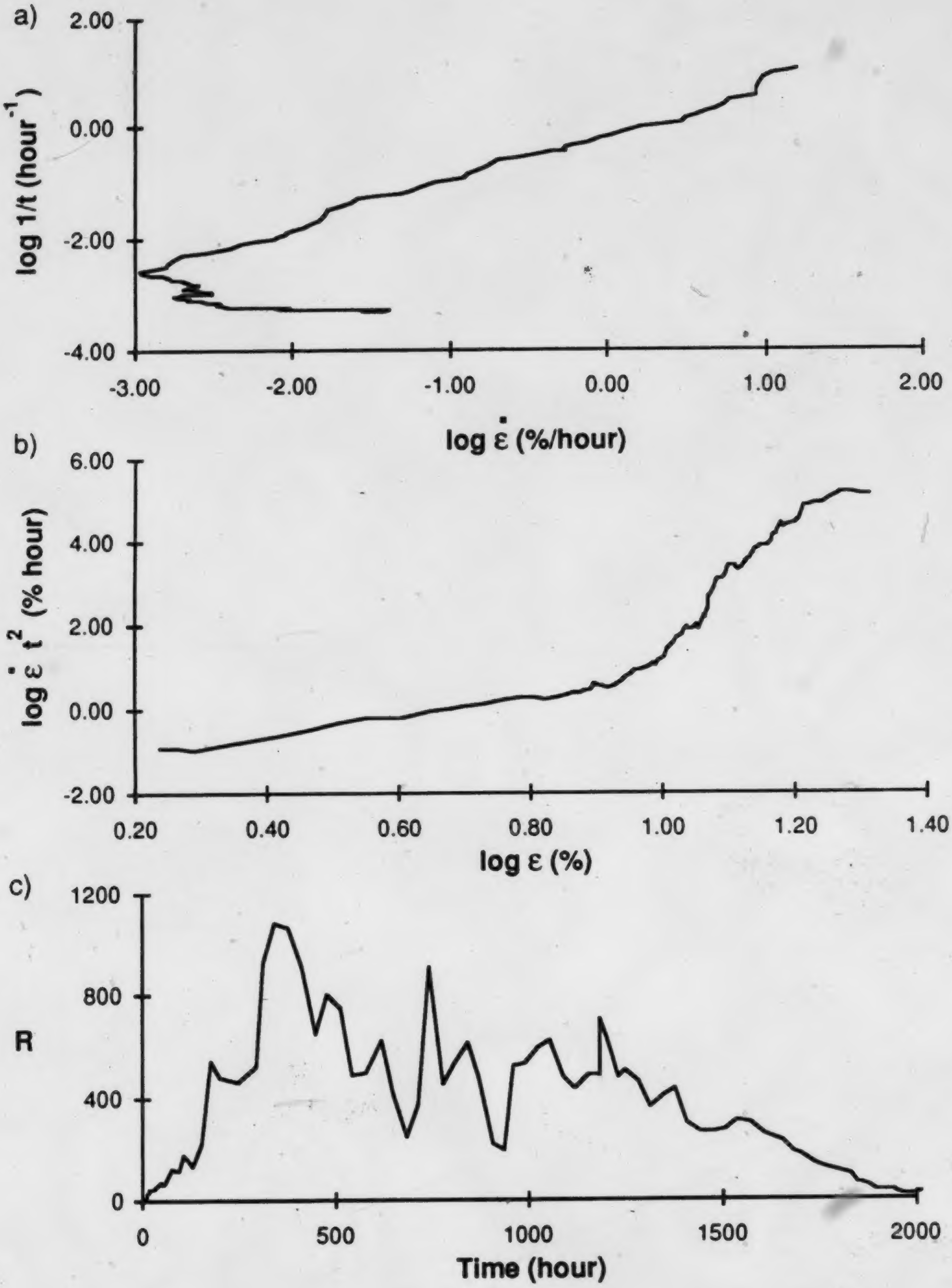

Figure D.31: Creep test #36 soil C 0 ppt at σ=1832 kPa
a) log 1/t vs log strain rate (Sayles, 1968)
b) log strain rate time^2 vs log strain (Vyalov, 1988)
c) R = dε / dt vs time (Berggren and Furuberg, 1985)

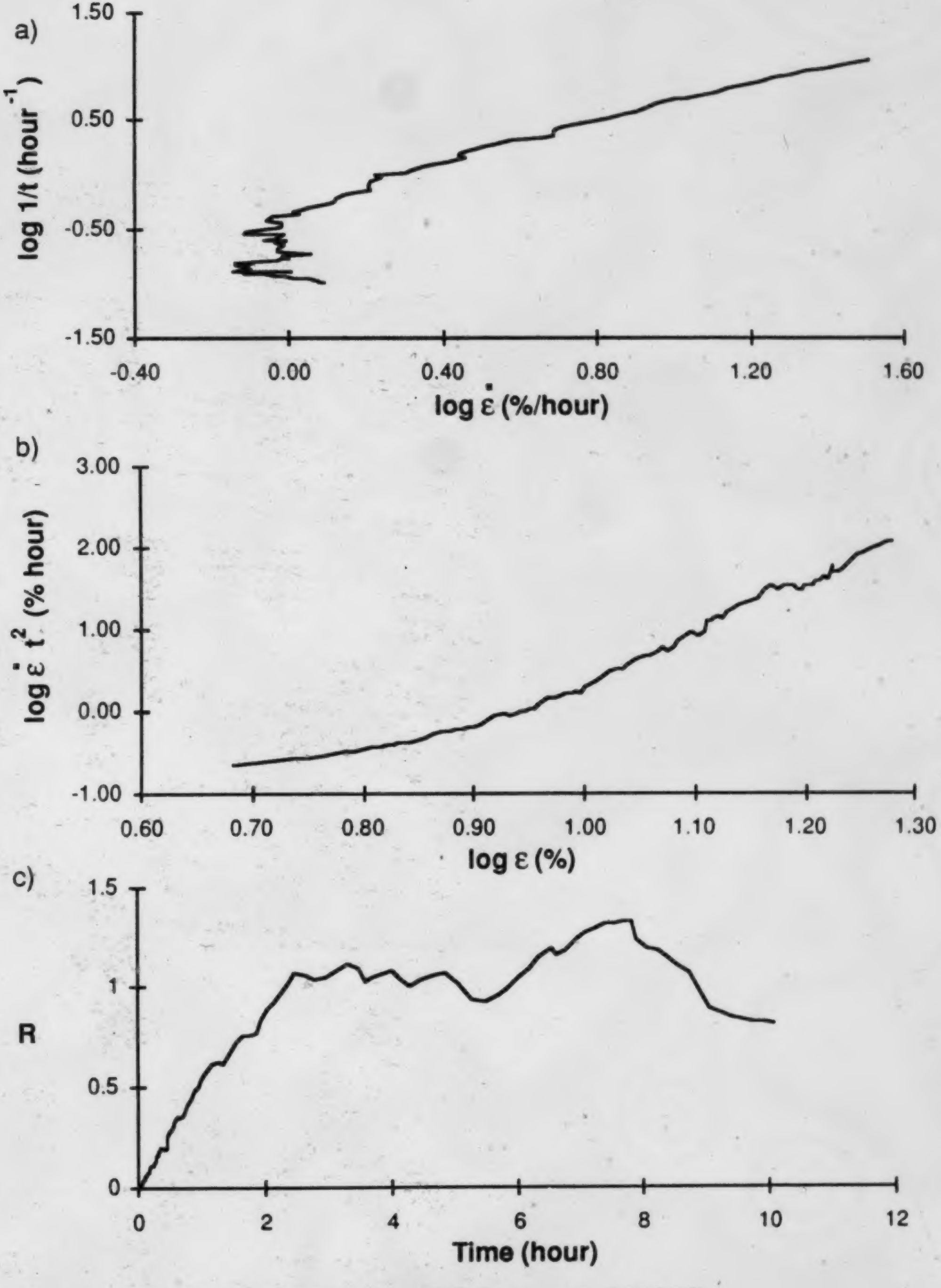

Figure D.32: Creep test CR-96 soil C 5 ppt at σ=2006 kPa
a) log 1/t vs log strain rate (Sayles, 1968)
b) log strain rate time^2 vs log strain (Vyalov, 1988)
c) R = dε / dt vs time (Berggren and Furuberg, 1985)

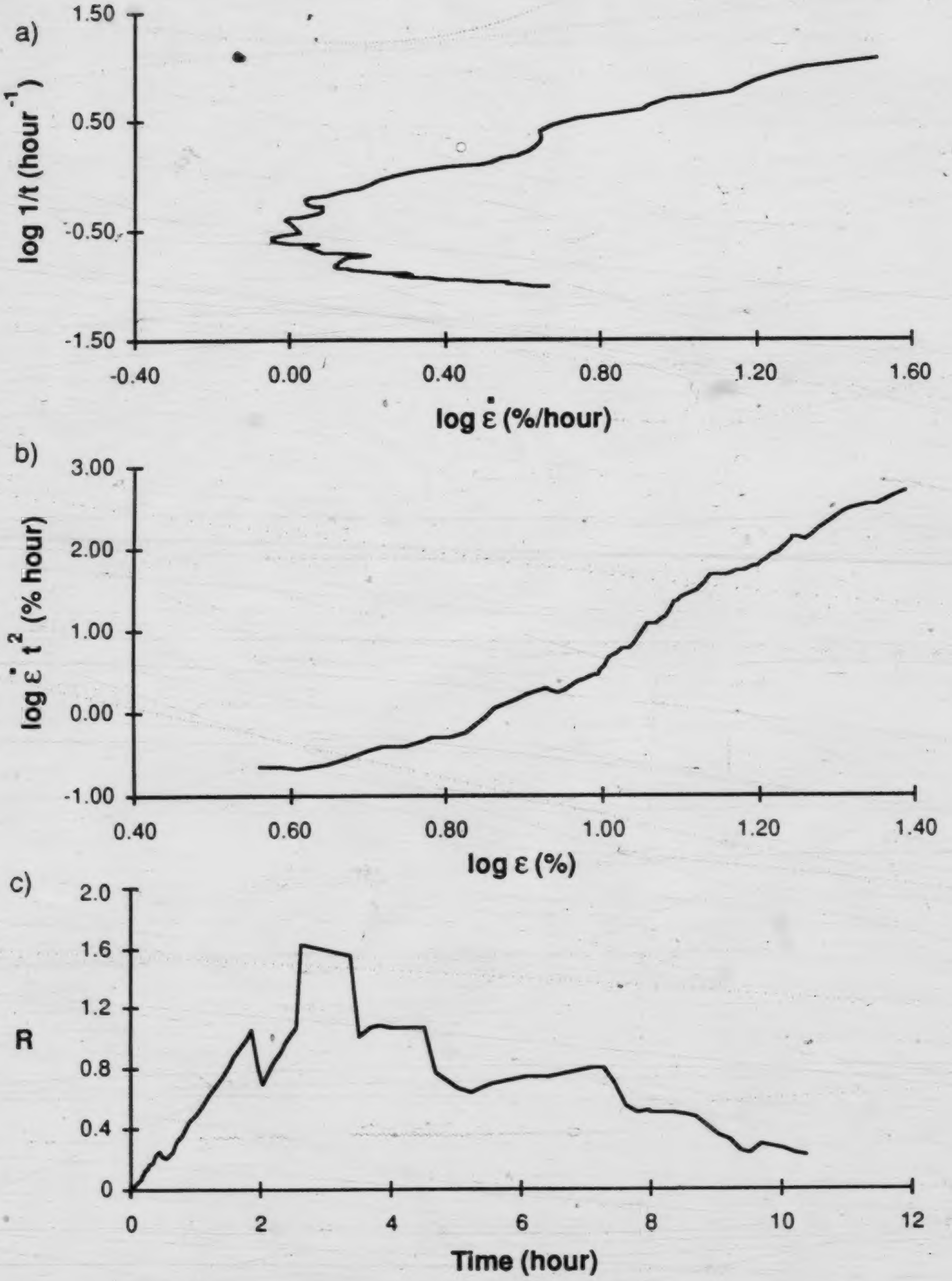

Figure D.33: Creep test CR-66 soil C 5 ppt at σ=1839 kPa
a) log 1/t vs log strain rate (Sayles, 1968)
b) log strain rate time^2 vs log strain (Vyalov, 1988)
c) R = dε / dt vs time (Berggren and Furuberg, 1985)

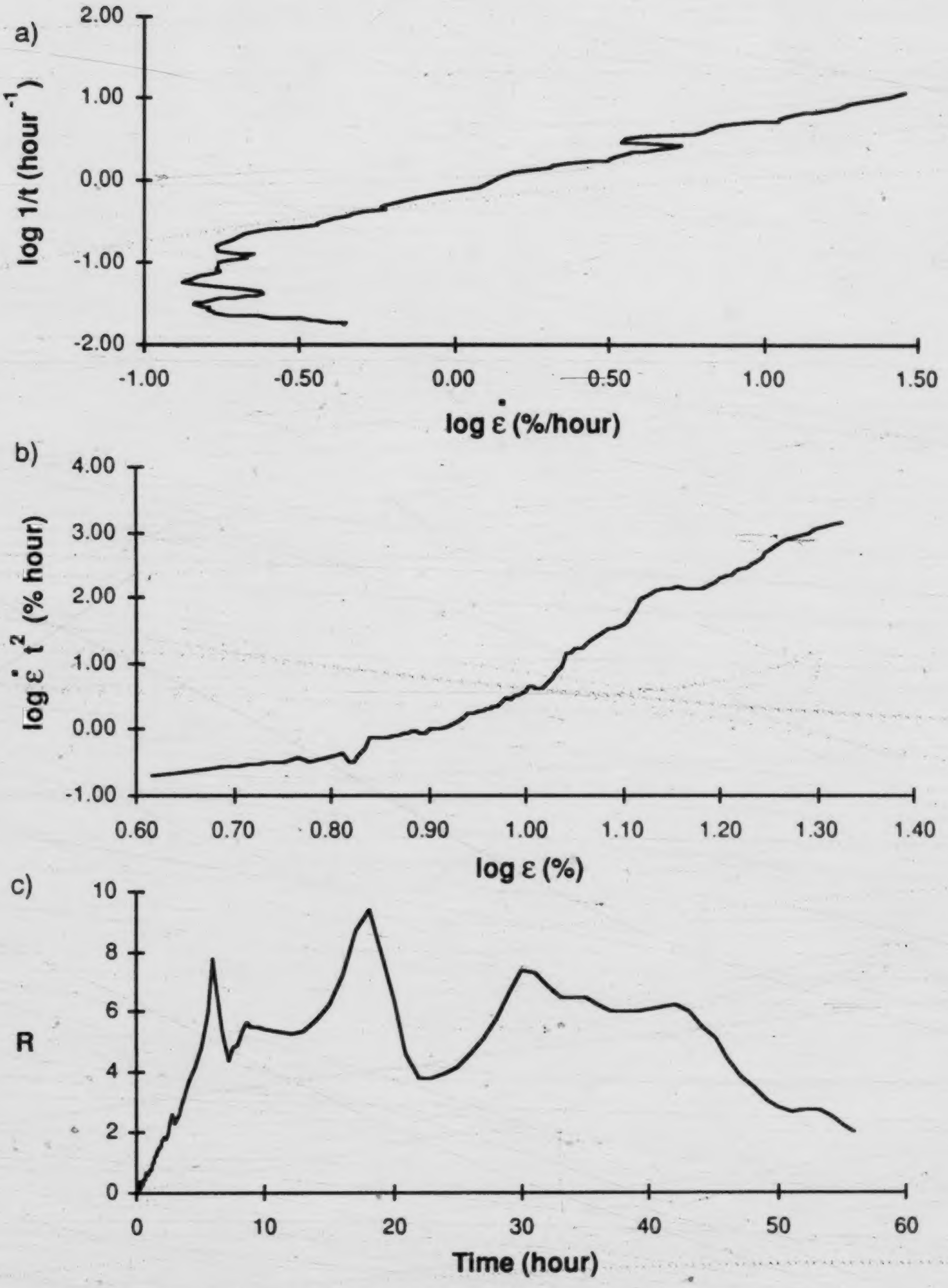

Figure D.34: Creep test CR-62 soil C 5 ppt at σ=1672 kPa
a) log 1/t vs log strain rate (Sayles, 1968)
b) log strain rate time^2 vs log strain (Vyalov, 1988)
c) R = dε / dt vs time (Berggren and Furuberg, 1985)

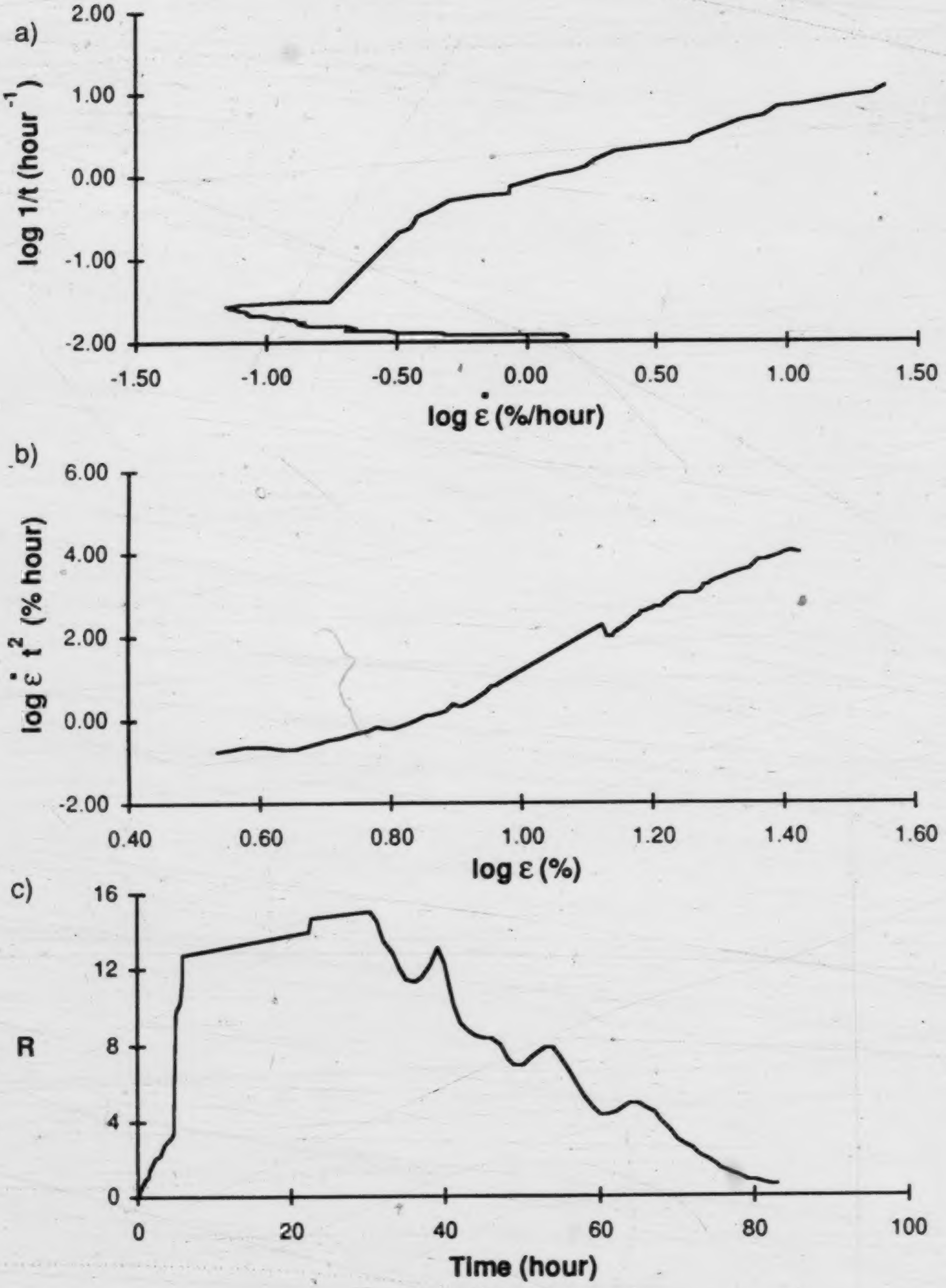

Figure D.35: Creep test CR-89 soil C 5 ppt at σ=1672 kPa
a) log 1/t vs log strain rate (Sayles, 1968)
b) log strain rate time^2 vs log strain (Vyalov, 1988)
c) R = dε / dt vs time (Berggren and Furuberg, 1985)

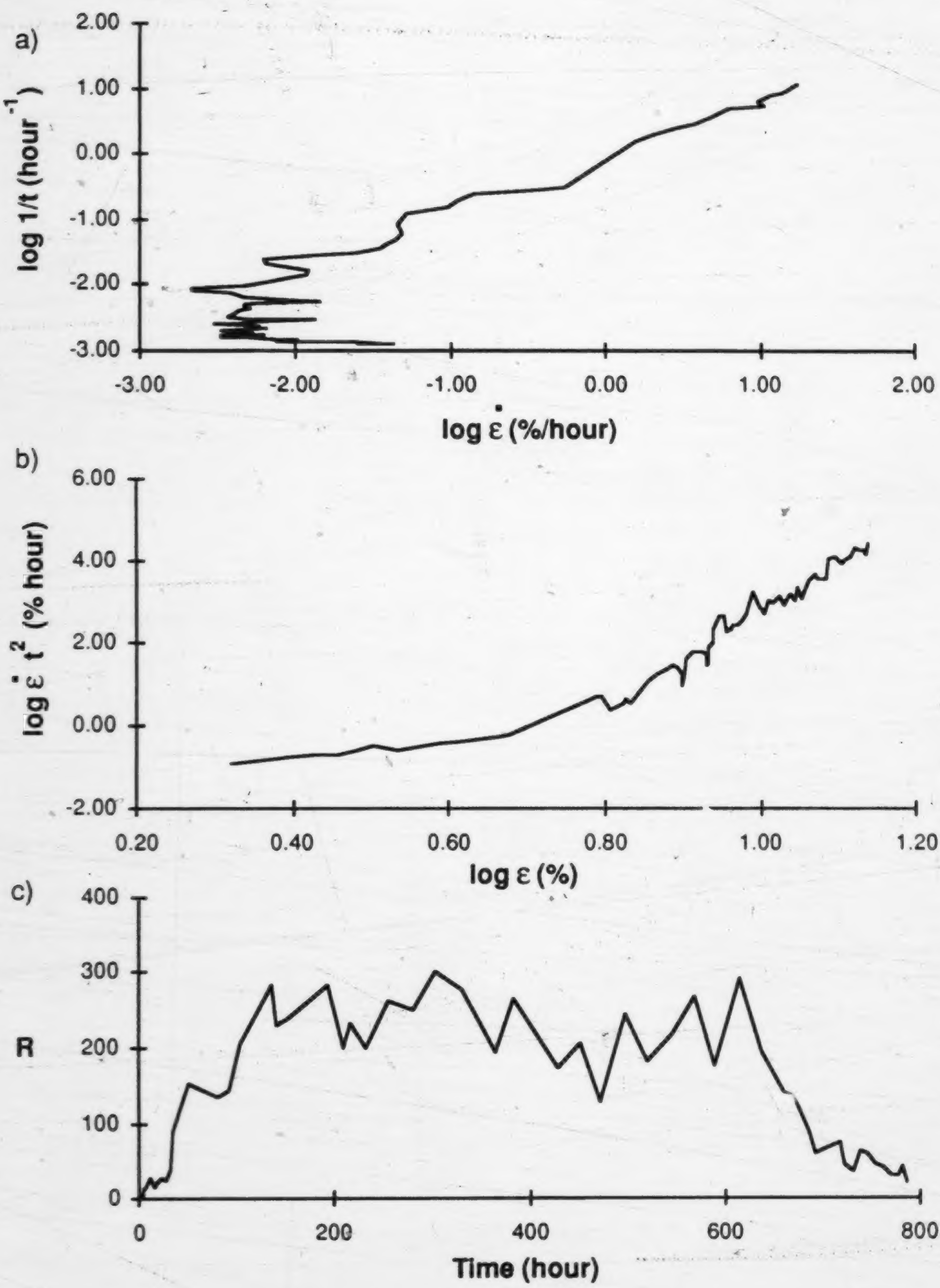

Figure D.36: Creep test CR-94 soil C 5 ppt at σ=1504 kPa
a) log 1/t vs log strain rate (Sayles, 1968)
b) log strain rate time^2 vs log strain (Vyalov, 1988)
c) R = dε / dt vs time (Berggren and Furuberg, 1985)

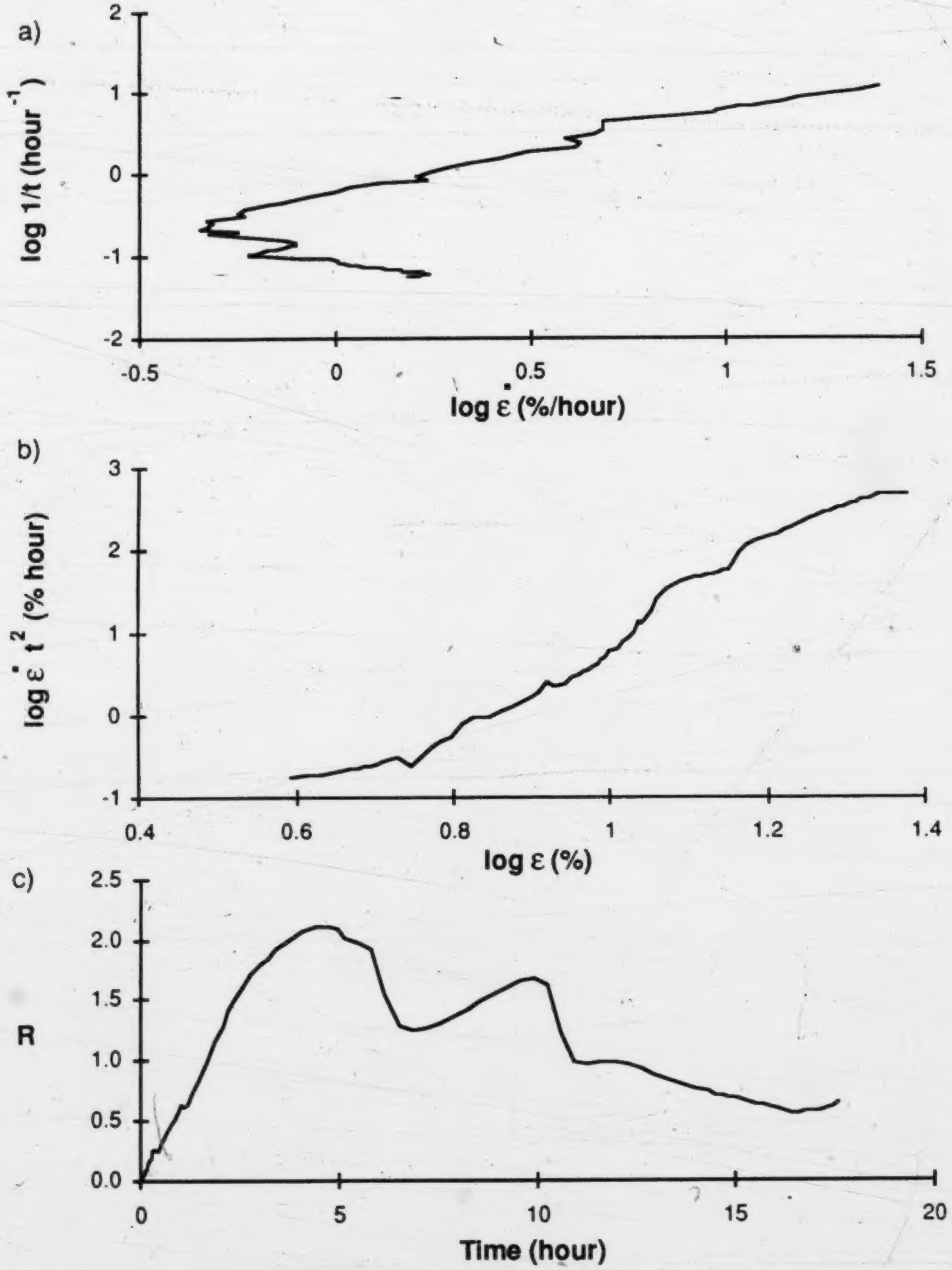

Figure D.37: Creep test CR-55 soil C 10 ppt at σ=1372 kPa
a) log 1/t vs log strain rate (Sayles, 1968)
b) log strain rate time^2 vs log strain (Vyalov, 1988)
c) R = dε / dt vs time (Berggren and Furuberg, 1985)

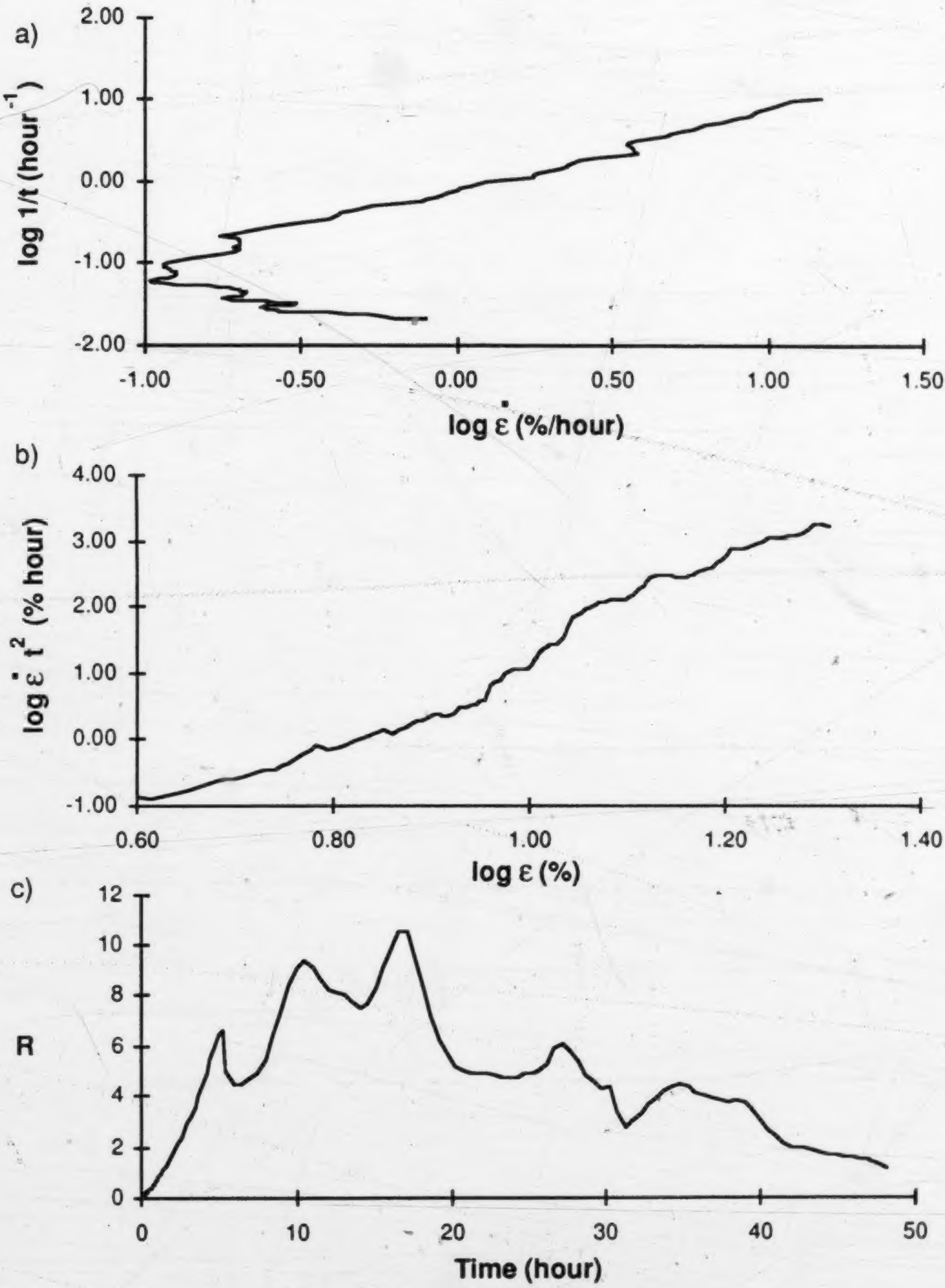

Figure D.38: Creep test CR-52 soil C 10 ppt at σ=1235 kPa
a) log 1/t vs log strain rate (Sayles, 1968)
b) log strain rate time^2 vs log strain (Vyalov, 1988)
c) R = dε / dt vs time (Berggren and Furuberg, 1985)

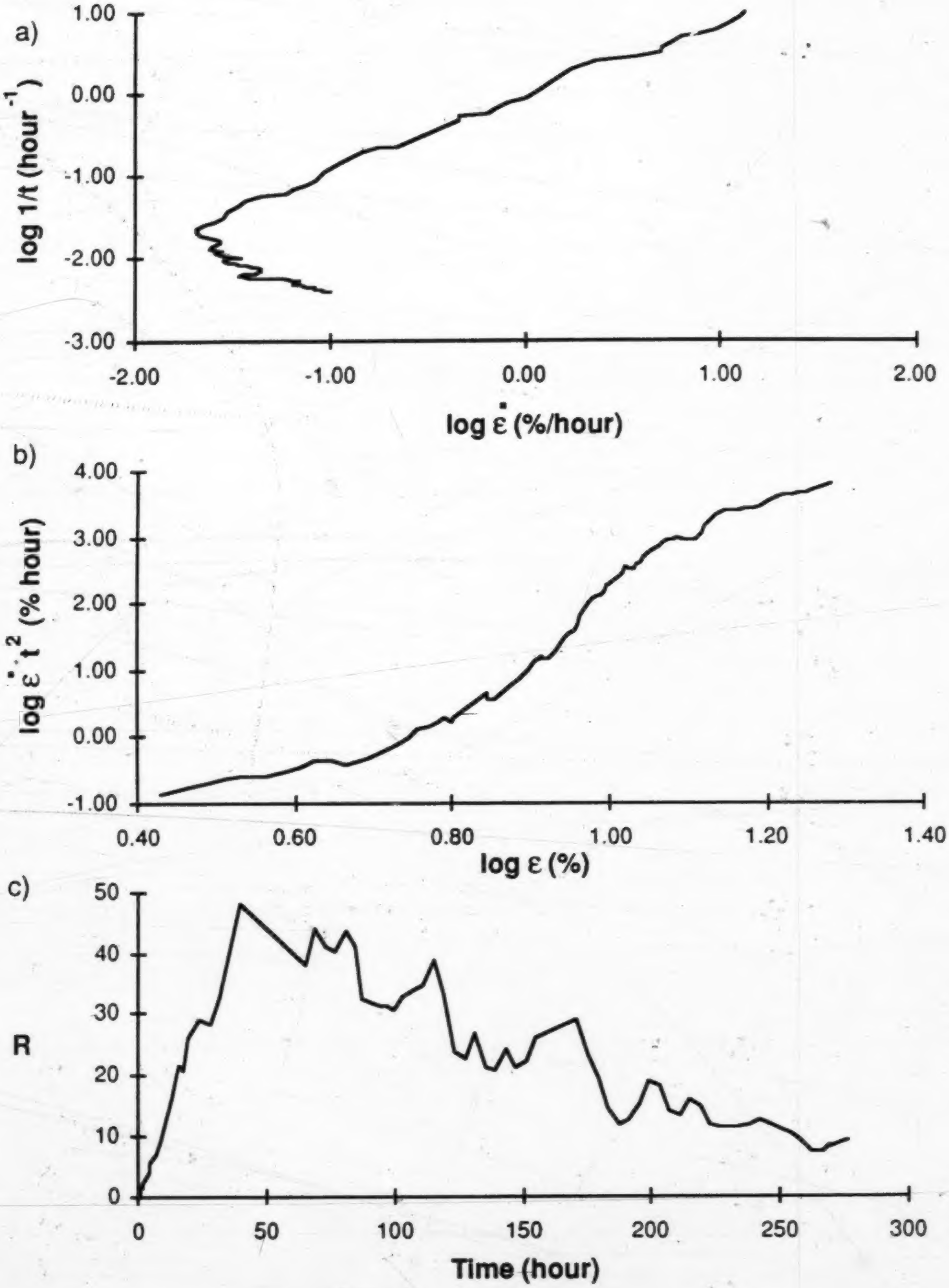

Figure D.39: Creep test CR-68 soil C 10 ppt at σ=1098 kPa
a) log 1/t vs log strain rate (Sayles, 1968)
b) log strain rate time^2 vs log strain (Vyalov, 1988)
c) R = $d\varepsilon / dt$ vs time (Berggren and Furuberg, 1985)

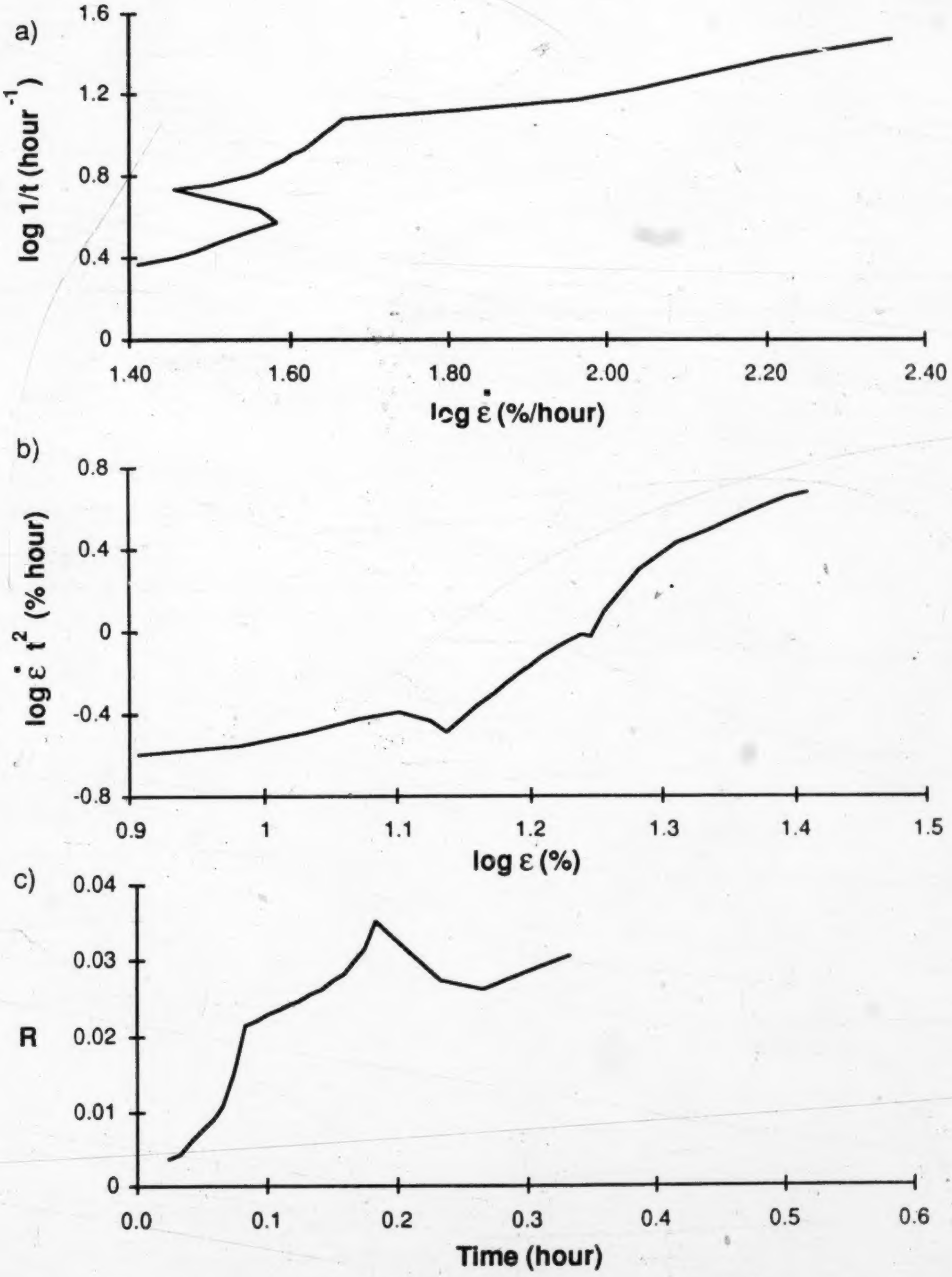

Figure D.40: Creep test CR-76 soil C 30 ppt at σ=1222 kPa
a) log 1/t vs log strain rate (Sayles, 1968)
b) log strain rate time^2 vs log strain (Vyalov, 1988)
c) R = dε / dt vs time (Berggren and Furuberg, 1985)

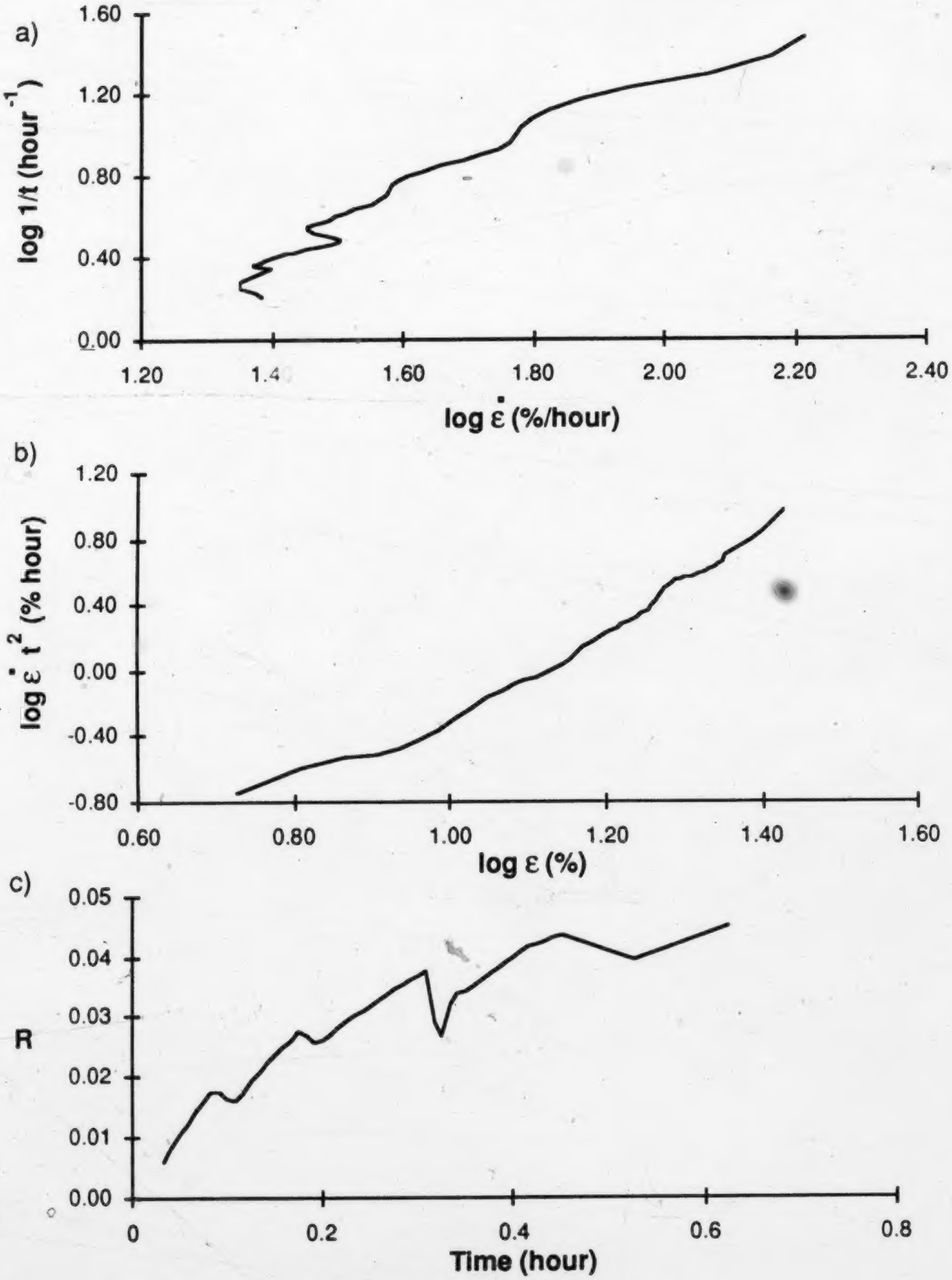

Figure D.41: Creep test CR-78 soil C 30 ppt at σ=1008 kPa
a) log 1/t vs log strain rate (Sayles, 1968)
b) log strain rate time^2 vs log strain (Vyalov, 1988)
c) R = dε / dt vs time (Berggren and Furuberg, 1985)

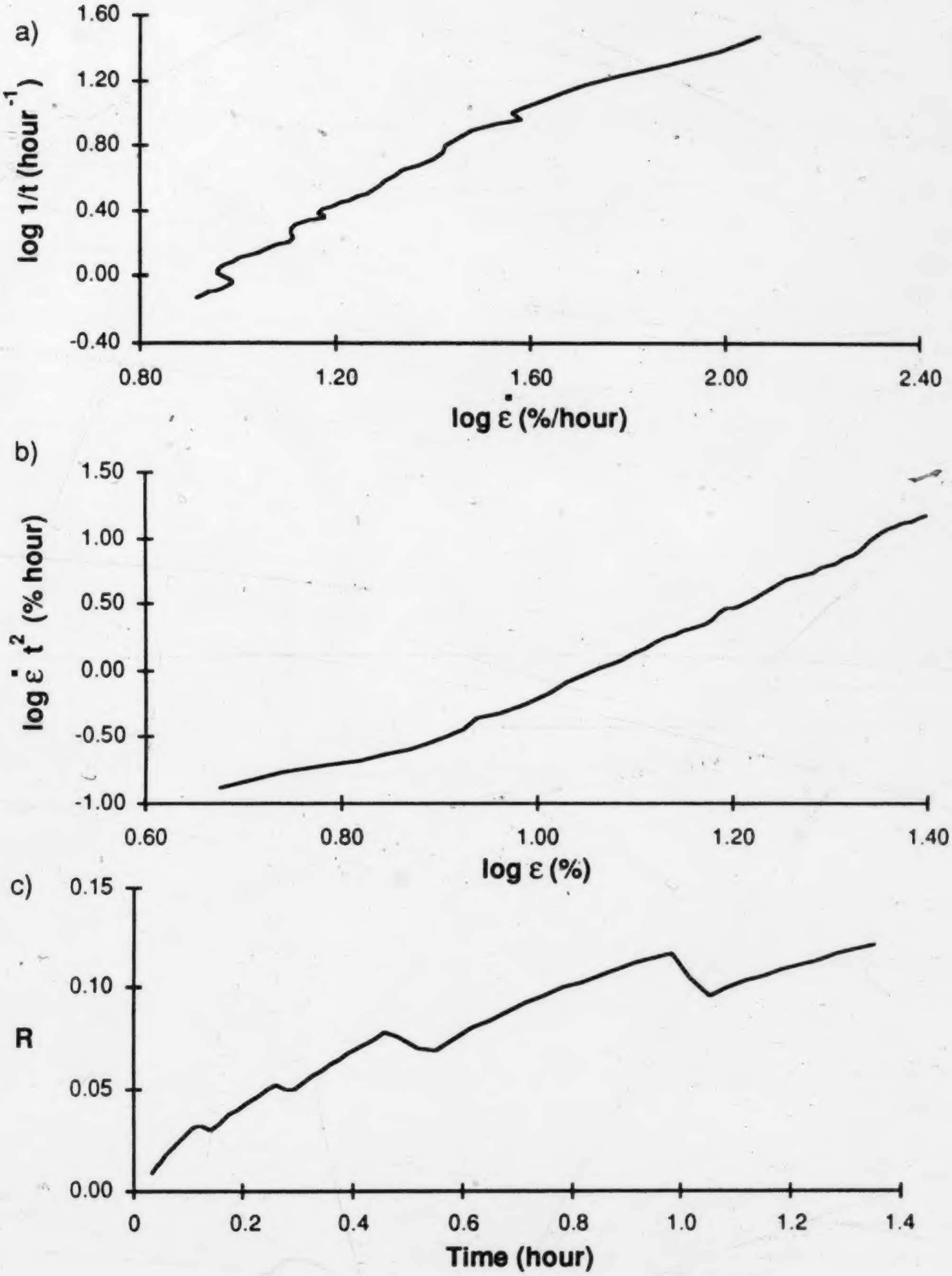

Figure D.42: Creep test CR-91 soil C 30 ppt at σ=794 kPa
a) log 1/t vs log strain rate (Sayles, 1968)
b) log strain rate time^2 vs log strain (Vyalov, 1988)
c) R = dε / dt vs time (Berggren and Furuberg, 1985)

APPENDIX E

STRAIN vs TIME PREDICTIONS
by
SAYLES's (1968)
VYALOV et al. (1988)
GARDENER et al. (1984)

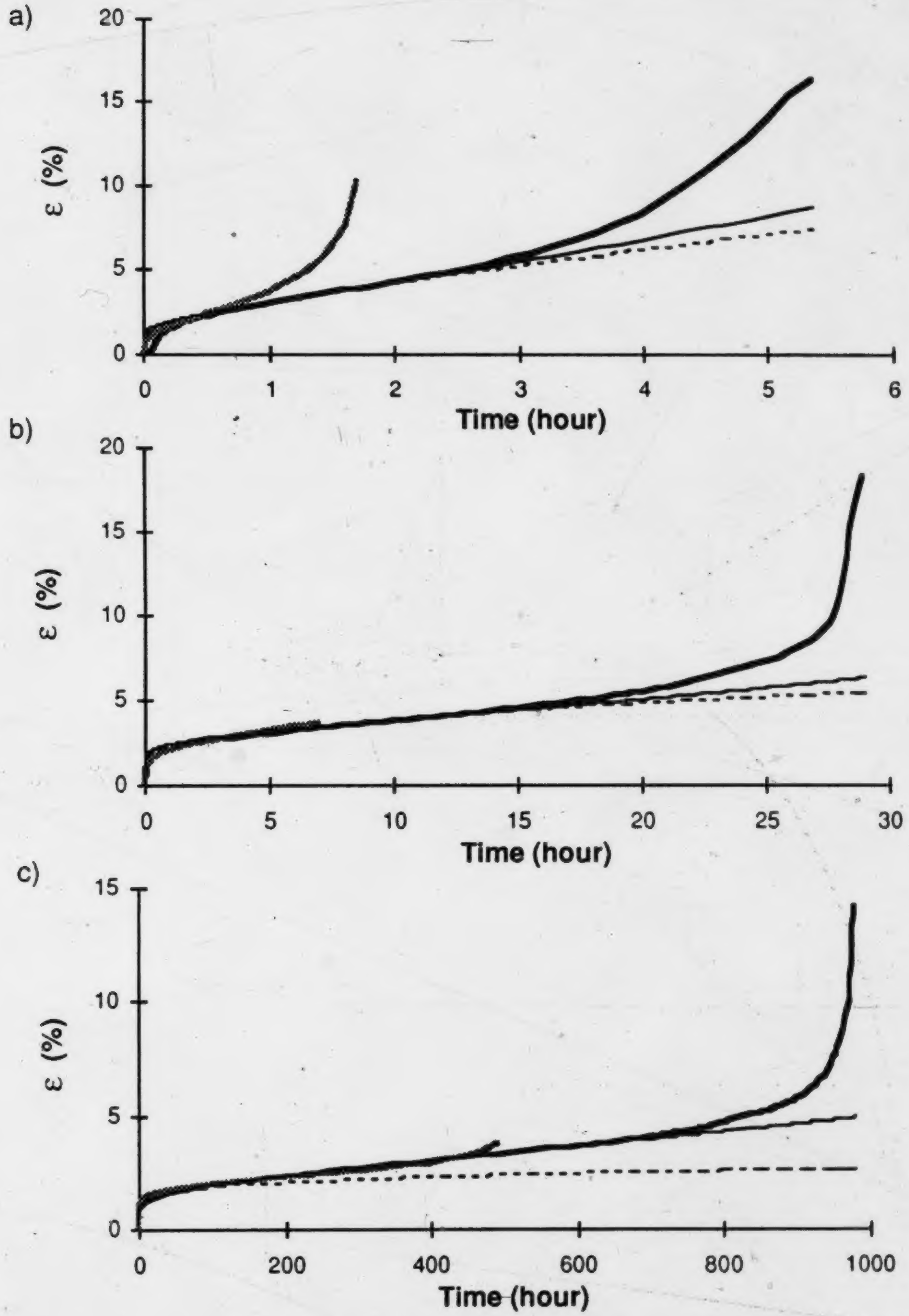

Figure E.1: Comparison between measured strain and predicted strain for soil A 0 ppt a) Test CR-45 b) Test CR-92 c)Test CR-95

▬ measured strain -- Sayles ▬ Vyalov — Gardener

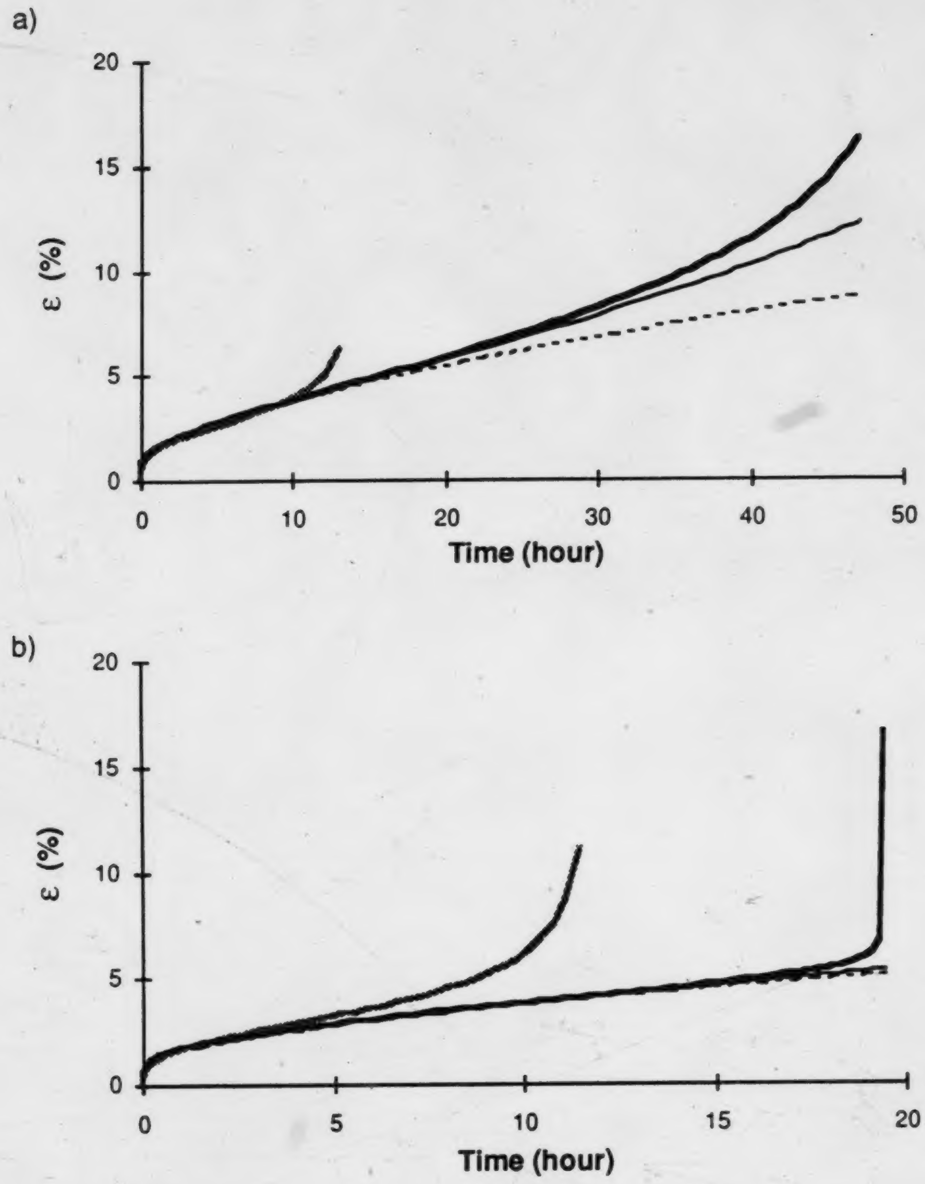

Figure E.2: Comparison between measured strain and predicted strain for soil A 5 ppt a) Test CR-59 b) Test CR-51

— measured strain -- Sayles — Vyalov — Gardener

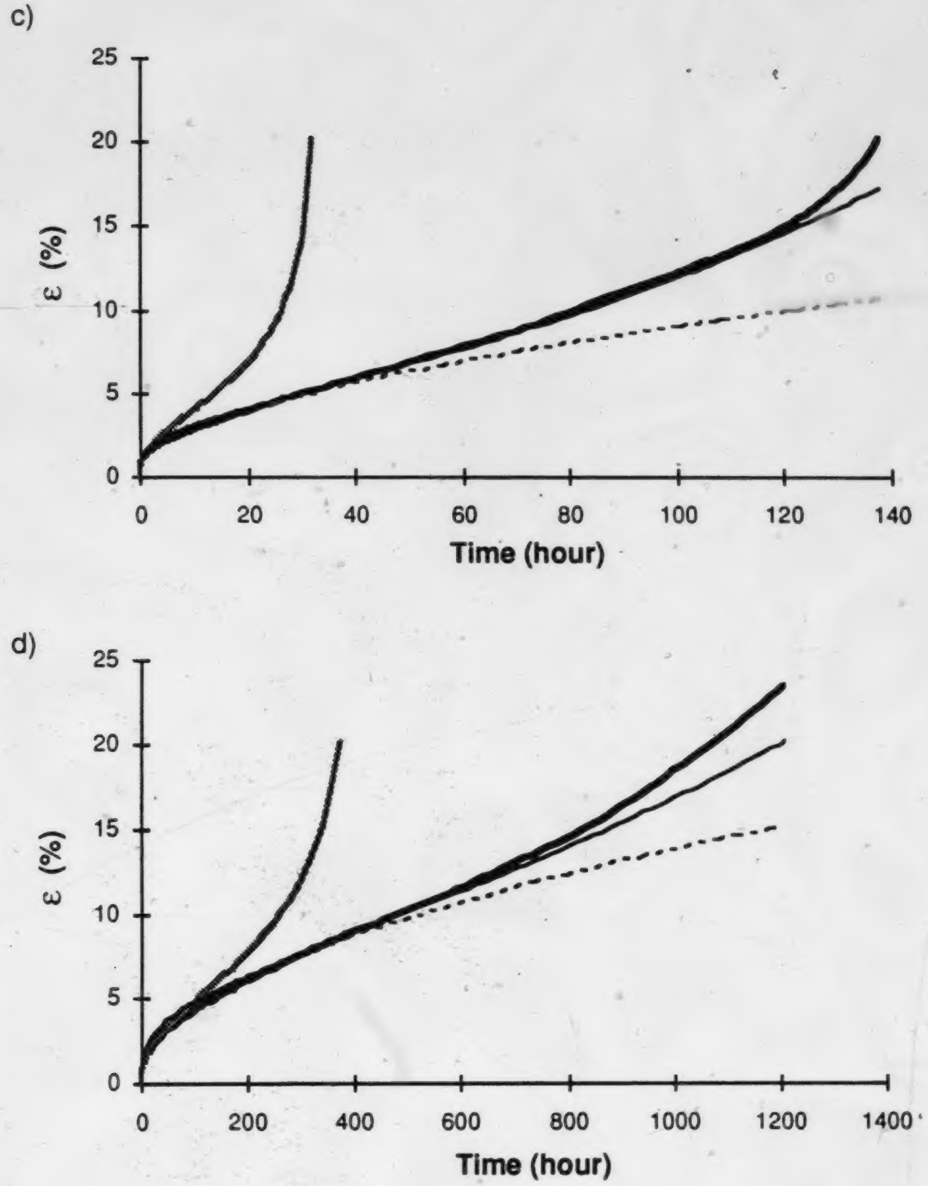

Figure E.2 con't:
Comparison between measured strain and predicted strain for soil A 5 ppt c) Test CR-60 d) Test CR-67
— measured strain -- Sayles — Vyalov — Gardener.

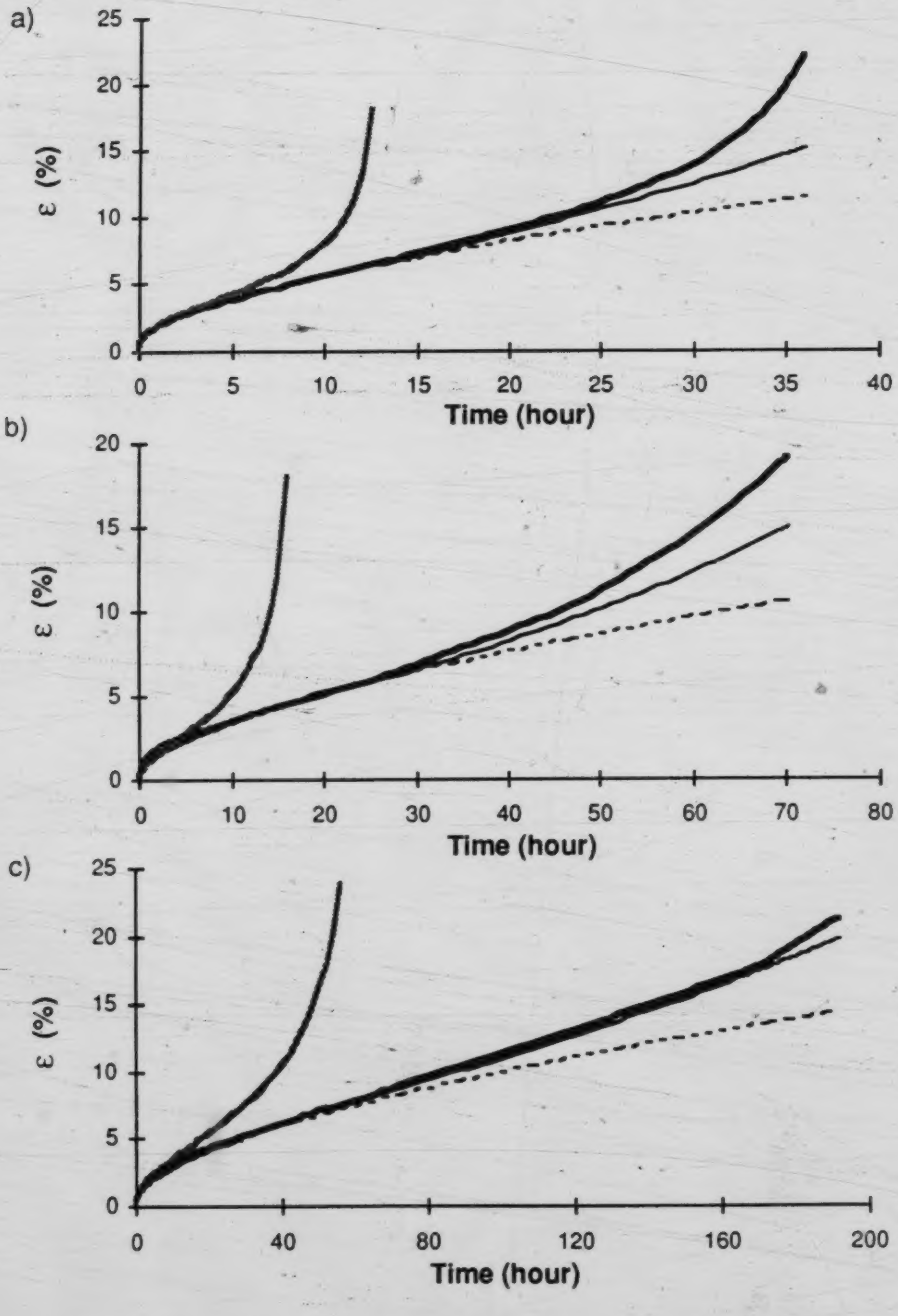

Figure E.3: Comparison between measured strain and predicted strain for soil A 10 ppt a) Test CR-86 b) Test CR-47 c)Test CR-87

— measured strain - - Sayles — Vyalov — Gardener

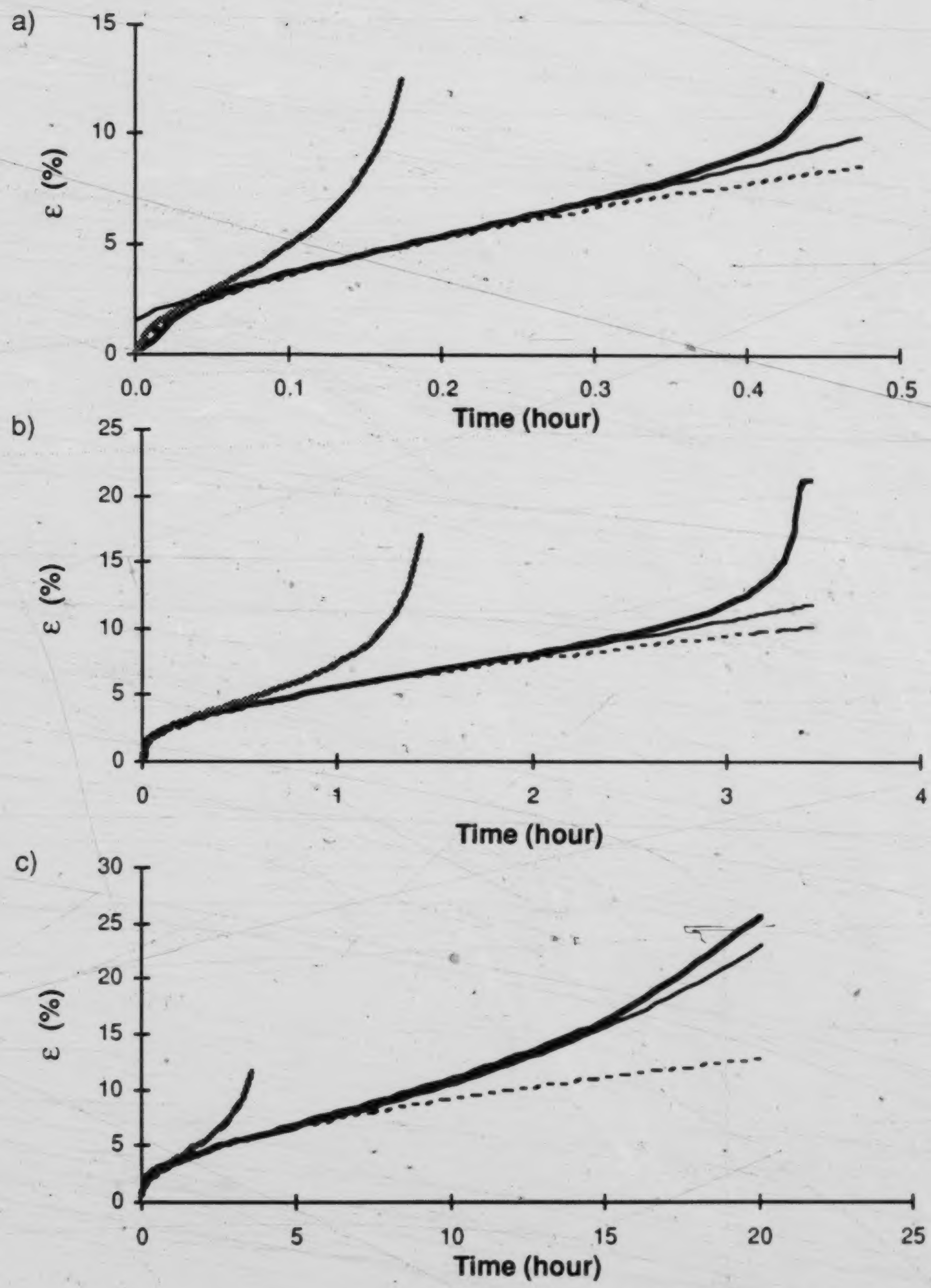

Figure E.4: Comparison between measured strain and predicted strain for soil A 30 ppt a) Test CR-64 b) Test CR-70 c)Test CR-72

— measured strain -- Sayles — Vyalov — Gardener

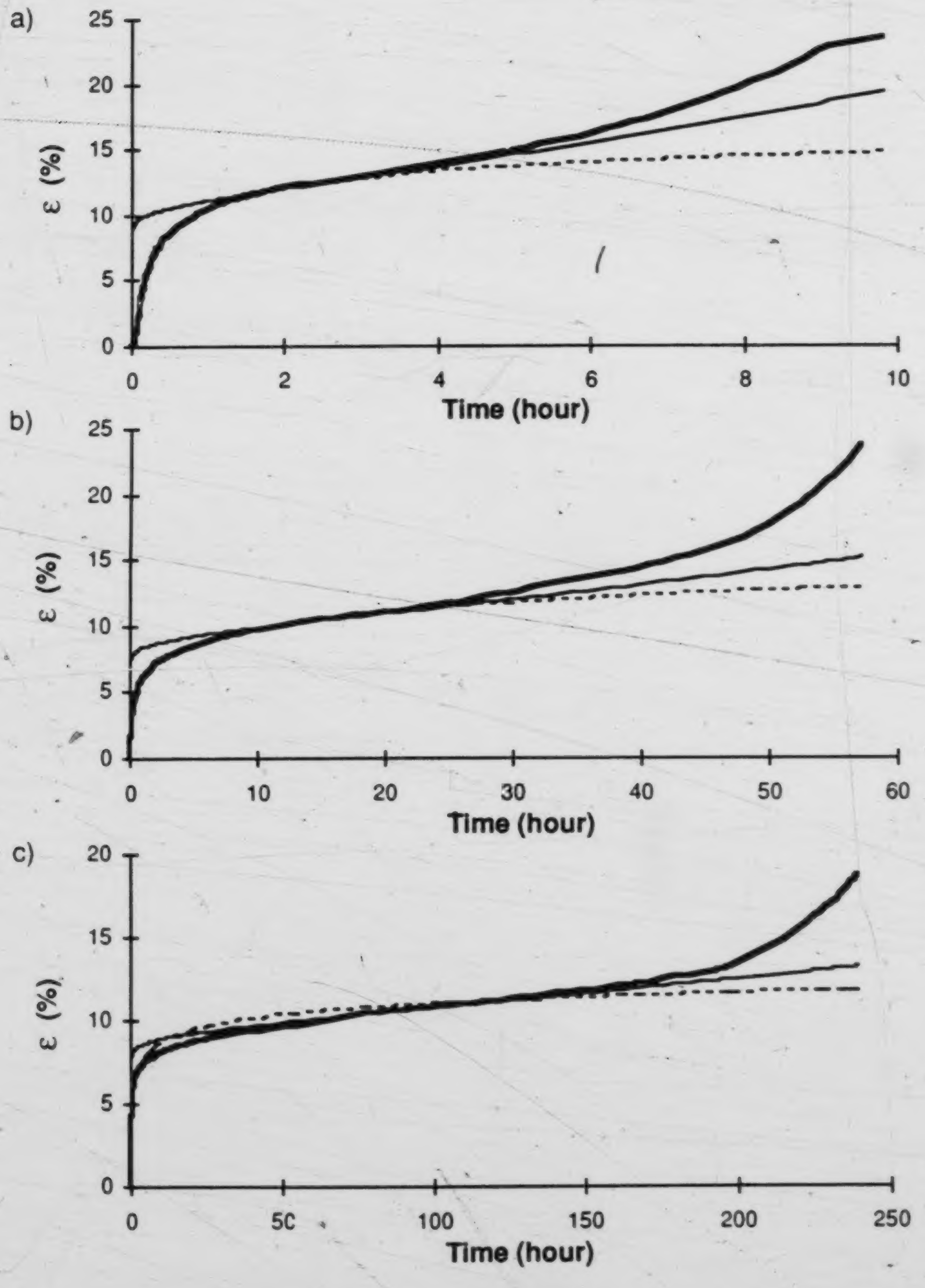

Figure E.5: Comparison between measured strain and predicted strain for soil B 0 ppt a) Test CR-83 b) Test CR-71 c)Test CR-81

▬ measured strain -- Sayles — Gardener

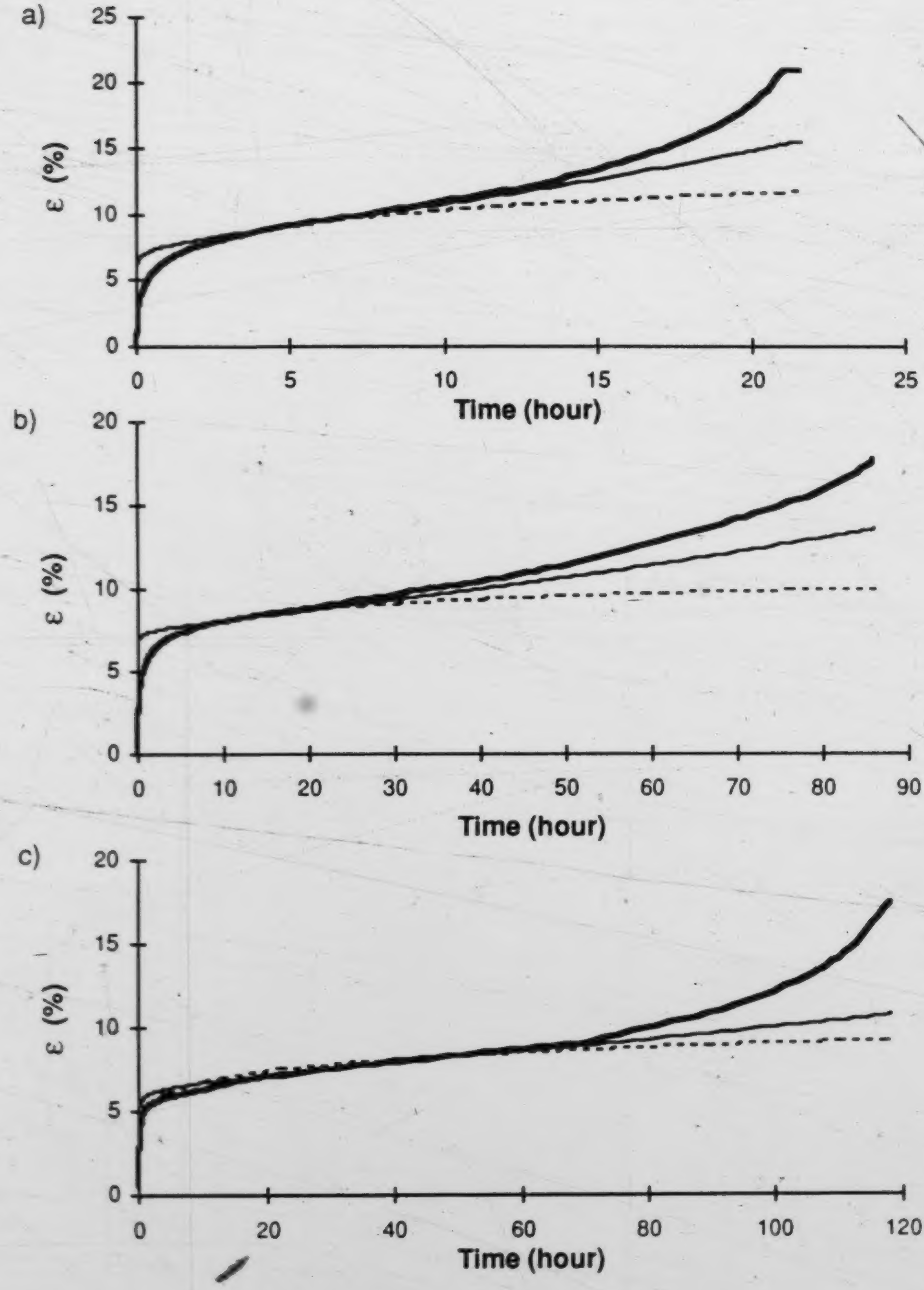

Figure E.6: Comparison between measured strain and predicted strain for soil B 5 ppt a) Test CR-84 b) Test CR-49 c)Test CR-9

— measured strain -- Sayles — Gardener

d)

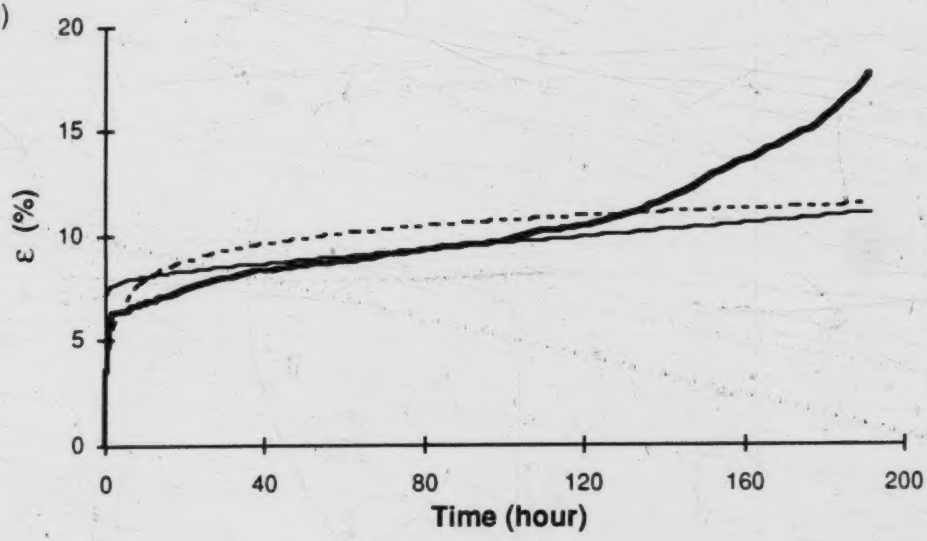

e)

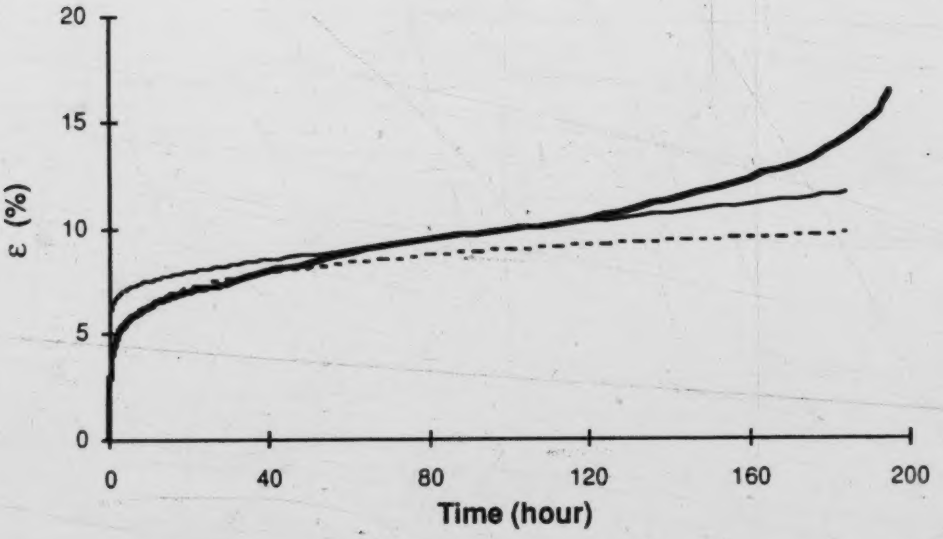

Figure E.6 con't:
Comparison between measured strain and predicted strain for soil B 5 ppt d) Test CR-17 e) Test CR-32
— measured strain -- Sayles — Gardener

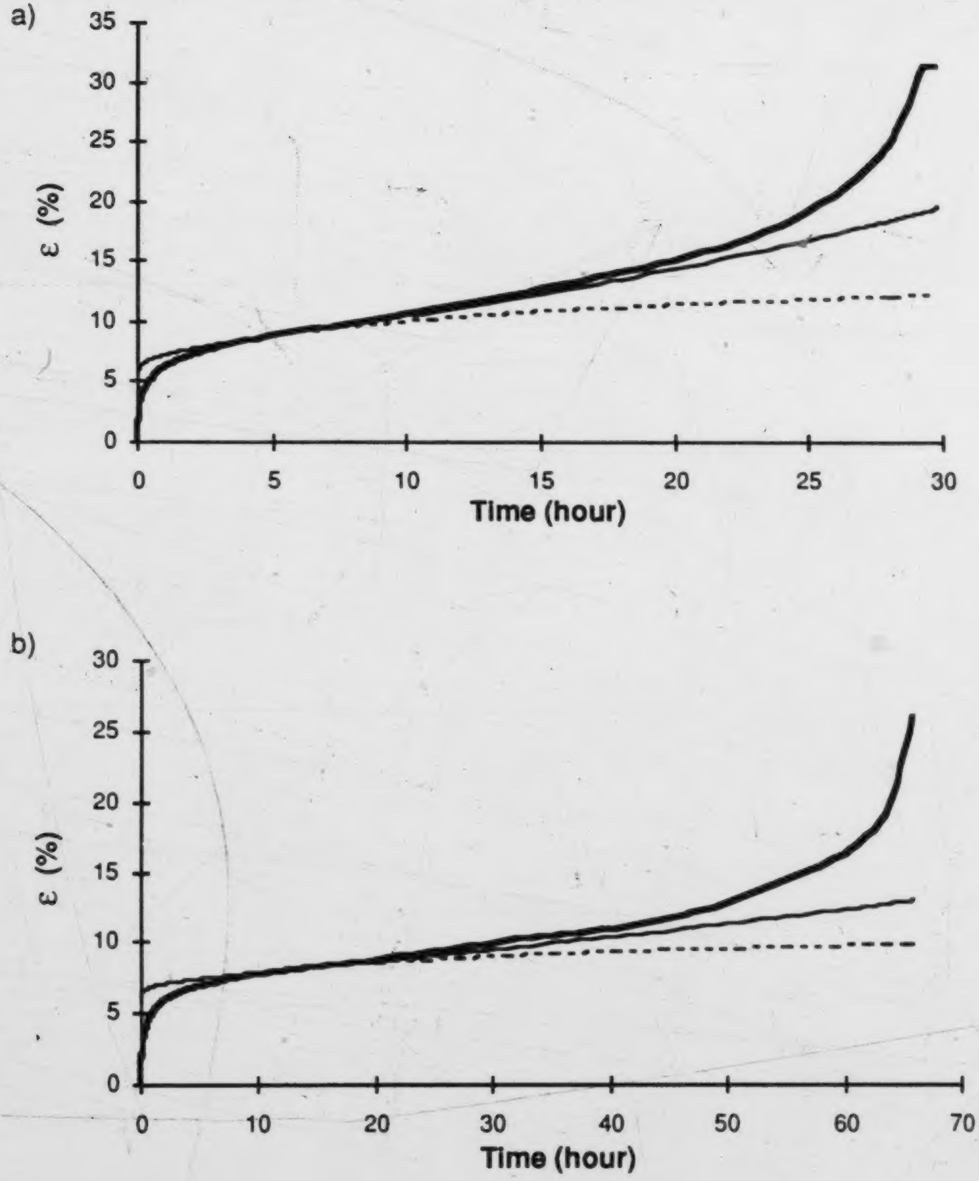

Figure E.7: Comparison between measured strain and predicted strain for soil B 10 ppt a) Test CR-82 b) Test CR-50

▬ measured strain -- Sayles — Gardener

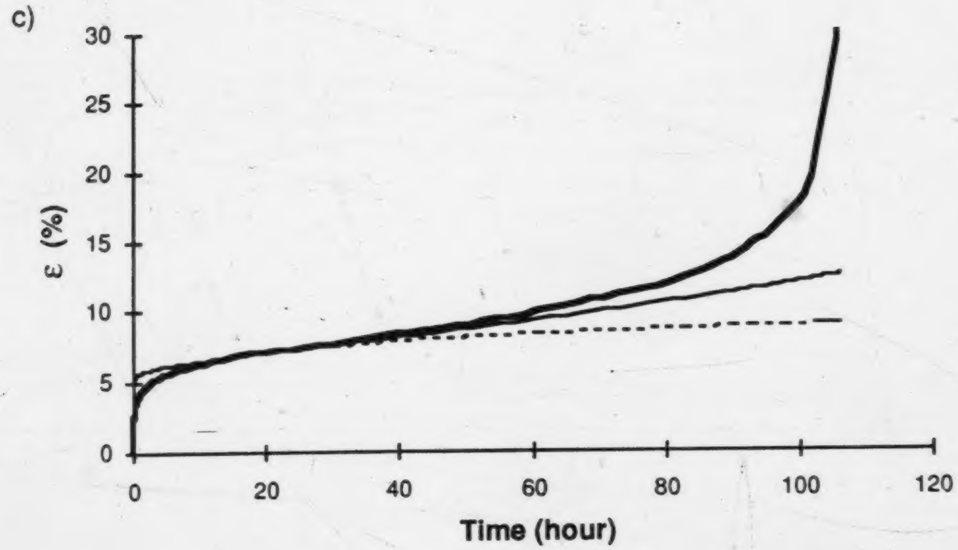

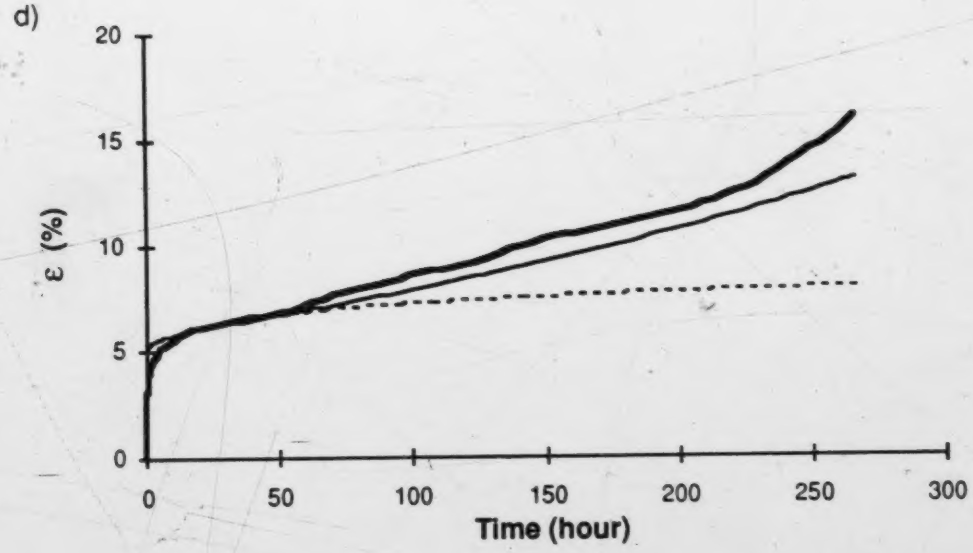

Figure E.7 con't:
Comparison between measured strain and predicted strain for soil B 10 ppt c) Test CR-33 d) Test CR-38
— measured strain -- Sayles — Gardener

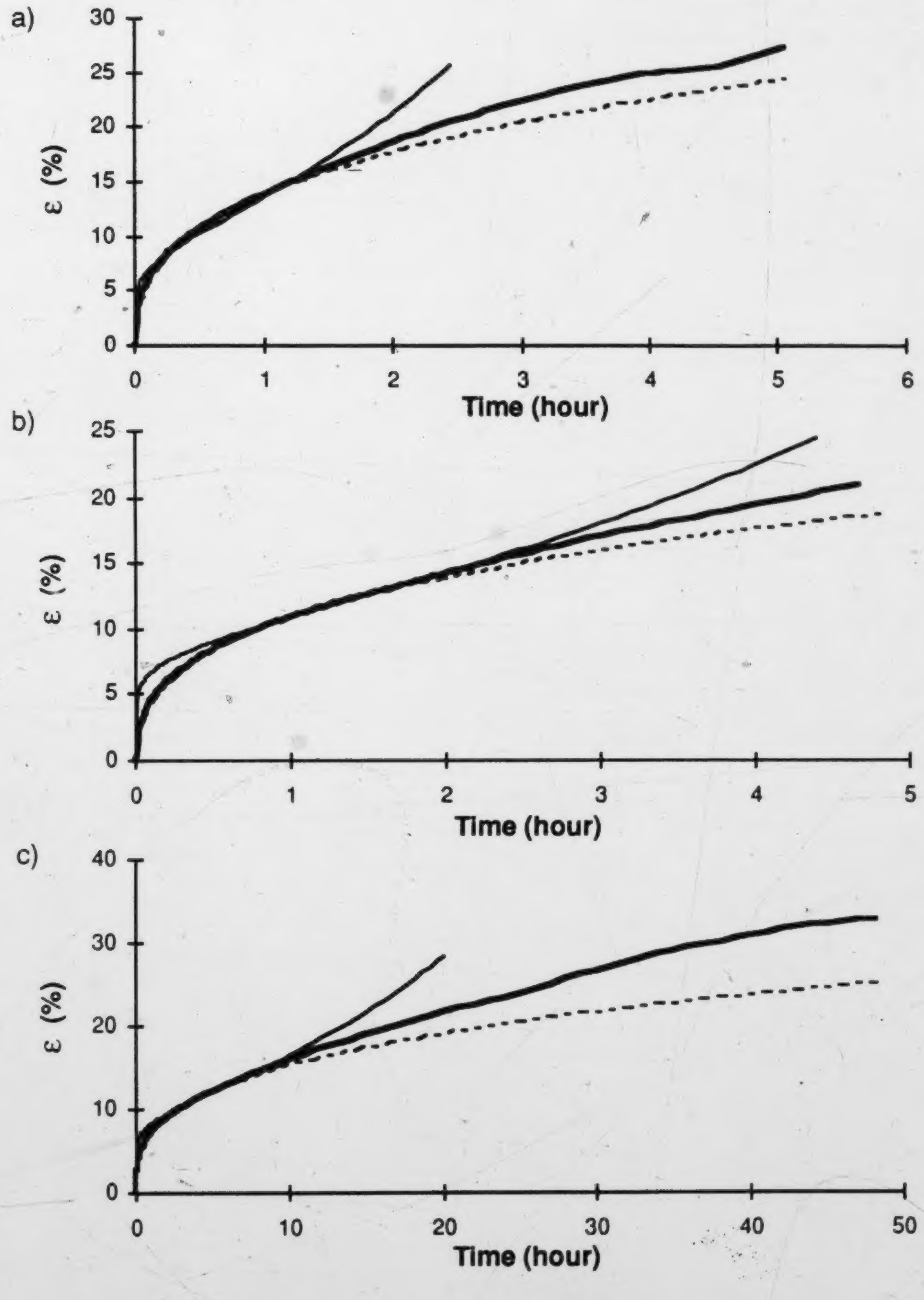

Figure E.8: Comparison between measured strain and predicted strain for soil B 30 ppt a) Test CR-75 b) Test CR-77 c)Test CR-88

▬ measured strain -- Sayles — Gardener

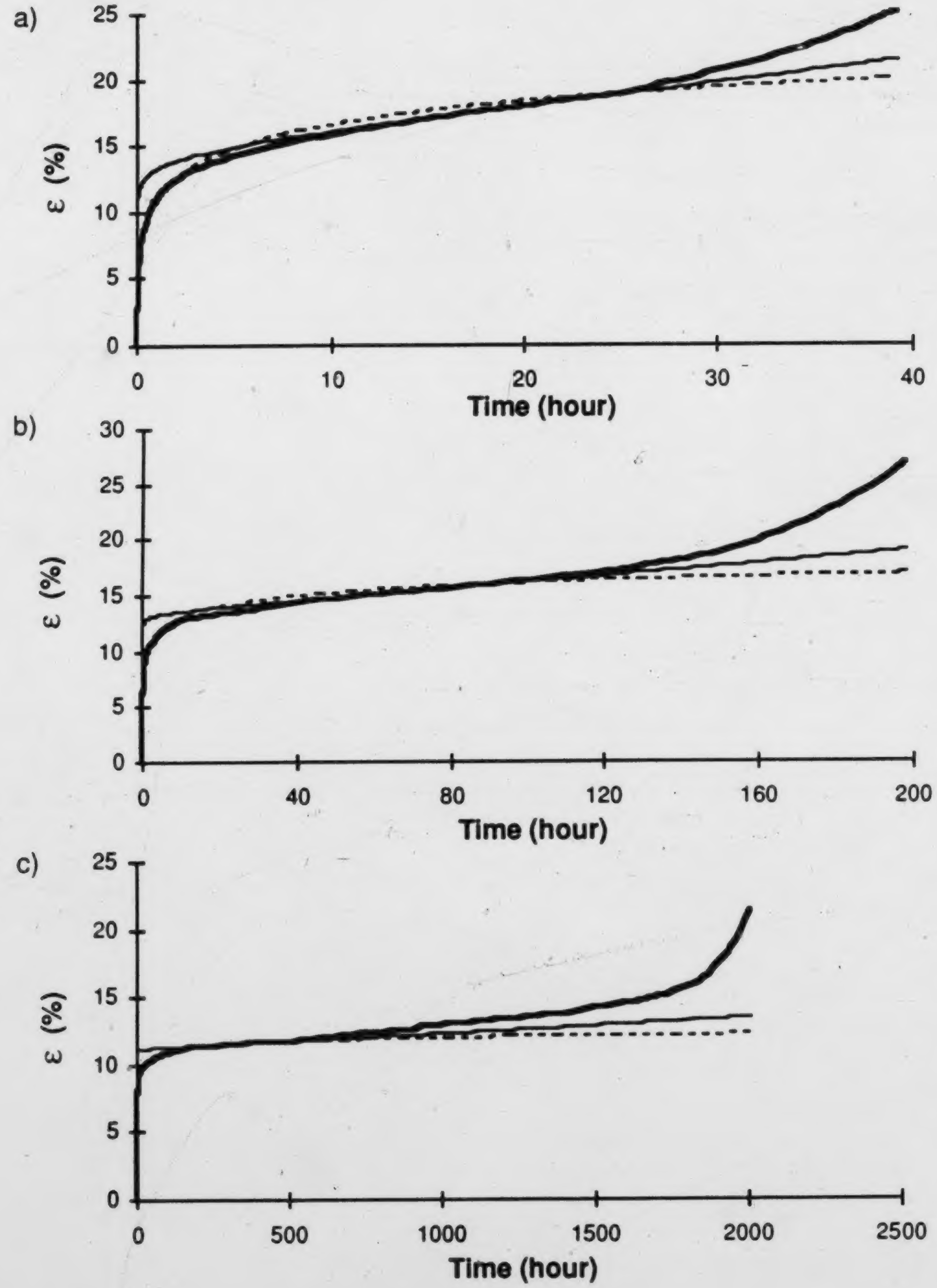

Figure E.9: Comparison between measured strain and predicted strain for soil C 0 ppt a) Test CR-79 b) Test CR-65 c)Test CR-36

▬ measured strain -- Sayles — Gardener

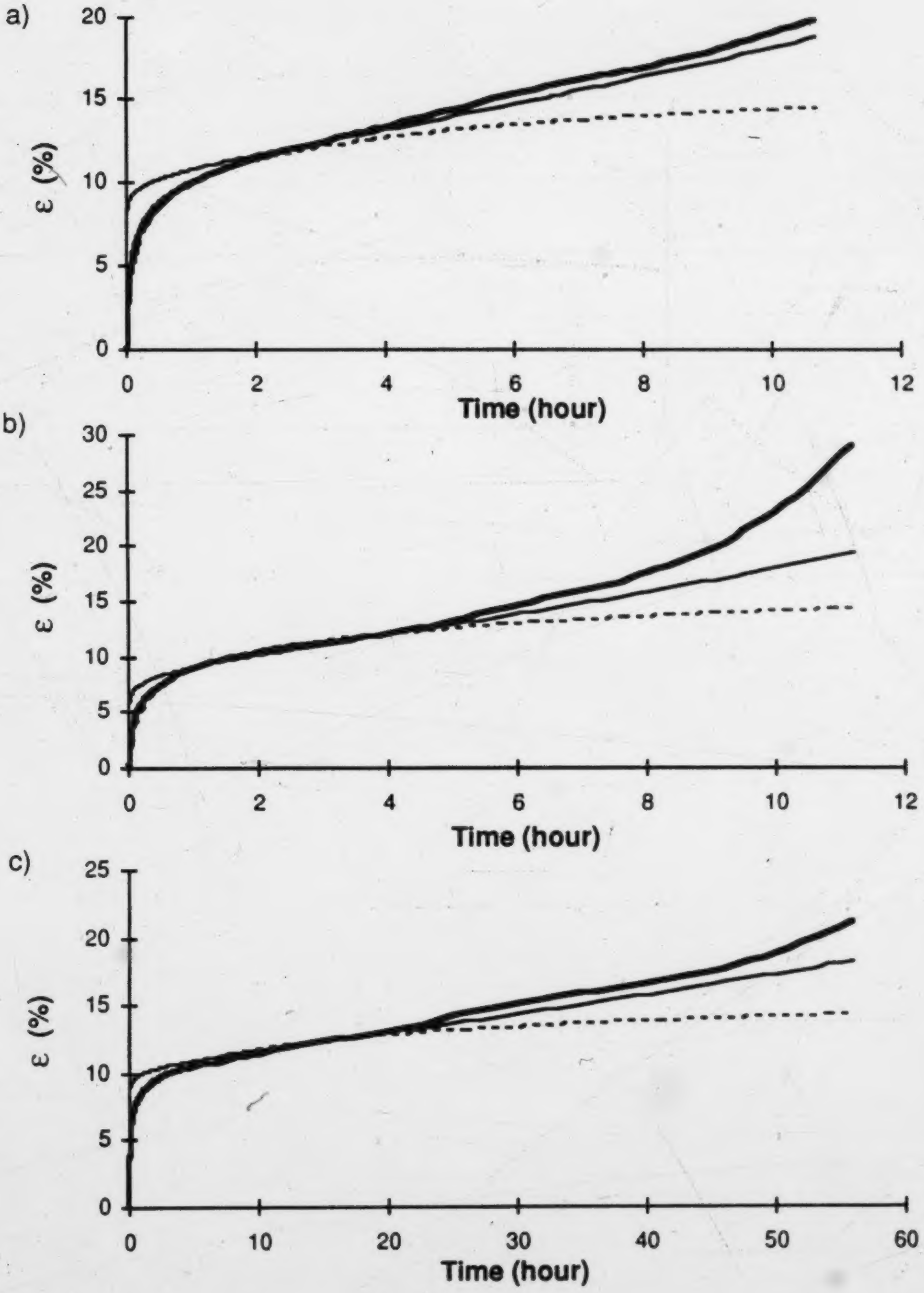

Figure E.10: Comparison between measured strain and predicted strain for soil C 5 ppt a) Test CR-96 b) Test CR-66 c)Test CR-62

— measured strain -- Sayles — Gardener

d)

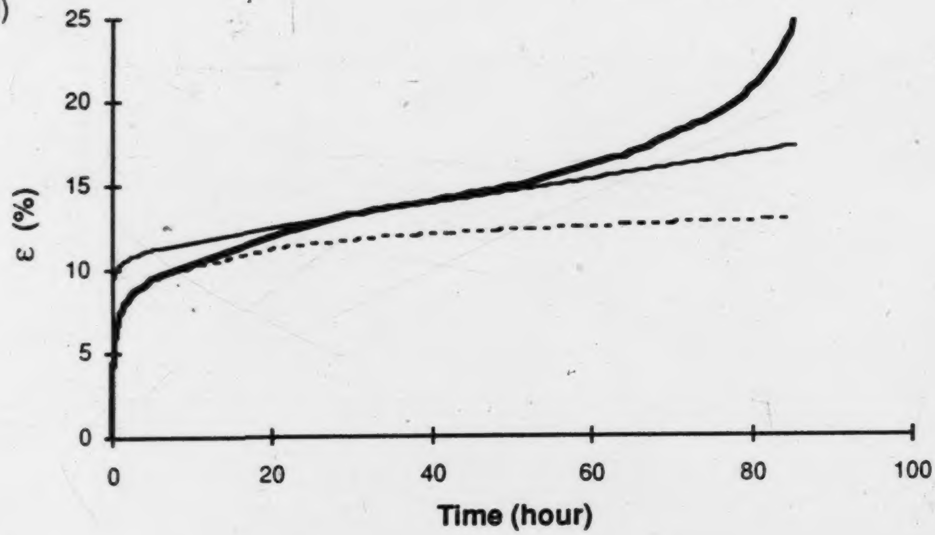

e)

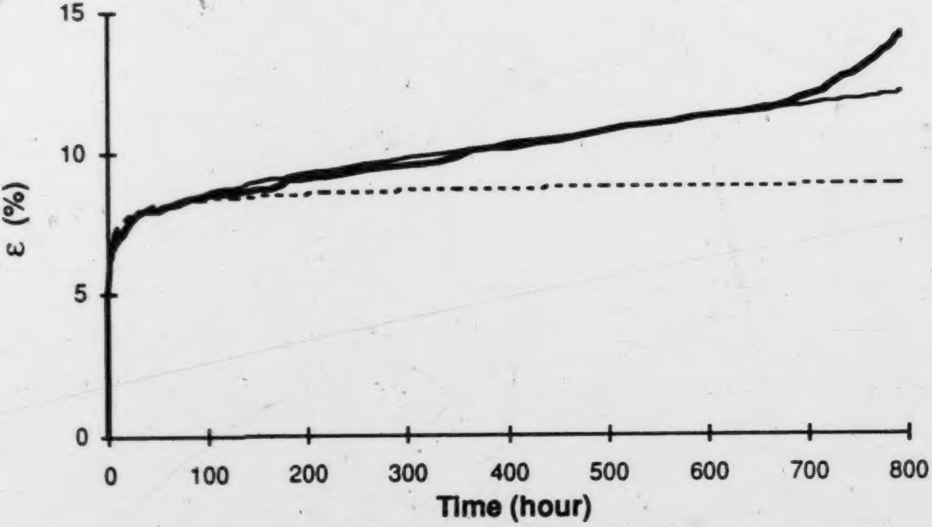

Figure E.10 con't:
Comparison between measured strain and predicted strain for soil C 5 ppt d) Test CR-89 e) Test CR-94
— measured strain -- Sayles — Gardener

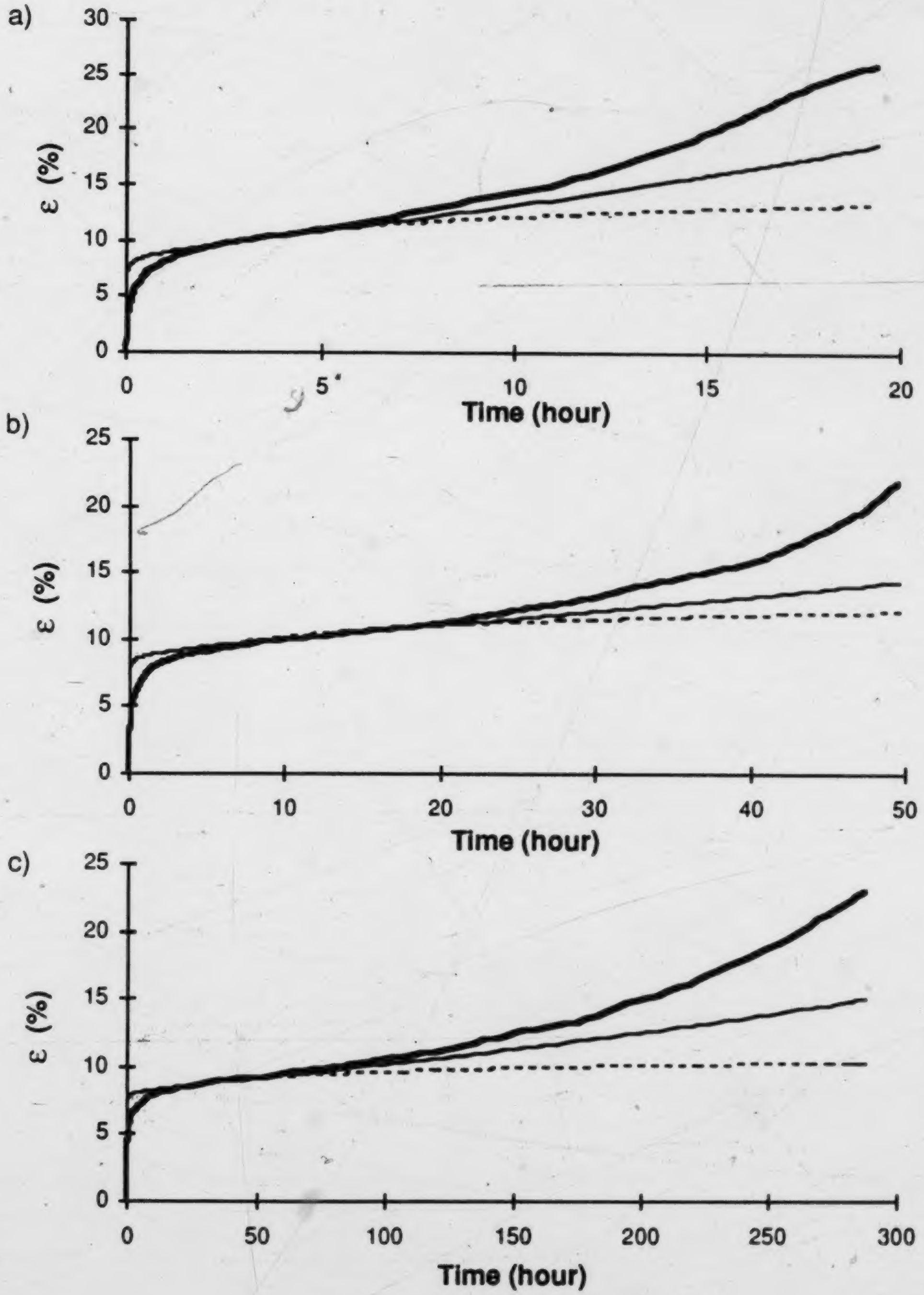

Figure E.11: Comparison between measured strain and predicted strain for soil C 10 ppt a) Test CR-55 b) Test CR-52 c)Test CR-68

━ measured strain -- Sayles — Gardener

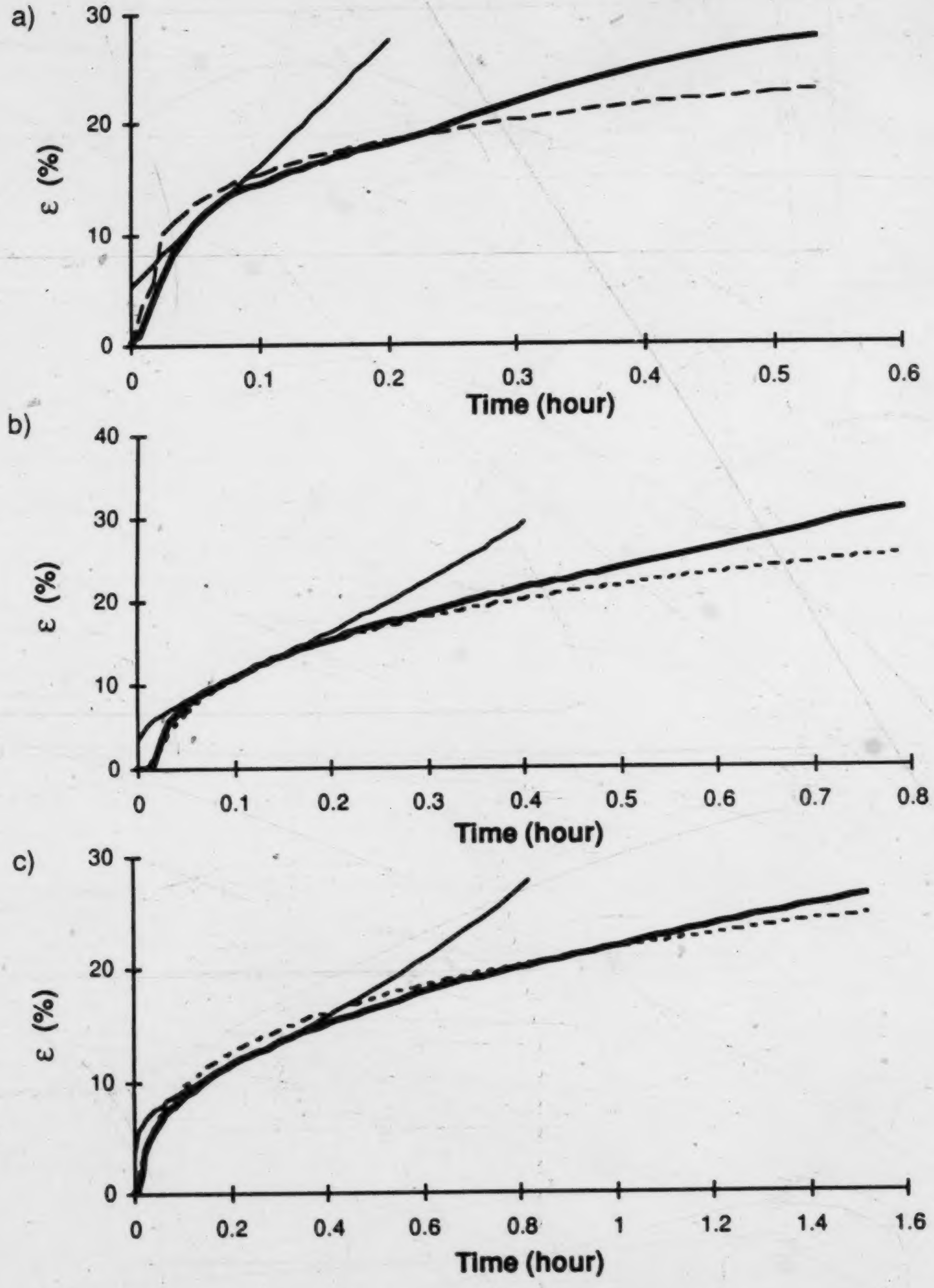

Figure E.12: Comparison between measured strain and predicted strain for soil C 30 ppt a) Test CR-76 b) Test CR-78 c)Test CR-91

▬ measured strain -- Sayles — Gardener